Examining the Impact of Caspase Activities in PD Animal Model & Differentiated ReNcell VM

Zahara Latif Chaudhry

Examining the Impact of Caspase Activities in PD Animal Model & Differentiated ReNcell VM

Zahara Latif Chaudhry

A Thesis Submitted in Partial Fulfilment of the Requirements for The Degree of

Doctor of Philosophy

in

Institute of Biomedical and Environmental Science and Technology

Faculty of Creative Arts, Technologies and Sciences

University of Bedfordshire

December 2015

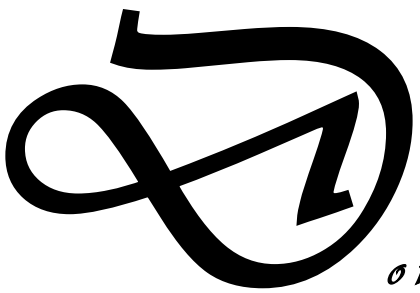

o not follow where the path may lead.

Go instead where there is no path and leave a trail

Ralph Waldo Emerson

In memory of my late father who has been my silent inspiration .....

.....My mother for her continuous confidence and optimism

.

I HOPE THIS ACHIEVEMENT WILL COMPLETE THE DREAM YOU HAD FOR ME ALL THOSE MANY YEARS AGO WHEN YOU CHOSE TO GIVE ME THE BEST EDUCATION YOU COULD.

Acknowledgements

I am indebted to the University of Bedfordshire for allowing me to read for this degree. I am grateful to my late father Mr Muhammed Latif Chaudhry and my brother Dr Qasim Chaudhry who provided funds to continue my studies. I would like to take the opportunity to thank my family, in particular my sisters for their moral support and much appreciated good sense of humour. I would like to give a special appreciation to my adorable friends for being the spring boards, role models, silent listeners, cheerleaders and pillars of strength that I have needed. I would like to offer my thanks to my supervisors for sharing their knowledge throughout the degree. I would like to thank Tiantian Zhang who provided PVC Research and my supervisor who provided RiT grant to partially support this thesis. I would like to thank our collaborators Jozef Langfort and Malgorzata Chalmoniuk at Dr Jozef Langfort laboratories Medical Research Centre, Polish Academy of Sciences, Warsaw, Poland, for providing PD animal samples for the initial part of this project. Lastly, I offer my gratitude to all of those who supported me in any respect during the completion of the project.

.

Abstract

Parkinson's disease (PD) is a neurodegenerative disorder that is characterised by uncontrollable shaking, muscular rigidity and cognitive impairment, due to low levels of dopamine caused by loss of dopamine containing neurons (DCN). The loss of DCN has been strongly associated with Caspase mediated apoptotic death. At present there are many studies that indicate exercise is beneficial in PD treatment, but there is a lack of research exploring the potential pathways, which exercise can activate and suppress to provide such positive and even negative effects.

This study is the first to explore the effect of treadmill exercise on the level of Caspases, along with CAMK-IV protein in different brain regions of MPTP-treated rat model, using WB analysis. The results of this research has demonstrated reduction or completely suppression of some active Caspases, as well as, elevated amount of CAMK-IV in different brain regions of exercised PD animal model. To determine how exercise is reducing and inhibiting activation of Caspases, the first step was to identify how Caspases are stimulated, using ReNcell VM stem cell line that had been differentiated and treated with 6OHDA.

The results of the study demonstrated 6OHDA triggered Caspase mediated apoptotic death of dDCN via PERK ER stress and NFκB classical pathway. IF, WB and cell viability analysis, using a wide range of inhibitors, showed that Caspase-2 is activated by the PERK pathway of ER stress and NFκB classical pathway in 6OHDA treated dDCN. 6OHDA triggered activation of Caspase- 8 by the classical pathway in NFκB mediated death of dDCN. 6OHDA triggered Caspase-4 activation but the exact mechanism involved remains to be identified. Only through understanding the molecular pathways regulating death of DCN in PD, new potential targets for therapy may be identified, which may ultimately reduce further death of DCN and slow PD progression. This proposed study has the potential to seek for more efficient drugs, which can suppress Caspase activation by targeting key targets in the pathways that the Caspases follow. These new specific targeted drugs could be used with treadmill exercise to achieve maximum effect, by slowing down or inhibiting further death of DCN.

Contents Page

List of Figures

Abbreviations

AIF	Apoptosis Initiating Factor
AMPA	αAmino 3 Hydroxyl 5 Methyl 4 Isoxalopropionate
Apaf-1	Apoptosis Activating Factor 1
ASC	Apoptosis associated Speck like protein containing a CARD
ASK-1	Apoptosis Signal Regulating Kinase 1
ATP	Adenosine 5 Triphosphate
ATF-4	Activating Transcription Factor 4
ATF-6	Activating Transcription Factor 6
BAK	Bcl-2 Antagonist Killer protein
BAX	BCL-2 Associated X protein
BCA	Bicinchoninic acid
BCL-2	B Cell Lymphoma 2
BDNF	Brain-Derived Neurotrophic Factor
BID	B Cell Lymphoma 2 Homology Domain 3 Interacting-Domain
BiP	Immunoglobulin Binding Protein
C	Control/ Untrained/ Untreated
CAD	Caspase Activated DNA
CAMK	Calmoduline Protein Kinase
CAMK-IV	Calmoduline Protein Kinase IV
CARD	Caspase Recruitment Domain
CHOP	C/EBP homologous protein
Compound A	7-[2-(cyclopropylmethoxy)-6-hydroxyphenyl]-5-[(3S)-3-piperidinyl]-1,4-dihydro-2H-pyrido[2,3-d][1,3]oxazin-2-one hydrochloride
DBS	Deep Brain Stimulation
DCF	2', 7'-dichlorofluorescin
DCFDA	2',7'-dichlorofluorescein diacetate

DCFH-DiOxyQ	Dichlorodihydrofluorescin DiOxyQ
DCN	Dopamine Containing Neurons
dDCN	Differentiated Dopamine Containing Neuron
DISC	Death Inducing Signal Complex
DMEM	Dulbecco's Modified Eagle Medium
DNA PK	DNA Dependent Protein Kinase
DOPAC	Dihydroxyphenylacetic acid
DTT	Dithiothreitol
DR-5	Death Receptor 5
E1	Ubiquitin Activating Enzymes
E2	Ubiquitin Conjugating Enzymes
E3	Ubiquitin Protein Lligase
ECL	Enhanced Chemiluminescent
EDEM	ER Degradation Enhancing α-Mannosidase
EGF	Epidermal Growth Factor
EGTA	Ethylene Glycol Tetraacetic Acid
eIF-2α	Eukaryotic translation initiation factor 2 subunit α
ELISA	Enzyme-linked immunosorbent assay
ER	Endoplasmic Reticulum
ERAD	Endoplasmic Reticulum Associated Degradation
ERO-1	ER Oxidoreductin 1
ERp-72	ER protein 72
ERp-61	ER protein 61
ERp-57	ER protein 57
ERp-44	ER protein 44
ERp-29	ER protein 29
ERSE	ER Stress Response Element
Ex	Exercise / Trained
FADD	Fas Associated Domain

FGF	Fibroblast Growth Factor basic
GADD34	Growth Arrest DNA Damage-inducible gene 34
GADD153	Growth Arrest DNA Damage-inducible gene 153
GAPDH	Gylceraldehyde-3-Phosphate Dehydrogenase
GDNF	Glial cell-Derived Neurotrophic Factor
HNE	4, Hydroxyl 2 Nonenal
HTRA-2	High Temperature Requirement A2
IAP	Inhibitor of Apoptosis Protein
ICAD	Inhibitor of Caspase-activated DNA
IF	Immunofluorescence
IκB	NFκB inhibitor
IKK	IκB kinase
IL-1β	Interleukin-1β
IL-6	Interleukin 6
IL-8	Interleukin 8
IMM	Inner Mitochondrial Membrane
IMS	Inner Membrane Space
iNOS	inducible Nitric Oxide Synthetase
IP	intraperitoneally
IRE-1	Inosital Requiring Enzyme 1
JNK	c- Jun-N-terminal kinases
L-DOPA	Levo Dopamine
LRRK-2	Leucine Rich Repeat Kinase 2
MAO	Monoamine Oxidase
MAOS	Membrane associated oxidative stress
MAPK	Mitogen Activated Protein Kinase
MPP+	1-Methyl 4-Phenylpyridinium
MPTP	1-Methyl 4-Phenyl 1, 2, 3, 6-Tetrahydropyridine

MTT	3-(4, 5-dimethylthiazolyl-2)-2, 5-diphenyltetrazolium bromide assay
NADH	Nicotinamide Adenine Dinucleotide(reduced)
NBD	NFκB essential modifier-Binding Domain
NEMO	NFκB Essential Modulator
NFκB	Nuclear Factor Kappa B
NIK	NFκB Inducing Kinase
Noxa	NADPH Oxidase Factor
NSC	Neural Stem Cell
6OHDA	6-hydroxydopamine
OMM	Outer Mitochondrial Membrane
Pael-R	Parkin Associated Endothelin Receptor like Receptor
PARP	Poly (ADP-Ribose) Polymerase
PBS	Phosphate Buffered Saline
PCD	Programmed cell death
PC 12	Pheochromocytoma cell line
PD	Parkinson's Disease
PD-Ex	Parkinson's Disease Exercise induced
PDI-5	Protein Disulphide Isomerise 5
PERK	Protein kinase RNA-like Endoplasmic Reticulum Kinase
PIDD	p53-Induced Death Domain
PINK-1	PTEN Induced Putative Kinase 1
PMCA	Plasma Membrane Calcium Pump
PMSF	Phenylmethylsulfonylfluoride
PTP	Permeability Transition Pore
p-JNK	phosphorylated JNK
p-EIF2α	phosphorylated EIF2α
p-PERK	phosphorylated PERK
p-IRE1	phosphorylated IRE1

PUMA	p53 Up-regulated Modulator of Apoptosis
PVDF	Polyvinylidene Difluoride
RCS	Reactive Chloride Species
RHD	Rel Homology Domain
RNS	Reactive Nitrogen Species
ROS	Reactive Oxidative Species
RIP	Receptor Interacting Protein
RT	Room Temperature
SDS-PAGE	Sodium dodecyl sulphate polyacrylamide gel electrophoresis
SN	Substantia Nigra
SNpc	Substantia Nigra pars compacta
tBID	truncate p15 BID
TDX	Thioredoxin
TH	Tyrosine Hydroxylase
TNF	Tumour Necrosis Factor
TRAF-2	Tumour necrosis factor Receptor Associated Factor 2
TRAP-1	TNF Receptor Associated Protein 1
TRB3	Tribbles Related Protein 3
TUNEL	Terminal deoxynucleotidyl transferase dUTP nick End Labelling
UPR	Unfolded Protein Response
UPS	Ubiquitin Proteasome System
USR	Unfolded Stress Response
WB	Western Blot
XBP-1	X Box-binding Protein 1
zIETDfmk	benzyloxycarbonyl -Ile-Glu(OMe)-Thr-Asp(OMe)-fluoromethylketone
zLEVDfmk	benzyloxycarbonyl -LE(OMe)VD (OMe)-fluoromethylketone

zVADfmk	carbobenzoxy-valyl-alanyl- (O-methyl)-fluoromethylketone
zVDVADfmk	benzyloxycarbonyl-Val-Asp(OMe)-Val-Ala-Asp(OMe)-fluoromethylketone

Chapter 1
Introduction: The role of Caspases and Caspase pathways in PD pathogenesis

1.0 Parkinson's disease (PD)

Parkinson's disease (PD) is a neurodegenerative disorder that affects 127000 people in the UK mostly aged over 50, although it is also able to affect people under age of 40. Patients diagnosed with PD have a lack of specific neurons that secrete the neurotransmitter dopamine in the pars compacta region of the substantia nigra (SNpc). Patients with PD have approximately 80% loss of dopamine containing neurons (DCN) at which time symptoms such as tremor, bradykinesia, rigidity and postural instability have already developed. The loss of dopamine interferes with normal control and coordination of movement. The most typical primary symptom that occurs is tremors at resting, which can affect the face, hands, arms or foot on one side of the body. Usually the PD patient may have constant shaking of one finger or hand when rested on their lap. Overtime it is possible that the tremor from one side of the body can progress to the opposite side. Often the tremor can be triggered by strong emotions such as stress or excitement (Gazewood et al 2013).

Muscle rigidity is consistent resistance of the muscles to passive displacement throughout the entire joint motion. Muscle rigidity may to be due to decreased activity of inhibitory interneurons in the spinal cord, which would increase the excitability of motor neurons. Another reason for muscle rigidity may be due to elastic properties of muscle that are changed in PD secondary to disuse, causing muscle to stiffen independently of neural activation. Muscle rigidity results in stiffness of the neck, arms, legs and torso, leading to a reduction in movement. In some cases the rigidity can result in pain. Rigidity can affect the facial muscles leading to a lack of expression in the PD patient which may cause problems in communication and can affect their social life (Weerkamp et al 2013, Gazewood et al 2013, Cesaro and Defebvre 2014).

Bradykinesia can cause lack of facial expression, difficulty in walking, speaking and getting into and out of chairs. Bradykinesia may be due to interference in cortical motor centres and excitatory circuits passing through the basal ganglia resulting in small and weak movements. The movement is slow and can interrupt the ease of carrying out daily tasks such as getting dressed, brushing teeth and cutting their

food. Speech can become slower and quieter causing problems in social situations. Repetitive movements such as finger tapping, typing and writing can become difficult for individuals suffering from PD due to the slowing of muscles. A significant symptom found in PD is the difficulty in maintaining a stable posture when standing upright. This increases the risk of falling which may cause injuries and sometimes hospitalisation. PD patients may also have difficulty in rising from a chair, pivoting and other balance movements. PD patients can often find it difficult to coordinate and plan ahead such as when walking (Weerkamp et al 2013, Cesaro and Defebvre 2014, Gazewood et al 2013).

Non motor systems such as lack of sleep, loss of smell, fatigue and depression have also been seen PD. PD patients that do not have a strong support system can suffer from nutritional deficiencies and become malnourished. Difficulty in swallowing food caused by the slow muscle movement can contribute to malnutrition. Fear, depression and anxiety can also be the result of diminished social life and lack of moral support. PD patients can also suffer from problems with memory and even dementia may occur. Freezing is a common sign in PD where the PD sufferer feels that they are temporarily immobile. Freezing can occur spontaneously in different situations such as walking, pivoting, going towards or sitting on a chair. This freezing symptom can increase the probability of the PD patient to fall (Weerkamp et al 2013).

The rate of progression of PD from its mild to advanced form varies for each patient. Furthermore, in some cases PD patients find non motor symptoms such as depression and fatigue more difficult to cope with on a daily basis then motor symptoms such as muscle rigidity. Due to the nature of PD it is difficult to obtain an early diagnosis as the majority of the symptoms have already developed in the patient. However, there is a scale to define the progression of PD and can aid to determine how far the disease has developed such as mild, moderate or advanced PD. Patients with mild PD often have the tremor symptom is present mostly on one side of the body. Mild PD patients also have some issues with movement, but can still carry out daily activities and there may be some changes in facial expression and walking. At this stage, exercise and medication such as levo dopamine (L-DOPA) therapy can improve

mobility, balance, depression and other PD symptoms effectively (Cesaro and Defebvre 2014, Gazewood et al 2013, LeWitt 2015).

The second stage of progression is moderate PD where there are episodes of freezing, issues with balance and tremors, rigidity or bradykinesia can occur on both sides of the body. Medication at the stage is still effective but side effects such as dyskinesias develop. Exercise still can improve and maintain good balance and movement. Advanced PD is the most severe form of PD, where the patient is unable to live independently by themselves and requires assistance to carry out all the daily activities. In advanced PD the patient is wheelchair bound or bedridden for the majority of the day. Cognitive memory is affected, which can result in memory loss, dementia and confusion. At this stage the side effects of the medication become more prominent (Cesaro and Defebvre 2014).

Although intensive research has been conducted the actual cause of PD is still unknown, therefore the treatment available at present is of limited quality (Tomlinson et al 2012, Gazewood 2013, Weekamp et al 2013, LeWitt 2015, Ganat et al 2012, Rodríguez-Nogales et al 2015, Cooper et al 2012, Machado et al 2012). However, a few theories to the aetiology of PD have been discussed. One of the many theories to the origin of PD is that PD may be the result of autoimmune cells that damage DCN of the brain. Speculating that the brain may spontaneously generate a chemical substance related to dopamine that can destroy nerve cells can extend this theory further. Further support for this view has come from an early investigation conducted by Bisaglia et al (2014), which suggested that nigral death could be the result of elevated levels of reactive oxidative species (ROS) and respiratory failure of the mitochondria.

Zuo et al (2013) demonstrated that there is an association between PD and the level of calcium in the mitochondria. A change in the level of calcium increases the possibility of cell apoptosis. Former work by Mattson at el (2000) and Cesaro and Defebvre (2014) suggested that imbalances in homeostatic levels of calcium in the endoplasmic reticulum (ER) induce increased levels of toxicity and death of neuron

cells. These results have been strongly correlated with neurodegenerative disorders.

Previous research conducted by Hald and Lotharius (2005), explored the relationship between inflammation and oxidative stress in PD. Monoamine oxidase induces catabolism of dopamine which is present inside the cell leading to the formation of dihydroxyphenylacetic acid (DOPAC), alongside hydrogen peroxide. Dopamine is subsequently converted to dopamine Y quinone via an antioxidant reaction, which takes place inside the cell. The formation of dopamine Y quinone interacts with protein sulphydryls causing an alteration in the redox buffer. The decrease in glutathione, increased outflow of hydrogen ions from the mitochondria and decreased levels of tyrosine hydroxylase (TH) contribute to the change in the content of the redox buffer. This modification decreases the ability of the buffer to remove oxidants caused by oxidative stress, leading to an accumulation of free radicals circulating the system, resulting in damage and destruction of neural cells. In addition, the impairment of adenosine triphosphate (ATP) synthesis can also participate in an increase in cell toxicity that causes the destruction of cells.

Hydroxyl radicals are formed from hydrogen peroxide through the Fenton reaction. The hydroxyl radicals' formed, increase and cause excessive levels of oxidative stress, leading to impairment and mass destruction of cells. In addition, an increase in 4-hydroxyl-2-nonenal (HNE) which is formed as a by-product in lipid metabolism induces a rise in oxidative stress and cell destruction, particularly in the SN of the PD individual. Excessive levels of HNE can alter the structure of proteins through covalent bonding. Furthermore, cell apoptosis and impairment of the mitochondria is the result of elevated levels of HNE in the system (Smith et al 2007).

Recent research by Chinta et al (2008) revealed that the general decrease in vitamin E and glutathione and an increase in iron in the SN, can contribute to the imbalance of the redox buffer. In addition, by products (super oxides, hydrogen peroxide and hydroxyls) formed during metabolism, contribute to the impairment of mitochondrial function and ATP synthesis. In the electron transport chain of the

mitochondria, complexes III and I produce the ROS super oxide. The super oxide is converted into hydrogen peroxide. As enzymes (peroxisomes) are destroyed, this contributes to an increase in hydrogen peroxide accumulation (as hydrogen peroxide cannot be removed). Subsequently, hydrogen peroxide enters the cytosol and can convert to hydroxyl by binding to ferrous ions. In addition, super oxides can interact with nitrogen oxides to produce peroxynitrite, which interfere with the normal function of key enzymes. This in turn can cause impairment of complexes I and IV in the electron transport chain of the mitochondria. The increase of free radicals can cause damage to the lipid bilayer of cells, resulting in the out flow of the cells inner content, which leads to cell lysis. In addition, peroxynitrite can induce fragmentation of DNA in cells as well as structural changes in amino acid residues of essential proteins.

Ischiropoulos (2003a 2003b) suggests that ROS promote the production of mutated α synuclein in protein inclusions and in Lewy bodies, which contributes to the pathogenesis of PD. The α synuclein are insoluble products, which can aggregate easily, and can interfere with the transport of dopamine. In addition, α synuclein combined with mitochondrial impairment can contribute to apoptosis and cell destruction. Former work, by Emerit et al (2004) suggests that the central nervous system is much more susceptible to the effects of oxidative stress then other body systems. As previously stated that ROS are produced as byproducts of metabolism, this increases the probability of elevated levels of oxidative stress to occur. Three enzymes (inducible nitrite oxide synthase, neuronal nitrate synthase and endothelial nitrite synthase) convert nitrite and promote an inflammatory response, which in turn results in the demethylation and degeneration of neurons. In addition, ROS can also be produced by elevated activity of glutamate receptors. The increase in receptor activation is due to an increased influx of calcium ions accumulating the system. As the receptors undergo excessive stimulation, this activates the arachidonic acid cascade pathway, resulting in the production of ROS. This in turn causes damage to the neuronal cells through the impairment of the mitochondria.

Previous work by Chandra et al (2002), suggested that oxidative stress can also be caused by oxidise substrates (such as P450 oxidase and xanthine oxidase), which can result in toxicity and cell lysis. As the

number of cells lysed increases, there is a decrease in synaptic activity. The total quantity of DCN is reduced substantially, causing PD symptoms in the individual. Inhibition or low levels of the enzyme glutamine synthetase prevent the conversion of excessive glutamate to glutamine, resulting in a buildup of glutamate in the cells. This reaction induces the production of more ROS and proteolytic enzymes, resulting in high rate of death of neuronal cells to take place within a short duration. The elevated levels of ROS induce opening of the permeability transition pore (PTP) of the mitochondria to open, allowing an increase in the movement of molecules into the cytosol. Due to the imbalance of key electrons in the mitochondria, factors such as pro-Caspases, apoptosis initiating factor (AIF) and cytochrome c are activated. These factors contribute to further damage and destruction to cells (Gazewood et al 2013).

1.1.1 PD and Brain Cortex

The brain cortex is the outer covering of the brain, and folds to form lobes (parietal, occipital, temporal and frontal lobe) which have different functions (Figure 1.1). In general the brain cortex is involved in thought and action. The frontal lobe participates in planning, reasoning, some speech, motor function, problem solving and movement. The parietal lobe plays a role in movement, sensation, handwriting and recognition, whilst the occipital lobe is associated with visual processing. The temporal lobe related with memory, and recognition of auditory stimuli such as music and speech (Martini and Ober 2006, Martini et al 2014).

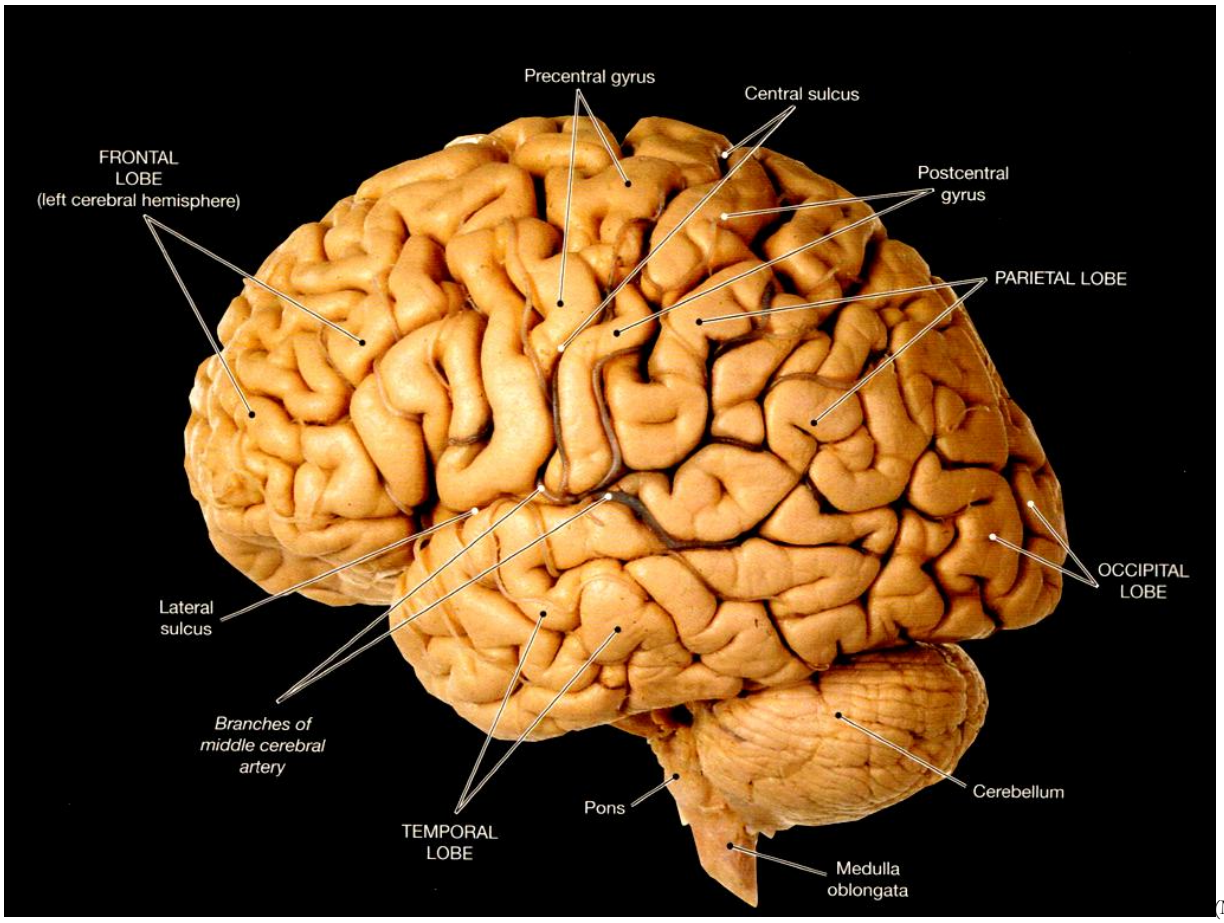

(Martini F.H, Ober W. C, 2006, Martinis Atlas of The Human Body, 7th edition, San Francisco, Pearson Benjamin Cummings Ed Ltd pp 24)

Figure 1.1: Lateral view of the brain cortex

The parietal, occipital, temporal and frontal lobes together form the brain cortex. Each lobe specialises and has a different function (Martini and Ober 2006).

Research by Brazhnik et al (2012) explored the electrophysiology of the motor cortex and midbrain in 6-hydroxydopamine (6OHDA) treated rats. 6OHDA-treated rats had suffered symptoms of freezing and difficulty in walking and turns on circular treadmill. Treadmill walking decreased the number of fluctuations of cortical oscillatory activity in the midbrain and motor cortex of 6OHDA-treated rats when compared to sedentary rats. Treadmill exercise was carried out and electrophysiological recordings of neuronal activity were documented. Rats underwent treadmill exercise for an hour, once a week for four weeks. For each session, rats walked on circular treadmill for 5 minutes followed by a 2 minute rest period. In addition, a change in the direction of the circular treadmill was carried out to determine its effect on the midbrain. The results showed that 6OHDA-treated rats that underwent treadmill exercise had reduced fluctuations of neuronal activity in the midbrain and improved motor control on the treadmill.

Ho et al (2011) found male Wister rats exhibited PD symptoms after administering 1-methyl 4-phenyl 1, 2, 3, 6-tetrahydropyridine (MPTP) injection. Immunohistochemical analysis revealed increased levels of interleukin-2 (IL-2) and lesions in the brain cortex, amydala and ventral and dorsal striatum. MPTP rats had suffered cognitive, motor and emotional impairment. The author concluded that the lesions found in MPTP brain cortex, amydala and striatum contributed to interference in normal cognitive, emotional and motor function. Previous work by Murray et al (2003) explored the effects of the α-amino-3-hydroxy-5-methyl-4- isoxazolepropionic acid (AMPA) agonist, LY503430 in MPTP mouse and 6OHDA rat PD model. Immunohistochemical analysis portrayed less lesions and intact tissue of the prefrontal cortex and ventral midbrain of 6OHDA-treated Sprague Dawley rats and MPTP mice that had been treated with LY503430, compared to 6OHDA and MPTP PD model that had not been treated with LY503430. Growth factors such as glial derived growth factor (GDNF) and brain-derived growth factor (BDNF) have a crucial role in neuronal growth. GDNF protects survival of neurons, whilst BDNF prevents structural damage in cells. Tissue analysis revealed low levels of BDNF in PD animal model. However, a two fold increase in BDNF was found in the brain cortex of 6OHDA rat and MPTP mouse model that had been treated with LY503430.

1.1.2 PD and Cerebellum

The cerebellum is comprised of the right and left cerebral hemisphere and plays a vital role in coordination of movement, posture and balance (Figure 1.2). The cerebellum stores routine patterns of movement (Martini and Ober 2006, Martini et al 2014). MRI testing has shown the cerebellum and striatum play a vital role in calculating and planning motor tasks and processing information from the temporal lobe of the brain in PD patients (Husarova et al 2011). Patients suffering from PD at early stage have reduced active cerebellum and striatum areas compared to healthy people (Husarova et al 2011). Minks et al (2011) determined if the cerebellum has a critical role in the development and progression of PD and if it can be used as a target in PD treatment. In the study twenty PD participants were given two motor tasks to complete (a ball test and nine hole peg test) and were assessed on how quickly they completed each task. Stimulation of the cerebellum improved the voluntary movements in PD.

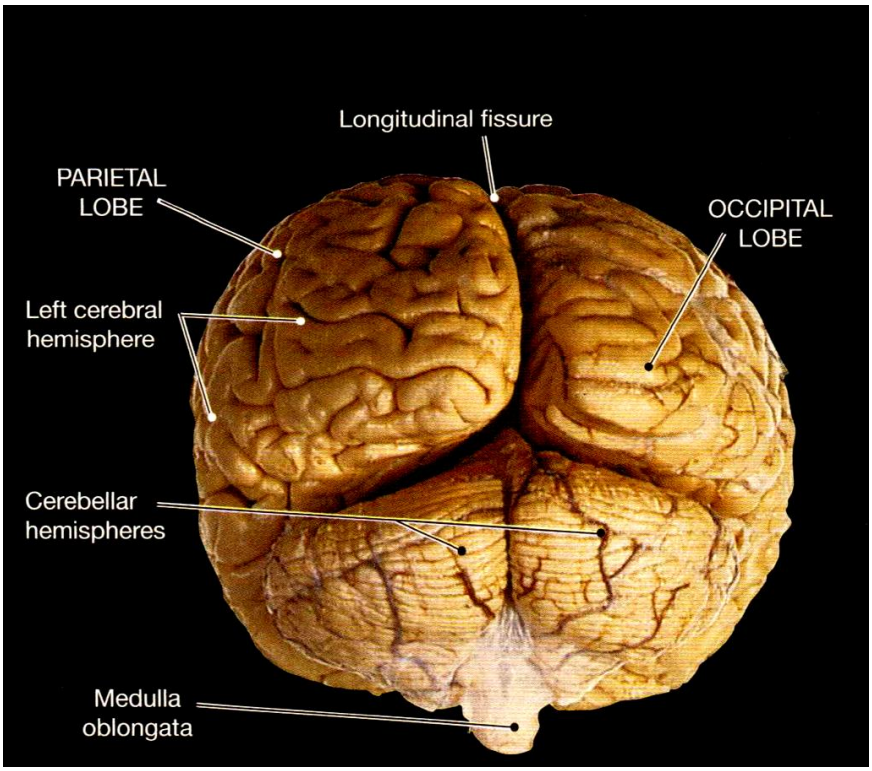

(Martini F.H, Ober W. C, 2006, Martinis Atlas of The Human Body, 7th edition, San Francisco, Pearson Benjamin Cummings Ed Ltd pp 23)

Figure 1.2 : Posterior view of the cerebellum

The cerebellum is comprised of the left cerebral hemisphere and the right cerebral hemisphere with a longitudinal fissure. Frequent cross talk occurs between the two hemispheres so controlled movements can be carried out (Martini and Ober 2006).

Rolland et al (2007) examined the impact of loss of neurons from the nigrostriatum on the cerebellum and basal ganglia in MPTP monkey and 6OHDA rat PD model. A reduction of thalamic neurons was found in the motor cortex in MPTP monkey and 6OHDA rat PD model may have contributed low activity levels of the thalamus. The amount of thalamocortical neurons that had received input from the cerebellum had decreased by half in 6OHDA rats compared to control. The decrease in cerebellum activity can contribute to reduced levels of stimulation in the SN pars reticulata, thereby effecting dopamine levels in cells. MRI imaging analysis found an increase in metabolic activity in the motor cortex of 6OHDA lesion rats compared to the control. The author suggests the cerebellum- thalamic pathway could provide a better target site in PD treatment. An increase in monoamine oxidase activity was found in the cerebellum, hippocampus and striatum of MPTP mice (Gal et al 2005).

Prevoius research by Shang et al (2004) found elevated levels of iron, nitric oxide, superoxide and active Caspase-3 levels in lysates of cerebellar neurons from MPTP rats. A reduction in the intracellular iron indicator, cytosolic aconitase was found in rats that had been injected with MPTP. A decrease in nitric oxidase synthase, superoxide synthase was detected in MPTP rat cerebellar neurons compared to control. Apoptotic death of MPTP cerebellar neurons was confirmed using terminal deoxynucleotidyl transferase dUTP nick end labelling (TUNEL) assay. Collectively the results indicated MPTP caused apoptotic death of rat cerebellar neurons via the accumulation of ROS, iron and a decrease in anti oxidant enzymes. The author concluded that the results of the study provide insight to how ROS can cause damage to neuronal cells in PD animal model (Shang et al 2004).

1.1.3 PD and Midbrain

The brainstem is comprised of pons, medulla and midbrain (Figure 1.3). The midbrain participates in eye movement, and body movement alongside vision and hearing (Martini and Ober 2006, Martini et al 2014). Immunofluorescence (IF) analysis has shown that DCN in the SNpc is more susceptible to 6OHDA damage compared to cholinergic neurons (Pienaar and Berg 2013). MPTP and 6OHDA promote increase in the concentration of zinc, leading to depleted ATP, essential growth factors resulting in damage of DCN in midbrain and striatum of PD rat animal model (Sheline et al 2013).

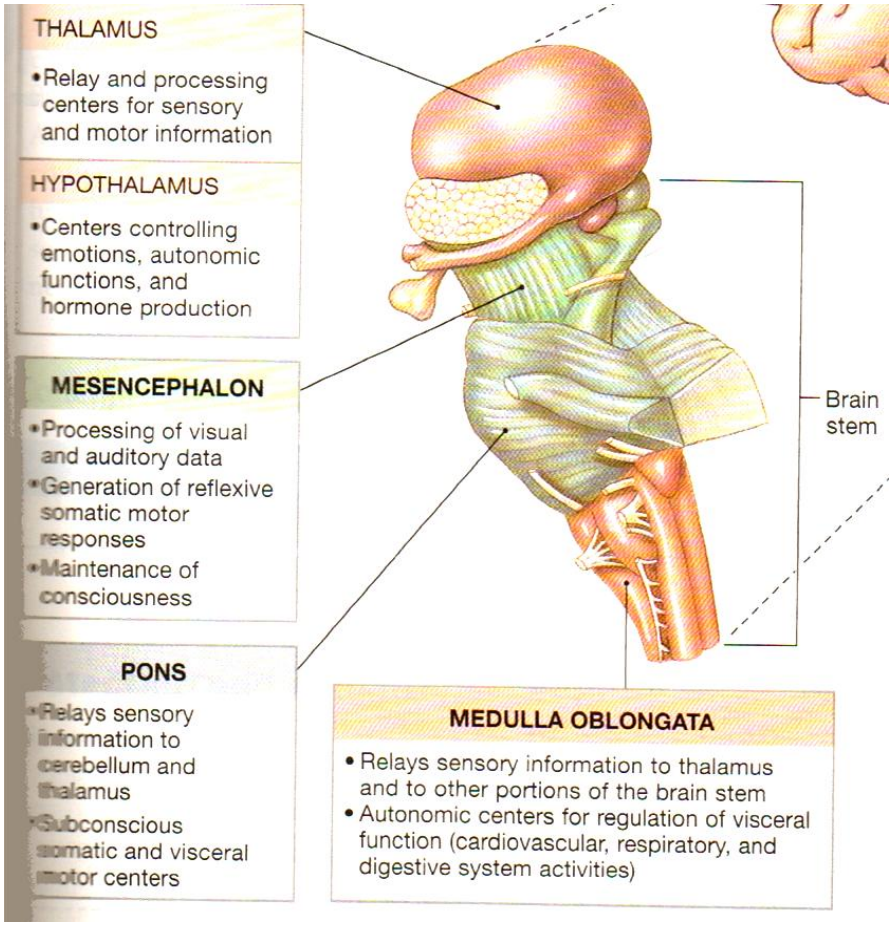

(Martini F.H, 2006, The Fundamentals Of Anatomy And Physiology, 7th edition, San Francisco, Pearson Benjamin Cummings Ed Ltd pp 461)

Figure 1.3 : Schematic view of the brainstem

The midbrain also known as the mesencephalon, pons and medulla oblongata form the brainstem. Each unit of the brainstem has specialised functions and are required in regulating normal bodily functions (Martini and Ober 2006).

Chung et al (2011) planted induced pluripotent stem cells into the midbrain of 6OHDA Sprague-Dawley rat model. 6OHDA rats that had undergone surgery had reduced PD symptoms and improved behaviour. Docosahexaenoic acid was combined with stem cells and aided to establish successful differentiation of DCN. An increase in neuroprotective genes such as BDNF, GDNF, Nurr1 and B cell lymphoma 2 (BCL-2) and decrease in Caspase-3 activity were found in the cells. The author emphasises that implantation of DCN into midbrain could be used as an alternative in PD (Chung et al 2011, Rath et al 2013).Cell derived from human ventral mesencephalon have better survival rate and functional abilities and have the potential to be used as grafts in brain of PD patients (Rath et al 2013).

Tanriover et al (2010) found a significant decrease of TH, GDNF and neurotonin in MPTP Wistar rats. A two fold increase in TH, GDNF and neurotonin was found in docosahexaenoic acid treated MPTP rats. docosahexaenoic acid increased GDNF and neurotonin and protected DCN from damage in SN of MPTP Wistar rats. In addition, docosahexaenoic acid treated MPTP rats had improved balance and motor co-ordination, when compared to MPTP rats (Tanriover et al 2010). Hacioglu et al (2012) found docosahexaenoic acid protected further neuronal damage in the SN in MPTP male Wistar rats. MPTP rats had poor co-ordination and balance compared to MPTP rats that had been treated with docosahexaenoic acid. MPTP docosahexaenoic acid rats had elevated levels of BCL-2, TH and had intact tissues compared to PD animal model. Immunohistochemical analysis showed loss of neurons and an abundance of fibrils accumulated in the midbrain of MPTP rats.

Decressac et al (2012) found high level of aggregated α-synuclein accumulated in lesions of the midbrain and striatum of 6OHDA rat. A decrease in TH was observed in the midbrain and striatum of 6OHDA rats when compared to the control. 6OHDA rats had slower performance, difficulty in walking and navigating around a maze when compared to control. Immunohistochemical analysis portrayed distorted axons and loss of neurons in the midbrain and striatum of PD animal model. 6OHDA, MPTP and rotenone encourage deletions of exons resulting in mutation of α-synuclein in PD model. A decrease in TH, proteasome function and increase in aggregated α-synuclein was observed in mesencephalic cultures, as well as striatum, SN and cortex of Sprague Dawley rats (Kalivendi et al 2010).

1.1.4 PD and Striatum

The striatum comprised of caudate nucleus and the putamen (Figure 1.4). The striatum is involved in movement, cognitive function and motor control, learning, and vision (Martini and Ober 2006, Martini et al 2014). The dorsal striatum plays a key role in decision making via integration of various corticostriatal regions of the striatum, which are able to process and analyse information such as sensorimotor, cognitive, and emotional efficiently in PD patients, as well as PD in vivo and in vitro models (Balleine et al 2007). Current work has shown the Chinese herb, medecassoside protected neurons from damage by increasing BDNF, BCL-2 and glutathione synthase in PD animal model. Hydroxysafflor yellow increased BDNF and GDNF levels, which protected neurons from oxidative damage in the striatum of 6OHDA rat. Hydroxysafflor yellow elevated dopamine levels in striatal neurons of PD animal model (Han et al 2013).

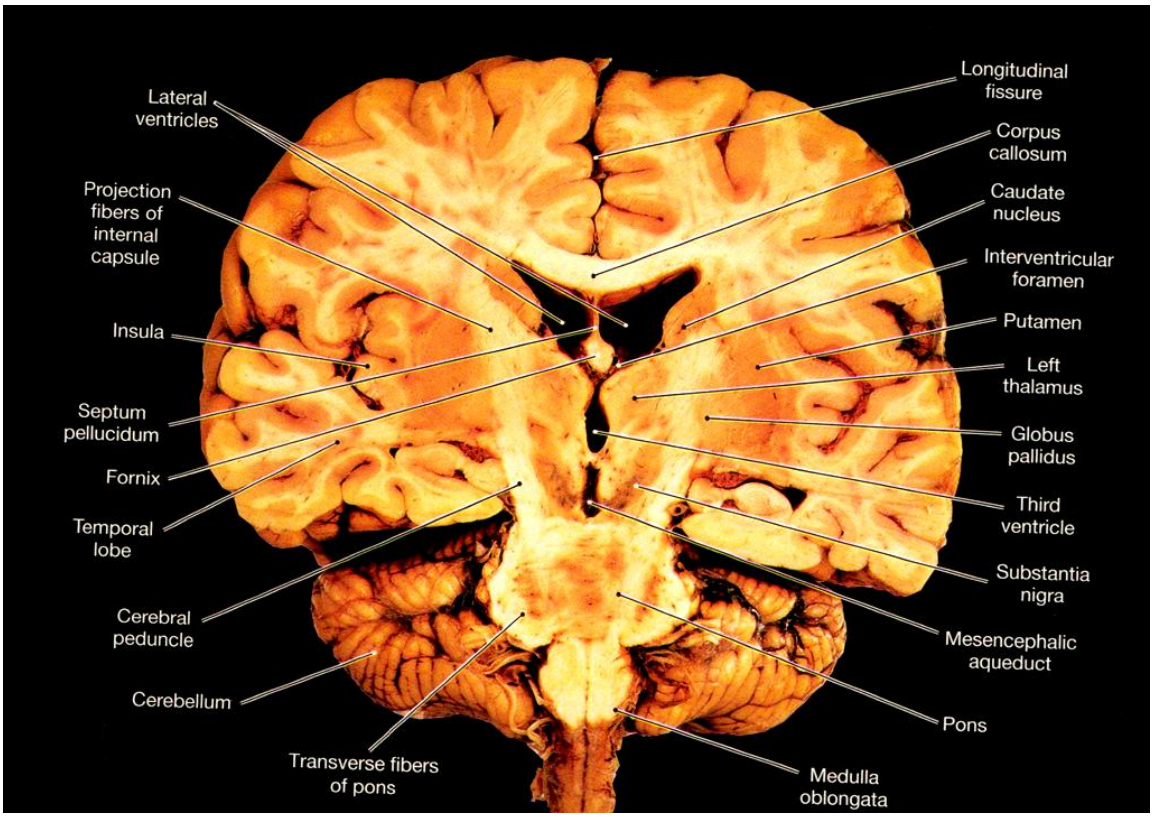

(Martini F.H, Ober W. C, 2006, Martinis Atlas of The Human Body, 7th edition, San Francisco, Pearson Benjamin Cummings Ed Ltd pp 18)

Figure 1.4 : Coronal section showing the mesencephalon as well as caudate nucleus and putamen of the striatum

The caudate nucleus and putamen form the striatum and is involved in regulating movement. Damage to the striatum has been associated with PD (Martini and Ober 2006).

Immunohistochemical analysis illustrated increased astrocytes, tumour necrosis factor (TNF) and oligomers of aggregated α-synuclein and reduced TH levels in the SN and striatum of MPTP and 6OHDA rats (Dimant et al 2013, Lee et al 2013). Nociceptin/ orphemin damage of neurons striatum of 6OHDA-treated rats. The protection of neurons provided by reduced nociceptin/ orphemin reduced the incidence of dyskinesias in PD animal model (Marti et al 2012).

Castro et al (2013) found elevated TNF, IL-1β and -10 and low levels of nerve growth factor in hippocampus and striatum of MPTP rats. Atorvastatin increased nerve growth factor in striatum and hippocampus in MPTP rats. MPTP had caused motor impairment, loss in sense of smell, slower pacing when walking and difficulty keeping a constant balance in PD animal model. Castro et al (2012) observed that lithium chloride and valporate protected neurons from ROS damage in the striatum and cortex of MPTP Wister rats. A decrease in TH and increase in fibrils was observed in lesions of striatum and cortex of PD rat model and rat mesencephalic cultures (Castro et al 2012, Kim et al 2014). Low levels of glutathione peroxidase, superoxide dismutase, dopamine, TH and proteasome activity was detected in SN, striatum and cortex of MPTP rats (Sonsalla et al 2013).

Aznavour et al (2012) found a decrease of active TH levels in the striatum of cats that had been induced with MPTP. MPTP cats had developed PD motor symptoms. PD patients have altered function of the basal ganglia causing difficulty in movement and carrying out daily activities. Functional MRI analysis of PD and non PD participants performing right hand movement tasks were carried out to detect any changes in movement initiation or inhibition in the striatum. It was found that PD patients had reduced motor activity in striatum and increased activity of pallidal at initiation stage, when compared to non PD patients. In addition, an increase in striatum cortical motor activity was found at resting stage in PD patients (Toxopeus et al 2012).

1.2.1 Diet

At present there is not enough strong clinical evidence demonstrating the impact of nutrition in PD. D'Orazio et al (2012) reviewed recent researched publications and found that alteration in diet can decrease the risk of many diseases such as cardiovascular, inflammatory and neurodegenerative disorders such as PD. Diets enriched with carotenoids (astaxanthin and fucoxanthin) reduce toxicity in cells by binding to ROS, toxins and heavy metals, which may cause pathology of cells. In addition, the binding of these β carotenoids protects peroxidation of lipids and phospholipids of cell membranes, which causes death of cells and other tissues. The increase of antioxidants in the diet such as vitamin E, vitamin C and phenols from fruits and vegetables reduce oxidants such as hydrogen peroxide, superoxynitrate, super oxide and nitric oxide, which are produced as by products in the cell (D'Orazio et al 2012, Mattson et al 2004).

1.2.2 Drug therapy and PD

PD patients are commonly treated with the drug L-DOPA combined with Carbidopa to ensure that L-DOPA is not converted to dopamine before reaching the blood brain barrier and so maximum dopamine can be used. L-DOPA is used at early stages and its treatment is effective for around 5 years. However, as PD advances over time L-DOPA becomes ineffective to the patient and produces more side effects, such as dystonia and dyskinesias(LeWitt 2015). Other drug treatments that are available include dopamine agonists (apomorphine, pramipexole and ropinirole), monoamine oxidase inhibitors (selegiline and rasagiline), and anticholinergic medication (trihexphenidyl and benztropine mesylate). The most current drug, safinamide is at phase three of clinical testing and has the potential to prevent and improve cognitive and motor impairment at early stage of PD. Safinamide irreversibly binds to and suppress monoamine oxidase (MAO), alongside inhibiting glutamate activity and dopamine reuptake, thereby increasing dopamine levels in the brain (Fabbri et al 2015). Isradipine has been shown to be neuroprotective in PD animal model by suppressing calcium channels and is currently at phase two in clinical trials (Rodríguez-Nogales et al 2015, Singer 2012).

1.2.3 Stem cell research and PD

Current research has explored the use of stem cells to produce neuronal grafts, as an option in PD treatment. DCN grafts were transplanted in 6OHDA-treated brain of PD rat, resulting in improvement of brain function (Aguila et al 2012). The transplantation of stem cells in PD patients could promote normal function of the brain. The presence of growth factors in stem cells leads to production of healthy stem lines. Stem cells lines that will be used in transplantation are specific DCN will have the potential to promote efficient synaptic communication and transmission in PD brain (Aguila et al 2012). Purification of stem cell prior to transplantation may decrease the probability of growing tumours leading to more successful grafts (Ganat et al 2012).

1.2.4 Deep brain stimulation and PD

Deep brain stimulation (DBS) is a surgical procedure that is used to reduce symptoms in patients suffering from severe PD, typically for eight to sixteen years. DBS is suitable for PD patients that are still responding to L-DOPA, are not cognitive impaired, have good health and have a supportive network. DBS reduced tremors, rigidity, dystonia, bradykinesia and dyskinesias in PD patients (Cooper et al 2012, Machado et al 2012). Six months of continuous DBS may be causing changes in pathways, which lead to step initiation suggesting that this may be the reason that DBS is able to decrease tremors but cannot improve gait or balance (Rocchi et al 2012). In contrast, a different study conducted by McNeely et al (2012) found combining drug therapy with DBS did not have any significant additional effects when compared to using one therapy, suggesting that similar pathways are influenced.

1.2.5 Exercise

At present there are extensive studies looking at the effect of different types of exercise, from Nordic walking, Alexandra technique, Tai Chi to various forms of dance, such as tango, waltz and ballet. Collectively, all types of exercise have indicated improved rigidity, hand movements, facial expression, learning, self confidence and better quality of life in PD patients (Fritz et al 2011, Stallibrass et al 2002, Hackney and Earhart 2009a, Hackney and Earhart 2007, Hackney and Earhart 2010, Li et al 2012, Earhart, 2009b, Dreu et al 2012). In addition, concurrent music can provide steady gait and can improve PD patients to carry out dual or multitask, as music can be used an external cue that develops recognition in transfers and mobility in PD (Brown et al 2010). Furthermore other approaches such as whole body massage, muscle strength exercise, participation in active theatre and community based exercise have shown positive effects in improving gait, mobility and balance (Heiberger et al 2011, Paterson et al 2005, Modugno et al 2010, C.Haas personal communication). Unconventional methods such as water based exercises have also shown signs in the improvement of postural stability, functional mobility, motor symptoms and reduced fear of falling in PD patients (Vivas et al 2011, Ayan and Cancela 2012).

Tomsilon et al (2012) analysed various exercise regimes (treadmill, cueing , dance , martial arts and physiotherapy) that were used in PD rehabilitation to determine which form of exercise was particularly suited in PD. Meta analysis revealed that there was no significant exercise regime that was preferred in PD treatment. In addition, exercise therapies used in patients suffering from PD were effective in overall treatment, when compared to PD patients that were not undergoing any exercise. PD patients that had exercise integrated into their treatment had better balance, mobility and improved gait compared to PD patients that led a sedentary lifestyle. Although the studies analysed by the author portray positive effects of exercise in PD, there were many factors which have to be considered such as small sample size, publication bias and not all studies were statistically significant.

Herman et al (2007) explored the effects of treadmill training on gait and mobility in PD rehabilitation. Treadmill training improved balance, gait and strength of muscles improving length of stride and velocity, which can decrease risk of freezing and falls. In the study, nine patients (suffering from mild to moderate PD), endured treadmill training for 30 minute session 4 times a week for 6 weeks. Evaluations and adjustments to treadmill speed were carried out at the end of each week, based on the patients speed whilst walking on normal ground. Patients had improved stride length, alongside stable walking speed on normal ground and a decrease in gait and number of falls was found. In addition, PD patients had an improved perception of their gait performance and had improved balance and mobility. The intensity and repetitiveness of treadmill training over a length of time provided the beneficial effects and may have contributed to better motor control.

Canning et al (2012) determined the effectiveness and viability of home based treadmill training in participants suffering from mild PD. Twenty PD participants were randomly allocated to either carry out home based treadmill training or usual physical activity for six weeks. Home based treadmill was carried out for 40 minutes four times a week for six weeks. Patients were supported by a safety harness and were asked to hold the treadmill handle bars at all times. Muscle soreness, tiredness, number of falls, intensity and adaptability of exercise were explored, before and after the six week training with another six week follow up. Home based treadmill training increased PD patient's confidence and quality of life. The main finding of the study showed that home based treadmill training was a safe and valid form of exercise which the mild PD patient could easily integrate into their lifestyle. PD patients will be able to use treadmill confidently as part of their exercise regime at home allowing flexibility and letting the PD patient work at their own pace. The screening and monitoring process will promote PD patients to carry out their exercise on the treadmill safely as possible.

1.2.5.1 Exercise in PD animal models

Research by Zigmond et al (2012) had shown exercise to have positive effects in rat PD animal model. To determine the effect of exercise, male rats were segregated into four groups' control, exercise, 6OHDA and 6OHDA exercised. Rats underwent treadmill exercise for 12 weeks followed by 6OHDA injection then another 8 weeks of treadmill running. WB analysis revealed a reduction of 47% TH and 49% TH in the SN and striatum in PD sedentary rats. Treadmill exercise prevented loss of TH positive striatal and SNpc neurons in PD Exercised induced (PD-Ex) rats. The author indicated that exercise may have increased gene expression of neurotrophic factors such as GDNF, BDNF, IGF1, FGF2 which protect DCN from damage by reducing ROS. Treadmill exercise may have promoted synthesis and release of dopamine by increasing the binding of dopamine receptors. Exercise promotes protection of synapses and increase superoxide dismutase, heat shock protein, catalase and glutathione peroxidase (Zigmond et al 2009, Frazzita et al 2013 Zigmond and Smeyne 2014).

El Ayadi and Zigmond (2011) explored the role ROS in DCN of PD mouse model. 6OHDA caused formation of apoptotic bodies, chromation condensation and membrane shrinkage of the cytoplasm in mice mesencephalic cultures, illustrating that ROS promotes apoptotic death of DCN via oxidative stress. Mild exposure to ROS can provoke gene expression of prosurvival genes such as superoxide dismutase and Bcl-2. WB showed that 6OHDA-treated with methamphetamine in mice mesencephalic cultures had decreased amount of phosphorylated JNK, indicating that 6OHDA increases ROS production leading to apoptotic death of DCN via JNK pathway.

Urgate et al (2003) showed that GDNF decreased 6OHDA toxicity in 6OHDA-treated mice mesencephalic cultures. Hoechst staining illustrated fragmentation of the nucleus and chromatin condensation, confirming 6OHDA promoted apoptotic death of DCN in PD animal model. GDNF protected a significant amount of DCN from neurotoxic damage indicating that oxidative stress contributes to death of DCN in PD animal model. Pothakos et al (2009) explored the influence of exercise in behaviour and coordination in PD mouse model. Mice were segregated into four groups, untreated, exercise, MPTP-treated and MPTP-treated with exercise. Mice underwent treadmill exercise

for 12 weeks. The results portrayed that MPTP-treated mice had reduced step length, took longer time to complete a maze task, and had problems with balance and co-ordination. MPTP-treated mice that had undergone endurance exercise had completed the maze task in a shorter time frame, had better memory, increased step length, had improved gait, balance and co-ordination, indicating that endurance exercise provided beneficial effects in PD animal model.

Immunohistochemical analysis demonstrated that lesions caused a decrease TH and loss of neurons from the striatum of MPTP-treated mice. High-performance liquid chromatography showed low levels of DOPAC in PD striatum but high DOPAC levels in PD-Ex striatum of PD mouse model. In addition, improved balance and motor performance was determined in Ex and PD-Ex. The author suggested that exercise promotes dopamine uptake, synthesis and release to be used by the synapses and reduces decay of dopamine (Petzinger et al 2007).

Gorton et al (2010) found that forced treadmill exercise had more beneficial effects then voluntary wheel running in PD animal model. MPTP mice underwent treadmill or running wheel exercise for an hour 5 days a week for 30 days. MPTP decreased GDNF in caudate putamen, cortex , midbrain and SNpc in mice. MPTP mice that underwent treadmill or wheel running had higher levels of GDNF in cortex, midbrain and SNpc. A decrease in striatal dopamine in was found in PD mice. An increase in dopamine levels were measured in striatal neurons of PD-Ex mice. Treadmill exercise had prevented further loss of DCN, dopamine decay, reduced anxiety and maximised dopamine usage and enabled the ease of turning in PD mice. An increase in distance and velocity in was found in voluntary wheel running compared to forced treadmill in PD-Ex mice.

Research has shown that four week treadmill exercise improved resting heart rate in MPTP-treated mice (Al-Jurrah et al 2007). MPTP mice that had carried out treadmill training had better respiratory, normal ECG and elevated levels of citrate synthase in cardiac and skeletal muscle. WB analysis demonstrated a decrease in DOPAC, dopamine and TH levels were determined in the striatum and SN of MPTP mice.

In comparison, MPTP exercised mice had an increase in TH positive neurons in striatum and SN of PD-Ex mice (Al-Jurrah et al 2007, Zhang et al 2013).

Immunohistochemical analysis had also shown a reduction of TH in striatum and SN of 6OHDA-treated rats (Anstrom et al 2007, Avila et al 2010). Work by Cohen et al (2003) found that exercise improved motor behaviour and protected neurons from damage in PD rat model. 6OHDA-treated rats had developed dyskineas and motor impairment. WB analysis showed an increase in dopamine, DOPAC and GDNF in the striatum of 6OHDA-treated exercised rats when compared to 6OHDA-treated sedentary rats. GDNF had protected striatal neurons from damage and increased the accumulation of dopamine to be used that improved motor activity in 6OHDA-treated rats (Zhang et al 2013a, Frazzita et al 2013). Howells et al (2005) found no significant difference protection of DCN from damage between 6OHDA-treated rats that underwent forced or voluntary exercise. 6OHDA-treated rats carried out exercise on a running wheel for one hour every day for two weeks. Immunohistochemical analysis revealed less lesions and increase in dopamine in the SNpc and striatum of exercised rats when compared to 6OHDA sedentary rats, indicating that exercise prevents loss and damage to DCN. Immunohistochemical analysis illustrated increased TH in the striatum of 6OHDA-treated rats that had treadmill exercise for an hour everyday for two weeks (Avila et al 2010).

Tillerson et al (2001) had found 6OHDA-treated rats had low levels of dopamine and DOPAC and increased lesions in striatum. An increase in dopamine and DOPAC levels were determined in striatal neurons in 6OHDA rats that underwent motor training rats when compared to sedentary rats. Further work had demonstrated exercise had decreased degeneration of DCN and reduced shaking in 6OHDA-treated rats when compared to 6OHDA-treated rats that did not exercise (Tillerson et al 2002). Research by Tajri et al (2010) had shown an increase in neurotrophic factors in exercised PD rat model. In the study, rats underwent treadmill exercise 30 minutes each day, 5 days a week for 4 weeks. Immunohistochemical analysis revealed lesions, loss TH positive neurons and damaged DCN in the SNpc and striatum of sedentary PD rats. In comparison, PD rats that had undergone treadmill exercise had intact tissues and more TH positive neurons in the SNpc and striatum. WB analysis revealed an

increase in BDNF and GDNF in striatum of exercised rats compared to sedentary rats. Cylinder and rotational test showed 6OHDA-treated rats had difficulty in turns and balance when compared to 6OHDA-treated rats that had exercised. Increase in GDNF promoted protection to neurons from damage (Frazzita et al 2013). Former research by Mabandla et al (2004, 2010) found that exercise had increase in the release of neurotrophins as well as promoting the protection of dopaminergic neurons of the SN of PD rat model. In the study Evan rats were segregated into two groups' 6OHDA-treated sedentary rats and 6OHDA-treated rats that underwent exercise. Rats underwent voluntary exercise on a running wheel for 30 minutes to 90 minutes every day for two weeks. 6OHDA-treated rats had reduced number of TH positive and dopamine levels in the SN. The author concluded that exercise had decreased loss of and protected DCN in 6OHDA-treated rats by releasing neurotrophins that protected neurons from damage.

Previous research (Yoon et al 2007) had investigated the effects of treadmill exercise in 6OHDA-treated rats in PD animal model. In the study, rats separated into four groups control, exercise, 6OHDA and 6OHDA exercised. Rats in exercised and 6OHDA-treated exercise underwent treadmill exercise 30 minutes a day for two weeks. Immunohistochemical analysis showed an increase of TH in the SNpc and striatum of exercised and 6OHDA-treated exercised group in PD rat model. The amount of TH was reduced by half in the SNpc and striatum of PD sedentary rats. An increase of TH was determined in the SNpc and striatum of PD rats that had completed treadmill exercise. Furthermore, destruction of nerve terminals of DCN, in SNpc was observed in rats that had been treated with 6OHDA. A loss of striatal fibres were observed in 6OHDA-treated rat, indicating that 6OHDA had successfully damaged neurons in PD animal model. The study highlighted that PD rat model is an adequate model to use to study PD pathogenesis. Moreover, the study demonstrated that treadmill exercise can prevent loss of neurons in the SN and striatum of PD animal model (Frazzita et al 2013).

The loss of DCN within the basal ganglia has been strongly associated with the activation of Caspases. Caspases (Caspase 1-14) are a family of cysteine proteases, which act as pro-apoptotic proteins that promote cell death, via activation of the Caspase cascade through the stimulation of various pathways. Initiator Caspases (Caspase-2,-8,-9 and-10) are able to activate executioner Caspases (Caspase-3,-6 and-7), resulting in death of cells via apoptotic routes (Figure 1.5). Moreover, Caspases can cleave and cause the stimulation of other members of the Caspase family resulting in eventual cell death. An imbalance between active pro-apoptotic:anti-apoptotic proteins results in pathogenesis. For example, prolonged stimulation of pro-apoptotic protein, such as Caspases, lead to programmed cell death, which contributes to apoptosis of DCN that lead to onset of PD (Altieri 2010, Nakamura et al 2012, Chowdhury et al 2008, Chaudhry and Ahmed 2014).

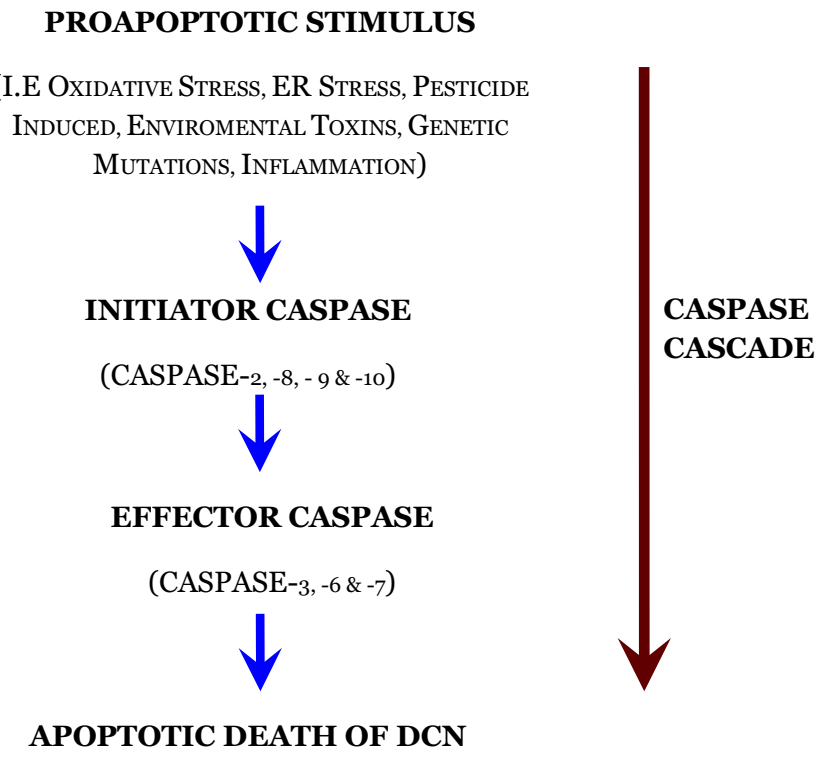

Figure 1.5 Caspase cascade

Figure showing overview of Caspase cascade which results in apoptosis. Initiator Caspases such as Caspases-2,-8,-9 and-10 activate downstream executer Caspases such as Caspases-3,-6 and-7 leading to eventual apoptotic cell death (McIlwain et al 2013, Chowdhury et al 2008, Nakamura et al 2012)

1.3.1 Caspase structure and activation

Caspases exist in most cells in a dormant state known as zymogens and can be activated through intrinsic or extrinsic routes such as mitochondrial, nuclear factor kappa beta (NFκB) and ER stress pathways. The Caspase structure consists of four main domains: an N terminal polypeptide, a large subunit, a small subunit and a linker region (Figure 1.6). The linker region functions to join the small subunit with large subunit and is comprised of aspartate residues. The large subunit and small subunit join to form the COOH terminal domain. Caspases can be categorized into two main types; initiator Caspases and effecter Caspases (as upstream and downstream respectively). The differentiation of these Caspases is based on their attributes, such as the role of action and participation in the proteolytic Caspase cascade. Initiator Caspases have long prodomains, which permit joining of proteases to their specific activators (Altieri 2010, Yan and Shi 2005).

Upon activation, the N terminal polypeptide and linker region of Caspases are dissociated, inducing the large subunit and small subunit to form an active enzyme complex (Figure 1.6). The complex consists of specific sequences, which combine to form an active site that recognizes particular substrates necessary for enzymatic stimulation. The N terminal polypeptide is composed of particular amino acid sequences, which makes the enzyme unique and highly specific. The inner recognition sites of Caspases can be activated via proteolysis, which can be triggered by Caspase substrates and in some cases other caspases. Caspases have diverse prodomains of different lengths and sequences, alongside distinct binding sites, causing a variation in substrate specificity (Fan et al 2005, McIlwain et al 2013). Activation of Caspases is achieved, via proteolytic cleavage of the linker regions between the large subunit and the small subunits of the enzyme, allowing the subunits to bind together, to form heterodimers stimulating activation (Venderova and Park 2012, McIlwain et al 2013).

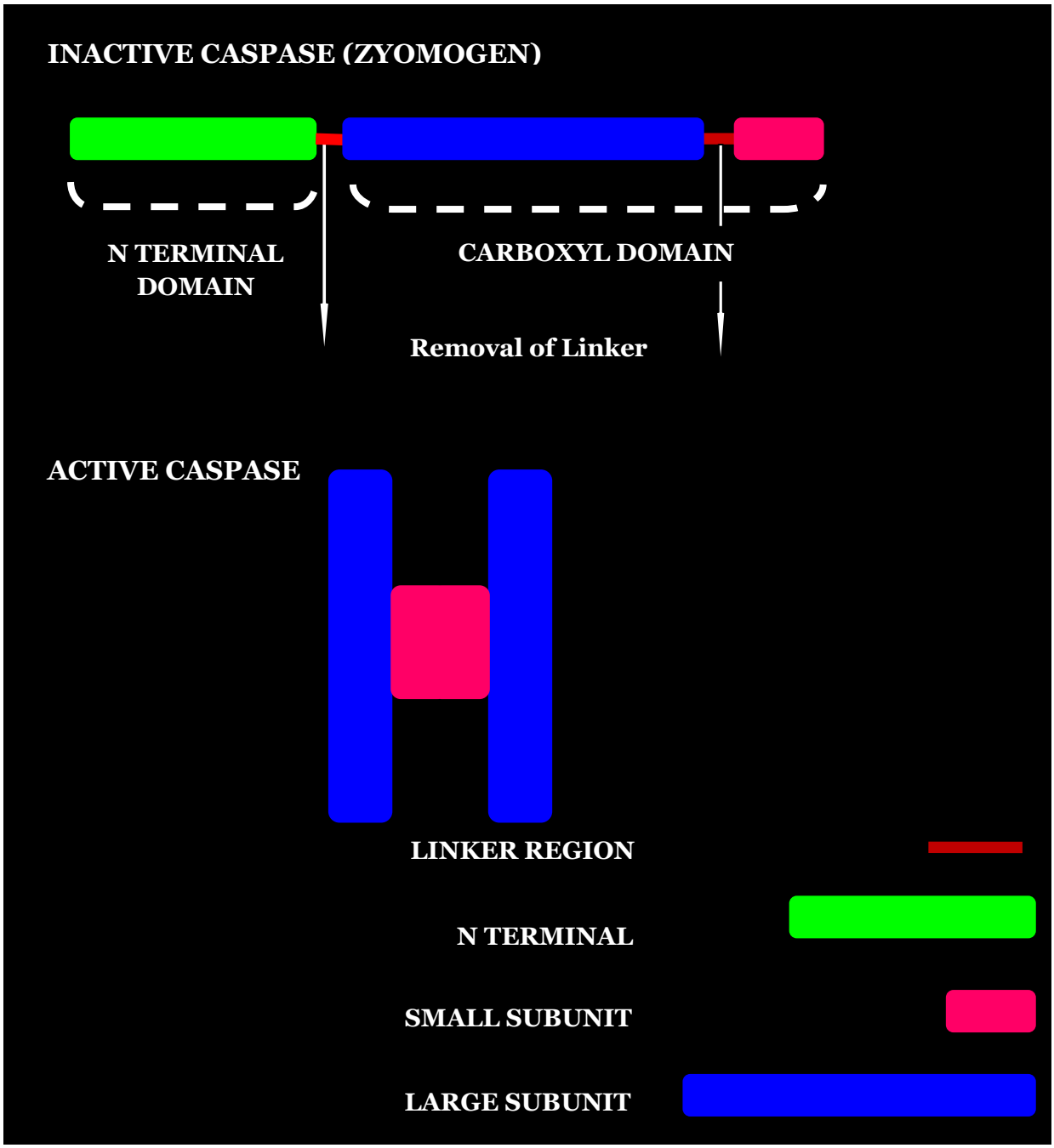

Figure 1.6 Caspase activation

The Caspase protein comprises of the N terminal domain and carboxyl domain. The carboxyl domain consists of the large and small subunit which is connected by a linker region. Caspase stimulation from inactive state (zymogen) to active state is achieved via proteolytic cleavage of the linker regions between the large and small subunits of the enzyme, allowing the subunits to bind together, to form heterodimers stimulating activation. Once a Caspase is activated, it triggers action of other Caspases, via the Caspase cascade, leading to apoptotic cell death (Altieri 2010, Venderova and Park 2012, McIlwain et al 2013, Yan and Shi 2005).

1.4 Different pathways (NFκB, ER stress, cJNK, p38) can stimulate activation of Caspases in DCN

Inflammation, oxidative stress, genetic mutation, calcium imbalance and toxins promote activation of intrinsic and extrinsic pathways. Activation of p38, JNK, and mutation of PTEN induced putative kinase 1 (PINK-1) gene triggers stimulation of intrinsic also known as the mitochondrial pathway. Activation of Caspases can be achieved through extrinsic routes, such as NFκB and ER stress pathway. Caspases can activate each other via a cascade reaction. Activation of NFκB stimulates Caspase-8 activity leading to stimulation of active Caspase-3. Active Caspase-1 can also activate NFκB indirectly leading to stimulation of other Caspases, such as, Caspase-8 followed by Caspase-3. Active Caspase-2 and active Caspase-8 participate in mitochondrial apoptosis pathway by converting B-cell lymphoma 2 homology domain 3 interacting-domain (BID) to truncate p15 BID (tBID). Subsequently, tBID binds to the pores of the mitochondria, thereby promoting the opening of mitochondrial PTP and release of cytochrome c. Cytochrome c binds to and stimulates Caspase-9, which in turn activates Caspase-3 (McIlwain et al 2013 Nakamura et al 2012, Chowdhury et al 2008, Chaudhry and Ahmed 2014).

Activation of JNK and p38 can provoke opening of mitochondrial PTP and release of cytochrome c leading to the activation of Caspases-9 and -3. Active Caspase-2 promotes release of cytokines such as IL- 6 and-8, leading to stimulation of microglia and death of neuronal cells via apoptotic routes. Oxidative stress, toxicity and mutations of specific genes, such as Parkin E3 ligase can damage the ubiquitin-proteasome system (UPS), resulting in elevated levels of aggregated incorrectly folded proteins, which accumulate to form Lewy bodies alongside stimulating activation of Caspase-12. Active Caspase-12 stimulates Caspase-9, which in turn results in stimulation of Caspase-3. Active Caspase-3 promotes fragmentation of DNA, shrinkage cell, formation of apoptotic bodies and death of cells. The mass destruction of DCN causes degeneration of neurones, resulting in PD (Nakamura et al 2012). Subsequent, pages describe such pathways (NFκB, mitochondrial and ER stress) and their role in Caspase activation in more detail.

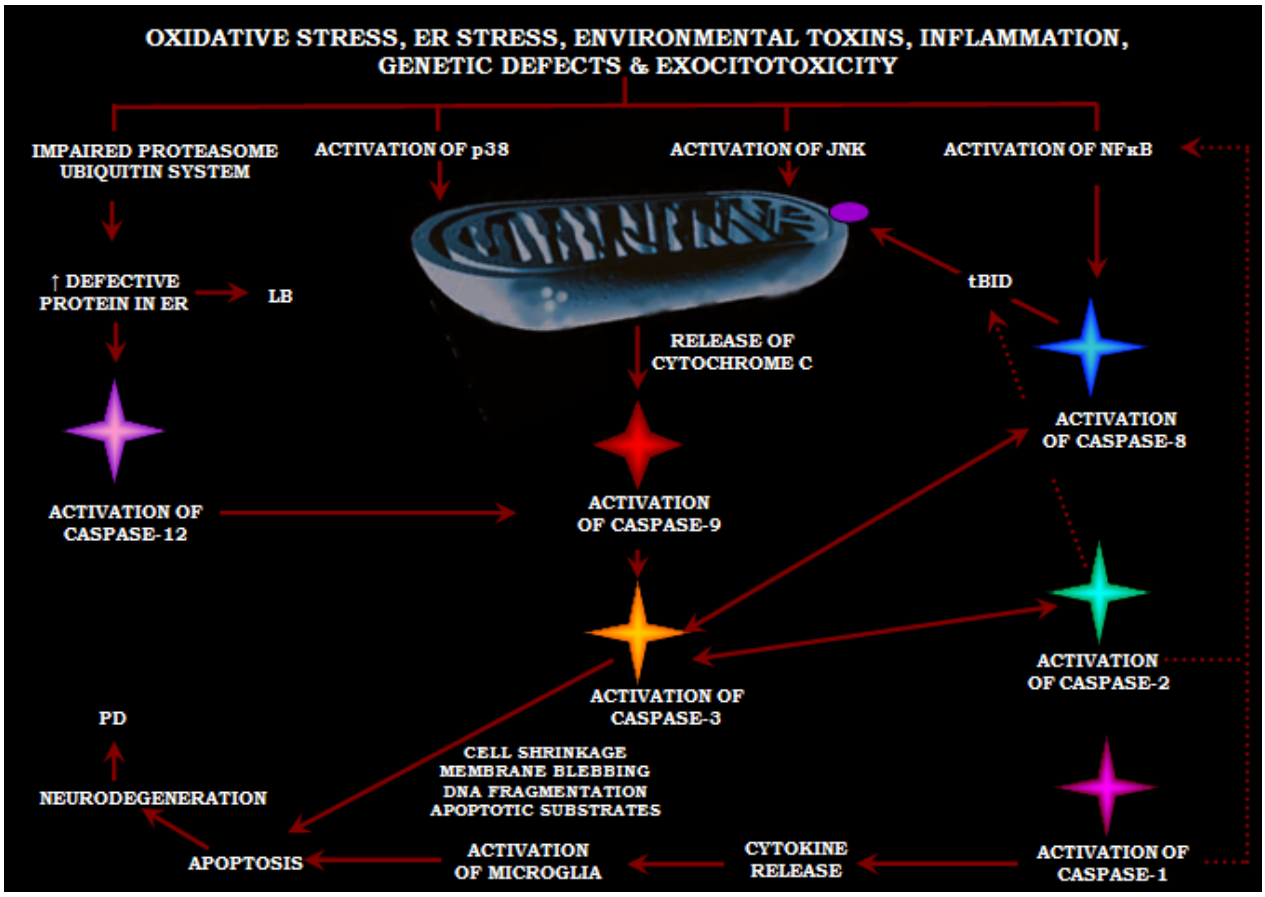

Figure 1.7: Caspase pathways that lead to cell apoptosis resulting in PD

Figure illustrates the involvement of various pathways that upon stimulation encourage cell death of DCN leading to the onset PD. Oxidative stress, environmental toxins, alongside genetic mutations and excitotoxicity can stimulate activation of different pathways such as inflammatory, JNK, NFκB, p38, and ER stress. Subsequently, this provokes motivation of initiator Caspases, leading to activation of other Caspases, resulting in cell death and disease and progression of PD Altieri 2010, Venderova and Park 2012, McIlwain et al 2013, Yan and Shi 2005, Nakamura et al 2012, Chowdhury et al 2008, Chaudhry and Ahmed 2014, Midwinter et al 2006, Flood et al 2011).

NFκB is an inducible transcription factor as it has the ability to bind to specific DNA sequences promoting transcription of genes that manufacture a variety of proteins. NFκB is present in an inactive form in virtually all cells and tissues. The NFκB family is comprised of five members such as p105, p100, p65, c-Rel and Rel B. p100 and p105 are precursors for the active p50 subunit and p52 subunits respectively, and are long proteins that possess glycine rich regions (Figure 1.8). The glycine rich regions of the p100 and p105 precursors are cleaved and release the N terminal segment of the proteins leading to the active p50 and p52 forms (Midwinter et al 2006, Chowdhury et al 2008).

In contrast, p65, c-Rel and Rel-B have transcriptional activation domain embedded within their C terminal region that promotes activation and regulation of these proteins in a different way. The p65, c-Rel and Rel-B proteins can form homodimers and heterodimers with each other via their transcriptional activation domains. As the p50 and p52 homodimers lack the transcriptional activation domains they are unable to stimulate transcription when bound to DNA in the nucleus. In order for transcription to occur p50 or p52 need to form heterodimers with p65, c-Rel or Rel-B (Hayden and Ghosh 2009, Mattson et al 2000).

Normally, the C terminal Rel homology domain (RHD) binds to the ankyrin repeats that are situated within the IκB, which prevents stimulation of NFκB proteins The RHD of the NFκB family proteins is comprised of 300 residues at the C terminal and contains all the elements necessary for the proteins to bind to DNA, to form dimers and to bind to IκB proteins. The RHD contains the nuclear localising signal which promotes the binding of DNA when NFκB is activated, resulting in transactivation of different target genes (Chowdhury et al 2008, Flood et al 2011).

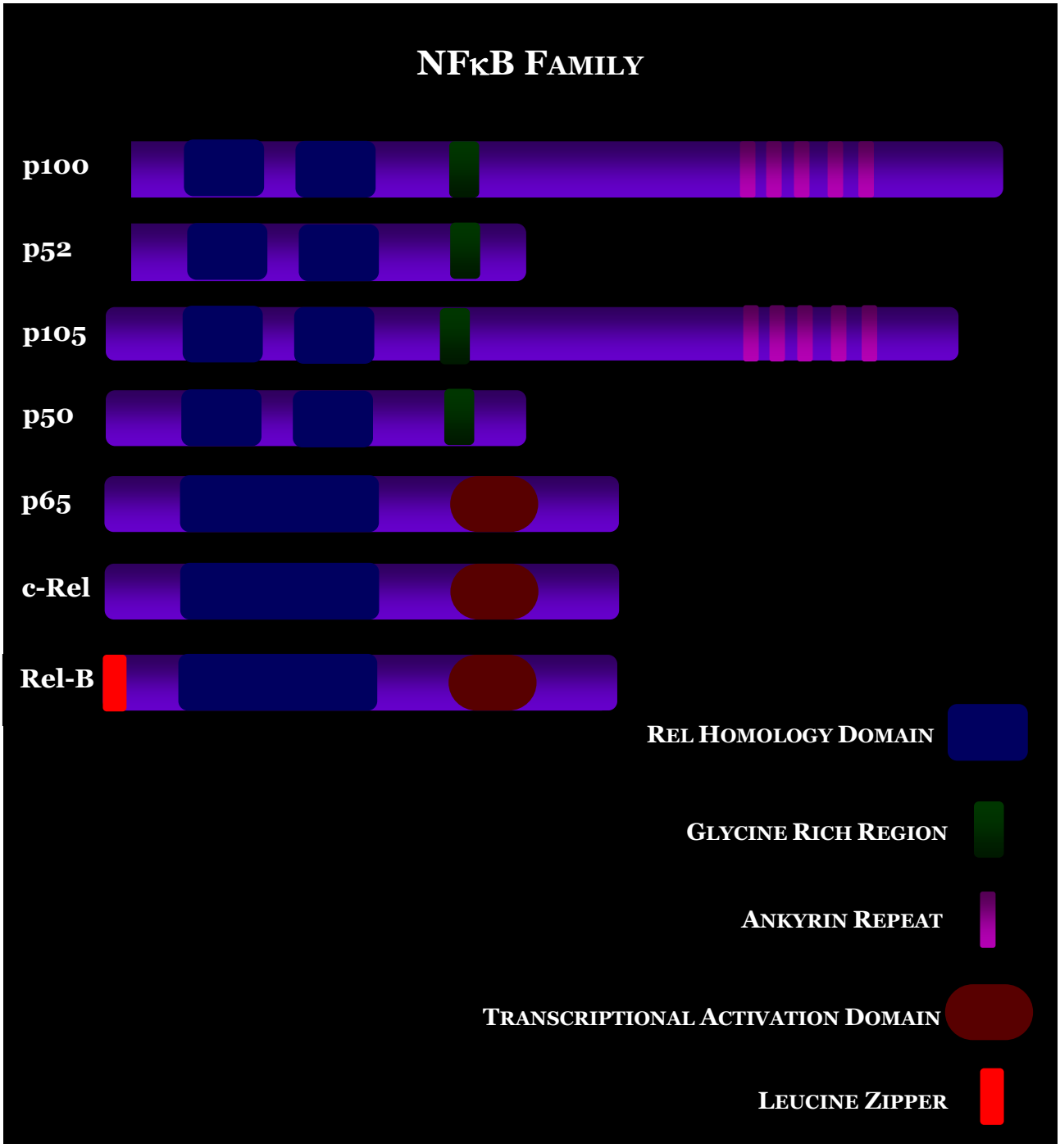

Figure 1.8: Structure of NFκB proteins

The precursor's p105, p100 and p65, c-Rel and Rel-B are the part of the NFκB family and are present in the cytoplasm in an inactive form. The ankyrin repeats of p105 and p100 inhibit activation of these precursors. The transcriptional activation domain of p65, c-Rel and Rel-B promote different variation of dimers to be formed. Rel Homology domain binds to DNA, to form dimers and to bind to IκB proteins (Midwinter et al 2006, Chowdhury et al 2008).

The IκB family is also comprised of five members known as IκB-α, IκB-β, IκB-γ, IκB-ε and Bcl-3 (Figure 1.9). The IκB proteins regulate NFκB by binding to and suppressing NFκB activation. IκB consist of 5-10 ankyrin repeats that bind to the RHD of NFκB and conceal the nuclear localization signal of NFκB. The amino terminal of IκB-α, IκB-β and IκB-γ all have a regulatory domain that contains two serines. During IκB degradation the serine residues are phosphorylated by ubiquitin. IκB-α phosphorylates at serine 32 and serine 36, whilst IκB-β phosphorylates serine 19 and serine 23. The N terminal regulatory domain of IκBs comprise of lysine residues which bind to polyubiquitin chain and are subsequently degraded (Memet 2006).

IκB proteins can bind to different combinations of NFκB proteins. IκB-α and IκB-β binds to and suppresses the p50:p65 combination or p50:c-Rel combination of NFκB proteins, which are found in most cell types. IκB-ε binds and inhibits homodimers such as p65:p65 or c-Rel:c-Rel form of NFκB, which are found in fewer cells. IκB-γ inhibit the homodimer precursor p50:p50 in mouse model and its function is yet to be determined. Bcl-3 is different to members of the IκB family as it can inhibit and also promote activation of the complex it binds to. Bcl-3 binds to homodimers p50:p50 or p52:p52 and promotes transcriptional activation when they enter the nucleus. The ankyrin repeats embedded in the C terminal of p100 and p105 function as inhibitors and cleavage at the glycine region converts p100 and p105 to the active p52 and p50 forms. The inhibitory protein IκB binds to and suppresses the nuclear localising signal on NFκB proteins thereby inactivating NFκB:IκB complex in the cells cytoplasm. When cells are stimulated IκB is phosphorylated and catabolised, allowing the release and activation of NFκB. NFκB enters the nucleus and binds to NFκB promoter binding sites on genes thereby encouraging NFκB response in gene expression (Midwinter et al 2006, Ghosh et al 2007).

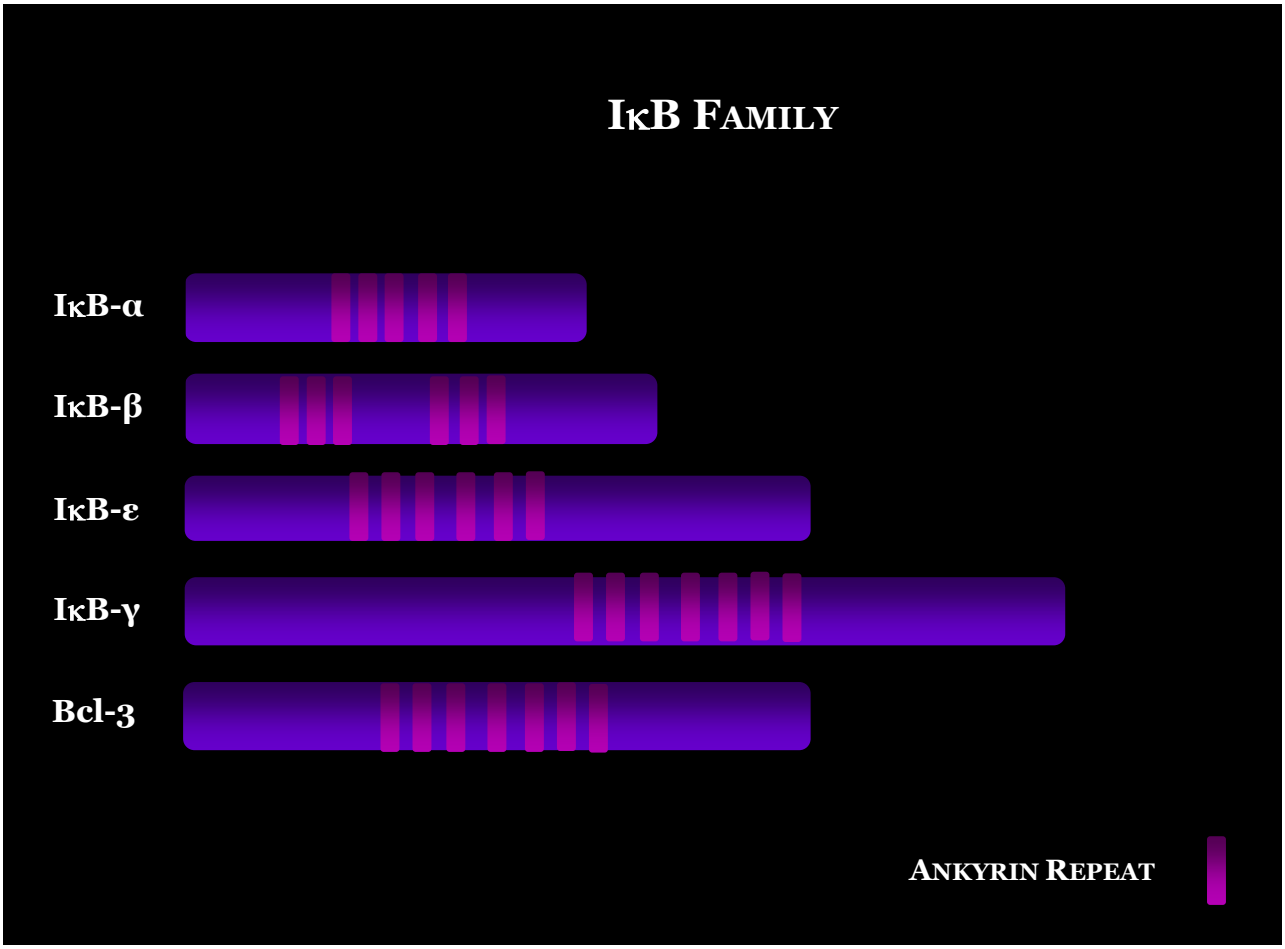

Figure 1.9: Structure of IκB proteins

IκB-α, IκB-β, IκB-γ, IκB-ε and Bcl-3 are all part of the IκB family which inhibit the activation of NFκB proteins. IκB proteins can bind and suppress different combinations of NFκB proteins in the cytoplasm of cells (Midwinter et al 2006, Chowdhury et al 2008, Memet 2006).

The IKK (IκB kinase) complex (700- 900 kDa) is composed of two catalytic subunits IKK-α, IKK-β and the regulatory subunit NFκB essential modulator (NEMO). IKK-α and IKK-β share 52% genetic sequence and 65% catalytic domains. IKK-α and IKK-β contain a leucine zipper for protein – protein interactions, a helix loop helix domain which has a regulatory function and a kinase domain (Figure 1.10). External stimuli promote leucine zipper of IKK-α and IKK-β to form dimers. The helix to helix domain of IKK-α and IKK-β interact with kinase domain. In addition, NEMO triggers autophosphorylation of serine residues in the activation loop of IKK-α and IKK-β, leading to formation of dimers and binding of NEMO. IKK-α:IKK-β dimer binds to NEMO, via the NEMO binding domain in IKK-α and IKK-β, producing a NEMO:IKK-α:IKK-β structure, known as the IKK complex. IKK complex phosphorylates the N terminal region of IκB at the serine residues 32 and 36. Degradation of IκB occurs at the lysine 21 and 22 residues by 26S proteasome. Degradation of IκB exposes the nuclear localisation signal, which results in activation of NFκB (Ghosh et al 2007, Li et al 2008).

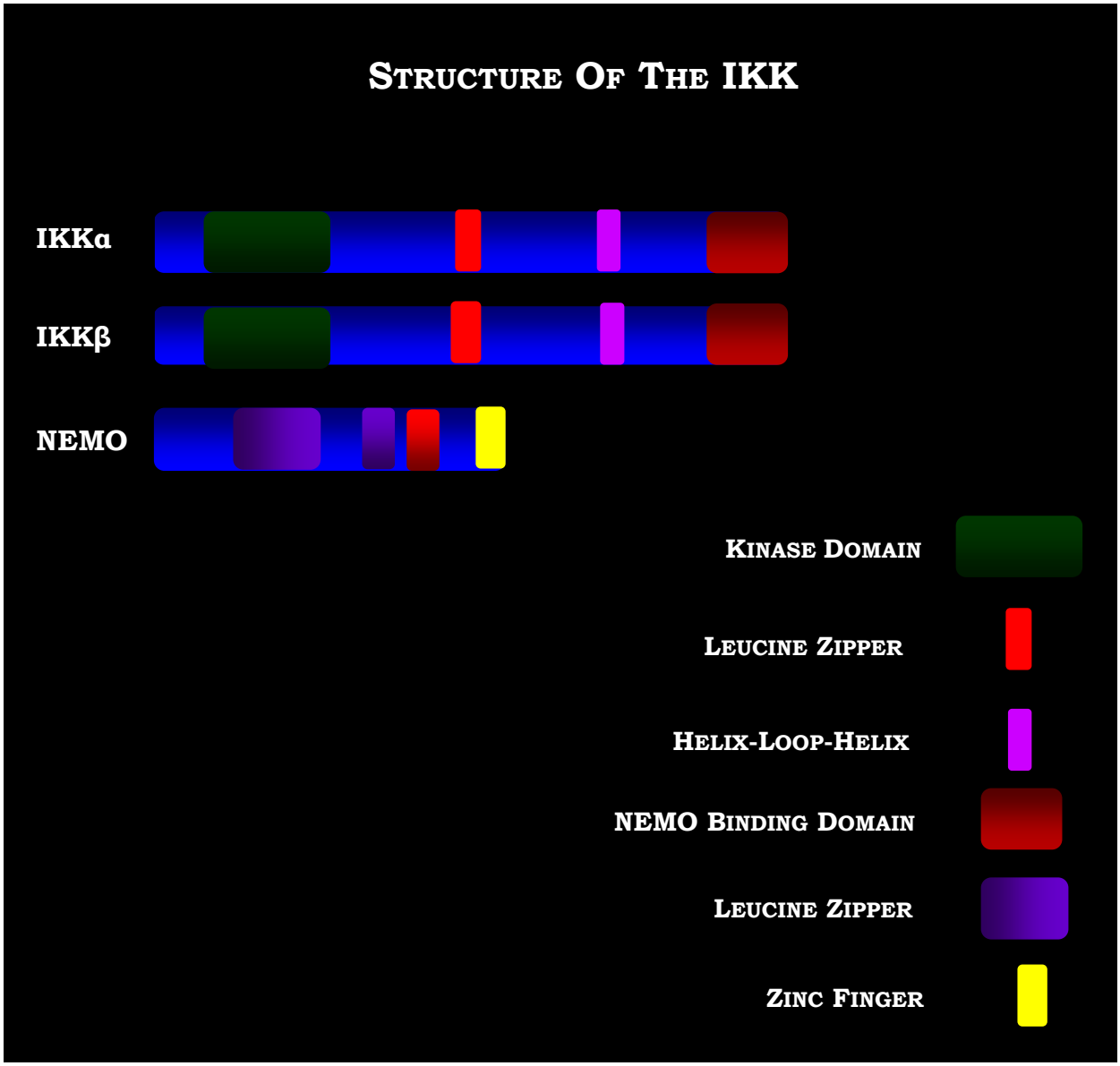

Figure 1.10: Structure of IKK proteins

IKK-α, IKK-β and NEMO are all part of the IKK proteins that form to make the IKK complex. IKK-α and IKK-β are the catalytic segment, whilst NEMO is the regulatory segment of the IKK complex. External stimuli promote the dimerization of IKK-α and IKK-β, followed with binding of NEMO via the NEMO binding domain which is embedded in the IKK-α and IKK-β structures (Ghosh et al 2007, Li et al 2008).

Extensive research has shown that NFκB plays a key role in anti apoptotic pathways mainly in cancer cell lines (Section 1.5.3). Recent studies have shown that NFκB is involved in triggering apoptotic death of cells (Section 1.5.4). External stimuli such as environmental toxin, ROS, TNF, IL, ligands and lymphotoxin B are all able to trigger IKK complex to stimulate cytoplasmic NFκB activation, either through the classical, alternative or atypical pathway (Figure 1.11 and discussed below). Active NFκB enters the nucleus to promote transcription of different proteins such as Caspases, cytokines, receptors, growth factors, adhesion molecules and chemokines (Flood et al 2011).

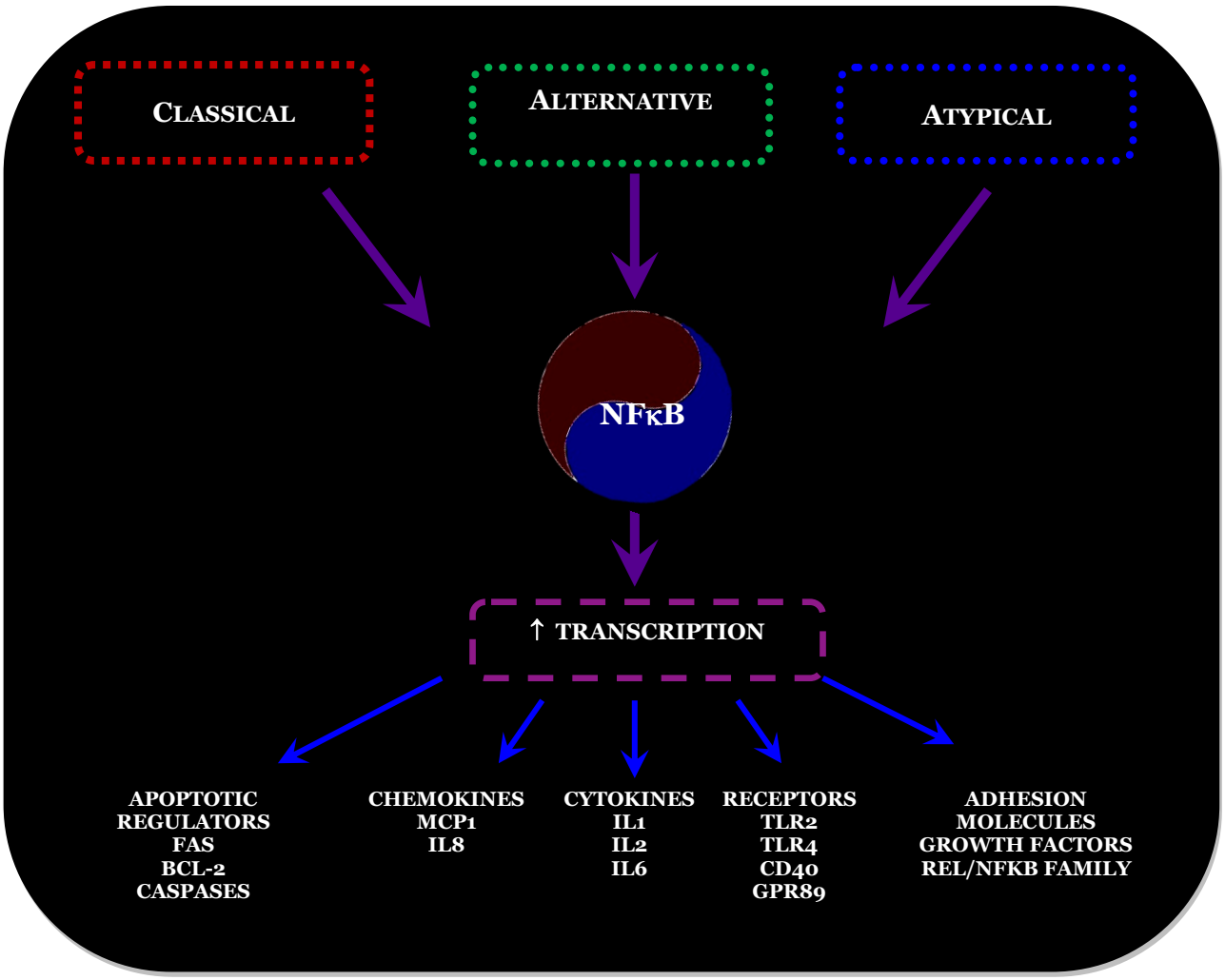

Figure 1.11: Active NFκB increases transcription of different genes

Different stimuli trigger activation of IKK complex, via classical, atypical or alternative pathway that results in stimulation of NFκB. Active NFκB provokes transcription of a wide variety of genes such as chemokines, cytokines, surface receptors, adhesion molecules and apoptotic regulators, which are used for different responses such as inflammatory (Chaudhry and Ahmed).

1.5.1 Classical Pathway triggers NFκB activation

In the classical pathway, external stimuli such as oxidative stress, ROS, TNF trigger activation of the protein NEMO. Active NEMO binds to IKK-α and IKK-β forming the IKK complex (Figure 1.12). This IKK complex interacts and degrades IκB of IκB of IκB:NFκB via proteasome degradation. IKK complex phosphorylates serine residues 32 and 36 at the N terminal region of IκB from the NFκB:IκB complex. Phosphorylated IκB binds to the E3IκBα complex, which sends a signal to the ubiquitin protein E2 conjugating protein. The binding of E2 conjugating protein to IκB results in degradation of IκB occurs at the lysine 21 and 22 residues by 26S proteasome (Li et al 2008, Ghosh et al 2007).

The release and degradation of IκB exposes the nuclear localisation signal, which results in activation of NFκB protein (p50:p65) through the formation of dimers. The nuclear localisation signal translocates active NFκB from the cytoplasm into the cell nucleus. Subsequently, active NFκB binds to the promoter and induces transcription of various genes (Li et al 2008, Ghosh et al 2007). The classical pathway, promotes NFκB to enhance expression of apoptotic genes, such as FAS ligand, which activates Caspase-8 in cells (Krumschnabel et al 2009, Li et al 2008, Reynolds et al 2007). For example, NFκB promotes transcription of inducible nitric oxide synthetase (iNOS), which participates in the increase of intracellular calcium concentration in damaged cells, alongside ROS and nitric oxide production (Mattson and Mark 2007, Panet et al 2001). In addition, NFκB promotes transcription of inhibitors of apoptosis, cytokines and neurotrophic factors (Lee et al 2001, Mattson and Meffet 2006).

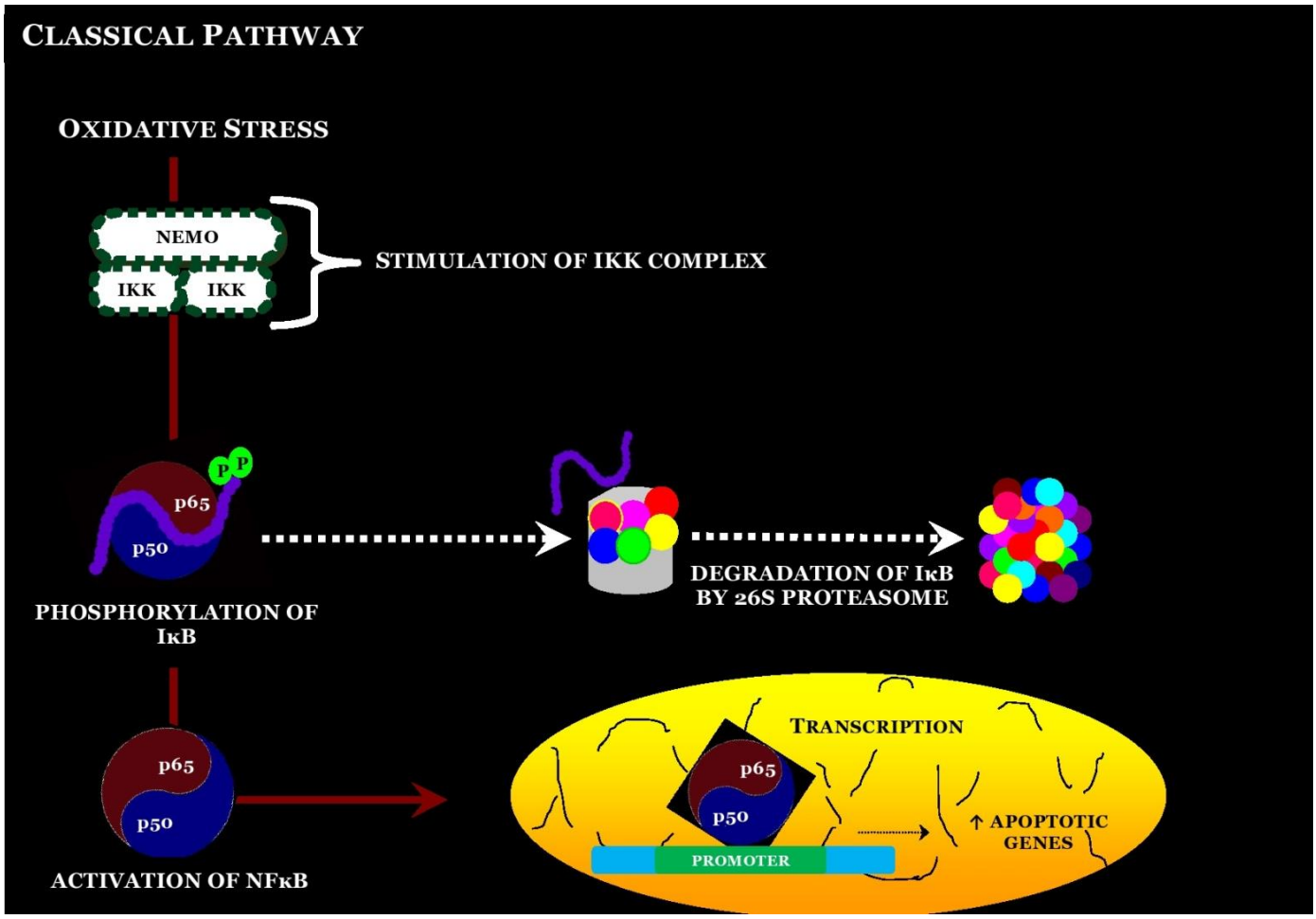

Figure 1.12: The Classical Pathway of NFκB

In the cytoplasm of resting cell, IκB binds to and inhibits NFκB activation. External signals cause the activation of NEMO which binds to IKK-α and IKK-β forming the IKK complex. IKK complex binds to and releases IκB from the IκB:NFκB complex, through phosphorylation. Phosphorylated IκB is degraded by proteasome 26S. The release of IκB exposes the nuclear localisation signal which promotes dimerization of p65:p50 (NFκB proteins) and translocation of active p65:p50 from the cytoplasm to the nucleus. Active p65:p50 binds to specific DNA sequences resulting in transcription of genes (Midwinter et al 2006).

1.5.2 The Alternative Pathway

In the alternative pathway, members of the TNF family such as lymphotoxin b, trigger NFκB inducing kinase (NIK) activation. Active NIK binds to and activates IKK-α:IKK-α forming the IKK complex. IKK complex phosphorylates and removes IκB from the p52:IκB:Rel-B complex. IκB is catabolised by proteasome 26S and p52:Rel-B is activated through dimerization. The p52: Rel-B dimer leaves the cytoplasm to enter the nucleus where it binds to DNA promoter site through and up regulates transcription of specific genes (Lee et al 2001, Jia and Misra 2007).

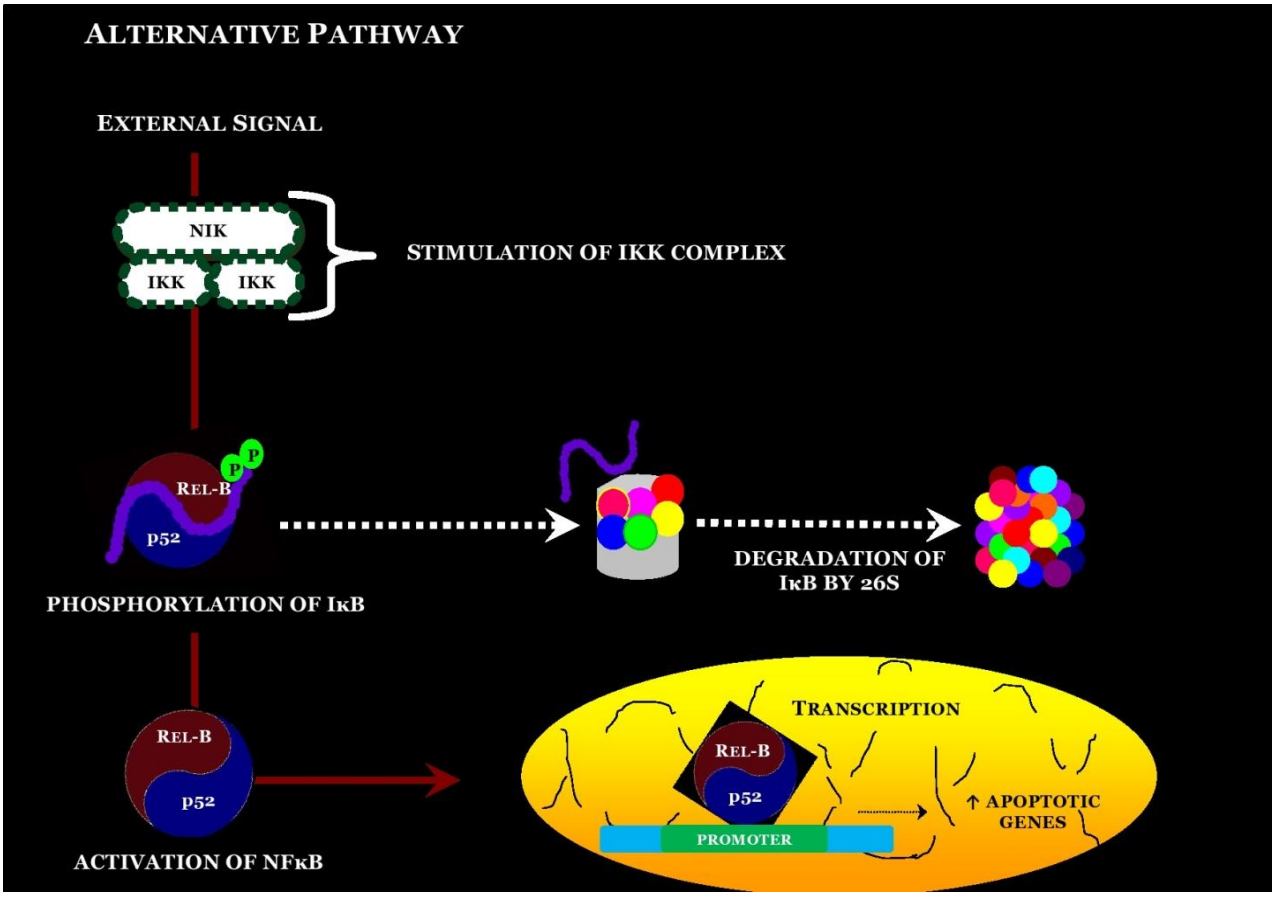

Figure 1.13: Alternative Pathway NFκB

Extracellular stimuli triggers cell surface receptors resulting in NIK activation. Subsequently, NIK binds to and dimerises IKK-α forming the IKK complex. IKK complex phosphorylates and releases IκB, which is subsequently degraded by ubiquitinylation. As the inhibitor IκB is removed, p52 forms dimer with Rel-B and the p52:Rel-B dimer translocates to the nucleus promoting transcription of proteins (Midwinter et al 2006).

Recent work by Lee et al (2007) suggests the presence of a third pathway, known as the atypical pathway, can also activate NFκB. This pathway is stimulated by UV radiation, which promotes proteasomes to degrade IκB-α through phosphorylation, resulting in the release and activation of NFκB. Active NFκB enters the nucleus, binds to the promoter of DNA, initiating the process of transcription of cytokine receptor genes and cytokine genes. The negative feedback system is used to catabolise the increased levels of NFκB so that the level of transcription ceases. This is achieved by producing new IκB-α proteins that attach to NFκB (Mattson et al 2000).

1.5.3 The role of NFκB in PD pathogenesis

The role of NFκB in cell death and survival is controversial (Yamamoto and Gaynor 2001, Cassarino et al 2000, Hunot et al 1997, Gao et al 2002, Flood et al 2007, Zhang et al 2012, DeErausquin et al 2003, Henn et al 2007, Ghosh et al 2007). A 60% increase in NFκB activity was found in human SH-SY5Y neuroblastoma cells treated with MPTP, when compared to untreated cells. Translocation of NFκB and increase in NFκB binding activity was detected in the nucleus of treated cells. NFκB increased expression of superoxide dismutase and promoted cell survival rather than death of MPTP-treated SH-SY5Y cells (Cassarino et al 2000). Furthermore, Parkin activated NFκB by phosphorylation of IκB, thereby promoting transcription of pro survival genes. However, mutant Parkin phosphorylates IκB and activate NFκB, which caused death of human SH-SY5Y neuroblastoma cells (Henn et al 2007). Research by Lee et al (2001) found that NFκB activation protected auto oxidized dopamine PC12 cells from apoptotic cell death in PD model. PC12 cells that had been transfected with p65 and p50 units of NFκB had greater resistance to apoptotic death caused by auto oxide dopamine, when compared to PC12 cells that had not been transfected.

In contrast, work by Gao et al (2002) found NFκB activity promoted death of DCN in SN, through the inflammatory pathway. A selective loss of DCN and increase of active microglia was observed using double IF analysis, in ventral mesencephalic cultures of male Fischer rats that had been treated with the

inflammagen lipopolysaccharide. An increase in ROS such as superoxide and nitrite and IL were found in treated DCN cultures compared to untreated cultures. The authors suggested that the increase in ROS and NFκB levels may result in selective and progressive death of DCN, which is relevant in neurodegenerative diseases such as PD.

Previous research by Ghosh et al (2007) suggests that loss of dopamine secreting cells can be prevented by selectively suppressing activation of NFκB. The mice used in the study were induced with the MPTP, to generate animal models that had PD symptoms. There was a significant increase in NFκB activity found in SNpc of the MPTP induced mice. These findings were also established in PD patients, indicating that increased stimulation of NFκB may play a vital role in the onset of PD. Double IF analysis showed high levels of p65 in astrocytes and microglia of midbrain of six to eight weeks old male mice that had been injected with MPTP, when compared to mice that received saline injection. Double IF analysis showed elevated levels of p65 in microglia the SN of PD patients when compared to age matched controls. The MPTP mice were administered with peptide NBD (NFκB essential modifier-binding domain) injection intravenously to see if there was a difference in the level of NFκB activity. A decrease in the level of NFκB was found in the SN of the MPTP induced mice, indicating that the peptide NBD had successfully suppressed NFκB activity. The NBD injection had prevented the binding of NEMO to IKK so the IKK complex could not be formed, thus the activity of NFκB was suppressed. Furthermore, a decrease in the activation of microglia in the SN and an increase in overall motor function was found in the MPTP-induced mice via the administration of peptide NBD injection. The author also suggested that the reduced level of NFκB through the NBD injection, had improved the quantity and secretion of dopamine secreting cells in the nigra of MPTP induce mice. In this way, the peptide NBD can be used therapeutically in the treatment of PD patients, via selectively suppressing the activation of NFκB.

In addition, high levels of iNOS in SN along with increased nitrite in cerebrospinal fluid have been found in PD patients, indicating inflammatory damage of DCN. Active microglia produce cytokines IL-6 and-1β as well as nitric oxide and ROS that trigger IKK complex, leading to NFκB activation, via the release and degradation of IκB. The ATP competitive inhibitor Compound A (7-[2-(cyclopropylmethoxy)-6-hydroxyphenyl]-5-[(3S)-3-piperidinyl]-1,4-dihydro-2H-pyrido[2,3-d][1,3]oxazin-2-one hydrochloride), competitively inhibits IKK-β kinase ability to phosphorylate IκB, thereby preventing NFκB activation and reducing death of DCN in SN in MPTP mouse model (Flood et al 2007, Zhang et al 2012).

DeErausquin et al (2003) found active NFκB level in DCN of PD patients and suggested that excitotoxicity may have promoted stimulation of NFκB. In addition, an increased in NFκB translocation , ROS production, calcium levels and decrease IκB expression was found in rat mesencephalic cultures that were exposed to glutamate receptor AMPA. IF analysis portrayed a significant loss of dendrites of rat mesencephalon DCN that were treated with AMPA, indicating that toxicity destroyed DCN. This shows that NFκB has a dual role as it can protect and promote DCN from apoptotic death (Yamamoto et al 2001).

Previous work by Hunot et al (1997) had indicated that ROS triggers NFκB activation leading to apoptotic death of DCN via oxidative stress. Double IF and Immunohistochemical analysis revealed p65 NFκB translocation and staining in mesencephalon DCN of post-mortem brains of PD patients as well as in mesencephalon rat cultures that had been treated with ceremide. IF analysis showed increased levels of ROS and formation of apoptotic bodies in ceremide induced mesencephalic cultured cells using a specific molecular probe, 2',7'-dichlorodihydrofluorescein diacetate (DCDHF-DA) that emits a green light when it is oxidised. This strongly indicates that ROS is able to trigger NFκB activation and apoptotic death of DCN through inflammatory pathway.

1.5.4 NFκB pathway and Caspase Activation

NFκB has been strongly correlated with PD, through oxidative stress and the inflammatory pathway (Figure 1.14 and discussed on pages 39-41). NFκB promotes complex formation between the pro apoptotic protein ASC (apoptosis associated speck like protein containing a CARD) and Ipaf a member of Apoptosis activating family -1 (Apaf-1). The ASC: Ipaf formation binds to and activates Caspase-8, which in turn stimulates Caspase-3 (Mattson et al 2000, Mattson and Meffert 2006, Jia and Misra, 2007, Yamamoto et al 2001, Masumoto et al 2003).

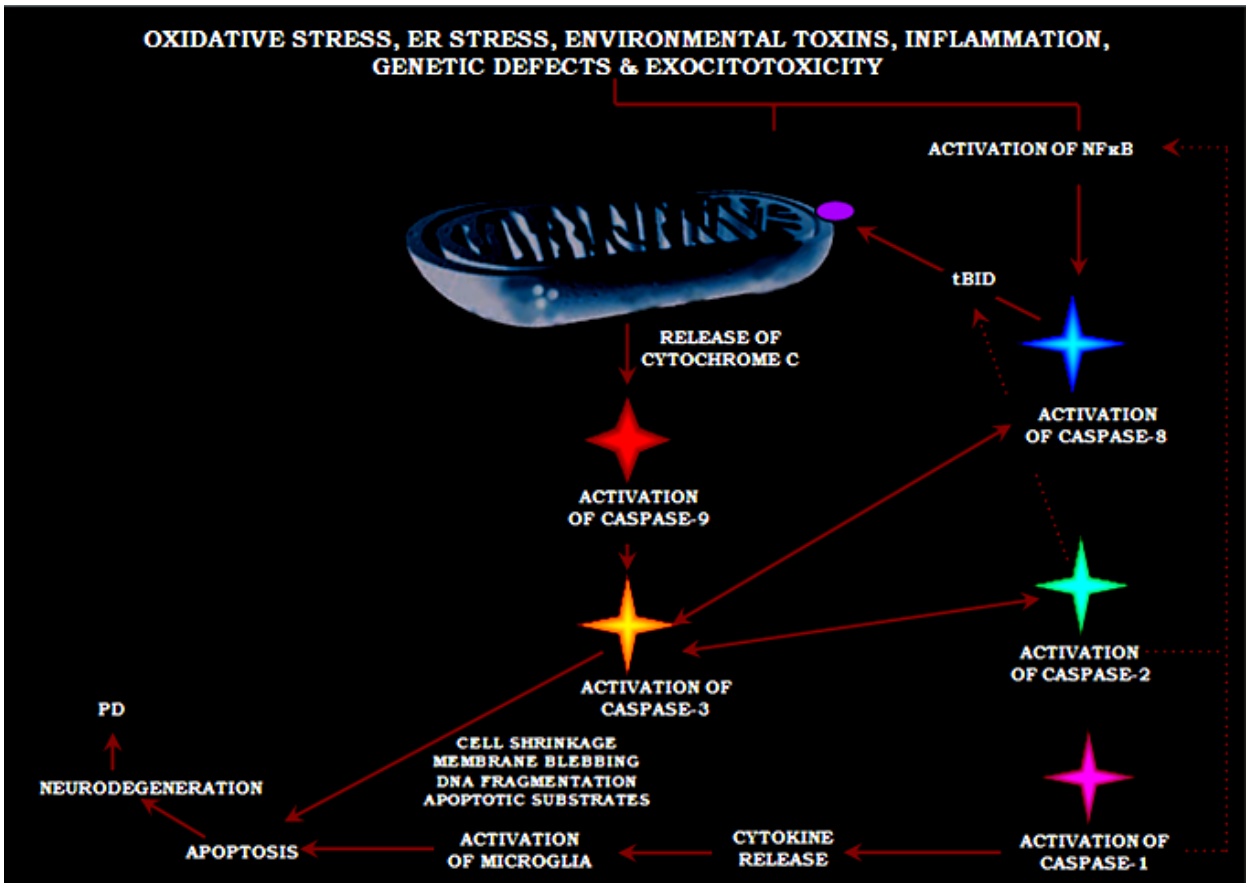

Figure 1.14 : Exploring Caspase activation in the NFκB pathway

NFκB can be activated by different Caspases and can also promote activation of other Caspases via intrinsic (mitochondrial) route and extrinsic route leading to death of DCN and PD onset. Active Caspase-2 can trigger NFκB activation which stimulates activation of Caspase-8 followed by Caspase-3 activation, resulting in death of DCN and PD onset. Oxidative stress promotes protein misfolding and aggregation leading to DCN to become more susceptible to cell death (Giasson and Lee 2001).

Oxidative stress depletes ATP and nicotinamide adenine dinucleotide (NADH) levels resulting in a decrease in TH and glutathione along with impairment of complex I of the mitochondria. Malfunction of the mitochondria leads to defects in ubiquitination. This contributes to the increase of Caspases-1,-3 and -8 stimulation leading to loss of cells in the pars compacta of PD brain (Williams et al 2005, Chandra and Orreius 2002, Chaudhry and Ahmed 2014).

1.5.4.1 Caspase-2 and NFκB pathway

Caspase-2 is a unique member of the Caspase family as it possesses a dual function, to promote or suppress cell death (Figure 1.14). Caspase-2 is able to promote apoptosis via stimulating Caspase-3 activation either directly or indirectly triggering NFκB activation (which subsequently activates Caspase-8 followed by Caspase-3 activation). Moreover, Caspase-2 can promote formation of tBID (a pro apoptotic protein) which translocates to the mitochondrial membrane. The binding of tBID induces rearrangement of the lipid channels on the mitochondria, causing pores to form, thereby releasing the component cytochrome c. Cytochrome c binds to Apaf-1 via oligomerization, forming an apoptosome. The apoptosome recruits and thereby stimulates Caspase-9 followed by Caspase-3 activation. In addition, Caspase-2 prevents apoptosis by increasing Bcl-2 (anti apoptotic protein) activity (Wilms et al 2007, Chaudhry and Ahmed 2014)

Lamkanfi et al (2006 and 2007) suggests that NFκB interacts with the prodomain of Caspase-2 forming complexes with NFκB through the recruitment of receptor interacting protein 1 (RIP). Caspase-2 comprises of a p53-induced death domain (PIDD) which is activated in response to DNA damage. PIDD is able to bind to the RIP1 forming a PIDDosome complex which attaches and activates Caspase-2. The PIDD:RIP1:Caspase-2 complex is able to trigger NFκB stimulation, promoting the transcription of pro-survival genes. However, substantial damage to DNA may result in Caspase-2 to

switch from protective to apoptotic function, promoting NFκB to increase transcription of pro apoptotic genes. More specifically research has shown that Caspase-2 is able to promote mitogen activated protein kinase (MAPK) and NFκB activation (Kumar 2007).

1.5.4.2 Caspase-3 and NFκB pathway

Active Caspases-3 and-8 levels were found in DCN of the SN in post mortem brain of PD patients (Anderson 2001). Karunakaran and Ravindranath (2009) discovered that p38 can influence activation of NFκB in midbrain of MPTP-treated mice. Western blot (WB) analysis revealed that IκB phosphorylation and translocation of NFκB was prevented when p38 inhibitor, SB239063 was used in midbrain of PD animal model, indicating that p38 triggers the phosphorylation of IκB resulting in activation of NFκB. In addition, increased p65 NFκB was found in the nucleus of MPTP mouse midbrain that had not been treated with the p38 inhibitor SB239063. WB analysis showed an increase in Caspase-3 activity in the midbrain of PD animal model that had not been treated with p38.

Research by Jia and Misra (2007) observed NFκB activation in the nucleus, alongside increase in hydrogen peroxide, Caspase-3 activation and production of superoxide in zinc ethylene bisdithiocarbamate fungicide (zineb), treated human neuroblastoma cells. The elevated ROS production, such as hydrogen peroxide and superoxide, alongside increased lipid peroxide was able to trigger activation of Caspases via NFκB route leading to death of cells via apoptotic pathway. Moreover, reduced stimulation of antioxidant enzymes such as, superoxide dismutase and catalase were found in cells exposed to the pesticide zineb, suggesting that oxidative stress is able to trigger NFκB apoptotic route and suppress antioxidant activity, leading to death of neuronal cells. The authors suggested that their findings are providing support for oxidative stress theory of PD pathogenesis, as environmental toxins may cause death of DCN and develop PD by inhibiting stimulation of antioxidant and activating pathways such as NFκB. The accumulation of hydrogen peroxide interacts with superoxides leading to further manufacture of hydroxyl radicals, increasing lipid peroxidation and degradation of DNA and proteins (Karunakaran and Ravindranath 2009, Henn et al 2007).

1.5.4.3 Caspase-1 and NFκB pathway

Caspase-1 indirectly activates apoptosis via triggering NFκB stimulation (thereby allowing Caspase-8 followed by Caspase-3 activation), and by promoting catabolism of the Parkin gene, E3 ligase. The breakdown of E3 ligase induces impairment of UPS. The UPS plays an essential role in the degradation of incorrectly folded and defective proteins (see Section 1.7.2 for further details). It has been shown that 6OHDA triggers phosphorylation of IκB and translocation of p65 to the nucleus in SH-SY5Y neuroblastoma cells. IF and WB analysis that revealed 6OHDA triggered Caspase-3 activation and death of DCN through NFκB pathway (Xiang et al 2011). Work by Panet et al (2001) revealed that NFκB triggers apoptotic death of 6OHDA-treated dopamine induced PC12 cells. Elevated levels of translocated p65 NFκB was found in 6OHDA-treated cells by flow cytometry analysis. A specific NFκB inhibitor SN-50 was able to decrease apoptotic death of 6OHDA-treated cells suggesting that 6OHDA triggers NFκB mediated death of cells. In addition, Caspase-1 inhibitor ICE and Caspase-3 inhibitor, CPP32, had decreased death of 6OHDA induced cells indicating that Caspases-3 and -1 are active in apoptotic death of 6OHDA induced cells. WB analysis showed an increase in survival in 6OHDA cells that had been treated with either the Caspase-3 inhibitor or Caspase-1 inhibitor. The study indicated that ROS triggers NFκB activation and activation of Caspases-3 and -1, resulting in apoptotic death of DCN.

1.5.4.4 Caspase-8 and NFκB pathway

NFκB triggers expression of FAS ligand, leading to Caspase-8 activation and death of cells via apoptotic route (Mattson et al 2000, DeErausquin et al 2003). In addition, stimulation of the FAS receptor encourages activation of FAS death domain by cleavage of cysteine residues. Active FAS binds to and activates the death domain of Fas-associated death domain containing protein (FADD). Subsequently, active FADD binds to the death effecter domain of Caspase-8, thereby triggering activation of Caspase-8. FADD also promotes Caspase-8 binds to the death-inducing signalling complex (DISC), which interacts with activate NFκB (Lamkanfi et al 2006 and 2007). However, studies by Mattson and Meffert (2006)

and Masumoto et al (2003) show that active NFκB triggers Caspase-8 activation, leading to apoptotic cell death).

Research by Ho et al (2009) found that mutated leucine rich repeat kinase 2 (LRRK-2) interacts and triggers FADD leading to Caspase-8 activation and death of mouse cortical neurons. Caspase-8 induces apoptosis intrinsically via converting BID to tBID which translocate onto the membrane of the mitochondria, allowing the membrane PTP to open (Kruidering and Evan 2000). Research by Hartmann et al (2001) indicated that higher levels of Caspase-8 were found in the SN of PD patients when compared to normal individuals. This suggests that Caspase-8 activity contributes to the loss of DCN leading to the onset of PD. Prolonged stimulation of NFκB may have caused Caspase-8 activation resulting in cell apoptosis via the inflammatory pathway.

The mitochondria play a vital role in production of ATP, cellular processes and serves as a reservoir for calcium storage. The mitochondrial respiratory chain possesses electron carriers (NADH/succinate) that transfer electrons to complexes in inner mitochondrial membrane (IMM). The transfer of electrons from complex 1 to complex 3, across the IMM forms a proton and electrochemical gradient, which aids to create the transmembrane potential of the mitochondria. The mitochondrial transmembrane potential, subsequently aids to create ATP production in complex 5. Impairment of the electron transport chain has been observed in fibroblasts and muscle of PD patients. Complex 1-3 produce ROS as a by product. During oxidative stress, oxygen and nitric oxide interact with accumulated ROS, forming peroxynitrite, which induces impairment of complexes 1-5, as well as increases leakage of proteins, leading to collapse of the membrane potential and impairment of the mitochondria (Jin et al 2012, Pislar et al 2013).

The mitochondrial PTP is the opening and closing of a pore that permits ions and other solutes to traverse the inner membrane of the mitochondria (Figure 1.15). The opening of the mitochondrial PTP can be caused by various stimuli (such as elevated levels of oxidants, inorganic phosphates or calcium) (Chandra and Orrenius 2002). Hyperpolarisation of the IMM allows an increase in osmalarity and inner membrane potential. Cardiolipin, is a negatively charged phospholipid found embedded between the inner and outer membranes of the mitochondria. Cardiolipin binds cytochrome c to the IMM. However, during oxidative stress, the cardiolipin acyl chains are oxidised, allowing the release of cytochrome c from the IMM and into the cytosol. Hexokinases II and III prevent release of cytochrome c, thus dissociation of bound hexokinase triggers cytochrome c to translocate into the cytosol (Addobbo et al 2009, Cheng et al 2010). The release of cytochrome c promotes Caspase activation and eventual death of the cell through the intrinsic route. Activated Caspases can induce changes in adjacent mitochondria, leading to a higher level of cytochrome c release (Soreq et al 2012).

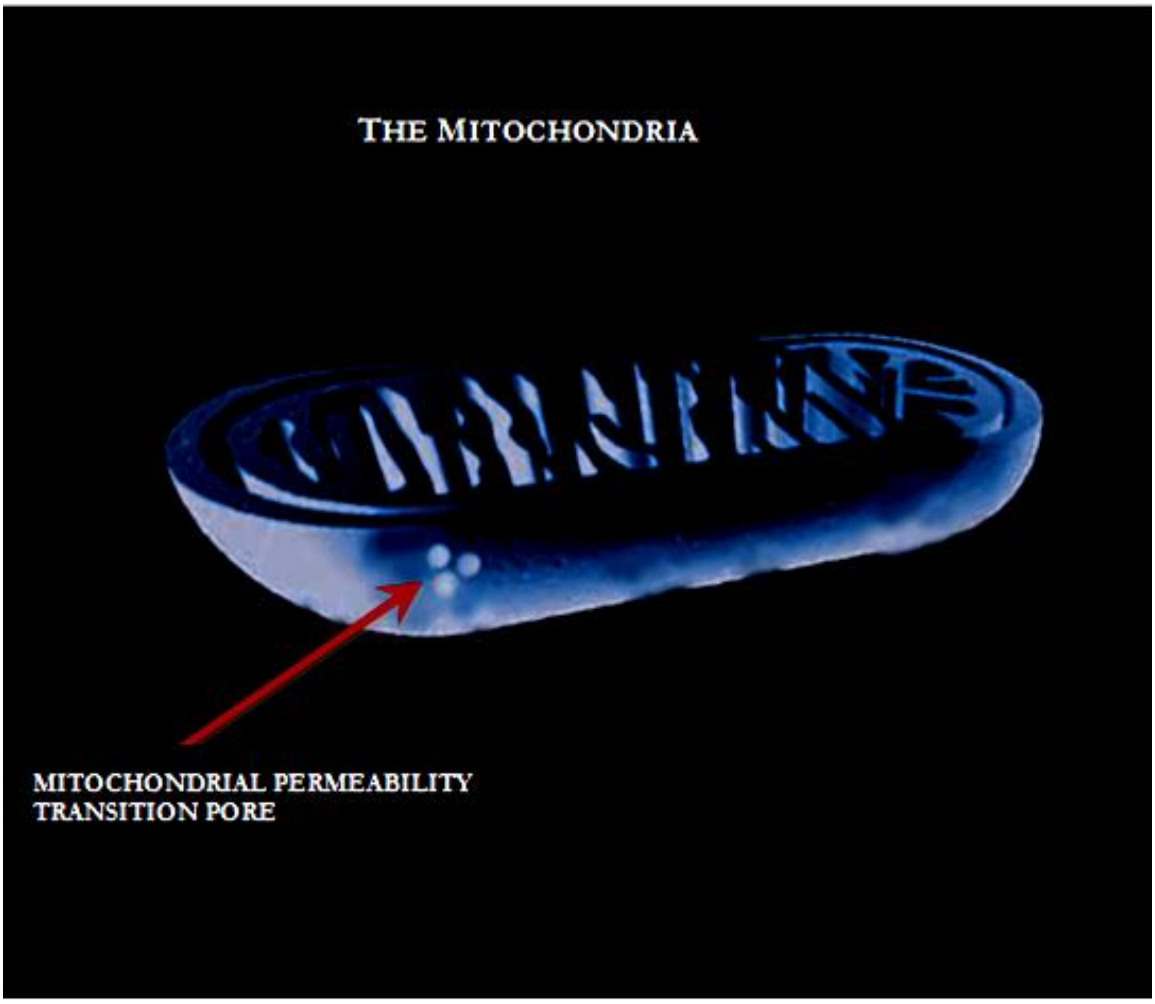

Figure 1.15 : The mitochondrial permeability transition pore (PTP)

Opening of the mitochondrial PTP causes an osmotic shift and peroxidation of cardiolipin, thereby releasing cytochrome c. The opening of the mitochondrial PTP and release of cytochrome c are the first steps to promote the activation of Caspases leading to mitochondrial mediated cell death (Chandra and Orrenius 2002, Soreq et al 2012, Addobbo et al 2009, Cheng et al 2010, Chaudhry and Ahmed 2014).

1.6.1 The mitochondria and Caspase-9 activation

Oxidative stress, inflammation, genetic mutation can encourage the activation of one of the major pathways, such as the mitochondrial also known as the intrinsic pathway via the stimulation of different proteins. JNK and p38 are a group of MAPKs that play an essential role in apoptosis and are found in neuronal tissue. Activation of JNK has been strongly associated with development of neurodegenerative disorders, particularly PD (Cassarino 2000, Chaudhry and Ahmed 2014). In the JNK pathway, release of cytochrome c promotes binding of Caspase-9 to the JNK domain, forming complexes that stimulate Caspase-9, which in turn cleaves and activates Caspase-3 (Figure 1.16). In the p38 pathway, cytochrome c released from the mitochondrial PTP, encourages binding of the cytosolic protein, Apaf-1 to bind to Caspase-9, forming complexes that permit activation of Caspase-9. Subsequently, Caspase-9 stimulates Caspase-3 activity resulting in apoptosis of DCN (Chen 2008).

Genetic mutation of specific genes such as PINK-1 or Parkin gene can result in impairment of the mitochondria leading to the release of cytochrome c. In the presence of ATP, cytochrome c induces the zymogen, pro-Caspase-9 to bind to Apaf-1, leading to the activation of Caspase-9. Subsequently, Caspase-9 promotes Caspase-3 activation resulting in cell death. (Kroemer and Blomgren 2007, Yang et al 2008, Fahn and Sulzer 2004, Haque et al 2008).

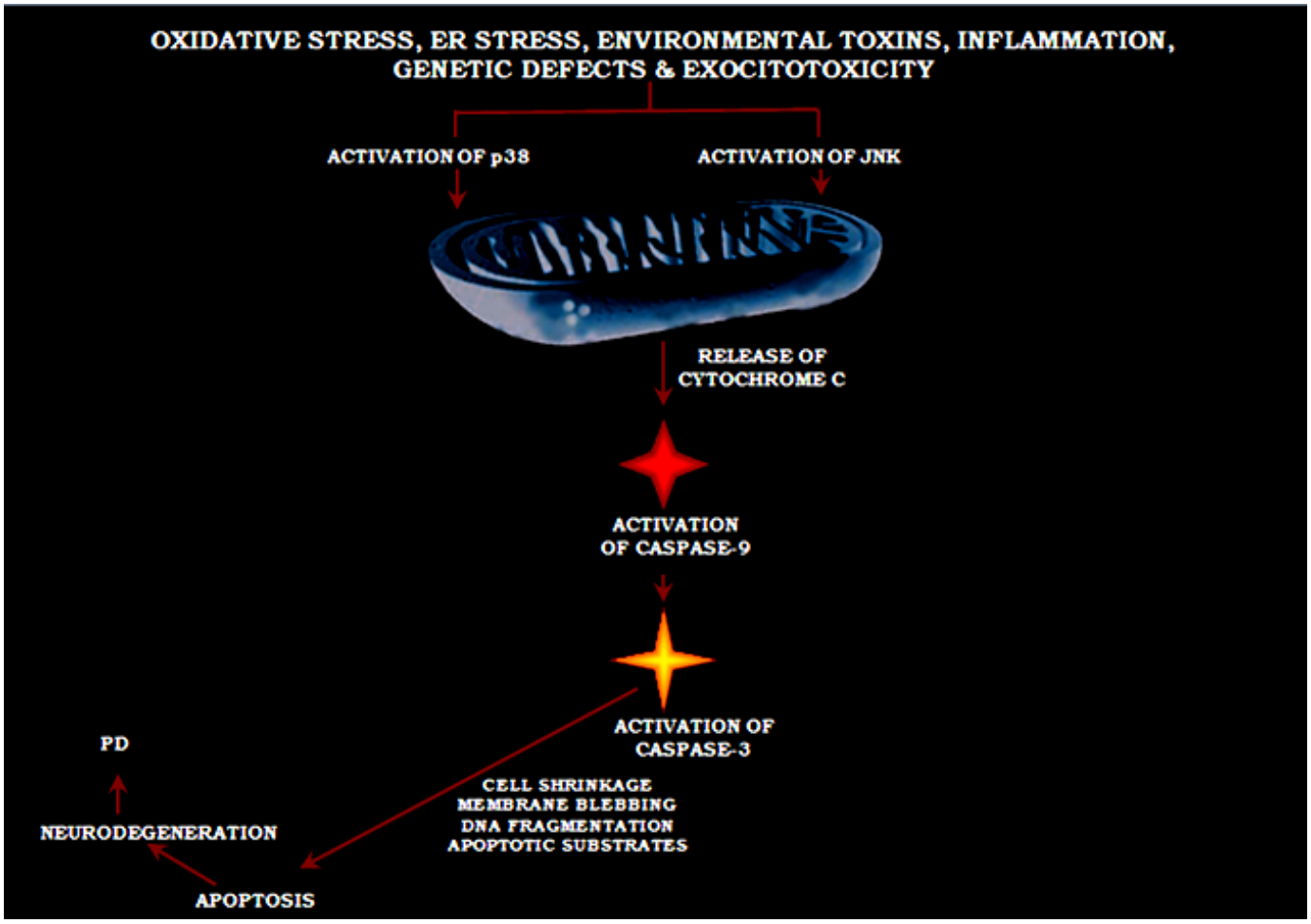

Figure 1.16: Exploring the mitochondrial pathway

Activation of p38 and JNK, alongside mutation of PINK-1 gene trigger opening of mitochondrial PTP releasing cytochrome c. A decrease in ATP levels and the difference in the permeability of mitochondria's inner membrane induce the opening of the PTP; thereby releasing cytochrome c. Cytochrome c binds to Apaf-1 via oligomerization in presence of ATP forming apoptosome. The apoptosome (cytochrome c:Apaf-1) recruits Caspase-9 binding and activation in the presence of ATP. Caspase-9 subsequently allows Caspase-3 activation to occur, resulting in mitochondrial mediated in DCN (Addabbo et al 2009, Andrabi et al 2008, Chaudhry and Ahmed 2014).

1.7 ER Secretory Pathway

The ER is a site for calcium storage and gated release in response to hormones, growth factors and oxidative protein folding. Secretory, membrane proteins and glycoproteins comprised of N glycan coating which plays a vital role in the folding, transportation and metabolism are synthesised in the ER. ER chaperones such as protein disulphide isomerise 5 (PDI-5), ER protein 72 (ERp-72), ERp-61, ERp-57, ERp-44, ERp-29, calnexin and calreticulin involved in proper formation of protein. PDI-5, ERp-72, ERp-61, ERp-57, ERp-44, ER-p29 are folding enzymes involved in disulphide bond formation in ER. Secretory proteins processed in the ER are transported to the Golgi apparatus and receive various modifications by enzymes located there (i.e. modifications of oligosaccharide chains and processing of peptide chains). Correctly folded proteins are transported to the Golgi body, whilst unfolded proteins are retained in the ER. Incorrectly folded proteins expose hydrophobic amino acid residues that should be located inside the protein and tend to form protein aggregates that possess toxic properties (Pereira 2013, Sano and Reed 2013).

The ER is the first compartment in the secretory pathway, which is responsible for the protein synthesis, modification and delivery. Proteins enter the ER on ribosomes that are translating mRNAs in polypeptide transients across the membrane of the ER where they enter in an unfolded state (Figure 1.17). Subsequently, the unfolded proteins undergo a process of proper oxidative folding and exit from the ER, via ER Golgi intermediate compartment in vesicles that traffic to the Golgi body. In the Golgi body, sugars are added to the correctly folded proteins to enable specific functions of the protein, prior to exocytosis in the plasma membrane or secreted to the extracellular matrix. Proteins that are incorrectly folded are either retained in the ER or degraded in the ER by the UPS. Polypeptides are extracted from the ER membrane and delivered to the cytosol for degradation by the proteasome through the ER associated protein degradation (ERAD) process (Sano and Reed 2013, Matus et al 2008).

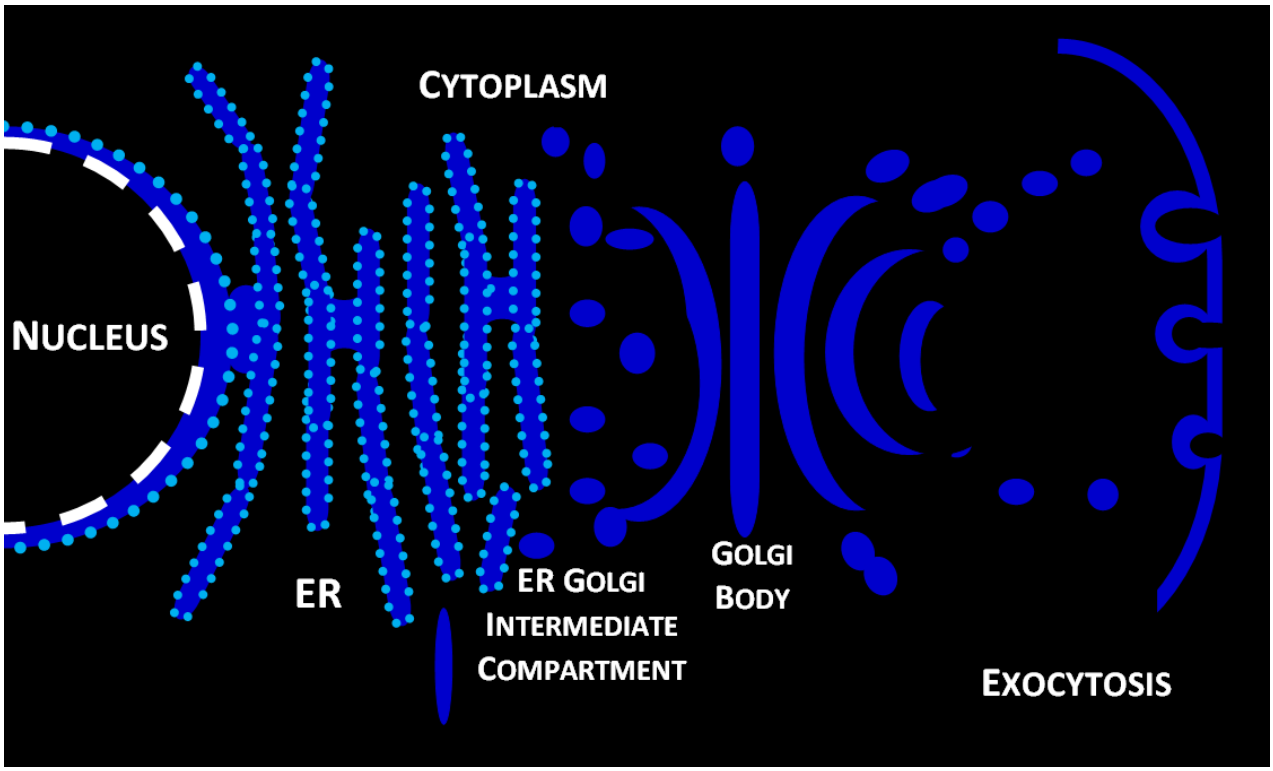

Figure 1.17 : The Secretory Pathway

In the ER, newly synthesised proteins undergo correct folding to ensure the production of mature functional proteins and to remove any potential formation of aggregates. Subsequently, the correctly folded mature proteins move from the ER to the Golgi body where they are modified and are then released to their specific locations. Proteins that are incorrectly folded are sensed by the ERAD pathway and then are subsequently degraded by the UPS (Wang and Takahasi 2007, Matus et al 2008, Pereira 2013, Sano and Reed 2013).

1.7.1 ERAD process

Incorrectly folded proteins are retained via the ERAD process and are progressed to the cytoplasm. The ERAD process comprises of four steps; recognition, retro-translocation, ubiquitination and degradation. ER stress occurs when ERAD fails to remove large amounts of incorrectly folded proteins that aggregate and become toxic (Pereira 2013).

At recognition stage, correctly and incorrectly folded proteins are identified by ER chaperones in the calnexin and calreticulin cycle. Calnexin and calreticulin are involved in the folding of glycoprotein, via the calnexin and calreticulin cycle. Calnexin is a transmembrane protein and calreticulin luminal protein. In the calnexin and calreticulin cycle, specific oligosaccharides are added to polypeptides to carry out its functional properties. Following the addition of oligosaccharides, the enzymes glucosidase I and II remove excess residues, before calnexin and calreticulin bind to the fold the protein. The correctly folded protein is released from the calnexin and calreticulin cycle to the Golgi body. In addition, ER chaperones such as ER degradation enhancing α-mannosidase like protein (EDEM), osteosarcoma-9 and XTP3 transactivated gene B identify and differentiate incorrectly folded polypeptides, from the correctly folded peptides (Pereira 2013, Sano and Reed 2013).

The following step in ERAD is retro-translation, where the disulphide bonds of incorrectly folded proteins are cleaved by ER chaperones, PDI-5 and immunoglobulin binding protein (BiP). The unfolded structure is removed from the ER channels into the cytosol via derlin-1, p97 and valocin interacting membrane protein 1. Removal of sugars embedded in the incorrectly folded protein occurs, prior to UPS detection and degradation (Pereira 2013, Yoshida 2007)

1.7.2 UPS

The UPS degrades a variety of intracellular proteins which have been incorrectly manufactured and have become unfolded/incorrectly folded proteins. The unfolded proteins are transferred from the ER to cytoplasm. In the presence of ATP, E1 (ubiquitin activating enzymes) binds to E2 (ubiquitin conjugating enzymes), which subsequently binds to E3 (ubiquitin protein ligase) to form a polyubiquitin chain that binds to defective proteins, which provokes a degradation signal (Figure 1.18). The degradation signal promotes 26S proteasome to catabolises target protein via proteolysis (Kahns et al 2003, Yamamoto et al 2005). 26S proteasome consists of two main domains (19S cap and 20S core). The 19S domain identifies polyubiquitinated substrates and engulfs the polyubiquitinated chain, thereby triggering the process of protein degradation (Omura et al 2006, Giasson and Lee 2003, Wang and Takahasi 2007).

Parkin is also known as E3 ligase and plays a role in UPS. Parkin is comprised of two domains; two C terminal RING domains and an N terminal ubiquitin like domain. The C terminal is where the E2 enzyme can attach to it and the N terminal detects the protein which is to be targeted for degraded via ubiquitination (Kim et al 2003).

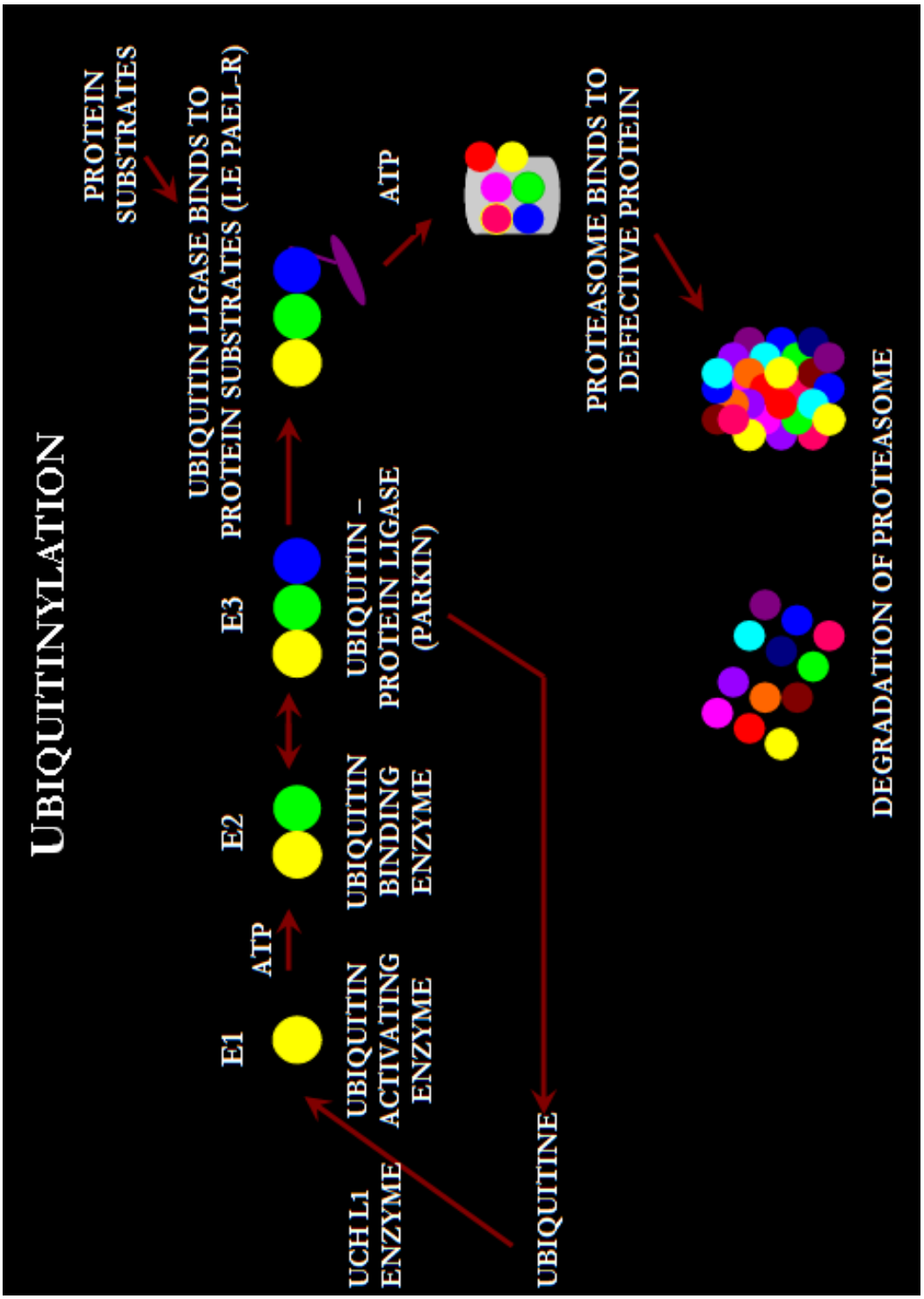

Figure 1.18: Ubiquitin-Proteasome System (UPS)

Figure showing the process of protein degradation by UPS. In the presence ATP, E1 binds to E2 followed by E3 forming a complex that can create polyubiquitin chain on defective proteins, which wraps around the defective protein, triggering a degradation signal. The proteasome is activated by the signal, binds to and catabolises the defective protein, which is embedded with the polyubiquitin chain, resulting in degradation of the protein (Yoshida 2007, Wang and Takahasi 2007).

Furthermore, when proteins are folded incorrectly, the hydrophobic regions are exposed, resulting in the formation of aggregates such as fibrils that are toxic and trigger ER stress (Figure 1.19 Rochet 2007, Yoshida 2007, Doyle et al 2011). Mutated DNA sequence causes the incorrect translation and formation of protein strands which produce a defective unfolded protein. The malfunctioning proteins accumulate and form β pleated sheets consisting of oligomers. The increase in protofibrils subsequently increases β amyloid levels allowing the formation of fibrils. The insoluble fibrils are able to aggregate and precipitate to form Lewy bodies, which is a key attribute found in PD patients (Doyle et al 2011, Skovronsky et al 2006, and Moore et al 2005).

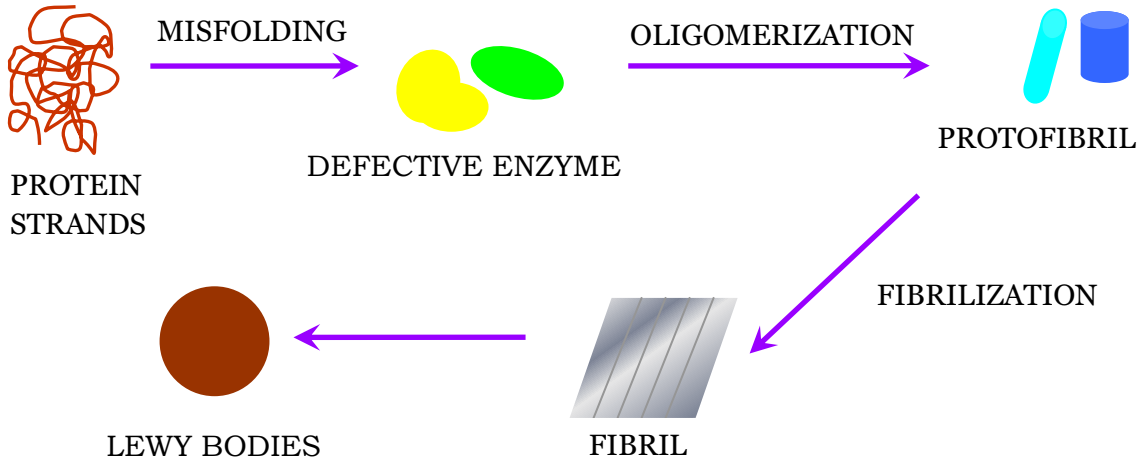

Figure 1.19: Formation of Lewy Bodies

Unfolded proteins that are not degraded by UPS are oligomerised and become insoluble fibrils that form Lewy bodies – a common feature found in PD pathogenesis (Doyle et al 2011).

1.7.3 ER Stress Pathway

ER stress response can by triggered by; proteasome activity inhibition, cytosolic calcium accumulation and disruption of disulphide bind formation. ER stress response has four mechanisms to cope with mechanisms of accumulated unfolded proteins. The first step of ER stress is suppression of protein synthesis, which prevents any further accumulation of incorrectly folded proteins. The next step is transcriptional induction of ER chaperone genes to increase folding capacity. The following step is transcriptional induction of ERAD component genes to increase ERAD activity. The final step is induction of apoptosis to safely dispose of cells injured by ER stress to ensure the survival of the adjacent cells (Hetz 2012, Sano and Reed 2013).

ER stress promotes activation of ERAD and Unfolded Protein Response (UPR). Subsequently, UPR triggers activation of the ER transmembrane proteins; Inosital requiring enzyme 1 (IRE-1), PKR-like ER kinase (PERK) and activating transcription factor 6 (ATF-6). UPR and ERAD work together to restore protein homeostasis. (Cali et al 2011, Lindholm et al 2006, Oakes et al 2006, Oshitari et al 2008). The UPR inhibits manufacturing of more incorrectly folded proteins by suppression of protein translation. In addition, protein chaperones are stimulated, allowing the refolding of incorrectly folded proteins (Doyle et al 2011).

IRE1, ATF-6 and PERK contribute to ER mediated cell death and survival (Figure 1.20). In normal cells, BiP is attached to the luminal domains of IRE-1, ATF-6 and PERK, suppressing activation of these proteins and ER stress related pathways. During ER stress, BiP disassociates from IRE-1, PERK and ATF-6, thereby activating their individual pathways. Current research has shown that ER stress triggers these pathways as a domino effect rather than stimulating these pathways at the same time. ER stress triggers IRE1α route, followed by stimulation of ATF-6 pathway and finally activation of the PERK pathway. The activation of IRE-1, PERK and ATF-6 encourages removal of unfolded proteins, thereby restoring homeostasis of the ER and promoting cell survival (Jing et al 2012, Szegezdi et al 2006).

1.7.3.1 IRE-1 pathway

IRE-1 consists of a luminal portion and a cytoplasmic portion and both have specific functions. The luminal portion senses unfolded proteins, whilst the cytoplasmic portion comprises of the kinase domain and RNase domain. The imbalance of incorrectly folded chaperones and proteins triggers IRE-1 stimulation. Activated IRE-1 promotes mRNA splicing for the transcription factor X box-binding protein 1 (XBP-1), resulting in translation of mature XBP-1. Subsequently, mature XBP1 is translocated to the nucleus, where it enhances transcription of PERK inhibitor $P58^{IPK}$, ER chaperones, ERAD proteins, C/EBP homologous protein/growth arrest and DNA damage-inducible gene 153 (CHOP/GADD153) and factors involved in protein degradation. $P58^{IPK}$ suppresses PERK translation thereby aiding to decrease the total level of accumulating protein and restoring ER homeostasis (Jing et al 2012, Holtz and O'Malley 2003, Kudo 2003 and Doyle et al 2011) .

In addition, activated IRE-1 binds to the adaptor protein (tumour necrosis factor receptor associated factor 2) TRAF-2, promoting the binding of apoptosis signal regulating kinase 1 (ASK-1) resulting in the formation of the IRE-1:TRAF-2:ASK-1 complex. The complex triggers MAPK activity followed by activation of JNK protein, via a series of cascade reaction, resulting in ER mediated cell apoptosis. Research has shown JNK activation can promote CHOP activation, as well as activation of Caspase-12, leading to apoptotic death (Jing et al 2012, Yoshida 2007 Doyle et al 2011, Oshitari et al 2008, Shibata and Kobayashi 2008). In addition, elevated levels of ROS can oxidise and cleave thioredoxin (TDX) of the ASK-1:TDX complex, allowing the release and activation of ASK-1 and active ASK-1 activates JNK (Malhotra and Kaufman 2007). Furthermore activated IRE-1 stimulates RIDD, which degrade mRNA proteins. IRE-1α can bind to Bcl-2 antagonist killer protein (BAK) and Bim, leading to mitochondrial apoptosis (Doyle et al 2011, Jing et al 2012, Ozcan and Tabas 2012).

1.7.3.2 ATF-6 pathway

ATF-6 comprises of the luminal portion and a cytoplasmic portion and both have specific functions. The luminal portion senses unfolded proteins, whilst the cytoplasmic portion contains the kinase domain and a transcription activating domain. During ER stress, BiP disassociates from ATF-6 exposing the Golgi localisation signal sequence on ATF-6. Activated ATF-6 moves to the Golgi apparatus, via vesicular transport. In the Golgi apparatus ATF-6 is cleaved by site 1 serine protease and site 2 metalloprotease, forming a cytoplasmic ATF-6 fraction (Ozcan and Tabas 2012, Yoshida 2007). The ATF-6 fraction translocates to the nucleus and binds to ER stress response element (ERSE), thereby promoting transcription of UPR genes, such as CHOP and XBP-1, alongside ER chaperones such as calrecticulin GRP78, GRP97 and BiP (Yoshida 2007).

1.7.3.3 PERK pathway

PERK has a luminal portion and a cytoplasmic portion and both have specific functions. PERK luminal portion senses unfolded proteins, whilst the cytoplasmic portion contains the kinase domain that activates after dissociation of BiP. Activated PERK promotes phosphorylation and inactivation of α subunit of eukaryotic translation initiation factor 2 subunit α (eIF-2), preventing further translation of new proteins, thereby reducing the amount of proteins accumulating in the ER. In addition, PERK promotes translation of activating transcription factor 4 (ATF-4), through phosphorylation of eIF-2. Subsequently, ATF-4 enters the nucleus and stimulates transcription of genes which restore ER homeostasis (Jing et al 2012, Rochet 2007, Wang and Takahashi 2007, Matus 2008).

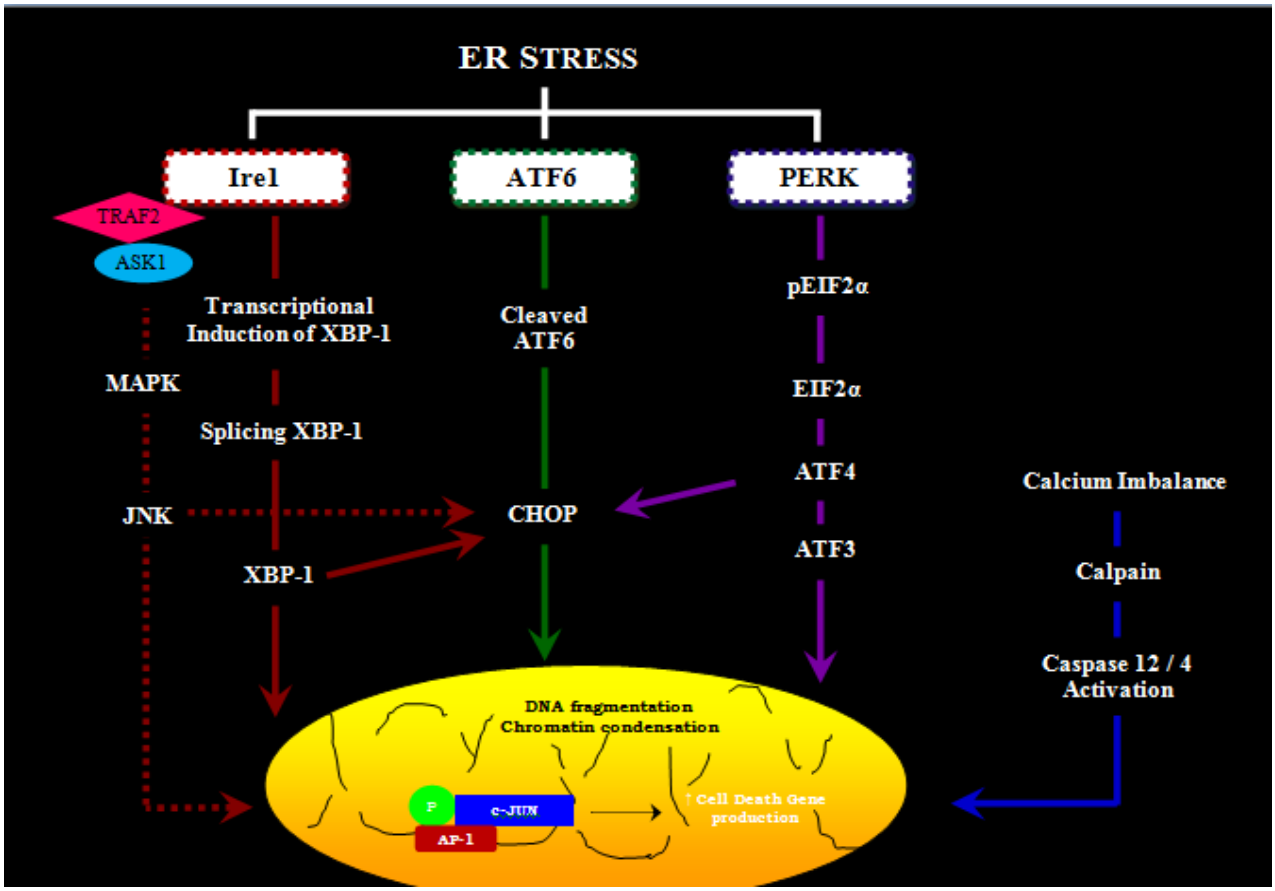

Figure 1.20: The involvement of ER stress in apoptosis

Figure showing the involvement of PERK, ATF-6 and IRE-1 transmembrane proteins triggered in ER stress. Active IRE-1 promotes transcriptional induction, splicing and formation of mature XBP1, which in turn activates CHOP protein. Furthermore, TRAF-1 and ASK-1 bind to IRE-1 to form a complex which triggers activation of MAPK followed by stimulation of JNK. Subsequently, active JNK promotes manufacture of cell death genes alongside activation of CHOP. In PERK pathway, α subunit of eIF-2, is inhibited via phosphorylation leading to stimulation of ATF-4 resulting in CHOP activation. In the ATF-6 pathway, ATF-6 is cleaved triggering activation of CHOP. Active CHOP provokes activates growth arrest and DNA damage-inducible gene 34 (GADD34), TRB3 and death receptor 5 (DR-5) eventually resulting in death of cells (Hetz 2012, Sano and Reed 2013, Cali et al 2011, Lindholm et al 2006, Oakes et al 2006, Oshitari et al 2008, Doyle et al 2011, Yoshida 2007, Jing et al 2012, Szegezdi et al 2006, Malhotra and Kaufman 2007, Yamaguchi and Wang 2004, Szegezdi et al 2006, Rochet 2007, Wang and Takahashi 2007, Matus 2008, Holtz and O'Malley 2003, Ghosh et al 2012).

1.7.4 The role of CHOP in ER mediated death

If PERK, ATF-6 and IRE-1 pathways are not effective to restore ER homeostasis, the final step is the activation of apoptotic pathway. The main factor to the triggering of the apoptotic pathway is stimulating activation of CHOP. Activated CHOP promotes transcription of growth arrest and GADD34, tribbles-related protein 3 (TRB3), ER oxidoreductin 1(ERO-1) and DR-5, contributing to death of cells via apoptotic pathway (Tiwary et al 2010, Szegezdi et al 2006, Malhotra and Kaufman 2007, Yamaguchi and Wang 2004).

In ER mediated apoptosis, GADD34 regulates ER protein and eIF2-α biosynthesis, whilst, TRB3 inhibits Akt, leading to stimulation of transcription factor FOXO3a, promoting activation of p53 up-regulated modulator of apoptosis (PUMA) and neutrophil NADPH oxidase factor (Noxa), resulting in death of cells (Jing et al 2012, Zhou et al 2009, Doyle et al 2011, Ghosh et al 2012, Galehdar et al 2010). In addition, active DR-5 promotes activation of Caspase cascade resulting in cell death via apoptotic route. JNK can promote DR-5 stimulation increasing ER mediated death of cells (Oyadomari and Mori 2004, Tiwary et al 2010, Yamaguchi and Wang 2004)

Increased levels of ERO-1 encourage a hyperoxidative environment in the ER. Active ERO-1 stimulates the opening of the ER channel IP3R1, which promotes the release of calcium from the ER to the cytoplasm (Pagani et al 2000, Malhotra and Kaufman 2007, Jing et al 2012). The excessive accumulation of calcium in the cytoplasm can result in the binding of calcium binding proteins, such as Calpain, which can activate Caspases. Hyperoxidation of ER leads to leakage of hydrogen peroxide to the cytoplasm, promoting increased levels of cytoplasmic ROS. Elevated ROS levels suppress ER disulphide isomerases thereby adding to accumulation of incorrectly folded proteins. CHOP can increase BCL-2 associated X protein (BAX) levels and Bim levels, inhibiting BCL-2 enhancing apoptotic cell death. In addition, the activation of PUMA and Noxa can inhibit BCL-2 activity (Malhotra and Kaufman 2007, Doyle et al 2011, Ghosh et al 2012).

1.7.5 ER stress and Caspases

The ER stores calcium and alteration of calcium homeostasis promotes abnormal protein folding leading to ER stress (Hara and Snyder 2007). Neurotransmitter receptor stimulation induces calcium ion release from the ER into the cytosol in neuronal cells. Research has shown that translocation of Caspase-7 from the cytosol to the ER surface provokes activation of the well known ER stress related protein Caspase-12. Activated Caspase-12 in turn activates Caspase-9 and then Caspase-3. Imbalance of calcium promotes translocation of Calpain from the cytosol to the ER membrane, which cleaves and activates Caspase-12 (Fan et al 2005, Chaudhry and Ahmed 2014).

Mutations of specific genes, such as mutation of α-synuclein have been strongly related to PD pathogenesis (Section 1.10). A study conducted by Smith et al (2005) revealed that mutation of the α synuclein gene, elevated Caspases-3, -9,-12 and ROS levels in PC12 cells. In addition, a reduction in proteasome activity and increase in defective proteins was found. The main findings suggested that mutant α-synuclein participates in apoptotic pathways, such as ER stress and mitochondrial dysfunction pathway (Figure 1.27). Substantial levels of DNA, protein and lipid damage caused by ROS and oxidative stress was found in PD patients. Elevated levels of incorrectly folded proteins present in oligodendrocytes can stimulate the activity of Caspase-12 through ER stress (Nakagawa and Yuan 2000). ER stress stimulates the UPR, enabling PERK to activate Caspase-12. Subsequently, Caspase-12 in turn activates Caspase-9 followed by Caspase-3, resulting in cell death (Sharma and Gow 2007, Sooka et al 2007).

Research by Oda et al (2007) found Calpain activated Caspase-4 in tunicamycin (a well known ER stress inducer) induced SK-N-SH cells. In addition, death of SH-SY5Y cells was observed via activation of Caspase-12 through the stimulation of CHOP pathway in ER mediated stress. Furthermore, active Caspase-4 induce ER mediated death of thapsigargin treated and tunicamycin treated SK-N-SH cells but not in SH-SY5Y cells. In contrast, SH-SY5Y cells induced with thapsigargin or tunicamycin was able to stimulate Caspase-12 apoptotic death via ER stress route.

Caspase dependent cell death in DCN cells has also been associated with ER stress pathway (Figure 1.21). The ER is an organelle which stores calcium alongside folding and modification of proteins. Excessive calcium levels promote increase in Calpain activity resulting in Caspase stimulation. Translocation of Calpain from the cytosol to the ER membrane cleaves and activates Caspase-12 (Ghribi et al 2003, Omura et al 2006, Nakagawa and Yuan 2000). Genetic mutation of specific genes such as Parkin permits continuous stimulation of Parkin Associated Endothelin Receptor like Receptor (Pael-R), which in turn promotes ER stress, and contributes to formation of Lewy bodies in PD patients. This is due to the fact that mutant Parkin has impaired E3 ligase therefore Pael-R cannot be degraded (Omura et al 2006).

In addition, Caspase-12 can be stimulated by other factors such as a mutation of Parkin, impairment of UPS or defect in the ER. Defect in ER elevates the quantity of incorrectly folded proteins. Incorrectly folded proteins are usually catabolised by UPS. Mutation of Parkin gene disrupts the degradation of incorrectly folded proteins which contributes to ER stress and Caspase-12 activation. The defective proteins can also form Lewy bodies which can be seen in PD patients. The elevated levels of incorrectly folded proteins provoke Caspase-12 activation which in turn stimulates Caspase-9 followed by Caspase-3 motivation. Furthermore, the elevated level of defective proteins induces further ROS production, which contributes to mitochondrial impairment via complex I inhibition alongside ATP depletion. ROS can trigger proliferation of cytokines which activate microglia therefore causing higher level of cell apoptosis (Friedlander 2003, Kadowaki and Nishitoh 2013, Shimoke et al 2004).

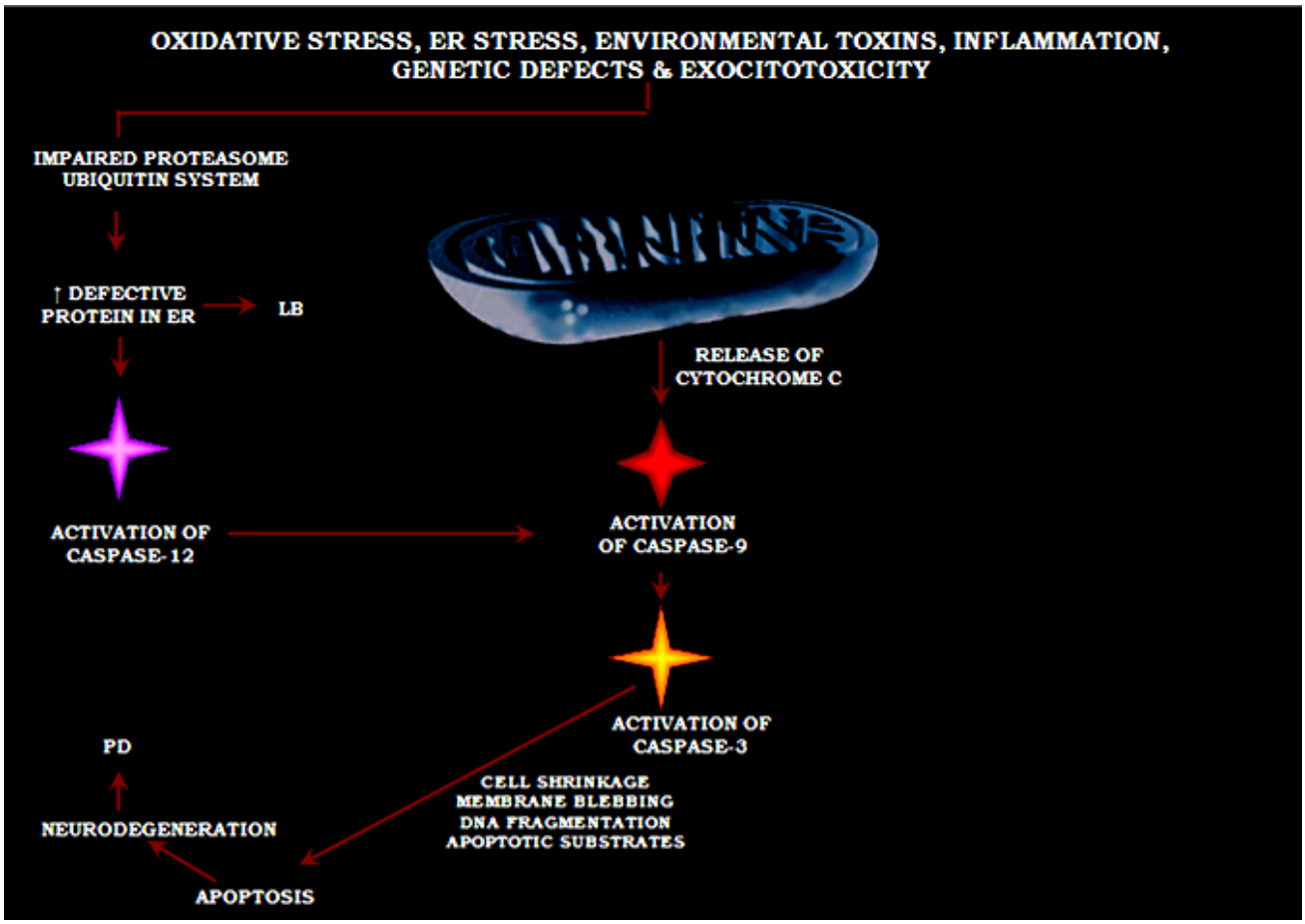

Figure 1.21 ER stress triggers Caspase dependent death of DCN resulting in PD

Calcium imbalance and ER stress promotes activation of Caspases via extrinsic route leading to death of DCN and PD onset. Imbalance of calcium promotes activation of Calpains which activates Caspase-12. Subsequently, Caspase-12 activates Caspase-9 which stimulates Caspase-3 activation resulting in neuronal death. Impairment of UPS leads to accumulation of defective proteins which aggregate and forms Lewy bodies and activation of Caspase-12. Production of ROS derived from defective proteins can alter calcium homeostasis, promoting activation of calcium binding protein, Calpains. Calpain triggers Caspases-12 and-4, leading to Caspase-9 activation, followed by Caspase-3 activation, resulting in apoptosis. The high levels of ROS caused by accumulated incorrectly folded proteins can lead to impairment of mitochondria, leading to complex one inhibition and depletion of ATP. Impairment of mitochondria leads to activation of Caspase-9 through the binding of cytochrome c. Active Caspase-9 in turn binds to and triggers Caspase-3 stimulation, permitting death of cells via apoptotic route (Doyle et al 2011, Chaudhry and Ahmed 2014, Yoshida 2007).

1.8 The role of Calcium in PD

Recent research has shown a connection between calcium and ER stress (Subramaniam and Chesselet 2013, Malhotra and Kaufman 2007, Chowdhury et al 2008, Friedlander 2003, Kadowaki and Nishitoh 2013).Excessive calcium leads to cell death via multiple potential pathways, including mitochondrial dysfunction, oxidative stress, ER dysfunction and abnormal calcium signalling (Figure 1.22). Ionic calcium is a critical signalling component in neurons and its cytoplasmic levels are tightly regulated. Calcium can be pumped to the extracellular components, mainly the ER and mitochondria (Subramaniam and Chesselet 2013). Mattson (2007) explored the relationship between intracellular calcium and the progression of PD. The homeostatic imbalance of calcium promotes cell death of DCN via direct and indirect pathways. Apoptosis of DCN via oxidative stress, aggregation of α synuclein and perturbed energy metabolism induces a homeostatic imbalance of calcium ions. The alteration in the level of calcium ions present results in the impairment of neural communication and activity in the brain, leading to the pathogenesis of PD (Mattson et al 2004, Mattson 2007).

Research conducted by Ton et al (2007) has shown no association between the use of antihypertensive drugs such as beta blockers and calcium channel blockers and the progression of PD. These findings do not support the notion that apoptosis of neural cells caused by the calcium dependent pathway can be prevented by the use of calcium channel blockers. A study performed by Bowser and Khakh (2004) portrays the importance of intracellular calcium in neuronal activity caused with the use of exogenous ATP. The results of the study show that an increase of intracellular calcium was achieved in interneurons of the striatum of mouse hippocampus by use of exogenous ATP. The increase of intracellular calcium subsequently generated action potentials leading to increased neural activity and release of neurotransmitter.

An increase in physical and mental exercise and a decrease in calorie intake promotes an increase in neural activity, leading to an influx of calcium ions. The higher level of calcium present promotes activation of transcription factors and protein kinases. Activation of kinases helps to mediate stress

resistance, energy metabolism and plays a crucial role in maintaining ion homeostasis, thereby promoting neurogenesis and survival of neural cells. An excessive level of cellular calcium induces toxicity resulting in mass destruction of neuronal cells (Figure 1.22). This was revealed in cultured Schwaan cells and oligodendrocytes, where cell death occurred due to toxic calcium levels. The findings suggested that the increase release glutamate (via overactive glutamate receptors) had induced an excessive increase of calcium, which had resulted in neural apoptosis (Subramaniam and Chesselet 2013).

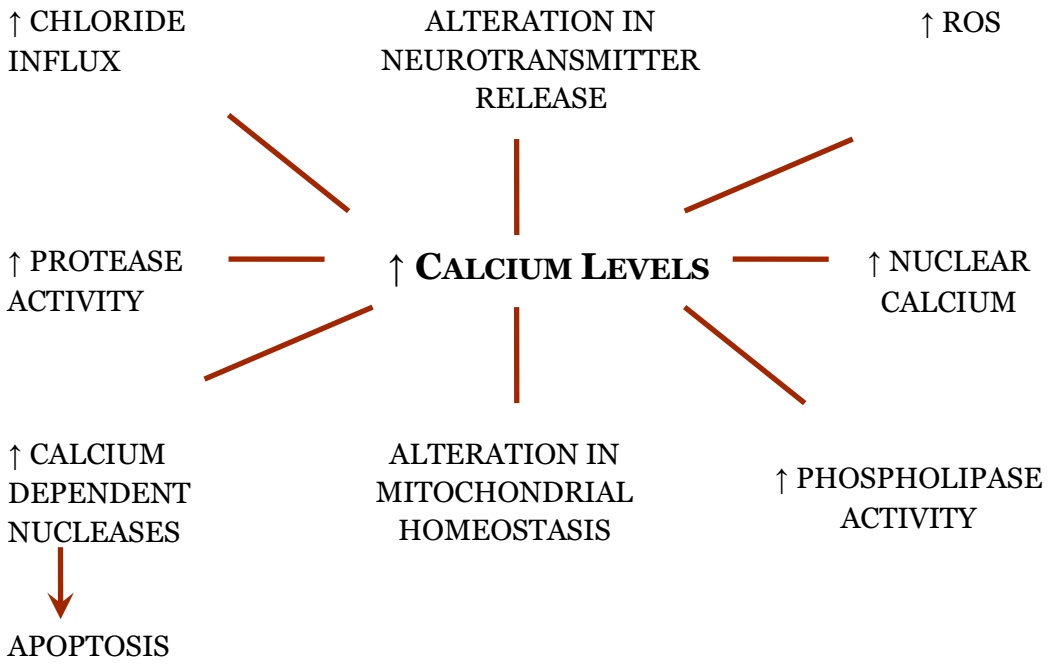

Figure 1.22: Calcium mediated cell apoptosis

Figure showing different factors that are involved in increased calcium levels resulting in cell apoptosis (as shown in text).

Calcium activates Calpain and Caspase activation. Membrane associated oxidative stress (MAOS) caused oxidative stress results in catabolism of lipid components of the membrane. Calcium activates BAX and p53 alongside release of cytochrome c and Caspase stimulation (Mattson 2007). In addition calcium can activate nitric oxidase synthase to produce nitric oxide. Subsequently, nitric oxide is able to suppress complex IV of the mitochondria, resulting in further elevation of ROS levels. The enhanced ROS levels can contribute to the leakage of calcium ions from the ER and mitochondria into the cytosol (Malhotra and Kaufman 2007).

Overexpression of BCL-2 reduces intracellular calcium in the ER. In addition, BAX and BAK encourage the transfer of calcium from the ER thereby maintaining calcium homeostasis. When stimulated by apoptotic factors, the lipid units of the mitochondria change their structural shape. In contrast, ceramide channels are held together in ceramide columns via hydrogen bonding. In excitotoxicity, the plasma membrane calcium pump (PMCA) and Na/Ca exchanger can be cleaved by Caspases, resulting in cell death. Cleavage of PMCA and Na/Ca exchanger allows influx and elevated intracellular calcium levels, preventing opening of the mitochondrial PTP (Subramaniam and Chesselet 2013, Doyle et al 2011, Malhotra and Kaufman 2007).

.

Final events of apoptosis

Stimulation of intrinsic or extrinsic pathways encourages activation of Caspases resulting apoptotic death of cells. The final steps involved in apoptotic cell death are crucial and require the activation of Caspase-3. Activation of Caspase-3 induces DNAses causing DNA fragmentation. In addition, Caspase-3 causes catabolism of proteins, thereby destroying the cytoskeleton of DCN. Caspase-3 inhibits DNA repair enzymes; therefore the structure of the cell cannot be repaired, resulting in cell apoptosis. Cell apoptosis causes an accumulation of ROS, which can damage and cause death to nearby cells. This can lead to a mass destruction of DCN, and thereby the development of PD (Chowdhury et al 2008).

Caspase-3 catabolises proteins that comprise to make the cytoskeletal structure, fodrin and actin, resulting in loss of cellular shape alongside loss of cellular adhesion, contributing to the decrease in cell volume and production of apoptotic bodies. Moreover, Caspase-3 activates Caspases-6 and -7, which play a vital role in cell apoptosis via digestion of specific cellular structures (Figure 1.23). Caspase-6 promotes the digestion of fibrous proteins, which is essential for the nuclear structure, and function, such as lamins, causing nuclear shrinkage and budding of the cell resulting in the formation of apoptotic bodies. Caspase-7 digests poly (ADP-ribose) polymerase (PARP), therefore DNA repair cannot be achieved. Caspase-3 can catabolise the DNA repair enzyme, DNA dependent protein kinase (DNA PK) into fragments, thereby preventing the cell to repair itself resulting in cell death (Venderova and Park 2012).

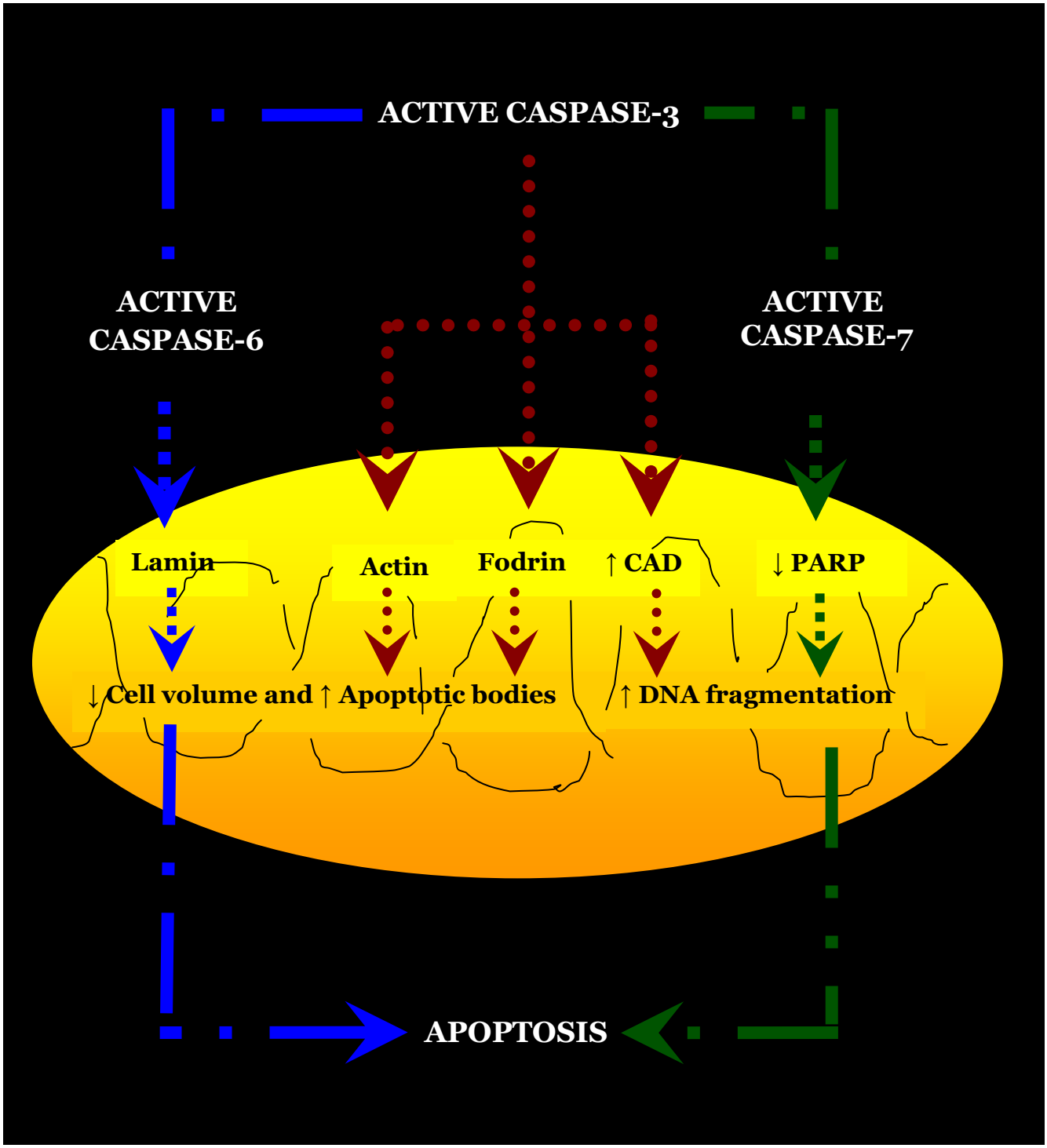

Figure 1.23 : Apoptotic events caused by Caspase-3

Caspase-3 promotes formation of apoptotic bodies' increase in fragmentation of DNA and decrease in cell volume, via breakdown of actin and fodrin, alongside activation of Caspase-activated DNA (CAD), Caspases-6 and -7 (blue lines and green lines correspondingly). The formation of apoptotic bodies, chromatin condensation and breakdown of the cell structure, leads to release of ROS, affecting neighbouring cells, resulting in mass destruction of DCN in PD pathogenesis. In normal cells the

DNAse complex is comprised of CAD and ICAD (inhibitory CAD) and is found to be inactive state. Caspase-3 cleaves ICAD from the CAD:ICAD complex, thereby initiating activity of DNAse, which promotes catabolism of nuclear DNA and chromatin resulting in decrease in cell volume and cell death. Subsequently, other organelles such as rough ER and Golgi complex are degraded via Caspases (by catabolism of Bap31, alongside golgin-160 and GRASP65). Moreover, the production of ROS during apoptosis promotes further destruction of nearby cells. ROS produced by the apoptotic cell are released and attack the phospholipid bilyar components of adjacent cells, promoting the formation of pores. Subsequently, the ROS are able to penetrate through the pores and cause further destruction to the cell via proteolysis of essential proteins and nucleic acids, resulting in further cell death. A mass destruction in DCN caused by prolonged Caspase-activation can contribute to the onset of PD (Venderova and Park 2012, Chowdhury et al 2008, Chaudhry and Ahmed 2014).

The morphology, presence and activation of specific proteins in apoptotic cells differ greatly when compared to normal cells (Figure 1.24). The ion content in normal cells aids to maintain the cellular structure of the cell to remain intact. A high level of potassium and a low level of sodium are found inside normal cells, so that an electrolyte balance can be maintained from the extracellular environment. Apoptotic cells are exposed to a hypertonic environment, which possesses an increase in extracellular osmotic strength. The increase in extracellular osmotic strength and imbalance of electrolytes, results in leakage of water and potassium ions inside the cell, causing the cell to shrink. The loss of potassium ions inside the cell activates Caspases and nucleases causing a loss in the cells architecture and subsequent apoptosis (Perier et al 2012).

In addition, the phospholipid, phosphatidylserine is found embedded in the inner membrane of normal cells. However, in apoptotic cells phosphatidylserine redistributes from the inner membrane to both the inner and outer membrane, causing a loss of membrane asymmetry. The reallocation of phosphatidylserine triggers the phagocytosis response signal for macrophages. Furthermore, the impairment of the vital organelle, the mitochondria promotes the stimulation of the Caspase cascade in apoptotic cells, which is achieved through the intrinsic route. Moreover, Caspase and nuclease activity is stimulated in apoptotic cells but not in normal cells (Perier et al 2012, Venderova and Park 2012).

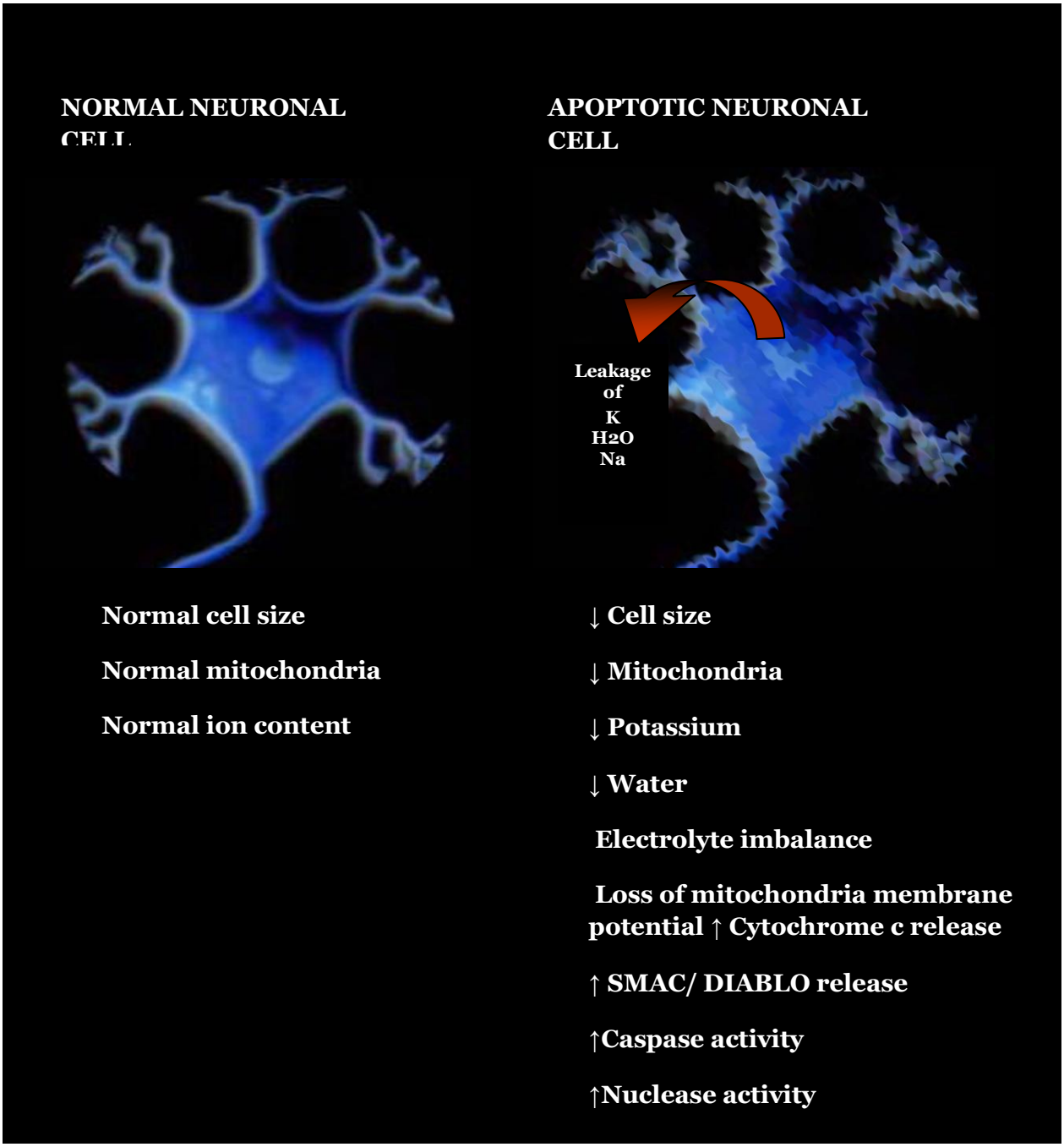

Image of neuron adapted and modified from Martini F.H, 2006, The Fundamentals of Anatomy and Physiology, 7th edition, San Francisco, Pearson Benjamin Cummings Ed Ltd pp 380

Figure 1.24: A comparison in morphology of Normal and Apoptotic cells

The normal cell is able to maintain is cellular structure due to homeostatic ion content and normal mitochondrial function, therefore Caspase and nuclease activity are not stimulated. In contrast, the apoptotic cell has a shift in ion content and mitochondrial dysfunction, thus there is an increase in activity of Caspases and nucleases (Perier et al 2012, Venderova and Park 2012).

In contrast, cells undergoing necrosis lose their architecture, via exposure to a hypotonic environment, causing the cell to swell and finally lyse. A short term injury to the cells promotes the cells to die via necrotic pathway. Necrotic cells can also trigger an inflammatory response when the wall of the cell is ruptured. In contrast, parts of the apoptotic cells break away in buds, which are eventually engulfed by phagocytes (Figure 1.25). Death of cells can be achieved via the necrosis or apoptosis route. Elevated levels of ROS promote necrosis, whilst lower ROS levels trigger apoptosis. In the current study, the involvement of Caspases was observed in PD model. The death of DCN was examined and determined if death of DCN was apoptotic or necrotic route (Perier et al 2012, Venderova and Park 2012, Chowdhury et al 2008).

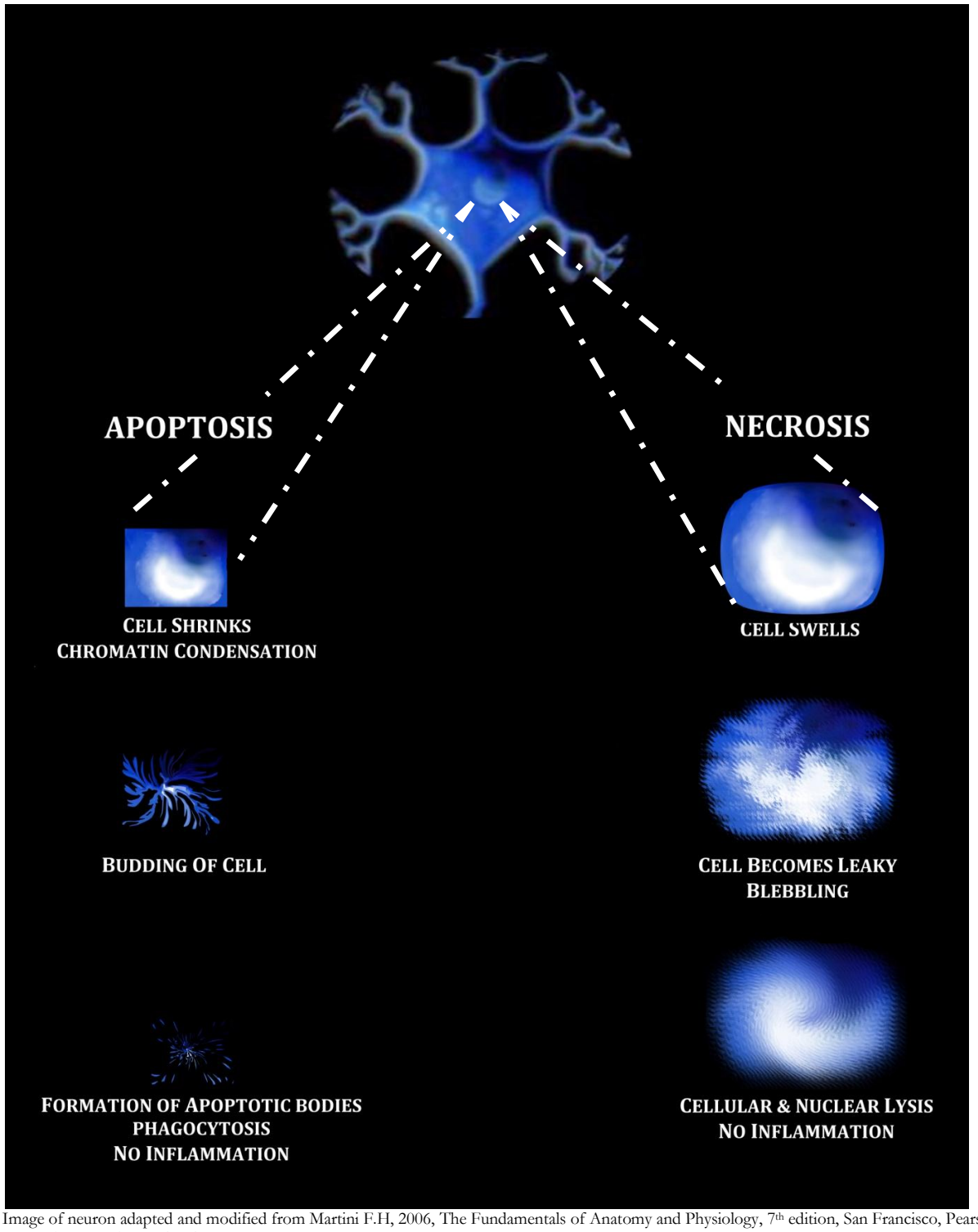

Image of neuron adapted and modified from Martini F.H, 2006, The Fundamentals of Anatomy and Physiology, 7th edition, San Francisco, Pearson Benjamin Cummings Ed Ltd pp 380

Figure 1.25: A comparison in morphology of Necrotic and Apoptotic cells

During normal apoptotic death there is cell shrinkage and chromatin condensation, leading to budding and formation of apoptotic bodies, which are phagocytised. In necrotic cell death, the cell swells, leading to leakage and blebbling resulting in cell lysis and inflammation (Perier et al 2012, Venderova and Park 2012, Chowdhury et al 2008).

Elevated ROS levels can contribute to mutations of essential genes such as mitochondrial, ER stress related and PD related genes such as Parkin and α synuclein. The rise of ROS such as superoxides, hydroxyls and nitric oxide accumulating in DCN promote cleavage of DNA bases, via extracting hydrogen atoms and thereby, causing a shift in genetic sequence and production of mutated genes. The mitochondrion is more susceptible to oxidative stress, as oxidants such as superoxide anion are often produced in the mitochondria's inner membrane (Bogaerts et al 2008, Kroemar and Blomgren 2007).

Research has shown that defects in mitochondrial genes contribute to the onset of PD (pages 75-78). Synaptic terminals have abundant levels of mitochondria present; therefore a significant level of ROS and ATP is also available in these areas (Kroemar and Blomgren 2007, Chaudhry and Ahmed 2014, Yang et al 2008, Bogaerts et al 2008). A study conducted by Bender et al (2006) revealed that higher levels of mitochondrial DNA deletions were found in PD patients, when compared to the control. Located in brain, various tissues and specifically in the matrix and inner membrane space (IMS) of the mitochondria, DJ-1 functions as an anti oxidant by reducing hydrogen peroxide levels (Figure 1.26). Frameshift and missense mutations, alongside deletions and insertions of DJ-1 gene, contribute to early onset PD. Mutational DJ-1 leads to increase in oxidative stress and mitochondrial impairment, causing degeneration of DCN, resulting in PD (Bogaerts et al 2008, Yang et al 2008, Kroemar and Blomgren 2007).

LRRK-2 also known as dardarin, is found in brain striatum and frontal cortex and is associated with nigrostriatal dopamine system. LRRK-2 functions as a kinase, which is located in the outer mitochondrial membrane (OMM) and cytoplasm (Figure 1.26). Mutated LRRK-2 which is found in the outside of the mitochondria contributes to toxicity and death of neurons that has been associated with PD (Bogaerts et al 2008, Yang et al 2008, Kroemar and Blomgren 2007).

HTRA-2 (high temperature requirement A2) is proapoptotic protease found in the IMS of the mitochondria, which plays a vital role in mitochondrial homeostasis (Figure 1.26). External stimuli such as environmental toxins, provokes HTRA-2 gene to transfer from the IMS to the cytosol, leading to Caspase activation (via disassociation of Caspase:IAP). Overexpression of HTRA-2 in mice has shown severe loss of motor neurons, via stimulation of the mitochondrial apoptosis pathway, resulting in symptoms similar to that of PD. Moreover, degeneration of striatal neurons caused by stimulation of Caspases has been observed in mice (Bogaerts et al 2008, Yang et al 2008, Kroemar and Blomgren 2007). Mutated HTRA-2 is translocated from the IMS to the cytoplasm where it promotes Caspase meditated death of cells via apoptotic pathway (Kroemar and Blomgren 2007, Chaudhry and Ahmed 2014).

PINK-1 gene is located in the OMM and IMM and functions to decrease ROS levels and suppresses cytochrome c. Mutation of PINK-1 and mutation of Parkin allows production of ROS and release of cytochrome c, promoting death of cells via apoptotic route. Genetic mutation in Parkin and PINK-1 gene has been strongly associated with the progression of PD, via mitochondrial dependent cell apoptosis (Fahn and Sulzer 2004, Chien et al 2013, Cookson 2004). PINK-1 reduces oxidative stress levels by inducing TNF receptor associated protein 1 (TRAP-1) phosphorylation. TRAP-1 protects mitochondrial DNA damage, via acting as a chaperone (Yang et al 2008, Kroemer and Blomgren 2007). The view can be supported further by Wood-Kaczmar et al (2008) who found increased oxidative stress and mitochondrial impairment of knockout PINK-1 in human DCN and neuroblastoma cell line. Decreased releases of dopamine in the striatum of PINK-1 deficient mice have also been found (Nakamura and Edwards 2007, Kroemer and Blomgren 2007). In vivo and in vitro studies have revealed elevated neuronal loss caused by mutated PINK-1 gene that has endured MPTP treatment (Haque et al 2008, Wood-Kaczmar et al 2008, Jin et al 2012).

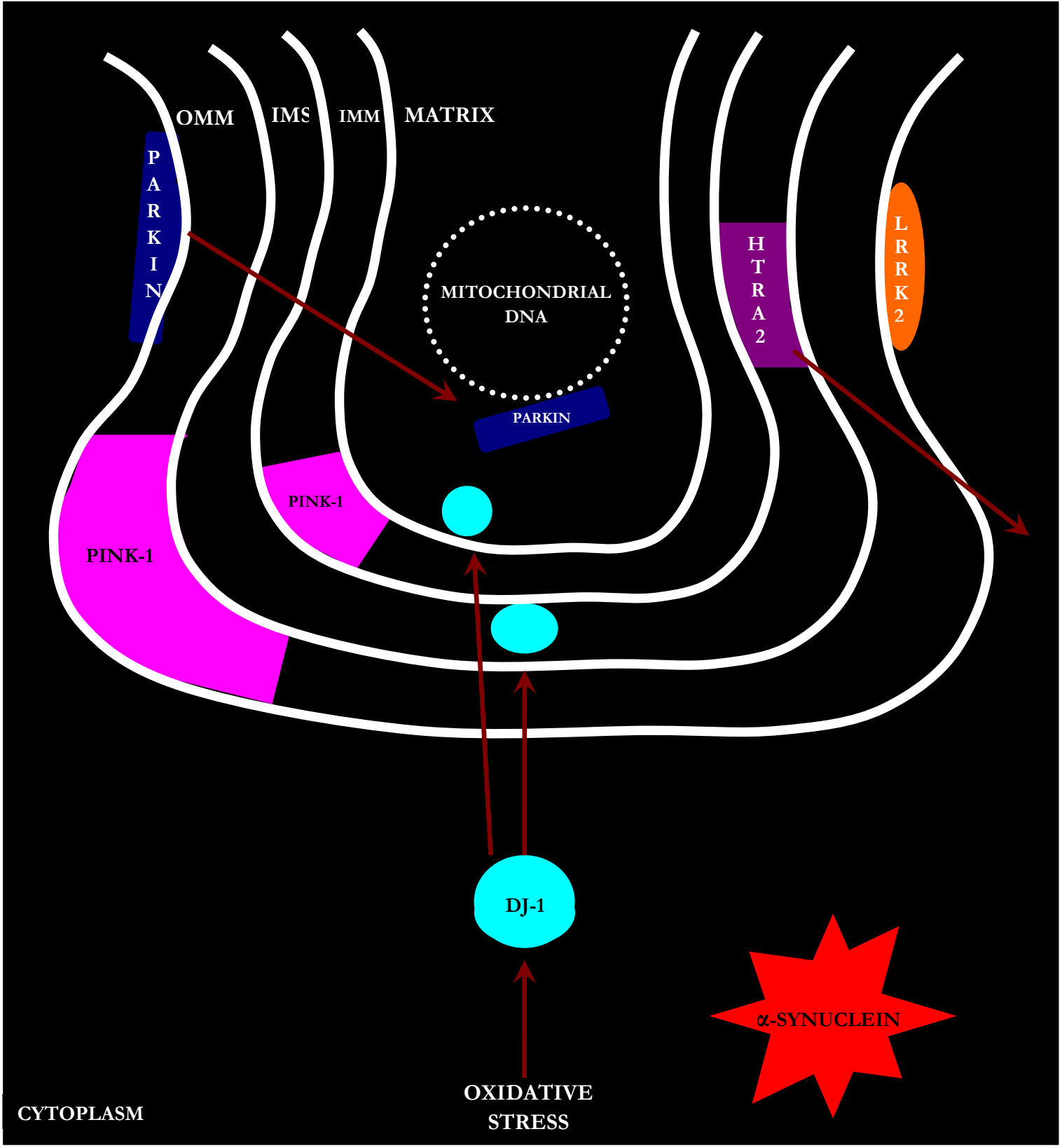

Figure 1.26: The role of mutant mitochondrial genes in PD

Figure showing the different mutated genes in relation to the mitochondria in PD pathogenesis. Oxidative stress promotes mutated DJ-1 gene to travel from the cytoplasm to the IMS and to the mitochondrial matrix, where it allows production of ROS. Mutated HTRA-2 is translocated from the IMS to the cytoplasm where it promotes Caspase meditated death of cells via apoptotic pathway. Mutated LRRK-2 which is found in the outside of the mitochondria contributes to toxicity and death of

neurons. PINK-1 gene is located in the OMM and IMM and functions to decrease ROS levels and suppresses cytochrome c. Mutation of PINK1 and mutation of Parkin allows production of ROS and release of cytochrome c, promoting death of cells via apoptotic route (Bogaerts et al 2008, Yang et al 2008, Kroemar and Blomgren 2007, Chaudhry and Ahmed 2014, Cookson 2005, Samann et al 2009, Inamdar et al 2007, Matsuda et al 2013).

1.10.1 Gene mutation and Caspase activation in PD

The mitochondrion is more susceptible to oxidative stress, as oxidants such as superoxide anion are often produced in the IMM(Kroemer and Blomgren 2007). Figure 1.27 indicates that mutation of PINK-1 promote mitochondrial impairment and the release of cytochrome c. Cytochrome c activates Caspase-9 followed by Caspase-3 leading to chromatin condensation alongside DNA fragmentation , resulting in destruction of DCN (Kroemer and Blomgren 2007, Yang et al 2008, Fahn and Sulzer 2004, Haque et al 2008). IF analysis has shown degeneration of neurons and increase in Caspase activation in knockout PINK-1 in tunicamycin treated rat cortical neurons , indicating a strong link between ER stress, PINK-1 suppression and activation of Caspases (Samann et al 2009). In addition, the lack of histones in mitochondrial DNA, permit mitochondria to be more vulnerable to oxidative stress. The increased levels of hydrogen peroxide, leads to lipid peroxidation, whilst elevated levels of peroxynitrate results in DNA damage. Reduced levels of DNA polymerase was observed in PD animal model, suggesting suppression of DNA excision repair function (Yang et al 2008, Fahn and Sulzer 2004, Kroemar and Blomgren 2007). The majority of mutations of the PINK-1 gene are missense mutations that are autosomal in PD patients (Cookson 2005). Furthermore defects in PINK-1 have resulted in degeneration of muscles via mitochondrial apoptotic route (Inamdar et al 2007, Matsuda et al 2013).

Parkin plays a vital role in maintaining mitochondrial homeostasis, alongside UPR in ER. Mutation of Parkin gene can result in ER stress or oxidative stress induced cell death (Perez et al 2005, Perez and Palmiter 2005). Defects of Parkin gene result in impairment of UPS inducing a rise in incorrectly folded proteins and triggering of the unfolded stress response (USR) leads to activation of Caspase-12 (Figure 1.27). Subsequently, active Caspase-12 stimulates Caspase-9 followed by Caspase-3 stimulation, inducing apoptotic cell death and release of ROS. Elevated levels of ROS damage nearby cells causing a mass destruction of DCN contributing to the onset of PD (Shimoke et al 2004, Chowdhury et al 2008, Shibata and Kobayashi 2008, Kudo 2003). As described in Figure 1.27 active Caspases encourage stimulation of other Caspases, via a cascade reaction, leading to cell death. IF analysis had showed enlargement of followed by collapse of the mitochondria in mutated Parkin and PINK-1 Drosophila cell lines and tissues, indicated that Parkin and PINK-1 are required to stabilize maintenance of mitochondria, thereby suppressing cell death of neuronal cells, via preventing the release of cytochrome c (Poole et al 2008, Yang et al 2008, Cookson et al 2008, Lim and Tan 2007).

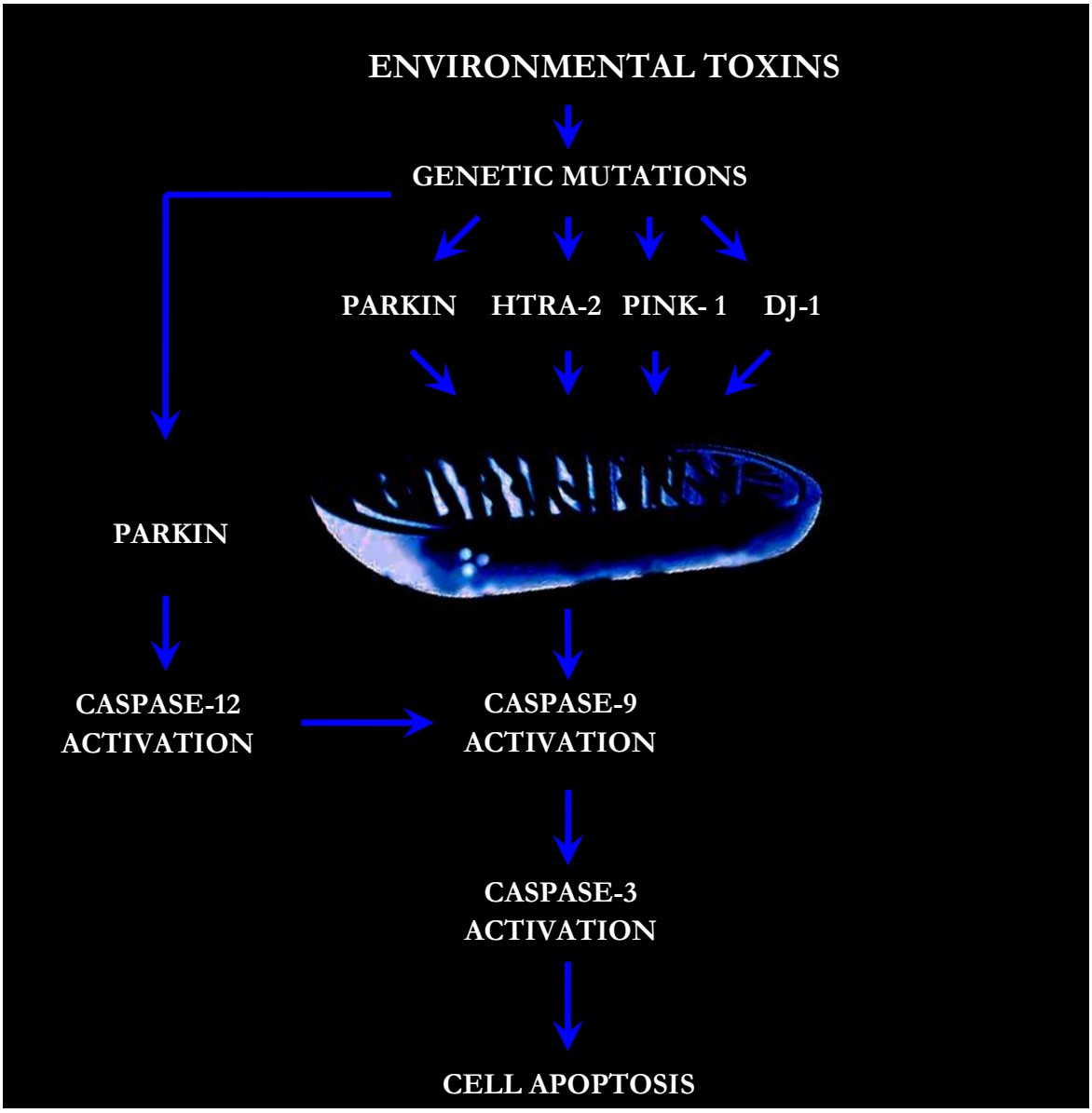

Figure 1.27: Environmental toxins cause mutations of genes resulting in Caspases dependent apoptotic death of DCN

Environmental toxins can contribute to mutations of various genes (Chae 2004). Mutated Parkin can activate Caspases through intrinsic and extrinsic route resulting in apoptotic cell death. Mutated Parkin (E3 ligase) leads to activation of Caspase-12, which leads to a cascade reaction of Caspases (Caspase-9 activation followed by activation of Caspase-3) resulting in cell apoptosis. Mutated PINK-1 and Parkin provoke cytochrome c release, leading to activation of Caspases-9 and-3, resulting in apoptotic dell death. Mutation of HTRA-2 activates Caspases through translocation of HTRA-2 from the IMS to the cytosol. Mutation of DJ-1 gene leads to elevated ROS and mitochondrial impairment, resulting in stimulation of Caspases and mitochondrial mediated death of neuronal cells (Cookson et al 2008, Chowdhury et al 2008, Shibata and Kobayashi 2008)

1.10.2 The Role ROS in Caspase activation

Exposure to environmental toxins (such as MPTP exposure), oxidative stress and inflammation can trigger activation of various pathways such as JNK, p38 and NFκB pathway, which subsequently initiates the activation of Caspases, leading to cell apoptosis and resulting in development of diseases such as PD (Wang et al 2005). Furthermore, an imbalance in ROS:antioxidant enzymes contribute to cell death, leading to the onset of PD. Accumulation of ROS such as superoxides promotes manufacture of peroxynitrate, leading to damage of DNA damage, chromatin condensation, lipid peroxidation, contributing to mutation of E3 ligase, which results in the impairment of the UPS. UPS dysfunction allows the accumulation of incorrectly folded proteins and other toxic compounds resulting ER stress mediated cell death and PD onset. ER stress can activate Calpain activation resulting in stimulation of Caspases (Matus et al 2008, Sano and Reed 2013, Figure 1.28).

Increased levels of reactive nitrite species (RNS) and reactive chloride species (RCS) can directly activate Caspase mediated cell death (Nakamura et al 2012, Chowdhury et al 2008). Furthermore, injured neurons release signal that stimulate microglial activation that release cytokines (such as IL-6,-β and -α), which stimulates Caspase activation. In addition, cytokines promotes expression of iNOS, provoking the formation of nitric oxide with superoxide resulting in manufacturing of peroxynitrate (Chowdhury et al 2008, Figure 1.28). In addition, increased iron levels encourage Caspase mediated cell death. Iron encourages the conversion of hydrogen peroxide to hydroxide contributing to stimulation of Caspase mediated cell death. Increase in iron, ROS and decrease in anti oxidative such as glutathione enhance the production of superoxides, which permit oxidative damage of proteins, DNA and lipids resulting in cell death (Moron and Castilla-Cortazar 2012).

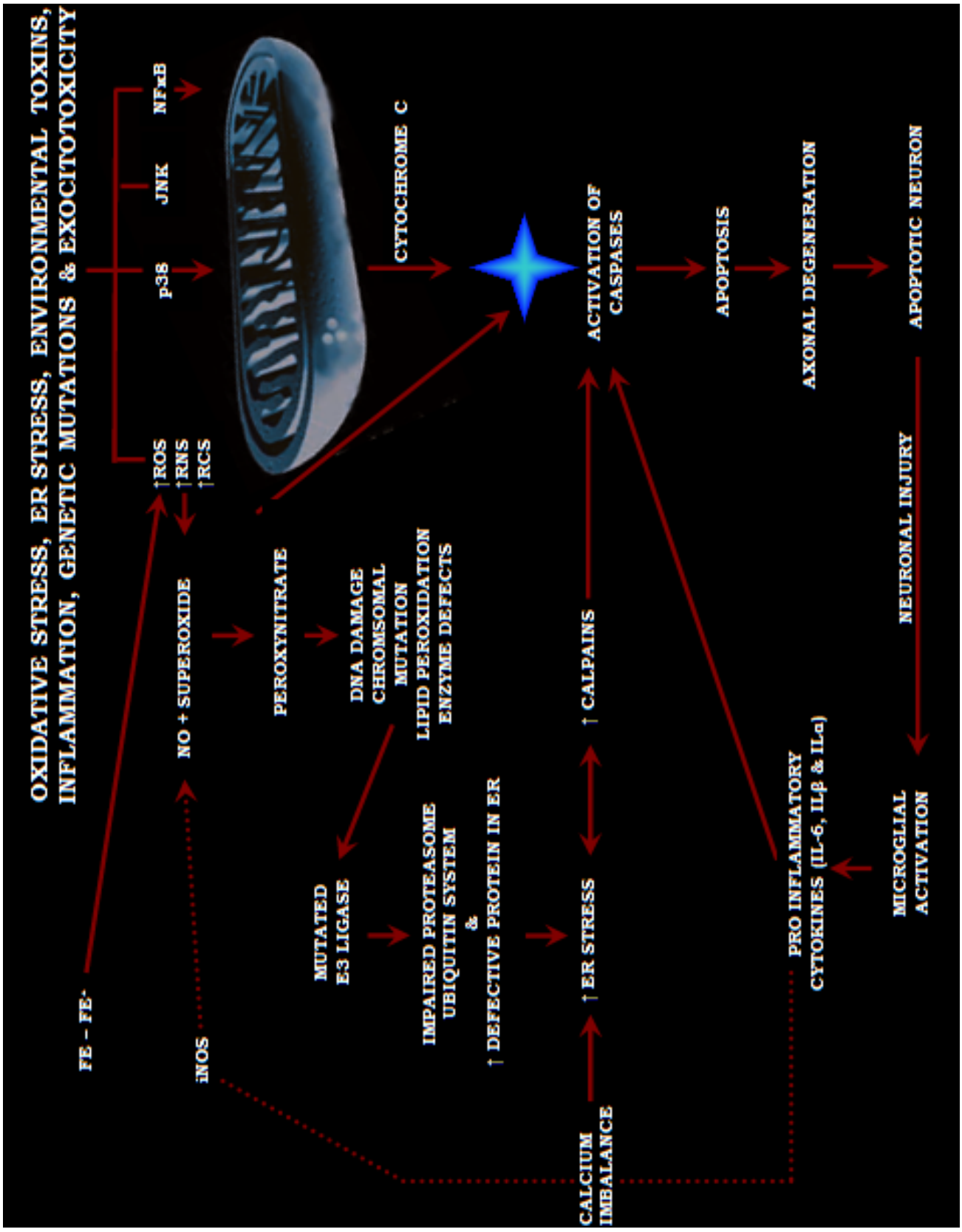

Figure 1.28: The involvement of ROS in Caspase mediated cell death

Figure showing the involvement of ROS in Caspase activation and cell apoptosis. Iron can promote hydrogen peroxide to convert to hydroxyl radicals contributing to oxidative stress by increasing manufacture of ROS. Elevated ROS promotes nitric oxide to bind to superoxide to produce

peroxynitrate which results in damage to DNA, mutation of chromosomes, lipid peroxidation and enzyme defects. Mutation of E3 ligase caused by peroxynitrate damage leads to impairment of UPS, resulting in high levels of defective proteins, accumulating in the ER promoting ER stress. ER stress can activate Calpains (and vice versa) leading to motivation of other Caspases, via Caspase cascade reaction, resulting in axonal degeneration via apoptotic pathway. The apoptotic neuron triggers injury signal that activates microglia promoting release of cytokines such as IL-6 and-8. Subsequently, IL provokes Caspase activation, as well as increase expression of iNOS, which promotes formation of nitric oxide. Exposure to excessive RNS provoke high nitric oxide levels (via excitoxicity) that interact with superoxide to produce peroxynitrate and radicals which can dysfunction complex IV followed by Complex I activity of the mitochondria, leading to mitochondrial mediated apoptosis through Caspase activation (Moron and Castilla-Cortazar 2012, Chowdhury et al 2008, Wang et al 2005, Matus et al 2008, Sano and Reed 2013, Hetz 2012).

Research by Liou et al (2005) found a significant rise in Calpain, AIF, Caspases-9 and-3 activities in MPTP-treated PC12 cells. In addition, a substantial increase in JNK pathway stimulation was found in these cells. The results of this study suggested that the increased accumulation of Calpain in cells provoked AIF. AIF entered the cytosol and adhered to the mitochondrial surface, promoting the release of cytochrome c leading to activation of Caspases-9 and-3, resulting in cell death. These findings were also found in MN9D cells. DNA fragmentation, chromatin condensation and presence of apoptotic bodies that was observed in both cell lines confirmed that cell death occurred via mitochondrial dependent apoptosis pathway. The enhanced release of cytochrome c, alongside impaired ATP levels, encouraged production of ROS, which contributed to further cell death.

The protein, α synuclein is abundantly found in presynaptic terminals of neurons and in cerebral spinal fluid and plays a vital role in synaptic maturation and neuronal plasticity (Chowdhury et al 2008). A study conducted by Smith et al (2005) revealed that mutant α synuclein elevated Caspases-3, -9, -12 and ROS levels in PC12 cells. In addition a reduction in proteasome activity was found. The main findings of the study suggested that mutant α synuclein participates in both ER stress and mitochondrial dysfunction pathways. Substantial levels of DNA, protein and lipid damage caused by ROS and oxidative stress was found in PD patients. ER stress stimulated USR, enabling PERK (an ER transmembrane kinase) to activate Caspase-12. Subsequently, Caspase-12 activated Caspase-9, followed by stimulation of Caspase-3, resulting in cell death.

1.11 The Use of MPTP-Treated Rat Animal Model in PD Pathogenesis

Present and past research has shown the use of MPTP-treated and 6OHDA-treated rat model to investigate PD pathogenesis (Section 1.2.5.1). Recent research by Xu et al (2013) has demonstrated the direct use of MPTP in brain of rat model to study neurotoxicity and has provided further insight into PD pathogenesis. MPTP treatment in rats had reduced the expression of BCL-2, BDNF, glutathione synthase and dopamine antioxidants. In addition, MPTP rats has shown damaged DCN, difficulty in movement and coordination , strongly indicating that MPTP rat model is a relevant model for investigating PD pathogenesis (Frazzita et al 2013). Immunohistochemical analysis has revealed loss of neurons, accumulation of fibrils and increase in lesions formed in the SNpc region of rat brain that had been treated directly with MPTP and 6OHDA, when compared to untreated rats. A decrease in number of TH positive neurons and dopamine levels were seen in SNpc of 6OHDA-treated rats compared to MPTP rats, indicating that 6OHDA-treated rat model is preferable to study the advanced stage of PD, where a prominent sign of memory impairment is observed. The author suggested that MPTP rat model is suitable model to study early onset of PD as its motor symptoms and loss of neurons are similar to that of early phase PD (Ferro et al 2005).

Bellissimo et al (2004) investigated the memory performance of MPTP-treated rats with relevance to PD. The author showed administration of MPTP in the brains of rats exhibited signs that are typically seen in PD and can be used as a model to study and explore PD pathogenesis. Current research by Friend and Keefe (2013) have used PD rat model to examine damage to striatal neurons caused by exposure to methamphetamine. Methamphetamine had decreased dopamine levels in the striatum in PD rat model. Perez et al (2002) demonstrated that mutated α-synuclein had decreased TH, dopamine, DOPA and dopamine synthesis in homogenates of rat striatum, indicating that the effect of genetic mutation can be studied using PD rat model.

MPTP animal model is considered as a suitable model to use when referring to PD as it has the advantage of portraying the complex mechanisms, which contribute to PD pathogenesis. The rodent

MPTP model demonstrates the neurochemical and neuropathological changes which occur in PD, whilst monkey MPTP model provides significant information on behavioural changes in PD (Bohlen and Halbach 2006). Recent research by Bazzu et al (2013) explored the regulation of D1 dopamine receptor in MPTP PD rat model. The study also found MPTP reduced TH activity in SNpc of rats. Bazzu et al (2013) research has used the systemic administration of MPTP in rats which is a newly developed model to study PD pathogenesis. This project which has been in collaboration with Professor Jozef Langford has used systemic administration of MPTP to develop a new PD rat model which brings uniqueness and originality to this thesis.

1.12 The use of ReNcell VM in previous studies

Previous research in PD has relied on the use of animal models and different cell lines, which have advantages and some limitations(Kroemer and Blomg 2007). ReNcell VM is a progenitor cell line derived from the midbrain of fourteen week old human foetus, which has recently been established to be used as an ideal model to study PD (Donato et al 2007). The transcription factor, myc used in ReNcell VM provides more karotype phenotype stability even after different passages decreasing the variability which other cell lines and donor tissues have to encounter. This increases the reliability in results and can be used to study the effect of different drugs , neurotoxicity and neurological diseases. Research by Donato et al (2007) has shown positive staining for the neurotransmitter TH, alongside the release of dopamine from these cells. TH converts precursor L-DOPA to dopamine in the brain and reduced TH levels in PD brain has been observed. Additionally, work by Massachusetts (2008) has explored the relationship of mutant PINK-1 (gene that has been strongly associated with Caspase activation) in PD using this dopaminergic cell line. Massachusetts' results demonstrated the mechanistic link of mutant PINK-1 gene and PD onset by suppressing PINK-1 in ReNcell VM. PINK-1 suppression in ReNcell VM increased ROS levels, leading to the collapse of the mitochondria and activation of Caspase resulting in death of DCN. These vital markers (mitochondrial impairment, presence of Caspases and ROS) of cell death have been found in other cell lines and PD animal models, supporting its suitability as a model to study PD (Kroemer and Blomg 2007, Yang et al 2008, Fahn and Sulzer 2004, Haque et al 2008). Thus, ReNcell VM offers a better representation of DCN therefore providing a gateway of new possibilities which animal models and other cell lines have been limited to.

1.13 Investigating Caspase Death Mechanisms in PD model

Current research has shown that exercise in PD patients indicates improvement in not only decreasing key features that are present in PD such as gait, tremors and bradykinesia, but they also improve quality of life of the PD patient in terms of forming social networks and can integrate well into the PD patients lifestyle (Heiberger et al 2011, Fritz et al 2011, Vivas et al 2011, Ayan and Cancela 2012, Hackney and Earhart 2009a, Hackney and Earhart 2007, Hackney and Earhart 2010, Li et al 2012, Modugno et al 2010, Dreu et al 2012, Brown et al 2010). Although there are extensive clinical studies carried out on treadmill exercise in PD patients (Section 1.2.5), there is a lack of biochemical understanding to how exercise is affecting PD patients at a cellular level. What key proteins can exercise affect and can different types of exercise increase or decrease these proteins has not yet been determined.

There is a lack of research exploring the potential pathways, which exercise can activate and suppress to provide such positive and even negative effects. Only through discovering what key proteins are important in Caspase activation and establishing, which pathways Caspases are involved in that result in death of DCN, can improved therapies and treatments be created. In addition, establishing which pathways the Caspases follow and understanding the key events that occur in Caspase activation new targets for treatment can be achieved. These new specific targeted drugs could be used with treadmill exercise to achieve maximum effect, by slowing down or inhibiting further death of DCN.

Aim: The current study explores the effect of treadmill exercise on Caspases, along with CAMK-IV protein in different brain regions of MPTP rat model, using WB analysis. More specifically, to determine the effect treadmill exercise had on activation of Caspases-1,-2,-3,-8,-9 and -12 in the cerebellum, brain cortex, midbrain and striatum of PD animal model.

The study explores the potential pathways that results in Caspase mediated death of dopamine containing neurones in relevance to Parkinson's disease. It is an attempt to identify the major pathways which cause Caspase mediated death and to establish key proteins involved in each pathway with the

motive to eventually find targets that can be used and manipulated to safely slow down apoptotic death of differentiated ReNcell VM stem cell line.

Objectives

WB analysis was used to determine the presence and absence of activated Caspase-1, -2, -3, -8, -9 and -12 in cerebellum, brain cortex, midbrain and striatum of PD-Ex animal model.

To establish differentiated ReNcell VM as a suitable PD model to study cell death mechanisms with administration of 6OHDA.

Co localisation studies, IF, WB and Caspase colorimetric analysis was performed to demonstrate 6OHDA triggers Caspase mediated death of dDCN.

Cell viability, double IF and WB analysis using specific inhibitors were used to identify specific potential pathways that promotes Caspase activation resulting in apoptotic death of 6OHDA dDCN.

More specifically, salubrinal, IKK , benzyloxycarbonyl-Val-Asp(OMe)-Val-Ala-Asp(OMe)-fluoromethylketone (zVDVADfmk) , benzyloxycarbonyl -LE(OMe)VD (OMe)- fluoromethylketone (zLEVDfmk) and benzyloxycarbonyl -Ile-Glu(OMe)-Thr-Asp(OMe)-fluoromethylketone (zIETDfmk) inhibitors were used to determine role of PERK, NFκB, Caspases-2, -4 and -8 in PD cell model.

Chapter 2:
Materials and Method

2.0 General Reagents

Following suppliers were used for the reagents including Sigma Dorset UK, Millipore Hertfordshire UK, Abcam Cambridge UK, Vector Laboratories Peterborough UK, Perbio Science Northumberland UK, Xograph Gloucestershire UK, Invitrogen Paisley UK, Fisher Scientific Leicestershire UK and Severn Biotech Worcestershire UK. A more detailed description of all reagents can be found in Appendix 1.

2.1 Antibodies

Primary and secondary antibodies; (AB1872) Anti-Caspase-1, (AB7979) Anti-Caspase-2, (AB3623, 04-439) Anti-Caspase-3, (AB52183, AB97318)Anti-Caspase-4, (AB25897)Anti-Caspase-8, (04-444) Anti-Caspase-9, (AB62484) Anti-Caspase-12, (04-1078) Anti CAMK-IV, (MAB3026) Anti-NFκB, (12-348) Goat-Anti-Rabbit HRP, (AP192P) Donkey-Anti-Mouse HRP, (MAB318, AB152) Anti-TH, (AP192F) Donkey-Anti-Mouse IgG FITC, (AB6791)Sheep-Anti-Rabbit IgG FITC, (AQ300F) Sheep-Anti-Mouse IgG FITC, (AP123R) Goat-Anti-Rabbit IgG Rhodamine, (AQ300R) Sheep-Anti-Mouse IgG Rhodamine were purchased from Abcam Cambridge UK and Millipore Hertfordshire UK. A more detailed description of all antibodies can be found in Appendix 1.

2.2 Inhibitors

Inhibitors; (SC-202332) Salubrinal, (401479) IKK, (218744) zVDVADfmk, (218755) zLEVDfmk, (218759) zIETDfmk, (G7351) zVADfmk were obtained from Santa Cruz Biotechnology Heidelberg Germany, Merck Chemicals Nottingham UK and Promega Southampton UK correspondingly. A more detailed description of all inhibitors can be found in Appendix 1.

The IKK inhibitor used in this project was specifically chosen as it irreversibly binds to IKK-α and IKK-β complex thereby preventing activation of NFκB of the classical pathway in cells (Merck Chemicals Ltd UK 2011). Salubrinal selectively inhibits protein phosphatase 1 (PP1) which prevents the dephosphorylation of eIF2-α, thereby preventing activation of PERK pathway of ER mediated death of cells (Santa Cruz Biotechnology 2011). The inhibitor zVADfmk irreversibly binds to fluoromethylketone

peptide sequence α-aspartyl-α-glutamylvalylaspartic acid of Caspase protein thereby preventing death of dDCN (Promega 2010). zVDVADfmk irreversibly binds to fluoromethylketone peptide sequence Benzyloxycarbonyl-Val-Asp(OMe)-Val-Ala-Asp(OMe)-fluoromethylketone of Caspase-2, resulting in suppression of Caspase-2 activity in cells(Merck Chemicals Ltd UK 2008). The specific Caspase-4 inhibitor zLEVDfmk, reversibly binds to aldehyde peptide sequence N-Acetyl-L-leucyl-L-α-glutamyl-N-[(2S)-1-carboxy-3-oxo-2-propanyl]-L-valinamide blocking the Caspase-4 activity in cells (Merck Chemicals Ltd UK 2011). The Caspase-8 inhibitor, zIETDfmk irreversibly binds to fluoromethylketone peptide sequence of the Caspase-8 protein, resulting in suppression of Caspase-8 activity in cells (Merck Chemicals Ltd UK 2011).

2.3 Animal work

Procedure for training and MPTP injection were carried out by collaborators Jozef Langfort and Malgorzata Chalmoniuk at Dr Jozef Langfort laboratories Medical Research Centre, Polish Academy of Sciences, Warsaw, Poland. All experimental procedures involving rat care and experimentation were performed in accordance with the European Communication Council Directive. Protocols for the care and use of laboratory animals were approved by local Ethical Committee for Animal Experiments at Nenki Institute, Warsaw, Poland (Ethical Approval Appendix 2). For this study, special consideration was given to use the minimum number of animals required to achieve statistical significance and all efforts were made to minimize animal suffering. Rats were housed in temperature controlled room under 12 hour daylight/ night cycle at animal breeding facility. Rats were fed rodent chow and water ad libitum to consume at regular intervals.

2.3.1 Segregation and treatments of rats

The following procedure was carried out by collaborators Jozef Langfort and Malgorzata Chalmoniuk at Dr Jozef Langfort laboratories Medical Research Centre, Polish Academy of Sciences, Warsaw, Poland. For the study, eight weeks old Wistar male rats (250g-290g) from the animal breeding facility within the Polish Academy of Sciences, Medical Research Centre were used (n=4 for each group). The rats were segregated to endure four conditions; control (untreated and un-trained (C), trained (Ex), MPTP-

treated (PD) and PD-Ex (MPTP-treated and trained). Rats that were segregated to the C group received saline injection intraperitoneally (i.p.) and remained sedentary. In the Ex group rats ran on motor-driven rodent treadmill for 28 m x min^{-1} for 1 hour every day for 6 weeks and received saline injection (i.p.). In the PD group, rats did not exercise and after 6 weeks rats received three injections of MPTP in saline at 2 hours intervals in a total dose 60mg/kg (i.p.). In the PD-Ex group, ran on motor-driven rodent treadmill for 28 m x min^{-1} for 1 hour every day for 6 weeks. Following completion of the 6^{th} week of training, rats received three injections of MPTP in saline at 2 hours intervals in a total dose 60mg/kg (i.p.). Rats were sacrificed on 14 days after the MPTP injection. Prior to sacrifice, all rats were deeply anaesthetised with sodium pentobarbital. Rats were sacrificed by decapitation and the brains were removed. The entire brain was quickly removed from the skull and dissected on an ice-cold glass petri dish. The brains were preserved with 30% sucrose with phosphate buffer. Different parts of brain were snap-frozen in liquid nitrogen and stored at -80°C and shipped to the University of Bedfordshire, Luton, UK.

2.3.2 BCA Protein Assay

Protein concentration of all samples (C, Ex, PD and PD-Ex) was determined using Bicinchoninic acid (BCA) method. All studied regions i.e. cerebellum, brain cortex, midbrain and striatum) from each sample was placed on ice, whilst carrying out homogenisation. Samples were homogenised in presence of homogenising buffer (20mM Tris HCl pH 7.4, 2mM EGTA, 1mM DDT, protease inhibitors containing 1μg/ml leupeptin, 2μg/ml antipain, 2μg/ml chymostatin, 2μg/ml pepstatin, 3mM benzamidine, 200μg/ml phenylmethylsulfonylfluoride (PMSF), using Dounce homogeniser. All samples were transferred to labelled centrifuge tubes. Homogenised samples were ultracentrifuged at 100 000 x g for 70 minutes at 4°C. The supernatant was removed and BCA (Pierce Biotechnology Rockford IL USA) protein assay was carried out. Serial dilutions of BSA standards and homogenised samples were prepared in 96 well plates. Working reagent, containing sodium carbonate anhydrous and copper II sulphate pentahydrate, was added to all wells and the microplate was incubated in 37°C incubator for 30 minutes. The absorbance was detected using the programme Stingray at 570nm wavelength (microplate reader). The data was analysed and the amount of protein was determined prior to WB analysis.

2.3.3 Protein Detection and Measurement using WB

Sodium dodecyl sulphate polyacrylamide gel (SDS-PAGE;12%) was prepared using vertical gel casting chamber and then transferred to electrophoresis tank. Loading buffer and dithiothreitol (DTT) were added to 50µg of protein from all samples (C, Ex, PD and PD-Ex group) were centrifuged at 1000 RMP for 5 minutes. Subsequently, all samples were placed in hot plate at 100°C for 5 minutes, before loading onto 12% SDS gel. SDS Running buffer was added to the electrophoresis tank and all samples were SDS PAGED at 200 volts for an hour. The blot module was assembled and transfer buffer was added prior to carrying out immunoblotting at 350 mAmps for 90 minutes. Coomaisse Brilliant Blue was used to stain the resolving gel whereas the nitrocellulose membrane was stained with Ponceau stain solution to determine successful transfer of proteins. Non-specific binding was blocked by incubating the nitrocellulose membrane with 1% milk solution for 30 minutes. Subsequently, the membrane was incubated with primary antibody cleaved Anti-Caspase-3 antibody (1:1500, Millipore Hertfordshire UK) overnight at 4°C. Serial washes of the membrane were performed using Phosphate Buffered Saline Tween 20 (PBS-T). The membrane was incubated with secondary antibody, Goat-Anti-Rabbit HRP (1:1000, Millipore Hertfordshire UK) for 2 hours at room temperature (RT). Enhanced chemiluminescent (ECL, Perbio Science Northumberland UK) comprising of 1.5ml Peroxide Solution & 1.5ml Luminol Enhancer Solution was prepared and transferred onto the membrane for 5 minutes. The membrane was wrapped in cling film and placed into the cassette along with a Kodak X-ray film (FMXOB0101824, Xograph Gloucestershire UK). The membrane was exposed to the X-ray film for 5 minutes before developing. Kodak X-ray film was placed in Kodak developer solution for 4 minutes, rinsed under tap water followed by placing into Kodak fixing solution for 8 minutes. Band analysis was carried out using a densitometer (GS800, Bio-Rad Hertfordshire UK) which is described in further detail below (Section 2.3.4). For each experiment the membrane was reprobed with the house keeping gene Gylceraldehyde-3-Phosphate Dehydrogenase (GAPDH) via strip and reprobe method (Section 2.3.5). It was essential that GAPDH was used as a reference guide to normalise the data prior to statistical analysis (Section 2.3.4).

2.3.4 Detection and Statistical Analysis

Band analysis was carried out using a densitometer (GS800, Bio-Rad Hertfordshire UK). Blots of good quality, which had less background noise, were scanned using GS800 scanner. Immunoblots were detected and quantified using Quantity One analysis software. The band lanes and each band was detected automatically using Quantity One software at default settings and the raw densitometric intensity values were obtained. The densitometric values for the experimental samples were normalised against the house keeping gene, GAPDH to determine the densitometric ratio , prior to carrying out statistical analysis (T test $p<0.05$, ANOVA $p<0.05$). A total of five independent experiments were conducted and the average of all three experiments was determined to finalise the end conclusion.

2.3.5 Strip and Reprobe of Membrane using Different Antibodies

To determine the presence and absence other Caspase proteins such as Caspase-1,-2,-3, -8,-9 and -12 and CAMK-IV (in some cases), as well as using the house keeping gene GAPDH as a reference guide, the membrane was stripped of the antibody by incubating the membrane with stripping buffer (1mM EGTA, 200mM glycine) for 20 minutes followed by serial wash with PBS Tween 20. Reprobing the membrane with a different antibody was achieved by incubating the membrane with the primary antibody (active Anti-Caspase-9, 1:1000, Millipore Hertfordshire UK) and secondary antibody (Goat-Anti-Rabbit HRP, 1:1000, Millipore Hertfordshire UK). The subsequent steps to develop Caspase-9 via X-ray film were achieved using the same conditions as stated above (Section 2.3.3).

2.4 ReNcell VM Human Neural Progenitor Cell Line

ReNcell VM is a newly developed cell line derived from human ventral mesencephalon brain region of fourteen week old foetus, which has the ability to differentiate into dopaminergic/dopamine containing neurons (dDCN) purchased from Millipore Hertfordshire
UK (SCM008).

2.4.1 Preparation of laminin coated flasks, well plates and chamber slides

To ensure that ReNcell VM Human Neural Progenitor cells adhered to the surface, 96 well plates, 2 well chamber slides, 8 well chamber slides, T75 and T25 flasks were coated with Laminin from Engelbreth-Holm-Swarm murine sarcoma basement membrane (L2020 Sigma Dorset UK) in Dulbecco's Modified Eagle Medium (DMEM) (D5796 Sigma Dorset UK) (20 μg/ml) and were left to incubate in 37°C 5% CO_2 incubator for four hours. Following 4 hour incubation, excess laminin solution was removed from the coated tissue culture ware and the apparatus were rinsed with PBS.

2.4.2 Culturing of ReNcell VM

Prewarmed ReNcell Neural Stem Cell (NSC) maintenance media (SCM005, Millipore Hertfordshire UK) was transferred into T75 laminin coated flask and left in 37°C incubator. ReNcell VM vial was thawed in 37°C water bath and transferred to a sterile 15 ml conical tube with use of 1 ml pipette. Prewarmed ReNcell NSC Maintenance Medium (comprised of human tansferrin, putrescine dehydrochloride, tri iodo thyronine, L thyroxine, progesterone, DMEM/F12, glutamine, L glutamine, human serum albumin, human recombinant insulin, tri-iodo-insulin, sodium selenite, heparin and corticosterone) was gradually added to the 15ml conical tube containing ReNcell VM. Cells were resuspended and centrifuged at 12000 RMP for 5 minutes at 4°C. The supernatant was removed and cells were suspended in 5ml of ReNcell NSC Maintenance Medium (pre-warmed to 37°C) containing freshly added Epidermal Growth Factor (EGF) (GF144, Millipore Hertfordshire UK) and Fibroblast Growth Factor basic, human recombinant (FGF) (GF003, Millipore Hertfordshire UK). ReNcell VM was pipetted into the laminin-coated T75 tissue culture flask that was pre-incubated in the 37°C incubator. ReNVM cells were left to

incubate overnight at 37°C in 5% CO_2 incubator. The medium was replaced the following day with fresh ReNcell NSC Maintenance Medium (prewarmed to 37°C) containing 0.4µl FGF and 3µl EGF. The medium (containing FGF and EGF) for ReNcell VM was changed every other day and cells were left to grow until they were 80% confluent.

2.4.3 Sub culturing of ReNcell VM

ReNcell VM was left to grow until they were 80% confluent after which they were subcultured in freshly prepared laminin coated flasks. Pre warmed ReNcell NSC Maintenance Medium containing 0.4µl FGF and 3µl EGF was added to the freshly prepared laminin coated flasks and was left at 37°C 5% CO_2 incubator. The old ReN media was removed from laminin-coated T75 flasks containing the confluent layer of ReNcell VM cells. Cold PBS was pipette slowly into the flask from the side to avoid detaching the cells. PBS was used to wash the cells after which the PBS was discarded. To detach ReNVM cells 3 ml of accutase (A6964, Sigma Dorset UK) was added to the flask and was left to incubate for 5 minutes in a 37°C incubator. The detached cells were transferred into a 15ml centrifuged tube and the cells were centrifuged at 12000 RPM for 5 minutes at 4°C. The supernatant was discarded and ReNcell NSC Maintenance Medium containing 0.4µl FGF and 3µl EGF was added to the cells. Cells were counted using a haemocytometer. Cells were plated in fresh laminin-coated flasks in ReNcell NSC Maintenance Medium containing 0.4µl FGF and 3µl EGF. The next day freshly prepared ReNcell NSC Maintenance Medium containing 0.4µl FGF and 3µl EGF replaced the old medium and cells were left to incubate as normal. The medium was exchanged with fresh ReNcell NSC Maintenance Medium containing FGF and EGF every other day.

2.4.4 Preparation of ReNcell VM stocks

To prepare stocks of ReNcell VM old medium was removed from laminin-coated T75 flasks containing the confluent layer of ReNcell VM cells. Cold PBS was added to the flask to wash cells. After cells were washed PBS was discarded and 3ml of accutase was added to the flask and was left to incubate in a 37°C incubator for 5 minutes. Prewarmed ReNcell NSC Maintenance Medium was added to the flask

containing detached cells. ReNcell VM was centrifuged at 12000R PM for 5 minutes at 4°C and the supernatant was discarded. ReNVM NSC Freezing Medium (SCM007, Millipore Hertfordshire UK) was added to the cells (1ml) and cells were aliquoted into labelled 1.5ml cryovials. All cryovials were placed in alcohol bath (containing isopropanol) and stored at -80°C.

2.5 General Methods for PD cell model

2.5.1 Drug treatment

Initially the concentration of each inhibitor had to be established prior to carrying out the main experiments. To determine appropriate concentration range for each inhibitor previous research was explored that had used the specific inhibitor. The concentration of the inhibitor was determined whilst the exposure time was kept at 2 hour time interval to coordinate with 6OHDA (H116, Sigma Dorset UK) drug treatment.

For all neurotoxicity experiments dDCN were approximately 80% confluent when exposed to 100µM 6OHDA for 2 hours. Subsequently, drug treatment was stopped with the removal of the media containing 100µM 6OHDA and replaced with fresh ReNcell maintenance media. Untreated and treated dDCN were left in 37°C CO_2 incubator overnight. The following day the main experiment was carried out. For some assays dDCN were exposed to 100µM 6OHDA as well as an inhibitor such as IKK, salubrinal or Caspase specific. In other experiments dDCN were treated with 100µM 6OHDA, along with a combination of two or more specific inhibitors.

2.5.2 Determining Caspase expression in 6OHDA dDCN

dDCN were cultured in laminin coated 8 well chamber slides until they had reached 80% confluence. dDCN were treated with 6OHDA with or without a specific inhibitor or with two inhibitors for 2 hours. Subsequently, drug treatment was stopped by removing the old media and replacing it with fresh ReNcell maintenance media. Untreated and treated dDCN were left overnight in CO_2 incubator for recovery (Chaudhry and Ahmed 2013).

Untreated and treated dDCN underwent fixation with 4% paraformaldyde for 15 minutes prior to washing with cold PBS. Subsequently, dDCN were treated with Triton X-100 for 10 minutes and blocked with 10% goat serum (S-1000, Vector Labs Peterborough UK). dDCN were serial washed with cold PBS (3 x 5 minutes) and were left to incubate overnight with primary antibodies at 4°C. The following morning, dDCN were washed with PBS (3 × 5 minutes) and incubated with secondary antibodies for two hours at RT. Cells were mounted using vectorshield mounting medium (158127, Vector Labs Peterborough UK) and were viewed under a Meiji MT6000 fluorescent microscope (Mazurek Warwickshire, UK) (Chaudhry and Ahmed 2013).

dDCN and 6OHDA dDCN were counted under x 20 magnification in 5 fields of vision per area (1.428mm x 1.092mm) of untreated and treated dDCN. The FITC excitation wavelength of 470nm and emission wavelength of 520nm demonstrated cells that were positively stained with green dye. In comparison, cells that were red stained were due to rhodamine excitation of 550nm and emission wavelength of 640nm. To analyse co localisation data effectively, cells that were in the same field and were stained positive for red dye and green dye were counted dDCN. Cell numbers are expressed as the mean per selected field from the wells. Three independent experiments were performed for each sample prior to statistical analysis (T test, $p<0.05$) (Chaudhry and Ahmed 2013).

2.5.3 Determining the amount of Caspase activation in 6OHDA dDCN using WB analysis

dDCN were grown in laminin coated T25 flasks until they had reached 80% confluence. dDCN were exposed to100µM 6OHDA and treated different inhibitors such as zVADfmk, IKK or salubrinal inhibitor for 2 hours. Fresh media was replaced and dDCN were left to recover overnight at 37°C in CO_2 incubator. Cells were detached from laminin coasted flasks with the aid of accutase and collected in labelled centrifuge tubes. Cells were centrifuged at 12000RPM for 8 minutes and the supernatant was removed. The pellet containing the cells was lysed with lysis buffer (HEPES, NaCl, EGTA, glycerophosphate 10% glycerol, 1% Triton,1mM PMSF, 1mM DTT, protease inhibitors) and protein concentration was measured using the BCA kit (Pierce Biotechnology Rockford IL USA).

Fifty micrograms protein was loaded on 12% gel prior to SDS PAGE (40 minutes at 200 volts), followed by immunoblotting on PVDF membrane (90 minutes at 350mAmps).To ensure complete transfer of

proteins from the resolving gel to PVDF membrane, immmunostaining was carried out. The PVDF membrane was stained with Ponceau whilst the gel was stained with Coomassie brilliant blue. The membrane was blocked with 1% skimmed milk for an hour followed by incubation with primary antibodies overnight at 4°C. The next day the membranes were washed with PBS-T (3 x 2 minutes), prior to incubation with secondary antibody for an hour at RT. After washing the membranes with PBST, ECL HRP solution (Perbio Science Northumberland UK) was added to the membrane for 4 minutes, prior to exposing the membrane to X ray. X ray was scanned in densitometer scanner (GS800 Biorad Hertfordshire UK). Band detection and statistical analysis was carried out using the same methods previously described in Section 2.3.4. In addition, to normalise the data prior to statistical analysis the PVDF membrane was reprobed with GAPDH via strip and reprobe method (Section 2.3.5).

2.5.4 Determining activation of Caspases-2,-4 and-8 in NFκB classical pathway and ER stress using in 6OHDA dDCN via 3-(4, 5-dimethylthiazolyl-2)-2, 5-diphenyltetrazolium bromide assay (MTT) assay

dDCN were grown in 96 well plates and were left until 80% confluence. dDCN were treated with different combinations of inhibitors along with 6OHDA for 2 hours after which fresh media was replaced and cells were left to recover overnight (Section 2.5.1). The following day old media was replaced with fresh media prior to the addition of 10µl of MTT (BT30006 Cambridge BioScience Cambridge UK) per well. All samples were left to incubate at 37°C for 4 hours in a 37°C CO_2 incubator. The formazan complex formed was broken by pipetting the dye crystals up and down in each well. Subsequently, samples were placed in microplate reader and the programme Stingray was used to determine the readings of samples at 575nm wavelength. The readings were normalised prior to statistical analysis at $p<0.05$ using ANOVA and student T test. A total of 24 replicates were made for each untreated and treated dDCN per experiment. A total of three independent experiments were conducted and the average of all three experiments was determined to finalise the end conclusion.

Chapter 3
The Effect of Treadmill Exercise on Caspases in PD Animal Model

3.0 PD and CAMKIV

Calmoduline is a ubiquitous calcium binding proteins, which activates enzymes and undergoes conformational changes upon binding with calcium ion. Calcium/calmodulin-dependent protein kinases (CAMKs) have been found in all eukaryotic cells. CAMK-IV is a multifunctional enzyme that plays an essential role in release and synthesis of neurotransmitters, axonal transport and regulating signal transduction in neural cells (Wayman et al 2008).

Redmond and Gosh (2005) explored the role of CAMK-IV in the growth of dendrites in corticol neurons and found CAMK-IV stimulated growth of dendrites, via calcium dependent mechanisms. Ribar et al (2000) observed the appearance of symptoms such as tremors, and loss of motor control in CAMK-IV knockout mice which correlate with the symptoms of PD.

Research by Suntoo et al (2003) has shown that during exercise calcium ions are released from the sarcoma of muscle cells and bind to calcium binding proteins CAMKs. The binding of CAMKs during exercise suppresses activation of the Caspase pathway, thereby preventing cell death. The study indicated that exercise had increased dopamine synthesis in the brain of PD animal model, via the calmodulin dependent pathways. The level of calcium in the serum had increased significantly, resulting in the transfer of calcium to the brain, inducing the synthesis of dopamine. The elevated levels of dopamine regulated a diverse range of brain functions, indicating that exercise may improve some symptoms of PD.

Research by Akimoto et al (2004) signifies that CAMKs have a role in skeletal muscle plasticity. When the levels of CAMK-IV were compared to mice that were in an exercise state to mice that were sedentary, it was found that the mice that were active had increased levels of CAMK-IV present in the skeletal muscle. This contributed to the higher rate of contractibility of skeletal muscle and, in addition fibre switching was observed.

3.1 Exercise, Caspase and PD

In the last few years, much progress has been made in understanding the effect of physical exercise on improvement of different diseases including PD (Chapter 1 Section 1.2.5). Exercise has been shown to improve neuromuscular interaction, neurogenesis and trophic factors, leading to initiate functional and morphological changes in both normal and injured brain (Chapter 1 Section 1.2.5). These changes are predominantly found in various motor regions of the brain that include motor cortex, basal ganglia, cerebellum and red nucleus (Graybiel 2005, De Zeeuw and Yeo 2005, Holschneider et al 2007).

Lee et al (2003) found that treadmill exercise had decreased Caspase-3 activity in the striatum of intracerebral haemorrhaged rats. Rats underwent treadmill exercise for 30 minutes every day for 10 days. The results showed that sedentary rats had greater loss of neurons in the striatum, increased Caspase-3 activity and bigger size haemorrhage compared to rats that had exercised. Exercise had decreased the size of haemorrhage, lowered Caspase-3 activity and prevented loss of striatal neurons.

IF analysis has shown an increase in Caspase-3 activation, formation of apoptotic bodies and degeneration neurons of spinal cord in rotenone induced rats. TUNEL staining confirmed that rotenone induced apoptotic death of spinal neurons in rats. WB analysis demonstrated high levels of active Calpain and Caspase-3 in spinal cord rotenone treated rat homogenates, signifying that rotenone triggered apoptotic death of spinal cord neurons via Caspase and Calpain mediated death in PD rat model (Samantary et al 2003).

IF analysis revealed loss of TH positive cells of 6OHDA and MPTP-treated rat mesencephalic cultures. The broad Caspase inhibitor zVADfmk had prevented loss of TH positive cells in the midbrain of 6OHDA and MPTP rat, indicating that loss of DCN is Caspase mediated. WB analysis had revealed increase in active Caspases-3 and -9 as well cytochrome c in PD rat animal model, indicating Caspase mediated death of DCN is via intrinsic pathway (Han et al 2003).

Immunohistochemical and WB analysis revealed high levels of Caspase-3 in MPTP-treated rat mesencephalon cultures, demonstrating that Caspase-3 is active in DCN of PD animal model. IF analysis revealed formation of apoptotic bodies and loss of TH positive cells, indicating MPTP triggered Caspase mediated death of DCN in the midbrain of PD rat model (Hartmann et al 2000). WB analysis showed high levels of active Caspases-3 and 9 in MPTP-treated striatum mice homogenates, indicating that MPTP triggered activation of Caspases-3 and -9 in striatum of mice in PD animal model. IF analysis revealed formation of apoptotic bodies, destruction and loss of striatal neurons in MPTP mice, signifying that MPTP triggered apoptotic death of cells (Zhang et al 2013b).

WB analysis revealed elevated amounts of cytochrome c and BAX and a decrease of BCL-2 in striatum of 6OHDA-treated rat. Lipid peroxidation of 6OHDA-treated rat striatum was confirmed with lipid peroxidation markers thiobarbituric. Caspase specific assays measured elevated levels of Caspases-3 and -9 activity in 6OHDA-treated striatum of PD rat model. Enzyme-linked immunosorbent (ELISA) analysis revealed higher levels of cytokines TNF-α and IL-1β in 6OHDA-treated rat striatum. The antioxidant, piperine had inhibited lipid peroxidation, TNF-α, -1β, cytochrome c, BAX, Caspases-3 and -9 activities in the striatum of 6OHDA-treated rats, indicating 6OHDA triggers Caspase-3 and 9 mediated apoptotic death of striatal neurons, through mitochondrial and inflammatory routes via oxidative stress (Shrivastava et al 2013).

Elevated Capases-3,-8 and -9 activities were found in heart ventricle homogenates of hypoxic sedentary rats. WB analysis demonstrated decrease in BCL-2 and increase in BAX levels in non exercised hypoxic rats. Treadmill running for an hour everyday for 5 weeks had decreased lipid peroxidation, BAX, mitochondrial swelling, Caspases-3,-8 and -9 activities whilst increasing superoxide dismutase and BCL-2 levels in the heart ventricles of hypoxic rats. These findings signified that exercise can prevent Caspase mediated apoptotic death of the heart (Magalhaes et al 2014).

Schulz (2006) suggested that to facilitate survival of nigrostriatal dopaminergic neurons, the major Caspase stimulation pathway (the mitochondrial apoptosis pathway) should be suppressed, as prevention of individual Caspases can only encourage short term survival of neuronal cells. Murlastis et al (2007) observed that exercise reduced ER stress in Ischemic Sprague- Dawley rats, when compared to the control. In addition, reductions in ER stress protein levels were found in the exercised Ischemic rats when compared to the sedentary rats. Furthermore, mice which endured regular exercise had an increased quantity of dendritic growth in cortical neurons and synapses present when compared to the control group. In addition, a decrease in DNA oxidative damage and lipid peroxidation was found (Mattson et al 2004)

3.2 Relevance of Treadmill Exercise on Caspases in MPTP animal model

Current research shows that exercise is an effective treatment and reduces symptoms of PD (Ayan and Cancela 2012, Heiberger et al 2011, Fritz et al 2011, Vivas et al 2011, Hackney and Earhart 2010, Li et al 2012, Dreu et al 2012,). There are extensive clinical studies carried out on treadmill exercise in PD patients, showing that treadmill exercise decreases PD symptoms, at the same time, it has positive effect on the quality of life of PD patients in terms of forming social networks (Paterson et al 2005, Brown et al 2010, C.Haas personal communication). Overall, exercises show some improvement in decreasing key features of PD, such as gait, tremors and bradykinesia (Chapter 1 Section 1.2.5). Although there are extensive clinical studies carried out on treadmill exercise in PD patients, there is a lack of biochemical understanding as to how exercise is affecting PD patients at a cellular level. Effect of exercise on expression or inhibition of different proteins has not been determined yet. There is a lack of research exploring the potential pathways, which exercise may activate and suppress to provide such positive and even negative effects.

The current study is the first to explore the effect of six week treadmill exercise on active Caspases, along with CAMK-IV protein in different brain regions. More specifically, the level of various Caspases (Caspase-1,-2,-3,-8,-9 and -12) was explored in different brain regions such as cerebellum, brain cortex, midbrain and striatum of C, Ex, PD and PD-Ex animal model. The presence and absence of different Caspases along with CAMK-IV in brain regions of PD animal model after undergoing six week treadmill exercise was carried out to determine the influence of exercise and its beneficial effects in PD so that new therapies can be made.

Aim: To determine the presence and absence of active and cleaved Caspases-1,-2,-3,-8,-9,-12 and CAMK-IV in PD-Ex brain cortex, cerebellum, midbrain and striatum of PD rat animal model.

3.3 Method : Determining the Effect of Endurance Exercise on Caspase and CAMK-IV Activities in C, Ex, PD and PD-Ex Animal Model

3.3.1 Endurance training, segregation and treatment of rats

Procedure for training, segregation and MPTP injection performed by collaborators Jozef Langfort and Malgorzata Chalmoniuk at Dr Jozef Langfort laboratories Medical Research Centre, Polish Academy of Sciences, Warsaw, Poland. Rats were housed in temperature controlled room under 12 hour daylight/ night cycle at animal breeding facility. Rats were fed rodent chow and water ad libitum to consume at regular intervals.

For the study, eight weeks old Wistar male rats) were segregated into four groups (n=4 for each group) to endure four conditions; control (untreated and un-trained (C), trained (Ex), MPTP-treated (PD) and PD-Ex (MPTP-treated and trained). Rats that were categorised to the C group received saline injection (i.p.) and remained sedentary (Figure 3.1). In the Ex group rats ran on motor-driven rodent treadmill for 28 m x min-1 for 1 hour every day for 6 weeks and received saline injection (i.p.). In the PD group, rats did not exercise and after 6 weeks rats received three injections of MPTP in saline (i.p.) at 2 hours intervals in a total dose 60mg/kg. In the PD-Ex group, rats ran on motor-driven rodent treadmill for 28 m x min-1 for 1 hour every day for 6 weeks. Following completion of the 6th week of training, rats received three injections of MPTP in saline (i.p.) at 2 hours intervals in a total dose 60mg/kg. Rats were sacrificed on 14 days after the MPTP injection. Prior to sacrifice, all rats were deeply anaesthetised with sodium pentobarbital. Rats were sacrificed by decapitation and the brains were removed and regions were dissected on ice. Different brain regions were collected, snap-frozen in liquid nitrogen and stored at -80°C prior to being shipped to the University of Bedfordshire, Luton, UK.

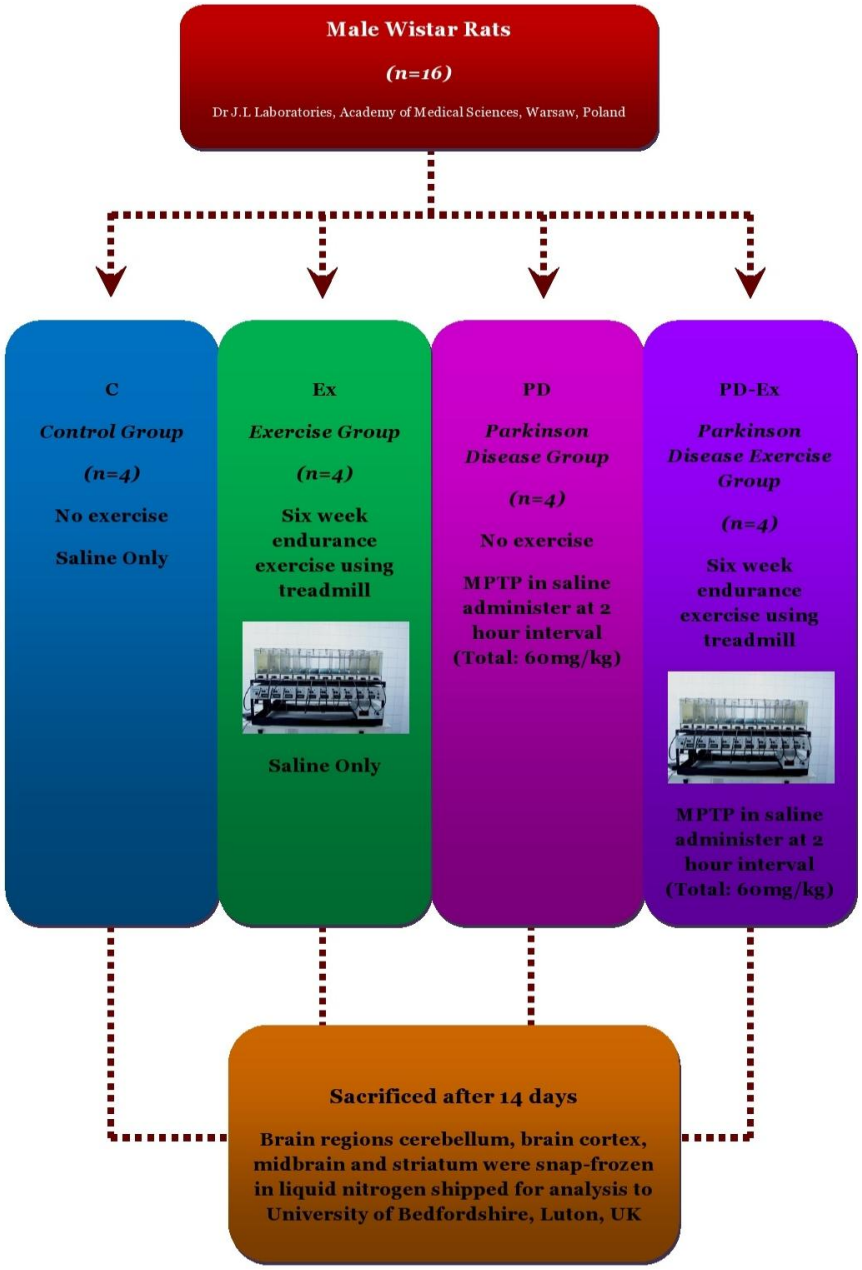

Figure 3.1 : Segregation and treatments of C, Ex, PD, PD-Ex groups in PD animal model

Sixteen male Wistar rats were categorised in groups of four and each segregated group (C, Ex, PD, PD-Ex) was exposed to specific conditions. Rats in the C group remained sedentary and received saline injection (i.p.). Ex group underwent treadmill training every day for one hour for six weeks and received saline injection (i.p.). PD group did not exercise and received systemic MPTP injection in saline (i.p.). PD-Ex group had undergone treadmill training every day for an hour for six weeks. After completion of treadmill exercise PD-Ex group received systemic MPTP injection in saline (i.p.). Procedures carried out by collaborators Jozef Langfort and Malgorzata Chalmoniuk at Dr Jozef Langfort laboratories Medical Research Centre, Polish Academy of Sciences, Warsaw, Poland.

3.3.2 BCA Protein Assay and WB

All brain regions i.e. cerebellum, brain cortex, midbrain and striatum from each group were homogenised followed by ultracentrifuged at 100 000 x g for 70 minutes at 4°C. The supernatant was removed and protein concentration was determined via BCA (Pierce Biotechnology Rockford IL USA) protein assay. All samples (50µg protein) were loaded on 12% SDS gel and were SDS-PAGED at 200 volts for an hour. Proteins were transferred from the resolving gel to nitrocellulose membrane via immunoblotting (350 mAmps for 90 minutes), followed by 30 minute blocking with 1% milk solution. Subsequently, the membrane was incubated with primary and secondary antibodies for overnight at 4°C and 2 hours at RT respectively. Primary antibodies; Anti-Caspase-1(1:50, Abcam Cambridge UK), Anti-Caspase-2 (1:250, Abcam Cambridge UK), Anti-Caspase-3 (1:1000, Millipore Hertfordshire UK), Anti-Caspase-8(1:1000, Abcam Cambridge UK), Anti-Caspase-9 (1:1000, Millipore Hertfordshire UK, Anti-Caspase-12 (1:500, Abcam Cambridge UK), Anti-CAMK-IV(1:2500, Millipore Hertfordshire UK), and secondary antibody Goat-Anti-Rabbit HRP (1:1000, Millipore Hertfordshire UK) were used. Membranes were incubated with ECL solution (Perbio Science Northumberland UK) for 5 minutes, prior to exposure and development via X-ray film (FMXOB0101824, Xograph Gloucestershire UK). Band analysis was carried out using a densitometer (GS800, Bio-Rad Hertfordshire UK). Blots were normalised against GAPDH prior to statistical analysis (ANOVA $p<0.05$, T test $p<0.05$ Chapter 2 Section 2.3.4). In some instances stripping and reprobing with other antibodies was carried out (Chapter 2 Section 2.3.5). A more detailed account of these procedures and reagents used can be found in Chapter 2 Section 2.1 and Section 2.3 and Appendix 1 correspondingly.

3.4 Results

The aim for this part of the project was to determine the effect of six week treadmill exercise on Caspases-1, 2,-3,-8,-9 and -12 in the cerebellum, brain cortex, midbrain and striatum of PD animal model. Caspase-1 was not detected in any regions (brain cortex, striatum, cerebellum and midbrain) of C, Ex, PD and PD-Ex Rat. This indicated that Caspase-1 was not present in the brain in this PD model. To ensure that Caspase-1 was not present in PD animal model the PVDF membrane was stripped and reprobed with another antibody GAPDH. The membrane showed positive staining of GAPDH antibody. In addition, the antibody concentration to detect Caspase-1 was increased to maximise any binding of Caspase-1 from the samples, but there was no presence of Caspase-1 in the brain regions of C, Ex, PD and PD-Ex group. Furthermore, the sample concentration was also increased so that the Caspase-1 protein present in the samples would bind to the antibody. However, there was detection of Caspase-1 from the highly concentrated antibody. Ponceau staining of PVDF membrane and Coomaisse staining of the resolving gel had showed successful transfer of all the proteins in the gel onto the membrane. Fewer washes with PBST were carried out between antibody incubation times to determine if Caspase-1 protein was detected in PVDF membrane. Furthermore, a lower concentration of blocking buffer containing 0.1% milk solution was used as it may have been that the blocking reagent had blocked all the specific and non specific binding sites. Different blocking buffer was also tried but still there was no detection of Caspase-1 in the brain regions of C, Ex, PD and PD-Ex group. Collectively, the work suggested that Caspase-1 is not detected in any regions of the brain in PD animal model.

WB analysis was performed to detect and measure the amount of active Caspase-2 in the brain cortex of PD-Ex animal model. Caspase-2 is an initiator Caspase, which when activated promotes stimulation of other downstream proteins such as Caspase-3 resulting in cell death (Chaudhry and Ahmed 2014). ANOVA ($p<0.01$) and T test ($p<0.05$) had shown a difference in the amount of Caspase-2 present in brain cortex of PD and PD-Ex animal model. A 32% increase in the amount of active Caspase-2 was detected in the brain cortex of PD sedentary rats, indicating that MPTP may have triggered Caspase-2 activation in the brain cortex. In contrast, a significant reduction in active Caspase-2 levels was present in brain cortex of PD-Ex group, indicating that exercise may have reduced active Caspase-2 activation in brain cortex of PD animal model (Figure 3.2).

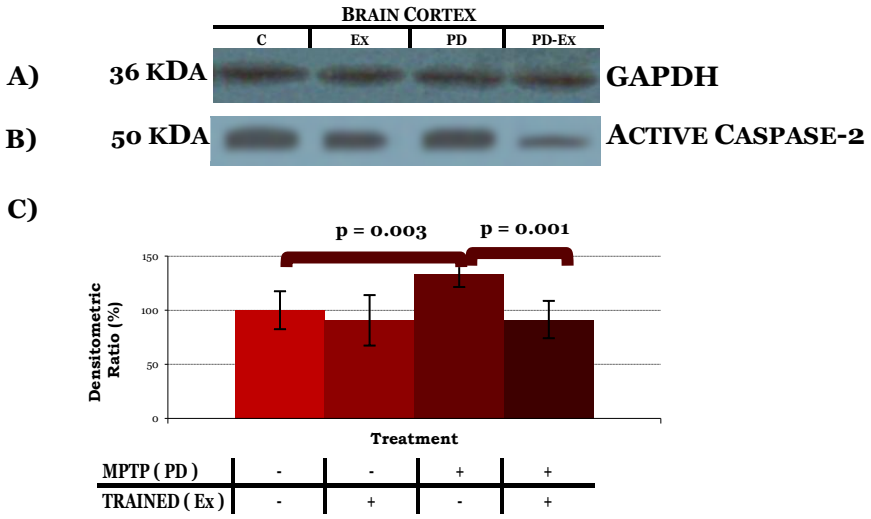

Figure 3.2: The effect of Exercise on active Caspase-2 in brain cortex of PD animal model

A) Illustrative example of GAPDH in brain cortex of PD animal model

B) Illustrative example of active Caspase-2 in brain cortex of PD animal model

C) Active Caspase-2 was present in the brain cortex of C, Ex, PD and PD-Ex rats. A significant amount of active Caspase-2 had decreased (41% reduction) in brain cortex of PD-Ex group compared to PD brain cortex ($p<0.01$), indicating that treadmill exercise may have reduced active Caspase-2 in the brain cortex of PD animal model. Means of five experiments ± SEM shown. Table of densitometry values and statistical analysis can be found in Figure 3.3, Appendix 3.

WB analysis was carried out to determine the effect of treadmill exercise on Caspase-3 in the brain cortex in PD animal model. Caspase-3 is a late marker of apoptotic death in cells and has been associated with death of DCN in PD pathogenesis in vivo and in vitro analysis (Chaudhry and Ahmed 2014). A significant rise in cleaved Caspase-3 was observed in brain cortex of PD rats that did not undergo treadmill exercise, suggesting that MPTP may have triggered Caspase-3 dependent death in the brain cortex (ANOVA $p<0.05$, T test $p<0.05$). In contrast, endurance exercise had reduced Caspase-3 levels in PD-Ex brain cortex, indicating that exercise may have reduced Caspase-3 activity in the brain cortex, thereby reducing apoptotic death of neurons (Figure 3.4).

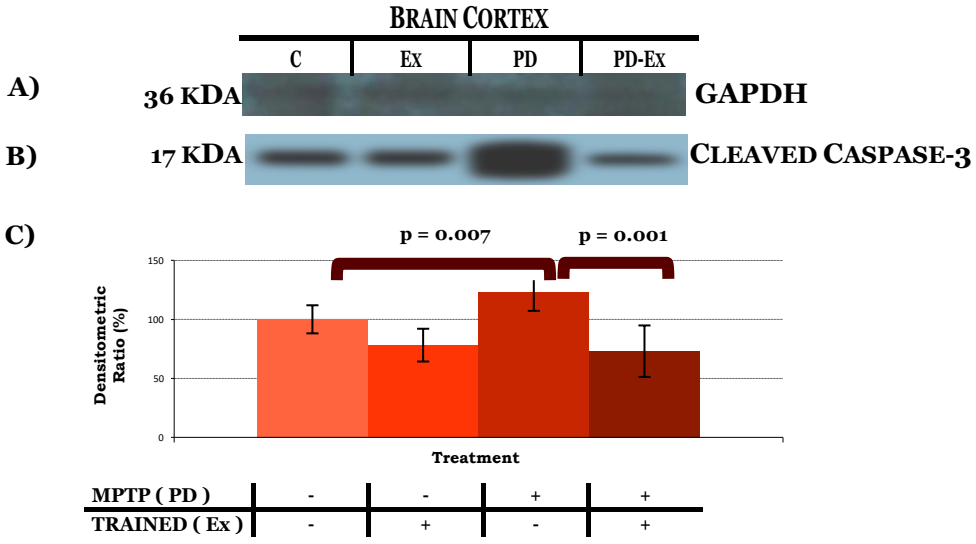

Figure 3.4 : Treadmill Exercise reduces cleaved Caspase-3 in PD animal brain cortex

A) Illustrative example of GAPDH in brain cortex of PD animal model

B) Illustrative example of cleaved Caspase-3 in brain cortex of PD animal model

C) Cleaved Caspase-3 was present in the brain cortex of C, Ex, PD and PD-Ex rats. A 22% decrease of cleaved Caspase-3 amount was detected in brain cortex of Ex group when compared to the C group. In comparison, 23% increased level of Caspase-3 was detected in brain cortex of sedentary PD samples, indicating that MPTP can increase Caspase-3 levels in brain cortex of PD model. On the other hand, Treadmill exercise significantly decreased cleaved Caspase-3 levels in brain cortex of PD-Ex group (50 % reduction, $p<0.01$) compared to PD group. Means of five experiments ± SEM shown. Table of densitometry values and statistical analysis can be found in Figure 3.5, Appendix 3.

To further explore the effect of exercise on Caspases in the brain cortex in PD animal model, Caspase-8 protein was examined. Caspase-8 is another initiator Caspase, which upon activated promotes stimulation of other downstream proteins such as Caspase-3 resulting in death of DCN (Chaudhry and Ahmed 2014). The results illustrated presence of high levels of active Caspase-8 in brain cortex of PD rats, highlighting that MPTP may have triggered activation of the initiator Caspase-8, which may result in activation of other proteins via the Caspase cascade (ANOVA $p<0.05$, T test $p<0.05$). In comparison, a significant decrease in Caspase-8 was measured in PD-Ex group, indicating that exercise might have promoted survival and have reduced death of cortical neurons in PD rat samples (Figure 3.6).

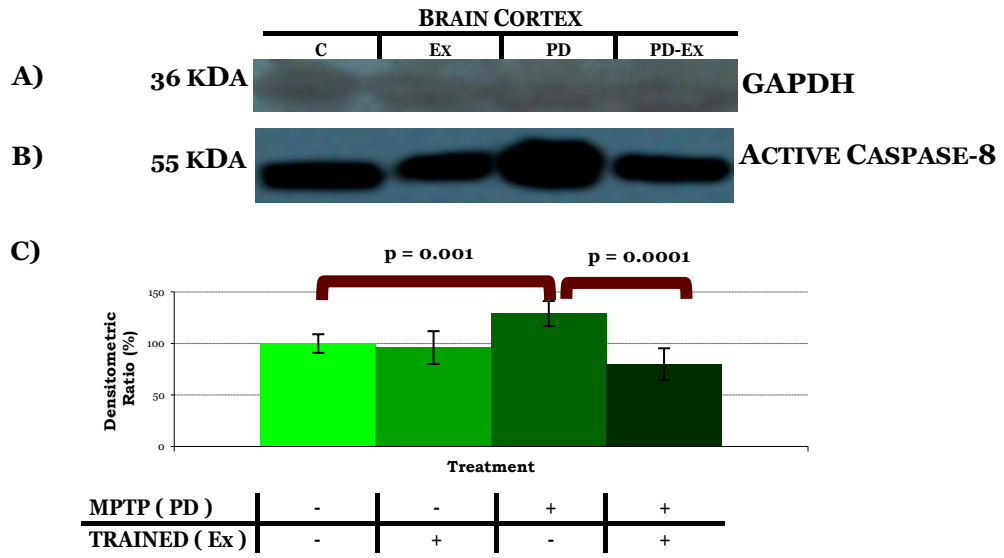

Figure 3.6 : Low levels of Caspase-8 found in exercised brain cortex of PD animal model

A) Illustrative example of GAPDH in brain cortex of PD animal model

B) Illustrative example of active Caspase-8 in brain cortex of PD animal model

C) Active Caspase-8 was present in the brain cortex of C, Ex, PD and PD-Ex rats. Similar Caspase-8 levels were found in brain cortex of sedentary (C group) and exercise (Ex group) rats. The amount of Caspase-8 had increased in brain cortex of PD rats that did not exercise by 29%. A significant decrease in Caspase-8 levels was found in brain cortex of PD rats that endured treadmill exercise for six weeks (49% reduction, $p<0.01$), compared to PD group. Means of five experiments ± SEM shown. Table of densitometry values and statistical analysis can be found in Figure 3.7, Appendix 3.

WB analysis was used to determine the amount of active Caspase-9 present in the brain cortex of C, Ex, PD and PD-Ex rats. Previous research has shown activation of Caspase-9 to be associated with the mitochondrial pathway leading to activation of other downstream proteins such as Caspase-3 resulting in cell death (Fan et al 2005, Chaudhry and Ahmed 2014). Similar levels of active Caspase-9 were detected in brain cortex of the C, Ex and PD group, indicating that MPTP had no significant influence on Caspase-9 activity in brain cortex ($p>0.05$). Interestingly, a significant rise in the amount of active Caspase-9 was measured in the brain cortex of PD-Ex group when compared to PD group ($p<0.05$), suggesting that treadmill exercise may have triggered Caspase-9 activity in brain cortex in PD animal model (Figure 3.8).

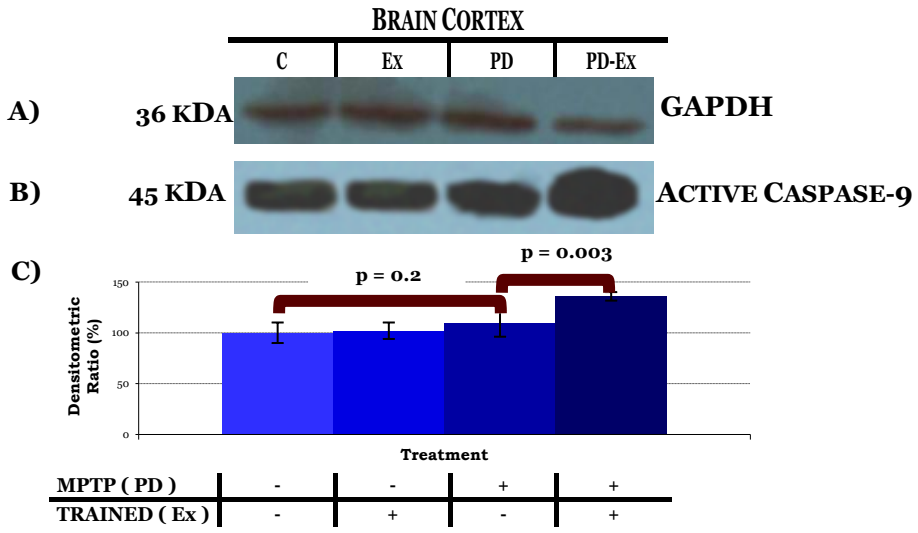

Figure 3.8 : Endurance exercise can increase active Caspase-9 levels in brain cortex of PD animal model

A) Illustrative example of GAPDH in brain cortex of PD animal model

B) Illustrative example of active Caspase-9 in brain cortex of PD animal model

C) Active Caspase-9 was present in the brain cortex of C, Ex, PD and PD-Ex rats. Similar amount of active Caspase-9 were in brain cortex of C, Ex and PD animal model (100%, 102% and 109%). A siginifcant increase of active Caspase-9 levels were determined in brain cortex of PD-Ex group compared to PD group (26% increase, $p<0.01$). Means of five experiments ± SEM shown. Table of densitometry values and statistical analysis can be found in Figure 3.9, Appendix 3.

The influence of endurance exercise on the amount of Caspase-12 in brain cortex in PD animal model was determined via WB analysis. Activation of Caspase-12 has been associated with ER stress pathway that contributes to death of cells (Doyle et al 2011, Yoshida 2007). In addition, active Caspase-12 promotes Caspase-9 stimulation, bypassing the intrinsic mitochondrial route, resulting in Caspase-3 activation and cell death (Fan et al 2005). Elevated levels of cleaved Caspase-12 were detected in brain cortex of PD sedentary rats when compared to the C group, indicating that MPTP may have trigger Caspase-12 activation in brain cortex of PD rat (ANOVA $p<0.05$, T test $p<0.05$). Furthermore, a significantly reduced the amount of cleaved Caspase-12 was measured in the brain cortex of PD-Ex group, suggesting that exercise may have decreased cell death associated with Caspase-12 activation (Figure 3.10).

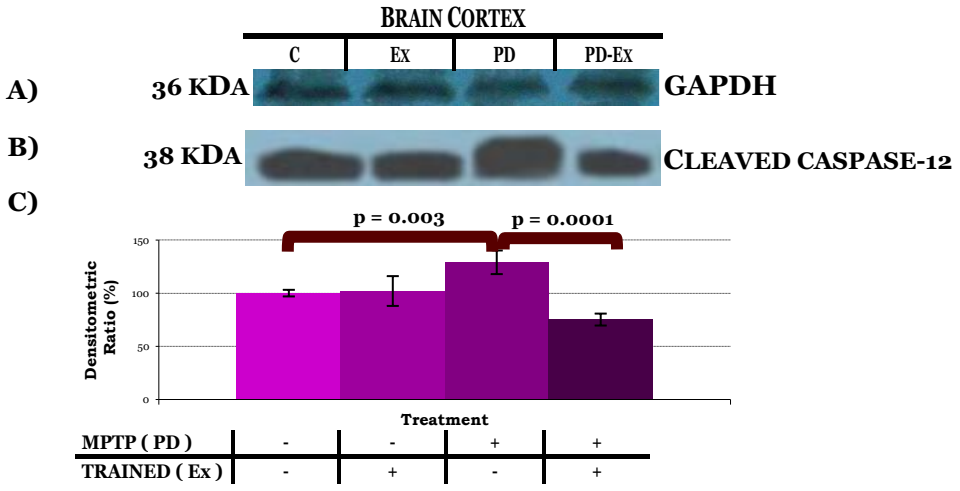

Figure 3.10 : Cleaved Caspase-12 is decreased exercised brain cortex of PD animal model

A) Illustrative example of GAPDH in brain cortex of PD animal model

B) Illustrative example of cleaved Caspase-12 in brain cortex of PD animal model

C) Cleaved Caspase-2 was present in the brain cortex of C, Ex, PD and PD-Ex rats. Caspase-12 was found in similar levels in brain cortex of C and Ex group. A 29% increase in the amount of Caspase-12 was found in brain cortex of PD rats indicated MPTP had triggered Caspase-12 activity in rat brain cortex ($p<0.01$). A 54% decrease in Caspase-12 levels was measured in brain cortex of PD-Ex rats compared to PD rats ($p<0.01$). Means of five experiments ± SEM shown. Table of densitometry values and statistical analysis can be found in Figure 3.11, Appendix 3.

The current study was extended further by investigating the presence and absence of active Caspases in the cerebellum of C, Ex, PD and PD-Ex rats. There was no significant difference in the amount of active Caspase-2 in the cerebellum of PD rats compared to the C group ($p>0.05$), suggesting that MPTP had not promoted Caspase-2 activation in the cerebellum of PD animal model. In contrast, a significant decrease ($p<0.05$) in active Caspase-2 levels was determined in the cerebellum of PD-Ex group when compared to the PD group; this indicated that exercise may have reduced Caspase-2 activity in the cerebellum (Figure 3.12).

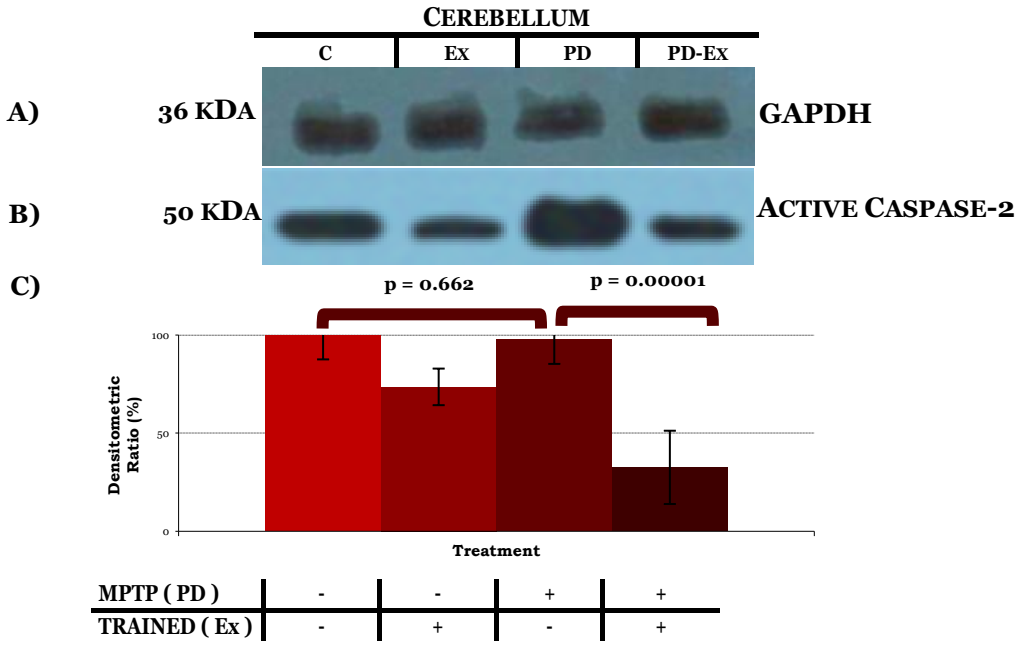

Figure 3.12: The effect of Exercise on Caspase-2 in cerebellum of PD animal model

A) Illustrative example of GAPDH in cerebellum of PD animal model

B) Illustrative example of active Caspase-2 in cerebellum of PD animal model

C) Active Caspase-2 was present in the cerebellum of C, Ex, PD and PD-Ex rats. No significant difference in the amount of active Caspase-2 was present in the C and PD rat cerebellum ($p>0.05$). Graph shows a reduction in the amount of active Caspase-2 (66% decrease) present in the cerebellum of PD rats that underwent treadmill training ($p<0.05$), compared to PD sedentary rats. Means of five experiments ± SEM shown. Table of densitometry values and statistical analysis can be found in Figure 3.13, Appendix 3.

WB analysis was used to measure the amount of cleaved Caspase-3 levels in the cerebellum of PD and PD-Ex animal model. The results demonstrate an increase in the amount of cleaved Caspase-3 in the cerebellum of PD group compared to C group (ANOVA $p<0.05$, T test $p<0.05$), indicating that MPTP up regulated Caspase-3 activity in the cerebellum. Furthermore, there was a lower amount of cleaved Caspase-3 present in cerebellum of PD-Ex group compared to PD group, indicating that exercise may have lowered Caspase-3 activity in the cerebellum of PD animal model (Figure 3.14).

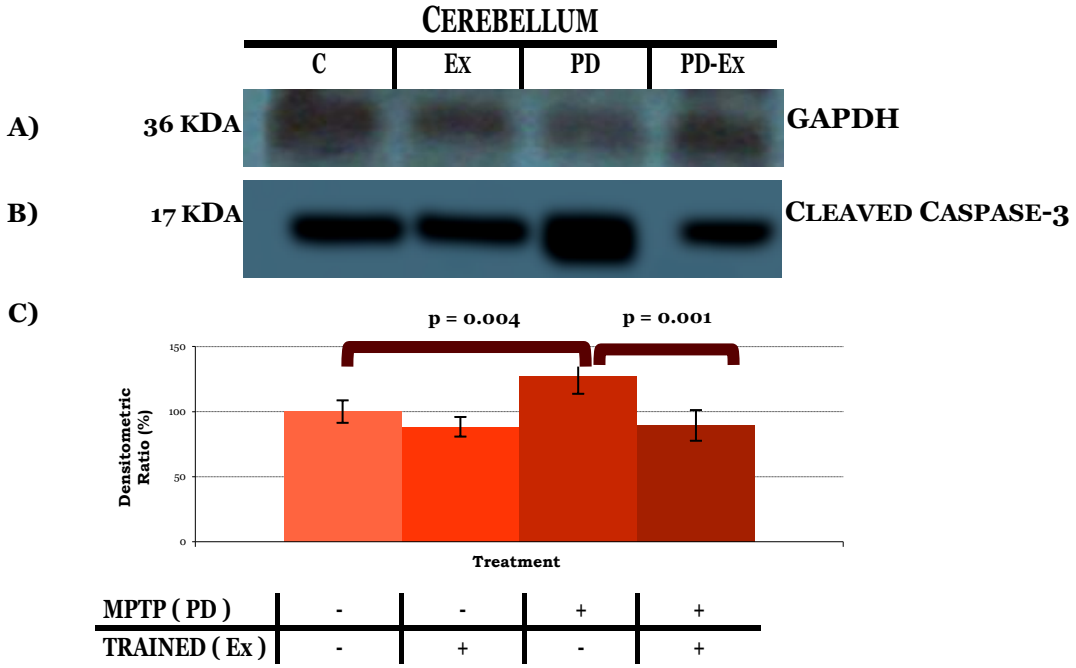

Figure 3.14 : Cleaved Caspase-3 is reduced in cerebellum of PD-Ex animal model

A) Illustrative example of GAPDH in cerebellum of PD animal model

B) Illustrative example of cleaved Caspase-3 in cerebellum of PD animal model

C) Cleaved Caspase-3 was present in the cerebellum of C, Ex, PD and PD-Ex rats. Graph shows MPTP had increased the amount of cleaved Caspase-3 in the cerebellum of PD group compared to C group (27% increase, $p<0.01$), signifying that MPTP triggers Caspase-3 activity in cerebellum of PD animal model. In comparison, a 38% decrease in cleaved Caspase-3 was measured in cerebellum of PD-Ex rat compared to PD group ($p<0.05$). Means of five experiments ± SEM shown. Table of densitometry values and statistical analysis can be found in Figure 3.15, Appendix 3.

The influence of endurance exercise on the amount Caspase-8 in cerebellum in PD animal model was determined via WB analysis. Elevated levels of active Caspase-8 were detected in cerebellum of PD sedentary rats when compared to the C group, indicating that MPTP may have triggered Caspase-8 activity (ANOVA $p<0.05$, T test $p<0.05$). A significant decrease in active Caspase-8 was measured in the cerebellum of PD-Ex group compared to PD group suggesting that endurance exercise may have decreased Caspase-8 activity in the cerebellum of PD animal model (Figure 3.16).

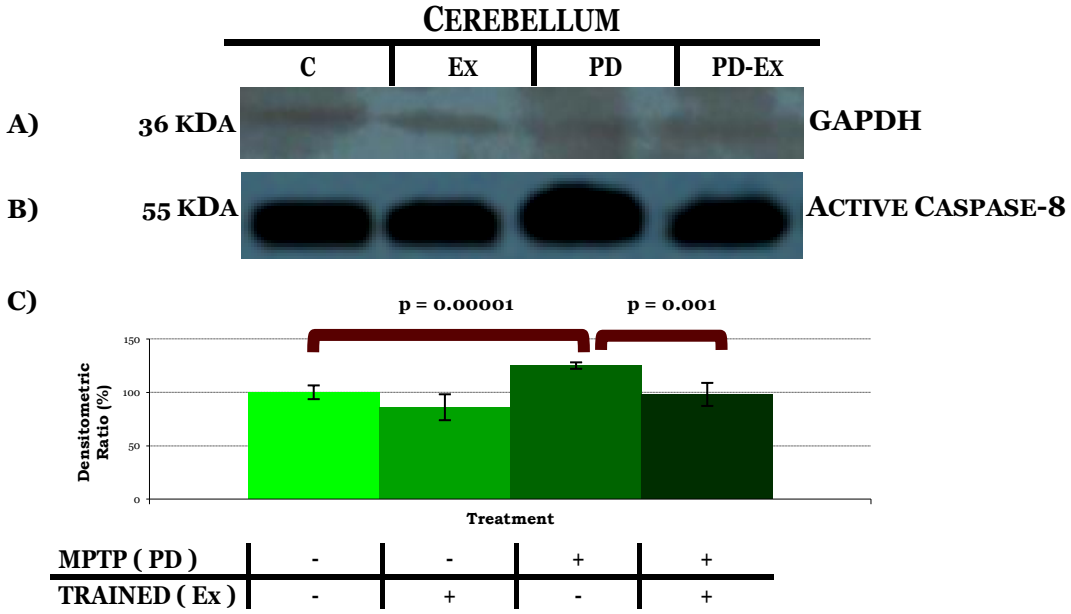

Figure 3.16 : Active Caspase-8 is decreased in cerebellum of PD-Ex animal model

A) Illustrative example of GAPDH in cerebellum of PD animal model

B) Illustrative example of active Caspase-8 in cerebellum of PD animal model

C) Active Caspase-8 was present in the cerebellum of C, Ex, PD and PD-Ex rats. Graph shows sedentary PD rats had higher amount of active Caspase-8 present in the cerebellum compared to C cerebellum (25% increase, $p<0.01$). In contrast a 27% decrease in active Caspase-8 levels was measured in the cerebellum of PD rats that underwent treadmill training ($p<0.01$) when compared to PD group. Means of five experiments ± SEM shown. Table of densitometry values and statistical analysis can be found in Figure 3.17, Appendix 3.

The amount of active Caspase-9 level was determined in the cerebellum of PD rats that underwent endurance exercise, using WB analysis. No difference in the amount of active Caspase-9 was found in the cerebellum of the PD group compared to the C group ($p>0.05$), indicating that MPTP did not increase Caspase-9 levels in the rat cerebellum. In contrast to the other Caspases explored, such as Caspases-2,-3 and-8, which showed decreased the levels of these Caspases in PD-Ex group, an increase in active Caspase-9 was in cerebellum of PD-Ex group ($p<0.05$), indicating that treadmill exercise may have increased Caspase-9 activity in the cerebellum of PD animal model (Figure 3.18).

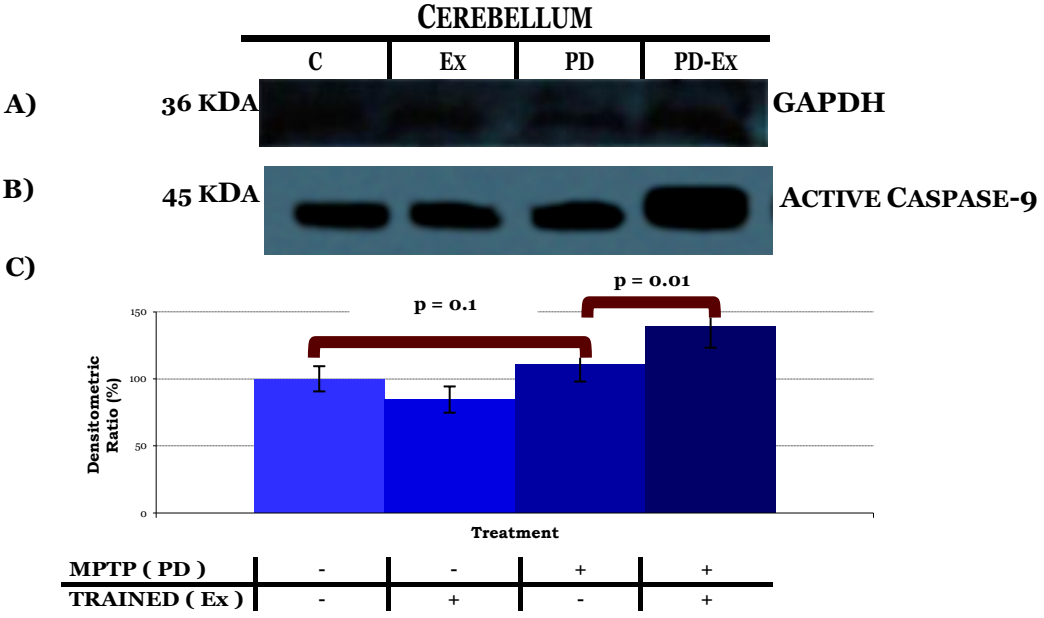

Figure 3.18 : Active Caspase-9 is increased exercised cerebellum of PD animal model

A) Illustrative example of GAPDH in cerebellum of PD animal model

B) Illustrative example of active Caspase-9 in cerebellum of PD animal model

C) Active Caspase-9 was present in the cerebellum of C, Ex, PD and PD-Ex rats. Similar level of active Caspase-9 was determined in C and MPTP-treated cerebellum (100%, 111% $p>0.05$), suggesting that MPTP did not amplify Caspase-9 activity in the cerebellum. A 28% increase of active Caspase-9 was observed in the PD-Ex cerebellum compared to the PD group ($p<0.05$). Means of five experiments ± SEM shown. Table of densitometry values and statistical analysis can be found in Figure 3.19, Appendix 3.

WB analysis was used to determine the amount of cleaved Caspase-12 present in the cerebellum of C, Ex, PD and PD-Ex rats. The results demonstrate elevated levels of cleaved Caspase-12 in the cerebellum of PD sedentary rats compared to C group ($p<0.05$) indicating that MPTP may have further increased Caspase-12 activity in the cerebellum. In contrast, a significant reduction in cleaved Caspase-12 was measured in the cerebellum of PD-Ex group compared to PD group ($p<0.05$), indicating that exercise may have lowered Caspase-12 activity in the cerebellum of PD animal model (Figure 3.20).

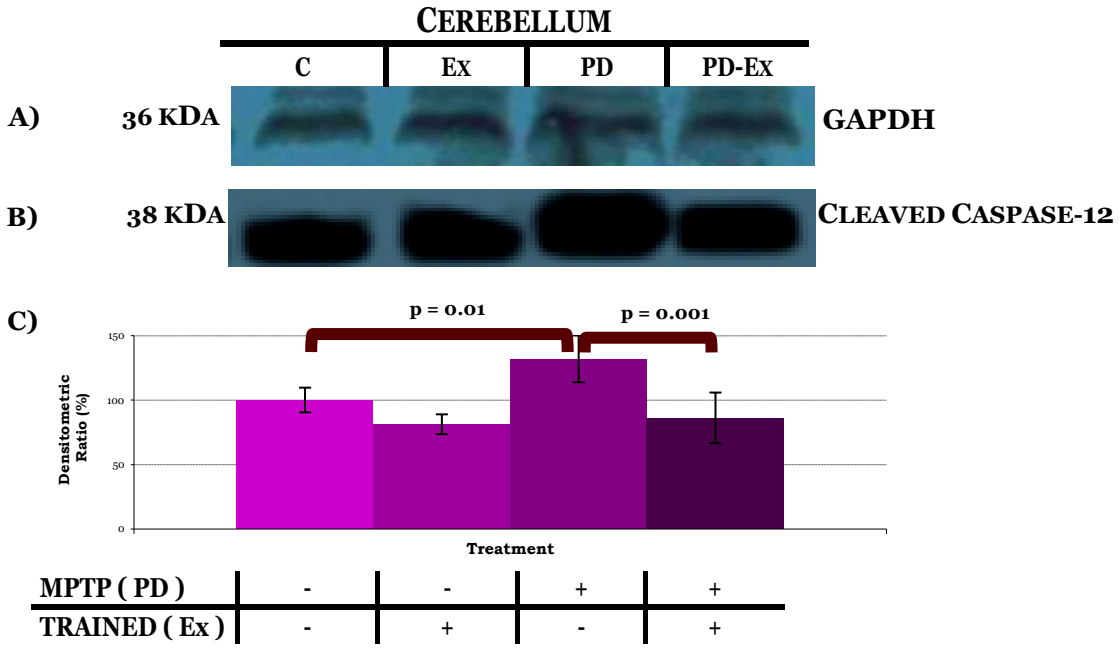

Figure 3.20 : Low levels of cleaved Caspase-12 detected in exercised cerebellum of PD animal model

A) Illustrative example of GAPDH in cerebellum of PD animal model

B) Illustrative example of cleaved Caspase-12 in cerebellum of PD animal model

C) Cleaved Caspase-12 was present in the cerebellum of C, Ex, PD and PD-Ex rats. A 32% increase in cleaved Caspase-12 was detected in cerebellum of PD animal model compared to C group ($p<0.05$). Cleaved Caspase-12 levels were decreased by 46% in cerebellum of PD-Ex group compared to PD group brain ($p<0.01$). Means of five experiments ± SEM shown. Table of densitometry values and statistical analysis can be found in Figure 3.21, Appendix 3.

The results had shown some changes in the amount of specific Caspases after six week treadmill exercise in cerebellum and brain cortex of PD animal model. However, the midbrain that contains the SN, may give a better indication of the influence of exercise on active Caspases in PD. The next aim was to determine the effect of exercise on Caspases in the midbrain of PD animal model. The results portray a significant increase in the amount of active Caspase-2 present in midbrain of PD rats ($p<0.01$), highlighting that MPTP may have triggered activation of the initiator Caspase-2, which may result in activation of other proteins via the Caspase cascade. In comparison, Caspase-2 was absent in the midbrain of PD-Ex group, indicating that endurance exercise may have completely inhibited Caspase-2 activity in the midbrain of PD animal model (Figure 3.22).

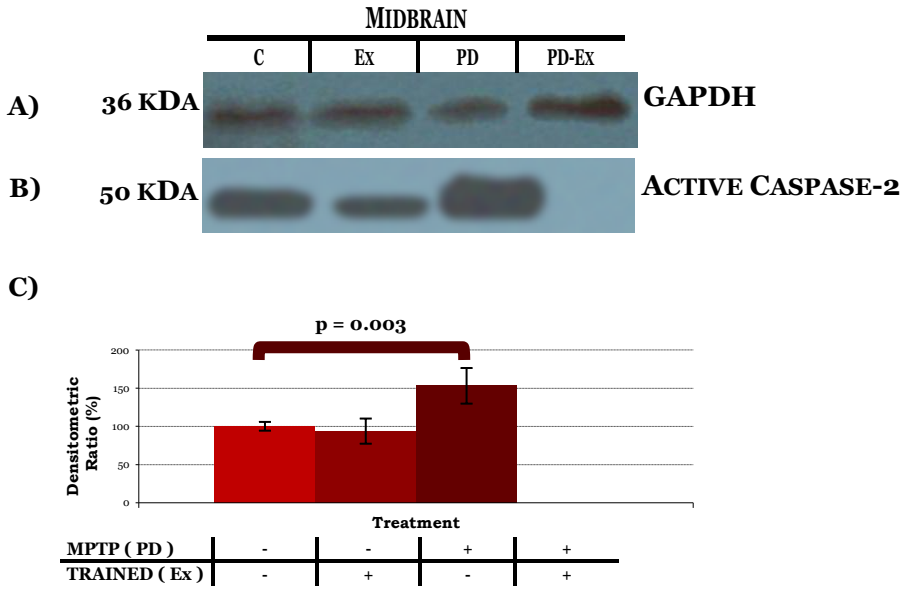

Figure 3.22 : Caspase-2 is absent in exercised midbrain of PD animal model

A) Illustrative example of GAPDH in midbrain of PD animal model

B) Illustrative example of active Caspase-2 in midbrain of PD animal model

C) Active Caspase-2 was present in the midbrain of C, Ex, and PD animal model. The midbrain of C and Ex group rats had similar levels of active Caspase-2. A significant increase (53% increase) in the amount of active Caspase-2 was found in midbrain of PD animal model compared to C group ($p<0.01$). Active Caspase-2 was absent in midbrain of PD rats that underwent treadmill exercise. Means of five experiments ± SEM shown. Table of densitometry values and statistical analysis can be found in Figure 3.23, Appendix 3.

WB analysis was used to determine the amount of cleaved Caspase-3 present in the midbrain of C, Ex, PD and PD-Ex rats. The results portray a rise in cleaved Caspase-3 levels in the midbrain of sedentary PD rat, compared to C group, indicating that MPTP may have promoted further activation of Caspase-3 in the midbrain ($p<0.01$). A significant decrease in cleaved Caspase-3 was measured in the midbrain of PD-Ex group, compared to PD group, signifying that exercise may have encouraged the decrease of Caspase-3 activity in the midbrain ($p<0.01$, Figure 3.24).

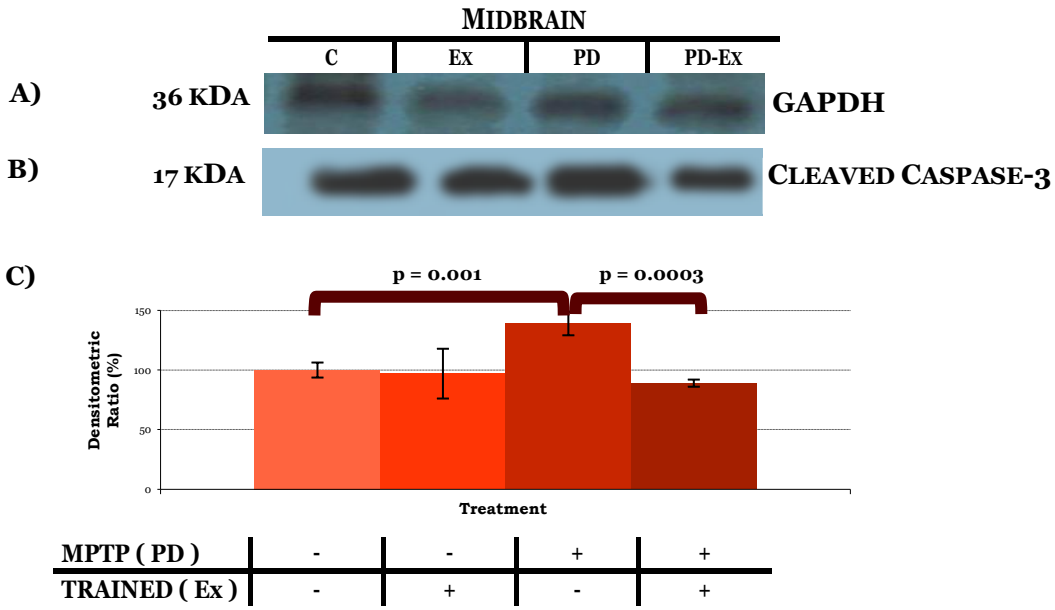

Figure 3.24: Reduced cleaved Caspase-3 Amount determined in PD-Ex rat midbrain

A) Illustrative example of GAPDH in midbrain of PD animal model

B) Illustrative example of cleaved Caspase-3 in midbrain of PD animal model

C) Cleaved Caspase-3 was present in the midbrain of C, Ex, PD and PD-Ex rats. Elevated amount of cleaved Caspase-3 (39% increase) was observed in midbrain of PD animal model. A significant decrease in cleaved Caspase-3 was found in the midbrain of PD rats that underwent endurance exercise (50% reduction, $p<0.01$) when compared to midbrain of PD sedentary rats. Means of five experiments ± SEM shown. Table of densitometry values and statistical analysis can be found in Figure 3.25, Appendix 3.

WB analysis was performed to detect and measure the amount of active Caspase-8 in the midbrain of PD and PD-Ex animal model. Elevated levels of active Caspase-8 were detected in the midbrain of PD sedentary rats, indicating that MPTP may have further enhanced Caspase-8 stimulation in the midbrain of PD animal model (ANOVA $p<0.05$, T test $p<0.05$). In contrast, active Caspase-8 was not detected in the midbrain of PD rats that underwent six week treadmill training, indicating that exercise may have inhibited Caspase-8 activation in the midbrain (Figure 3.26).

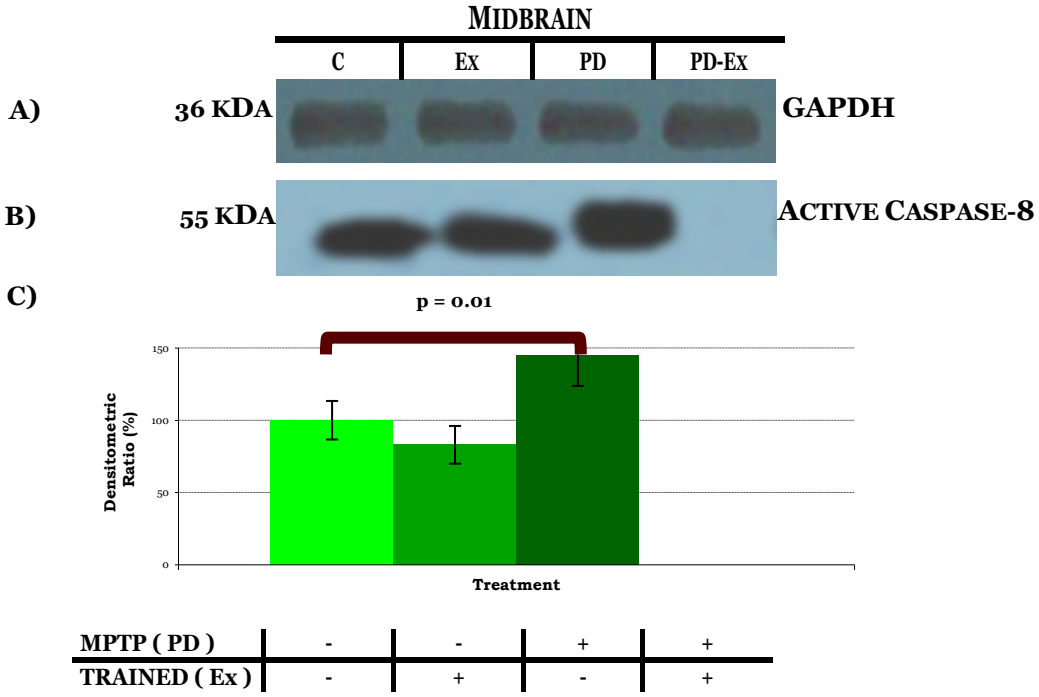

Figure 3.26 : Active Caspase-8 is absent in exercised midbrain of PD animal model

A) Illustrative example of GAPDH in midbrain of PD animal model

B) Illustrative example of active Caspase-8 in midbrain of PD animal model

C) Active Caspase-8 was present in the midbrain of C, Ex, PD and PD-Ex rats. Reduced levels of active Caspase-8 (17% decrease) were observed in midbrain of Ex group, when compared with C group. A 45% increase of active Caspase-8 was found in midbrain of PD animal model compared to C group ($p<0.05$). Active Caspase-8 was absent in midbrain of PD-Ex animal model. Means of five experiments ± SEM shown. Table of densitometry values and statistical analysis can be found in Figure 3.27, Appendix 3.

The influence of endurance exercise on the amount active Caspase-9 in midbrain in PD and PD-Ex animal model was determined via WB analysis. Elevated levels of active Caspase-9 were detected in midbrain of PD sedentary rats when compared to the C group ($p<0.01$), indicating that MPTP further stimulates Caspase-9 activation in the midbrain of PD rat. Furthermore, a reduction in the amount of active Caspase-9 was measured in the midbrain of PD-Ex group when compared to the PD group, suggesting that exercise may have decreased Caspase-9 activity in the midbrain of PD animal model (Figure 3.28).

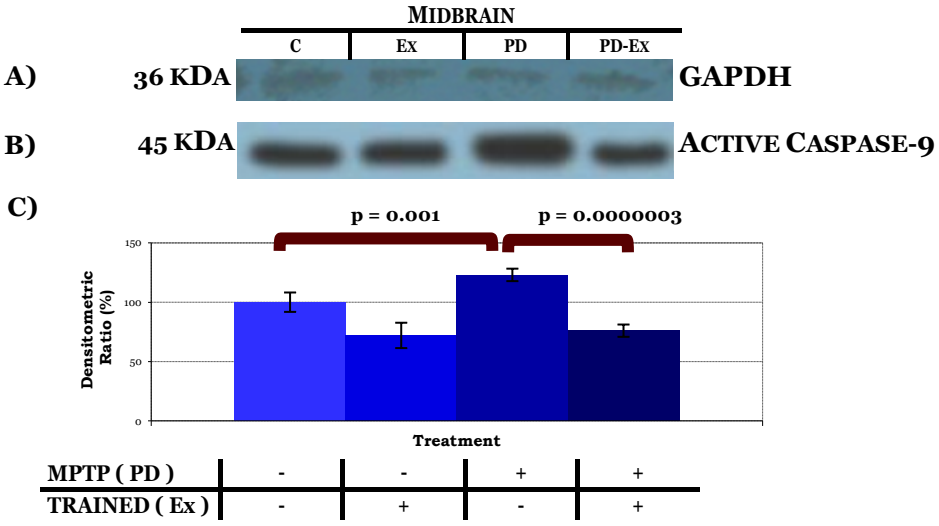

Figure 3.28 : Reduced levels of active Caspase-9 levels in PD-Ex rat midbrain

A) Illustrative example of GAPDH in midbrain of PD animal model

B) Illustrative example of active Caspase-9 in midbrain of PD animal model

C) Active Caspase-9 was present in the midbrain of C, Ex, PD and PD-Ex rats. A lower amount of active Caspase-9 was present in Ex group when compared to C group, indicating that exercise may have decreased Caspase-9 activity by 28% in rat midbrain. High levels of active Caspase-9 (23% increase) were measured in the midbrain of Parkinsonian rats when compared to C group, indicating that MPTP amplifies Caspase-9 activity in the midbrain of PD animal model. A 47% decrease in the amount of active Caspase-9 was detected in midbrain of PD-Ex group when compared to PD group ($p<0.05$). Means of five experiments ± SEM shown. Table of densitometry values and statistical analysis can be found in Figure 3.29, Appendix 3.

WB analysis was used to determine the amount of cleaved Caspase-12 present in the midbrain of C, Ex, PD and PD-Ex rats. The results illustrated elevated levels of cleaved Caspase-12 in the midbrain of PD sedentary rats compared to C group ($p<0.01$) indicating that MPTP further increased Caspase-12 activity in the midbrain. In contrast, a significant reduction in cleaved Caspase-12 was measured in the midbrain of PD-Ex group compared to PD group ($p<0.01$), indicating that exercise may have lowered Caspase-12 activity in the midbrain of PD animal model (Figure 3.30).

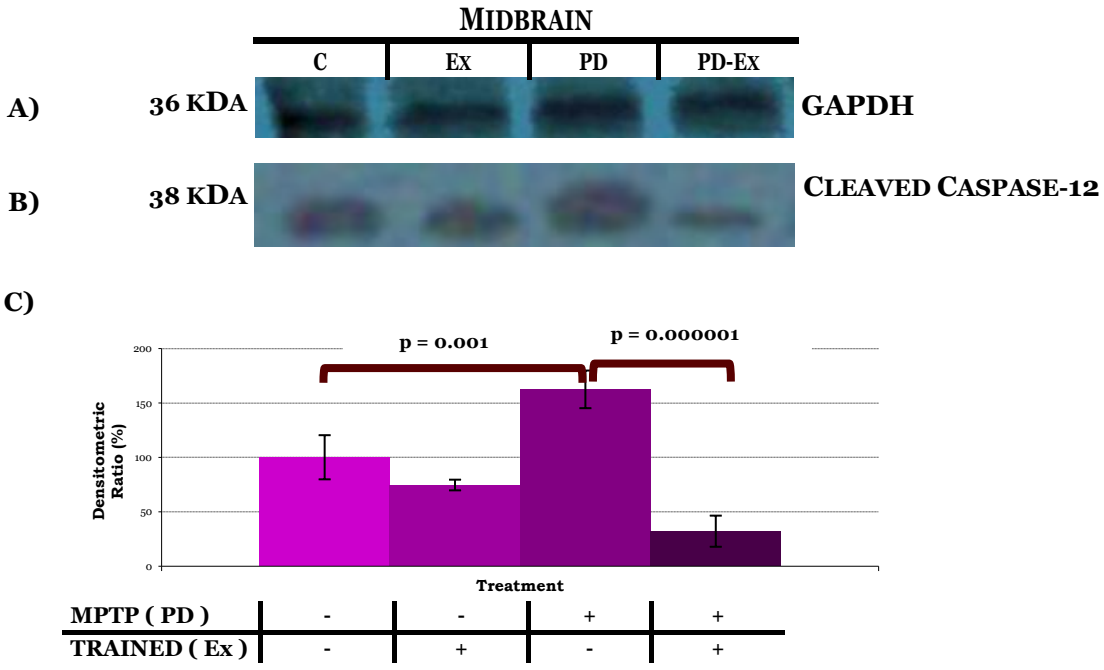

Figure 3.30 : Endurance exercise lowered cleaved Caspase- 12 levels in rat PD midbrain

A) Illustrative example of GAPDH in midbrain of PD animal model

B) Illustrative example of cleaved Caspase-12 in midbrain of PD animal model

C) Cleaved Caspase-12 was present in the midbrain of C, Ex, PD and PD-Ex rats. A 26% reduction in cleaved Caspase-12 was observed in the midbrain of Ex group, when compared to C group. Elevated levels of cleaved Caspase-12 (62% increase, $p<0.05$) were found in midbrain of PD group when compared to C group. A significant decrease in cleaved Caspase-12 levels was found in the midbrain of PD rats that underwent treadmill exercise compared to sedentary PD rats ($p<0.05$). Means of five experiments ± SEM shown. Table of densitometry values and statistical analysis can be found in Figure 3.31, Appendix 3.

The final region that was explored was the striatum, which is associated with PD. WB analysis was used to detect and measure the level of active Caspase-2 in the striatum of PD-Ex animal model (Figure 3.32). A significant rise in the amount of active Caspase-2 was present in striatum of PD rats that did not undergo treadmill exercise, suggesting that MPTP further stimulated Caspase-2 activity in PD rat striatum (ANOVA $p<0.05$, T test $p<0.05$). In contrast, Caspase-2 was absent in PD-Ex striatum, indicating that exercise may have suppressed Caspase-2 activity in the striatum in PD animal model.

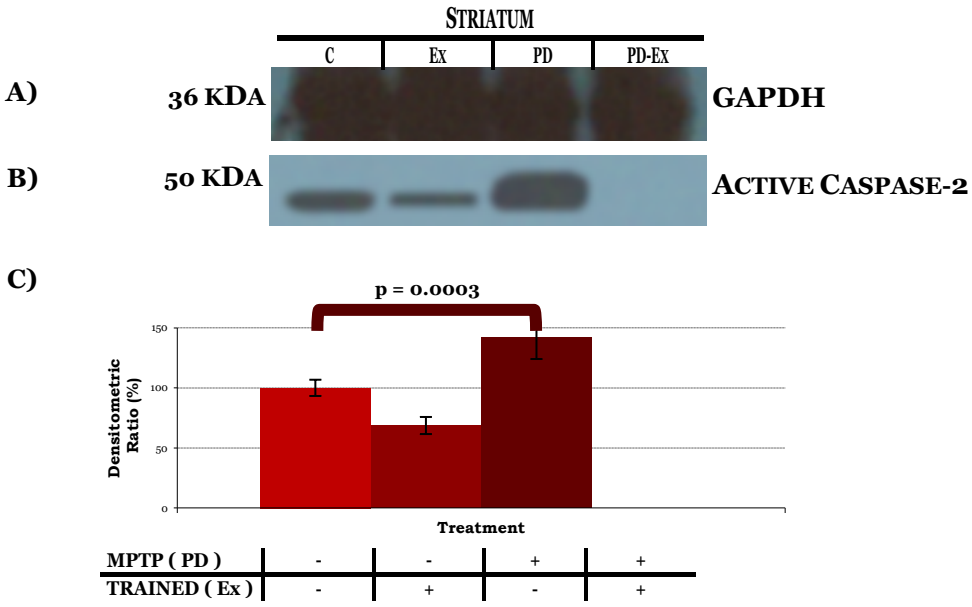

Figure 3.32 : Caspase-2 is absent in exercised striatum of PD animal model

A) Illustrative example of GAPDH in striatum of PD animal model

B) Illustrative example of active Caspase-2 in striatum of PD animal model

C) Active Caspase-2 was present in the striatum of C, Ex and PD rats. A 31% decrease in active Caspase-2 was detected in the striatum of rats that had done endurance exercise when compared to sedentary rats. Furthermore, a higher amount of active Caspase-2 was found in striatum of PD group, when compared to C group, indicating that MPTP amplified Caspase-2 activity in the striatum of PD animal model (42% increase, $p<0.05$). Active Caspase-2 was not detected in striatum of PD rats that had endured treadmill exercise Means of five experiments ± SEM shown. Table of densitometry values and statistical analysis can be found in Figure 3.33, Appendix 3.

The influence of endurance exercise on the amount cleaved Caspase-3 in striatum in PD animal model was determined via WB analysis. The results illustrated elevated levels of cleaved Caspase-3 in the striatum of PD rats that did not exercise compared to C group ($p<0.01$) indicating that MPTP further increased Caspase-3 activity in the striatum. In contrast, a significant reduction in cleaved Caspase-3 was measured in the striatum of PD-Ex group compared to PD group ($p<0.01$), indicating that exercise may have lowered Caspase-3 activity in the striatum of PD animal model (Figure 3.34).

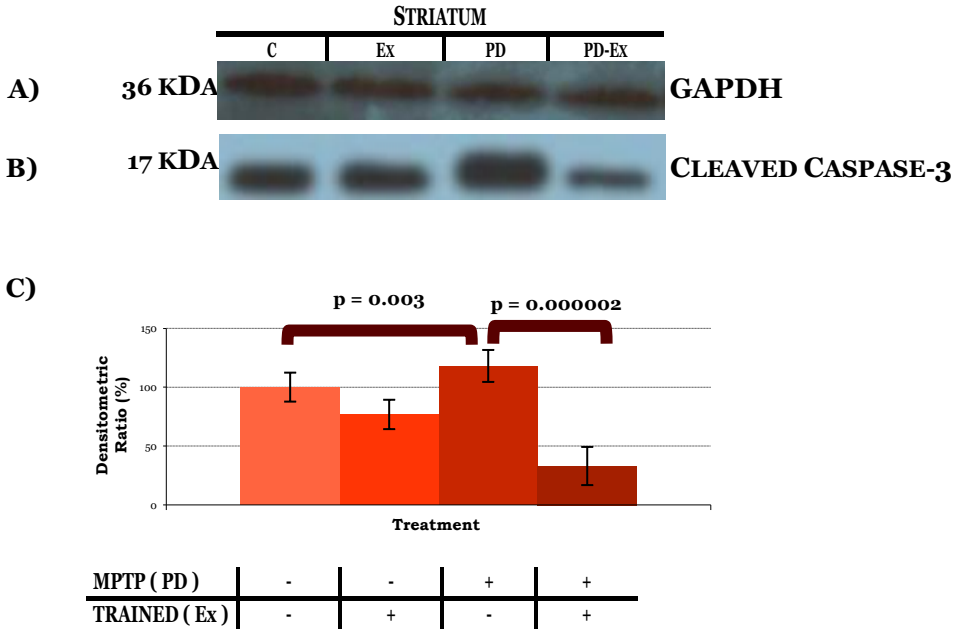

Figure 3.34 : Low levels of cleaved Caspase-3 found in striatum of PD-Ex animal model

A) Illustrative example of GAPDH in striatum of PD animal model

B) Illustrative example of cleaved Caspase-3 in striatum of PD animal model

C) Cleaved Caspase-3 was present in the striatum of C, Ex, PD and PD-Ex rats. A 23% decrease in the amount of cleaved Caspase-3 was determined in the striatum of Ex group when compared to C group. The amount of cleaved Caspase-3 levels had increased by 18% in the striatum of PD group when compared to C group ($p<0.05$). Low levels of cleaved Caspase-3 were observed in striatum of PD rats that underwent six week endurance exercise ($p<0.05$), when compared to PD group. Means of five experiments ± SEM shown. Table of densitometry values and statistical analysis can be found in Figure 3.35, Appendix 3.

The amount of active Caspase-8 was determined in the striatum of PD-Ex animal model. Elevated levels of active Caspase-8 were detected in the striatum of PD sedentary rats, indicating that MPTP increases Caspase-8 activation in striatum of PD animal model (ANOVA $p<0.05$, T test $p<0.05$). In contrast, active Caspase-8 was not detected in the striatum of PD rats that underwent six week treadmill training, indicating that exercise may have inhibited Caspase-8 activity in the striatum of PD animal model (Figure 3.36).

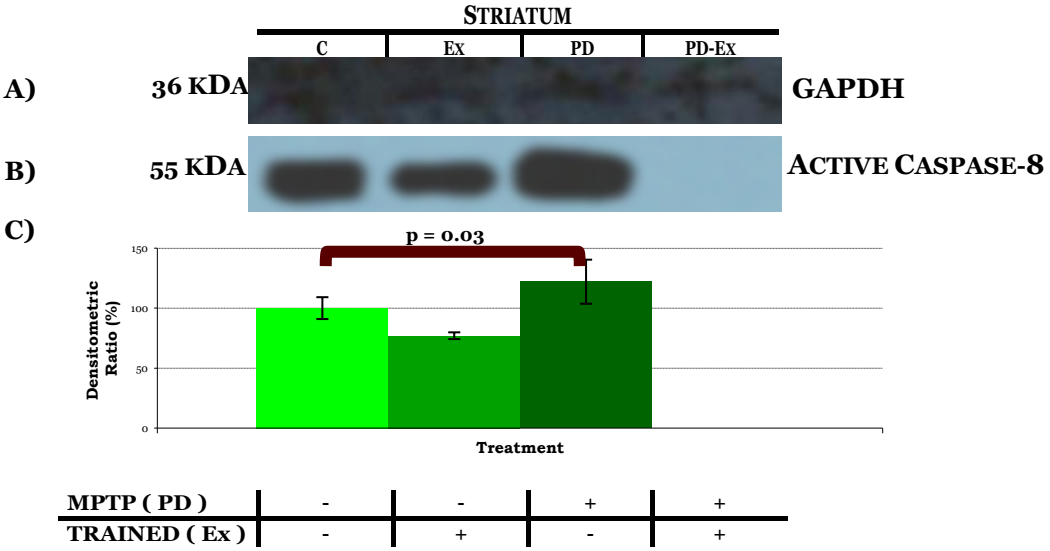

Figure 3.36 : Active Caspase-8 is absent in exercised striatum of PD animal model

A) Illustrative example of GAPDH in striatum of PD animal model

B) Illustrative example of active Caspase-8 in striatum of PD animal model

C) Active Caspase-8 was present in the striatum of C, Ex and PD rats. A reduced amount of active Caspase-8 (23% decrease) was detected in the striatum of Ex rat group when compared to C rat group. A 22% rise in active Caspase-8 levels was found in striatum of non exercised PD animal model when compared to the C group ($p<0.05$). Active Caspase-8 was not detected in the striatum of exercised PD animal model. Means of five experiments ± SEM shown. Table of densitometry values and statistical analysis can be found in Figure 3.37, Appendix 3.

WB analysis was carried out to determine the amount of active Caspase-9 levels present in the striatum of C, Ex, PD and PD-Ex animal model (Figure 3.38). The results showed that the amount of active Caspase-9 had increased in striatum of PD rats, when compared to C group, highlighting that MPTP may have triggered activation of the mitochondrial associated Caspase-9 protein in the striatum of PD animal model (ANOVA $p<0.05$, T test $p<0.05$). Additionally, the amount of active Caspase-9 had significantly reduced in PD-Ex group, when compared to PD group ($p<0.01$), indicating that endurance exercise may have decreased Caspase-9 activity in the striatum of PD animal model.

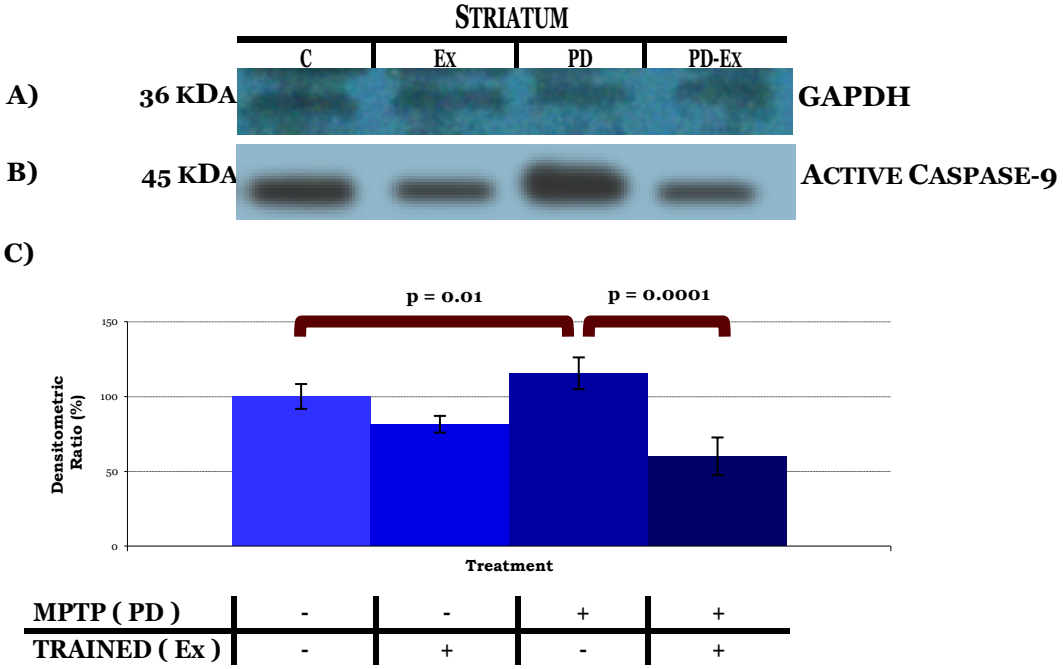

Figure 3.38 : Exercise decreases active Caspase-9 in the striatum of PD animal model

A) Illustrative example of GAPDH in striatum of PD animal model

B) Illustrative example of active Caspase-9 in striatum of PD animal model

C) Active Caspase-9 was present in the striatum of C, Ex, PD and PD-Ex rats. A 19% decrease in active Caspase-9 was found in striatum of Ex group, when compared to the C group. In contrast, an increased amount of active Caspase-9 was found in the striatum of sedentary PD rats when compared to the C group (15% increase, $p<0.05$). A 55% decrease in active Caspase-9 was determined in striatum of PD-Ex group when compared to PD group ($p<0.01$). Means of five experiments ± SEM shown. Table of densitometry values and statistical analysis can be found in Figure 3.39, Appendix 3.

WB analysis was used to investigate if there was an increased or decreased active Caspase-12 levels in the striatum of PD animal model. A significant rise in cleaved Caspase-12 was present in the striatum of PD group, when compared to the C group; highlighting that MPTP may have amplified further activation of the ER associated Caspase-12 protein in the striatum of PD animal model (ANOVA $p<0.05$, T test $p<0.05$). In comparison, Caspase-12 was absent in PD-Ex group, indicating that exercise may have inhibited Caspase-12 activity in the striatum of PD animal model (Figure 3.40).

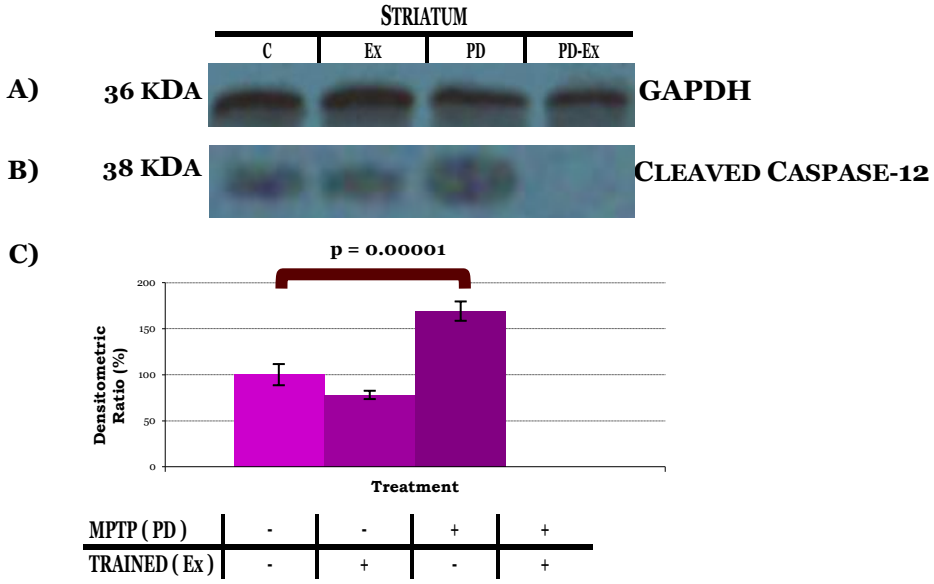

Figure 3.40 : Cleaved Caspase-12 is absent in exercised striatum of PD animal model

A) Illustrative example of GAPDH in striatum of PD animal model

B) Illustrative example of cleaved Caspase-12 in striatum of PD animal model

C) Cleaved Caspase-12 was present in the striatum of C, Ex, and PD rats. The striatum of Ex group had lower levels of Caspase-12 (22% decrease) present, when compared to C group. Elevated levels of cleaved Caspase-12 (69% increase, $p<0.01$) were found in striatum of PD group when compared to C group. Cleaved Caspase-12 was not detected in striatum of PD rats that underwent treadmill exercise. Means of five experiments ± SEM shown. Table of densitometry values and statistical analysis can be found in Figure 3.41, Appendix 3.

The results had indicated a general decrease the level of different Caspases in different brain regions in PD-Ex animal model (Figure 3.2- Figure 3.6, Figure 3.10-Figure 3.16, Figure 3.20-Figure 3.38). The next aim was to determine the effect of exercise on the presence of calcium binding protein, CAMK-IV in these brain regions of PD animal model. The results demonstrated no significant difference in the amount of active CAMK-IV in the cerebellum of PD animal model, when compared to the control ($p>0.05$), indicating that MPTP did not substantially increase or decrease CAMK-IV activity in the cerebellum. A significant increase ($p<0.05$) in the amount of active CAMK-IV was measured in the cerebellum of PD-Ex group, compared to PD group indicating that exercise may be increasing CAMK-IV activity in cerebellum of PD animal model (Figure 3.42).

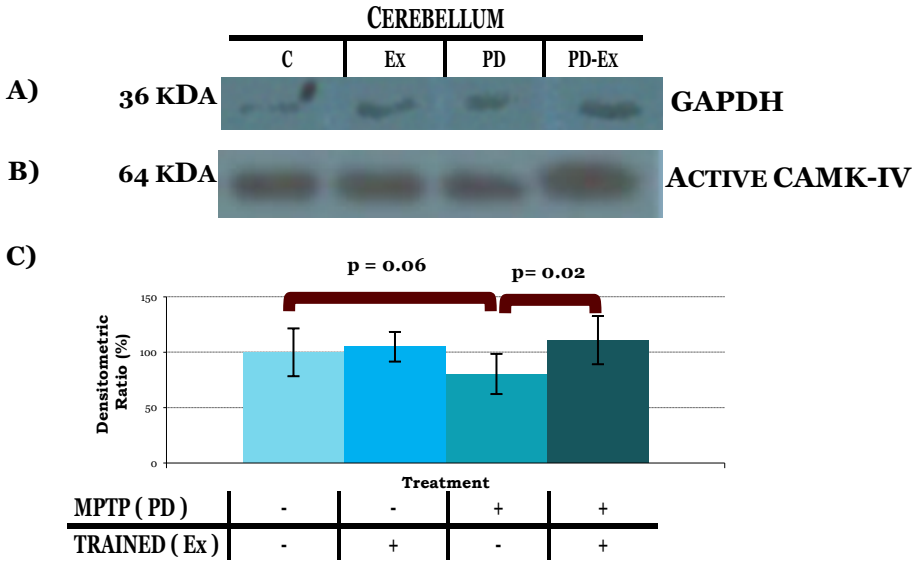

Figure 3.42 : The effect of Exercise on active CAMK-IV levels in PD rat cerebellum

A) Illustrative example of GAPDH in cerebellum of PD animal model

B) Illustrative example of active CAMK-IV in cerebellum of PD animal model

C) Active CAMK-IV was present in the cerebellum of C, Ex, PD and PD-Ex rats. A 4% increase in the amount of active CAMK-IV was determined in the cerebellum of Ex group, when compared to C group. The amount of active CAMK-IV levels had decreased by 20% in the cerebellum of PD group when compared to C group ($p>0.05$). An increase active CAMK-IV was determined in PD-Ex cerebellum by 31 % ($p<0.05$), when compared to PD group. Means of five experiments ± SEM shown. Table of densitometry values and statistical analysis can be found in Figure 3.43, Appendix 3.

WB analysis was carried out to detect and measure CAMK-IV activity in the brain cortex of PD animal model that had undergone endurance exercise (Figure 3.44). No significant difference in the amount of active CAMK-IV was measured in brain cortex of PD sedentary rats when compared to the C brain cortex, indicating that MPTP did not notably up regulate or down regulate CAMK-IV activity in the brain cortex of PD animal model. In comparison, a significant increase in active CAMK-IV was detected in PD-Ex group, indicating that exercise may be promoting an increase in CAMK-IV activity in brain cortex of PD animal model (T test $p<0.05$).

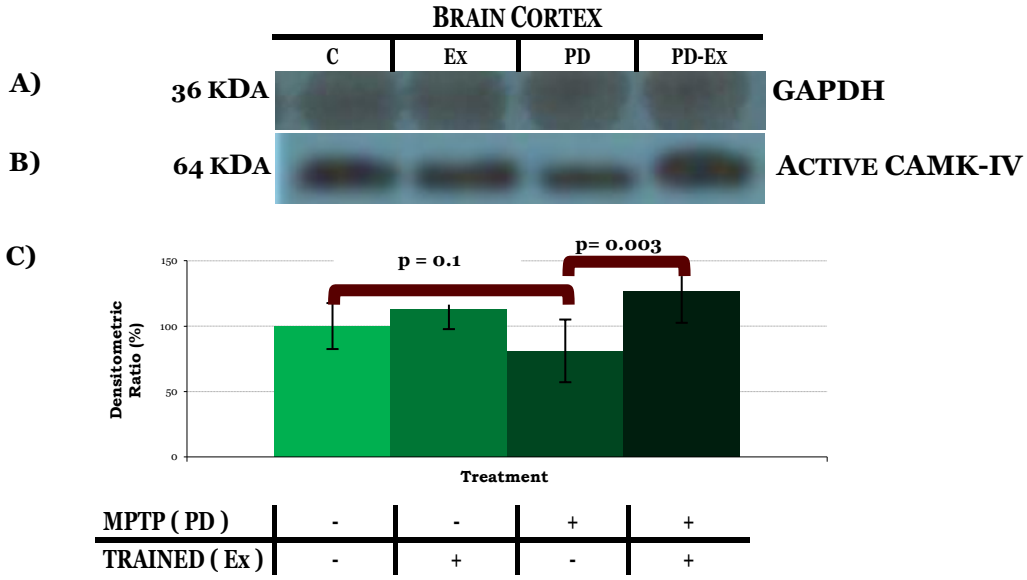

Figure 3.44 : Active CAMK-IV is increased exercised brain cortex of PD animal model

A) Illustrative example of GAPDH in brain cortex of PD animal model

B) Illustrative example of active CAMK-IV in brain cortex of PD animal model

C) Active CAMK-IV was present in the brain cortex of C, Ex, PD and PD-Ex rats. A similar level of active CAMK-IV was measured in the brain cortex of Ex group and C group. The amount of active CAMK-IV levels had reduced by 19% in the brain cortex of PD group when compared to C group ($p>0.05$). High levels active CAMK-IV was determined in PD-Ex brain cortex (44% increase, $p<0.05$), when compared to PD group. Means of five experiments ± SEM shown. Table of densitometry values and statistical analysis can be found in Figure 3.45, Appendix 3.

WB analysis was used to determine the amount of CAMK-IV present in the midbrain of C, Ex, PD and PD-Ex rats (Figure 3.46). Endurance exercise, consisting of six week treadmill training had shown a decrease of active CAMK-IV in the midbrain of PD group, when compared to the C group($p<0.05$); highlighting that MPTP may have discouraged further activation of CAMK-IV protein in the midbrain of PD animal model. In comparison, high levels of active CAMK-IV were present in PD-Ex group, suggesting that exercise may have promoted CAMK-IV activity in the midbrain of PD animal model (ANOVA $p<0.05$, T test $p<0.05$).

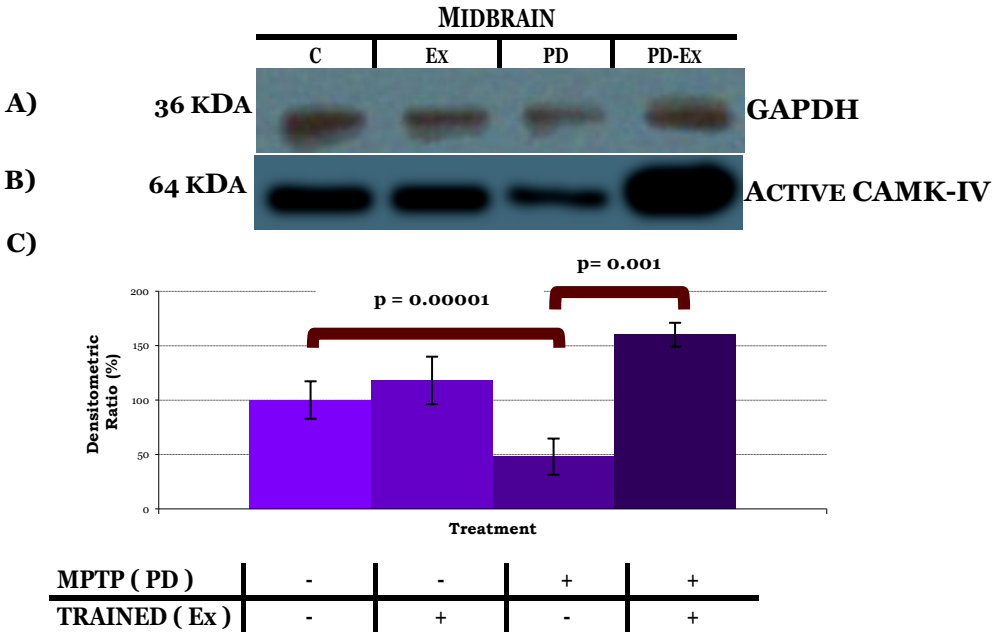

Figure 3.46 : Treadmill exercise amplifies CAMK-IV activity in midbrain PD animal model

A) Illustrative example of GAPDH in midbrain of PD animal model

B) Illustrative example of active CAMK-IV in midbrain of PD animal model

C) Active CAMK-IV was present in the midbrain of C, Ex, PD and PD-Ex rats. An increase in the amount of active CAMK-IV (18% increase) was found in the midbrain of Ex rat group, when compared to Ex rat group. CAMK-IV levels had diminished by 52% in the midbrain of PD rats when compared to C midbrain ($p<0.01$). High levels of active CAMK-IV were observed in midbrain of PD rats that underwent six week endurance exercise ($p< 0.01$) when compared to PD sedentary rats. Means of five experiments ± SEM shown. Table of densitometry values and statistical analysis can be found in Figure 3.47, Appendix 3.

Further work was carried out to determine if endurance exercise had an increase or decrease of active CAMK-IV in the striatum of PD animal model (ANOVA $p<0.05$, T test $p<0.05$). The results showed a significant amount of active CAMK-IV had decreased in striatum of PD rats, when compared to C group, highlighting that MPTP may interfere with the activation of CAMK-IV protein in the striatum of PD animal model ($p<0.01$). Additionally, the amount of active CAMK-IV had significantly increased in PD-Ex group, when compared to PD group ($p<0.01$), indicating that endurance exercise may have increased CAMK-IV activity in the striatum of PD animal model (Figure 3.48).

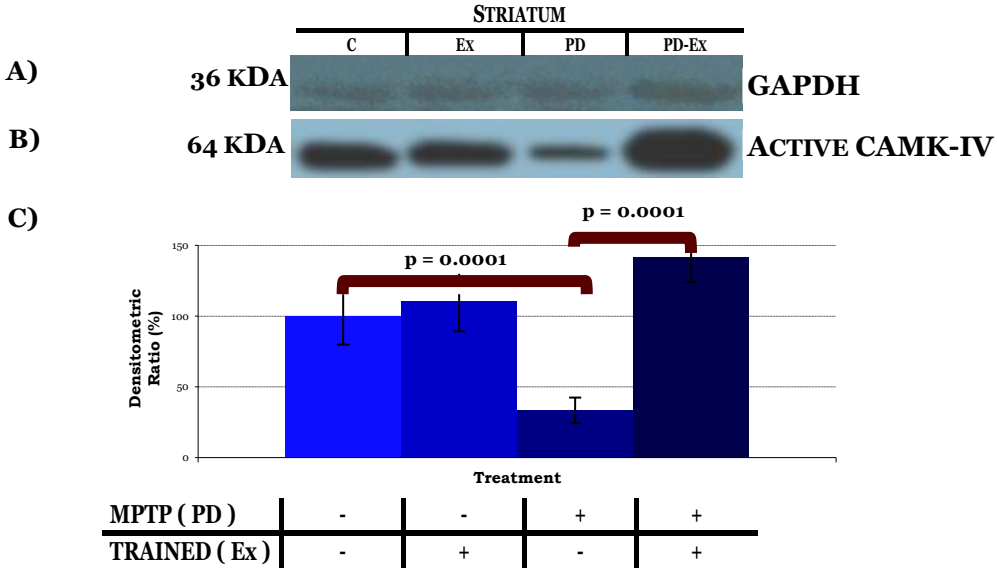

Figure 3.48 : Elevated Active CAMK-IV levels in exercised striatum of PD animal model

A) Illustrative example of GAPDH in striatum of PD animal model

B) Illustrative example of active CAMK-IV in striatum of PD animal model

C) Active CAMK-IV was present in the striatum of C, Ex, PD and PD-Ex rats. An 11% increase in active CAMK-IV was determined in rat striatum of Ex group when compared to C group. The amount of active CAMK-IV levels had reduced by 67% in the striatum of PD group when compared to C group ($p<0.01$). High levels active CAMK-IV was determined in PD-Ex striatum ($p<0.01$), when compared to PD group. Means of five experiments ± SEM shown. Table of densitometry values and statistical analysis can be found in Figure 3.49, Appendix 3.

3.5 Discussion

This is the first study to determine the effect of six week treadmill exercise on Caspases -1,-2,-3,-8,-9 and -12 in the cerebellum, brain cortex, midbrain and striatum of PD animal model. In general there was a decrease in Caspase activity in different brain regions of PD rats that underwent six week endurance exercise (Figure 3.2- Figure 3.6, Figure 3.10-Figure 3.16, Figure 3.20-Figure 3.38).

A study conducted by Lin et al (2000) showed that Caspase-1 was present in low levels in untreated mouse mesencephalic cultures brain. WB analysis illustrated that Caspase-1 was present in the midbrain of mouse model. In comparison, higher levels of Caspase-3 followed by Caspase-12 were found in the untreated midbrain of mouse model. In contrast, work carried out by Usha et al (2000) Caspase-1 was not detected in the SN of MPTP-treated mice. MPTP was administered twice at day 1, 2 and 7 prior to extracting DNA of the SN and nucleus caudate putamen of mice. DNA fragmentation was confirmed in SN and nucleus caudate putamen of MPTP mice using DNA ladder after SDS-PAGE, indicating apoptotic death of DCN. However, immunohistochemical studies did not detect presence of Caspase- 1 activity in the SN of MPTP mouse model. In comparison, high levels of cleaved Caspase-3 were found in MPTP-treated SN, indicating that MPTP triggers activation of Caspase-3 leading to DNA fragmentation and death of DCN. The results of the current study provide further support to Usha et al (2000) study as Caspase-1 was absent in all regions of C , Ex, PD and PD Ex animal model.

In a previous study, WB analysis demonstrated an increased in Caspases-3 and -7 in with MPTP-treated rat cerebellum, indicating that MPTP triggered death of neurons, via apoptotic route as Caspase-3 is a well known apoptotic marker (Iwashita et al 2007, Shang et al 2004). Similarly, the results of the current study had shown an increase of Caspases-3,-8 and-12 activities in cortex and cerebellum regions that were treated MPTP, indicating that MPTP stimulated Caspase activation in cerebellum region of PD animal model (Figure 3.4-Figure 3.6, Figure 3.10, Figure 3.14-Figure 3.16 and Figure 3.20). Furthermore, the current study is the first to demonstrate MPTP did not significantly enhance stimulation of Caspases-2 and -9 in the cerebellum of PD animal model (Figure 3.12 and Figure 3.18). The reduction of

active and cleaved Caspases-2,-3,-8 and-12 in PD-Ex rat cerebellum and cortex, indicated that endurance exercise may have decreased Caspase activity in the cerebellum of PD animal model (Figure 3.2-Figure 3.6, Figure 3.10-Figure 3.16 and Figure 3.20).

Lumini-oliveira et al (2009) investigated the effect of treadmill training on skeletal muscles in male Wistar rats. Rats underwent endurance exercise using motor driven treadmill for one hour 5 days a week for a total of 14 weeks. Results showed increased activation of the mitochondria apoptosis marker Caspase-9, increased mitochondria PTP opening, cytochrome c, succinate, swelling of mitochondria and calcium accumulation in skeletal muscle homogenates of exercised rat, indicating apoptotic death of skeletal muscle cells were due to mitochondrial pathway. The author concluded that apoptotic death of muscle cells was required to improve overall muscle strength and function in rats.

In the current study, an unexpected finding was determined when exploring Caspase-9 activity in the cerebellum of PD animal model. An increase in active Caspase-9 was determined in PD-Ex cortex and cerebellum, indicating that endurance exercise may have increased Caspase-9 activity in the cerebellum of PD animal model (Figure 3.8 and Figure 3.18). Similar to Lumini-oliveira et al (2009) research, the increase of Caspase-9 activation in cerebellum and cortex by endurance exercise may be associated to the specific role of Caspase-9 in mitochondrial pathway (Chowdhury et al 2008). Although, ROS level was not directly determined in this study, MPTP is known to cause a high acculturation of ROS production by inhibiting mitochondrial complexes, which contributes to stimulation of the apoptotic death (Shang et al 2004, Xu et al 2013).

Lo et al (2012) found MPTP-treated rat mesencephalic cultures had increased levels of ROS, Caspase-9 and -3 activities, when compared to untreated cultures, indicating that MPTP promotes Caspases-9 and 3 activation in midbrain of PD animal model. Immunohistochemical analysis revealed large inclusions and decrease in TH levels in MPTP rat midbrain when compared to untreated midbrain. IF and flow cytometry analysis showed positive staining with Annexin confirming MPTP triggered apoptotic death of neurons. Previous research by Pain et al (2008) has shown increased Caspase-9 activity in the

midbrain and SN of MPTP-induced PD rat model. WB analysis revealed an increase and amount of active Caspases-9 and -3 in midbrain and SN of MPTP induced rats, suggesting MPTP triggered activation of Caspases-9 and-3 in midbrain and SN. IF analysis showed large lesions, loss of neurons as well as increased expression of Caspases-9 and -3 in MPTP-treated midbrain and SN. Moreover, a reduction of caspases-9 and-3 was determined in MPTP midbrain sections that had been treated with a JNK inhibitor TAT-JBD, indicating that MPTP promotes activation of caspases-9 and -3 through JNK pathway resulting in loss of midbrain and striatal neurons. Similarly to the findings of Pain et al (2008) and Lo et al (2012), the current study had illustrated high Caspases-9 and -3 levels as well as Caspase-12 in the midbrain of PD animal model, indicating that MPTP had amplified Caspases-3, -9 and -12 activation in the midbrain (Figure 3.24, Figure 3.28-Figure 3.30).

WB and Colorimetric assays revealed increase of Caspase-3 activity in 6OHDA-treated rat mesencephalic culture, indicating Caspase-3 is actively involved in death of DCN of PD animal model. Furthermore, immunohistochemical analysis revealed a decrease in TH level of MPTP-treated rat mesencephalic culture, indicating that MPTP decreased dopamine levels in the midbrain of PD rat (Kim et al 2012). In comparison to Pain et al (2008) and Kim et al (2002) research, the current study showed a reduction in Caspases-3, -9 and -12 were observed in midbrain of MPTP rats that had endured six week treadmill exercise, suggesting that exercise may have reduced activation of Caspases in the midbrain of PD animal model (Figure 3.24, Figure 3.28-Figure 3.30).

Previous research by Hartmann et al (2001) has shown the suppression of Caspase-8 activity had reduced neuronal apoptotic death of MPTP-treated rat mesencephalic cultures. TUNEL, WB and Colorimetric assays illustrated an increase of Caspase-8 activities in MPTP-treated rat midbrain when compared to untreated midbrain, suggesting that an increase in Caspase-8 activation resulting in apoptotic death of neurons in the midbrain of PD animal model. Immunohistochemical analysis portrayed a decrease in TH expression, loss of neurons and presence of fibrils in MPTP rat midbrain (Hartmann et al 2001). In comparison, the current study demonstrated that MPTP further promoted activation of Caspases-2 and -8 in MPTP-treated rat midbrain (Figure 3.22 and Figure 3.26).

Furthermore, absence of Caspases-2 and -8 in the PD-Ex midbrain indicated that exercise may have suppressed Caspase-2 and -8 activities in the midbrain of PD animal model (Figue 3.22 and Figuer 3.26). The exact mechanism of how this could be achieved is unclear.

Former work by Choi et al (2011) showed increase of nitrate, ROS and Caspase-3 activities in 6OHDA rat mesencephalic cultures and MPTP rat striatum, signifying that oxidative stress promotes death of neurons in PD animal model. Furthermore, immunohistochemical analysis showed decrease of TH expression and damage to striatal neurons and mesencephalic culture exposed with MPTP. In the current study, high levels of active and cleaved Caspases-2,-3,-8,-9 and -12 were determined in MPTP-treated rat striatum, indicating that MPTP promoted up regulation of Caspase activity in the striatum (Figure 3.32-Figure 3.40). Similar to Choi et al (2011), the current study showed an increase of Caspase-3 level in the rat striatum that had been treated with MPTP (Figure 3.34). This is the first study demonstrating the absence of Caspases-2,-8 and -12 in PD-Ex striatum, signifying that six week treadmill exercise may have suppressed Caspases-2,-8 and -12 activities in the striatum PD animal model (Figure 3.32, Figure 3.36 and Figure 3.40).

WB and IF analysis showed decrease of Caspase-8 and -3 levels in the liver of rats that had endured treadmill training for an hour every day for five weeks. A decrease in mitochondrial swelling and ROS levels were also determined in liver homogenates of rats that had exercised compared to non exercised rats, indicating that exercise had positive effects (Ascensao et al 2012). Although ROS level was not measured in this study, treadmill exercise may have reduced accumulation of ROS, which may have decreased activation of Caspases in these brain regions in PD animal model. Research by Ascensao et al (2011) had shown that treadmill exercise decreased Caspases-3 and -9 activities and increased superoxide dismutase in rat heart and liver homogenates, indicating that exercise can reduce oxidative stress and loss of cells. Based on a similar idea by Ascensao et al (2011), in the current study endurance exercise may have increased levels of antioxidants, which may have reduced ROS accumulation resulting in a decrease in activation of Caspases in brain regions of PD animal model.

Collectively, the results indicated that six weeks treadmill exercise had reduced the level of specific Caspases in different brain regions in PD animal model (Figure 3.2-Figure 3.6, Figure 3.10-Figure 3.16, Figure 3.20-Figure 3.40). More specifically, exercise had greatly affected the midbrain and striatum of PD animal model by either significantly inhibiting or completely suppressing Caspase-2, -3, -8, -9 and -12 activities (Figure 3.22 –Figure 3.40). However, as the original sample size (n=16) is small these findings must be looked at with caution. A larger sample size (n=50) would be a more realistic representation of these findings. In addition, knockdown of specific Caspases such as Caspase-2, -3, -8, -9 and -12 in PD-Ex animal model would give a better representation if exercise can indeed suppress Caspases activation or if there is an different factor such as GDNF, BDNF is involved in suppression of Caspase activation.

To develop this project further, the amount of CAMK-IV was determined in cerebellum, brain cortex, midbrain and striatum of C, Ex, PD and PD-Ex group (Figure 3.42-Figure 3.48). Previous work has shown that during exercise, calcium ions from the sacroplasma of muscle are released into the bloodstream, where they bind to calcium binding proteins, CAMKs. The level of calcium:CAMK-IV complexes formed contributes to the activation of the CAMK cascade pathway, resulting in increased synthesis of neurotransmitter TH which is required to release dopamine (Suntoo et al 2003).

At present there is no study that specifically explores the amount of CAMK-IV in the cerebellum, brain cortex, midbrain and striatum of Parkinsonian rats that had undergone endurance exercise. A decrease in active CAMK-IV was found in MPTP rat cerebellum and brain cortex, but this reduction of active CAMK-IV was not significant (Figure 3.42-Figure 3.44). In contrast, a significant increase in active CAMK-IV was determined in PD-Ex cerebellum and brain cortex, indicating that treadmill exercise may have increased CAMK-IV activity in cerebellum and brain cortex of PD animal model (Figure 3.42-Figure 3.44). Low levels of active CAMK-IV were measured in MPTP-treated midbrain and striatum, indicating that MPTP significantly reduced CAMK-IV activity in the midbrain and striatum of PD animal model (Figure 3.46-Figure 3.48). Higher levels of active CAMK-IV were determined in PD-Ex midbrain and striatum, indicating that treadmill exercise may have further increased CAMK-IV activity in the midbrain and striatum of PD animal model (Figure 3.46-Figure 3.48).

See et al (2001) explored the link between CAMK-IV and Caspase induced apoptosis in granule cells of the cerebellum of mouse model. Active CAMK-IV promoted survival of neurons and prevented cell death caused by potassium deprivation in granuale cells. CAMK-IV encouraged cell survival via CAMK-IV: CREB and maintaining electrolyte homeostasis, thereby decreasing the probability of Caspase dependent apoptosis in potassium deprived cells. The decrease levels of Caspases in PD-Ex regions may be due to the participation of CAMK proteins, which inhibit Caspase activation and may promote neuronal survival. Additionally, treadmill exercise may have increased the amount of CAMK-IV in different brain regions of PD animal model, by encouraging the binding of calcium to CAMK-IV, which may have resulted in production and release of dopamine. This could aid to decrease the symptoms such as tremor, which is associated with PD pathogenesis. In addition, previous research has indicated that the calcium-CAMK complex suppresses the stimulation of Caspase activation, through an unknown mechanism (See et al 2001).

The results of the study are similar to research carried out by H.Ali (personal communication), who had found increased levels of CAMK II (another member of the CAMKs family) in muscles of exercised rats. In addition, WB analysis had shown increased levels of CAMK-II in the midbrain of PD rats that had underwent endurance exercise. The author concluded that CAMK-II activity is amplified by treadmill exercise and can protect DCN from further damage in the PD midbrain. The author had also explored the effect of treadmill exercise on CAMK-II in the striatum. WB analysis had shown a significant rise in CAMK-II in PD-Ex striatal DCN, indicating that exercise increases CAMK II activity in striatal DCN (H.Ali, personal communication). The findings of the current study are in parallel to H.Ali's research. WB analysis revealed low levels of CAMK-IV in MPTP induced PD rat striatum, indicating that MPTP reduced CAMK-IV activation which may have contributed to loss of striatal neurons (Figure 3.48). Treadmill exercise may have increased CAMK-IV activity and may lead to protection of neurons in the in the midbrain and striatum of PD animal model (Figure 3.46-Figure 3.48).

Collectively the results indicated that MPTP increased activities of Caspases and decreased CAMK-IV activation in cerebellum, brain cortex, midbrain and striatum in PD animal model model (Figure 3.42-Figure 3.48). Overall, six weeks treadmill exercise had decreased Caspase activation and increased CAMK-IV activation in these regions in PD model (Figure 3.50). More specifically, endurance exercise had significantly reduced Caspase-2, -3, -8,-9 and -12 activities, whilst increasing CAMK-IV activity in the rat striatum and midbrain of PD animal model model (Figure 3.22 –Figure 3.40 and Figure 3.46-Figure 3.48). The increased activation CAMK-IV may have reduced activation of Caspases through a mechanism which has yet to be established. Exercise may have suppressed Caspase activity through a CAMK-IV route or it may have inhibited Caspase activation by inhibiting a pathway which is common to all Caspases, thereby preventing further loss of cells in these regions (Suntoo et al 2003, Wayman et al 2008, See et al 2001, Reymond and Ghosh 2005).

Former research (McIlwain et al 2013) has shown that Caspase activation is associated with both intrinsic and extrinsic pathways (Chapter 1 Section 1.3- 1.10). The absence of specific Caspases such as Caspase-2, -8 and -12 in PD-Ex midbrain and striatum, indicated that exercise may have the potential to suppress NFκB and ER stress pathways (Figure 3.50). A study carried out by Mattson et al (2004) revealed mice, which endured regular exercise had an increased quantity of dendritic growth in cortical neurons and synapses present when compared to the control group. In addition, a decrease in DNA oxidative damage and lipid peroxidation was found. In the current study, it is possible that treadmill exercise may aid in reducing ROS and promote growth of dendrites and improve synaptic communication. The improvement of efficient synaptic communication and dopamine release could potentially decrease some symptoms, such as muscle rigidity and facial palsy, thereby improving muscle tone and coordinated movement in PD. Additionally, this current study has shown that treadmill exercise increased CAMK-IV level and may be involved in the process that results in release of dopamine from neurons (Figure 3.50).

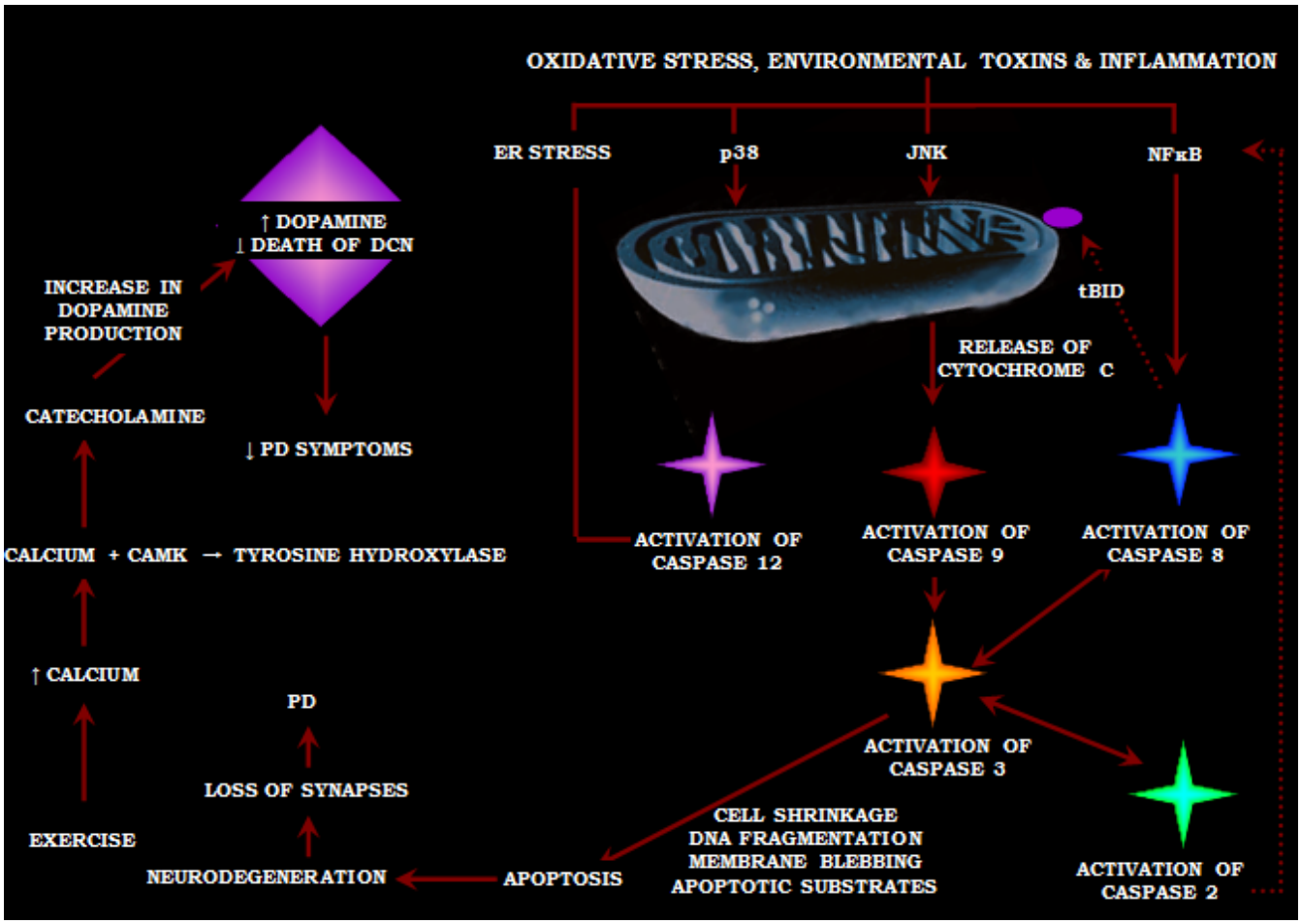

Figure 3.50 : The Potential Effect of Exercise on CAMK and Activation of Caspases via Mechanisms of Cell Death

Environmental toxins, oxidative stress and inflammation are able to trigger intrinsic (mitochondrial) or extrinsic (NFκB and ER) pathways promoting the activation of specific Caspases. Activation of Caspases results in apoptotic death of DCN, causing degeneration of neurons and the loss of synaptic communication leading to PD pathogenesis. Exercise encourages calcium binding to CAMKs which promote production of TH leading to synthesis of catecholamines such as dopamine. CAMKs can suppress Caspase activation through an unknown mechanism. Increased dopamine levels and decreased death of DCN can reduce some symptoms of PD such as muscle rigidity (See et al 2001, Suntoo et al 2003, Reymond and Ghosh 2005, Ribar et al 2000, Wayman et al 2008, Akimoto et al 2003).

The results of this research had addressed the need to explore the Caspase family and how they are activated in greater detail. The results have opened up further questions as to how different Caspases are activated, do they all have a common stimulus or are they activated by specific events, such as, mitochondrial collapse, ER stress or NFκB over activity. There have not been any studies which explore the possibilities of cross talk of Caspase specific pathways in DCN. In order to determine how exactly exercise may reduce or suppress Caspase activation in cells, the process of activation of Caspases needs to be established first. Through understanding how Caspases are activated can key proteins be identified and targeted to suppress Caspase mediated death and promote survival of cells. Following this, how exercise can effect Caspase pathways can then be discovered and at which time point exercise suppresses Caspase activation can be determined. Treadmill exercise may have decreased ROS level leading to a decrease in stimulation of Caspases and Caspase pathways which may reduce and protect death of cells (See et al 2001, Suntoo et al 2003, Reymond and Ghosh 2005, Ribar et al 2000, Wayman et al 2008, Akimoto et al 2003 Figure 3.50).

There also exists a possibility that exercise may be suppressing upstream proteins such as PERK, Calpain or NFκB, or unknown proteins that trigger activation of Caspases or it may be directly targeting the Caspases itself. In addition, treadmill exercise may be indirectly suppressing Caspases by activating other proteins that effect Caspases. For example, exercise may be triggering activation of CAMK-IV and the activation of CAMK-IV may directly suppressed Caspase activation and not exercises itself. Exercise may be acting as an initiator that triggers different proteins or maybe it activates specific proteins that directly suppress Caspase activation which may lead to a decrease in death of DCN. Another possibility is that exercise triggers proteins, which stimulate other proteins that activate another generation of proteins leading to suppression of Caspases (Chaudhry and Ahmed 2014, See et al 2001, Suntoo et al 2003, Reymond and Ghosh 2005, Ribar et al 2000, Wayman et al 2008).

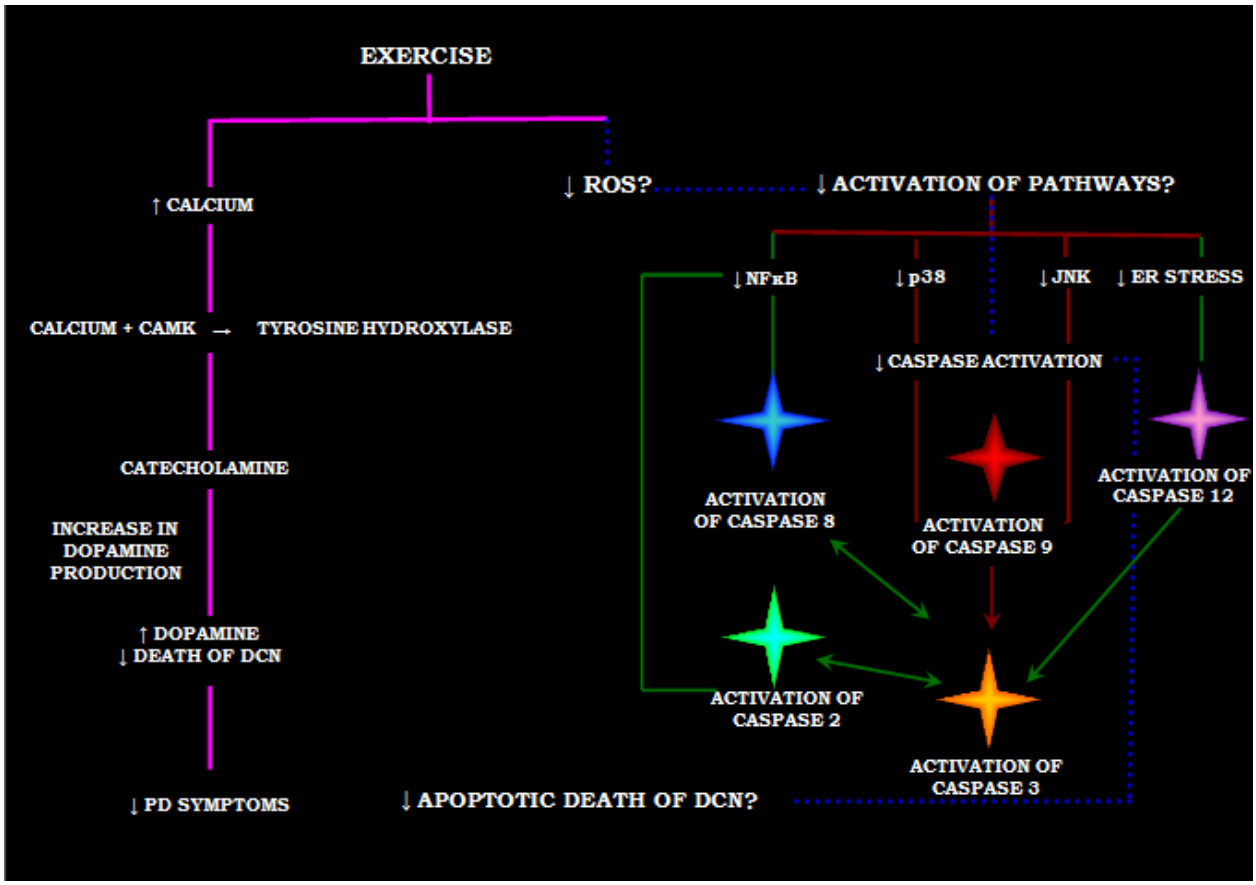

Figure 3.51: Exercise may decrease activation of Caspases by effecting ER and NFκB pathway

Exercise promotes release and binding of calcium to CAMK leading to TH synthesis. Elevated TH increases dopamine levels in the brain that may reduce symptoms of PD (pink lines). Exercise may also decrease ROS levels which may lead to a reduced stimulation of pathways such as JNK, ER stress, NFκB and p38 pathway, resulting in decreased activation of Caspases and apoptotic death of DCN (blue lines). The effect of ROS on the ER stress and NFκB pathway alongside specific Caspases-2,-8 and -12 will be further explored in DCN (green lines).

3.6 Conclusion

At present, there are many studies that indicate that exercise is beneficial in PD treatment from a social aspect as well as decreasing PD symptoms such as rigidity, gait and improvement in balance (Chapter 1 Section 1.2.5 and Section 3.1). However, there is a lack of research exploring how exactly exercise can provide such benefits. To date there is no research that investigates the potential pathways, which exercise may be influencing to provide such positive and even negative effects. The current study explores the effect of treadmill exercise on active Caspases, along with CAMK-IV protein in specific brain regions (Figure 3.2-Figure 3.48).

Treadmill exercise may have had positive effects in PD animal model via presence of CAMK-IV and absence of various Caspases in different regions (brain cortex, cerebellum, midbrain and striatum) of the brain (Figure 3.2-Figure 3.48). The activation of CAMK-IV may inhibit Caspase activation in the brain cortex, midbrain and striatum, through exercise may help to reduce further cell death (Suntoo et al 2003 and Figure 3.50). CAMK may also encourage increase dopamine synthesis and release alongside inducing communication from the preganglionic neuron to the postganglionic neuron (Suntoo et al 2003, Akimoto et al 2004, Redmond and Gosh 2005, Ribar et al 2000, Wayman et al 2008).

The improvement of efficient synaptic communication and dopamine release may have the potential to decrease some symptoms (such as muscle rigidity and facial palsy) thereby improving muscle tone and coordinated movement in PD (Akimoto et al 2004, Suntoo et al 2003, Redmond and Gosh 2005). Stimulation of intrinsic (mitochondrial) or extrinsic (ER stress or NFκB) pathways trigger activation of specific pathways (Chaudhry and Ahmed 2014, Hetz 2012, Sano and Reed 2013, Cali et al 2011, Oshitari et al 2008, Doyle et al 2011, Yoshida 2007, Jing et al 2012, Malhotra and Kaufman 2007, Holtz and O'Malley 2003). Manipulation of these pathways may inhibit Caspase activation, thereby reducing death of DCN (Figure 3.51). The effect of ROS on the ER stress and NFκB pathway alongside specific Caspases-2,-8 and -12 will be further explored in DCN in following Chapters.

Chapter 4
Examining Caspase Activation using ReNcell VM stem cells: Exploring Cell Death Pathways

Previous work by Miljan (2007) had compared the neural stem cell lines ReNcell VM and ReNcell CX. ReNcell VM is derived from the ventral mesencephalon region, whilst ReNcell CX is generated from the cortical regions of the fourteen week old human foetus brain. Both ReNcell VM and ReNcell CX maintain a stable genotype and phenotype across many passages during cell culture as they are transduced with the oncogene myc. In addition, both cell lines have a reliable competency to differentiate into neuronal cells. Moreover, withdrawal of growth factors EGF and FGF promote differentiation to occur in both cell lines (Miljan 2007).

Following differentiation, ReNcell CX cells were spread across the plate whereas differentiated ReNcell VM cells were grown in clusters and formed neurospheres. Furthermore, WB analysis showed ReNcell lines were positive for the neural stem marker nestin. In addition, WB and IF analysis illustrated that only differentiated ReNcell VM cells were positively stained for TH, indicating that ReNcell VM and not ReNcell CX can differentiate into DCN. The formation of neurospheres after differentiation promotes the generation of action potentials in ReNcell VM line. Differentiated ReNcell VM had constant active currents that were inhibited by tetrodotoxin, indicating the presence of active sodium and potassium voltage channels are required to generate action potentials in these cells (Donato et al 2007).

Differentiated ReNcell VM has been used to study PD pathogenesis at a cellular level (Miljan et al 2008). An increase in glutathione, free radicals and death of cells were observed in differentiated ReNcell VM that had PINK-1 gene suppressed. Electron microscopy portrayed abornmalities in the mitochondria and aggregation of toxic deposits in PINK-1 gene suppressed ReNcell VM, indicating mutation of PINK-1 promotes cell death via oxidative stress which has also been found in other PD models. Furthermore, research by Massachusetts (2008) had demonstrated mechanistic link of mutant PINK-1 gene and PD onset by suppressing PINK-1 in ReNcell VM.

The results from the previous Chapter showed mostly decreased activation of different Caspases in different brain regions of PD animal model (Chapter 3 Figure 3.2- Figure 3.6, Figure 3.10-Figure 3.16, Figure 3.20-Figure 3.38). This finding subsequently posed further questions that needed to be answered. The main question arise from the results obtained from the animal model was how does treadmill exercise reduce activation of Caspases, is exercise directly suppressing Caspases itself or is it inhibiting the pathway of Caspases. Furthermore, is exercise inhibiting specific proteins, which indirectly suppress Caspase activation, thereby reducing death of DCN? The initial step to answer these questions was to examine how Caspases are activated in DCN. More specifically, the aim was to determine which pathway or pathways are causing Caspase activation and can these pathways encourage stimulation of each other?

In attempt to answer these questions, the first step was to establish how Caspases are activated in DCN of PD model. To achieve this, the aim was to explore the pathway or pathways that trigger Caspase activation in DCN of PD model. Specifically; the aim was to determine the activation of Caspases in 6OHDA induced differentiated ReNcell VM (dDCN). 6OHDA is a well known neurotoxin used in PD animal and cell models, which produces ROS that selectively destroys DCN and inhibits the mitochondrial electron chain complexes I and IV, leading to neuronal damage by producing ROS. 6OHDA induces neurotoxicity onto the nigrostriatal dopaminergic system, thereby promoting death of DCN, therefore can establish a good model to study PD pathogenesis (Denault et al 2007).

As there are many pathways such as intrinsic and extrinsic that can potentially trigger Caspase activation leading to death of DCN, the aim of this project was to explore the potential involvement of the ER stress and NFκB pathways in Caspase activation of 6OHDA induced DCN. There has been extensive research already done on the intrinsic route, mitochondrial pathway in PD pathogenesis compared to ER stress and NFκB (Chapter 1 Section 1.4 -1.7). The aim was to look at the impact that ER stress and NFκB pathway has on Caspase activation and if it can result in death or protection of 6OHDA induced dDCN. The effect of ROS on the ER stress and NFκB pathway alongside specific Caspases will be further explored in DCN in subsequent Chapters.

This research is the first to demonstrate the involvement of Caspase activation and pathways in differentiated ReNcell VM. In order to determine the key proteins and what pathways trigger Caspase activation in DCN, a PD model had to be established. Subsequently, Caspase activation and apoptotic death of the established PD model had to be confirmed before reaching the main aims of this study. The following pages demonstrate and confirm that Caspases-2,-3, and -8 follow Caspase mediated death of 6OHDA-treated dDCN.

Main Aim: To demonstrate 6OHDA triggered Caspase mediated apoptotic death of dDCN.

4.2.1 Differentiation of ReNcell VM to dDCN

ReNcell VM were cultured and differentiated into DCN (dDCN) after withdrawal of EGF (GF144, Millipore Hertfordshire UK) and FGF (GF003, Millipore Hertfordshire UK). As recommended by the manufacturer (Millipore Hertfordshire UK). The medium was changed every second day and cells were left for 2–3 days to grow until they had reached 80% confluence. To determine if dDCN had successfully differentiated into dDCN, the common marker TH (MAB318, 1:1500, Millipore Hertfordshire UK) was used. dDCN were fixed with 4% parformaldehyde for 15 minutes and were washed with cold PBS. Subsequently, dDCN were treated with Triton X-100 for 10 minutes and blocked with 10% goat serum (S-1000, Vector Labs Peterborough UK) for 40 minutes prior to primary antibody Anti-TH (1:1500, Millipore Hertfordshire UK) incubation for overnight at 4°C. The following morning, dDCN were washed with PBS (3 × 5 minutes) and incubated with secondary antibody Donkey-Anti-Mouse IgG FITC (1:500, Millipore Hertfordshire UK) for two hours at RT. Cells were mounted using vectorshield mounting medium (158127, Vector Labs Peterborough UK) and were viewed under a Meiji fluorescent microscope (Mazurek Warwickshire UK). Statistical analysis was carried out as described in Chapter 2 Section 2.5.2. A more detailed account of the reagents used can be found in Chapter 2 Section 2.1 and Appendix 1.

4.2.2 Administration and optimisation of 6OHDA in dDCN

dDCN were exposed to different concentrations of 6OHDA (50μM, 100μM, 150μM and 200μM) at different time intervals (30min, 1 hour, 1 hour 30 min, 2 hour, 2 hour 30min, 3 hour, 3 hour 30 minute, 4 hour and 5 hour). After each given exposure time, 6OHDA drug treatment was stopped by removing 6OHDA and replacing with fresh media. Optimisation of 6OHDA was carried out using MTT assay (BT30006, Cambridge BioScience, Cambridge UK) and the absorbance was read at 570nm using microplate reader.

4.2.3 Determining apoptosis in dDCN using TUNEL Assay

To determine if 6OHDA stimulates death of dDCN via apoptotic or necrotic pathway TUNEL assay (482830K**,** Trevigen Maryland USA) was used. Various inhibitors (salubrinal, IKK, zVADfmk, zVDVADfmk, zLEVDfmk and zIETDfmk) were used with 6OHDA to determine if the inhibitor protects 6OHDA mediated death of dDCN. A more detailed account of the reagents used can be found in Chapter 2 Section 2.2 and Appendix 1.

4.2.3.1 Administration and inhibition of dDCN

dDCN were cultured and treated with 100µM 6OHDA, 100µM 6OHDA and 30µM salubrinal (Santa Cruz Biotechnology Heidelberg Germany), 100µM 6OHDA and 70µM IKK (Merck Chemicals Nottingham UK), 100µM 6OHDA and 50µM zVADfmk (Promega Southampton UK), 100µM 6OHDA and 20µM zLEVDfmk (Merck Chemicals Nottingham UK), 100µM 6OHDA and 80µM zIETDfmk (Merck Chemicals Nottingham UK), 100µM 6OHDA and 20µM zVDVADfmk (Merck Chemicals Nottingham UK), for 2 hours after which the given treatments were replaced with fresh media. dDCN were left overnight in CO_2 incubator at 37°C.

4.2.3.2 TUNEL assay used to verify apoptotic death of dDCN

6OHDA-treated and untreated dDCN were centrifuged at 1000 x g for 7 minutes at RT followed by fixing with 3.7% formaldehyde for 7 minutes. Subsequently, dDCN plate was centrifuged at 1000 x g for 7 minutes at RT and dDCN were washed with PBS. 100% methanol was placed in dDCN for 20 minutes at RT, after which dDCN were washed with PBS. Treated and untreated dDCN were centrifuged as normal and the PBS was replaced with Protein K and was left to incubate for 15 minutes. TACSNucleaseTM Solution was added to the untreated samples and was incubate for 40 minutes. All samples were washed twice with PBS followed by centrifugation. Hydrogen peroxide (30%) was added to treated and untreated dDCN for 4 minutes to suppress endogenous activity. Treated and untreated dDCN were washed with distilled water and were centrifuged at 1000 x g for 5 minutes. Labelling buffer was added to all dDCN for 5 minutes following centrifugation. The labelling buffer was replaced with labelling Reaction solution. The microplates were placed in a humidified chamber to incubate for an

hour at 37°C. TdT Stop Buffer was added to all samples for 5 minutes to stop labelling reaction after which the microplates were centrifuged and the buffer was removed. Treated and untreated dDCN were serial washed with PBS and then centrifuged 1000 x g for 5 minutes. Treated and untreated dDCN were incubated with HRP Solution for 10 minutes. PBST (0.1%) was used to wash samples followed by centrifuging the plate between each wash. Subsequently, TACS-Sapphire was added to treated and untreated dDCN and the samples were incubated for 30 minutes in the dark. The addition 0.2 N HCl was used to stop the reaction and the absorbances were read at 450 nm. Statistical analysis (ANOVA $p<0.05$, T test at $p<0.05$) was carried out to determine the apoptotic death of 6OHDA-treated dDCN.

4.2.4 6OHDA triggers Caspase mediated death of dDCN

To determine if 6OHDA provoked Caspase mediated death of dDCN, the CaspACE assay system kit (G7351, Promega Southampton UK) was used. In addition, IF analysis was carried out to determine if Caspase-2(Abcam Cambridge UK), Caspase-3(04-439, Millipore Hertfordshire UK) and Caspase-8 (Abcam Cambridge UK) are activated expressed in 6OHDA TH positive cells.

4.2.4.1 Determining the effect of zVADfmk on 6OHDA-treated dDCN

To check if 6OHDA stimulated Caspase mediated cell death in dDCN, Caspase detection kit was used following manufacturer's instructions (G7351 caspACE assay system, Promega Southampton UK). Briefly, cells were treated with 100μM 6OHDA in the presence of 50μM zVADfmk for 2 hours, after which fresh media was replaced and cells were left to recover overnight. Cells were washed in ice cold PBS, resuspended in lysis buffer, following freeze thaw cycles to produce lysates. The lysates were centrifuged and the extracts obtained were detected for Caspase activity using DEVD-pNA substrate via the colorimetric method, absorbance was measured at 405nm.

4.2.4.2 Determining presence of Caspases-2,-3 and-8 in untreated (-6OHDA) and treated (+6OHDA) dDCN

IF was used to determine if Caspases-2,-3 and-8 are expressed in untreated and treated 6OHDA dDCN with similar methodology as described above (Section 4.2). The primary antibodies; cleaved Anti-

Caspase-3 (1:1000, Millipore Hertfordshire UK), active Anti-Caspase-2 (1:2000, Abcam Cambridge UK), active Anti-Caspase-8 (1:2000, Abcam Cambridge UK), and Anti-TH (1:1500, Millipore Hertfordshire UK) were used overnight at 4C. Secondary antibodies; Donkey-Anti-Mouse IgG FITC (1:500, Millipore Hertfordshire UK), Goat-Anti-Rabbit IgG Rhodamine (1:2500 Millipore Hertfordshire UK) were used for two hours at RT prior to mounting and viewing the cell under the IF microscope. Three independent experiments were performed for each sample. Semi quantitative analysis ($p<0.05$, T test) to determine the change in TH positive and Caspase positive dDCN was carried out as described in Chapter 2 Section 2.5.2. A more detailed account of the reagents used can be found in Chapter 2 Section 2.1 and Appendix 1.

4.2.4.3 Caspases-2 and-8 can stimulate Caspase-3 activation of 6OHDA dDCN

The dDCN were treated with 100μM 6OHDA and 50μM zVADfmk as described above. Cells were lysed and protein concentration was measured using the BCA kit (Pierce Biotechnology, Rockford, IL, USA). Fifty micrograms protein was loaded on 12% gel prior to SDS PAGE, followed by immunoblotting on PVDF membrane. The membrane was blocked with 1% skimmed milk for an hour followed by incubation with primary antibodies; cleaved Anti Caspase-3 (1:1500, Abcam Cambridge UK), active Anti-Caspase-2 (1:2500, Abcam Cambridge UK), active Anti-Caspase-8 (1:1000, Abcam Cambridge UK) for overnight incubation at 4^{o}C. The following day, membranes were incubated with secondary antibody, Goat-Anti-Rabbit HRP (1:1000, Millipore Hertfordshire UK) for an hour at RT. After washing the membranes with PBST, the ECL HRP detection system was employed as described by the supplier (Perbio Science Northumberland UK). Immunoblots bands were quantified with a densitometer scanner (GS800, Biorad Hertfordshire UK). Five independent experiments were performed for each treatment. Statistical analysis was carried out at $p<0.05$ using student T test followed by strip and reprobe with the house keeping gene GAPDH (Chapter 2 Section 2.3.4 and Chapter 2 Section 2.3.5 correspondingly). A more detailed account of the reagents used can be found in Chapter 2 Section 2.2 and Appendix 1.

ReNcell VM was differentiated in to dopaminergic cells by withdrawal of growth factors (EGF and FGF) after two weeks of culture. To ensure that the cells were dopaminergic, the dopamine marker TH was used. Figure 4.1 portrays positive TH staining which indicates that the cells had been successfully differentiated into dopaminergic cells (Chaudhry and Ahmed 2013).

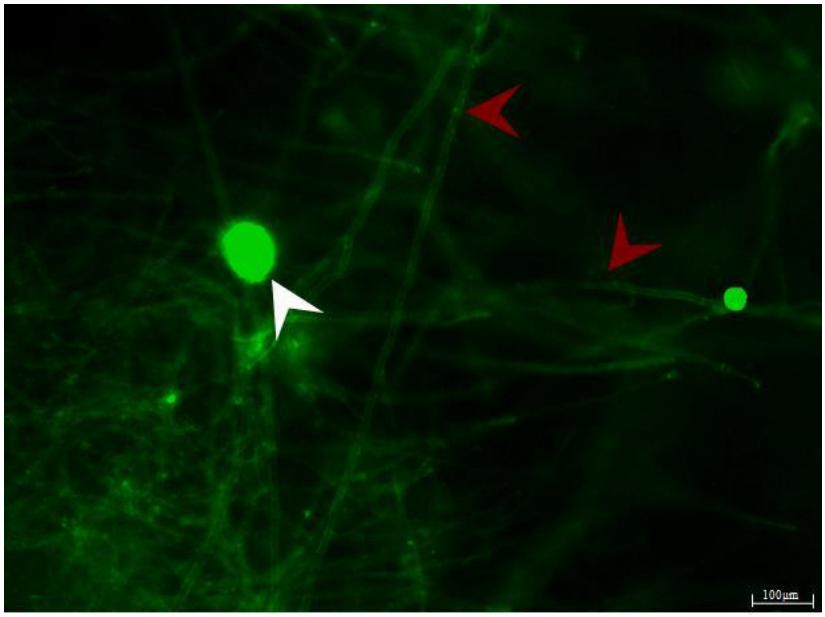

Figure 4.1: Differentiated ReNVM cells are dopaminergic

To ensure that cells had differentiated into DCN, TH, a marker for dopaminergic neurons was used. The Figure shows positive staining for TH indicating successful differentiation of ReNcell VM into dDCN. The cell body (white arrow) and dendrites (red arrow) showed positive staining for TH.

The next aim was to establish a suitable PD model with the administration of the neurotoxin 6OHDA in dDCN. 6OHDA is transported into the nerve terminals via dopamine transporter. At the nerve terminals of DCN, 6OHDA produced ROS resulting in degradation of dopaminergic cells. 6OHDA was used to induce neurotoxicity, thereby subsequent experiments could be carry out successfully when exploring cell death mechanisms in dDCN. Various concentrations of 6OHDA (50µM, 100µM, 150µM and 200µM) were used at different time intervals (30min, 1 hour, 1 hour 30 min, 2 hour, 2 hour 30min, 3 hour, 3 hour 30 minute, 4 hour and 5 hour) to determine the optimal conditions to create PD model for further neurotoxicity experiments. Figure 4.2 illustrated a significant decrease in 6OHDA-treated dDCN, when compared with untreated 6OHDA dDCN (Chaudhry and Ahmed 2013).

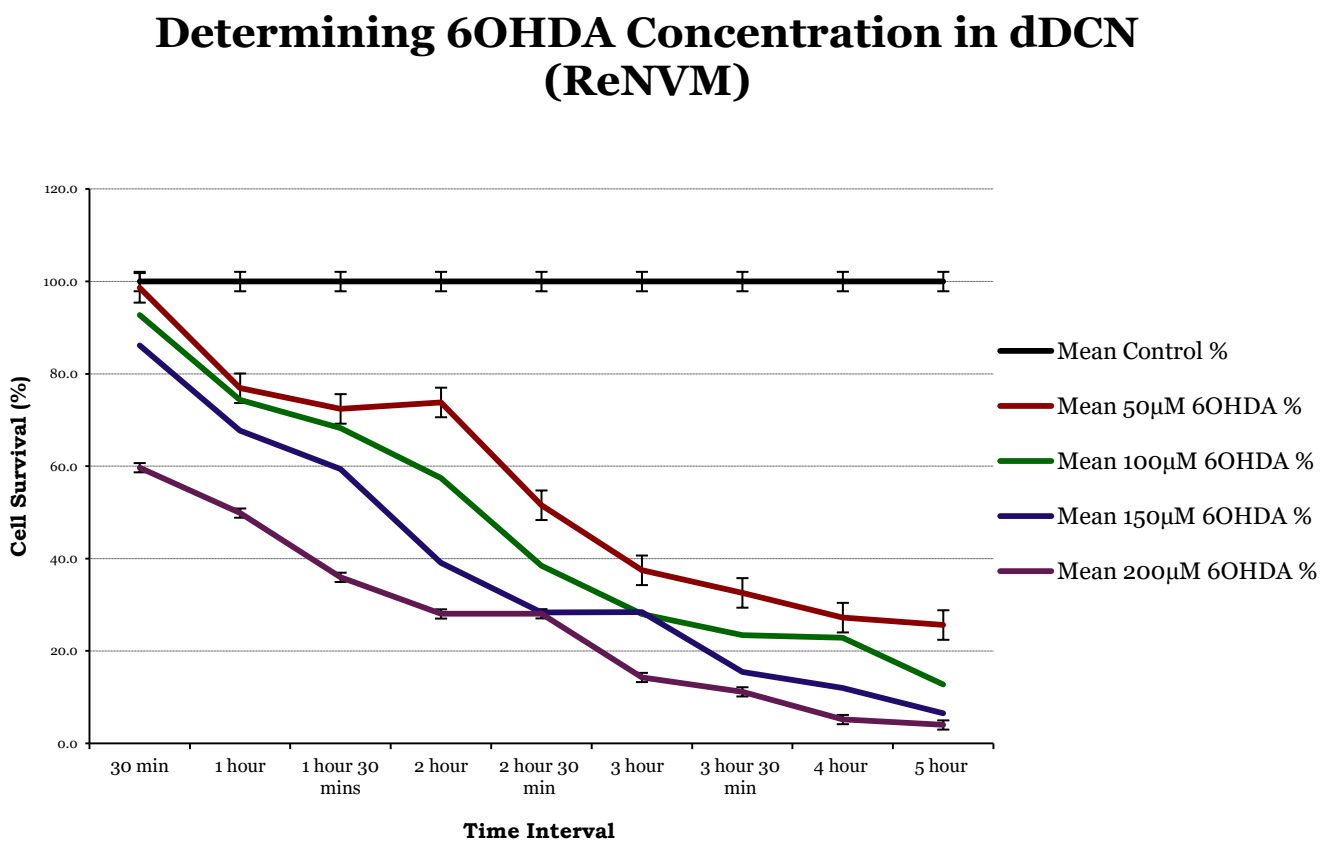

Figure 4.2: 6OHDA toxicity in dDCN

Optimisation of 6OHDA was carried out using MTT assay. Various concentrations of 6OHDA (50µM, 100µM, 150µM and 200µM) were used at different time intervals (30min - 5 hour) to determine the optimal conditions. The Figure illustrates a significant decrease of cell survival in 6OHDA-treated

dDCN, when compared with untreated dDCN. dDCN exposed at 200μM had 59.1% survival in cell number at 30 minute time interval, when compared to dDCN treated with 50μM 6OHDA (98.6%) , 100μM 6OHDA (92.7%) and 150μM 6OHDA (86.2%) at the same time interval. Administration of 6OHDA at 30 minute time interval was too early to detect the effect of Caspases and there was above 85% survival of dDCN (when using concentration 50μM, 100μM and 150μM 6OHDA). Although administration of 200μM 6OHDA at 30 minute time interval showed 59.1% dDCN survival the exposure was quick and the effect of Caspases may have been lost, therefore this concentration was not used. After cells had been exposed to 6OHDA for three hours at different concentrations, there was a significant reduction in dDCN survival (less than 30% cell number), therefore the effect of Caspases would be hard to determine as most cells have died. In addition, it would be hard to determine effect of Caspases if the number of dDCN to begin with was less than 30%, therefore this time frame and concentrations of 6OHDA were not used. To establish a suitable PD a balance was required to see the effect Caspases had on 6OHDA dDCN and to have enough dDCN to use in the experiments. The optimal conditions used to induce neurotoxicity in dDCN in order to establish a PD model for further work, was to treat dDCN with 100μM 6OHDA at 2 hour time interval. Administration of 100μM 6OHDA at 2 hour time interval in dDCN provided the balance to see the effect of Caspases in adequate number of cells (57% dDCN survival). Table of values can be found in Figure 4.3, Appendix 4.

To determine if 6OHDA caused induction of Caspases-2, 3 and 8 in treated dDCN double IF study using Anti Caspases-2,-3,-8 along with Anti-TH antibody was carried out (Chaudhey and Ahmed 2013, Figure 4.4). The presence of Caspases in untreated dDCN was not surprising as Caspases are required for normal cellular function. Figure 4.4 shows positive staining of Caspases-2,-3 and -8 of 6OHDA-treated dDCN. A loss in dendrites and formation of apoptotic bodies was observed in all 6OHDA-treated cells, suggesting 6OHDA had destroyed dendrites of DCN. Active Caspase-2 (red stain) was expressed approximately half of untreated dDCN. In 6OHDA dDCN, Caspase-2 was actively expressed in more TH positive dDCN. Cleaved Caspase-3 (red stain) was expressed in low levels of TH positive dDCN. In contrast, a significant increase in the number of cleaved Caspase-3 was observed in 6OHDA-treated dDCN. Similar findings were established when determining Caspase-8 expression in untreated and 6OHDA-treated dDCN. Active Caspase-8 (red stain) was present in less than half of TH positive dDCN (green stain).6OHDA-treated dDCN had elevated levels of active Caspase-8 present indicating 6OHDA promotes an increased induction of Caspase-8 in dDCN.

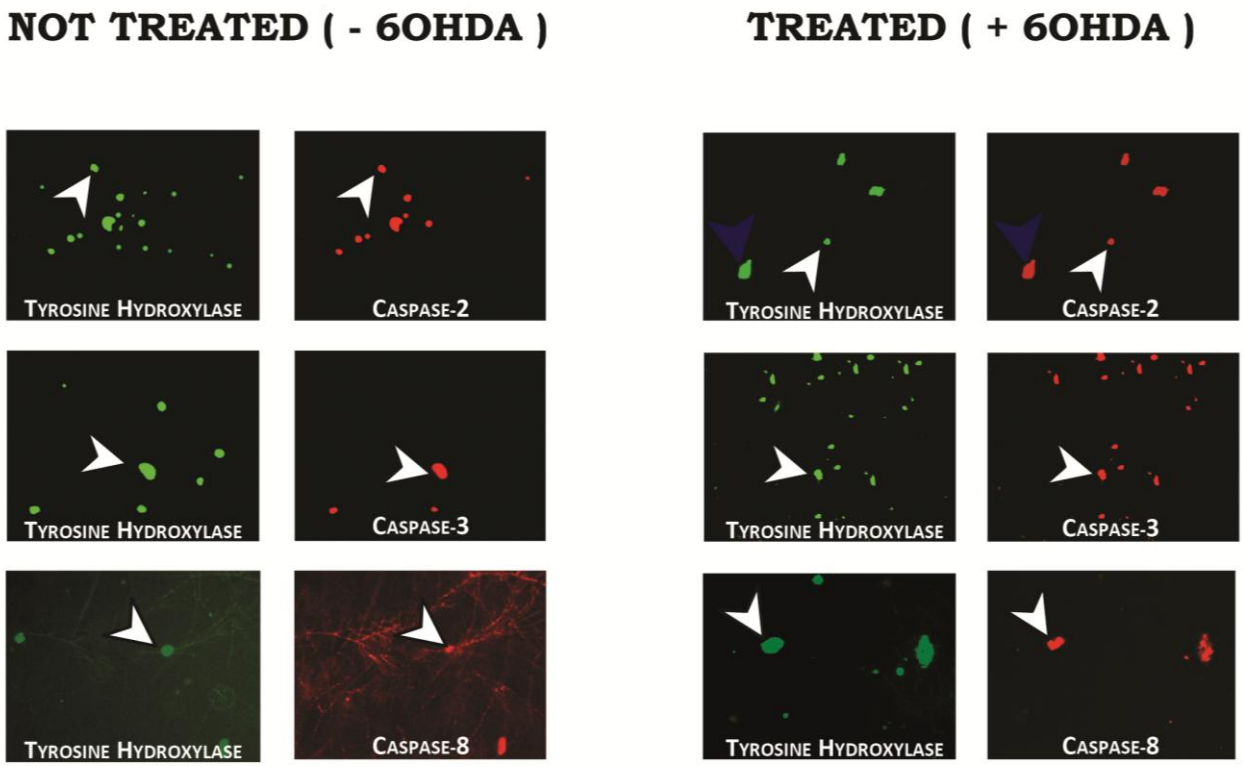

Figure 4.4 : 6OHDA triggered Caspase-2, -3 and -8 activation in dDCN

Active Caspase-2 (red stain) expression was found in more in half of untreated TH positive (green stain) dDCN. Active Caspase-2 expression was increased in TH positive 6OHDA-treated dDCN, suggesting 6OHDA caused activation of Caspase-2 resulting in cell death. In comparison, cleaved Caspase-3 (red stain) was observed in all 6OHDA-treated dDCN, but was found only in some untreated dDCN, indicating that 6OHDA enhanced Caspase-3 mediated cell death. Moreover, active Caspase-8 (red stain) was expressed in some untreated dDCN, indicating that in normal cellular processes active Caspase-8 is present. Active Caspase-8 was present in more 6OHDA-treated dDCN, compared to untreated dDCN, indicating that 6OHDA provokes Caspase-8 activity in dDCN.

Positive staining for cell bodies (White Arrow) and budding of apoptotic bodies (Blue Arrow) was observed in untreated (- 6OHDA) and treated (+ 6OHDA) dDCN.

Quantification analysis revealed that 6OHDA stimulated the increase in active Caspases-2,-3 and -8 in dDCN (Figure 4.5). 6OHDA had elevated the proportion of Caspase-2 in TH positive 6OHDA-treated dDCN, indicating an increase in Caspase-2 activity. A significant increase in the proportion of TH cells that were Caspase-3 positive in treated dDCN signified that 6OHDA promoted induction of Caspase-3 resulting in death of dDCN. An increase in the proportion of active Caspase-8 in TH positive 6OHDA-treated dDCN, demonstrated that 6OHDA stimulates further Caspase-8 activity in dDCN.

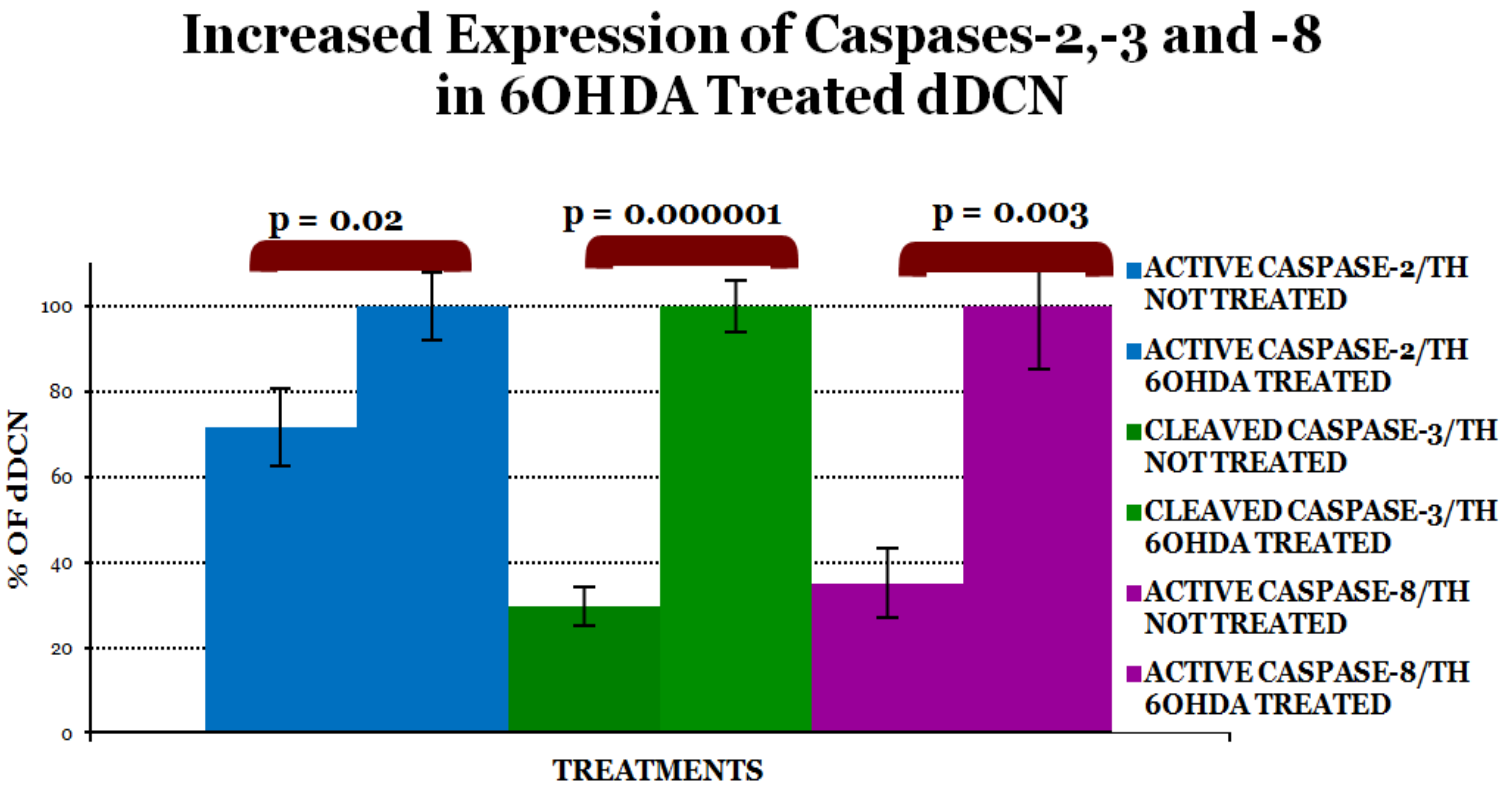

Figure 4.5: 6OHDA amplified expression of activated Caspases-2,-3 and-8 in dDCN

Graph showing that the proportion of active Caspase-2 TH positive, cleaved Caspases-3 TH positive and activated Caspase-8 TH positive cells had significantly increased after 6OHDA treatment ($p<0.05$). Means of five experiments ± SEM shown. Table of values and statistical analysis can be found in Figure 4.6, Appendix 4.

Co-localisation studies revealed the presence of Caspase-2 and -3 in the same cell in untreated and treated dDCN (Chaudhry and Ahmed 2013, Figure 4.7). Active Caspase-2 was present in more untreated dDCN, compared to cleaved Caspase-3. However, in 6OHDA-treated dDCN, more cells were stained positive for Caspase-3 compared to Caspase-2. 6OHDA may have triggered Caspase-2, leading to the activation of Caspase-3 in dDCN. In contrast, low levels of Caspase-3 and -8 were found in untreated dDCN. A significant increase in the number of cells that were both Caspase-3 and -8 positive increased in 6OHDA-treated dDCN. 6OHDA may have provoked activation of upstream Caspase-8, which subsequently led to activation of downstream Caspase-3 in dDCN.

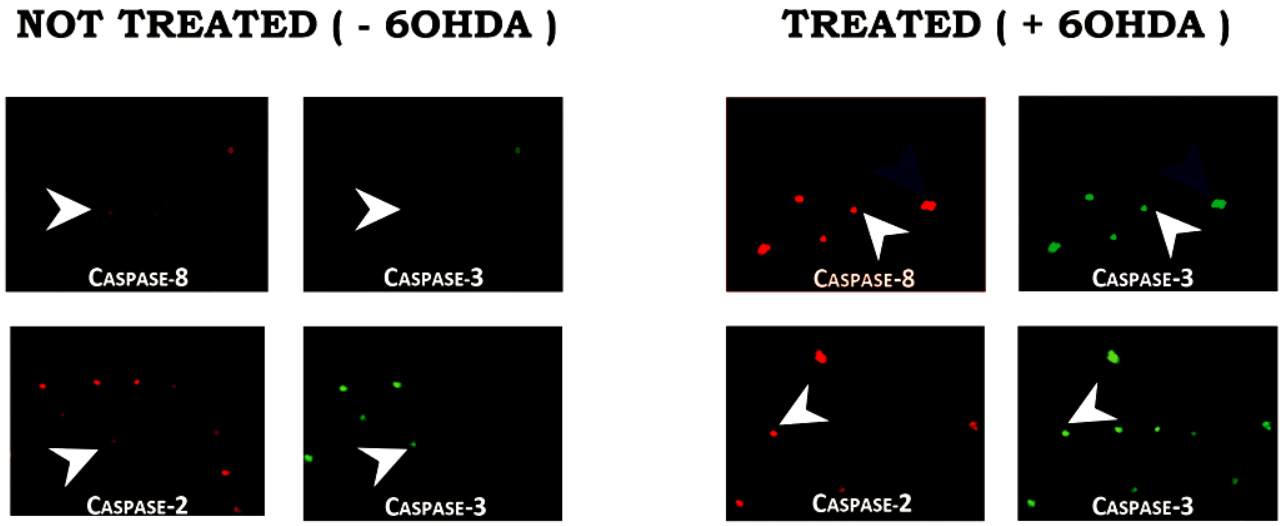

Figure 4.7 : 6OHDA triggered activation of Caspase-2, -8 and followed by Caspase-3 in dDCN

Double IF staining signified the presence of higher expression of Caspase-2 (red stain), compared with Caspase-3 (green stain) in untreated dDCN. In contrast, 6OHDA-treated dDCN showed more Caspase-3 and less Caspase-2 expression. Untreated dDCN revealed low levels of active Caspase-8 positive (red stain) and active Caspase-3 positive (green stain) cells. A significant rise in active Caspase-3 and-8 expressions was determined in 6OHDA-treated dDCN. Collectively the results indicate 6OHDA stimulates activation of Caspases-2 and -8 followed by Caspase-3 in dDCN. Positive staining for cell bodies (White Arrow) in untreated (- 6OHDA) and treated (+ 6OHDA) dDCN. Table of values and statistical analysis can be found in Figure 4.8, Appendix 4.

To investigate if 6OHDA could cause Caspase-mediated cell death of dDCN, a broad Caspase-inhibitor zVADfmk was used. zVADfmk significantly reduced level of dying cells that had been treated with 6OHDA ($p < 0.05$, Figure 4.9). zVADfmk irreversibly binds to the cysteine residue of Caspases, thereby decreasing Caspase-activation and Caspase-dependent cell death of 6OHDA dDCN. The result successful demonstrated 6OHDA caused cell death of dDCN and the death of cells is Caspase dependent, therefore it is a good model to use to study Caspases in PD.

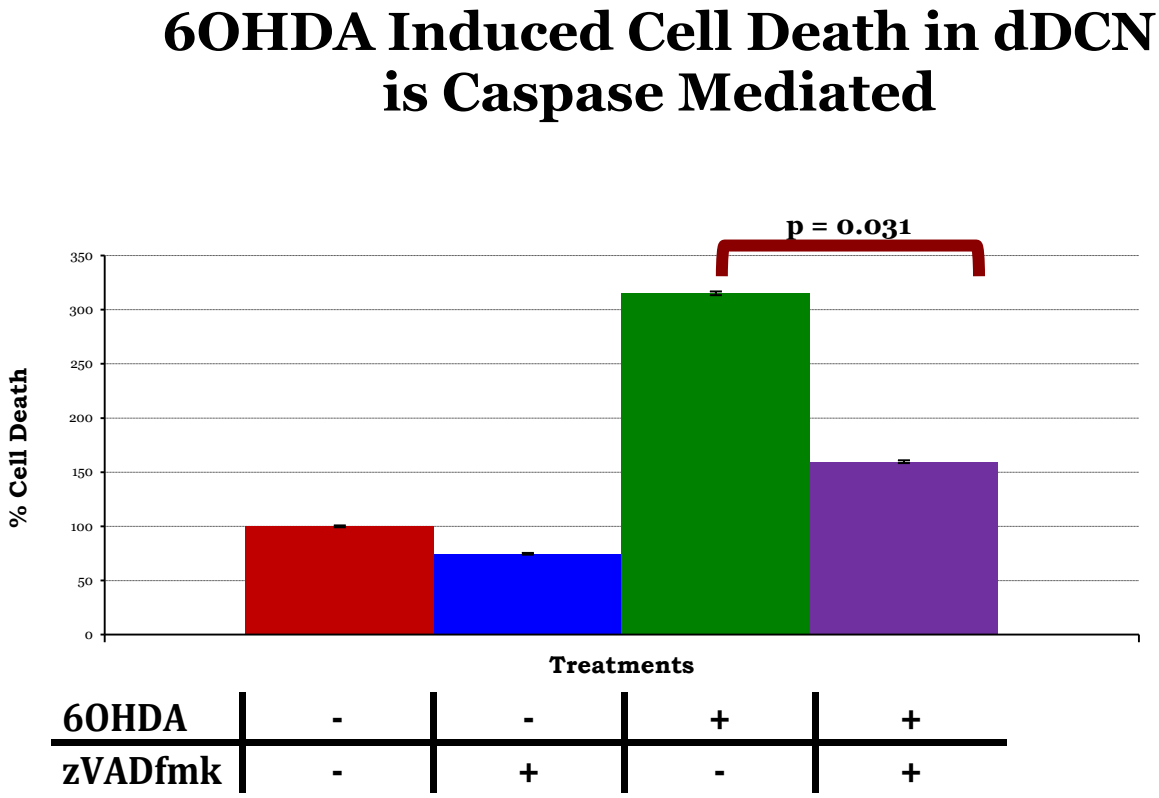

Figure 4.9: Determining the effect of zVADfmk in 6OHDA-treated dDCN

Graph showing that the common Caspase inhibitor zVADfmk considerably reduced cell death by approximately 50% ($p<0.05$) of dDCN, which had been treated with 6OHDA and zVADfmk (purple bar), when compared to dDCN treated with 6OHDA only (green bar). Means of five experiments ± SEM shown. Table of values and statistical analysis can be found in Figure 4.10, Appendix 4.

The next aim was to identify which Caspases are stimulated by 6OHDA in dDCN. In order to determine if specific Caspases can be inhibited following 6OHDA-induced toxicity in dDCN, the universal inhibitor, zVADfmk was used. zVADfmk significantly reduced activation of Caspase-2 (Figure 4.11), Caspase-3 (Figure 4.13) and Caspase-8 (Figure 4.15) in 6OHDA-treated dDCN. zVADfmk reduced the amount of active Caspase-2 in 6OHDA-treated dDCN by 41%, when compared to dDCN that were treated with 6OHDA only (Figure 4.11, $p<0.05$). Similarly, zVADfmk decreased cleaved Caspase-3 and active Caspase-8 by 88% and 74% respectively compared to 6OHDA treated dDCN (Figure 4.13, $p<0.05$ and Figure 4.15, $p<0.05$). Collectively, the results suggested that all studied Caspases-2,-3 and-8 play an active role in 6OHDA-mediated death of dDCN. This supports data obtained from IF analysis and confirms the involvement of these Caspases in this PD model.

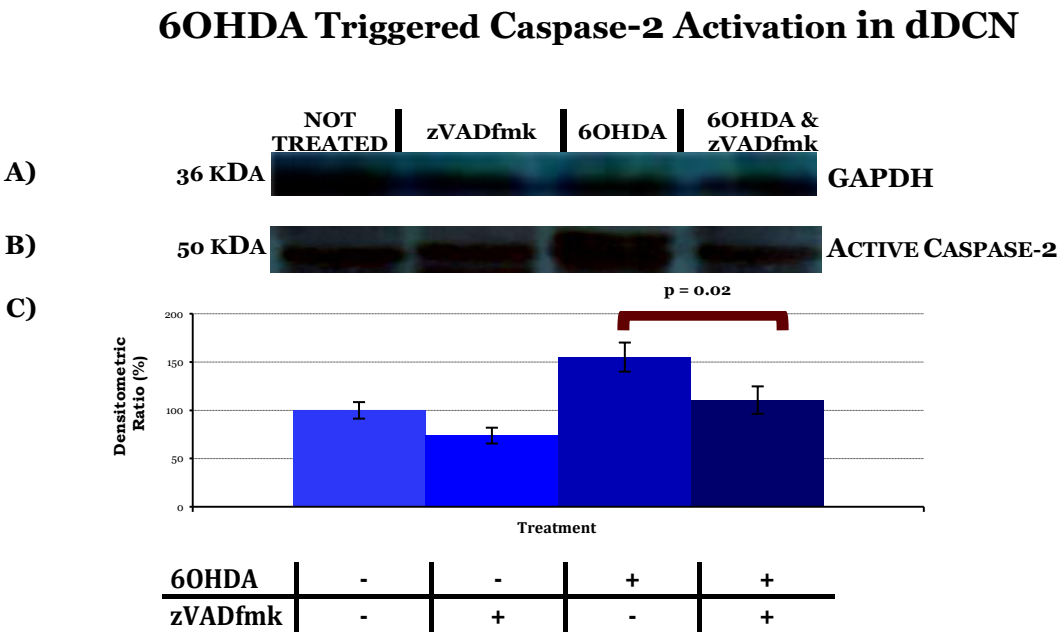

Figure 4.11: zVADfmk decreased the amount of active Caspase-2 in 6OHDA-treated dDCN

A) Illustrative example of GAPDH in untreated, zVADfmk, 6OHDA, zVADfmk+6OHDA treated dDCN.

B) Illustrative example of active Caspase-2 in untreated, zVADfmk, 6OHDA, zVADfmk+6OHDA treated dDCN.

C) Graph showing the common Caspase inhibitor zVADfmk significantly reduced amount of active Caspase-2 (41 % reduction, $p<0.05$) of treated 6OHDA dDCN, when compared to dDCN treated with 6OHDA only. Means of five experiments ± SEM shown. Table of densitometry values and statistical analysis can be found in Figure 4.12, Appendix 4.

6OHDA Triggers Caspase-3 Activation in dDCN

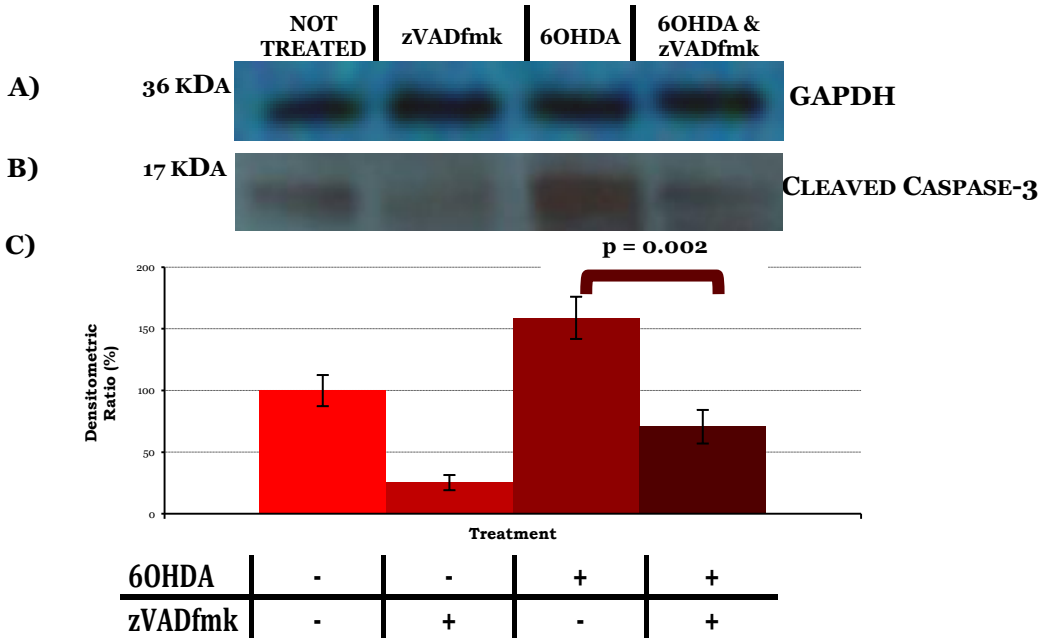

Figure 4.13: zVADfmk decreased cleaved Caspase-3 levels in 6OHDA-treated dDCN

A) Illustrative example of GAPDH in untreated, zVADfmk, 6OHDA, zVADfmk+6OHDA treated dDCN.

B) Illustrative example of cleaved Caspase-3 in untreated, zVADfmk, 6OHDA, zVADfmk+6OHDA treated dDCN.

C) Graph showing zVADfmk significantly decreased cleaved Caspase-3 in treated dDCN (88% reduction, $p<0.05$), compared to 6OHDA-treated dDCN. Means of five experiments ± SEM shown. Table of densitometry values and statistical analysis can be found in Figure 4.14, Appendix 4.

6OHDA Stimulates Caspase-8 Activation in dDCN

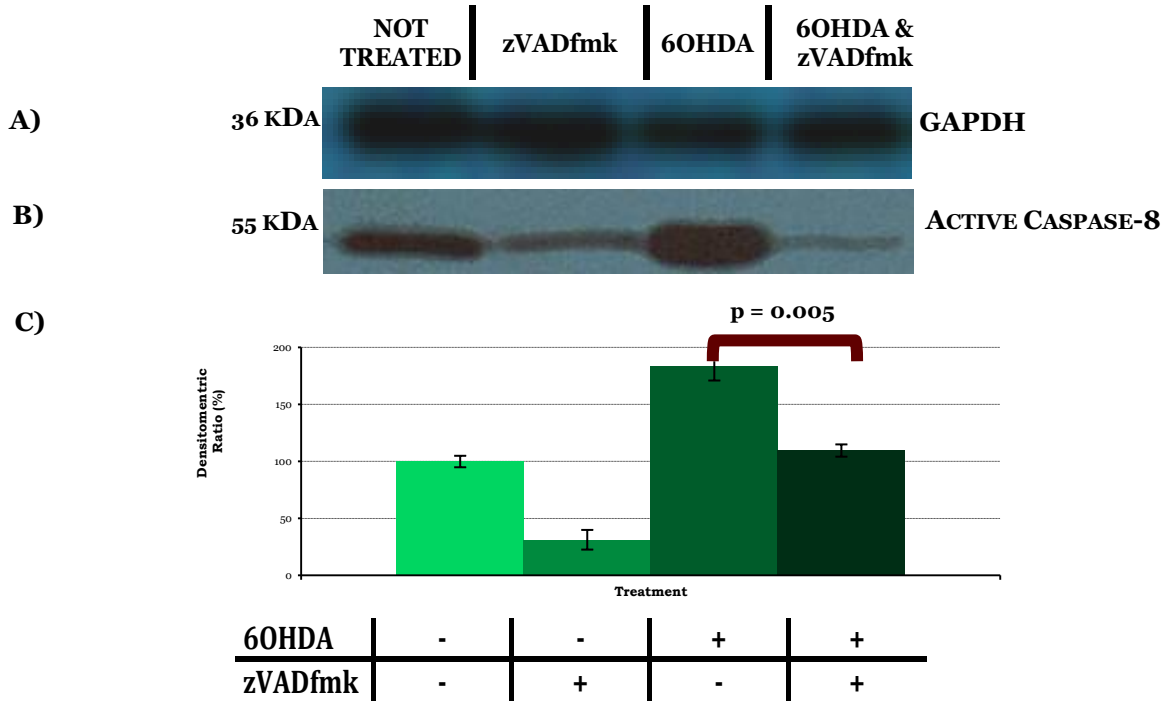

Figure 4.15: 6OHDA stimulates increased Caspase-8 activity in dDCN

A) Illustrative example of GAPDH in untreated, zVADfmk, 6OHDA, zVADfmk+6OHDA treated dDCN.

B) Illustrative example of active Caspase-8 in untreated, zVADfmk, 6OHDA, zVADfmk + 6OHDA treated dDCN.

C) Graph showing zVADfmk reduced active Caspase-8 in 6OHDA mediated death (74% reduction, $p<0.05$) compared to 6OHD induced dDCN. Means of five experiments ± SEM shown. Table of densitometry values and statistical analysis can be found in Figure 4.16, Appendix 4.

The results had indicated 6OHDA triggers Caspase mediated death of dDCN. The subsequent aim was to determine if 6OHDA caused death of dDCN by necrosis or apoptosis pathway, using TUNEL assay. In the damaged cell, the activation of Caspase-3 catabolises the ICAD of the ICAD-CAD complex, thereby releasing and activating CAD (refer to page 68-70 for further details). Active CAD splices DNA into fragments, which is a key trait of apoptotic death. The Tacs TdT enzyme detects the DNA fragments of the damaged cell. The results showed that 6OHDA significantly encouraged death of dDCN through apoptotic pathway ($p<0.01$, Figure 4.17). IF and WB analysis had shown 6OHDA triggered activity of Caspases-2, 3 and-8 in dDCN. To further explore this area a more interesting method was used. 6OHDA dDCN were treated with different types of inhibitors to gain a better understanding which proteins are present in the apoptotic cell death pathways.

ANOVA and T test analysis ($p<0.05$) revealed a significant difference the level of apoptotic death of 6OHDA dDCN with different treated inhibitors. Salubrinal a specific inhibitor of the PERK ER stress pathway had prevented 6OHDA-treated dDCN from apoptotic death. 6OHDA triggered 36% apoptotic death of salubrinal treated dDCN, indicating that the PERK ER stress pathway is a potential pathway involved in cell death ($p<0.01$, Figure 4.17). dDCN that were treated with 6OHDA and the specific IKK inhibitor that suppresses the activation of the NFκB classical pathway, had shown 65% apoptotic cell death ($p<0.01$, Figure 4.17). Previous data had shown the universal inhibitor, zVADfmk had decreased Caspases-2,-3 and -8 activities in 6OHDA dDCN. 6OHDA+ zVADfmk treated dDCN had 25% apoptotic death of dDCN, confirming that 6OHDA triggers Caspases resulting in death of dDCN via apoptotic rather than necrotic routes ($p<0.01$, Figure 4.17).

The results had shown Caspase-2 was active in 6OHDA dDCN. This finding was extended further using a Caspase-2 specific inhibitor zVDVADfmk. 6OHDA+zVDVADfmk treated dDCN shown 34% apoptotic cell death, confirming its involvement in apoptotic death of dDCN ($p<0.01$, Figure 4.17). Similarly, Caspase-8 specific inhibitor, zIETDfmk was used in 6OHDA-treated dDCN. 6OHDA+zIETDfmk treated dDCN, had 61% level of apoptotic cell death, indicating that 6OHDA stimulates Caspase-8 activity resulting in death of dDCN via apoptosis ($p<0.01$, Figure 4.17). To extend the idea of Caspase mediated death of 6OHDA dDCN further, another potential Caspase was explored. zLEVDfmk is an inhibitor that can specifically inhibit Caspase-4 activity. 6OHDA+zLEVDfmk treated dDCN, had shown 44% apoptotic cell death, indicating that 6OHDA triggers Caspase-4 activity in dDCN ($p<0.01$, Figure 4.17).

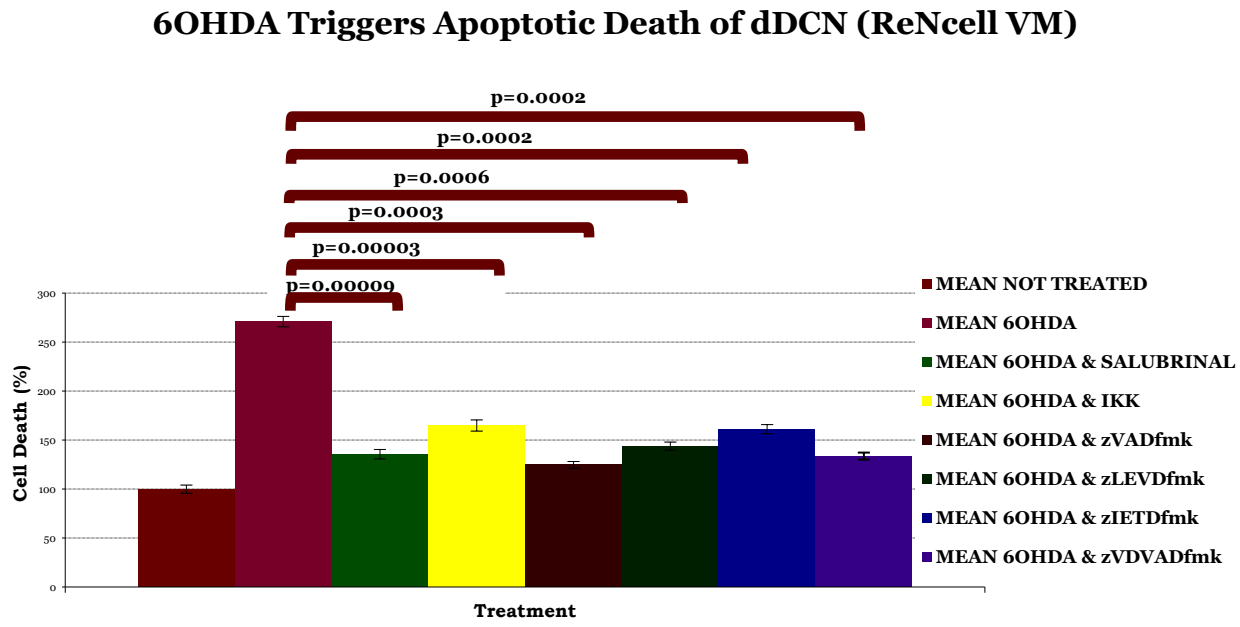

Figure 4.17: 6OHDA provokes apoptotic death of dDCN

To determine if 6OHDA stimulated death of dDCN via apoptotic or necrotic pathway, TUNEL assay was used. Various inhibitors (salubrinal, IKK, zVADfmk, zVDVADfmk, zLEVDfmk and zIETDfmk) were used with 6OHDA, to determine if the inhibitor decreased 6OHDA mediated death of dDCN. 6OHDA triggered death of dDCN, via apoptotic route. The graph illustrates that different inhibitors reduced apoptotic death of dDCN at various rates. Proportion of apoptotic dDCN was determined by TUNEL absorbance at 450nm. Means of three experiments ± SEM shown. Table of values and statistical analysis can be found in Figure 4.18, Appendix 4.

6OHDA triggered NFκB, PERK, Caspases-2,-3,-4 and -8 activities resulting in apoptotic death of dDCN (Figure 4.19). The results have demonstrated 6OHDA promotes activation of Caspases-2 and -8 leading to stimulation of Caspase-3 dDCN. 6OHDA may have stimulated a variety of pathways or these pathways may be interlinked resulting in apoptotic death of dDCN. Furthermore, Caspases-2,-3,-4 and -8 may be involved in one or many of these pathways or may be activating one another resulting in apoptotic death of 6OHDA-treated dDCN.

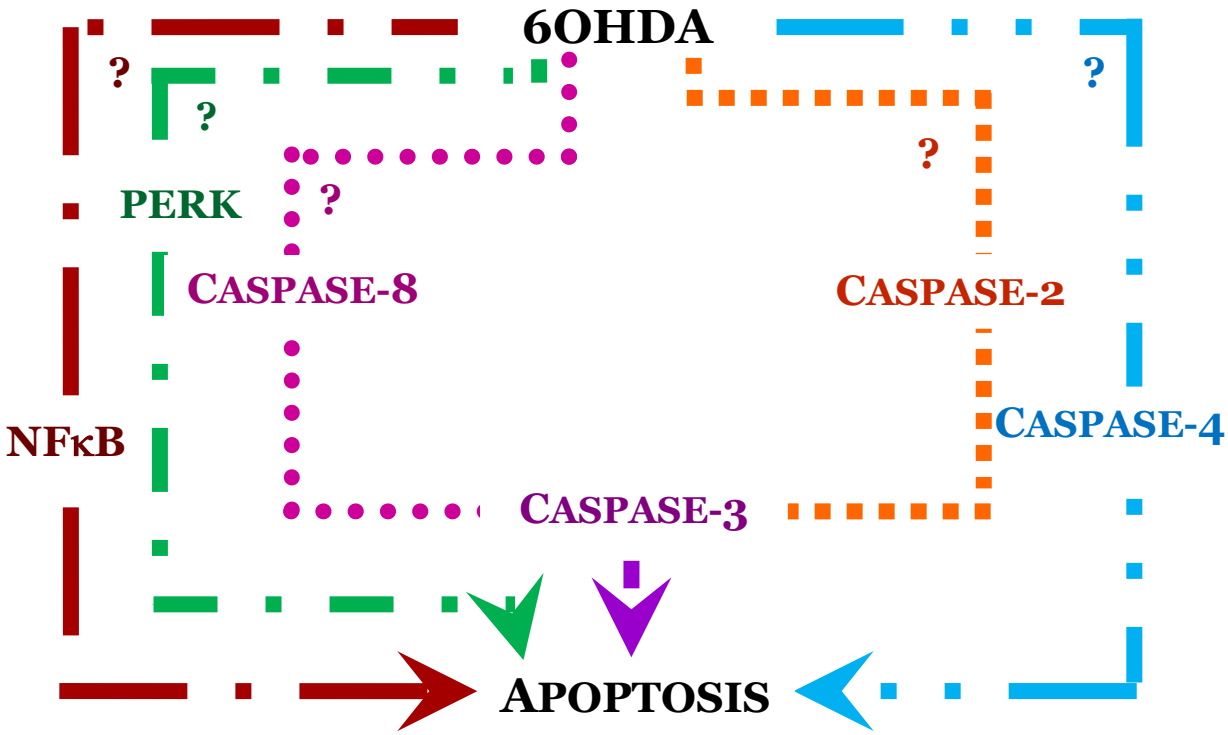

Figure 4.19: 6OHDA promotes apoptotic death of dDCN via different pathways

6OHDA triggered Caspase mediated apoptotic death of dDCN. The results have indicated 6OHDA stimulates NFκB classical pathway, PERK ER stress pathway and Caspases-2,-3,-4 and -8 that eventually result in apoptotic death of dDCN. The next steps are to identify if these Caspases pathways are related to NFκB pathway or PERK ER stress pathway in 6OHDA-treated dDCN. Furthermore, the remainder of this study is to determine how 6OHDA triggers Caspase activity and if there is any cross talk between these Caspases or the different pathways that result in death of dDCN via apoptotic route.

4.4 Discussion

The aim of the current study was to establish successful PD model to investigate cell death mechanisms using ReNcell VM that had differentiated into DCN. Figure 4.1 shows positive staining for TH indicating that after the withdrawal of growth factors EGF and FGF, ReNcell VM had successfully differentiated into DCN. This method was adopted from research by Donato et al (2007) who had used TH as a marker to determine if the ReNcell VM had differentiated into DCN after removal of growth factors. In Donatos et al (2007) research it was found that the dDCN from the ReNcell VM had grown in bunches which allowed them to form neurospheres and promoting the generation of action potentials. In addition, research by Jaegar et al (2013) further demonstrated undifferentiated ReNcell VM was shown to be spread across the plate with many cell bodies of round appearance and short axons and dendrites, whilst differentiated ReNcell VM had grown in bunch like manner, with longer dendrites and axons and smaller cell bodies. In the current study, dDCN had also grown in a bunch like state with elongation of axons, dendrites and formation of neurospheres similar to Donato et al (2007) and Jaegar et al (2013) research.

The production of ROS has been strongly linked to PD pathogenesis, via the oxidative stress theory (Shih et al 2011). In order to make a suitable model to study PD, the initial step was to optimise the concentration of 6OHDA in dDCN. PD patients suffer from an 80% loss of DCN in the SNpc region of the brain. However, if this model to study PD, had 80% loss of DCN, it would be difficult to study cell death mechanisms as the majority of cell death had already occurred. Therefore, an earlier time frame was required and a 50% loss of DCN was chosen as there would be enough cells to carry out experiments and determine the cell death mechanisms occurring in DCN (Figure 4.2).

The current study is the first to demonstrate 6OHDA stimulates Caspase mediated death via apoptotic route in ReNcell VM that had been differentiated into DCN (Chaudhry and Ahmed 2013). Current research by Jaegar et al (2013) had demonstrated positive staining for apoptosis in differentiated ReNcell VM and formation of apoptotic bodies using Hoechst staining. Moreover, WB analysis showed an

increase in cleaved Caspase-3 and BAX activity in 6OHDA dDCN, indicating that 6OHDA stimulated BAX and Caspase-3 activity resulting in death of dDCN. The findings from the current study confirmed 6OHDA triggered death of dDCN through an apoptotic rather than a necrotic route using TUNEL assay (Figure 4.17). TUNEL assay detected death of dDCN by measuring the amount of fragmented DNA caused by active Caspase-3. 6OHDA triggered Caspase-3 a well known apoptotic marker, which promoted the breakdown of ICAD-CAD complex via the catabolism of ICAD Venderova and Park 2012, Chowdhury et al 2008, Chaudhry and Ahmed 2014). The release of CAD encouraged the splicing of DNA into fragments resulting in breakdown of the cells architecture of 6OHDA dDCN (see page 68-72). In addition, this is the first study to demonstrate that 6OHDA triggered NFκB, PERK, Caspases-2,-4 and -8 activity resulting in death of dDCN using TUNEL assay. The results further emphasise 6OHDA promoted death of dDCN, via apoptotic route as an increase of cleaved Caspase-3 was found in dDCN after exposure to 6OHDA. This finding was further highlighted in IF analysis where the destruction of dendrites and membrane blebbing was observed in 6OHDA-treated dDCN (Figure 4.4).

Research by Li et al (2010) showed positive staining for condensed nuclei in apoptotic ReNcell CX that were treated with 6OHDA using Hoechst 33342. 6OHDA-treated ReNcell CX cells had shown apoptotic cell death using Annexin V FITC stain via IF analysis. Annexin V FITC detected phosphatidylserine on the outer membranes of cells indicating 6OHDA triggered apoptosis in ReNcell CX. Propidium iodide positive staining was found in nuclear and chromatin of apoptotic cells of ReNcell CX cell line. WB analysis detected a rise on Caspases-3 and-8 in 6OHDA-treated ReNcell CX, indicating that 6OHDA promotes Caspase mediated death of ReNcell CX cells.

Although the current study used differentiated ReNcell VM then ReNcell CX, similar findings were determined to the above study. Comparable to Li et al (2010) research, IF and WB analysis illustrated 6OHDA had enhanced activation Caspases-2,-3 and -8 activation in dDCN (Figuer 4.4 –Figure 4.7 and Figure 4.11-Figure 4.15). Furthermore, co-localization studies had shown that 6OHDA triggers activation of Caspases-2 and-8 followed by Caspase-3 in dDCN (Figure 4.7). In addition, the Caspase

inhibitor, zVADfmk substantially reduced active Caspases-2,-3 and -8 in 6OHDA-treated dDCN, indicated that 6OHDA amplified activation of Caspases-2,-3 and -8 in dDCN (Figure 4.9). Collectively, the results illustrated that a successful PD model had been established to study cell death pathways which result in Caspase mediated apoptotic death of 6OHDA dDCN (Chaudhry and Ahmed 2013).

4.7 Conclusion

Results from the previous Chapter showed presence and absence of many active Caspases in brain regions of PD animal model (Chapter 3 Figure 3.2- Figure 3.6, Figure 3.10-Figure 3.16, Figure 3.20-Figure 3.38). However, as the findings of active Caspases varied from each brain region after exercise in PD animal model, it was difficult to determine whether exercise had directly caused the decrease of active Caspase or if there was another factor involved. It had become clear that a better understanding of Caspases and how they are activated needed to be established. In order to determine how Caspases are stimulated and which routes they follow, the first step was to establish if Caspases are present in differentiated ReNcell VM. 6OHDA had successfully promoted Caspase mediated death of dDCN, establishing an accomplished PD model to study cell death mechanisms (Chaudhry and Ahmed 2013). IF, WB and zVADfmk confirmed 6OHDA triggered Caspase mediated apoptotic death of dDCN (Chaudhry and Ahmed 2013). Results from the TUNEL assay aided to give a better insight to potential pathways such as NFκB classical pathway, PERK ER stress pathway, Caspases-2,-3,-4 and -8 that cause apoptotic death of 6OHDA dDCN (Figure 4.17- Figure 4.19). The subsequent aim was to identify how and if these Caspases, PERK ER stress and NFκB pathways are influenced by each other in 6OHDA-treated dDCN. Furthermore, the remainder of the current study was to determine how 6OHDA triggers Caspase activity and if there is any cross talk between these Caspases or the different pathways that result in death of dDCN via apoptotic route. The following Chapter explored the potential role of NFκB classical pathway and its involvement with specific Caspases such as Caspases-2,-4 and -8 in 6OHDA dDCN.

Chapter 5
6OHDA triggers Caspase mediated death of dDCN via NFκB pathway: A tale of Two Caspases

5.0 NFκB pathway in Caspase activation and PD pathogenesis

The role of NFκB in cells is controversial as activation of NFκB can promote or prevent death of DCN (Ghosh et al 2007, Yamamoto and Gaynor 2001, Cassarino et al 2000, Hunot et al 1997, Gao et al 2002, Flood et al 2007, Zhang et al 2012, DeErausquin et al 2003, Henn et al 2007). Research by Asanuma et al (2004) found elevated levels NFκB and cytokines in striatum and cerebrospinal fluid of PD patients. In addition, an increase in ferrous ions, alongside a decrease in glutathione oxidase was found in SN and striatum of PD patients. Collectively the author concluded microglial activation and release of ROS such as hydrogen peroxide promotes motivation of NFκB, promoting release of cytokines and activation of pro apoptotic proteins, such as Caspases that result in death of DCN. In contrast, work by Cassarino et al (2000) had shown that increased translocation of NFκB in MPTP-treated human SH-SY5Y neuroblastoma cells had increased expression of superoxide dismutase which promoted survival rather than death of DCN. Furthermore, PC12 cells that had been transfected with p65 and p50 units of NFκB had greater resistance to apoptotic death caused by auto oxide dopamine when compared to PC12 cells that had not been transfected, demonstrating that NFκB has a dual role as it can protect and promote DCN from death (Cassarino et al 2000).

Research by Li et al (2008) showed that an increase amount of translocated p65 NFκB was found in SNpc region of 6OHDA-treated rat via IF analysis. TUNEL staining had confirmed that 6OHDA had triggered an apoptotic pathway, leading to death of DCN in SN in PD animal model. Bilobalide reduced death of DCN in SN of 6OHDA-treated rats when compared to control (6OHDA induced brain that had no bilobalide). In addition, bilobalide decreased the level of translocated p65 NFκB in SN that was caused by 6OHDA treatment, suggesting that 6OHDA triggers NFκB activation resulting in apoptotic death of DCN in the SN of PD animal model. In addition, bilobalide has the ability to prevent further apoptotic death of DCN in the SN of PD model by inhibiting the activation of NFκB (Li et al 2008).

An increase in NFκB and Caspase-3 activity was observed in cultured PC12 cells, when exposed to high ROS levels and dopamine metabolites. Translocation of p65 and p50 NFκB proteins was also observed after dopamine treatment, indicating that NFκB aids to promote Caspase mediated apoptotic death of neurons in the SN of PD patients (Jia and Misra 2007, Tanaka et al 2001). Previous work by Asanuma et al (2004) suggested that activated microglia and hydrogen peroxide stimulates NFκB, allowing release of cytokines and activation of pro apoptotic proteins such as Caspases. Elevated levels of NFκB and cytokines were found in striatum and cerebrospinal fluid of PD patients.

Furthermore, WB analysis revealed elevated BAX, p53, Caspase-3, cytochrome c, p65 NFκB levels in murine stem cells that had been exposed to L-DOPA. Flow cytometry , Annexin staining and cell viability assays revealed apoptotic death of cells that had been exposed to L-DOPA at 12 and 24 hours, indicating that L-DOPA is causing death of cells, through activation of Caspase-3 in NFκB and mitochondrial mediated apoptotic cell death. A significant decrease in Caspase-3, cytochrome c, BAX and p65 NFκB levels were measured in cells that had been treated with L-DOPA and pergolide. Pergolide had partially suppressed apoptotic cell death from occurring by inhibiting L-DOPA toxicity (Liu et al 2004).

Previous research has shown a link between the Caspase activation and NFκB pathway. WB analysis, IF and luciferase activity showed increased levels of active Caspases-7,-8, -10 and p65 NFκB levels in transfected cells extracts. In addition, there were no significant changes in Caspases-1, -2 and -9 levels, suggesting that NFκB had encouraged activation of Caspases-7, -8 and -10 in cells (Chaudhary et al 2000).

5.1 Determining the relevance of NFκB pathway in 6OHDA-treated dDCN

Results from the previous Chapter indicated that 6OHDA triggered Caspase mediated apoptotic death of dDCN (Chapter 4 Figure 4.4-Figure 4.19). Furthermore, 6OHDA stimulated activation of Caspases-2,-3 and -8 in dDCN, but how these Caspases are stimulated had not yet been established (Chapter Figure 4.4). The remainder of this project was to identify, which specific pathways were stimulating Caspase activation in 6OHDA-treated dDCN. More specifically, the aim was to determine if 6OHDA triggered one main pathway or several pathways were involved and if any of these pathways overlapped, or encouraged further activation of each other, leading to activation of Caspases, which resulted in apoptotic death of dDCN.

The findings from Chapter 4 suggested NFκB pathway is involved in death of 6OHDA-treated dDCN (Figure 4.17-Figure 4.19). The initial aim of this Chapter was to confirm 6OHDA triggers NFκB pathway in dDCN and if NFκB classical pathway is the main route that results in apoptotic death of dDCN. Another aim was to determine if suppression of NFκB classical pathway using IKK can reduce death and increase survival of 6OHDA-treated dDCN.

Previous research has already suggested a link between NFκB and Caspases-2,-3 and 8 activation in DCN (Chapter 1 Section 1.5.4). The aim of the current study was to identify specific Caspases that trigger or are activated by NFκB classical pathway in 6OHDA dDCN. To date there have not been any studies that have looked at these specific Caspases, along with NFκB in differentiated ReNcell VM stem cell line. This study focuses on the role of Caspases-2,-4,-8, in relation to NFκB classical pathway in 6OHDA-treated dDCN, using specific inhibitors IKK, zLEVDfmk, zIETDfmk and zVDVADfmk.

Main Aim: To determine if 6OHDA triggered Caspase activation through NFκB mediated apoptotic death of dDCN.

5.2 Method : The involvement of NFκB classical pathway in 6OHDA mediated death of dDCN

5.2.1 Determining presence of NFκB in untreated and treated 6OHDA using IF analysis

IF was used to establish if cleaved NFκB (MAB3026 Millipore Hertfordshire UK) is present in TH positive dDCN after exposure to 100μM 6OHDA. dDCN were grown and exposed to 100μM 6OHDA for 2 hours, after which fresh media was replaced and cells were left to recover overnight. Cells were fixed with 4% parformaldehyde for 15 minutes and were washed with cold PBS. Subsequently, cells were treated with Triton X (10 minutes) and blocked with 10% goat serum for 40 minutes prior to primary antibody (Anti-TH 1:1500, Millipore Hertfordshire UK) and cleaved Anti-NFκB -(1:1500, Millipore Hertfordshire UK) incubation, overnight at 4°C and secondary antibody (Sheep Anti-Rabbit IgG FITC 1:800, Millipore Hertfordshire, UK) (Sheep-Anti-Mouse IgG Rhodamine, 1:300, Millipore Hertfordshire UK) incubation for two hours at RT. Cells were mounted using vectorshield mounting medium and were viewed under a Meiji fluorescent microscope.

Furthermore, Co-localisation studies were performed to determine if NFκB and Caspases were present in the same cell by using primary antibodies Anti-NFκB (1:1500, Millipore Hertfordshire UK), cleaved Anti-Caspase-3 (1:1000, Millipore Hertfordshire UK), active Anti-Caspase-2 (1:2000, Abcam Cambridge UK), active Anti-Caspase-8 (1:2000, Abcam Cambridge UK), and secondary antibodies, Sheep-Anti-Mouse IgG FITC (1:2000 Millipore Hertfordshire UK), Goat-Anti-Rabbit IgG Rhodamine (1:2500, Millipore Hertfordshire UK). The expression of active Caspases-2,-4,-8 and NFκB were determined in cells that were treated with 6OHDA + IKK dDCN. dDCN and 6OHDA dDCN were treated with either 70 μM IKK and with specific Caspase inhibitors such as 80μM zIETDfmk, 20μM zVDVADfmk and 20μM zLEVDfmk as described in Section 2.5.3 and stained for IF. A more detailed account of the reagents used can be found in Chapter 2 Section 2.1 Appendix 1.

5.2.2 Detecting NFκB amount in untreated and 6OHDA-treated dDCN using WB analysis

dDCN were grown and exposed to 100μM 6OHDA in dDCN, after which fresh media was replaced and cells were left to recover overnight. Cells were lysed and protein concentration was measured using the BCA kit. Fifty micrograms protein was loaded on 12% gel prior to SDS PAGE, followed by immunoblotting on PVDF membrane. The membrane was blocked with 1% skimmed milk for an hour followed by incubation with primary antibody, cleaved Anti-NFκB (1:5000, Millipore, Hertfordshire, UK)

for overnight at 4°C. The membranes were washed with PBST and incubated with Donkey-Anti-Mouse HRP (1:6000, Millipore, Hertfordshire, UK) for an hour at RT. After washing the membranes with PBST, antibody binding was detected using ECL and immunoblots bands were quantified with a densitometer scanner (GS800, Biorad). Statistical analysis was carried out at $p<0.05$ using student T test followed by strip and reprobe with the house keeping gene GAPDH (Chapter 2 Section 2.3.4 and Chapter 2 Section 2.3.5 correspondingly). Five independent experiments were performed for each treatment.

Furthermore, cells were treated with 100μM 6OHDA and 70μM IKK as described below (Section 5.2.3). Primary antibodies, cleaved Anti-NFκB (1:5000, Millipore Hertfordshire, UK), active Anti-Caspase-2 (1:2500, Millipore Hertfordshire UK), active Anti-Caspase-4 (1:4000, Abcam Cambridge UK), active Anti-Caspase-8 (1:1000, Millipore Hertfordshire, UK) along with secondary antibodies Donkey-Anti-Mouse HRP (1:6000, Millipore Hertfordshire UK), Goat-Anti-Rabbit HRP (1:1000, Millipore Hertfordshire UK) were used to detect the presence, absence and level of protein in untreated and 6OHDA-treated dDCN. Statistical analysis was carried out as described in Chapter 2 Section 2.3.4. A more detailed account of the reagents used can be found in Chapter 2 Section 2.1 - Section 2.2 and Appendix 1.

5.2.3 Measuring NFκB Caspases-2,-3 and -8 activities in 6OHDA-treated dDCN

Optimal conditions for the IKK treatment (70μM for 2 hours exposure) were determined by treating 100μM 6OHDA dDCN with different IKK concentrations (10μM - 120μM) and measuring cell survival using MTT assay (BT30006, Cambridge Bioscience, UK). For further analysis in determining if Caspases-2,-4, and -8 are active in NFκB classical pathway in untreated and treated dDCN, the IKK inhibitor was used. dDCN and 6OHDA dDCN were treated with either or both 70μM IKK or Caspase inhibitors such as Caspase-2 inhibitor (20μM zVDVADfmk), Caspase-4 inhibitor (20μM zLEVDfmk), Caspase-8 inhibitor (80μM zIETDfmk)for 2 hours, prior to measuring cell survival using MTT assay and statistical analysis as described in Chapter 2 Section 2.5.4. A more detailed account of the reagents used can be found in Chapter 2 Section 2.2 and Appendix 1.

The aim was to determine if 6OHDA triggers death of dDCN via NFκB pathway. Double IF analysis was done to determine if NFκB was actively present in untreated and 6OHDA-treated dDCN. Cleaved NFκB was present in untreated TH positive dDCN, indicating that NFκB is active normal cellular processes (Figure 5.1). The presence of cleaved NFκB in untreated DCN is not surprising as NFκB is a diverse transcription factor, which is required for many other cellular functions. Administration of 100μM 6OHDA in cells, led to the destruction of dendrites in TH positive dDCN. The presence of p65 subunit of NFκB in majority TH positive treated dDCN indicated that 6OHDA enhanced further activation of NFκB in TH positive dDCN.

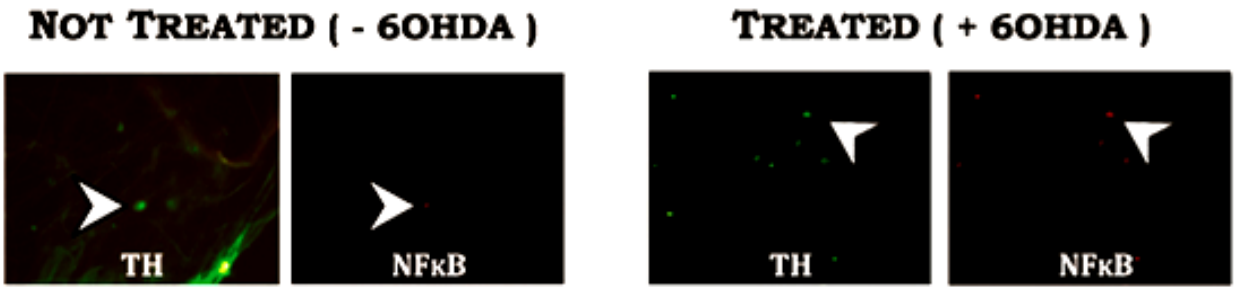

Figure 5.1: Presence of NFκB in untreated and 6OHDA-treated dDCN

Figure shows positive staining for TH (green) for untreated and treated dDCN, indicating that cells are dopaminergic. Positive staining for cleaved p65 subunit NFκB (red) was found in untreated and treated dDCN. Untreated dDCN had lower proportion of cleaved NFκB in TH positive cells. However, in 6OHDA-treated dDCN there was an increase in the number of cleaved NFκB present in TH positive cells, indicating that 6OHDA promoted further NFκB activity. The cell body (white arrow) showed positive staining in untreated (- 6OHDA) and treated (+ 6OHDA) dDCN.

Quantitative analysis portrayed a difference in the number of p65 NFκB cells expressed in TH positive untreated and 6OHDA-treated and untreated dDCN. P65 NFκB was expressed in 54% of TH positive dDCN, indicating that NFκB is active in normal cellular processes. 6OHDA significantly increased the proportion of cleaved NFκB in dDCN, illustrating 6OHDA triggers further activation of NFκB in dDCN ($p<0.05$, Figure 5.2).

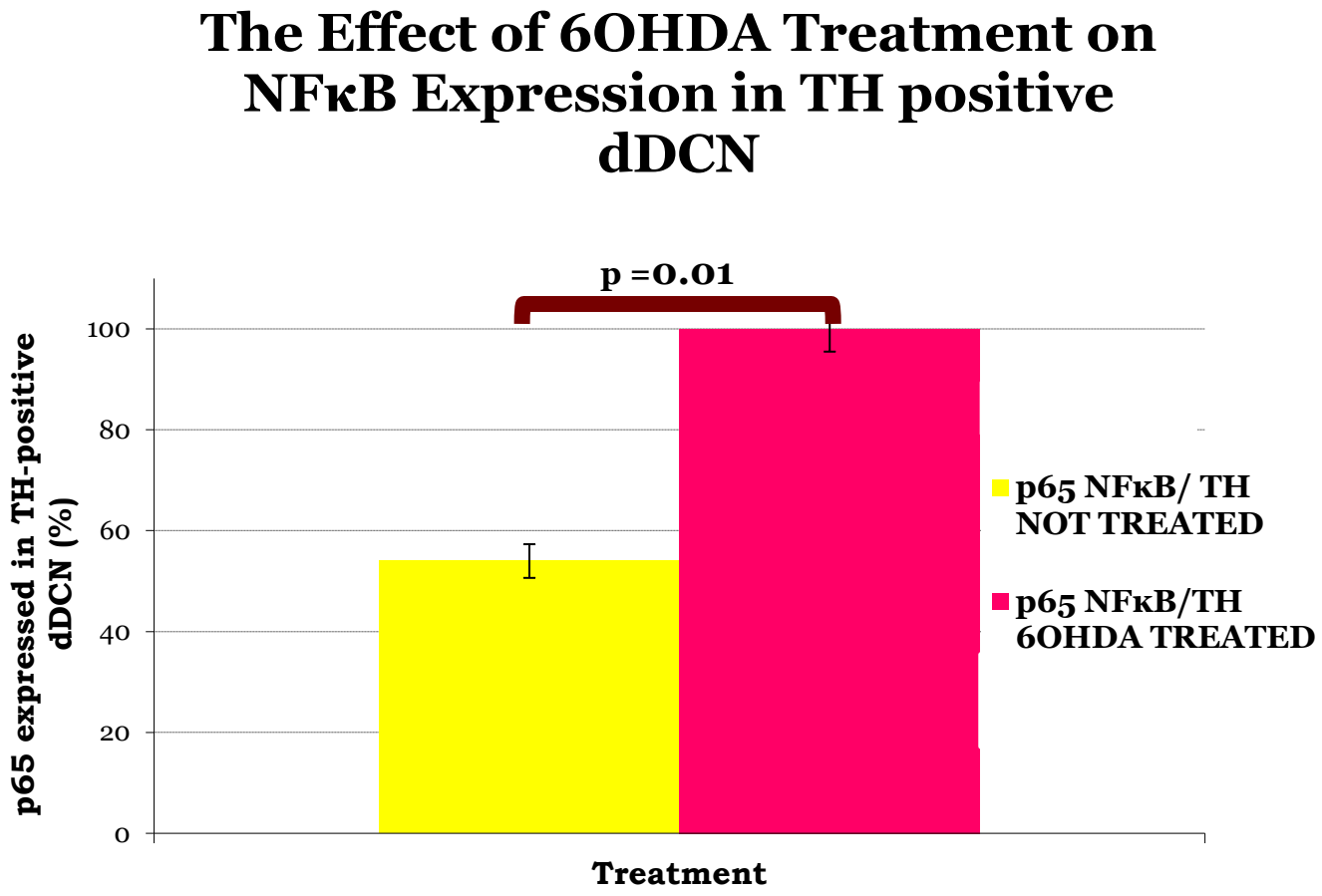

Figure 5.2 6OHDA amplifies NFκB activity in dDCN

Graph illustrating the proportion of p65 NFκB expressed in TH positive untreated and treated dDCN. p65 NFκB was expressed in approximately 54% of TH positive untreated dDCN. However, more cells expressed p65 NFκB after exposure to 6OHDA, indicating that 6OHDA further enhances NFκB activity in dDCN. Means of three experiments ± SEM shown. Table of values and statistical analysis can be found in Figure 5.3, Appendix 5.

To quantify the amount of NFκB present in 6OHDA-treated and untreated dDCN, WB analysis was performed. Cleaved NFκB was present in 6OHDA untreated dDCN, further confirming that NFκB is actively present in DCN because it may be transcribing genes that are needed for other cellular processes. Furthermore, WB analysis showed a substantial increase in the amount of cleaved NFκB present in 6OHDA-treated dDCN compared to untreated dDCN($p<0.05$), indicating that 6OHDA amplified NFκB activation in more than half of dDCN (Figure 5.4).

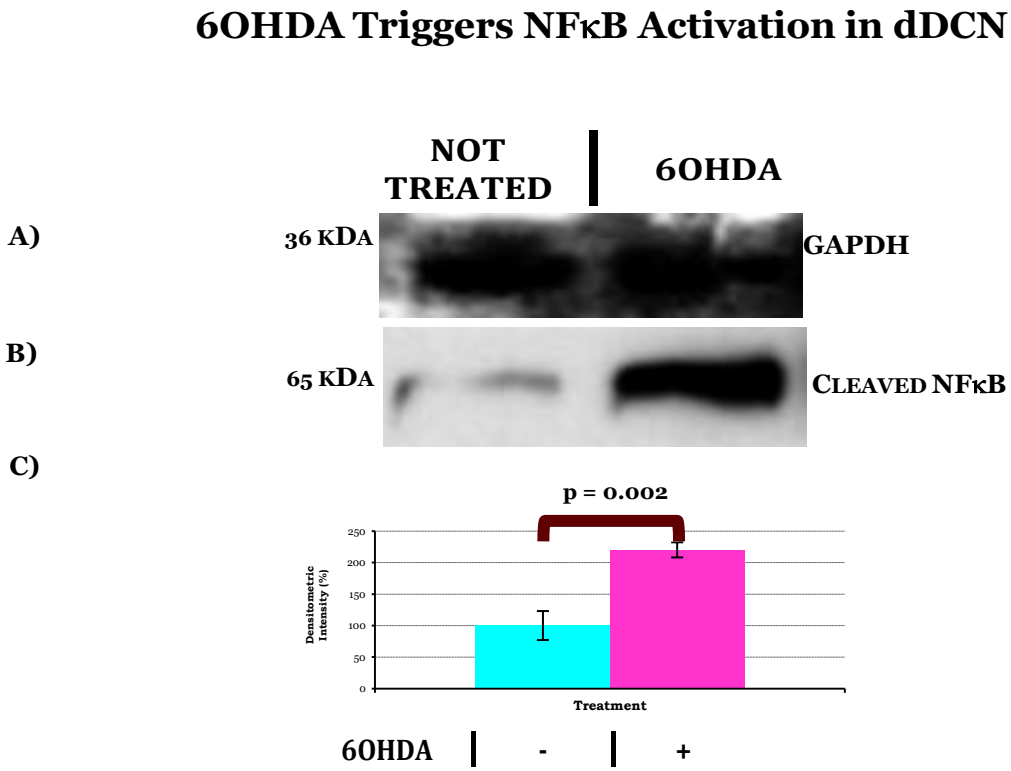

Figure 5.4: 6OHDA provokes further activation NFκB in dDCN

A) Illustrative example of cleaved GAPDH in untreated and 6OHDA treated dDCN.

B) Illustrative example of cleaved NFκB in untreated and 6OHDA treated dDCN.

C) Graph showing the amount of cleaved NFκB, which is present in 6OHDA untreated and treated dDCN. A significant increase in cleaved NFκB levels was found in dDCN that were treated with 6OHDA. The blue bar represents dDCN that were not treated with 6OHDA. The pink bar symbolises dDCN that were treated with 100μM 6OHDA. Means of five experiments ± SEM shown. Table of densitometry values and statistical analysis can be found in Figure 5.5, Appendix 5.

Co localisation studies were carried out to determine if specific Caspases, along with NFκB, were present in the same untreated and 6OHDA-treated dDCN. Active Caspase-2 and cleaved NFκB were present in many of the same untreated dDCN. However, the amount of active Caspase-2 present in NFκB positive dDCN substantially increased after 6OHDA treatment. Fewer untreated cells were Caspase-3 positive than were p65 NFκB positive, whereas there were many cells positive for Caspase-3 after 6OHDA treatment. Likewise, active Caspase-8 positive cells were more frequent in NFκB positive 6OHDA dDCN than in untreated p65 NFκB positive dDCN. 6OHDA triggered a further increase in Caspase-2,-3 and -8 and NFκB activity in the same cell location of dDCN (Figure 5.6).

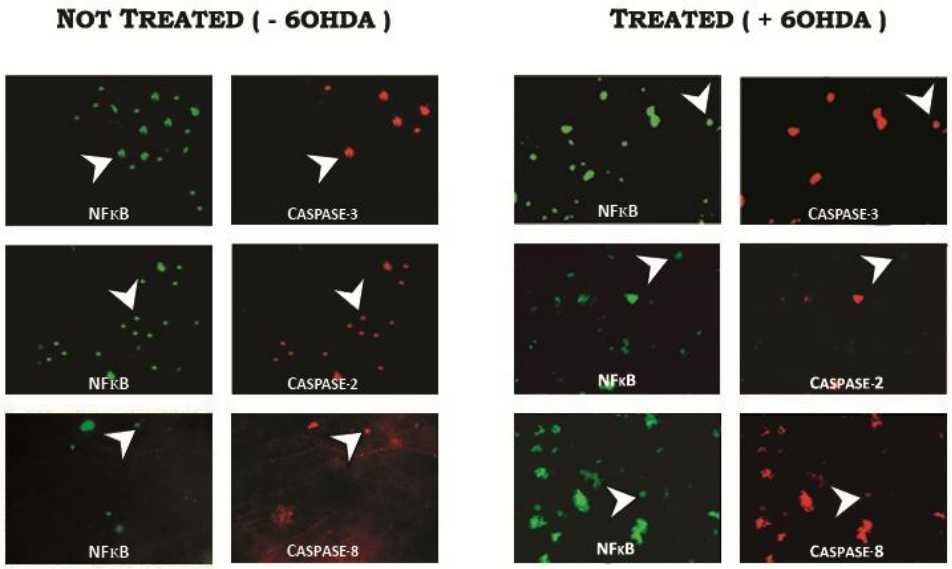

Figure 5.6: Presence of active Caspases-2,-3 and-8 in NFκB positive untreated and 6OHDA-treated dDCN

Figure shows positive staining for NFκB (green) and positive staining for Caspases-2,-3 and -8 (red) in untreated and treated 6OHDA dDCN. Caspase-2 was located in many p65 NFκB positive untreated dDCN. A higher expression of cleaved Caspase-3 was observed in p65 NFκB positive 6OHDA treated dDCN when compared to untreated dDCN. Caspase-8 was found in low levels in untreated dDCN, but an increase of Caspase-8 was determined in p65 NFκB positive 6OHDA treated dDCN. Positive staining for cell bodies (White Arrow) in untreated (-6OHDA) and treated (+ 6OHDA) dDCN.

Quantitative analysis revealed a positive correlation between Caspase-2,-3,-8 and NFκB in treated dDCN. ANOVA and T test analysis revealed statistical difference in the proportion of p65 positive cells that express active Caspases in dDCN before and after exposure to 6OHDA (Figure 5.7). The graph portrayed 20-45% of untreated p65 positive cells expressed these Caspases-2, -3 and -8 in dDCN (45%, 31% and 34% respectively).. However, after 6OHDA treatment 50-100% of p65 positive cells expressed Caspases-2,-3 and -8 ($p<0.05$).Collectively the results shown a positive indication that Caspases-2,-3 and -8 are involved in NFκB mediated death of 6OHDA dDCN.

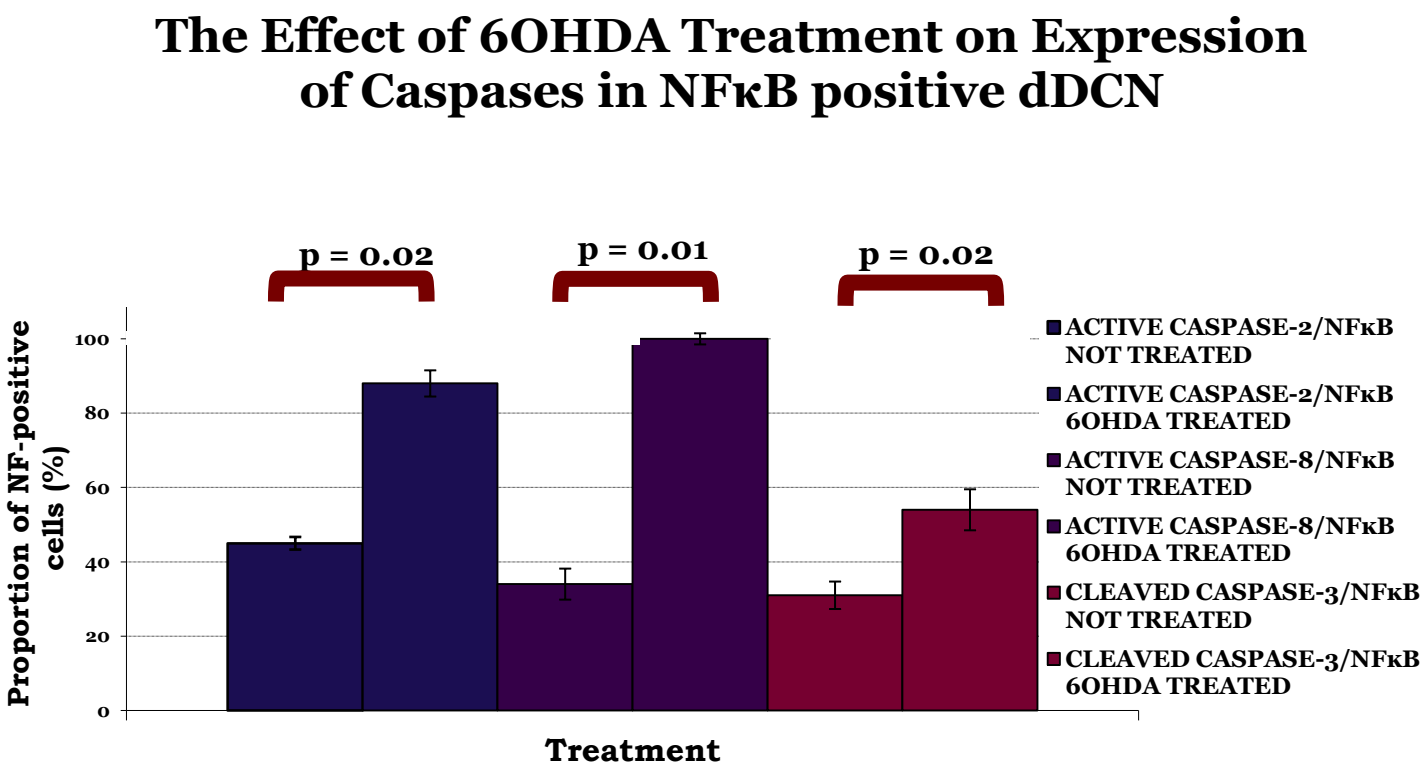

Figure 5.7: 6OHDA amplified active Caspases-2,-3 and -8 expression in NFκB positive dDCN

Graph showing the proportion of p65 NFκB positive cells that expressed active Caspases-2,-3 and-8 in untreated and 6OHDA-treated dDCN. The proportion of active Caspases-2,-3 and-8 was expressed in less than half of p65 positive untreated dDCN. There was a significantly increased proportion of active Caspases-2,-3 and-8 expressed in more than half of p65 NFκB positive cells after 6OHDA treatment. 6OHDA increased induction of cleaved NFκB in dDCN, suggesting involvement of NFκB pathway in

death of dDCN.. Means of three experiments ± SEM shown. Table of values and statistical analysis can be found in Figure 5.8, Appendix 5.

An IKK inhibitor that specifically suppresses the NFκB classical pathway was used in dDCN that had been treated with 6OHDA. This was carried out to determine if 6OHDA triggered NFκB classical pathway in dDCN. Different concentrations of IKK inhibitor was used in dDCN that had been treated with 6OHDA dDCN. IKK had prevented the classical pathway of NFκB in 6OHDA-treated dDCN, demonstrating that 6OHDA stimulates NFκB classical pathway. Prevention of NFκB classical pathway significantly promoted more survival of 6OHDA-treated dDCN ($p<0.05$). Even at a high concentration, IKK did not completely inhibit death of all 6OHDA-treated dDCN, indicating that 6OHDA triggers another route or many other routes that result in apoptotic death of dDCN, as death of dDCN was still occurring (Figure 5.9).

Increasing IKK Concentration does not Completely Prevent Death of 6OHDA Treated dDCN

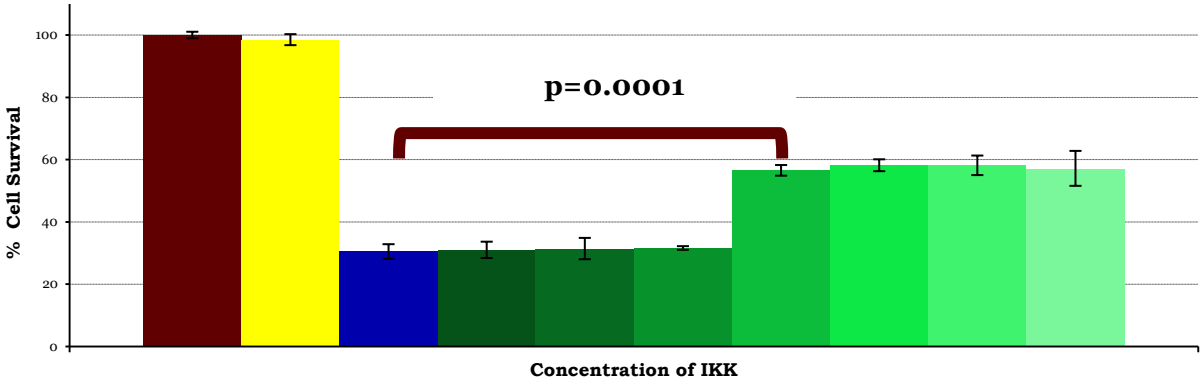

IKK	-	+	-	10μM	30μM	50μM	70μM	80μM	100μM	120μM
6OHDA	-	-	+	+	+	+	+	+	+	+

Figure 5.9: IKK can prevent death of 6OHDA-treated dDCN

Determining if further survival of 6OHDA-treated dDCN can occur by increasing the concentration of inhibitor IKK. A rapid increase in the amount of cells survived in 6OHDA-treated dDCN, was found when 6OHDA dDCN were treated with 70μM IKK, indicating that the NFκB classical pathway is involved in death of 6OHDA dDCN. The increase in IKK inhibitor dose from 80μM IKK to 120μM IKK did not provide further cell survival of 6OHDA dDCN, indicating other routes are causing death

of dDCN. Means of three experiments ± SEM shown. Table of values and statistical analysis can be found in Figure 5.10, Appendix 5.

To confirm that 6OHDA triggers additional pathways other then NFκB classical pathway which results in death of dDCN, two inhibitors were used. A universal Caspase inhibitor zVADfmk and a specific NFκB inhibitor IKK were used to determine if death of 6OHDA-treated cells is caused by one Caspase pathway (NFκB pathway) or if other pathways are also contributing to the death of dDCN. IKK significantly suppressed death of 6OHDA-treated dDCN. However, zVADfmk significantly further prevented death of 6OHDA-treated dDCN. The increase in cell survival was found when zVADfmk was used additionally to IKK, suggesting that two different cell death pathways are activating and causing apoptotic cell death of dDCN. This indicates that although NFκB classical pathway is important in apoptotic death of dDCN, there are other Caspase related pathways that are also contributing to death of 6OHDA-treated dDCN (Figure 5.11).

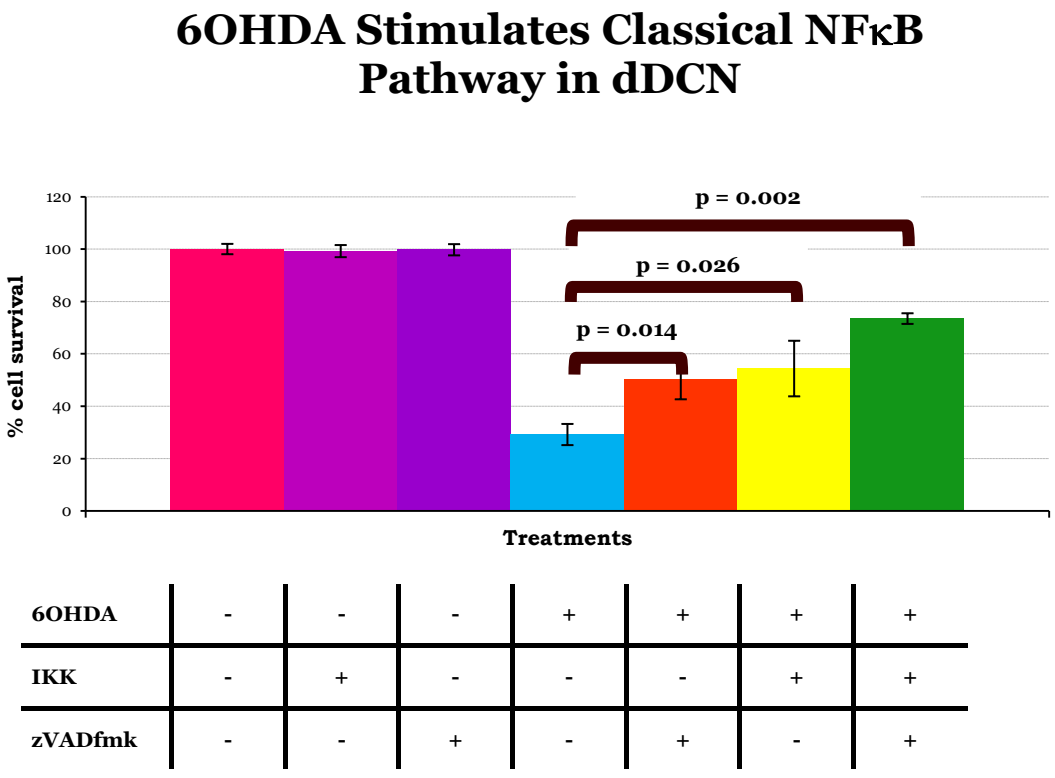

Figure 5.11: zVADfmk and IKK decreased death of 6OHDA-treated dDCN

6OHDA dDCN that were treated with zVADfmk and IKK had more survival of cells (73% cell survival) by inhibiting NFκB and Caspase mediated death. Proportion of cells surviving was determined by MTT

absorbance at 570nm. Means of three experiments ± SEM shown. Table of values and statistical analysis can be found in Figure 5.3, Appendix 5.12.

The classical, alternative and atypical pathway stimulate NFκB activation. To further confirm that 6OHDA triggers the activation of NFκB classical pathway and not the NFκB alternative or NFκB atypical pathway in treated dDCN, the NFκB classical pathway inhibitor, IKK was used. IKK inhibitor was to determine if complete suppression of NFκB could be achieved by inhibiting the classical pathway in 6OHDA dDCN. IKK inhibited activation of NFκB by suppressing the NFκB classical pathway in 6OHDA untreated and treated dDCN (Figure 5.13).

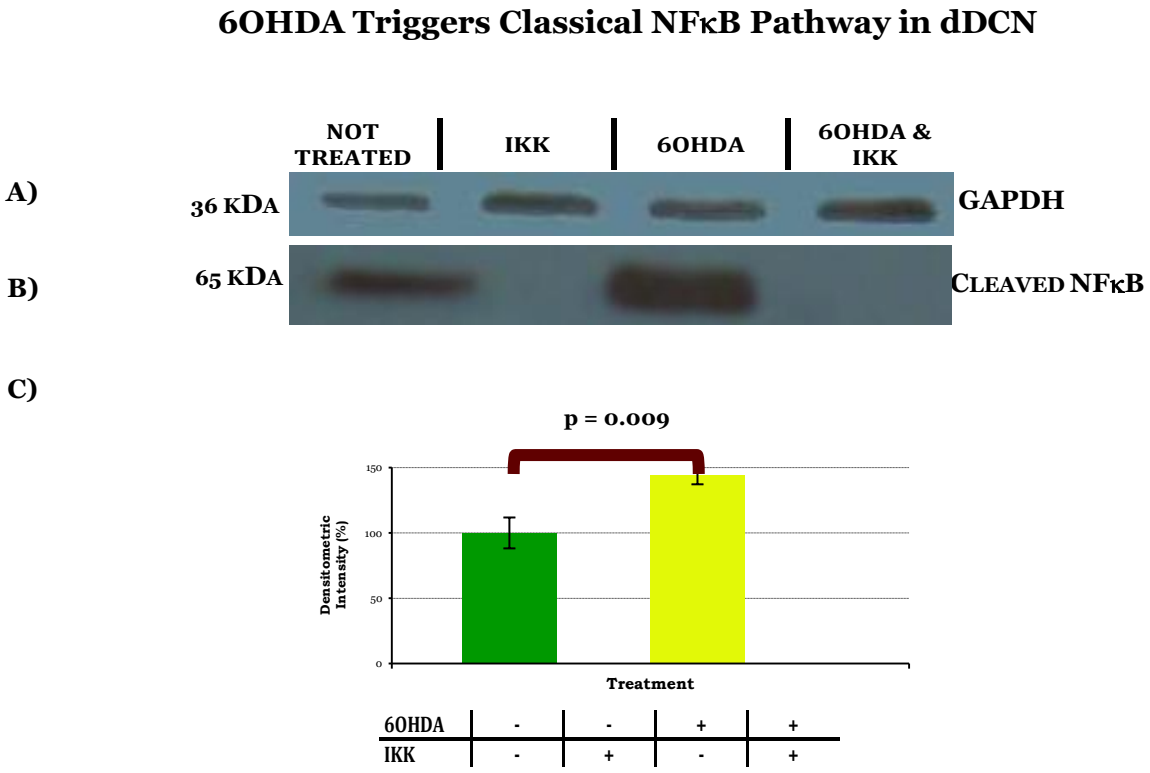

Figure 5.13: The effect of IKK on cleaved NFκB in untreated and 6OHDA-treated dDCN

A) Illustrative example of GAPDH in untreated, IKK, 6OHDA, IKK + 6OHDA treated dDCN.

B) Illustrative example of cleaved NFκB in untreated, IKK, 6OHDA, IKK + 6OHDA treated dDCN.

C) Quantitatively, a significant increase in cleaved NFκB was detected in 6OHDA-treated dDCN compared to untreated dDCN ($p<0.01$). The absence of cleaved NFκB was observed in IKK treated, 6OHDA+IKK treated dDCN; suggest that NFκB classical pathway is actively involved in death of

dDCN. Means of three experiments ± SEM shown. Table of densitometry values and statistical analysis can be found in Figure 5.3, Appendix 5.14

Results from previous Chapter had shown that Caspase-8 is active in 6OHDA-treated dDCN. In addition, results from double IF analysis had shown a strong positive correlation in active Caspase-8 and NFκB positive dDCN. To determine the importance of Caspase-8 activation in NFκB mediated cell death in 6OHDA dDCN, cells were treated with specific Caspase-8 inhibitor zIETDfmk and IKK inhibitor. The results demonstrated that 6OHDA dDCN that were treated with zIETDfmk, IKK or both IKK and zIETDfmk had similar levels of cell survival, suggesting 6OHDA triggered NFκB and Caspase-8 activation via the same pathway in dDCN (Figure 5.15).

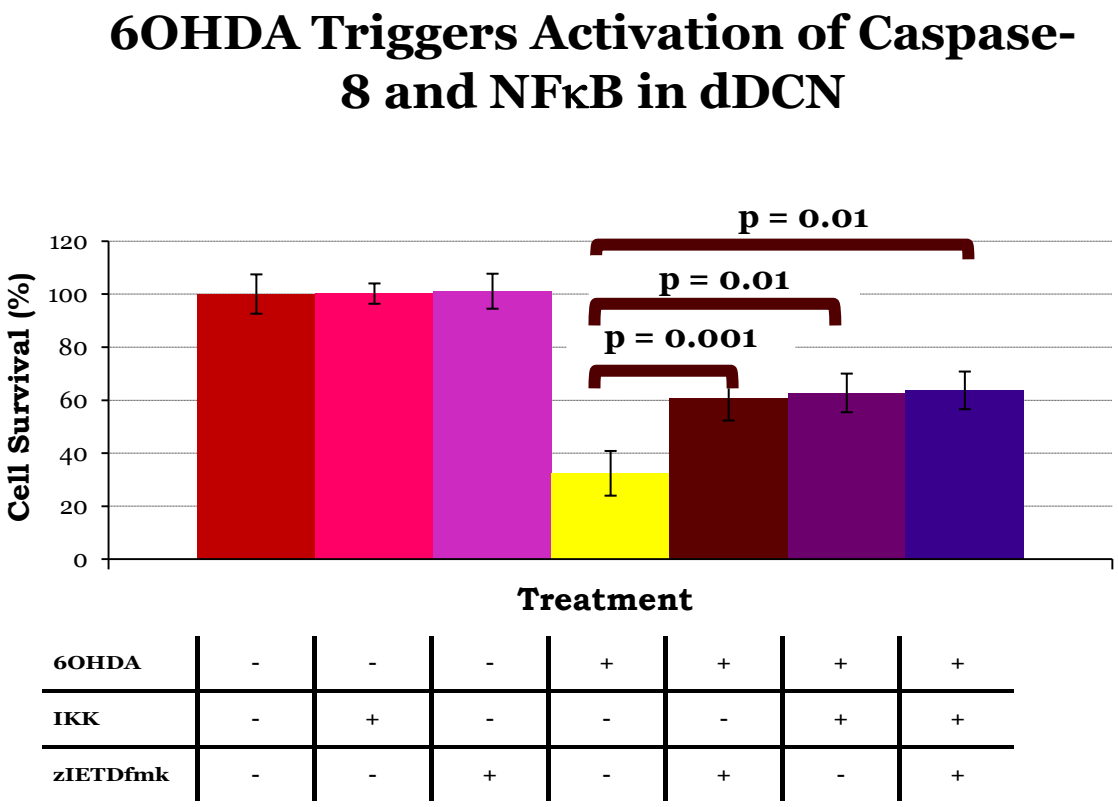

Figure 5.15: Determining Caspase-8 activity in 6OHDA-treated dDCN

zIETDfmk inhibited Caspase-8 activity and promoted 63% survival of 6OHDA-treated dDCN. IKK promoted 61% survival of 6OHDA-treated dDCN by suppressing NFκB classical pathway. The combination of zIETDfmk and IKK promoted similar survival of (64% cell survival) of 6OHDA-treated dDCN, indicating no additional benefit of targeting both Caspase-8 and NFκB. Proportion of

cells surviving was determined by MTT absorbance at 570nm. Means of three experiments ± SEM shown. Table of values and statistical analysis can be found Figure 5.3, Appendix 5.16

Further analysis was carried out to determine if combining IKK and zIETDfmk inhibitors can promote more survival of 6OHDA-treated dDCN can be achieved, then just using one inhibitor. The combination of IKK and zIETDfmk inhibitor had no additional benefit to further increase survival of 6OHDA-treated dDCN, indicated that Caspase-8 and NFκB are following the same NFκB classical pathway ($p>0.05$, Figure 5.17).

	Treatment 1	Treatment 2	Treatment 3	Treatment 4	
	6OHDA	6OHDA IKK	6OHDA zIETDfmk	6OHDA IKK zIETDfmk	p-value obtained
Comparison 1	+	+	-	-	0.001
Comparison 2	+	-	+	-	0.01
Comparison 3	+	-	-	+	0.01
Comparison 4	-	+	+	-	0.62
Comparison 5	-	+	-	+	0.472
Comparison 6	-	-	+	+	0.852

Figure 5.17: IKK suppressed Caspase-8 activity in 6OHDA-treated dDCN

There was no further cell survival of 6OHDA dDCN, was determined when zIETDfmk was added with IKK ($p>0.05$, comparison 6), indicating Caspase-8 and NFκB are both following the NFκB classical pathway. Similarly there was no additional benefit in survival of 6OHDA dDCN when IKK was added to zIETDfmk ($p>0.05$ comparison 5), indicating that the IKK is targeting both Caspase-8 and NFκB activity in dDCN. There was no additional benefit of more cell survival when Caspase-8 inhibitor and NFκB inhibitor were combined, signifying there is one pathway that was contributing to death of 6OHDA dDCN. Furthermore, only the IKK inhibitor was required to be used to suppress the same pathway so survival of 6OHDA dDCN could be achieved. Proportion of cells surviving was determined

by MTT absorbance at 570nm. Means of three experiments ± SEM shown. Table of values and statistical analysis can be found in Figure 5.3, Appendix 5.16

Co-localisation studies were carried out to investigate if suppression of Caspase-8 activity can inhibit NFκB activation or vice versa in dDCN. Caspase-8 was found active in only in untreated and 6OHDA-treated dDCN (Figure 5.18). Active Caspase-8 was present in a greater proportion of 6OHDA-treated dDCN, indicating that 6OHDA triggers Caspase-8 in dDCN. Furthermore, active Caspase-8 was absent in IKK treated, zIETDfmk treated, 6OHDA+IKK treated, 6OHDA+ zIETDfmk treated, 6OHDA+IKK +zIETDfmk treated dDCN. However, NFκB was present in 6OHDA+zIETDfmk treated dDCN, demonstrating that inhibiting Caspase-8 activation using zIETDfmk inhibitor did not suppress NFκB classical pathway in dDCN. This indicated that activation of Caspase-8 is dependent upon stimulation of NFκB resulting in death of dDCN.

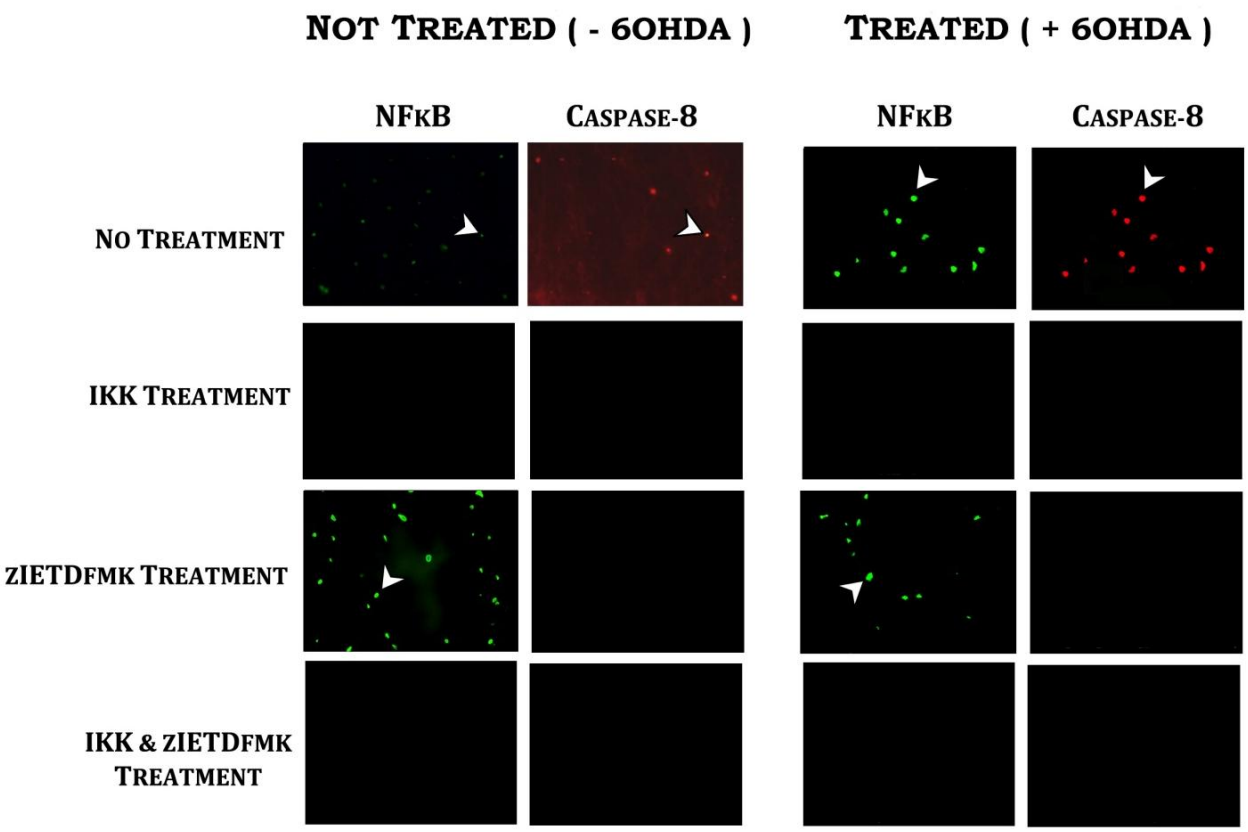

Figure 5.18: The effect of IKK on active Caspase-8 expressed in NFκB positive untreated and 6OHDA-treated dDCN

NFκB was present in untreated and 6OHDA-treated dDCN (green). There were more NFκB positive cells in 6OHDA-treated dDCN, when compared to untreated (-6OHDA) dDCN, suggesting 6OHDA further enhances translocation of NFκB resulting in death of dDCN, via NFκB classical route. Active Caspase-8 was present in untreated and 6OHDA-treated dDCN (red). There were more active Caspase-8 positive cells in 6OHDA-treated dDCN, when compared to untreated (- 6OHDA) dDCN, signifying that 6OHDA provokes up regulation of Caspase-8 activity in dDCN. Furthermore, active Caspase-8 was present in the same NFκB positive cells which had been exposed to 6OHDA, suggesting that NFκB and Caspase-8 interact with one another leading to death of dDCN.

NFκB was absent in IKK treated, 6OHDA+IKK treated dDCN, confirming that 6OHDA triggers NFκB activation via NFκB classical pathway and suppression of NFκB classical pathway can inhibit NFκB mediated death of dDCN. Similarly, active Caspase-8 was not detected in IKK treated, 6OHDA+IKK treated dDCN. This indicates that inhibiting the NFκB pathway can suppress Caspase-8 activity in dDCN. Stimulation of Caspase-8 is dependent on activation of NFκB classical pathway in dDCN.

NFκB was present in zIETDfmk treated, 6OHDA+ zIETDfmk treated dDCN, suggesting that suppression of Caspase-8 activity does not influence NFκB activation and NFκB activation is independent of Caspase-8 stimulation in dDCN. In contrast, active Caspase-8 was absent in zIETDfmk treated, 6OHDA+zIETDfmk treated dDCN, signifying that zIETDfmk had competitively inhibited Caspase-8 activity in dDCN. NFκB was absent in IKK+zIETDfmk treated, 6OHDA+IKK+zIETDfmk treated dDCN. Caspase-8 was not found in IKK+zIETDfmk treated, 6OHDA+ IKK+ zIETDfmk treated dDCN. IKK had suppressed both NFκB and Caspase-8 activity in untreated and 6OHDA-treated dDCN. Caspase-8 activation can be suppressed by directly inhibiting Caspase-8 or via inhibiting NFκB classical pathway in untreated and 6OHDA-treated dDCN. Positive staining for cell bodies (White Arrow) in untreated (- 6OHDA) and treated (+ 6OHDA) dDCN. Table of values and statistical analysis can be found in Figure 5.19, Appendix 5.

WB analysis was carried out to confirm that IKK inhibitor can completely suppress activation of Caspase-8 in 6OHDA-treated dDCN. Active Caspase-8 was found in untreated and 6OHDA-treated dDCN. A higher amount of active Caspase-8 was detected in 6OHDA-treated dDCN, suggesting 6OHDA triggered further activation of Caspase-8 in dDCN. Active Caspase-8 was not detected in IKK treated, 6OHDA+IKK treated dDCN, suggesting inhibiting NFκB classical pathway can also inhibit activation of Caspase-8 in dDCN (Figure 5.20).

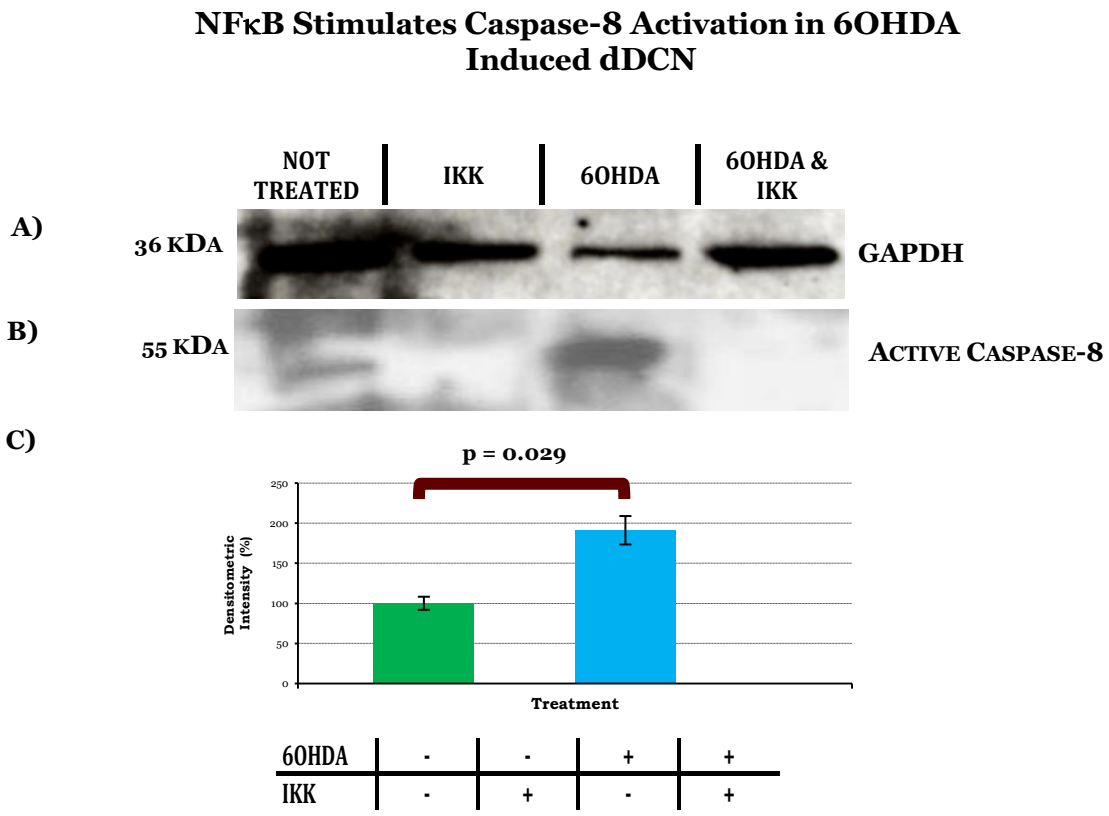

Figure 5.20 : The effect of IKK on active Caspase-8 in untreated and 6OHDA-treated dDCN

A) Illustrative example of GAPDH in untreated, IKK, 6OHDA, IKK + 6OHDA treated dDCN.

B) Illustrative example of active Caspase-8 in untreated, IKK, 6OHDA, IKK + 6OHDA treated dDCN.

C) Quantitatively, a higher amount of active Caspase-8 was detected in 6OHDA-treated dDCN compared to untreated dDCN ($p<0.05$). The absence of active Caspase-8 in IKK treated, 6OHDA+IKK treated dDCN, suggest that Caspase-8 activity is dependent upon NFκB classical pathway. Means of three experiments ± SEM shown. Table of densitometry values and statistical analysis can be found in Figure 5.21, Appendix 5.

Results from previous Chapter had illustrated that the proportion of active Caspase-2 increased in 6OHDA dDCN. In addition, co localisation studies had shown a high expression of active Caspase-2 present in NFκB positive dDCN. The subsequent aim was to determine if suppression of Caspase-2 activity, using specific Caspase-2 inhibitor zVDVADfmk could slow death and increase survival of 6OHDA dDCN. The results demonstrated that 6OHDA+ zVDVADfmk treated, 6OHDA+ IKK + zVDVADfmk dDCN had similar levels of cell, suggesting 6OHDA stimulates NFκB and Caspase-2 through the same route in dDCN (Figure 5.22).

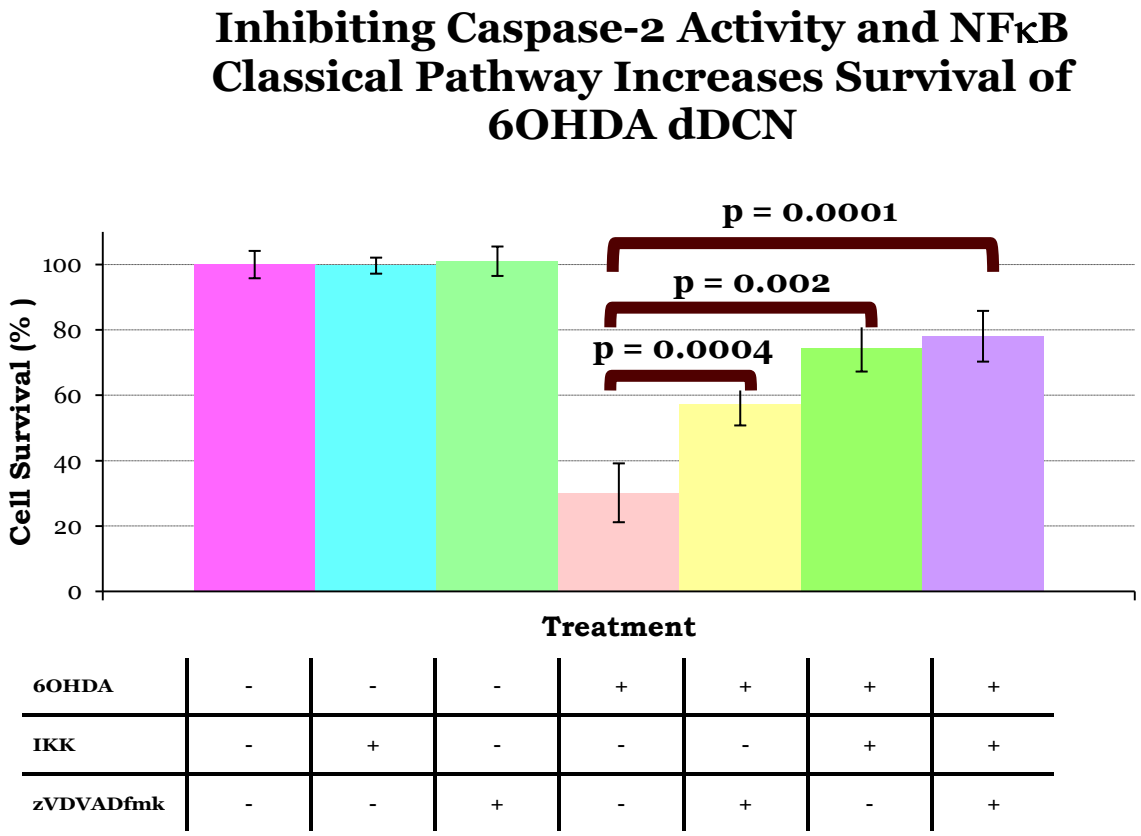

Figure 5.22: Determining Caspase-2 activity in 6OHDA-treated dDCN

6OHDA triggered Caspase-2 activation in dDCN. 6OHDA+ IKK treated dDCN promoted 57% survival by inhibiting the NFκB classical pathway ($p<0.05$). A further increase in cell survival, via suppressing Caspase-2 activity was found in 6OHDA+zVDVADfmk treated dDCN (75% cell survival $p<0.05$). 6OHDA+IKK+ zVDVADfmk treated dDCN promoted 78% cell survival ($p<0.05$), by inhibiting activity of Caspase-2 and NFκB classical pathway. Proportion of cells surviving was determined by MTT absorbance at 570nm. Means of three experiments ± SEM shown. Table of values and statistical analysis can be found in Figure 5.23, Appendix 5

A closer examination of the results confirmed that Caspase-2 and NFκB are activated in the same pathway in 6OHDA-treated dDCN. Suppressing Caspase-2 pathway in addition to NFκB classical pathway had no added effect to more cells surviving, indicating that there one pathway ($p>0.05$). 6OHDA+ IKK+ zVDVADfmk treated dDCN did not provide further cell survival, suggesting 6OHDA triggers Caspase-2 and NFκB classical pathway activity through the same mechanism, resulting in death of dDCN (Figure 5.24).

	Treatment 1	Treatment 2	Treatment 3	Treatment 4	
	6OHDA	6OHDA IKK	6OHDA zVDVADfmk	6OHDA IKK zVDVADfmk	p-value obtained
Comparison 1	+	+	-	-	0.0004
Comparison 2	+	-	+	-	0.002
Comparison 3	+	-	-	+	0.0001
Comparison 4	-	+	+	-	0.03
Comparison 5	-	+	-	+	0.004
Comparison 6	-	-	+	+	0.449

Figure 5.24: 6OHDA triggers Caspase-2 activation in dDCN via NFκB classical pathway

There was no further cell survival when zVDVADfmk was added to 6OHDA+ IKK treated dDCN (Comparison 6 $p>0.05$), indicating Caspase-2 and NFκB are both following the same pathway. There was no additional benefit of more cell survival when Caspase-2 and NFKB inhibitors were combined, signifying that there is one pathway that was contributing to death of 6OHDA dDCN. This can be explained as if the pathways were different a greater survival of 6OHDA-treated dDCN would have occurred when both inhibitors were used together. Proportion of cells surviving was determined by MTT absorbance at 570nm. Means of three experiments ± SEM shown. Table of values and statistical analysis can be found in Figure 5.23, Appendix 5

Co localisation study was carried out to determine if active Caspase-2 and cleaved NFκB were present in the same dDCN and if Caspase-2 is acting upstream or downstream in NFκB classical pathway (Figure 5.25). Active Caspase-2 was detected in only untreated and 6OHDA-treated dDCN. Furthermore, active Caspase-2 was absent in IKK treated, zVDVADfmk treated, 6OHDA+IKK treated, 6OHDA+zVDVADfmk treated, 6OHDA+IKK +zVDVADfmk dDCN. However, NFκB was present in zVDVADfmk treated dDCN, 6OHDA+zVDVADfmk treated dDCN, indicating NFκB is activated upstream and Caspase-2 is activated downstream in 6OHDA-treated dDCN, as Caspase-2 inhibitor did not inhibit NFκB activity.

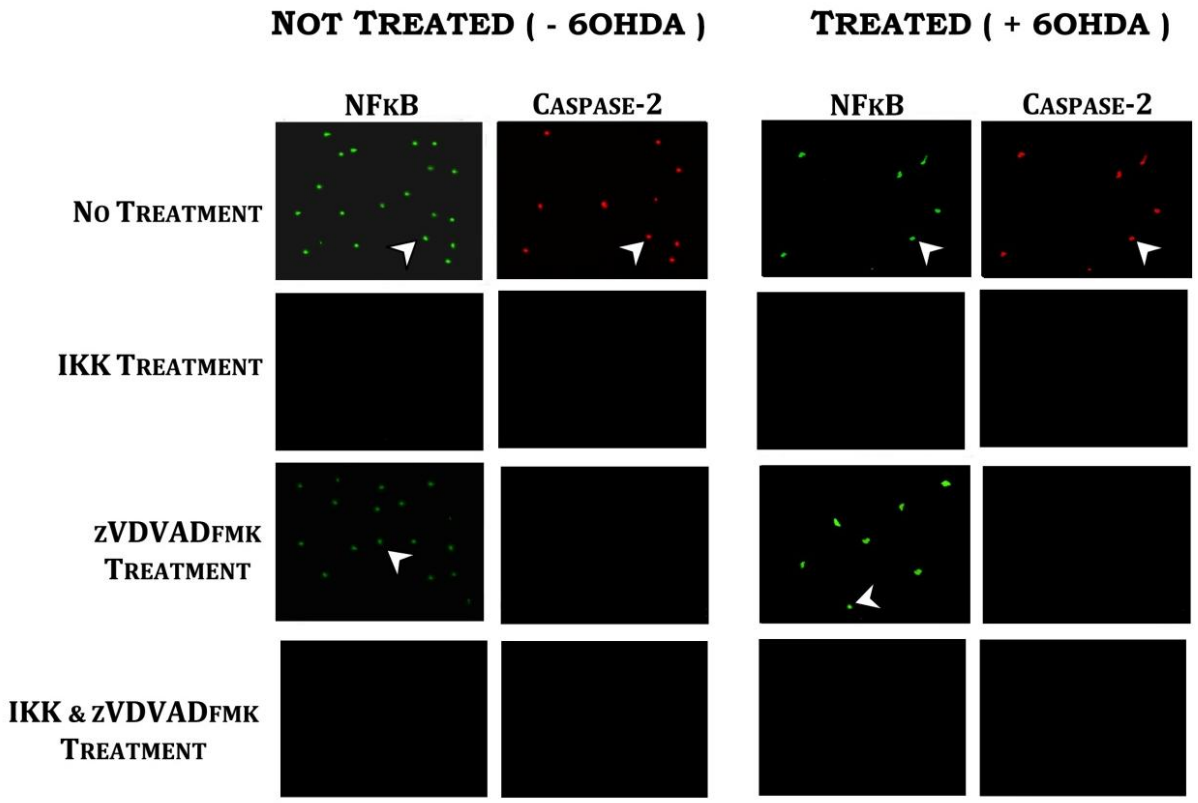

Figure 5.25: IKK can inhibit Caspase-2 activation in untreated and 6OHDA-treated dDCN

NFκB was present in untreated and 6OHDA-treated dDCN (green). There were more NFκB positive cells in 6OHDA-treated dDCN, when compared to untreated (-6OHDA) dDCN, suggesting 6OHDA further enhances NFκB expression resulting in death of dDCN. Active Caspase-2 was present in untreated and 6OHDA-treated dDCN (red). NFκB and Caspase-2 were present in the same cell bodies in 6OHDA-treated dDCN, indicating 6OHDA promotes further interactions of Caspase-2 and NFκB in resulting in death of dDCN.

NFκB was absent in IKK treated dDCN, 6OHDA+IKK treated dDCN, signifying that inhibiting IKK complex suppresses NFκB classical pathway in dDCN. Similarly, active Caspase-2 was not detected in IKK treated dDCN, 6OHDA+IKK treated dDCN. This indicates that NFκB is acting as upstream and by inhibiting the NFκB classical pathway; activation of Caspase-2 can also be suppressed in dDCN. NFκB was present in zVDVADfmk treated, 6OHDA+zVDVADfmk treated dDCN, suggesting that even with the suppression of Caspase-2; the NFκB classical pathway is still active in dDCN. In contrast, active Caspase-2 was absent in zVDVADfmk treated, 6OHDA+zVDVADfmk treated dDCN, signifying that Caspase-2 activity is successfully suppressed in dDCN when using Caspase-2 inhibitor. NFκB was absent in IKK+ zVDVADfmk treated dDCN, 6OHDA+IKK+zVDVADfmk treated dDCN. Caspase-2 was not found in IKK+ zVDVADfmk treated dDCN, 6OHDA+IKK + zVDVADfmk treated dDCN. IKK had suppressed both NFκB and Caspase-2 activity in untreated and 6OHDA-treated dDCN. Caspase-2 activation can be suppressed by directly inhibiting Caspase-2 or via inhibiting NFκB classical pathway in untreated and 6OHDA-treated dDCN. IKK inhibitor is more effective in minimising death of 6OHDA dDCN via suppressing both NFκB and Caspase 2 activation. Positive staining for cell bodies (White Arrow) in untreated (- 6OHDA) and treated (+ 6OHDA) dDCN. Table of values and statistical analysis can be found in Figure 5.26, Appendix 5.

To confirm if IKK inhibitor suppressed Caspase-2 activation of treated dDCN, WB analysis was carried out (Figure 5.27). An increase of active Caspase-2 was measured in 6OHDA-treated dDCN, compared to untreated dDCN, demonstrating that 6OHDA amplified Caspase-2 activation in dDCN. Active Caspase-2 was absent in IKK treated, 6OHDA+IKK treated dDCN, indicating that activation of Caspase-2 follows the NFκB classical pathway in dDCN. IKK suppressed Caspase-2 activation in dDCN, illustrating that 6OHDA triggers stimulation of Caspase-2 resulting in NFκB mediated death of dDCN.

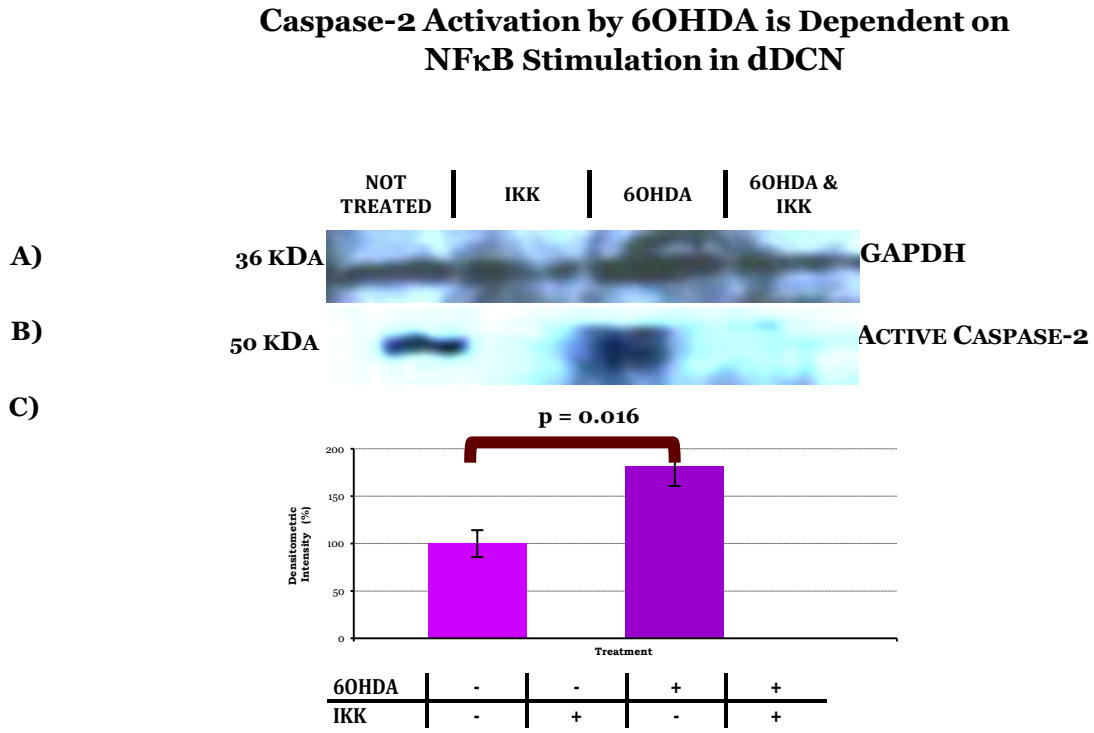

Figure 5.27: IKK suppressed activation of Caspase-2 in untreated and 6OHDA-treated dDCN

A) Illustrative example of GAPDH in untreated, IKK, 6OHDA, IKK + 6OHDA treated dDCN.

B) Illustrative example of active Caspase-2 in untreated, IKK, 6OHDA, IKK + 6OHDA treated dDCN.

C) Quantitatively, a significant increase in active Caspase-2 was detected in 6OHDA-treated dDCN, compared to untreated dDCN ($p<0.05$). The absence of active Caspase-2 in IKK treated, 6OHDA+IKK treated dDCN, suggest that Caspase-2 activity is dependent upon NFκB classical pathway. Means of three experiments ± SEM shown. Table of densitometry values and statistical analysis can be found in Figure 5.28, Appendix 5.

The results had showed that 6OHDA triggers activation of Caspases-2 and-8, via NFκB classical pathway. In addition, the findings had shown that NFκB is acting upstream and these two Caspases are activated downstream in the NFκB classical pathway in 6OHDA-treated dDCN. It was of interest to determine the impact of suppressing NFκB, Caspases-2 and -8 activities would have on cell death and survival of 6OHDA-treated dDCN. ANOVA and T test analysis indicated a significant difference in survival of 6OHDA dDCN that were treated with zVDVADfmk, zIETDfmk and IKK ($p < 0.01$, Figure 5.29, Appendix 5).

No additional effect in cell survival was measured in 6OHDA zIETDfmk +IKK treated dDCN, suggesting that activation of Caspase-8 is completely dependent on NFκB classical pathway and blocking NFκB classical pathway will suppress Caspase-8 activation in dDCN. There was no significant difference to slow death and promote cell survival in 6OHDA+ zIETDfmk +IKK dDCN, indicating that the use of IKK inhibitor can suppress both NFKB and Caspase-8 activity in dDCN($p > 0.01$, Figure 5.30).

zVDVADfmk and IKK reduced death of 6OHDA-treated dDCN compared to IKK alone ($p<0.05$ Figure 5.30). Combining IKK and zVDVADfmk, increased protection of 6OHDA-treated dDCN from apoptotic death 6OHDA-treated dDCN using IKK on its own. IKK, zVDVADfmk and zIETDfmk inhibited activation of NFκB, Caspases-2 and-8 in 6OHDA-treated dDCN. However, the combination of zVDVADfmk with IKK did not completely suppress death of 6OHDA-treated dDCN, indicating 6OHDA is promoting activation of other pathways.

6OHDA Triggers Caspases-2 and-8 in Classical NFκB Pathway

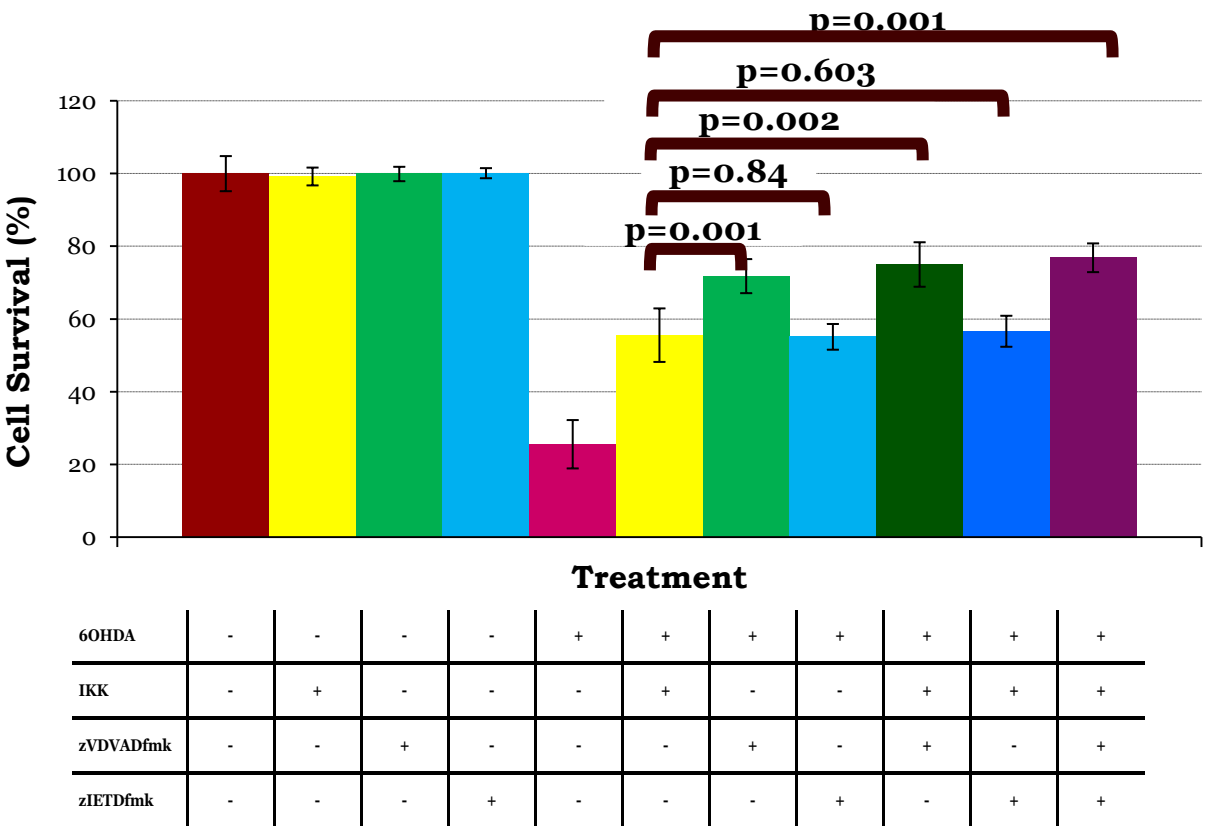

6OHDA	-	-	-	-	+	+	+	+	+	+	+
IKK	-	+	-	-	-	+	-	-	+	+	+
zVDVADfmk	-	-	+	-	-	-	+	-	+	-	+
zIETDfmk	-	-	-	+	-	-	-	+	-	+	+

Figure 5.30: Suppression of Caspases-2,-8 and NFκB classical pathway promote further protection and survival of 6OHDA-treated dDCN

IKK suppressed Caspase-8 and NFKB pathway of 6OHDA-treated dDCN. IKK and zVDVADfmk protected more cells from death of 6OHDA-treated dDCN, indicating that both these inhibitors are required to suppress Caspase-2 and NFκB activity in dDCN. IKK and zVDVADfmk inhibitor was more effective to slow death and increase survival of 6OHDA-treated dDCN then zIETDfmk inhibitor. Proportion of cells surviving was determined by MTT absorbance at 570nm. Means of three experiments ± SEM shown. Table of values and statistical analysis can be found in Figure 5.29, Appendix 5.

A further analysis of the findings showed increased levels of cell survival of 6OHDA+IKK+ zVDVADfmk treated dDCN, compared to 6OHDA+IKK+zIETDfmk treated dDCN (Figure 5.31). A closer examination of Caspase-2 activity in relation to NFκB classical pathway indicated that Caspase-2 is dependent on stimulation of NFκB classical pathway (Figure 5.31). There amount cell survival of 6OHDA+IKK+zVDVADfmk treated dDCN, compared to 6OHDA+zVDVADfmk treated dDCN (Comparison 9 $p>0.05$), is not statistically significant, indicated activation of Caspase-2 is dependent on NFκB pathway. This indicates 6OHDA stimulates Caspases-8 and-2 activation separately in NFκB classical pathway and that neither Caspases are dependent on each other to become activated.

	Treatment 1	Treatment 2	Treatment 3	Treatment 4	Treatment 5	Treatment 6	
	6OHDA IKK	6OHDA zVDVADfmk	6OHDA zIETDfmk	6OHDA IKK zVDVADfmk	6OHDA IKK zIETDfmk	6OHDA IKK zVDVADfmk zIETDfmk	p-value obtained
Comparison 1	+	+	-	-	-	-	0.001
Comparison 2	+	-	+	-	-	-	0.848
Comparison 3	+	-	-	+	-	-	0.002
Comparison 4	+	-	-	-	+	-	0.063
Comparison 5	+	-	-	-	-	+	0.001
Comparison 6	-	-	-	+	+	-	0.003
Comparison 7	-	-	-	+	-	+	0.522
Comparison 8	-	-	-	-	+	+	0.002
Comparison 9	-	+	-	+	-	-	0.247
Comparison 10	-	-	+	-	+	-	0.482

Figure 5.31: 6OHDA triggers activation of Caspases-2 and-8 independently in NFκB Classical pathway of dDCN

No additional survival and death of cells was determined in 6OHDA+zVDVADfmk+IKK treated dDCN, when compared to 6OHDA+IKK+zVDVADfmk+ zIETDfmk treated dDCN (Comparison 7

p>0.05), indicating that IKK can successfully inhibit Caspase-8 and NFκB activity in 6OHDA-treated dDCN. A difference in survival and death of cells was determined in 6OHDA+ zIETDfmk +IKK treated dDCN, when compared to 6OHDA+IKK+zVDVADfmk+ zIETDfmk treated dDCN (Comparison 8 p<0.05), indicating that IKK and zVDVADfmk need to be used together to successfully inhibit Caspase-2 and NFκB activity in 6OHDA-treated dDCN. There was no difference in cell survival in 6OHDA+zVDVADfmk treated dDCN compared to 6OHDA+IKK+zVDVADfmk treated dDCN, indicating that 6OHDA triggers Caspase-2 activation through NFκB mechanisms causing apoptotic death of dDCN (Comparison 9 p>0.05). Similarly there was no added effect when cells were treated with 6OHDA+IKK+ zIETDfmk , compared to 6OHDA+zIETfmk indicating that Caspase-8 is depended upon NFκB activation in 6OHDA-treated dDCN (Comparison 10 p>0.05).Proportion of cells surviving was determined by MTT absorbance at 570nm. Means of three experiments ± SEM shown. Table of values and statistical analysis can be found in Figure 5.29, Appendix 5.

Collectively, the results suggest that 6OHDA triggers NFκB mediated death of dDCN. 6OHDA stimulates NFκB activation, which in turn stimulates Caspases-2 and-8 activities in dDCN (Figure 5.32). The results have shown that NFκB is activated upstream, whilst Caspases are activated downstream in 6OHDA-treated dDCN. IKK inhibitor has the ability to completely suppress NFκB classical pathway which subsequently inhibits Caspases-2 and-8 activities in 6OHDA-treated dDCN.

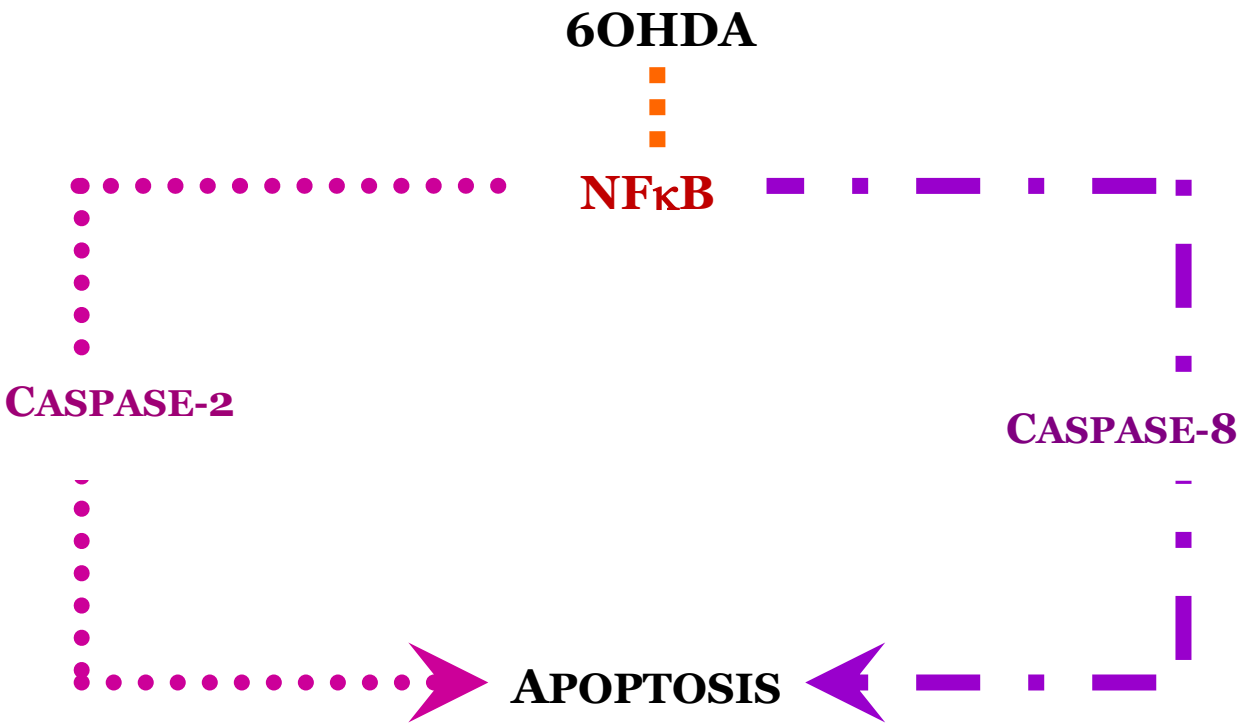

Figure 5.32 : NFκB activates Caspases-2 and -8 in 6OHDA mediated death of dDCN

Figure showing active Caspases-2 and-8 is involved in NFκB mediated cell death of 6OHDA-treated dDCN. The activation of Caspases-2 and-8 is independent of each other in NFκB classical pathway of 6OHDA-treated dDCN. NFκB promoted activation of Caspases-2 and-8 separately in 6OHDA-treated dDCN.

Results from previous Chapter had shown Caspase-4 inhibitor, zLEVDfmk had decreased apoptotic death of 6OHDA-treated dDCN, indicating 6OHDA triggered Caspase-4 activation in dDCN. The significance of Caspase-4 activity was determined in NFκB meditated death of dDCN. The findings illustrated that further cell survival was achieved in 6OHDA+IKK+zLEVDfmk treated dDCN, indicating 6OHDA triggers Caspase-4 and NFκB activation via different mechanisms dDCN (Figure 5.33).

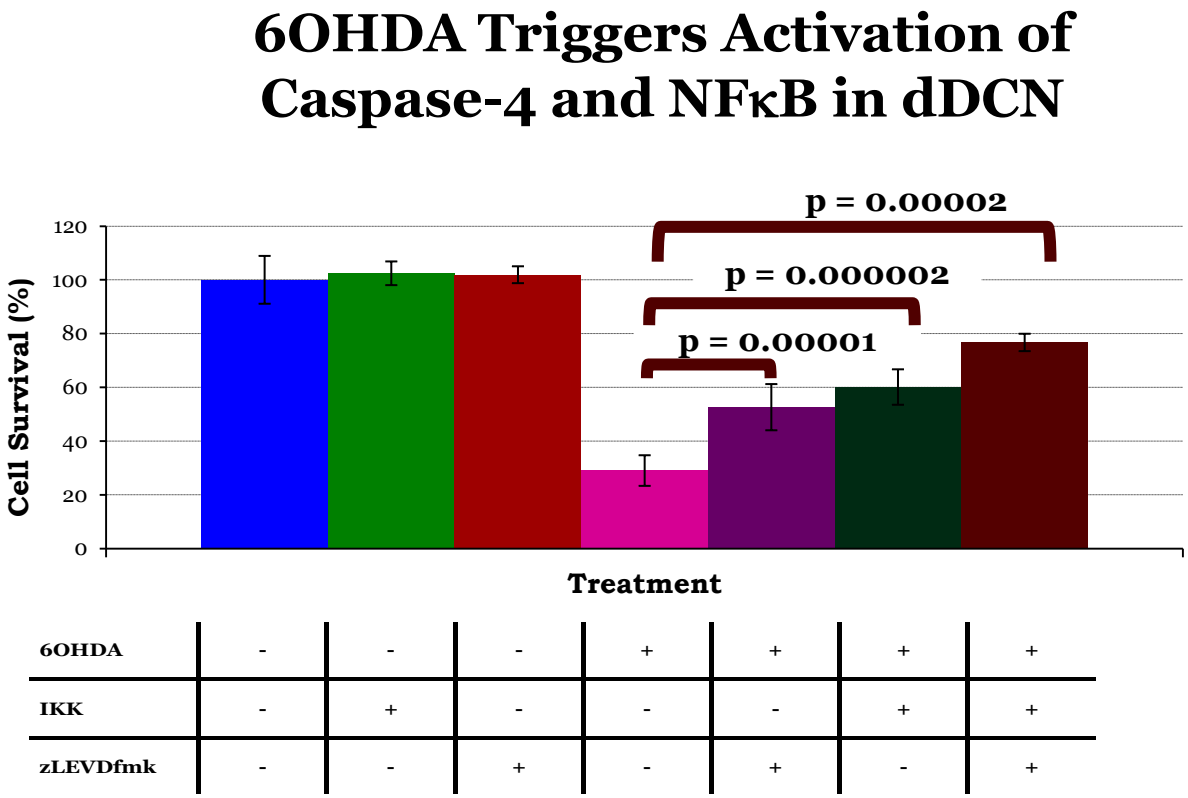

Figure 5.33 : Determining Caspase-4 activation in 6OHDA-treated dDCN

Cells were treated with 6OHDA+IKK, 6OHDA+zLEVDfmk, 6OHDA+IKK+zLEVDfmk, to determine if suppression of Caspase-4 and NFκB activity promoted survival of dDCN. 6OHDA+IKK treated dDCN promoted 53% cell survival by inhibiting the NFκB classical pathway. A further increase in cell survival, via suppressing Caspase-4 activity was found in 6OHDA+zLEVDfmk treated dDCN (60% cell survival). 6OHDA+IKK+zLEVDfmk treated dDCN promoted more cell survival (77% survival), by inhibiting both Caspase-4 and NFκB classical pathway activities. Proportion of cells surviving was determined by MTT absorbance at 570nm. Means of three experiments ± SEM shown. Table of values and statistical analysis can be found in Figure 5.34, Appendix 5

It was important to further explore to if Caspase-4 activity is influenced by NFκB classical pathway in 6OHDA dDCN. More survival and reduced death of cells was achieved in 6OHDA+zLEVDfmk +IKK treated dDCN. Suppression of Caspase-4 pathway in addition to NFκB classical pathway had an added effect in more cells surviving, indicating that there are two pathways. The results suggested that Caspase-4 is not following NFκB classical pathway and could be activated by another pathway, resulting in death of 6OHDA-treated dDCN (Figure 5.35).

	Treatment 1	Treatment 2	Treatment 3	Treatment 4	
	6OHDA	6OHDA IKK	6OHDA zLEVDfmk	6OHDA IKK zLEVDfmk	p-value obtained
Comparison 1	+	+	-	-	0.00001
Comparison 2	+	-	+	-	0.000002
Comparison 3	+	-	-	+	0.00002
Comparison 4	-	+	+	-	0.001
Comparison 5	-	+	-	+	0.00002
Comparison 6	-	-	+	+	0.001

Figure 5.35: IKK does not suppress Caspase-4 activation in 6OHDA-treated dDCN

Survival of 6OHDA dDCN increased when IKK was added to zLEVDfmk, indicating that NFκB classical pathway does not influence stimulation of Caspase-4 in 6OHDA-treated dDCN (comparison 5 $p<0.01$). Further survival and decrease in death of 6OHDA dDCN was achieved when zLEVDfmk was added to IKK, indicating that 6OHDA stimulated Caspase-4 and NFκB classical pathways via different mechanisms (comparison 6 $p<0.01$). The additional effect of more cells survival when Caspase-4 inhibitor and IKK inhibitor were combined indicates that there are two pathways that are contributing to death of 6OHDA dDCN. Furthermore, both inhibitors are required to be used to suppress both pathways so more cell survival can be achieved. Proportion of cells surviving was determined by MTT absorbance at 570nm. Means of three experiments ± SEM shown. Table of values and statistical analysis can be found in Figure 5.34, Appendix 5.

Double IF analysis was carried out to determine if active Caspase-4 and cleaved NFκB are present in the same untreated and 6OHDA-treated dDCN (Figure 5.36). It was important to determine if the Caspase-4 inhibitor, zLEVDfmk suppressed cleaved NFκB in 6OHDA-treated dDCN. The results portrayed that active Caspase-4 was not often present in cells that were stained positive for p65 NFκB of untreated and 6OHDA-treated dDCN, indicating that NFκB and Caspase-4 activation are most likely not interacting with one another. Active Caspase-4 was present in untreated, IKK treated, 6OHDA-treated, 6OHDA+IKK treated dDCN, demonstrating that IKK did not suppress Caspase-4 activation in dDCN. This puts forward the notion that Caspase-4 is not following the NFκB classical pathway of 6OHDA-treated dDCN, indicating that another pathway is causing death of dDCN via Caspase-4 activation. 6OHDA triggers activation of Caspase-4 and NFκB through two separate signalling pathways causing apoptotic death of dDCN.

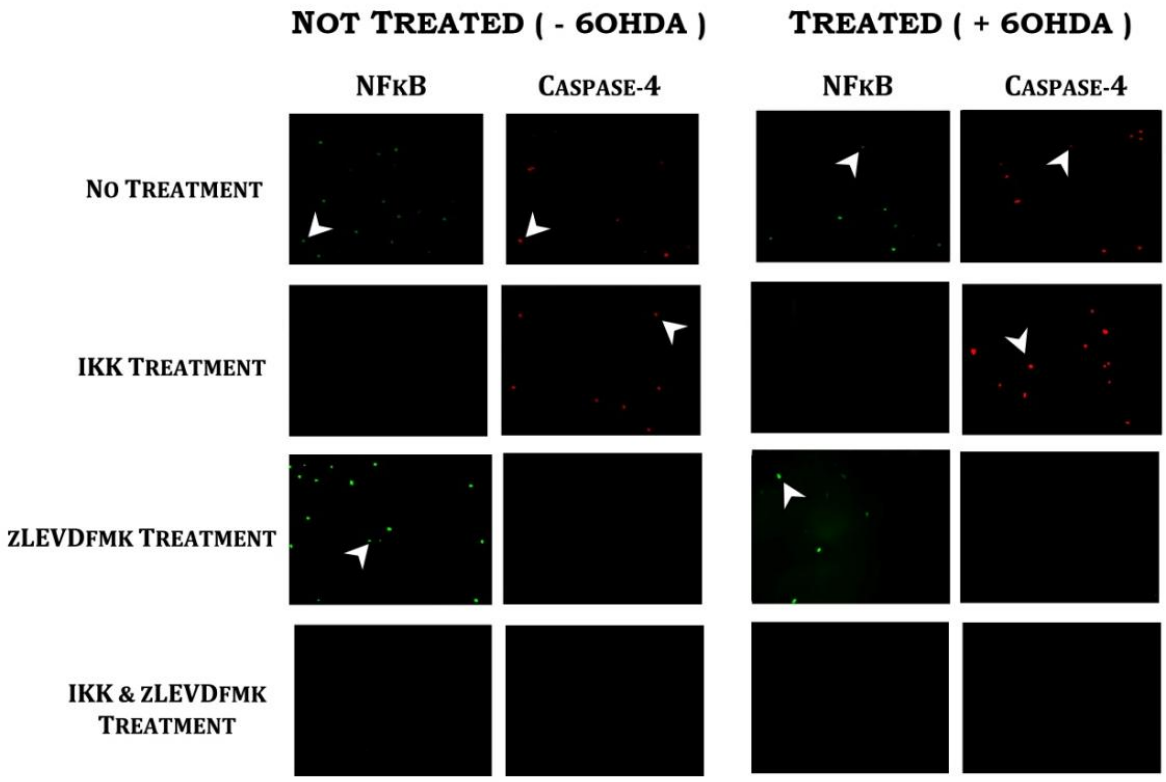

Figure 5.36: Determining the effect of IKK on Caspase-4 expressed in NFκB positive cells in 6OHDA-treated dDCN

Presence of cleaved NFκB was observed untreated and 6OHDA-treated dDCN (green). Active Caspase-4 was present in untreated and 6OHDA-treated dDCN (red). There were more cells that were stained

positive for active Caspase-4 in 6OHDA-treated dDCN, when compared to untreated (- 6OHDA) dDCN, indicating 6OHDA amplified activation of Caspase-4 in dDCN. Active Caspase-4 and cleaved NFκB were mostly detected in different untreated and 6OHDA-treated dDCN, suggesting there is a decreased possibility that Caspase-4 and NFκB interact with each other in dDCN.

NFκB was not detected in IKK treated, 6OHDA+IKK treated dDCN, suggesting NFκB is dependent on phosphorylation of IKK complex and removal of IκB so it can be activated in dDCN. In contrast, active Caspase-4 detected in IKK treated, 6OHDA+IKK treated dDCN, indicating that inhibiting the NFκB classical pathway does not influence Caspase-4 activity in dDCN. 6OHDA triggers Caspase-4 activity through a different pathway that is not related to NFκB classical pathway in dDCN.

NFκB was present in zLEVDfmk treated, 6OHDA+zLEVDfmk treated dDCN, suggesting that NFκB activation is independent of Caspase-4 stimulation in dDCN. The suppression of Caspase-4 activity does not influence NFκB activation in dDCN. In comparison, active Caspase-4 was absent in zLEVDfmk treated, 6OHDA+zLEVDfmk treated dDCN, signifying that zLEVDfmk had competitively suppressed Caspase-4 activity in dDCN. NFκB was absent in untreated and 6OHDA+IKK+ zLEVDfmk treated dDCN treated dDCN. Caspase-4 was not found in IKK+ zLEVDfmk treated, 6OHDA+IKK+zLEVDfmk treated dDCN. IKK had suppressed NFκB activity, whilst zLEVDfmk inhibited Caspase-4 activation in untreated and 6OHDA-treated dDCN. Positive staining for cell bodies (White Arrow) in untreated (- 6OHDA) and treated (+ 6OHDA) dDCN. Table of values and statistical analysis can be found in Figure 5.37, Appendix 5.

WB analysis was carried out to determine if IKK could suppress Caspase-4 activity in 6OHDA-treated dDCN (Figure 5.38). Active Caspase-4 was present in untreated, IKK treated, 6OHDA and 6OHDA+IKK treated dDCN. A higher amount of active Caspase-4 was detected in 6OHDA-treated dDCN compared to untreated dDCN, suggesting 6OHDA triggered further activation of Caspase-4 in dDCN. IKK did not prevent nor reduce the amount of Caspase-4 in 6OHDA-treated dDCN, illustrating that IKK does not influence Caspase-4 activation. The ineffectiveness of IKK against activation of Caspase-4 further supports the notion that Caspase-4 is independent of NFκB mediated death of treated dDCN. 6OHDA triggered Caspase-4 activation, but this was being achieved, through a different route and not via NFκB classical pathway.

Caspase-4 Activation by 6OHDA is not Dependent of NFκB Classical Pathway

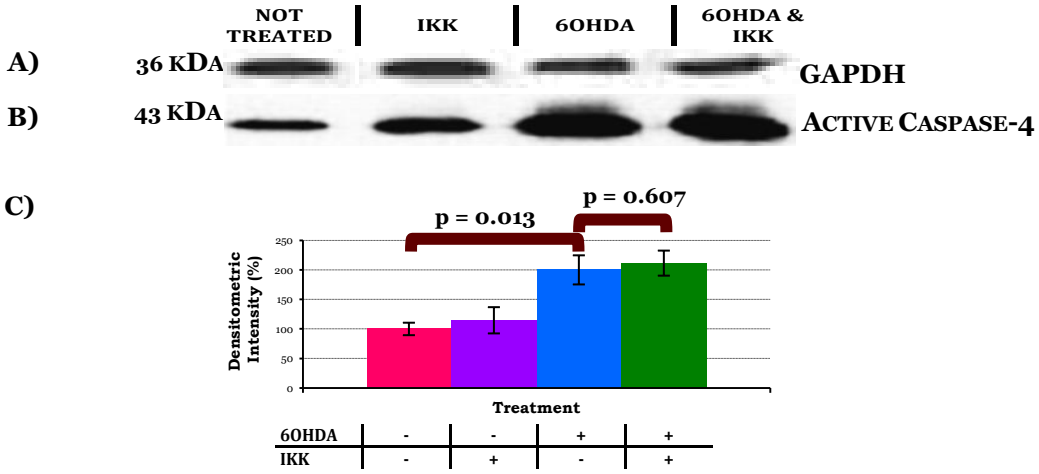

Figure 5.38: IKK does not inhibit Caspase-4 activation in 6OHDA-treated dDCN

A) Illustrative example of GAPDH in untreated, IKK, 6OHDA, IKK + 6OHDA treated dDCN.

B) Illustrative example of active Caspase-4 in untreated, IKK, 6OHDA, IKK + 6OHDA treated dDCN.

C) Quantitatively, a substantial increase in active Caspase-4 was detected in 6OHDA-treated dDCN, compared to untreated dDCN ($p<0.05$). IKK neither prevented nor reduced the amount of active Caspase-4 in present in IKK treated, 6OHDA+IKK treated dDCN ($p>0.05$), indicating that NFκB classical pathway does not influence Caspase-4 stimulation in 6OHDA-treated dDCN. Means of three experiments ± SEM shown. Table of densitometry values and statistical analysis can be found in Figure 5.39, Appendix 5.3.

The results showed NFκB classical pathway influences activation Caspases-2 and-8 but not of Caspase-4 in 6OHDA-treated dDCN. The next aim was to determine if maximum survival could be achieved by further suppression Caspases-2,-4,-8 and NFκB activities in 6OHDA-treated dDCN. 6OHDA dDCN were treated with different combinations of IKK, zVDVADfmk, zLEVDfmk and zIETDfmk. ANOVA analysis illustrated a considerable difference in survival of 6OHDA dDCN that were treated with zVDVADfmk, zIETDfmk, zLEVDfmk and IKK ($p < 0.01$, Figure 5.40, Appendix 5). Subsequent T tests were used to identify key inhibitors that had the most effect in promoting survival and slowing death of 6OHDA dDCN. The results demonstrate that the use of Caspase inhibitors, zLEVDfmk and zVDVADfmk, along with IKK provide more protection and survival of 6OHDA-treated dDCN then using a single inhibitor or two inhibitors ($p<0.05$ Figure 5.41).

Additional cell survival of 6OHDA dDCN was determined when IKK was added with zLEVDfmk, demonstrating that IKK has an additional effect to slow death and promote cell survival ($p<0.05$ Figure 5.41). More cell survival of was found in 6OHDA+IKK+zLEVDfmk treated dDCN, signifying that both inhibitors can promote further survival and slow death of 6OHDA dDCN, via suppressing two different routes. The additional effect of more cells survival when Caspase-4 inhibitor and NFκB inhibitor are combined indicates that there are two pathways that are contributing to death of 6OHDA dDCN.

In contrast, similar cell survival was determined in 6OHDA + IKK +zIETDfmk treated dDCN, when compared to 6OHDA + IKK treated dDCN or 6OHDA + zIETDfmk treated dDCN, indicating NFκB directly influences Caspase-8 activity ($p>0.05$ Figure 5.41). The amount of cell survival was not significant when zIETDfmk inhibitor was added to IKK inhibitor, suggesting the addition of zIETDfmk did not provide an additional effect to slow death and increase survival of 6OHDA-treated dDCN($p>0.05$ Figure 5.41). There was no significant difference to slow death and promote cell survival in 6OHDA + IKK + zIETDfmk treated dDCN, indicating that the use of IKK inhibitor can suppress both NFκB and Caspase-8 activity, therefore zIETDfmk is not required to inhibit death of dDCN.

A higher cell survival rate was determined in 6OHDA + IKK + zVDVADfmk treated dDCN when compared to 6OHDA + IKK treated dDCN $p<0.05$ Figure 5.41), indicating that Caspase-2 may be

activated by another pathway as well as NFκB pathway. This can be explained further as the results previously demonstrated that activation of Caspase-2 is dependent on stimulation of the NFκB pathway. However, cell survival analysis has shown that a greater survival of 6OHDA-treated dDCN, when both NFκB and Caspase-2 is suppressed, indicating that there may be another factor which can activate Caspase-2. Combining all inhibitors reduced death of treated dDCN then using solely IKK ($p<0.01$ Figure 5.41). The results suggest that IKK+ zVDVADfmk +zLEVDfmk provided better survival of 6OHDA-treated dDCN.

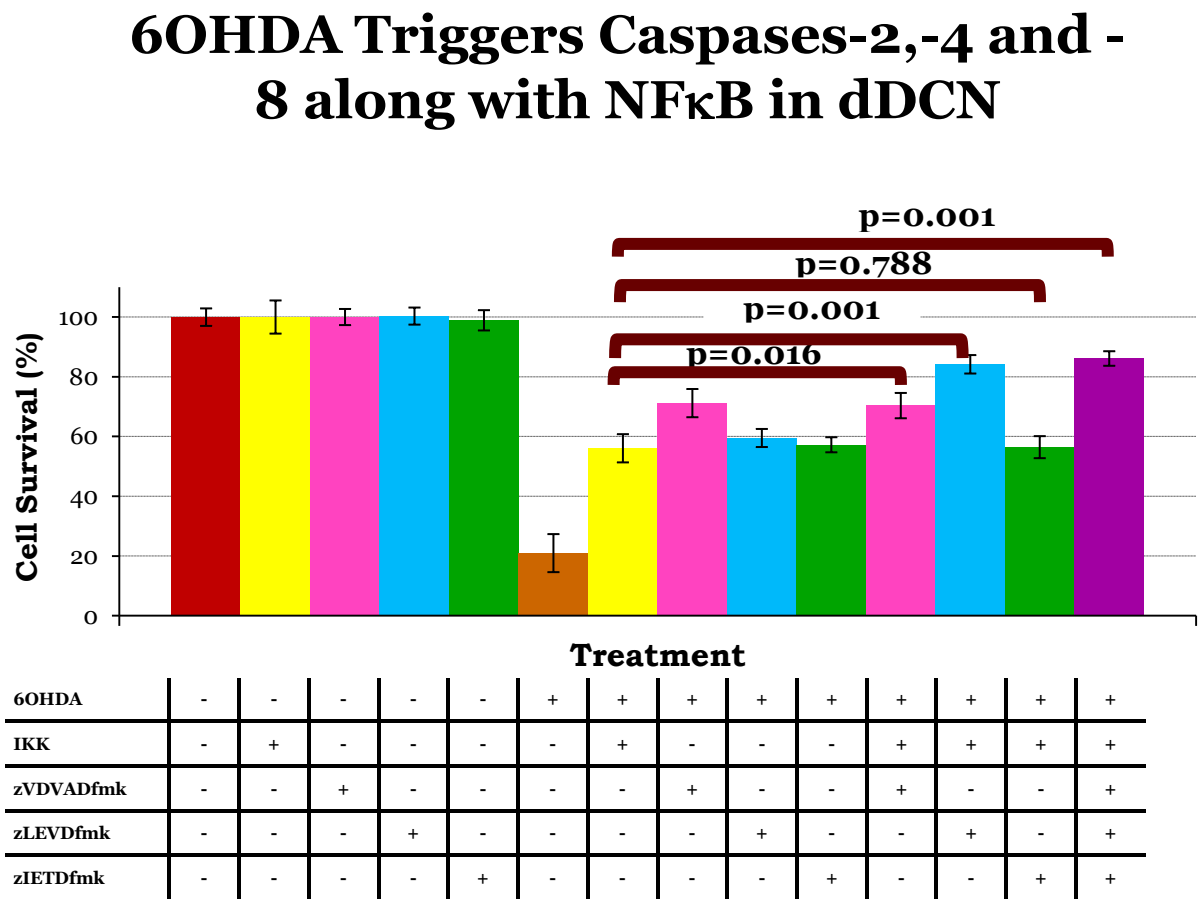

Figure 5.41: Suppression of Caspases-2,-4,-8 and NFκB classical pathway promoted further cell survival of 6OHDA-treated dDCN

6OHDA dDCN were treated with different combinations of IKK, zVDVADfmk, zLEVDfmk and zIETDfmk to determine if maximal cell survival could be achieved by suppression of Caspases-2,-4,-8 and NFκB activity. Similar cell survival was determined in 6OHDA+ IKK treated dDCN, 6OHDA+ zIETDfmk dDCN, 6OHDA +IKK + zIETDfmk dDCN (cell survival 56%, 57% and 56%). In comparison, further cell survival was achieved in 6OHDA-treated dDCN that were treated with

zVDVADfmk inhibitor (70%, cell survival). In addition, a greater cell survival was measured in 6OHDA + zLEVDfmk +IKK treated dDCN compared to IKK (84% cell survival). 6OHDA +IKK+ zVDVADfmk+ zLEVDfmk +zIETDfmk treated dDCN promoted 86% survival of cells. Proportion of cells surviving was determined by MTT absorbance at 570nm. Means of three experiments ± SEM shown. Table of values and statistical analysis can be found in Figure 5.40, Appendix 5.

The next aim was to determine if there was any cross talk between Caspase-2,-4,-8 and NFκB in the NFκB classical pathway of 6OHDA-treated dDCN (Figure 5.42, Appendix 5). More specifically the aim was to determine if activation of Caspase-4 could influence the others Caspases such as Caspase-2 and -8 in 6OHDA dDCN. To achieve this aim, a combination of different treatments consisting of specific inhibitors such as zVDVADfmk, zIETDfmk and IKK were used in 6OHDA-treated dDCN. Moreover, further survival of 6OHDA dDCN, was determined when IKK was added with zVDVADfmk and zLEVDfmk, demonstrating that these three inhibitors are required to be used to suppress pathways, thereby promoting cell survival and slowing death.

The results showed a greater cell survival was achieved in 6OHDA + IKK + zLEVDfmk+ zIETDfmk + zVDVADfmk treated dDCN,, when compared to 6OHDA +IKK + zVDVADfmk treated dDCN (Comparison 8, $p<0.01$, Figure 5.42, Appendix 5), indicating activation of Caspase-2 is dependent on NFκB classical pathway , but other pathways or factors cause death of in 6OHDA-treated dDCN. Collectively the data has demonstrated that 6OHDA stimulates NFκB classical pathway which promotes activation of Caspases-2 and-8 separately and one Caspase is not dependent on the other, resulting in death of dDCN. Although there was an increase in cell survival of 6OHDA +IKK + zLEVDfmk + zIETDfmk + zVDVADfmk treated dDCN, when compared to 6OHDA + IKK + zLEVDfmk treated dDCN, the increase was not statistically significant (Comparison 9, $p>0.05$, Figure 5.42, Appendix 5), indicating the greatest cell survival is achieved by combining IKK and zLEVDfmk with zVDVADfmk.

In comparison, a difference in cell survival measured in 6OHDA +IKK + zLEVDfmk+ zIETDfmk + zVDVADfmk treated dDCN, when compared to 6OHDA + IKK + zIETDfmk treated dDCN, indicating that activation of Caspase-8 is completely dependent on stimulation of NFκB classical pathway in 6OHDA dDCN and another factors and pathways are involved in death of 6OHDA dDCN (Comparison 10, $p<0.05$, Figure 5.42, Appendix 5). This finding emphasises that IKK inhibitor is more beneficial to use to block Caspase-8 activity and NFκB classical pathway compared to using zIETDfmk inhibitor, as the zIETDfmk inhibitor would suppress Caspase-8 activity only in 6OHDA-treated dDCN.

A comparison between 6OHDA+IKK+zLEVDfmk treated dDCN and 6OHDA+IKK+zVDVADfmk treated dDCN (Comparison 11, $p<0.05$, Figure 5.42, Appendix 5) revealed that Caspase-4 activity does not directly influence Caspase-2 activity and the stimulation of these Caspases are most likely through different mechanisms. Furthermore, 6OHDA+IKK+zVDVADfmk treated dDCN increased cell survival, when compared to 6OHDA+IKK+zIETDfmk treated dDCN (Comparison 12, $p<0.05$, Figure 5.42, Appendix 5), indicating activation of that Caspases-2 is not dependent on and activation on Caspase-8 and vice versa dDCN. 6OHDA+IKK+zLEVDfmk treated dDCN provided greater cell survival, when compared to 6OHDA+IKK+zIETDfmk treated with dDCN (Comparison 13, $p<0.01$, Figure 5.42, Appendix 5), indicating that 6OHDA triggers Caspases-4 and-8 activation in dDCN, through different mechanisms and one Caspase is not dependent on the other to be activated.

There was no significant difference in cell survival in 6OHDA +zVDVADfmk treated dDCN, when compared to 6OHDA + IKK + zVDVADfmk treated dDCN (Comparison 14, $p>0.05$, Figure 5.42, Appendix 5), confirming NFκB is required to stimulation Caspase-2 activity in dDCN. In contrast, there was a difference in cell survival of 6OHDA+zLEVDfmk treated dDCN, when compared to 6OHDA + IKK + zLEVDfmk treated dDCN, suggesting that NFκB and Caspase-4 follow different cell signalling pathways causing death of 6OHDA dDCN(Comparison 15, $p<0.01$, Figure 5.42, Appendix 5). Additionally, no additional effect in cell survival was found in 6OHDA+ zIETDfmk treated dDCN, when compared to 6OHDA + IKK + zIETDfmk treated dDCN, signifying NFκB and Caspase-8 follow the same apoptotic pathway in 6OHDA dDCN(Comparison 16, $p>0.05$, Figure 5.42, Appendix 5).

Collectively, the results demonstrate that 6OHDA triggered Caspases-2 and -8 activation resulting NFκB mediated death of dDCN. NFκB separately stimulated Caspases-2 and-8 activation in 6OHDA dDCN. Furthermore, another factor apart from NFκB classical pathway seems to activate Caspase-2 resulting in death of 6OHDA dDCN. IKK inhibitor completely suppressed Caspases-2 and -8 by preventing activation of NFκB in 6OHDA dDCN. Although it is has been confirmed that Caspase-4 plays an active role in death of 6OHDA-treated dDCN, the exact route and how Caspase-4 is activated in 6OHDA dDCN remains to be established. The results also suggest 6OHDA stimulates other route leading to apoptotic death of dDCN (Figure 5.43).

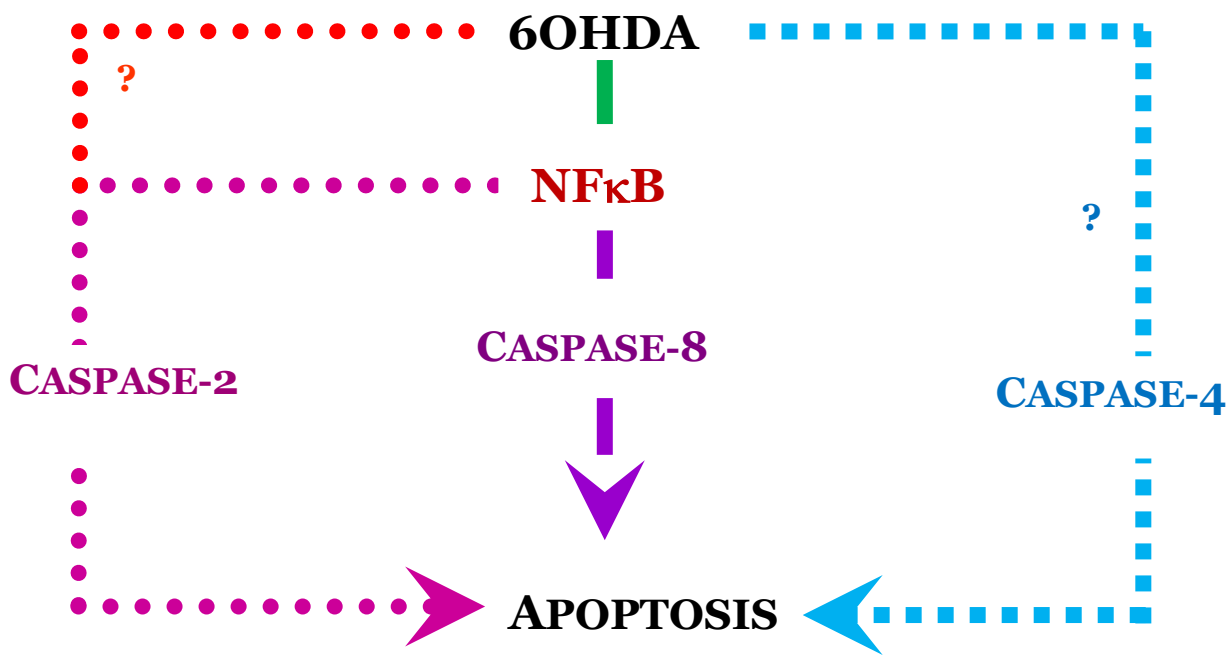

Figure 5.43: The involvement of Caspases-2,-4 and -8 in NFκB mediated death of 6OHDA-treated dDCN

6OHDA triggered NFκB classical pathway leading to activation of Caspases-2 and-8 in dDCN. NFκB classical pathway promoted activation of Caspases-2 and-8 independently in 6OHDA-treated dDCN. In comparison, NFκB classical pathway did not influence activation of Caspase-4, suggesting that Caspase-4 is active in another route (such as ER stress). In addition, the combination of Caspase-4 inhibitor and IKK increased cell survival of 6OHDA-treated dDCN, indicating that there are two separate pathways that are causing apoptosis of 6OHDA-treated dDCN.

5.4 Discussion

The main aim was to determine the influence of NFκB classical pathway in Caspase mediated death of 6OHDA-treated dDCN. The results demonstrated that 6OHDA triggers NFκB pathway leading activation of Caspases-2,-3 and -8 resulting in apoptotic death of dDCN (Figure 5.43). The results of the current study demonstrated that NFκB promotes apoptotic death rather than survival of 6OHDA-treated dDCN (Figure 5.1-Figure 5.13). Double IF and WB analysis illustrated 6OHDA amplified NFκB activity in dDCN (Figure 5.1-5.7). These finding are similar to previous work carried out by Ye et al (2013) and Xiang et al (2011) who had found that 6OHDA triggered phosphorylation of IκB and translocation of p65 to the nucleus in SH-SY5Y neuroblastoma cells. IF and WB analysis revealed 6OHDA triggered Caspase-3 activation and death of DCN through NFκB classical pathway (Ye et al 2013, Xiang et al 2011).

Work by Jia and Misra (2007) demonstrated increased Caspase-3 levels in zineb induced SHSY5Y cells, indicating that environmental toxin cause Caspase dependent death of neuronal cells. Quantificatation of p50 NFκB from nuclear extracts of zineb induced SHSY5Y cells was carried out using ELISA. Colorimetric analysis revealed increase hydrogen peroxide and superoxide, levels in pesticide induced neuronal cells. Furthermore, research by Tsui et al (2011) found an increase in Bax, cytochrome c, p38, NFκB, Caspase-3 levels in PC12 cells that had been exposed to hydrogen peroxide over a time course. WB analysis revealed elevated cleaved Caspase-3, PARP and NFκB p65 levels at 10, 12 and 24 hours demonstrating that exposure to toxins promotes apoptotic death of cells through over activity of NFκB. In comparison to Jia and Misra (2007) and Tsui et al (2011) the findings of this current study has demonstrated an increase in Caspase-3 activation that were expressed in NFκB cell of 6OHDA-treated dDCN, indicating that 6OHDA promotes Caspase-3 stimulation through NFκB pathway in dDCN (Figure 5.6-Figure 5.7).

The results of this study have shown an increase in p65 NFκB, Caspases-2,-3 and -8 in 6OHDA-treated dDCN (Figure 5.6-Figure 5.7). Furthermore, IF, WB and inhibitor analysis had demonstrated that activation of Caspase-2 and -8 was dependent on NFκB pathway and the suppression of NFκB pathway inhibited stimulation of thesis Caspases in 6OHDA dDCN (Figure 5.15-Figure 5.32). These findings are in parallel to research carried out by Liu et al (2004), who found increased levels of cytochrome c, p65 NFκB, Caspases-3,-8 and -9 in PC12 cells treated with MPTP, indicating that MPTP triggered activation of Caspases-3,-8 and -9 via mitochondrial and NFκB pathways resulting in cell death.

Work by Panet et al (2001) illustrated 6OHDA triggered NFκB mediated apoptotic death of dopamine induced PC12 cells. Furthermore, reduced death of 6OHDA cells was achieved using a specific NFκB inhibitor SN-50, suggesting that 6OHDA triggers NFκB mediated death of cells. Moreover, WB analysis showed an increase in survival of 6OHDA cells that had been treated with either the Caspases-3 or-1 inhibitor, signifying that ROS triggers NFκB activation and activation of Caspases-3 and -1, resulting in apoptotic death of DCN. Work by Masumoto et al (2003) had found NFκB over activity was encouraged by elevated levels of the pro apoptotic protein ASC. Elevated levels of Caspase-8 and NFκB p65 were determined in cells treated with ASC, indicating that over expression of ASC promoted apoptotic cell death through NFκB and Caspase-8 mechanisms.IKK had inhibited NFκB p65 and Caspase-8 apoptotic death of cells that had been exposed to ASC and Ipaf.

In comparison, the current study has illustrated 6OHDA triggers activation of NFκB classical pathway resulting in Caspase mediated apoptotic death of dDCN using specific inhibitors. IF, WB and inhibitor cell viability assays using NFκB, Caspases-2 and -8 specific inhibitors demonstrated NFκB stimulates Caspases-2 and -8 in 6OHDA dDCN (Figure 5.15-Figure 5.32). This study had also found that IKK had inhibited NFκB and Caspase-8 as well as Caspase-2 activation and apoptotic death of 6OHDA dDCN (Figure 5.18-Figure 5.20 and Figure 5.25-Figure 5.27).

Research by Wilms et al (2003) and Lamkanfi et al (2006 and 2007) demonstrated that Caspase-2 can trigger NFκB activation resulting in Caspase-3 activation and death of cells. Active Caspase-2 forms the PIDD:RIP-1:Caspase-2 complex that promotes NFκB stimulation. However, the findings of this research suggest that NFκB promotes activation of Caspase-2 in dDCN (Figure 5.32). IF, WB and inhibitor cell viability assays had demonstrated that suppression of NFκB pathway had inhibited Caspase-2 activation in dDCN, signifying that NFκB is activated upstream and Caspase-2 is stimulated downstream in 6OHDA dDCN (Figure 5.22-Figure 5.32).

Work by Ho et al (2009) has showed a decrease in death of cortical neurons from E16 mice that had knocked down Caspase-8. RNAi was used to inhibit and silence Caspase-8 activity in cortical neurons and WB analysis had shown that inhibition of Caspase-8 had reduced death of cortical neurons, emphasising that activation of Caspase-8 results in death of cortical neurons. Further work using WB analysis showed increased Caspase-8 levels and absence of Caspase-2 in striatal lysates of LRRK-2 PD patient. This indicated that mutated LRRK-2 promoted Caspase-8 dependent death of striatal DCN in PD.

In comparison, the results of the current study demonstrated 6OHDA had triggered Caspases-2 and-8 activation leading to death of dDCN (Figure 5.32). zVDVADfmk and zIETDfmk inhibited Caspases-2 and-8 activities thereby promoting survival and reducing death of 6OHDA-treated dDCN (Figure 5.30-Figure 5.32). In addition, the findings of this research have clearly demonstrated that NFκB stimulates activation of Caspases-2 and-8 leading to death of 6OHDA-treated dDCN (Figure 5.15-Figure 5.32). Ho et al (2009) research had collected specific PD brain samples that had been associated with mutated LRRK-2 gene so only the effect of mutated effect of LRRK-2 gene on Caspases could be determined. In comparison, this research focussed on specific Caspases and how they are activated after administration of 6OHDA, and therefore explored the environmental and not genetic aspect, which results in death of dDCN.

To date this is the first research that determined the effect of NFκB classical pathway on Caspase-4 activation in 6OHDA-treated dDCN. The aim of this research was to determine if 6OHDA triggers Caspase-4 activation resulting in NFκB mediated death of dDCN. The results demonstrated that 6OHDA triggered Caspase-4 activation, but this was not achieved through NFκB classical pathway (Figure 5.33-Figure 5.41). Overall, IF analysis had illustrated that Caspase-4 and NFκB were present mostly in different untreated and 6OHDA-treated dDCN, indicating that they are independent of each other (Figure 5.36). Further work using IKK had shown that Caspase-4 was still active in 6OHDA-treated dDCN, and IKK inhibitor was ineffective in suppressing Caspase-4 activation (Figure 5.36). WB analysis portrayed IKK inhibitor had no effect in suppressing Caspase-4 activity, signifying that Caspase-4 does not follow NFκB classical pathway (Figure 5.38). To confirm this, the combination of IKK and zLEVDfmk prevented further death and increased more cell survival of 6OHDA-treated dDCN, then using one inhibitor alone (Figure 5.33). The additional effect measured when combining both inhibitors highlighted that 6OHDA triggers NFκB and Caspase-4 activation through different pathways resulting in death of dDCN(Figure 5.33-Figure 5.34). NFκB did not inhibit all cell death, therefore it is plausible that another parallel death signalling pathway involved (Figure 5.9- Figure 5.11 and Figure 5.43). The next Chapter will attempt to determine what this other pathway is.

5.5 Conclusion

Collectively, the results have shown that 6OHDA had triggered activation of NFκB, via the classical pathway (Figure 5.1- Figure 5.4 and Figure 5.9-Figure 5.13). Subsequently, active NFκB promoted activation of Caspases-2 and-8 separately; resulting in death of 6OHDA-treated dDCN (Figure 5.32 and Figure 5.43). A closer examination using IF, WB and inhibitor cell viability assays illustrated that suppression of NFκB classical pathway inhibits stimulation of Caspases-2 and -8, resulting in an increase in survival of 6OHDA dDCN (Figure 5.15 –Figure 5.32). Furthermore, 6OHDA triggered Caspase-4 activation independently to the NFκB classical pathway causing apoptotic death of dDCN (Figure 5.33-Figure 5.38). Inhibitor cell viability assays revealed suppressing NFκB, Caspases-2 and-4 activation using IKK, zVDVADfmk and zLEVDfmk inhibitors resulted in slow death and a greater survival of 6OHDA dDCN (Figure 5.41- Figure 5.42). IF, WB and inhibitor cell viability assays revealed that NFκB classical pathways is one of the main routes that lead to Caspase mediated death of 6OHDA dDCN (Figure 5.1-Figure 5.4 and Figure 5.9-Figure 5.13). However, the results have also demonstrated that 6OHDA triggers other routes that result in apoptotic death of dDCN (Figure 5.9 – Figure 5.11 and Figure 5.43).

Chapter 6
6OHDA triggers ER mediated death of dDCN: The Legend of ER stress pathway

Activation of ER stress pathways is required in normal cellular processes (Chapter 1 Section 1.7). Research has shown that failure to remove defective proteins promotes formation of toxic aggregates provoking stimulation of the ER stress pathways; IRE-1, PERK and ATF-4, in aid to restore cell homeostasis and survival (Todd et al 2008). However, unsuccessful restoration of cell homeostasis encourages the activation of death mechanisms leading to ER mediated death of cells, which has been recently been associated with PD pathogenesis and is currently being explored (Oakes and Papa 2014).

6OHDA and 1-Methyl 4-Phenylpyridinium (MPP^+) can mimic the key attributes of PD (such as Lewy body formation, mitochondrial dysfunction and ROS production) and so are commonly used neurotoxins to study in vivo and in vitro PD models (Bohlen and Halbach 2006, Ferro et al 2005, Brazhnik et al 2012, Murray et al 2003, Pienaar and Berg 2013). Holtz and O'Malley (2003) found 6OHDA triggers stimulation of PERK, ATF-6 and IRE-1 pathways resulting ER mediated death of cells. WB and IF analysis revealed a substantial increase of active CHOP, BiP, XBP-1, p-JNK, p-EIF2α, p-PERK and Caspases-3 levels in 6OHDA-treated MN9D cells. A gradual increase in p-JNK, CHOP, XBP-1 and Caspase-3 were determined from 6 hour to 12 hours in 6OHDA-treated MN9D cells. In comparison elevated levels of p-EIF2α, BiP and Caspase-3 was determined in MPP^+ induced MN9D cells. The results demonstrated that 6OHDA and MPP^+ activated CHOP via UPR in MN9D cells. In addition, oxidative stress, impairment of the mitochondria and high accumulation of proteins were found in 6OHDA-treated and MPP^+ treated cells (Holtz and O'Malley 2003).

Research by Lee et al (2010) demonstrated elevated levels of CHOP, p-PERK, p-IRE-1, p-EIF2α and XBP-1 in tunicamycin induced SK-N-SH cells via WB and IF analysis. Colorimetric Caspase specific assays revealed a gradual increase of Caspases-4 and -3 activities in neuronal cells that had been treated with tunicamycin. Salubrinal significantly decreased p-EIF2α, CHOP, Caspases-3 and -4 activity and protected tunicamycin treated cells from damage (Lee et al 2010).

Research by Arduíno et al (2009) measured Caspase-2,-3,-4 and -9 activation using Caspase specific colorimetric substrates such as ac-VDVAD-fmk, ac-DEVD-fmk, ac-LEVD-fmk and ac-LEDH-fmk in lysates of MPTP induced neuronal cells. The results showed that Caspase-4 activity increased by 40% after 24 hours of MPTP exposure in neuronal cells. Furthermore, Caspase-2 activity increased by 30% in 6 hour MPTP induced cells and rose by a further 25% after 24 hour MPTP exposure to cells. Moreover, Caspases-3 and -9 activities were lower in 2 hour exposed MPTP-treated cells compared to untreated cells. However, a significant rise in the level of Caspases-3 and -9 activities was found in cells that had been exposed to MPTP after 24 hours. WB analysis revealed an increase in active BiP at 2 hour MPTP exposure, followed by gradual decrease of active BiP from 2 hour to 24 hour, where at 24 hours BiP was at normal basal levels. IF analysis demonstrated an increase in calcium levels in the ER and mitochondria of thapsigargin and MPTP-treated cells using Fura-2AM. Collectively the results demonstrated that MPTP triggers leakage of calcium from the ER into the mitochondria provoking activation of Caspases-2,-3,-4 and -9 resulting in death of neuronal PD cells.

Work by Colla et al (2012a) found that oligomers of α synuclein accumulated in the ER promoted activation of ER stress in transgenic mice model. WB analysis revealed high levels of aggregated α synuclein in ER microsomal and mitochondrial fractions alongside increased fragmentation of Golgi body in the midbrain of transgenic mouse model. Furthermore, the PERK inhibitor, salubrinal, decreased the amount of aggregated α synuclein in ER microsomal and mitochondrial fractions alongside reduced fragmentation of Golgi body of transgenic mouse model, indicating that aggregated α synuclein providing a signal to trigger ER stress. Further work (Colla et al 2012b) showed similar results in human brain tissues and in transgenic mouse model. WB and Immunohistochemical analysis showed elevated levels p-EIF, Caspases-12,-9 and -3 and aggregated α synuclein in human tissues and in ER microsomal neuroblastoma cell line. Salubrinal decreased the level of Caspases and accumulated toxic oligomers of α synuclein, indicating α synuclein triggers PERK pathway of ER stress leading to Caspase activation and death of DCN.

Work by Smith et al (2005) found that mutant A53T α synuclein accumulated in the ER promoted activation of ER stress in PC12 model. Further analysis using 2', 7'-dichlorofluorescein diacetate (DCFDA) probe indicated high ROS levels in the cytosol of mutant A53T α synuclein cells. Inhibitor analysis using specific zDEVDfmk, zIETDfmk and zLEHDfmk inhibitors determined the increased activation of Caspases-3 and-9 but not Caspase-8 in that mutant A53T α synuclein cells indicating that mutated form of α synuclein promoted activation of Caspase-3 and-9 dependent death of DCN. WB analysis revealed high levels of p-eIF2-α, GRP78, CHOP and Caspase-12 after 5 days in mutant A53T α synuclein PC12 cells. The author concluded that knock down of Caspase-12 increased cell survival, indicating that Caspase-12 participates in ER stress mediated death of DCN. Salubrinal partially inhibited death of DCN, indicating that ER stress caused death of DCN but other pathways such as the mitochondrial pathway also contributed to death of DCN. WB analysis demonstrated a significant increase in active p-EIF2α, ATF-4, CHOP and Caspase-3 in tunicamycin, thapsigargin and 6OHDA induced SH-SY5Y cells (Hara et al 2011). 6OHDA triggered a higher elevation in Caspase activity in cells compared to cells that were treated with tunicamycin or thapsigargin. A significant decrease was found in Caspase-3, p-EIF2α and CHOP in 6OHDA, tunicamycin and thapsigargin cells that had been treated with salubrinal (Hara et al 2011). Research by Chinta et al (2009) demonstrated that paraquat induced ER mediated death of DCN caused through oxidative stress. Oxidative stress contributed to the misfolding and impairment of proteins leading to initiation of ER stress. IF and WB analysis revealed the ability of salubrinal to protect neurons that had been treated with paraquat. Salubrinal had significantly reduced p-eIF2α, CHOP, XBP-1 and Caspase activation in paraquat induced N27 dopaminergic cell line. Furthermore, work by Jiang et al (2010) demonstrated that salubrinal had prevented ER stress mediated apoptosis, alongside accumulation and aggregation of α-synuclein in sodium butyrate treated PD cells. Sodium butyrate promoted accumulation of aggregated α-synuclein in SHSY5Y cells resulting in activation of Caspase-3. WB analysis showed high levels of cleaved Caspase-3 after 24 hours and IF analysis revealed aggregated deposits of incorrectly folded proteins in sodium butyrate treated cells. WB analysis demonstrated that salubrinal had suppressed death of sodium butyrate treated cells.

6.1 Determining the Relevance of PERK Associated ER stress Pathway in 6OHDA-treated dDCN

Chapter 5 had indicated that classical NFκB pathway plays a vital role in initiating death of 6OHDA-treated dDCN (Chapter 5 Figure 5.1-Figure 5.4 and Figure 5.9-Figure 5.13). In addition, the results had demonstrated that activation of Caspases-2 and -8 are dependent upon NFκB activation by 6OHDA in dDCN, indicating that NFκB is acting upstream to Caspases-8 and-2 (Chapter 5 Figure 5.15- Figure 5.31). It was also found that NFκB triggered activation of Caspases-2 and-8 through different routes and that Caspases-8 and-2 are not dependent, nor enhance each other's activation (Chapter 5 Figure 5.32 and Figure 5.43). In contrast, NFκB pathway did not affect activation of Caspase-4 in 6OHDA-treated dDCN and so the next aim was to determine how Caspase-4 is activated (Figure 5.43). It was also found that blocking classical NFκB pathway did not completely promote survival of 6OHDA dDCN and death of treated dDCN was still occurring (Chapter 5 Figure 5.9- Figure 5.11 and Figure 5.41-Figure 5.42). Similar to NFκB, the role of ER stress in cells is controversial as activation of PERK can promote or prevent death of DCN (Oakes and Papa 2014, Pereira 2013, Matus et al 2008, Todd et al 2008, Hetz 2012, Sano and Reed 2013).

Results from the Chapter 4 had shown the potential involvement of ER stress in apoptotic death of 6OHDA-treated dDCN (Chapter 4 Figure 4.17- Figure 4.19). The next aim was to explore the potential influence of PERK ER stress on Caspases-2,-4 and -8 in apoptotic death of 6OHDA-treated dDCN. At present there is no research that has explored the potential link between PERK ER stress and NFκB in DCN. The following Chapter investigates if NFκB classical pathway and PERK ER stress pathway encourages up regulation or have any impact on each other's pathway in treated 6OHDA dDCN.

Main aim: To determine if 6OHDA triggered activation of Caspases-2,-4 and -8 in PERK ER stress pathway resulting in apoptotic death of dDCN.

6.2.1 Determining if activities of PERK and Caspases-2,-4 and -8 in 6OHDA-treated dDCN

Similar methods were used as described in Chapter 5 to determine the influence of PERK pathway on each specific Caspase. Optimisation of salubrinal (Santa Cruz Biotechnology Heidelberg Germany) dose was established via treating 6OHDA dDCN with different concentrations of salubrinal (30μM - 120μM salubrinal) for 2 hour, after which fresh media was replaced and cells were left to recover overnight. dDCN and 6OHDA were cultured and treated 30μM salubrinal with different combinations of specific Caspase inhibitors such as 20μM zVDVADfmk (Merck Chemicals Nottingham UK), 20μM zLEVDfmk (Merck Chemicals Nottingham UK) or 80μM zIETDfmk (Merck Chemicals Nottingham UK) for 2 hours, after which fresh media was replaced and cells were left to recover overnight. Cells viability was determined and measured using MTT assay and statistical analysis as described in section 2.5.4.

To determine the potential link between NFκB and PERK ER mediated death of 6OHDA dDCN, cells were treated either with 30μM salubrinal, 70μM IKK and 50μM zVADfmk before measuring cell viability using MTT assay. ANOVA and T test ($p<0.05$) were performed as described in Chapter 2 Section 2.5.4. A more detailed account of the reagents used can be found in Chapter 2 Section 2.2 and Appendix 1.

6.2.2 Investigating if salubrinal can inhibit expression of active Caspases-2,-4 and -8 in 6OHDA-treated dDCN using IF analysis

dDCN and 6OHDA were cultured and treated 30μM salubrinal and specific Caspase inhibitors such as 20μM zVDVADfmk, 20μM zLEVDfmk or 80μM zIETDfmk for 2 hours, after which fresh media was replaced and cells were left to recover overnight. Cells were fixed with 4% parformaldehyde for 15 minutes and were washed with cold PBS. Subsequently, cells were treated with Triton X (10 minutes) and blocked with 10% goat serum for 40 minutes prior to overnight incubation primary antibodies Anti-TH (1:1500, Millipore Hertfordshire UK), active Anti-Caspase-2 (1:2000, Abcam Cambridge UK), active Anti-Caspase-4 (1:4000, Abcam UK), active Anti-Caspase-8 (1:2000, Abcam Cambridge UK) at 4°C. The

membrane was incubated with secondary antibodies Donkey-Anti-Mouse IgG FITC (1:500, Millipore Hertfordshire UK), Goat-Anti-Rabbit IgG Rhodamine (1:2500, Millipore Hertfordshire UK) for two hours at RT. Cells was mounted using vectorshield mounting medium and were viewed under a Meiji fluorescent microscope prior to statistical analysis as described in Chapter 2 Section 2.5.2. A more detailed account of the reagents used can be found in Chapter 2 Section 2.1 -Section 2.2 and Appendix 1.

6.2.3 Determining if salubrinal can inhibit active Caspases-2,-4 and -8 in PERK pathway in 6OHDA dDCN using WB analysis

dDCN were grown and treated 30μM salubrinal, 100μM 6OHDA, 100μM 6OHDA and 30μM salubrinal for 2 hours, after which the fresh media was replaced and cells were left to recover overnight in 37 ^{o}C CO_2 incubator. Cells were lysed and protein concentration was measured using the BCA kit. Fifty micrograms protein was loaded on 12% gel prior to SDS PAGE at 200 volts for 40 minutes, followed by immunoblotting on PVDF membrane. The membrane was blocked with 1% skimmed milk for an hour followed by incubation with primary antibodies, active Anti-Caspase-2 (1:2500, Millipore Hertfordshire UK), active Anti-Caspase-4 (1:300, Abcam Cambridge UK), and active Anti-Caspase-8 (1:1000, Millipore Hertfordshire UK) for overnight at 4^{o}C. The membranes were washed with PBST and incubated with Goat-Anti-Rabbit HRP (1:1000, Millipore Hertfordshire UK) for an hour at RT. After washing the membranes with PBST, ECL system was employed and immunoblots bands were quantified with a densitometer scanner. Statistical analysis was carried out at $p<0.05$ using student T test followed by strip and reprobe with the house keeping gene GAPDH (Chapter 2 Section 2.3.4 and Chapter 2 Section 2.3.5 correspondingly). Five independent experiments were performed for each treatment. A more detailed account of the reagents used can be found in Chapter 2 Section 2.1 - Section 2.2 and Appendix 1.

To determine if 6OHDA can trigger ER stress mediated apoptotic death in dDCN, the specific PERK inhibitor, salubrinal was used in untreated and 6OHDA-treated dDCN. Salubrinal was used to determine if it can increase cell survival or promote cell death via the ER stress pathway on 6OHDA-treated dDCN. Salubrinal prevented apoptotic death and promoted survival 6OHDA-treated dDCN (72% cell survival, $p<0.01$), compared to 6OHDA-treated dDCN, indicating that 6OHDA triggers death of dDCN, through an ER stress pathway. More specifically, 6OHDA activates PERK pathway leading to death of dDCN (Figure 6.1).

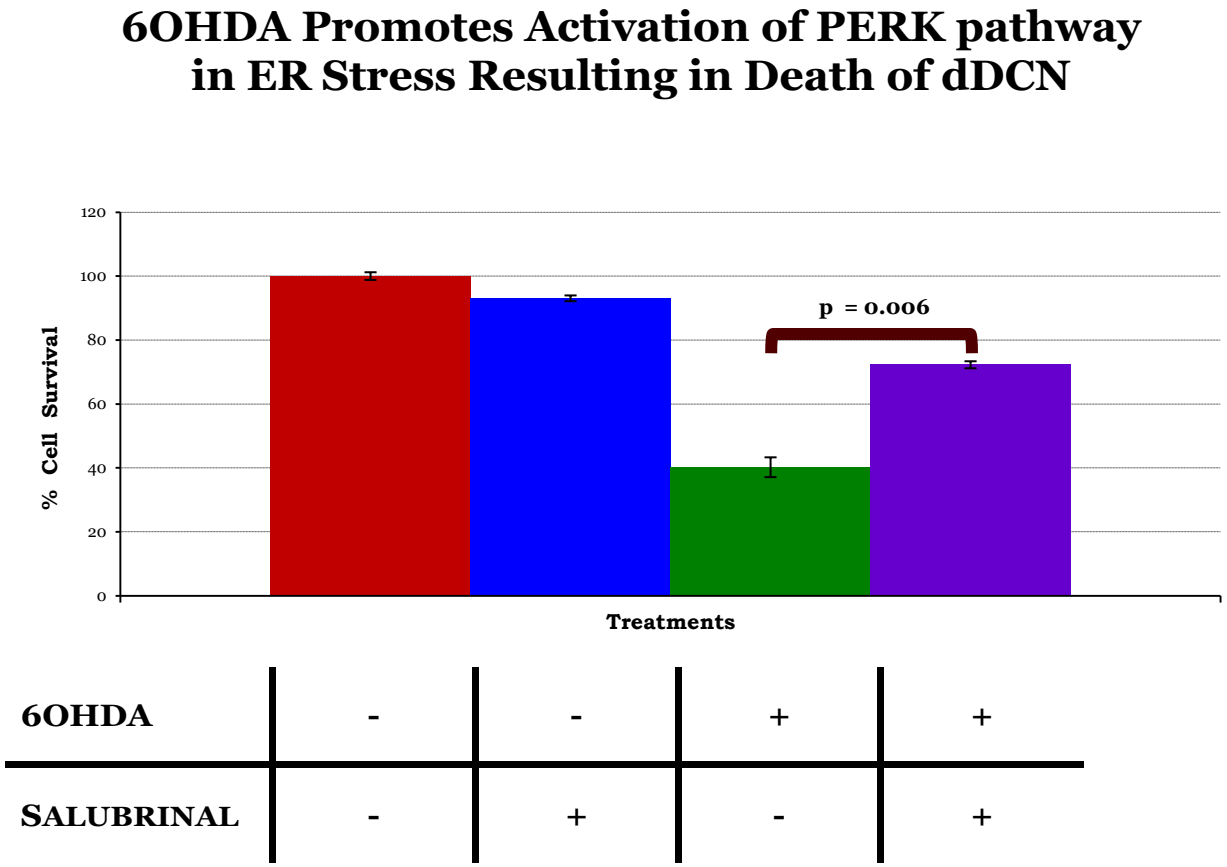

Figure 6.1 : Determining the effect of salubrinal in 6OHDA-treated dDCN

Salubrinal promoted survival of cells compared to cells that had been treated with 6OHDA by inhibiting the ER stress pathway, indicating the involvement of PERK pathway in dDCN. Proportion of cells surviving was determined by MTT absorbance at 570nm. Means of three experiments ± SEM shown. Table of values and statistical analysis can be found in Figure 6.2, Appendix 6.

To confirm if ER stress is not the only pathway which is causing death to 6OHDA-treated cells, different concentrations of salubrinal were used (30µM - 120µM). The results indicate that increasing the concentration of salubrinal did not completely inhibit death of 6OHDA-treated dDCN, strongly indicating that a second cell signalling pathway is involved which causes death of 6OHDA-treated dDCN (Figure 6.3).

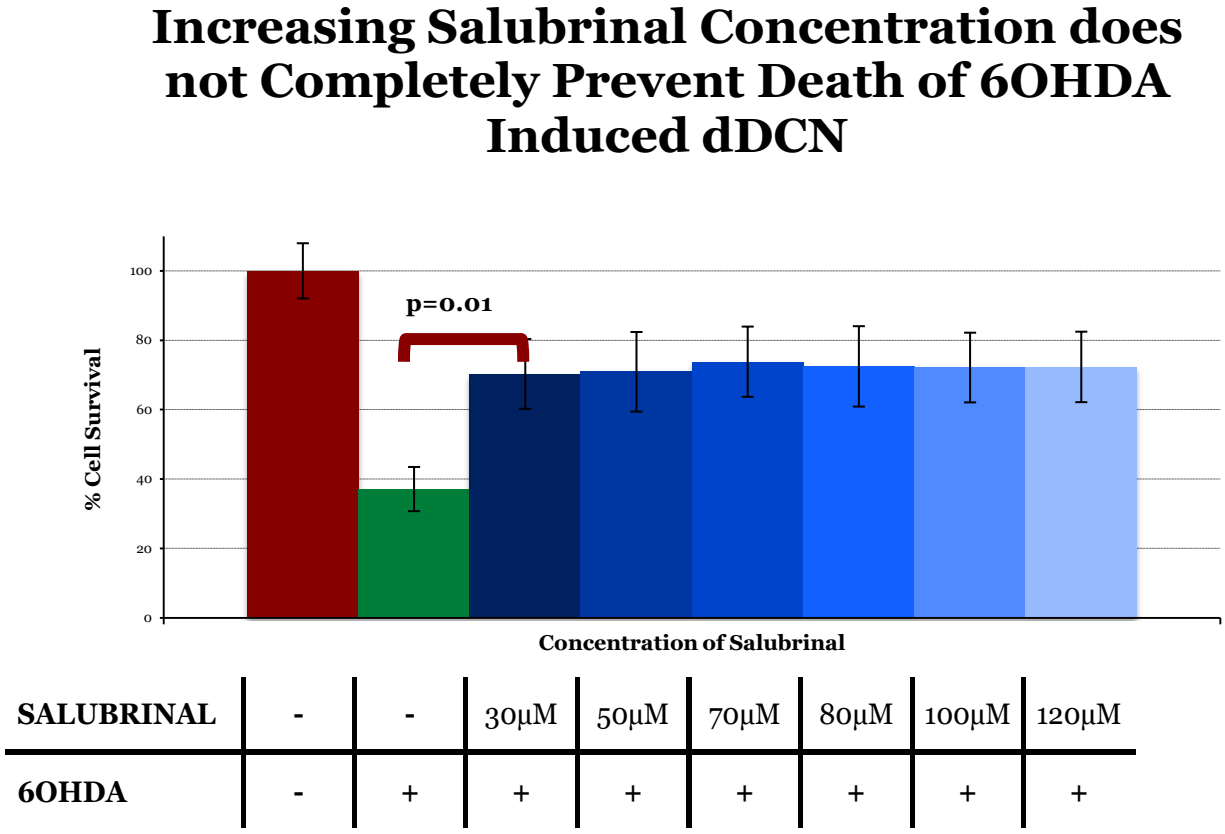

Figure 6.3 : Determining if further survival of 6OHDA-treated cells can occur by increasing the concentration of salubrinal

Graph shows similar levels of survival of 6OHDA-treated cells occur at different salubrinal concentrations (30µM - 120µM). A gradual increase in salubrinal concentration did not provide further survival of 6OHDA-treated dDCN. Proportion of cells surviving was determined by MTT absorbance at 570nm. Means of three experiments ± SEM shown. Table of values and statistical analysis can be found in Figure 6.4, Appendix 6.

To determine if suppression of UPR prevents activation of Caspases in 6OHDA dDCN, the broad Caspase inhibitor zVADfmk was used. In addition, the combination of zVADfmk and salubrinal was used to determine if the combination can provide more protection and decrease overall cell death of 6OHDA-treated dDCN (Figure 6.5). The combination of zVADfmk and salubrinal promoted further survival of 6OHDA-treated dDCN (91% cell survival) compared to using only zVADfmk (56% cell survival) or salubrinal (78% cell survival) on its own. The additional survival of treated dDCN when using both inhibitors indicated that ER stress is not the only pathway that is causing apoptotic death of dDCN. Furthermore, the results suggest that Caspase activation is still occurring even when UPR is inhibited in 6OHDA-treated dDCN (Figure 6.5).

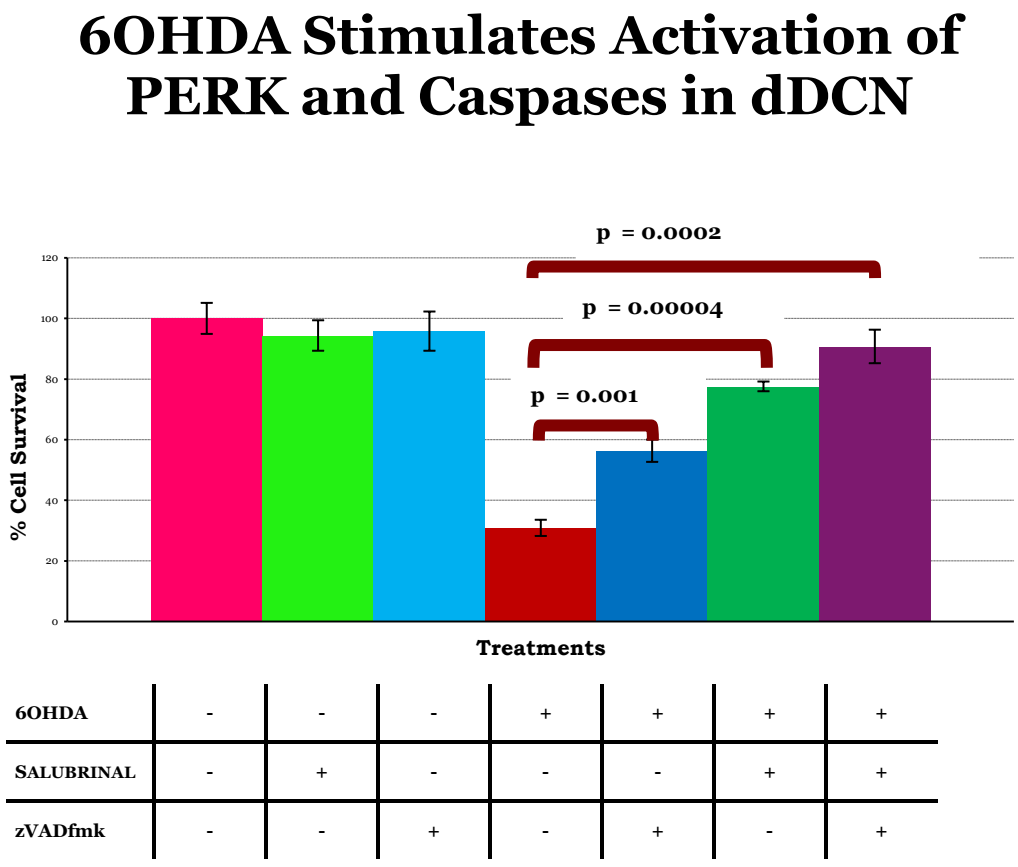

Figure 6.5: Determining the effect of salubrinal and zVADfmk on 6OHDA-treated dDCN

A significant increase in survival was determined in cells that had been treated 6OHDA +salubrinal+ zVADfmk treated dDCN (91% cell survival $p < 0.01$). Proportion of cells surviving was determined by MTT absorbance at 570nm. Means of three experiments ± SEM shown. Table of values and statistical analysis can be found in Figure 6.6, Appendix 6.

Chapter 5 had shown 6OHDA triggered Caspase-2 activation in dDCN, via NFκB classical pathway. The next aim was to determine if PERK pathway influences activity of Caspase-2 in 6OHDA-treated dDCN. To achieve this aim, zVDVADfmk and salubrinal inhibitor were used separately and together in 6OHDA-treated dDCN. The results demonstrated that 6OHDA dDCN that were treated with zVDVADfmk, salubrinal or both salubrinal and zVDVADfmk had similar levels of cell survival, suggesting 6OHDA triggered PERK and Caspase-2 activation via the same pathway in dDCN (Figure 6.7).

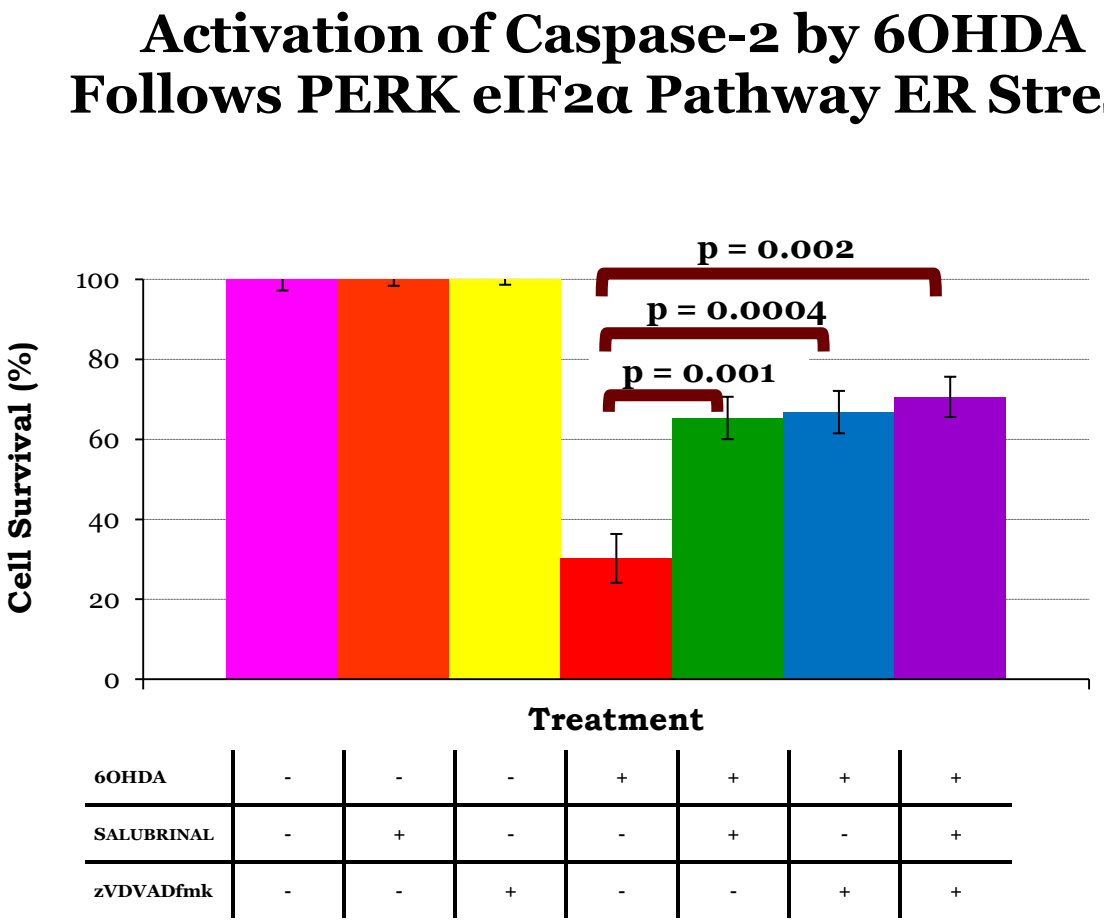

Figure 6.7 : Caspase-2 is active in ER stress pathway in 6OHDA-treated dDCN

A 65% cell survival rate was found in salubrinal treated dDCN, whereas 67% cell survival was measured in zVDVADfmk treated dDCN. A 71% cell survival was determined in 6OHDA+ salubrinal+ zVDVADfmk treated dDCN, suggesting no additional benefit of targeting both PERK ER Stress and Caspase-2. Proportion of cells surviving was determined by MTT absorbance at 570nm. Means of three experiments ± SEM shown. Table of values and statistical analysis can be found in Figure 6.8, Appendix 6.

A closer examination of the findings revealed no additional benefit in survival of 6OHDA-treated dDCN when both inhibitors were used. The results strongly signify that using salubrinal inhibitor can inhibit Caspase-2 activity and so zVDVADfmk is not required, suggesting that Caspase-2 is active in PERK ER stress pathway in dDCN (Figure 6.9).

	Treatment 1	Treatment 2	Treatment 3	Treatment 4	
	6OHDA	6OHDA SALUBRINAL	6OHDA zVDVADfmk	6OHDA SALUBRINAL zVDVADfmk	p-value obtained
Comparison 1	+	+	-	-	0.001
Comparison 2	+	-	+	-	0.0004
Comparison 3	+	-	-	+	0.002
Comparison 4	-	+	+	-	0.716
Comparison 5	-	+	-	+	0.199
Comparison 6	-	-	+	+	0.257

Figure 6.9 : Caspase-2 is active in ER stress mediated death of 6OHDA-treated dDCN

Suppressing Caspase-2 pathway did not provide more survival of 6OHDA dDCN, illustrating that Caspase-2 and PERK are one pathway. The survival of 6OHDA dDCN did not significantly increase when zVDVADfmk was added with salubrinal, demonstrating that zVDVADfmk does not have an additional effect to slow death and promote cell survival (Comparison 6 $p > 0.05$). No additional effect in cell survival was found when salubrinal was added to zVDVADfmk, indicating that PERK is following the same pathway as Caspase-2 in 6OHDA dDCN (Comparison 5 $p > 0.05$). Furthermore, the use of the salubrinal inhibitor can be used to suppress both Caspase-2 and PERK activity in 6OHDA dDCN. Proportion of cells surviving was determined by MTT absorbance at 570nm. Means of three experiments ± SEM shown. Table of values and statistical analysis can be found in Figure 6.8, Appendix 6.

Co-localisation studies were carried out to investigate if suppression of Caspase-2 activity can inhibit PERK activation in dDCN. Caspase-2 was found active in only in untreated and 6OHDA-treated dDCN (Figure 6.10). Active Caspase-2 was present in a greater proportion of TH-positive cells following 6OHDA treatment, indicating that 6OHDA triggers Caspase-2 in dDCN. Furthermore, active Caspase-2 was absent in salubrinal treated, zVDVADfmk treated, 6OHDA+salubrinal treated, 6OHDA+zVDVADfmk treated, 6OHDA+salubrinal+zVDVADfmk treated dDCN. This indicated that activation of Caspase-2 is dependent upon stimulation of PERK pathway resulting in death of dDCN via ER stress.

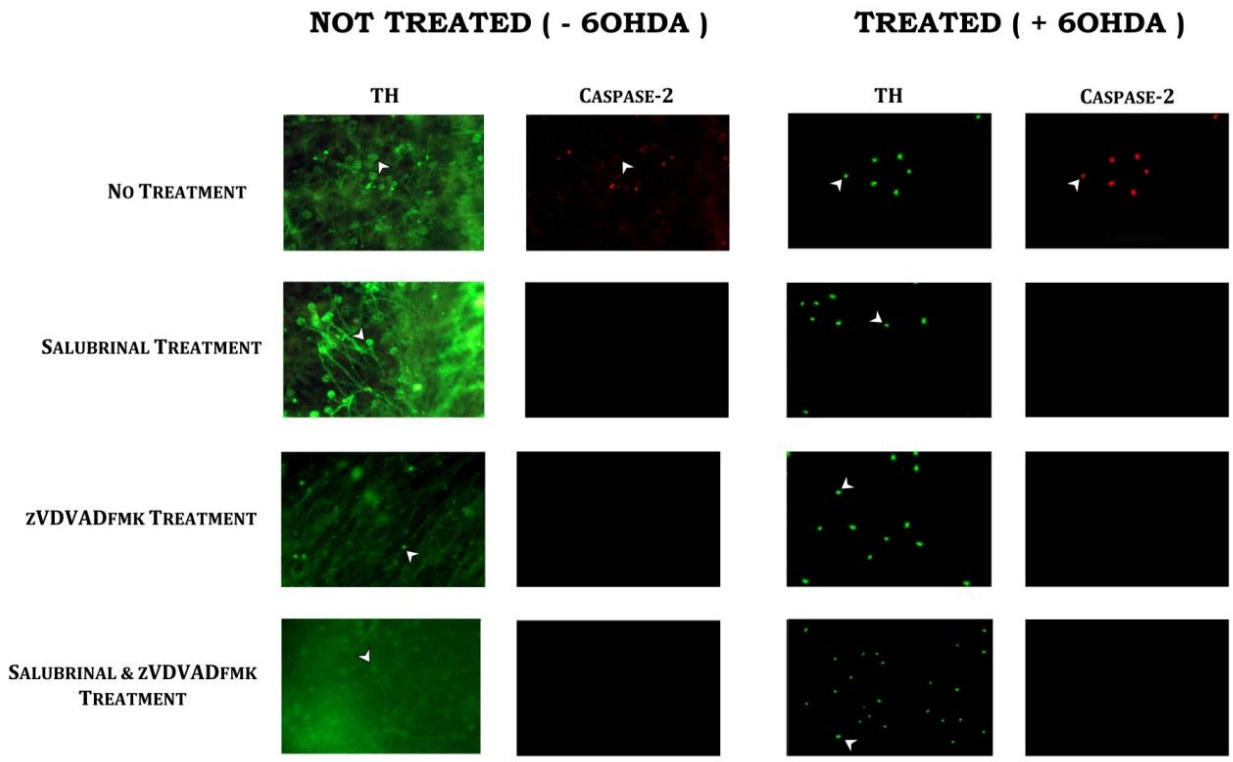

Figure 6.10 : Salubrinal and zVDVADfmk suppressed active Caspase-2 in 6OHDA-treated dDCN

TH was present in untreated and 6OHDA-treated dDCN (green). A loss of dendrites was observed in TH positive dDCN that had been exposed to dDCN. Active Caspase-2 (red stain) was present in untreated and 6OHDA-treated TH positive dDCN (red). There were more Caspase-2 positive cells present in 6OHDA-treated dDCN, compared to untreated dDCN. Active Caspase-2 was absent in salubrinal treated, 6OHDA+salubrinal treated dDCN. This indicates that inhibiting the PERK pathway

can suppress Caspase-2 activity in dDCN. Stimulation of Caspase-2 is dependent on activation of PERK ER stress pathway in dDCN. Furthermore, active Caspase-2 was absent in zVDVADfmk treated, 6OHDA+zVDVADfmk treated dDCN, signifying that Caspase-2 activity is successfully suppressed in dDCN when using Caspase-2 inhibitor. Active Caspase-2 was not detected in salubrinal+ zVDVADfmk treated, 6OHDA + salubrinal + zVDVADfmk treated dDCN. Caspase-2 activation can be suppressed by directly inhibiting Caspase-2 or via inhibiting PERK ER stress pathway in untreated and 6OHDA-treated dDCN. Positive staining for cell bodies (White Arrow) in untreated (- 6OHDA) and treated (+ 6OHDA) dDCN. Table of values can be found in Figure 6.11, Appendix 6.

To confirm if salubrinal can completely suppress Caspase-2 activation of treated dDCN WB analysis was carried out (Figure 6.12). Active Caspase-2 was absent in salubrinal treated, 6OHDA+salubrinal treated treated dDCN, indicating that 6OHDA triggers activation of Caspase-2 via PERK pathway in ER mediated death of dDCN.

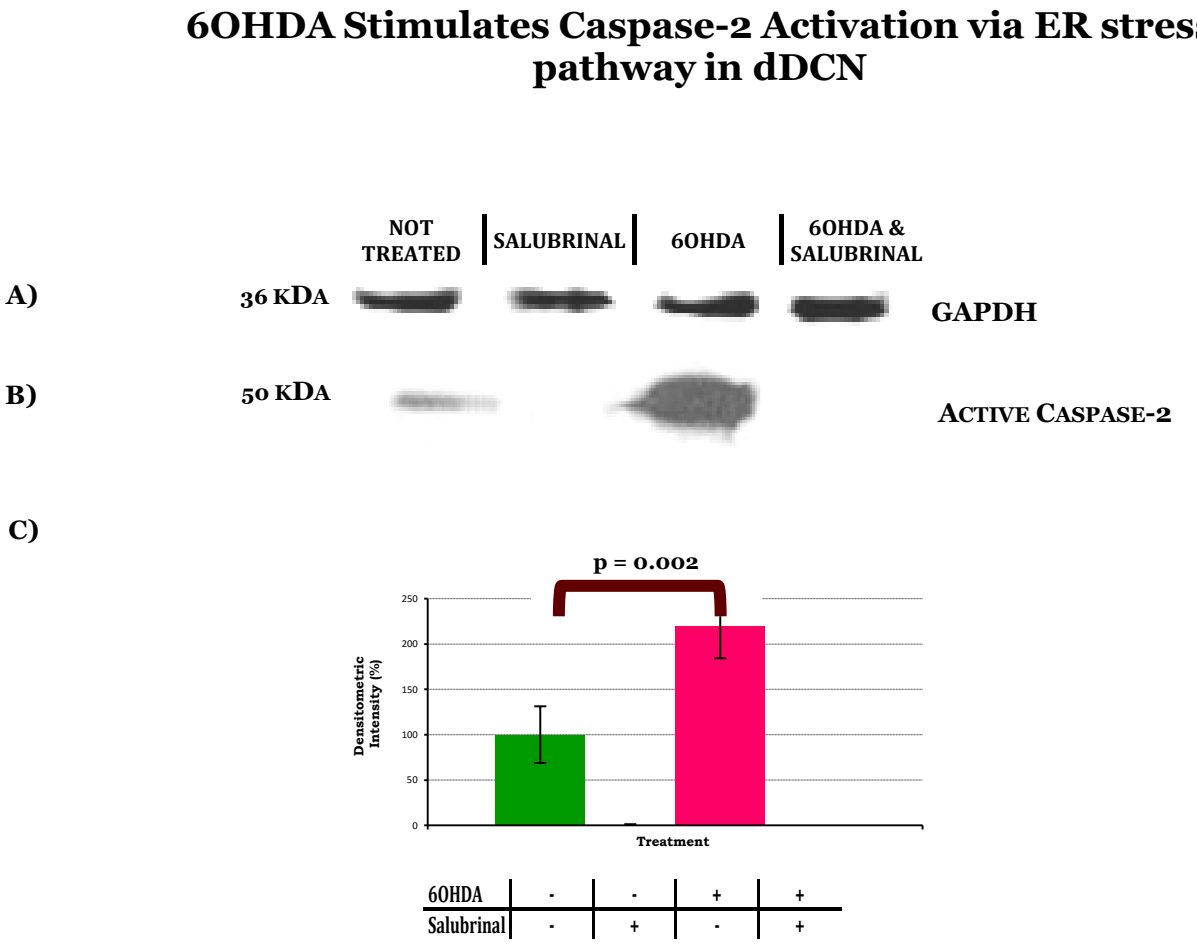

Figure 6.12 : Caspase-2 is suppressed by salubrinal in 6OHDA-treated dDCN

A) Illustrative example of GAPDH in untreated, salubrinal, 6OHDA, salubrinal + 6OHDA treated dDCN.

B) Illustrative example of active Caspase-2 in untreated, salubrinal, 6OHDA, salubrinal + 6OHDA treated dDCN.

C) Quantitatively, there was an increase in active Caspase-2 detected in 6OHDA-treated dDCN, compared to untreated dDCN ($p<0.05$). The absence of active Caspase-2 in salubrinal treated and 6OHDA+salubrinal treated dDCN, suggest that Caspase-2 activity is dependent upon PERK pathway. Means of five experiments ± SEM shown. Table of densitometry values and statistical analysis can be found in Figure 6.13, Appendix 6.

Recent research has shown that Caspase-4 is involved in ER mediated death of DCN. It was important to determine if Caspase-4 was involved in ER mediated death of 6OHDA-treated dDCN. The findings illustrated that further cell survival was achieved in 6OHDA+salubrinal+zLEVDfmk treated dDCN, indicating 6OHDA triggers Caspase-4 and PERK activation via different mechanisms dDCN (Figure 6.14).

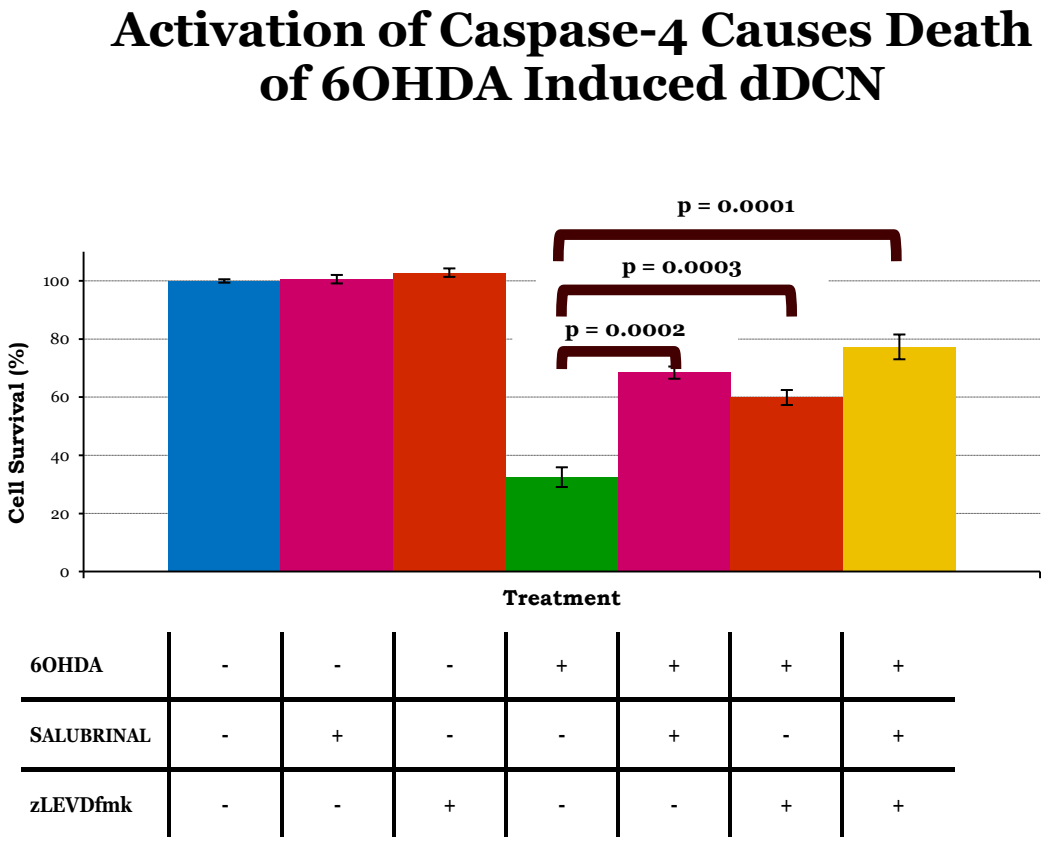

Figure 6.14 : 6OHDA triggered Caspase-4 activity in dDCN

A 68% cell survival was determined in 6OHDA+ salubrinal treated dDCN, showing 6OHDA triggered PERK pathway. A 60% cell survival was measured in 6OHDA+ zLEVDfmk treated dDCN, demonstrating 6OHDA triggered Caspase-4 activation in dDCN. A further 77% survival of 6OHDA+ salubrinal + zLEVDfmk treated dDCN, indicating that PERK pathway does not influence Caspase-4 activation in dDCN. zLEVDfmk in combination with salubrinal promoted further survival of 6OHDA-treated dDCN, indicating an additional benefit of targeting ER stress pathway and Caspase-4. Proportion of cells surviving was determined by MTT absorbance at 570nm. Means of three experiments ± SEM shown. Table of values and statistical analysis can be found in Figure 6.15, Appendix 6.

The aim was to determine if Caspase-4 activity is influenced by PERK ER stress pathway in 6OHDA dDCN, via use of salubrinal and zLEVDfmk inhibitors (Figure 6.16). The combination of salubrinal and Caspase-4 inhibitor provided further cell survival, suggesting that Caspase-4 is not following PERK pathway of ER stress and could be activated by another pathway, resulting in death of dDCN. Suppressing Caspase-4 pathway in addition to PERK pathway had an added effect in more cells surviving, indicating that there are two pathways.

	Treatment 1	Treatment 2	Treatment 3	Treatment 4	
	6OHDA	6OHDA SALUBRINAL	6OHDA zLEVDfmk	6OHDA SALUBRINAL zLEVDfmk	p-value obtained
Comparison 1	+	+	-	-	**0.0002**
Comparison 2	+	-	+	-	**0.0003**
Comparison 3	+	-	-	+	**0.0001**
Comparison 4	-	+	+	-	**0.007**
Comparison 5	-	+	-	+	**0.004**
Comparison 6	-	-	+	+	**0.001**

Figure 6.16 : Activation of Caspase-4 is independent of PERK pathway in 6OHDA dDCN.

Survival of 6OHDA dDCN increased when salubrinal was added to zLEVDfmk, indicating that PERK ER stress pathway does not influence stimulation of Caspase-4 in 6OHDA-treated dDCN (comparison 5 $p<0.01$). zLEVDfmk inhibited Caspase-4 activity promoting more survival of 6OHDA dDCN. Further cell survival of 6OHDA dDCN, was determined when zLEVDfmk was added with salubrinal (Comparison 6 $p<0.01$).The additional effect of more cells survival when Caspase-4 inhibitor and PERK inhibitor are combined indicates that there are two pathways that are contributing to death of 6OHDA dDCN. Furthermore, both inhibitors are required to be used to suppress both pathways so more cell survival can be achieved. Proportion of cells surviving was determined by MTT absorbance at 570nm. Means of three experiments ± SEM shown. Table of values and statistical analysis can be found in Figure 6.15, Appendix 6.

Double IF analysis was carried out to determine the presence and absence of Caspase-4 in untreated and 6OHDA-treated dDCN (Figure 6.17). Caspase-4 was present in untreated, salubrinal treated, 6OHDA-treated, 6OHDA+salubrinal treated dDCN, demonstrating that salubrinal did not suppress Caspase-4 activation in dDCN. This puts forward the notion that Caspase-4 is not following the PERK pathway of ER mediated death of dDCN, indicating that another pathway is causing death of dDCN via Caspase-4 activation. Furthermore, active Caspase-4 was absent in zLEVDfmk treated, 6OHDA+zLEVDfmk treated, 6OHDA+salubrinal+ zLEVDfmk treated dDCN. This shows that both Caspase-4 inhibitor and salubrinal need to be used to minimise death.

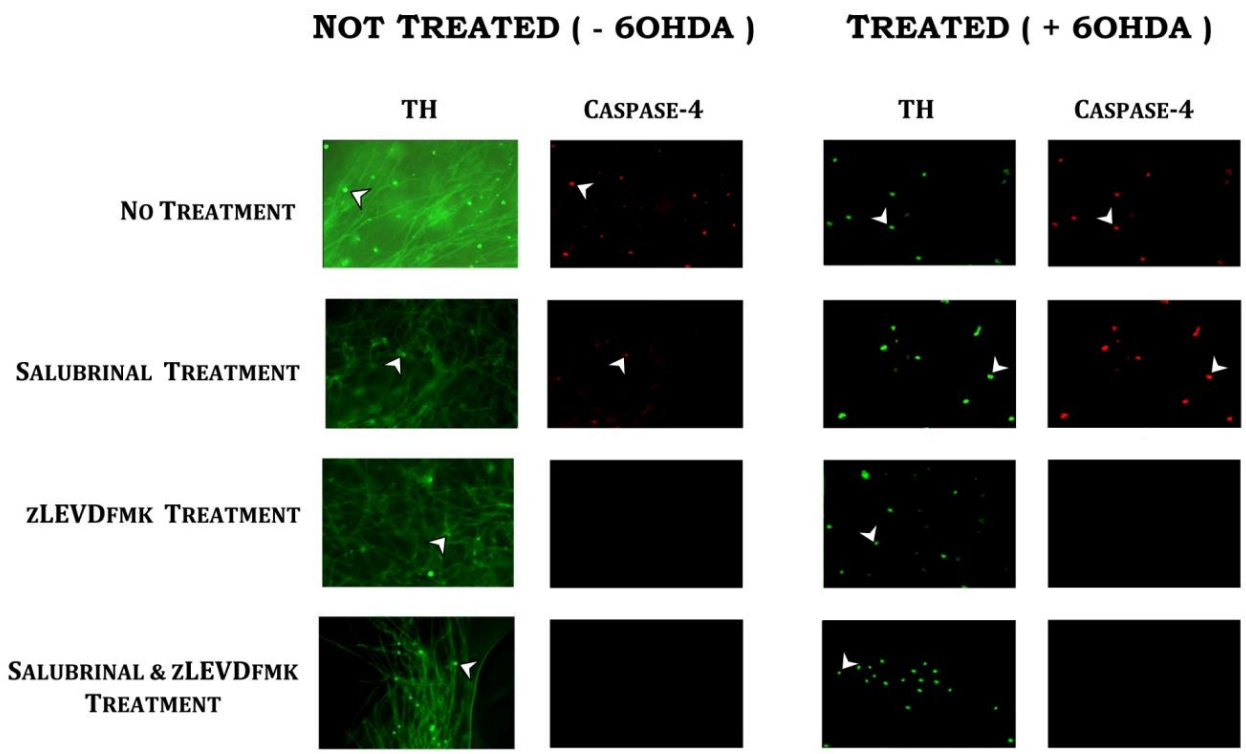

Figure 6.17: Salubrinal does not inhibit active Caspase-4 in 6OHDA-treated dDCN

Presence of TH positive cells was observed untreated and 6OHDA-treated dDCN (green).
Active Caspase-4 was present in the same TH positive cells of untreated and 6OHDA-treated dDCN, signifying that Caspase-4 is actively present in dDCN (red). There were more active Caspase-4 positive cells in present in TH positive 6OHDA-treated dDCN, when compared to TH positive untreated (-6OHDA) dDCN, indicating 6OHDA enhanced further activation of Caspase-4 in dDCN.

Active Caspase-4 detected in salubrinal treated, 6OHDA+salubrinal treated dDCN. This indicates that inhibiting the PERK ER stress pathway does not influence Caspase-4 activity in dDCN. Stimulation of Caspase-4 is independent on activation of PERK pathway in dDCN. In contrast, active Caspase-4 was absent in zLEVDfmk treated, 6OHDA+zLEVDfmk treated dDCN, signifying that Caspase-4 activity is successfully suppressed in dDCN when using Caspase-4 competitive irreversible inhibitor. Caspase-4 was not found in salubrinal+ zLEVDfmk treated, 6OHDA+salubrinal +zLEVDfmk treated dDCN. The Caspase-4 inhibitor, zLEVDfmk had directly suppressed Caspase-4 activation in untreated and 6OHDA-treated dDCN. Positive staining for cell bodies (White Arrow) in untreated (- 6OHDA) and treated (+ 6OHDA) dDCN. Table of values can be found in Figure 6.18, Appendix 6.

WB analysis was carried out to confirm if salubrinal could not suppress Caspase-4 activity in 6OHDA-treated dDCN (Figure 6.19). Active Caspase-4 was present in untreated, salubrinal treated, 6OHDA-treated, 6OHDA+salubrinal treated dDCN. An increase in the amount of active Caspase-4 was detected in 6OHDA-treated dDCN, compared to untreated dDCN. The ineffectiveness of salubrinal against activation of Caspase-4 further supports the notion that Caspase-4 is independent of ER mediated death of 6OHDA-treated dDCN. 6OHDA triggered Caspase-4 activation, but this was achieved, through a different route and not via PERK pathway.

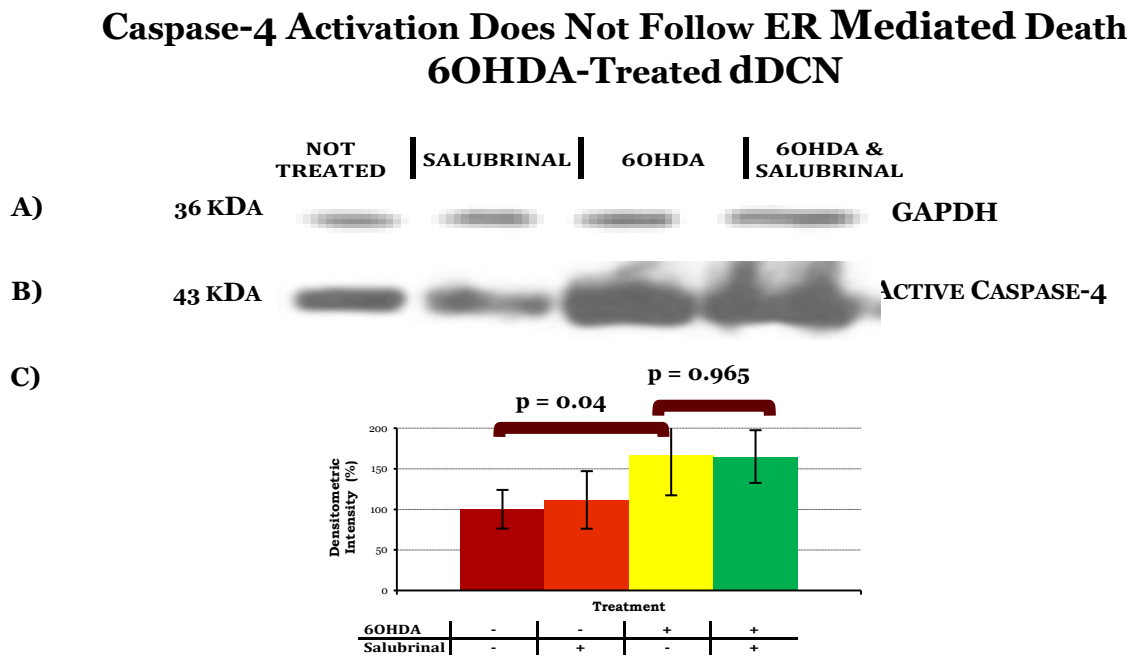

Figure 6.19 : PERK pathway does not influence Caspase-4 activation in 6OHDA dDCN

A) Illustrative example of GAPDH in untreated, salubrinal, 6OHDA, salubrinal + 6OHDA treated dDCN.

B) Illustrative example of active Caspase-4 in untreated, salubrinal, 6OHDA, salubrinal + 6OHDA treated dDCN.

C) Quantitatively, a 67% increase in active Caspase-4 was detected in 6OHDA-treated dDCN, compared to untreated dDCN ($p<0.05$). Salubrinal neither prevented nor reduced the amount of active Caspase-4 in present in salubrinal treated and 6OHDA+salubrinal treated dDCN ($p>0.05$), indicating that PERK pathway does not influence Caspase-4 stimulation in 6OHDA-treated dDCN. Means of five experiments ± SEM shown. Table of densitometry values and statistical analysis can be found in Figure 6.20, Appendix 6.

The involvement of Caspases-2,-4 and PERK activity was further determined in 6OHDA-treated dDCN, using different combinations of zVDVADfmk, zLEVDfmk and salubrinal (Figure 6.19). ANOVA analysis indicated a significant difference in survival of 6OHDA dDCN that were treated with zVDVADfmk, zLEVDfmk and salubrinal ($p < 0.01$, Figure 6.21, Appendix 6). Subsequent T tests were used to identify key inhibitors that had the most effect in promoting survival and slowing death of 6OHDA dDCN.

No additional effect in cell survival was measured in 6OHDA +zVDVADfmk +salubrinal treated dDCN, suggesting that activation of Caspase-2 is completely dependent on PERK and suppression of PERK ER stress pathway will inhibit Caspase-2 activation in dDCN. There was no significant difference to slow death and promote cell survival in 6OHDA+ zVDVADfmk +salubrinal dDCN, indicating that the use of salubrinal inhibitor can suppress both PERK and Caspase- activity in dDCN($p > 0.01$, Figure 6.22).

In comparison, additional cell survival of 6OHDA dDCN was determined when salubrinal was added with zLEVDfmk, demonstrating that salubrinal has an additional effect to slow death and promote cell survival. Further cell survival of 6OHDA+zLEVDfmk+salubrinal treated dDCN, signifying that both inhibitors can promote further survival and slow death of 6OHDA dDCN, via suppressing two different routes. The additional effect of more cells survival when Caspase-4 inhibitor and PERK inhibitor are combined indicates that there are two pathways that are contributing to death of 6OHDA dDCN ($p < 0.01$, Figure 6.22).

Activation of Caspase-2 but not Caspase-4 follows PERK Pathway of ER stress in 6OHDA induced dDCN

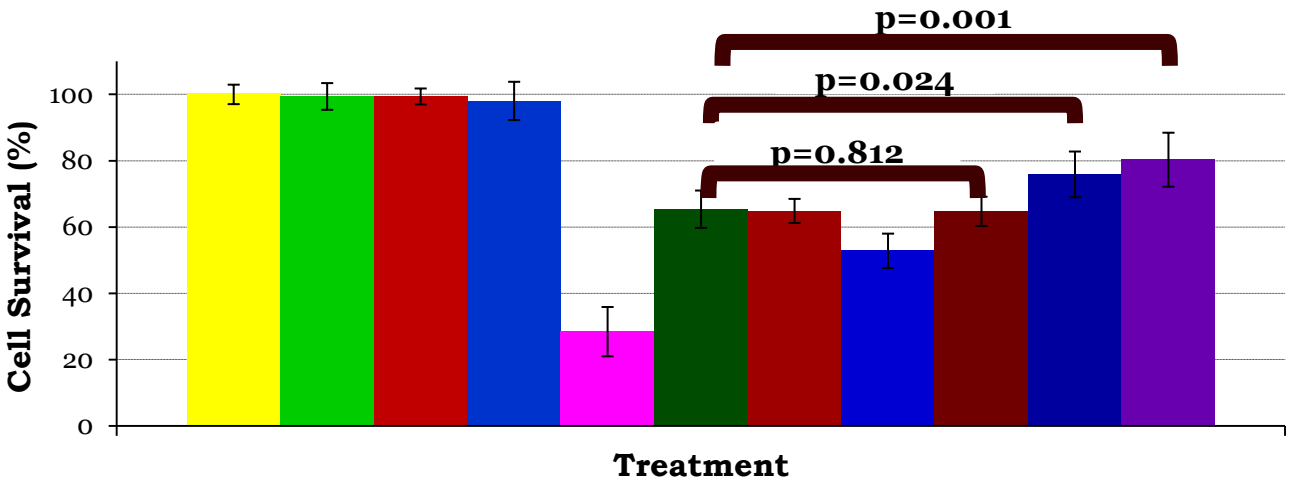

6OHDA	-	-	-	-	+	+	+	+	+	+	+
SALUBRINAL	-	+	-	-	-	+	-	-	+	+	+
zVDVADfmk	-	-	+	-	-	-	+	-	+	-	+
zLEVDfmk	-	-	-	+	-	-	-	+	-	+	+

Figure 6.22 : zLEVDfmk and salubrinal reduced further death of 6OHDA-treated dDCN

6OHDA triggered activation of PERK ER stress, Caspases-2 and -4 in dDCN. Salubrinal suppressed Caspase-2 and PERK pathway of 6OHDA-treated dDCN. A further increase in survival and decreased death was measured in 6OHDA+zLEVDfmk +salubrinal treated dDCN, indicating that Caspase-4 and PERK are separate pathways that are causing apoptotic death of 6OHDA-treated dDCN. Salubrinal and zLEVDfmk protected more cells from death of 6OHDA-treated dDCN, indicating that both these inhibitors are required to suppress two pathways that are causing apoptotic death of 6OHDA dDCN. Proportion of cells surviving was determined by MTT absorbance at 570nm. Means of three experiments ± SEM shown. Table of values and statistical analysis can be found in Figure 6.21, Appendix 6.

A closer examination of Caspase-4 activity in relation to PERK indicated that Caspase-4 is independent on stimulation of PERK pathway (Comparison 9 $p<0.05$ Figure 6.23). The amount cell survival of 6OHDA+salubrinal+zVDVADfmk treated dDCN, compared to 6OHDA+zVDVADfmk treated dDCN (Comparison 10 $p>0.05$), was not statistically significant, indicated activation of Caspase-2 is dependent on PERK pathway. The results demonstrated 6OHDA triggered activation of Caspases-2 and -4 via different pathways. Moreover, further survival of 6OHDA dDCN, was determined when salubrinal was added with zLEVDfmk, demonstrating that both inhibitors are required to be used to suppress pathways, promoting cell survival and slowing death.

	Treatment 1	**Treatment 2**	**Treatment 3**	**Treatment 4**	**Treatment 5**	**Treatment 6**	
	6OHDA SALUBRINAL	**6OHDA zVDVADfmk**	**6OHDA zLEVDfmk**	**6OHDA SALUBRINAL zVDVADfmk**	**6OHDA SALUBRINAL zLEVDfmk**	**6OHDA SALUBRINAL zVDVADfmk zLEVDfmk**	**p-value obtained**
Comparison 1	+	+	-	-	-	-	**0.825**
Comparison 2	+	-	+	-	-	-	**0.002**
Comparison 3	+	-	-	+	-	-	**0.812**
Comparison 4	+	-	-	-	+	-	**0.024**
Comparison 5	+	-	-	-	-	+	**0.001**
Comparison 6	-	-	-	+	+	-	**0.023**
Comparison 7	-	-	-	+	-	+	**0.008**
Comparison 8	-	-	-	-	+	+	**0.181**
Comparison 9	-	-	+	-	+	-	**0.003**
Comparison 10	-	+	-	+	-	-	**0.966**

Figure 6.23: The involvement of Caspases-4 and-2 activity in ER mediated 6OHDA dDCN

The additional effect of more cells survival when Caspases-2 and-4 inhibitors are combined indicates that there Caspase-2 and -4 are two separate pathways that are contributing to death of 6OHDA dDCN (Comparison 6

$p<0.05$). Furthermore, both inhibitors are required to be used to suppress both pathways so more cell survival can be achieved. A further increase in survival and reduction in death of cells was determined in 6OHDA+ zVDVADfmk+ salubrinal treated dDCN, when compared to 6OHDA+ salubrinal +zVDVADfmk+ zLEVDfmk treated dDCN (Comparison 7 $p<0.05$), demonstrating salubrinal + zLEVDfmk need to be used together to successfully inhibit Caspase-4 and PERK activity in 6OHDA-treated dDCN. In contrast, there was no significant difference observed in cell survival in 6OHDA+ zLEVDfmk + salubrinal treated dDCN, when compared to 6OHDA+ salubrinal +zVDVADfmk+ zLEVDfmk treated dDCN (Comparison 8 $p>0.05$), indicating PERK stimulates Caspase-2 activation in 6OHDA-treated dDCN. A greater benefit in cell survival was achieved when salubrinal and zLEVDfmk was used together as it successfully inhibited two separate pathways in 6OHDA-treated dDCN (Comparison 9, $p <0.05$). There was no additional benefit in reducing death of cells when zVDVADfmk and salubrinal inhibitor were combined, indicating that only the salubrinal inhibitor is required to suppress both PERK and Caspase-2 pathway in 6OHDA-treated dDCN (Comparison 10, $p>0.05$). Proportion of cells surviving was determined by MTT absorbance at 570nm. Means of three experiments ± SEM shown. Table of values and statistical analysis can be found in Figure 6.21, Appendix 6.

The results indicated that Caspase-2 is activated by ER mediated death of 6OHDA-treated dDCN (Figure 6.24). Specifically 6OHDA has been able to stimulate Caspase-2 activation through the PERK pathway of ER stress. Surprisingly, Caspase-4 was not active in PERK pathway of ER mediated death of 6OHDA-treated dDCN. This suggests that 6OHDA triggers Caspase-4 activation through a different route which may or may not be ER stress related. Before exploring other potential pathways that could be stimulated by 6OHDA, another Caspase of interest was explored, to determine it's involved in ER mediated death of dDCN.

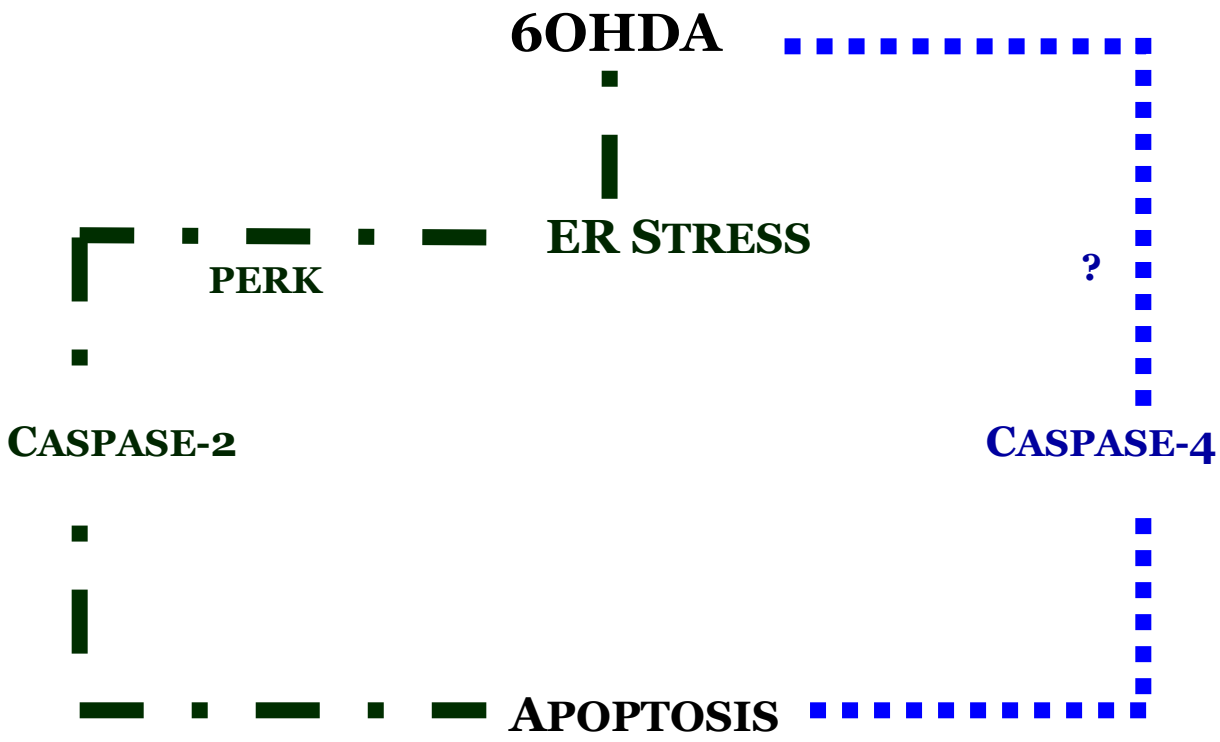

Figure 6.24 : The involvement of Caspases-2 and -4 in ER mediated death of 6OHDA-treated dDCN

Caspase-2 is involved in ER mediated cell death. Salubrinal was able to suppress Caspase-2 activity indicating that Caspase-2 is active in PERK pathway of ER stress. In comparison, Caspase-4 activity was not inhibited by salubrinal, suggesting that Caspase-4 is active in another route (such as ATF, IRE1) of the ER stress pathway or another pathway.

To date research has not investigated if Caspase-8 is associated with ER stress in DCN. It was essential to determine if Caspase-8 is active in the ER mediated death of 6OHDA-treated dDCN, using inhibitors salubrinal and zIETDfmk. The combination of salubrinal and zIETDfmk inhibitor had additional benefit to further increase survival of 6OHDA-treated dDCN, indicated that Caspase-8 and PERK are following different pathways (Figure 6.25)

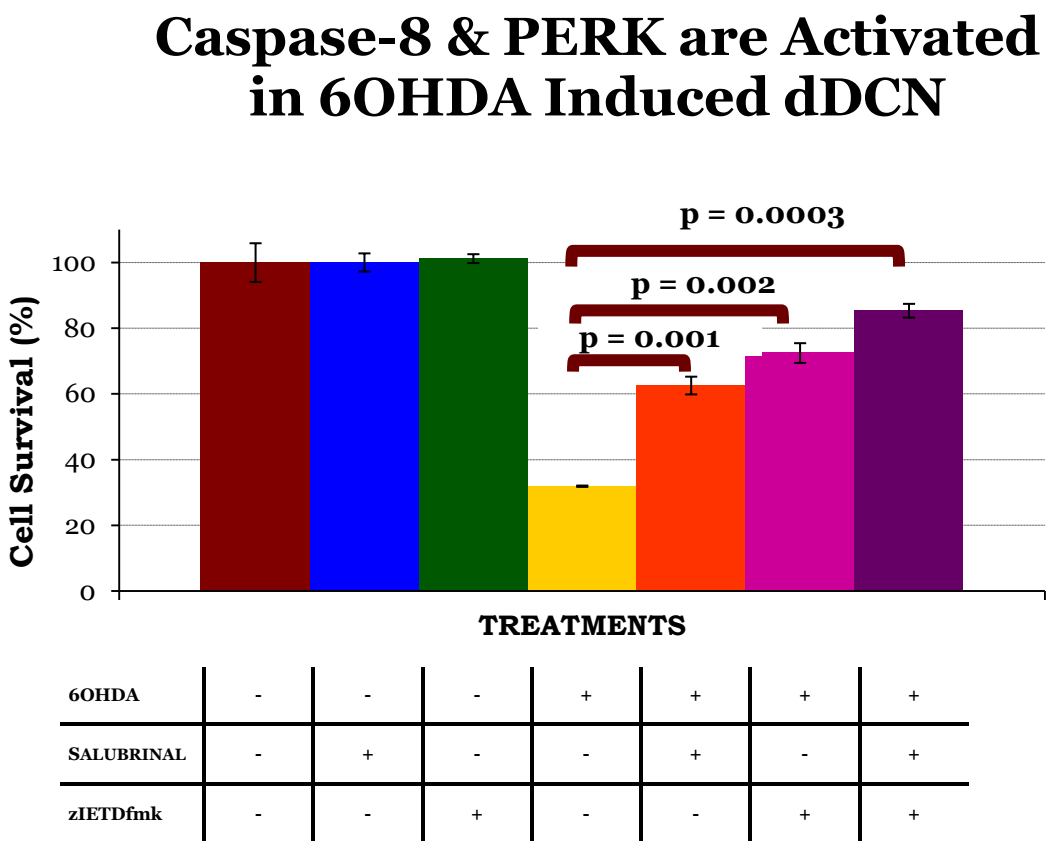

Figure 6.25: 6OHDA triggers Caspase-8 activation in dDCN

A 63% cell survival was determined in 6OHDA+ salubrinal treated dDCN, showing 6OHDA triggered PERK pathway. A 72% cell survival was measured in 6OHDA+ zIETDfmk treated dDCN, demonstrating 6OHDA triggered Caspase-8 activation in dDCN. A further 85% survival of 6OHDA+ salubrinal + zIETDfmk treated dDCN, indicating that PERK pathway does not influence Caspase-8 activation in dDCN. zIETDfmk in combination with salubrinal promoted further survival of 6OHDA-treated dDCN, indicating an additional benefit of targeting ER stress pathway and Caspase-8. Proportion of cells surviving was determined by MTT absorbance at 570nm. Means of three experiments ± SEM shown. Table of values and statistical analysis can be found in Figure 6.26, Appendix 6.

Further analysis of demonstrated an additional effect in cell survival of 6OHDA +salubrinal + zIETDfmk treated dDCN, suggesting that 6OHDA triggers Caspase-8 and PERK ER stress activity via different cell signalling mechanisms causing death of dDCN. Both salubrinal and zIETDfmk used together have an additional benefit to increase survival and reduce death of 6OHDA dDCN (Figure 6.27).

	Treatment 1	Treatment 2	Treatment 3	Treatment 4	
	6OHDA	6OHDA SALUBRINAL	6OHDA zIETDfmk	6OHDA SALUBRINAL zIETDfmk	p-value obtained
Comparison 1	+	+	-	-	0.001
Comparison 2	+	-	+	-	0.002
Comparison 3	+	-	-	+	0.0003
Comparison 4	-	+	+	-	0.007
Comparison 5	-	+	-	+	0.0004
Comparison 6	-	-	+	+	0.002

Figure 6.27: Caspase-8 is not involved ER stress pathway in 6OHDA-treated dDCN

Survival of 6OHDA dDCN increased when salubrinal was added to zIETDfmk, indicating that PERK ER stress pathway does not influence stimulation of Caspase-8 in 6OHDA-treated dDCN (Comparison 5 $p<0.01$). Further survival and decrease in death of 6OHDA dDCN was achieved when zIETDfmk was added to salubrinal, indicating that 6OHDA stimulated Caspase-8 and PERK ER stress pathways via different mechanisms (Comparison 6 $p<0.01$). The additional effect of more cells survival when Caspase-8 inhibitor and salubrinal inhibitor were combined indicates that there are two pathways that are contributing to death of 6OHDA dDCN. Furthermore, both inhibitors are required to be used to suppress both pathways so more cell survival can be achieved. Proportion of cells surviving was determined by MTT absorbance at 570nm. Means of three experiments ± SEM shown. Table of values and statistical analysis can be found in Figure 6.26, Appendix 6.

Double IF analysis was carried out to determine the presence and absence of Caspase-8 in untreated and 6OHDA-treated dDCN after treated with salubrinal. Caspase-8 was present in untreated, salubrinal treated, 6OHDA-treated and 6OHDA+salubrinal treated dDCN, indicating that salubrinal did not suppress Caspase-8 activation in dDCN. This strongly indicates that Caspase-8 is not following the PERK pathway of ER mediated death of dDCN (Figure 6.28).

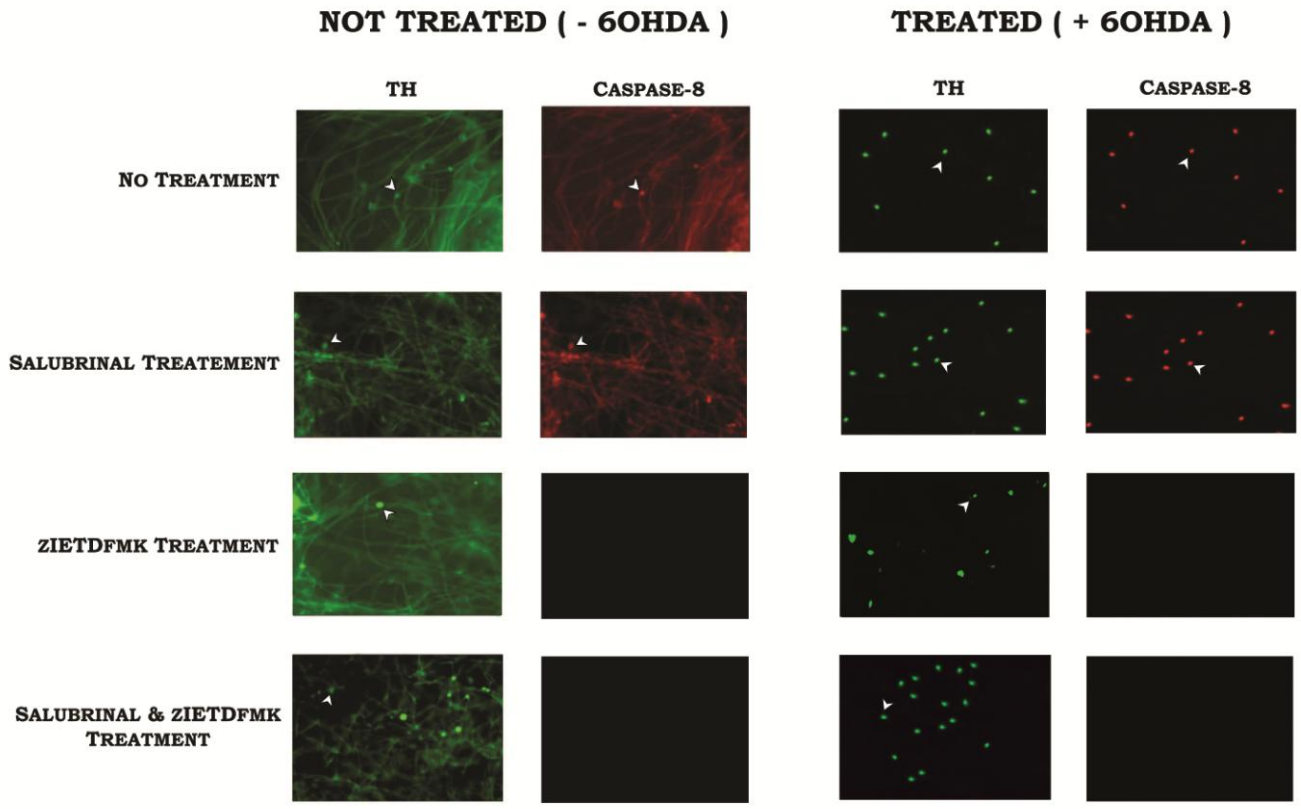

Figure 6.28 Salubrinal does not inhibit active Caspase-8 in 6OHDA-treated dDCN

Presence of TH positive cells was observed untreated and 6OHDA-treated dDCN (green).

Active Caspase-8 was present in untreated and 6OHDA-treated dDCN (red). An increase in the proportion of active Caspase-8 positive cells was determined in 6OHDA-treated dDCN, when compared to untreated (- 6OHDA) dDCN, indicating 6OHDA enhanced further activation of Caspase-8 in dDCN. Active Caspase-8 was present in the same TH positive cells of untreated and 6OHDA-treated dDCN, signifying that Caspase-8 is actively present in dDCN.

Active Caspase-8 was observed in salubrinal treated and 6OHDA+salubrinal treated dDCN, indicating that stimulation of Caspase-8 is independent from activation of PERK pathway in dDCN. In contrast, active Caspase-8 was absent in zIETDfmk treated and 6OHDA+zIETDfmk treated dDCN, signifying

that Caspase-8 activity is successfully suppressed in dDCN when using Caspase-8 inhibitor. Caspase-8 was not found in salubrinal+ zIETDfmk treated and 6OHDA+salubrinal+zIETDfmk treated dDCN. The Caspase-8 inhibitor, zIETDfmk had directly suppressed Caspase-8 activation in untreated and 6OHDA-treated dDCN. Positive staining for cell bodies (White Arrow) in untreated (- 6OHDA) and treated (+ 6OHDA) dDCN. Table of values can be found in Figure 6.29, Appendix 6.

WB analysis was carried out to determine if salubrinal inhibited Caspase-8 activity in 6OHDA-treated dDCN (Figure 6.30). Salubrinal did not prevent nor reduce the amount of Caspase-8 in 6OHDA-treated dDCN, illustrating that salubrinal does not influence Caspase-8 activation. The ineffectiveness of salubrinal against activation of Caspase-8 further supports the notion that Caspase-8 is independent of PERK pathway and does not follow ER mediated death of treated dDCN. 6OHDA triggered Caspase-8 activation but this was being achieved through a different route and not via PERK pathway.

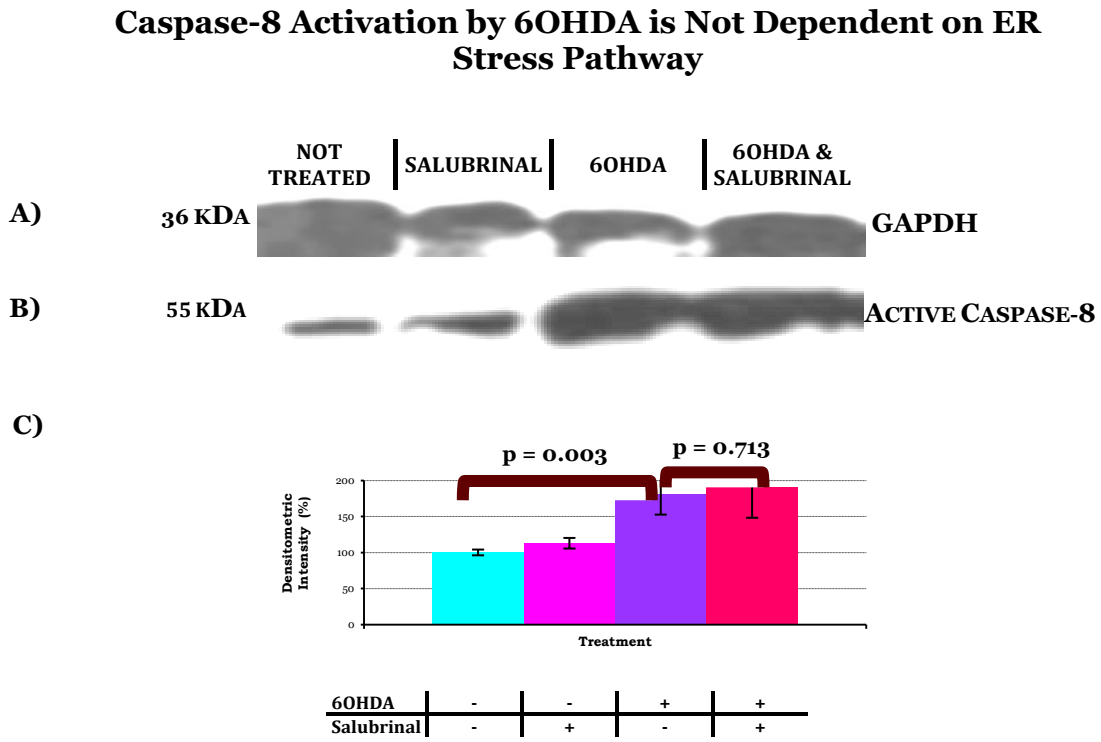

Figure 6.30 : PERK pathway does not suppress Caspase-8 activation in 6OHDA dDCN

A) Illustrative example of GAPDH in untreated, salubrinal, 6OHDA, salubrinal + 6OHDA treated dDCN.

B) Illustrative example of active Caspase-8 in untreated, salubrinal, 6OHDA, salubrinal + 6OHDA treated dDCN.

C) Quantitatively, an 81% increase in active Caspase-8 was detected in 6OHDA-treated dDCN, compared to untreated dDCN ($p<0.05$). Salubrinal neither prevented nor reduced the amount of active Caspase-8 in present in salubrinal treated, 6OHDA+salubrinal treated dDCN ($p>0.05$), indicating that PERK pathway does not influence Caspase-8 stimulation in 6OHDA-treated dDCN. Means of three experiments ± SEM shown. Table of densitometry values and statistical analysis can be found in Figure 6.31, Appendix 6.

To investigate if further survival of 6OHDA-treated dDCN could be achieved by suppression of Caspases-2,-4,-8 and PERK activity, 6OHDA-treated dDCN were treated with different combinations of salubrinal, zVDVADfmk, zLEVDfmk and zIETDfmk. ANOVA analysis illustrated a considerable difference in survival of 6OHDA dDCN that were treated with zVDVADfmk, zIETDfmk, zLEVDfmk and salubrinal ($p < 0.01$, Figure 6.32, Appendix 6). T tests were used to discover which inhibitors were most effective in promoting survival and reducing death of 6OHDA dDCN. The results demonstrate that the use of Caspase inhibitors, zLEVDfmk and zIETDfmk, along with salubrinal provide more protection and survival of 6OHDA-treated dDCN then using a single inhibitor or two inhibitors ($p<0.01$ Figure 6.33).

Similar cell survival was determined in 6OHDA+salubrinal treated, 6OHDA+zVDVADfmk treated, 6OHDA+salubrinal+zVDVADfmk treated dDCN (cell survival 64%, 61% and 66%), indicating PERK directly influences Caspase-2 activity. The amount of cell survival was not significant when zVDVADfmk inhibitor was added to salubrinal inhibitor, suggesting the addition of zVDVADfmk did not provide an additional effect to slow death and increase survival of 6OHDA-treated dDCN($p>0.05$ Figure 6.33). There was no significant difference to slow death and promote cell survival in 6OHDA+zVDVADfmk+salubrinal treated dDCN, indicating that the use of salubrinal inhibitor can suppress both PERK and Caspase-2 activity, therefore zVDVADfmk is not required to inhibit death of dDCN.

In comparison, more cell survival was achieved in 6OHDA + zLEVDfmk + salubrinal treated dDCN, compared to 6OHDA + salubrinal treated dDCN (77% cell survival, $p<0.01$ Figure 6.33). This showed that PERK does not influence Caspase-4 activity and suppression of Caspase-4 and PERK can provide additional benefit. There was a significant difference to slow death and promote cell survival in 6OHDA dDCN that were treated with both zLEVDfmk and salubrinal inhibitors, indicating that the use of both zLEVDfmk and salubrinal inhibitors can suppress both PERK and Caspase-4 activity in dDCN. The results demonstrate that the use of Caspase-4 inhibitors along with salubrinal promotes more protection and survival of 6OHDA-treated cells then using one inhibitor.

Furthermore, additional cell survival was determined in 6OHDA+ salubrinal+ zIETDfmk treated dDCN, compared to 6OHDA + salubrinal treated dDCN, demonstrating that salubrinal has an additional effect to slow death and promote cell survival ($p<0.01$ Figure 6.33). Further cell survival of 6OHDA dDCN, was determined when zIETDfmk was added with salubrinal, signifying that both inhibitors can promote further survival and slow death of 6OHDA dDCN, via suppressing two different routes. The additional effect of more cells survival when Caspase-8 inhibitor and PERK inhibitor are combined indicates that there are two pathways that are contributing to death of 6OHDA dDCN.

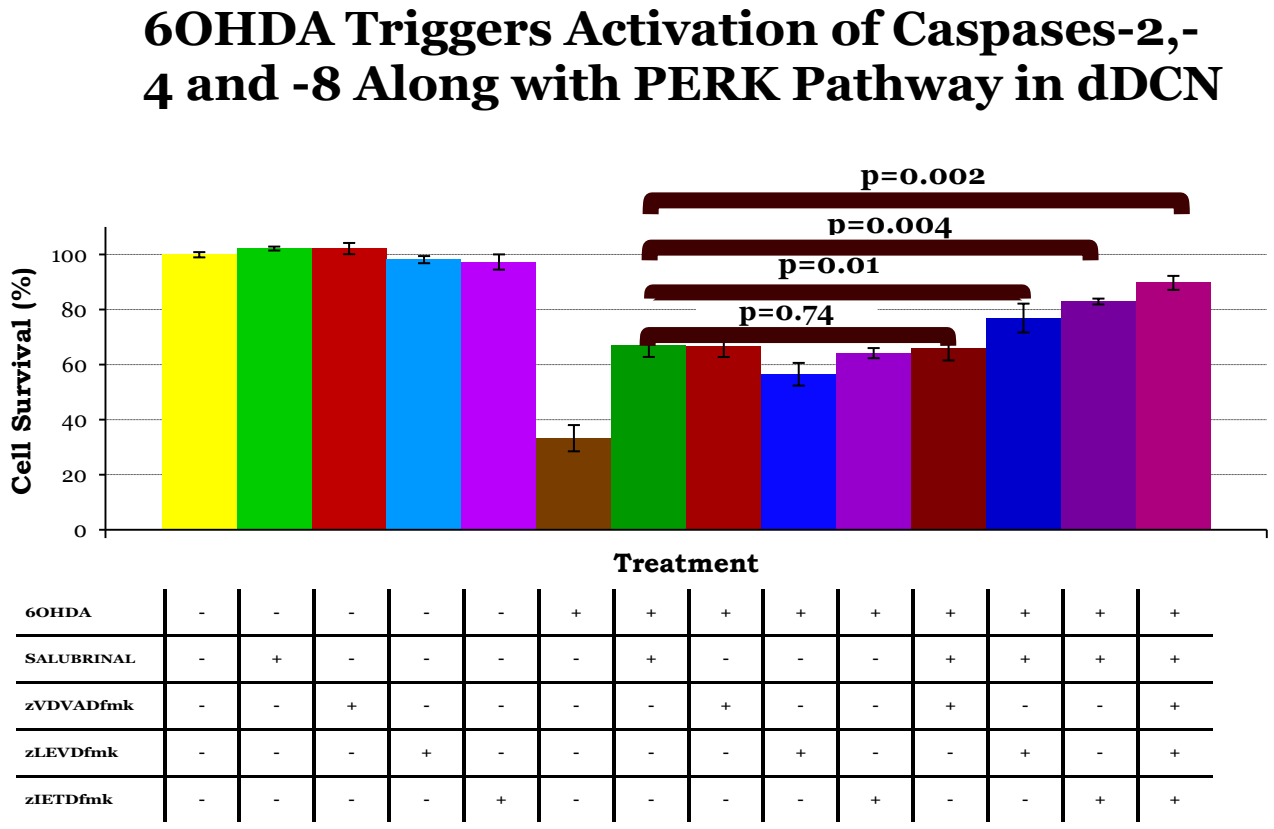

Figure 6.33 : zLEVDfmk zIETDfmk and salubrinal reduced death of 6OHDA dDCN

Untreated and 6OHDA-treated dDCN were treated with different combinations of salubrinal, zVDVADfmk, zLEVDfmk and zIETDfmk to determine if maximal cell survival could be achieved by suppression of Caspases-2,-4,-8 and PERK activity. The use of Caspase inhibitors, zLEVDfmk and zIETDfmk, along with salubrinal provide more protection and survival of 6OHDA-treated dDCN then using a single inhibitor or two inhibitors. Proportion of cells surviving was determined by MTT

absorbance at 570nm. Means of three experiments ± SEM shown. Table of values and statistical analysis can be found in Figure 6.32, Appendix 6.

A closer examination of the results portrayed that 6OHDA triggered activation of Caspases-2, -4 and -8 using diverse pathways (Figure 6.34, Appendix 6). Moreover, further survival of 6OHDA dDCN, was determined when salubrinal was added with zVDVADfmk and zIETDfmk, demonstrating that these three inhibitors are required to be used to suppress pathways, thereby promoting cell survival and slowing death.

The findings demonstrated more survival of cell in 6OHDA + salubrinal + zLEVDfmk+ zIETDfmk + zVDVADfmk treated dDCN,, when compared to 6OHDA +salubrinal + zVDVADfmk treated dDCN (Comparison 8, $p<0.01$, Figure 6.34, Appendix 6), indicating suppression of Caspase-4 and -8 as well as PERK reduces death of 6OHDA-treated dDCN.

Similarly, suppression of Caspases-8, 2 and PERK can decrease death of and promote survival of 6OHDA dDCN. cells that were treated with 6OHDA + salubrinal + zIETDfmk + zLEVDfmk dDCN had a higher survival rate compared to 6OHDA-treated + salubrinal + zLEVDfmk dDCN, showing using three inhibitors to reduce death of cells is more effective than using two inhibitors (Comparison 9, $p<0.01$, Figure 6.34, Appendix 6). Furthermore, 6OHDA + salubrinal + zLEVDfmk+ zIETDfmk + zVDVADfmk treated dDCN had increased cell survival, when compared to 6OHDA +salubrinal + zIETDfmk treated dDCN, indicating that the use of three inhibitors to suppress cell signalling pathways that cause death of dDCN is more effective than using two inhibitors (Comparison 10, $p<0.01$, Figure 6.34, Appendix 6).

The results portrayed a difference in cell survival between 6OHDA+salubrinal+zLEVDfmk treated dDCN and 6OHDA+salubrinal +zVDVADfmk treated dDCN (Comparison 11, $p<0.05$, Figure 6.34, Appendix 56), indicating Caspase-4 activity does not directly influence Caspase-2 activity and the stimulation of these Caspases are most likely through different mechanisms. Furthermore, a significant difference in cell survival was determined in 6OHDA+salubrinal+zVDVADfmk treated dDCN, when

compared to 6OHDA+salurbianl +zIETDfmk treated dDCN (Comparison 12, $p<0.01$, Figure 6.34, Appendix 6), indicating activation of that Caspases-2 is in dependent on and activation on Caspase-8 and vice versa dDCN. A significant increase in cell survival was determined in 6OHDA+salubrinal +zLEVDfmk treated dDCN, when compared to 6OHDA+salubrinal +zIETDfmk treated with dDCN (Comparison 13, $p<0.01$, Figure 6.36, Appendix 6), indicating that 6OHDA triggers Caspases-4 and-8 activation in dDCN, through different mechanisms and one Caspase is not dependent on the other to be activated.

There was no significant difference in cell survival in 6OHDA +zVDVADfmk treated dDCN, when compared to 6OHDA + salubrinal + zVDVADfmk treated dDCN (Comparison 14, $p>0.05$, Figure 6.34, Appendix 6), indicating activation of Caspase-2 is dependent on PERK pathway. Suppression of PERK pathway had inhibited Caspase-2 activity, indicating that the use of salubrinal inhibitor can suppress both PERK and Caspase-2 activity in 6OHDA-treated dDCN. In contrast, a difference in cell survival was found between 6OHDA+zLEVDfmk treated dDCN, compared to 6OHDA + salubrinal + zLEVDfmk treated dDCN, suggesting that PERK and Caspase-4 follow separate routes that result in the death of 6OHDA dDCN(Comparison 15, $p<0.01$, Figure 6.34, Appendix 6). This showed that the use of salubrinal and zLEVDfmk inhibitor is effective to reduce death and increase survival of 6OHDA dDCN. Additionally, an additional effect in cell survival was found in 6OHDA+ zIETDfmk treated dDCN, when compared to 6OHDA + salubrinal + zIETDfmk treated dDCN, signifying PERK and Caspase-8 follow the different apoptotic pathway in 6OHDA dDCN. Suppression of these two pathways using salubrinal and zIETDfmk inhibitors would be more efficient to reduce death of 6OHDA dDCN (Comparison 16, $p<0.05$, Figure 6.34, Appendix 6).

The results indicated that Caspase-2 is activated by ER mediated death of 6OHDA-treated dDCN. Specifically 6OHDA stimulated Caspase-2 activation through the PERK pathway of ER stress resulting in death of dDCN (Figure 6.35). In comparison, Caspases-4 and -8 were not active in PERK pathway of ER mediated death of 6OHDA-treated dDCN, suggesting 6OHDA triggers Caspases-4 and-8 activation, through a different route, which may or may not be ER stress related. It was also found that there was no cross talk between Caspases-2,-4 and -8 and each specific Caspase is stimulated by a different pathway in 6OHDA dDCN.

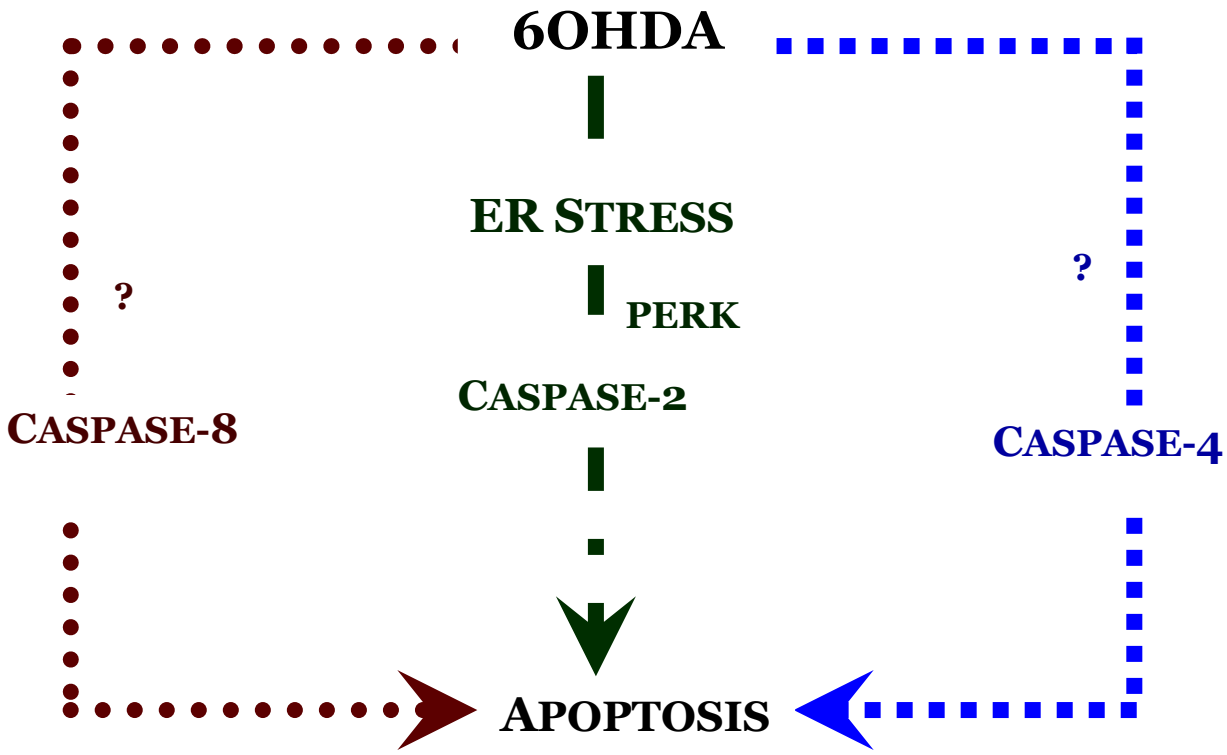

Figure 6.35 : 6OHDA triggers activation of Caspase-2 via PERK ER stress pathway and stimulation of Caspases-4 and-8 in dDCN

Caspase-2 is involved in PERK pathway of ER mediated death of 6OHDA-treated dDCN. Salubrinal suppressed Caspase-2 activity, indicating that Caspase-2 is active in PERK pathway of ER stress. In comparison, Caspases-4 and-8 activity was not inhibited by salubrinal, suggesting 6OHDA triggers Caspases-4 and- 8 activities via separate mechanisms resulting in apoptotic death of dDCN.

The results from the previous Chapter had shown that 6OHDA triggers an additional pathway apart from NFκB classical pathway in dDCN. The importance of NFκB activity was determined in PERK ER stress mediated apoptotic death of 6OHDA-treated dDCN. The findings illustrated that further cell survival was achieved in 6OHDA+IKK+salubrinal treated dDCN, indicating 6OHDA triggers PERK and NFκB activation via different mechanisms (Figure 6.36)

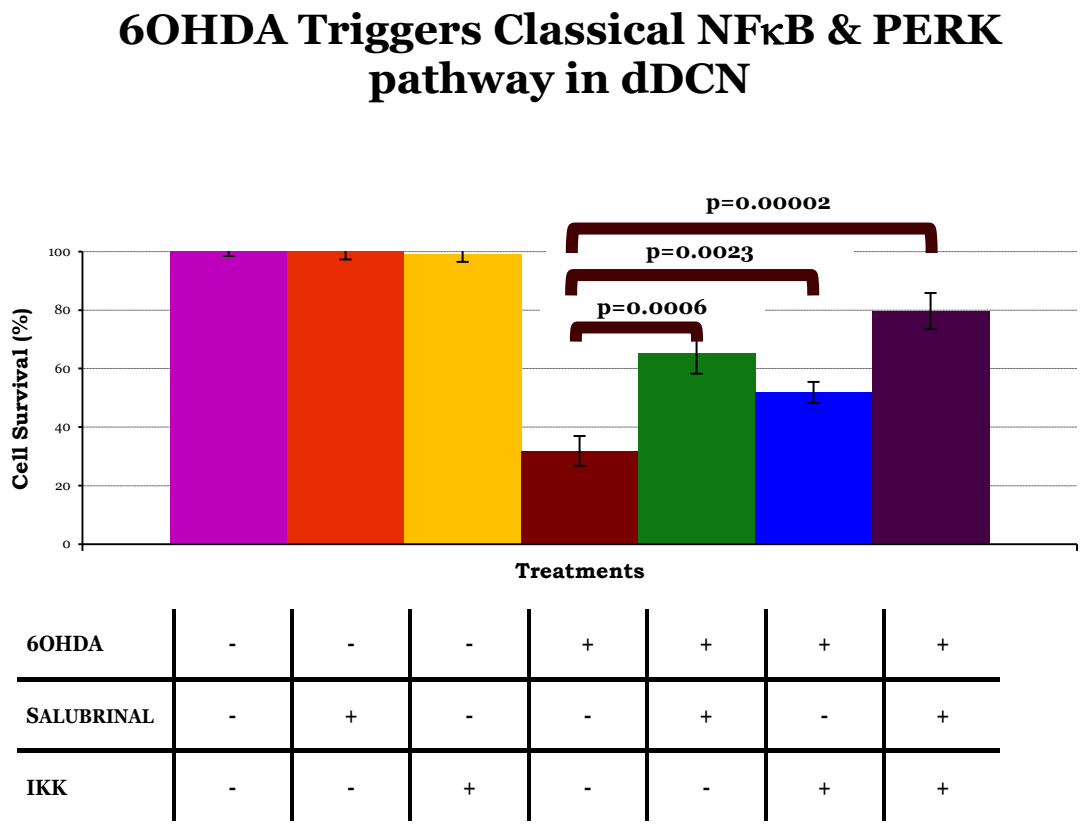

Figure 6.36: 6OHDA promotes NFκB and PERK ER Stress mediated death of dDCN

PERK activity in NFκB classical pathway were determined in untreated and 6OHDA-treated, 6OHDA+IKK, 6OHDA+salubrinal, 6OHDA+IKK+salubrinal treated dDCN. 6OHDA triggered PERK activation in dDCN. A 65% cell survival was determined in 6OHDA+salubrinal treated dDCN. A 52% cell survival was determined in 6OHDA+IKK treated dDCN. An 80% cell survival was determined in 6OHDA+IKK+salubrinal treated dDCN, indicating an additional benefit of targeting NFκB classical pathway and PERK pathway. Proportion of cells surviving was determined by MTT absorbance at 570nm. Means of three experiments ± SEM shown. Table of values and statistical analysis can be found in Figure 6.37, Appendix 6.

The combination of IKK and salubrinal was used to investigate if IKK and salubrinal follow the same pathway or if there is any cross talk in these pathways in 6OHDA-treated dDCN (Figure 6.38). Findings indicated that 6OHDA triggers NFκB mediated and ER mediated death of dDCN, via the NFκB classical pathway and PERK pathway (respectively). These results indicated that 6OHDA is provoking death of dDCN via two separate independent routes. This can be further explained by the fact that if ER stress and NFκB were following the same pathway, then the addition of IKK to salubrinal would not provide more survival of 6OHDA-treated dDCN. An additional effect in further survival of 6OHDA dDCN was measured when both IKK and salubrinal were used.

	Treatment 1	Treatment 2	Treatment 3	Treatment 4	
	6OHDA	6OHDA IKK	6OHDA SALUBRINAL	6OHDA IKK SALUBRINAL	p-value obtained
Comparison 1	+	+	-	-	0.0023
Comparison 2	+	-	+	-	0.0006
Comparison 3	+	-	-	+	0.00002
Comparison 4	-	+	+	-	0.0006
Comparison 5	-	+	-	+	0.0004
Comparison 6	-	-	+	+	0.0011

Figure 6.38: NFκB does not influence PERK activation in 6OHDAinduced dDCN

Additional cell survival of 6OHDA dDCN was determined when salubrinal was added with IKK, demonstrating that salubrinal has an additional effect to slow death and promote cell survival (Comparison 6, $p<0.01$). Further cell survival of 6OHDA dDCN, was determined when IKK was added with salubrinal, signifying that both inhibitors can promote further survival and slow death of 6OHDA dDCN, via suppressing two different routes (Comparison 5, $p<0.01$). The additional effect of more cells survival when NFKB inhibitor and PERK inhibitor are combined indicates that there are two separate pathways that are contributing to death of 6OHDA dDCN. Proportion of cells surviving was determined by MTT absorbance at 570nm. Means of three experiments ± SEM shown. Table of values and statistical analysis can be found in Figure 6.37, Appendix 6.

The results indicated that 6OHDA stimulated NFκB classical pathway and PERK pathway of ER stress resulting in death of dDCN. Furthermore, the findings demonstrated that there was no cross talk between PERK and NFκB activities suggesting that 6OHDA triggers these two pathways separately resulting in apoptotic death of dDCN (Figure 6.39).

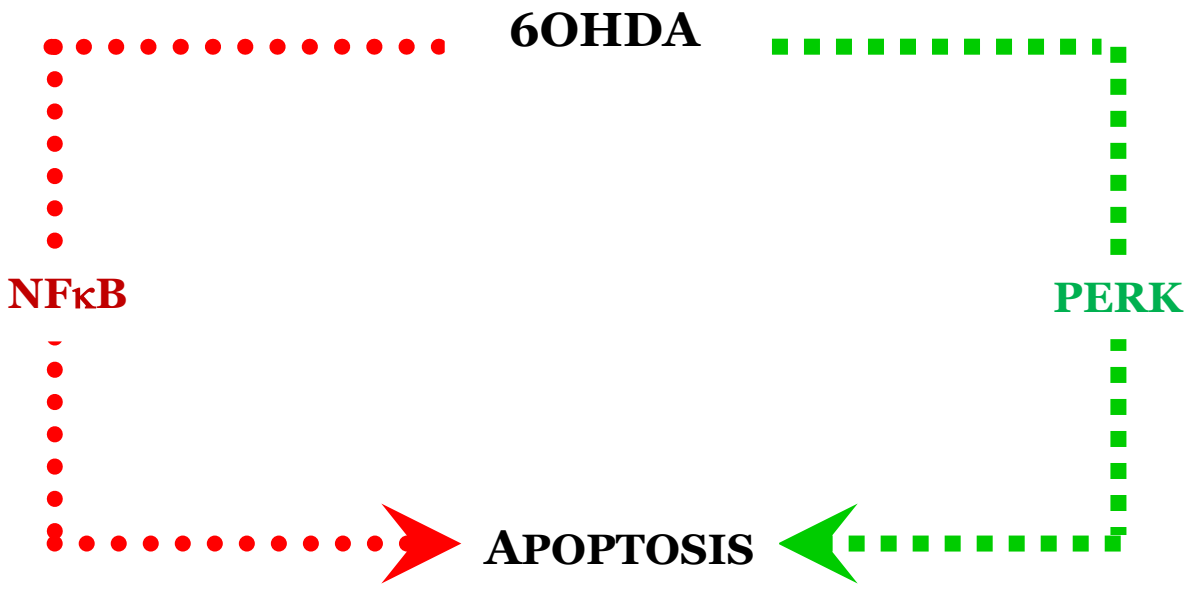

Figure 6.39: 6OHDA triggers PERK and NFκB classical pathway in dDCN

6OHDA stimulates activation of PERK and NFκB classical pathway, resulting in apoptotic death of dDCN. This finding was determined using specific inhibitors, salubrinal and IKK in 6OHDA-treated dDCN, using MTT assay. Salubrinal inhibited activation of PERK pathway and promoted survival of 6OHDA-treated dDCN. Similarly, IKK suppressed activation of NFκB classical pathway, thereby reducing 6OHDA-treated dDCN. The suppression of NFκB classical and PERK pathway had increased survival of 6OHDA-treated dDCN, suggesting that NFκB classical pathway does not influence PERK pathway and vice versa in 6OHDA-treated dDCN.

To determine if NFκB and ER stress were the main pathways that cause apoptotic death in

It was essential to determine if 6OHDA triggered a third pathway that significantly contributed to apoptotic death of dDCN. Suppression of PERK ER stress pathway promoted survival and slowed death of cells that had been treated with 6OHDA+salubrinal. Similarly, an increase in cell survival was measured in 6OHDA+IKK treated dDCN, via inhibiting NFκB activity. zVADfmk had slowed death and promoted survival of 6OHDA dDCN, signifying that 6OHDA triggered Caspase mediated apoptotic death of dDCN. More survival of cells was achieved when cells were treated with 6OHDA+IKK+salubiranl+zVADfmk, indicating that suppressing Caspases, NFκB and PERK pathways can reduced apoptotic death of dDCN (Figure 6.40).

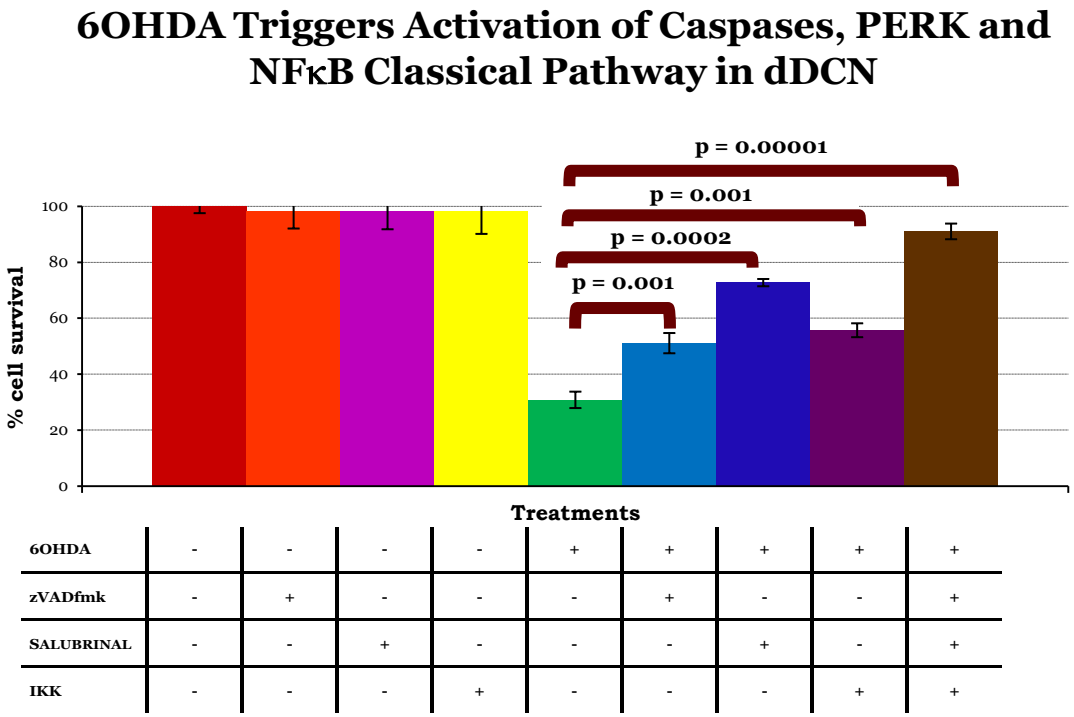

Figure 6.40: Salubrinal IKK and zVADfmk promoted further survival of 6OHDA dDCN

A 51% cell survival was found in 6OHDA+ zVADfmk treated dDCN, emphasising Caspase mediated death of 6OHDA dDCN. A 56% cell survival was determined in 6OHDA+IKK treated dDCN. A 73% cell survival was determined in 6OHDA+salubrinal treated dDCN. A 90% cell survival was determined in 6OHDA+zVADfmk+IKK+salubrinal treated dDCN, indicating an additional benefit of targeting NFκB, PERK and Caspases pathways. Proportion of cells surviving was determined by MTT absorbance at 570nm. Means of three experiments ± SEM shown. Table of values and statistical analysis can be found in Figure 6.41, Appendix 6.

A closer analysis of the results revealed 6OHDA triggered NFκB, PERK and Caspase pathways resulting in apoptotic death of dDCN. An additional effect in cell survival was measured in 6OHDA salubrinal +IKK +zVADfmk treated dDCN, suggesting that PERK and NFκB pathway cause death of 6OHDA dDCN, but there are other potential pathways that cause death of dDCN. 6OHDA triggers another pathway apart from PERK ER Stress and NFκB classical pathway that results in apoptotic death of dDCN. There is a high possibility that this potential pathway is related to Caspase-4 activation that is contributing to apoptotic death of dDCN (Figure 6.42).

	Treatment 1	Treatment 2	Treatment 3	Treatment 4	Treatment 5	
	6OHDA	6OHDA zVADfmk	6OHDA SALUBRINAL	6OHDA IKK	6OHDA zVADfmk SALUBRINAL IKK	p-value obtained
Comparison 1	+	+	-	-	-	0.001
Comparison 2	+	-	+	-	-	0.0002
Comparison 3	+	-	-	+	-	0.001
Comparison 4	+	-	-	-	+	0.00001
Comparison 5	-	+	-	-	+	0.00005
Comparison 6	-	-	+	-	+	0.0016
Comparison 7	-	-	-	+	+	0.0003

Figure 6.42: 6OHDA promoted PERK ER Stress, NFκB and Caspase mediated apoptotic death of dDCN

More cell survival was achieved when zVADfmk was added to 6OHDA+salubrinal+IKK treated dDCN, indicating that 6OHDA triggers another Caspase cell signalling pathway causing apoptotic death of dDCN (Comparison 5 $p<0.05$). A higher level of survival and decrease in death of cells was achieved when salubrinal was added to 6OHDA+IKK+zVADfmk, treated dDCN, demonstrating that salubrinal has an additional effect to slow death and promote cell survival (Comparison 6 $p<0.05$).Further cell

survival of cells was measured when IKK was added to 6OHDA+salubrinal+ zVADfmk treated dDCN, signifying that all three inhibitors can promote further survival and slow death of 6OHDA dDCN, via suppressing three different routes (Comparison 7 $p<0.01$). The additional effect of more cells survival when Caspase, NFKB and PERK inhibitors are combined indicates that there are three separate pathways that are contributing to death of 6OHDA dDCN. Proportion of cells surviving was determined by MTT absorbance at 570nm. Means of three experiments ± SEM shown. Table of values and statistical analysis can be found in Figure 6.41, Appendix 6

6.4 Discussion

One of the main aims was to determine the impact the PERK ER stress pathway had in 6OHDA dDCN. Collectively the results demonstrated 6OHDA triggers PERK pathway resulting in ER mediated death of dDCN (Figure 6.1-6.5). Furthermore, the PERK ER stress pathway was one of the major routes that caused apoptotic death rather than survival of dDCN, when triggered by 6OHDA (Figure 6.39). Moreover, activation of PERK promoted stimulation of Caspase-2 in 6OHDA dDCN (Figure 6.7-Figure 6.12).

These findings are similar to previous research by Arduíno et al (2009a) that demonstrated activation of Caspase-2 in tunicamycin treated neuronal cells using WB analysis. IF and WB analysis revealed PERK is an upstream protein which promotes activation of Caspase-2 in dDCN. IF, WB and inhibitor analysis demonstrated that suppression of PERK protein had inhibited Caspase-2 activation, resulting in an increase in survival of 6OHDA dDCN. Previous research by Jiang et al (2010) portrayed salubrinal had reduced Caspase-3 activity and protected cells from ER stress mediated apoptosis sodium butyrate treated PD cells. In comparison, the current study showed salubrinal had suppressed Caspase-2 activity leading to an increase in cell survival and slowing death of 6OHDA dDCN (pages 226-230).

Furthermore, work by Chinta et al (2009) demonstrated that salubrinal had decreased p-eIF2α, CHOP, XBP-1 and Caspase-3 activation in paraquat induced N27 dopaminergic cell line. Paraquat caused an increase of ROS in the cell which can lead to cell death via oxidative stress. 6OHDA has been known to promote elevated ROS levels provoking death of DCN. In the current study stimulation of PERK leading to Caspase-2 activity and death of dDCN may have been due to an elevation of ROS caused by 6OHDA. The elevated accumulation of ROS may have caused misfolding and impairment of proteins leading to initiation of PERK ER stress pathway, which promoted Caspase-2 activation leading to apoptotic death of dDCN. To confirm this, future studies could explore the levels and what types of ROS are involved in death of 6OHDA dDCN over a time frame. This would indicate at what point ROS accumulation can cause the ER stress pathway to switch from promoting cell survival to cell death.

Another factor that could be investigated is the impact salubrinal inhibitor has on ROS levels itself in 6OHDA-treated dDCN.

The current study is the first to determine if active Caspase-8 is involved in ER mediated death of 6OHDA dDCN. IF and WB analysis illustrated Caspase-8 activation in presence of the PERK inhibitor salubrinal, signifying that stimulation of Caspase-8 is achieved through a different pathway and is not connected to the PERK pathway in 6OHDA dDCN (Figure 6.28-Figure 6.30). A closer examination of Caspase-8 activation in relevance to PERK pathway in 6OHDA dDCN, revealed that suppressing PERK pathway and inhibiting Caspase-8 pathway promoted further cell survival of dDCN (Figure 6.25-Figure 6.27). In addition, the current study is the first to explore if there is any cross talk between Caspases-2,-4 and -8 with relevance to PERK ER mediated death of dDCN. Cell viability assays that had been treated with different combinations of inhibitor had shown that there was no cross talk between caspases-2,-4 and -8 in 6OHDA dDCN (Figure 6.33-Figure 6.35).

Work by Smith et al (2005) found that Caspase-12 participates in ER stress mediated death of DCN. Salubrinal partially inhibited death of DCN by suppression of Caspase-12, indicating that ER stress caused death of DCN but other pathways such as the mitochondrial pathway also contributed to death of DCN. In comparison, to work carried out by Smith et al (2005), Caspase-12 was not detected but Caspase-4 was active in 6OHDA-treated dDCN in the current study. However, Caspase-12 was present in PD-Ex (refer to Chapter 3) but not in found in 6OHDA dDCN, therefore another ER associated protein, Caspase-4 was used as a substitution. One possible reason why Caspase-12 was not detected in dDCN could be because the human cell has large deletions of essential homologous of Caspase-12, whilst in animal model all the essential codons to promote Caspase-12 protein are expressed so Caspase-12 is usually actively expressed in PD animal model and not in human PD model (Hertz 2009).

Similar to Smith et al (2005), this research has demonstrated that ER stress causes death of 6OHDA DCN but other pathways also contribute to death of dDCN. Suppression of PERK pathway as well as Caspases-4 and -8 can promote further survival of more cells, demonstrating the involvement of other

pathways (Figure 6.33-Figure 6.35). Smith et al (2005) suggested that the intrinsic pathway may be involved in death of DCN, whilst results from this research indicate an involvement of NFκB classical pathway. Another pathway that could be explored is the intrinsic pathway in relation to ER mediated and NFκB mediated death of dDCN.

A surprising outcome was achieved in the current study which illustrated the lack of relation of Caspase-4 in PERK ER mediated death of 6OHDA dDCN. IF and WB analysis had shown that salubrinal had not suppressed Caspase-4 activation in 6OHDA dDCN (Figure 6.17-Figure 6.19). Cell survival analysis using inhibitors had revealed activation of Caspase-4 pathway causes death of dDCN but the stimulation of Caspase-4 activity is independent from PERK pathway in 6OHDA-treated cells (Figure 6.14-Figure 6.16). These findings are in contrast to research carried out by Lee et al (2010) that illustrated increased levels of CHOP, p-PERK, p-IRE-1, p-EIF2α , XBP-1, Caspases-3 and -4 in tunicamycin treated SK-N-SH cells using colorimetric Caspase specific assays, indicating that Caspase-4 is triggered by PERK pathway. Furthermore, salubrinal had reduced Caspase-4 activity in tunicamycin treated SK-N-SH cells.

The reason for PERK pathway did not influence Caspase-4 activity in dDCN could be due to the type of neurotoxin used. 6OHDA may have triggered Caspase-4 pathway through calcium mechanisms instead of PERK pathway in dDCN. This potential idea can be supported by research performed by Arduíno et al (2009b) which had shown that MPTP leakage of calcium from the ER into the mitochondria provoked activation of Caspases-2,-3,-4 and -9 resulting in death of neuronal PD cells. WB and colorimetric assays had shown increased levels of Caspases-2,-3,-4 and -9 over a time course in MPTP PD cells.

Similarly, research by Higuchi et al (2005) has shown that calcium promoted Caspase-4 and Calpain activation in transgenic mice that had been injected with kainic acid. IF analysis revealed degeneration of axonal and dendrites as well as an up regulation of Caspase and Calpain activation signifying that elevated calcium levels provokes Calpain and Caspase stimulation resulting in degeneration of neuronal axons and. Although no work has been carried out in Calpain, Caspase and Caspase activation in dDCN,

it is plausible that calcium imbalance and Calpain proteins interact and effect Caspase activation and death of dDCN. It is possible that 6OHDA may have triggered Caspase-4 activation through a calcium related pathway in dDCN. Although suppression of Caspase-2 can be achieved by inhibiting the PERK pathway, further understanding of the PERK ER stress pathway in cell death and survival needs to be established. The PERK ER stress pathway is vital for normal cellular processes and so the complete suppression of this pathway may result in other potential problems.

Currently there has not been any research determining if there is a link between NFκB pathway and PERK ER stress pathway in 6OHDA-treated dDCN. The aim of this research was to investigate any cross talk of NFκB classical and PERK ER stress pathway in 6OHDA-treated dDCN. The results demonstrated that 6OHDA triggered NFκB classical pathway and ER stress pathway via independent different routes resulting in death of dDCN (Figure 6.36). Activation of NFκB pathway did not influence activation of ER stress pathway or vice versa, emphasising that the pathways are activated by 6OHDA independently in dDCN (Figure 6.39).

6.5 Conclusion

6OHDA triggers activation of PERK pathway resulting in ER mediated death of dDCN (Figure 6.1-6.5). IF and WB analysis revealed that stimulation of the PERK pathway encourages activation of Caspase-2 activity contributing to death of 6OHDA-treated dDCN (Figure 6.10-Figure 6.12). IF, WB and cell viability assays illustrated that suppression of PERK pathway inhibits stimulation of Caspase-2, resulting in an increase in survival of 6OHDA dDCN. IF, WB and cell viability assays demonstrated that 6OHDA triggered activation of Caspases-4 and-8 independently to the PERK ER stress pathway in dDCN. Suppression of PERK, Caspases-4 and -8, using a combination of salubrinal, zLEVDfmk and zIETDfmk inhibiters had protected DCN from death and significantly increased survival of 6OHDA-treated dDCN Figure (Figure 6.33-Figure 6.34). The PERK ER stress pathway is one of the main routes that contribute to apoptotic death of 6OHDA dDCN (Figure 6.35). However, 6OHDA provokes other potential pathways that result in Caspase mediated death of 6OHDA dDCN via apoptotic routes (Figure 6.40- Figure 6.42). Further research to identify other key proteins in the PERK ER stress pathway would aid to provide better targets to slow death and provide protection of DCN (Figure 7.1).

Furthermore, inhibitor cell viability assay have shown suppression of PERK ER Stress and NFκB classical pathway had resulted in a significant amount of survival and decrease in 6OHDA dDCN, indicating 6OHDA promotes NFκB and PERK ER mediated apoptotic death of dDCN (Figure 6.36). However, activation of NFκB and PERK pathway were independent of one another and 6OHDA had provoked activation of NFκB and PERK, via different routes (Figure 6.39).

Chapter 7:
General Discussion

Different types of exercise have been explored ranging from Nordic walking to dancing (tango, waltz, and foxtrot), muscle and strength resistance and different environments (land versus water) in PD patients (Fritz et al 2011, Stallibrass et al 2002, Hackney and Earhart 2009a, Hackney and Earhart 2007, Hackney and Earhart 2010, Li et al 2012, Earhart, 2009b, Dreu et al 2012, Vivas et al 2011). All these exercises have shown some improvement not only decreasing key features that are present in PD such as gait, tremors and bradykinesia, but also improving quality of life of the PD patient in terms of forming social networks and integrating well into their lifestyle. Although there are extensive clinical studies carried out on treadmill exercise showing improvement in PD symptoms (Tomsilon et al 2012, Herman et al 2007, Canning et al 2012). However, there is a lack of biochemical understanding to how exercise is affecting PD patients at a cellular level and on key proteins involved in the development and progression of PD. Hence, there is a lack of research exploring the potential pathways, which exercise can activate and suppress to provide such positive and even negative effects. The current study is the first to explore the effect of treadmill exercise on Caspases, along with CAMK-IV protein in different brain regions of MPTP rat model using WB analysis (Chapter 3 Figure 3.2-Figure 3.48).

The results of this research had demonstrated a general reduction or absence active Caspase as well as increase in active CAMK-IV levels in different brain regions of PD animal model that underwent endurance exercise (Chapter 3). More specifically, treadmill exercise may have inhibited activation of Caspases-2, -8 and -12 in the midbrain and striatum of PD animal model (Chapter 3 Figure 3.22, Figure 3.26, Figure 3.32, Figure 3.36 and Figure 3.40). There is a possibility that exercise may be acting as an initiator that triggers different proteins or it may activate specific proteins that directly suppress Caspase activation, leading to a decrease in death of DCN. There also exist the possibility that exercise triggers proteins, which in turn stimulate other proteins that activate another generation of proteins leading to suppression of Caspases, indicating that exercise reduces death of neuronal cells and that may be due to different Caspase pathways. To determine how exercise is reducing and inhibiting activation of Caspases, the first step was to investigate stimulation of Caspases. Only through discovering what key proteins are

important in Caspase activation and establishing which pathways Caspases are involved in that result in death of DCN, can improved therapies and treatments be created in the future. In addition, establishing which pathways the Caspases follow and understanding the key events that occur in Caspase activation new targets for treatment can be achieved. Exercise may have had decreased and suppressed specific Caspases, such as Caspases-12,-8 and -2 in PD animal models, putting forward an idea that suppression of specific pathways may inhibit and slow down the rate of death of DCN in PD (Chapter 3 Figure 3.2, Figure 3.6, Figure 3.10-Figure 3.16, Figure 3.20-Figure 3.26, Figure 3.3-Figure 3.36 and Figure 3.40). To explore this notion further in vitro work, using dopaminergic stem cells was employed.

In attempt to answer these questions, the first step was to establish how Caspases are activated in DCN of studied PD model. To achieve this, the aim was to identify the pathway or pathways that trigger Caspase activation in DCN of PD. It was important to determine how Caspase-2, -4 and -8 are activated and which pathways they follow were investigated using ReNcell VM stem cell line that had been differentiated in DCN and treated with 6OHDA (Chapter 4).

In the current study the universal Caspase inhibitor, zVADfmk had demonstrated that 6OHDA triggered Caspase mediated death of dDCN(Chapter 4, Chaudhry and Ahmed 2013). TUNEL staining had confirmed that 6OHDA triggered apoptotic death of dDCN. TUNEL assay with wide range inhibitors showed involvement of NFκB, PERK, Caspases-2,-4 and -8 in apoptotic death of 6OHDA dDCN (Chapter 4 Figure 4.17 and Figure 4.19). In addition, co localisation studies showed active Caspases-2,-3 and-8 were present in 6OHDA-treated dDCN, indicating 6OHDA triggers Caspases-2 and -8 followed by Caspase-3 in dDCN (Chapter Figure 4.4-Figure 4.7). WB analysis showed zVADfmk decreased Caspase-2,-3 and -8 levels in dDCN (Chapter 4 Figure 4.11-Figure 4.15). Therefore, it was appropriate to conclude that 6OHDA had triggered apoptotic death of dDCN successfully establishing a suitable PD model to investigate potential pathways that stimulate Caspases (Chapter 4, Chaudhry and Ahmed 2013).

In order to understand potential pathways which cause Caspase activation leading to death of dDCN, the NFκB pathway was explored (Chapter 5). The IKK inhibitor that is specific to prevent activation of NFκB classical pathway was used to explore the impact NFκB classical pathway has on Caspase activation in 6OHDA-treated dDCN(Chapter 5 Figure 5.15-Figure 5.43). Co-localisation studies illustrated that 6OHDA triggered activation of Caspases-2, -3 and -8, along with active NFκB expression in dDCN (Chapter 5 Figure 5.6). The specific NFκB inhibitor, IKK was used to investigate if the NFκB classical pathway promoted activation of Caspases-2, -4 and -8 resulting in apoptotic death of dDCN (Chapter 5 Figure 5.15- Figure 5.41). Cell viability, IF and WB analysis revealed that IKK inhibited Caspases-2 and-8 activities and promoted survival of treated dDCN (Chapter 5 Figure 5.15-Figure 5.32). In comparison, Caspase-4 was not affected by IKK inhibitor as IKK was not able to suppress Caspase-4 activity suggesting that Caspase-4 is stimulated via alternative pathway (Chapter 5 Figure 5.33-Figure 5.41). In addition, the combination of Caspase-4 inhibitor and IKK increased cell survival of 6OHDA-treated dDCN, indicating that there are two separate pathways that are causing apoptosis of 6OHDA-treated dDCN (Chapter 5, Figure 5.41-Figure 5.43).

Subsequently, it was essential to determine if ER stress was involved in Caspase activation in 6OHDA-treated dDCN (Chapter 6). Salubrinal, a specific inhibitor of the ER stress pathway was used to investigate if the PERK pathway promoted activation of Caspases-2,-4 and -8, resulting in apoptotic death of dDCN (Chapter 6 Figure 6.7-Figure 6.35). Cell viability, IF and WB analysis revealed that salubrinal inhibited Caspase-2 activity and promoted survival of treated dDCN. 6OHDA triggered activation of Caspase-2, via PERK pathway in dDCN (Chapter 6 Figure 6.7-Figure 6.12). In comparison, Caspases-4 and-8 was not inhibited by salubrinal suggesting that PERK pathway does not influence activation of these Caspases in 6OHDA-treated dDCN (Chapter 6 Figure 6.14-Figure 6.33). Collectively, the results illustrated that the PERK ER stress pathway plays a vital role in death of 6OHDA dDCN (Chapter 6 Figure 6.35). IF and cell viability assays using a range of specific inhibitors demonstrated that 6OHDA stimulates activation of Caspases-2,-4 and -8 independently and that there is no cross talk between these Caspases in dDCN (Chapter 6, Figure 6.7-Figure 6.35).

It was vital to investigate if NFκB classical pathway and ER stress pathway are dependent of each other and if one pathway provokes activation of the other pathway in 6OHDA-treated dDCN (Chapter 6). To achieve this aim, specific inhibitors, IKK and salubrinal were used to determine if NFκB and PERK ER stress pathway followed the same route or if they independently promoted death of 6OHDA-treated dDCN by separate routes. The results demonstrated that 6OHDA triggered NFκB classical pathway and ER stress pathway via independent different routes, resulting in death of dDCN. Activation of NFκB classical pathway did not influence activation of ER stress pathway or vice versa, emphasizing that both pathways are activated by 6OHDA independently (Chapter 6, Figure 6.39). To confirm this, the combination of IKK and salubrinal prevented further death and increased more cell survival of 6OHDA-treated dDCN then using one inhibitor alone (Chapter 6 Figure 6.36-Figure 6.42). The additional effect measured when combining both inhibitors highlighted that 6OHDA triggers NFκB and ER stress activation through different pathways resulting in death of dDCN. Inhibition of the PERK ER stress pathway using salubrinal and suppression of NFκB pathway using IKK gives a greater increase of cell survival, compared to inhibiting one pathway alone (Figure 6.36-Figure 6.42. 6OHDA equally triggers two main pathways the PERK ER stress and NFκB classical pathway resulting in death of dDCN (Chapter 6 Figure 6.36-Figure 6.42).

Results obtained from animal data and cell line illustrate the presence of Caspases in vivo and in vitro PD model. The findings from MPTP-treated animal model and 6OHDA-treated cell line demonstrate Caspase activation. MPTP-treated animal model demonstrated an increase in Caspases-2,-3,-8,-9 and -12 in different brain regions. In contrast, 6OHDA stimulated Caspases-2,-3,-4 and -8 in dDCN. In differentiated cell line, specific Caspases inhibitors such as zLEVDfmk, zVDVADfmk, zIETDfmk and zVADfmk were used to competitively inhibit Caspases activation. In PD animal model, endurance exercise was used to determine if it can act as a potential inhibitor to suppress Caspase activation in different brain regions. An increase in activity of the calcium binding protein CAMK-IV was found in the midbrain and striatum of MPTP-treated rats that underwent six week endurance exercise.

Prevention of PERK ER Stress and NFκB pathway had significantly increased survival and slowed death of 6OHDA-treated dDCN but there was still cell death occurring, indicating that it is possible that there is another potential route that is needed to be identified (Figure 7.1). Activation of Caspase-4 remains to be investigated and it is possible that calcium may influence Caspase-4 activity resulting in apoptotic death of dDCN (Figure 7.1). The final outcomes of both PD animal model and cell model indicate a positive direction to explore the impact of calcium for future studies. Calcium regulation plays a vital role in ER function. Calcium imbalance could lead to UPS and ER stress and activation of Caspase mediated death of dDCN. Research has shown Calpain can activate Caspases due to calcium imbalance (Ozcan and Tabas 2012). It is plausible that Calpain can activate Caspases resulting in apoptotic death of dDCN via calcium mechanisms.

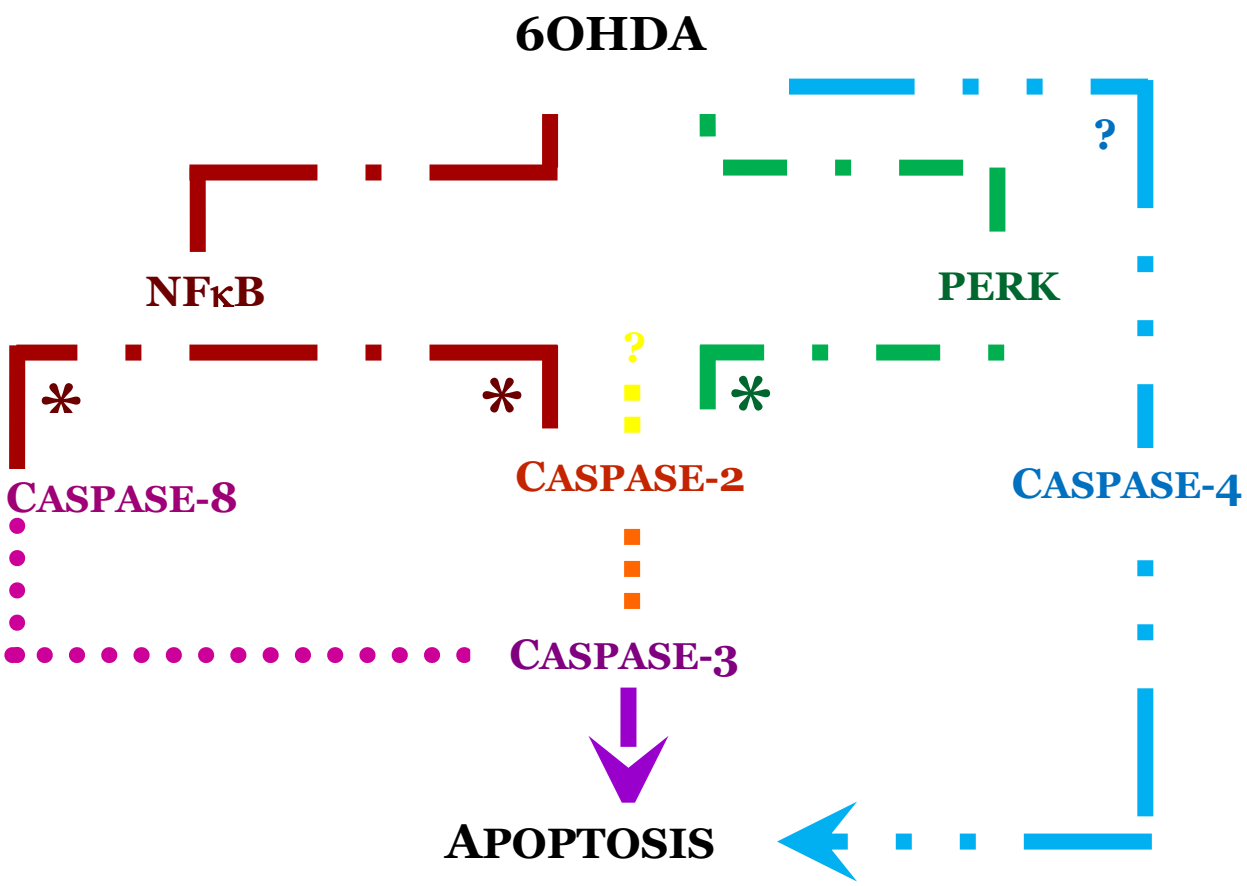

Figure 7.1 : 6OHDA Triggers Caspase Mediated Apoptotic Death of dDCN, via PERK ER stress and NFκB Pathway

It was important to determine how Caspases are activated, which pathways they follow and if there is a major or several pathways, which cause Caspase activation leading to death of dDCN.

6OHDA triggered activation of PERK ER Stress and NFκB classical pathway in dDCN. PERK ER Stress pathway stimulates activation Caspase-2 in 6OHDA-treated dDCN. NFκB classical pathway stimulates activation of Caspases-2 and -8 6OHDA-treated dDCN. 6OHDA stimulated Caspase-4 leading to apoptotic death of dDCN. Inhibition of PERK ER stress pathway suppresses Caspase-2 activity in 6OHDA-treated dDCN. Complete suppression of NFκB classical pathway inhibited Caspase-2 and -8 activation in 6OHDA-treated dDCN. Identifying proteins that are downstream from PERK ER stress and NFκB but are upstream from Caspases-2 and -8 will give a better understanding and provide potential targets that can be used to safely inhibit apoptotic death of DCN without disturbing normal cellular function.

The results from the current study have shown that 6OHDA triggers Caspase-2, -3, -4 and -8 activation via ER and NFκB mediated death of dDCN (Figure 7.1). Suppression of NFκB pathway and ER stress pathway using specific inhibitors IKK and salubrinal prevented downstream events to take place, such as Caspase activation, resulting in survival of dDCN. WB analysis demonstrated that exercise had shown a link between elevated CAMK-IV levels and reduced activation of Caspases in midbrain and striatum of PD animal model (Chapter 3 Figure 3.50-Figure 3.51). The results from the current study have exposed further questions that need to be explored, discovered and addressed (as discussed below). The results from the study have shown that PERK, and NFκB are upstream factors which cause death of dDCN, but the question remains how they are exactly activated (Figure 7.1). Do other proteins trigger activation of PERK, and NFκB or is there activation a direct result of elevated production of ROS caused by 6OHDA in dDCN? Even more curious is determining how ER stress and NFκB, which are both initially promoting survival of dDCN, can switch to provoking death of dDCN. Although the results show that ER stress pathway and NFκB pathway are triggered by 6OHDA separately, it may be that the two pathways have a common switch, that is more upstream, which when activated, results in death of dDCN.

Collectively, results from PD animal model and in dDCN have shown that calcium plays a crucial role in PD, and have shown the need to explore the influence of calcium in 6OHDA-treated DCN. A future aim would be to determine how calcium switches from having favourable to adverse effects in 6OHDA-treated dDCN. What key events are involved and are there several proteins that promote calcium to switch from encouraging cell survival to cause cell death of dDCN. Moreover, is elevated ROS production directly provoking the calcium switch, resulting in Caspases dependent death in dDCN or if there is a presence in a series of events that occur before calcium levels are increased? Calpain are calcium dependent proteins found in the cytosol of cells and have been associated with Caspase activation as a result of calcium imbalance and ER stress (Fan et al 2005, Higuchi et al 2005, Chaudhry and Ahmed 2014, Ozcan and Tabas 2012, Itohara and Saido 2005). To extend the current study, it would be of

interest to explore the role of Calpain in calcium-dependent death of dDCN. The aim could be to determine if Calpain works as an upstream protein, if it can activate a specific Caspase and its role in calcium or ER stress mediated death of 6OHDA-treated dDCN.

Calcium is vital for synaptic transmission as well as production of neurotransmitters, yet elevated calcium levels may trigger Caspases dependant death of dDCN (Cali et al 2011, Surmeier 2009, Subramaniam and Chesselet 2013, Cesaro and Defebvre 2014). Specifically, the concentration of calcium in the ER and cytosol could be measured to determine if 6OHDA can trigger leakage of calcium from the ER stores into the cytosol in a time frame of 0 to 24 hour cycle. The data obtained would provide important information at which time frame calcium can promote apoptotic death of DCN. The calcium inhibitor nimodipine may be used to determine if calcium levels have an influence in treated DCN (Li et al 2009). Another future aim would be to determine if Caspases-2,-4 and -8 were present in tunicamycin or thapsigargin induced dDCN. This would determine if PERK and changes in calcium level influence death of dDCN.

Although the results with the use of inhibitors, have clearly demonstrated that specific Caspases follow particular routes, a different approach could have also been used to understand the mechanism which activates Caspase in dDCN. ELISA Caspase specific assays (Life Technologies UK) could have been performed to detect and measure the level of Caspases-2, -3, -8 and -12 in 6OHDA dDCN. Electron microscopy could have been used to examine different layers of each brain region of PD animal model, in depth as this would provide further background on how treadmill exercise is affecting each brain region of PD animal model. Research has shown that PD patients find it difficult to express emotion, which may be due to disruption of the cranial nerves, more specifically the facial nerve being affected (Mu et al 2013, Thomas and Le 2004). Another exploration would be to determine the effect of Caspases and the pathways in relation to cranial nerves in PD in vitro and in animal model. Does activation of Caspases cause disruption of the facial nerve and to what extent is the damage? Are both

the ER stress pathway and NFκB pathway causing destruction of the facial nerve or if there is another pathway that contributing death of dDCN?

The complete suppression of PERK ER stress and NFκB classical pathway inhibited activation of Caspases-2 and -8 in 6OHDA dDCN. However, total inhibition of these pathways may contribute or ignite new problems at a cellular and physiological level, as both pathways are involved in a diverse range of processes that regulate healthy cells (Asanuma et al 2004, Cassarino et al 2000, Yamamoto and Gaynor 2001, Todd et al 2008, Oakes and Papa 2014, Sano and Reed 2013). Therefore, there is a need to further understand and define the involvement of other proteins that act downstream from NFκB and PERK, but upstream to the Caspases. These newly identified proteins would be better targets to safely suppress Caspase activation and slow death of 6OHDA dDCN, without impacting other cellular mechanisms (Figure 7.1).

It is essential to understand at which point NFκB and PERK switches from cell survival to apoptotic route need to be determined, which key markers and proteins are involved need to be established (Chaudhry and Ahmed 2014). To achieve this , a time interval study , could be carried out to identify which well known ER proteins such as PERK, eIF2-α, CHOP, XBP1, GRP78 and Caspases-2,-3,-4 and-8 are present in 6OHDA-treated dDCN. The presence and absence of these proteins may aid in establishing a pathway by indicating which proteins are present and absent at a particular time using the cleaved and active form of these proteins in WB analysis. The time interval would start at 0 times and the interval would be every half hour for a 24 hour cycle which would determine at which time frame each specific protein is either up regulated or down regulated, present or absent after treatment with 6OHDA. This set up could also be carried out when cells are treated with tunicamycin or thapsigargin for a 24 hours cycle and comparisons can be made. The results obtained would determine the involvement of key proteins that are acting upstream and/or downstream and would give a clearer image as to how Caspases are being activated in 6OHDA-induced dDCN. It may be that there is an upstream key protein that overlaps two proteins or is common in both PERK and NFκB pathway, which has the

potential to trigger the Caspases, can be revealed. Subsequently, this protein can be targeted and manipulated to prevent and slow death of dDCN. The NFκB pathway and PERK ER stress pathway are both vital in other normal cellular functions, therefore the total suppression of these pathways would inhibit specific Caspase activation, but it may hold the potential to cause other cellular abnormalities, which could be more disastrous. Taken this into account, a future aim would be to identify key proteins that act downstream from NFκB and PERK but act upstream from the Caspases, and to target these proteins (Figure 7.1).

In addition, isolation of cellular components such as mitochondria, ER , cytosol and nucleus may give a better understanding as to how 6OHDA can triggers Caspase activation and death of dDCN. Isolation of ER can be achieved using ER isolation kit (Sigma-Aldrich UK 2011) where suspended cells undergo a series of separation using centrifugation followed by fractionating the columns centrifuged x 600g for 10 minutes. The supernatant would be removed, and cells would be incubated for 20 minutes with hypotonic extraction buffer (10mM HEPES, 25mM potassium chloride, 1mM EGTA, analytical water, protease inhibitor cocktail) at 4°C. Subsequently, cells would be centrifuged x 600g for 10 minutes after which the supernatant would be removed. Isotonic buffer (10mM HEPES, 25mM potassium chloride , 1mM EGTA, 250mM sucrose, analytical water, protease inhibitor cocktail) would be added and cells would be homogenised using Dounce homogeniser. The homogenate would be centrifuged x 1000g for 15 minutes at 4°C. The supernatant would be transferred to another tube and the post mitochondrial fraction would be ultracentrifuged for 60 minutes x 100, 000g. The supernatant would be removed and the pellet (microsomal fraction) would be homogenised completely in isotonic extraction buffer. Microsomal fraction would contain the crude ER. Calcium activation kit could be used to measure the amount of calcium in the ER, cytosol, nuclei and mitochondria in untreated and treated DCN. Another method to measure amount of calcium in whole DCN is with the use of fluorescent probes. Treated and untreated cells could be collected and centrifuged at 1000rpm for 3 minutes. The old medium would be removed and cell pellet would be resuspended in Fluo4 direct assay buffer in 96 well plate. The plate

would be incubated at 37°C and 5% CO_2 for 60 minutes to allow the cells to settle. Finally, the fluorescence would be measured at excitation at 494 nm and emission at 516 nm.

The effect of 6OHDA caused in the purified cellular components can be looked at over a time interval and the effect of Caspases-2,-4 and -8 can be studied. To expand on this work Caspase and Calpain inhibitors can be used to determine if they can reduce death of 6OHDA-treated DCN. Calcium and Calpain involvement can be explored in 6OHDA dDCN and its involvement with Caspase activation and death of dDCN can be determined. This study has not explored the intrinsic pathway (mitochondrial) and its involvement in DCN. Is calcium a cause or effect of collapse of mitochondria? What is the impact of exercise on mitochondrial dependant activation of the Caspases in DCN? Previous research has shown that Caspase-12 can trigger Caspase-9 followed by Caspase-3 (Alteri 2010, Nakamura et al 2012, Chowdhury 2013, Chaudhry and Ahmed 2014, McIlwain et al 2013). In this study, Caspase-12 was looked at in animal model and was substituted with Caspase 4 in dDCN. It would be interesting to investigate if Caspase-4 able to promote Caspase-9 activation without the presence of the mitochondria. Does Caspase-12 or any other Caspases intensify death of DCN, via mitochondrial death of dDCN?

Another important aspect to determine is the amount and type of ROS that are causing death of dopaminergic neurons after 6OHDA treatment. This could be achieved using specific cellular ROS detection kit (Abcam UK 2015), which would measure the amount of ROS in the cell. After diffusion in to the cell, DCFDA is deacetylated by cellular esterases to a non-fluorescent compound, which is later oxidized by ROS into 2', 7'-dichlorofluorescin (DCF). DCF is a highly fluorescent compound, which can be detected by fluorescence spectroscopy with maximum excitation and emission spectra of 495nm and 529nm respectively. After cells have reached 85% confluence cells would treated as before (100µM 6OHDA 2 hour exposure). Cells would be collected, centrifuged and washed with cold PBS buffer following incubation with 20µM DCFDA for 30 minutes at 37°C in the dark. Cells would be washed again with PBS and supplementary buffer containing 10% FBS. Absorbance would be read at excitation

wavelength at 485 nm and emission wavelength at 535 nm. Quantitative analysis would be achieved using microplate reader to measure the amount of hydroxyl, peroxyl and other ROS activity inside the cell before and after treatment. Hydrogen peroxide may be used as a positive control.

Furthermore, the amount of ROS and RNS may be measured using Oxiselect InVitro ROS/RNS Assay kit (Cambridge Bioscience UK 2015). Cells would be treated with 6OHDA at 2 hours after reaching 85% confluence. Cells would be collected, centrifuged at 10000g for 5 minutes and washed with PBS. Fresh PBS would be added to the cells along with catalase. The quenching fluorogenic probe, dichlorodihydrofluorescin DiOxyQ (DCFH-DiOxyQ) would be added to the homogenate with priming solution, mixed and left to incubate for 30 minutes at RT. The stabilising solution would be added to the cells and mixed to stabilise to its reactive DCFH form. The RNS and ROS react to DCFH and is oxidised to DCF and absorbances would be measured at 485nm excitation wavelength. Quantitative analysis could be achieved to measure the levels of hydrogen peroxide, peroxyl radical, nitric oxide, and peroxynitrite anion against a DCF standard curve.

7.2 Clinical relevance

Although previous and current research has shown that treadmill exercise can decrease PD symptoms they have not been clear as to how exercise is able to cause such benefits. Furthermore current research has looked at the consequence of exercise but not the cause of the positive effects (Tomsilon et al 2012, Herman et al 2007, Canning et al 2012). Only through understanding how exercise can improve PD, can effective treatments be made. An in-depth knowledge on what impact exercise has on DCN, which pathways it can stimulate and suppress and specific proteins to inhibits or activate in DCN are crucial to understand.

The results from the proposed study will provide further answers to which pathways (ER, mitochondrial, NFκB) play a major role in regulating Caspases causing apoptotic cell death in PD, and if by inhibiting one or two major pathways can reduce further cell death in PD. Through understanding the molecular pathways regulating cell death in DCN in PD, new potential targets for therapy, such as specific drugs which target particular proteins of the major pathways, may be identified, which may ultimately reduce further death of DCN and slow PD progression (Figure 7.1). At present L-DOPA is used in combination with physical therapy as a form of treatment for PD patients (Singer et al 2012, LeWitt 2015, Pourmoghaddam et al 2015). This proposed study may have the potential to seek for more efficient drugs which can suppress Caspase activation by targeting key targets in the pathways that the Caspases follow. These new specific targeted drugs could be used with treadmill exercise to achieve maximum effect, by slowing down or inhibiting further death of DCN.

Reference

Abcam UK. (2015).*Cellular ROS Detection Assay Kit*. pp 1-24. London: Abcam.

Addabbo, F., Montagnani, M. and Goligorsky, M. S. (2009). Mitochondria and reactive oxygen species. *Hypertension* **53,** 885-892.

Aguila, J. C., Hedlund, E. and Sanchez-Pernaute, R. (2012). Cellular programming and reprogramming: Sculpting cell fate for the production of dopamine neurons for cell therapy. *Stem cells international* **2012,**.

Akimoto, T., Ribar, T. J., Williams, R. S. and Yan, Z. (2004). Skeletal muscle adaptation in response to voluntary running in Ca2+/calmodulin-dependent protein kinase IV-deficient mice. *Am. J. Physiol. Cell. Physiol.* **287,** C1311-9.

Ali H. The effect of endurance exercise on CAMK I and II activity in parkinsons disease. **verbal discussion on laboratory results (unpublished) in relation to CAMK in PD rat brain regions,**.

Al-Jarrah, M., Pothakos, K., Novikova, L., Smirnova, I. V., Kurz, M. J., Stehno-Bittel, L. and Lau, Y. (2007). Endurance exercise promotes cardiorespiratory rehabilitation without neurorestoration in the chronic mouse model of parkinsonism with severe neurodegeneration. *Neuroscience* **149,** 28-37.

Altieri, D. (2010). Survivin and IAP proteins in cell-death mechanisms. *Biochem. J.* **430,** 199-205.

Andersen, J. K. (2001). Does neuronal loss in parkinson's disease involve programmed cell death? *Bioessays* **23,** 640-646.

Andrabi, S. A., Dawson, T. M. and Dawson, V. L. (2008). Mitochondrial and nuclear cross talk in cell death. *Ann. N. Y. Acad. Sci.* **1147,** 233-241.

Anstrom, K. K., Schallert, T., Woodlee, M. T., Shattuck, A. and Roberts, D. (2007). Repetitive vibrissae-elicited forelimb placing before and immediately after unilateral 6-hydroxydopamine improves outcome in a model of parkinson's disease. *Behav. Brain Res.* **179,** 183-191.

Arduíno, D. M., Esteves, A. R., Cardoso, S. M. and Oliveira, C. R. (2009). Endoplasmic reticulum and mitochondria interplay mediates apoptotic cell death: Relevance to parkinson's disease. *Neurochem. Int.* **55,** 341-348.

Arduino, D. M., Esteves, A. R., Domingues, A. F., Pereira, C. M., Cardoso, S. M. and Oliveira, C. R. (2009). ER-mediated stress induces mitochondrial-dependent caspases activation in NT2 neuron-like cells. *BMB Rep.* **42,** 719-724.

Arduino, D., Silva, D., Cardoso, S. M., Chaves, S., Oliveira, C. R. and Santos, M. A. (2008). New hydroxypyridinone iron-chelators as potential anti-neurodegenerative drugs. *Front. Biosci.* **13,** 6763-6774.

Asanuma, M., Miyazaki, I., Diaz-Corrales, F. J., Miyoshi, K., Ogawa, N. and Murata, M. (2008). Preventing effects of a novel anti-parkinsonian agent zonisamide on dopamine quinone formation. *Neurosci. Res.* **60,** 106-113.

Asanuma, M., Miyazaki, I., Diaz-Corrales, F. J. and Ogawa, N. (2004). Quinone formation as dopaminergic neuron-specific oxidative stress in the pathogenesis of sporadic parkinson's disease and neurotoxin-induced parkinsonism. *Acta Med. Okayama* **58,** 221-234.

Ascensao, A., Goncalves, I., Lumini-Oliveira, J., Marques-Aleixo, I., Dos Passos, E., Rocha-Rodrigues, S., Machado, N., Moreira, A., Oliveira, P. and Torrella, J. (2012). Endurance training and chronic intermittent hypoxia modulate in vitro salicylate-induced hepatic mitochondrial dysfunction. *Mitochondrion* **12,** 607-616.

Ascensão, A., Lumini-Oliveira, J., Machado, N., Ferreira, R., Goncalves, I., Moreira, A., Marques, F., Sardao, V., Oliveira, P. and Magalhães, J. (2011). Acute exercise protects against calcium-induced cardiac mitochondrial permeability transition pore opening in doxorubicin-treated rats. *Clin. Sci.* **120,** 37-49.

Ascensao, A., Goncalves, I., Lumini-Oliveira, J., Marques-Aleixo, I., Dos Passos, E., Rocha-Rodrigues, S., Machado, N., Moreira, A., Oliveira, P. and Torrella, J. (2012). Endurance training and chronic intermittent hypoxia modulate< i> in vitro</i> salicylate-induced hepatic mitochondrial dysfunction. *Mitochondrion* **12,** 607-616.

Ascensão, A., Lumini-Oliveira, J., Machado, N., Ferreira, R., Goncalves, I., Moreira, A., Marques, F., Sardao, V., Oliveira, P. and Magalhães, J. (2011). Acute exercise protects against calcium-induced cardiac mitochondrial permeability transition pore opening in doxorubicin-treated rats. *Clin. Sci.* **120,** 37-49.

Avila, I., Parr-Brownlie, L. C., Brazhnik, E., Castañeda, E., Bergstrom, D. A. and Walters, J. R. (2010). Beta frequency synchronization in basal ganglia output during rest and walk in a hemiparkinsonian rat. *Exp. Neurol.* **221,** 307-319.

Ayán, C. and Cancela, J. (2012). Feasibility of 2 different water-based exercise training programs in patients with parkinson's disease: A pilot study. *Arch. Phys. Med. Rehabil.* **93,** 1709-1714.

Aznavour, N., Cendres-Bozzi, C., Lemoine, L., Buda, C., Sastre, J., Mincheva, Z., Zimmer, L. and Lin, J. (2012). MPTP animal model of parkinsonism: Dopamine cell death or only tyrosine hydroxylase impairment?–A study using PET imaging, autoradiography, and immunohistochemistry in the cat. *CNS neuroscience & therapeutics* **18,** 934-941.

Balleine, B. W., Delgado, M. R. and Hikosaka, O. (2007). The role of the dorsal striatum in reward and decision-making. *J. Neurosci.* **27,** 8161-8165.

Bazzu, G., Rocchitta, G., Migheli, R., Alvau, M. D., Zinellu, M., Puggioni, G., Calia, G., Mercanti, G., Giusti, P. and Desole, M. S. (2013). Effects of the neurotoxin MPTP and pargyline protection on extracellular energy metabolites and dopamine levels in the striatum of freely moving rats. *Brain Res.* **1538,** 159-171.

Bellissimo, M. I., Kouzmine, I., Ferro, M. M., de Oliveira, B. H., Canteras, N. S. and Da Cunha, C. (2004). Is the unilateral lesion of the left substantia nigra pars compacta sufficient to induce working memory impairment in rats? *Neurobiol. Learn. Mem.* **82,** 150-158.

Bender, A., Krishnan, K. J., Morris, C. M., Taylor, G. A., Reeve, A. K., Perry, R. H., Jaros, E., Hersheson, J. S., Betts, J. and Klopstock, T. (2006). High levels of mitochondrial DNA deletions in substantia nigra neurons in aging and parkinson disease. *Nat. Genet.* **38,** 515-517.

Bisaglia, M., Filograna, R., Beltramini, M. and Bubacco, L. (2014). Are dopamine derivatives implicated in the pathogenesis of parkinson's disease? *Ageing research reviews.*

Bogaerts, V., Theuns, J. and Van Broeckhoven, C. (2008). Genetic findings in Parkinson's disease and translation into treatment: A leading role for mitochondria? *Genes, Brain and behavior* .**7,** 129-151.

Bové, J., Prou, D., Perier, C. and Przedborski, S. (2005). Toxin-induced models of parkinson's disease. *NeuroRx* **2,** 484-494.

Bowser, D. N. and Khakh, B. S. (2004). ATP excites interneurons and astrocytes to increase synaptic inhibition in neuronal networks. *J. Neurosci.* **24,** 8606-8620.

Brazhnik, E., Cruz, A. V., Avila, I., Wahba, M. I., Novikov, N., Ilieva, N. M., McCoy, A. J., Gerber, C. and Walters, J. R. (2012). State-dependent spike and local field synchronization between motor cortex and substantia nigra in hemiparkinsonian rats *J. Neurosci.* **32,** 7869-7880.

Brown, L. A., de Bruin, N., Doan, J., Suchowersky, O. and Hu, B. (2010). Obstacle crossing among people with parkinson disease is influenced by concurrent music *J. Rehabil. Res. Dev.* **47,** 225-231.

Cali, T., Ottolini, D. and Brini, M. (2011). Mitochondria, calcium, and endoplasmic reticulum stress in parkinson's disease. *Biofactors* **37,** 228-240.

Cambridge BioScience UK. (2015). OxiSelect™ In Vitro ROS/RNS Assay Kit. pp1-11: San Diego.Cell Biolabs

Canning, C. G., Allen, N. E., Dean, C. M., Goh, L. and Fung, V. S. (2012). Home-based treadmill training for individuals with parkinson's disease: A randomized controlled pilot trial. *Clin. Rehabil.* **26,** 817-826.

Cassarino, D. S., Halvorsen, E. M., Swerdlow, R. H., Abramova, N. N., Parker, W. D.,Jr, Sturgill, T. W. and Bennett, J. P.,Jr. (2000). Interaction among mitochondria, mitogen-activated protein kinases, and nuclear factor-kappaB in cellular models of parkinson's disease *J. Neurochem.* **74,** 1384-1392.

Castro, A. A., Ghisoni, K., Latini, A., Quevedo, J., Tasca, C. I. and Prediger, R. D. (2012). Lithium and valproate prevent olfactory discrimination and short-term memory impairments in the intranasal 1-methyl-4-phenyl-1, 2, 3, 6-tetrahydropyridine (MPTP) rat model of parkinson's disease. *Behav. Brain Res.* **229,** 208-215.

Castro, A. A., Wiemes, B. P., Matheus, F. C., Lapa, F. R., Viola, G. G., Santos, A. R., Tasca, C. I. and Prediger, R. D. (2013). Atorvastatin improves cognitive, emotional and motor impairments induced by intranasal 1-methyl-4-phenyl-1, 2, 3, 6-tetrahydropyridine (MPTP) administration in rats, an experimental model of parkinson's disease. *Brain Res.* **1513,** 103-116.

Cesaro, P. and Defebvre, L. (2014). Drug treatment of early-stage (de novo and "honeymoon") parkinson disease. *Rev. Neurol. (Paris).*

Chae, H. J., Kim, H. R., Xu, C., Bailly-Maitre, B., Krajewska, M., Krajewski, S., Banares, S., Cui, J., Digicaylioglu, M., Ke, N. et al. (2004). BI-1 regulates an apoptosis pathway linked to endoplasmic reticulum stress. *Mol. Cell* **15,** 355-366.

Chan, C. S., Gertler, T. S. and Surmeier, D. J. (2009). Calcium homeostasis, selective vulnerability and parkinson's disease. *Trends Neurosci.* **32,** 249-256.

Chandra, J. and Orrenius, S. (2002). Mitochondria, oxygen metabolism and the regulation of cell death. **1233,** 259-272.

Chandra, D., Liu, J. W. and Tang, D. G. (2002). Early mitochondrial activation and cytochrome c up-regulation during apoptosis. *J. Biol. Chem.* **277,** 50842-50854.

Chaudhary, P. M., Eby, M. T., Jasmin, A., Kumar, A., Liu, L. and Hood, L. (2000). Activation of the NF-κB pathway by caspase 8 and its homologs. *Oncogene* **19,**.

Chaudhry, Z. L. and Ahmed, B. Y. (2013). Caspase-2 and caspase-8 trigger caspase-3 activation following 6-OHDA-induced stress in human dopaminergic neurons differentiated from ReNVM stem cells. *Neurol. Res.* **35,** 435-440.

Chaudhry, Z. L. and Ahmed, B. Y. (2014), The Role of Caspases in Parkinson's disease Pathogenesis: A brief look at the Mitochondrial Pathway, *Journal of Austin Alzheimer and Parkinson disease*, **1**, 4, 1-5.

Chen, G., Bower, K. A., Ma, C., Fang, S., Thiele, C. J. and Luo, J. (2004). Glycogen synthase kinase 3beta (GSK3beta) mediates 6-hydroxydopamine-induced neuronal death. *FASEB J.* **18,** 1162-1164.

Chen, L. H., Jiang, C. C., Watts, R., Thorne, R. F., Kiejda, K. A., Zhang, X. D. and Hersey, P. (2008). Inhibition of endoplasmic reticulum stress-induced apoptosis of melanoma cells by the ARC protein. *Cancer Res.* **68,** 834-842.

Chen, S., Zhang, X., Yang, D., Du, Y., Li, L., Li, X., Ming, M. and Le, W. (2008). D2/D3 receptor agonist ropinirole protects dopaminergic cell line against rotenone-induced apoptosis through inhibition of caspase-and JNK-dependent pathways. *FEBS Lett.* **582,** 603-610.

Cheng, A., Hou, Y. and Mattson, M. P. (2010). Mitochondria and neuroplasticity.

Chien, W., Lee, T., Hung, S., Kang, K., Wu, R., Lee, M. and Fu, W. (2013). Increase of oxidative stress by a novel PINK1 mutation, P209A. *Free Radical Biology and Medicine* **58,** 160-169.

Chinta, S. J., Poksay, K. S., Kaundinya, G., Hart, M., Bredesen, D. E., Andersen, J. K. and Rao, R. V. (2009). Endoplasmic reticulum stress-induced cell death in dopaminergic cells: Effect of resveratrol. *J. Mol. Neurosci.* **39,** 157-168.

Chinta, S. J., Rane, A., Poksay, K. S., Bredesen, D. E., Andersen, J. K. and Rao, R. V. (2008). Coupling endoplasmic reticulum stress to the cell death program in dopaminergic cells: Effect of paraquat. *Neuromolecular Med.* **10,** 333-342.

Choi, J. G., Kim, H. G., Kim, M. C., Yang, W. M., Huh, Y., Kim, S. Y. and Oh, M. S. (2011). Polygalae radix inhibits toxin-induced neuronal death in the parkinson's disease models. *J. Ethnopharmacol.* **134,** 414-421.

Chung, H., Chung, H. Y., Bae, C. W., Kim, C. J. and Park, S. (2011). Ghrelin suppresses tunicamycin- or thapsigargin-triggered endoplasmic reticulum stress-mediated apoptosis in primary cultured rat cortical neuronal cells. *Endocr. J.* **58,** 409-420.

Chowdhury, I., Tharakan, B. and Bhat, G. K. (2008). Caspases - an update *Comp. Biochem. Physiol. B. Biochem. Mol. Biol.* **151,** 10-27.

Cohen, A. D., Tillerson, J. L., Smith, A. D., Schallert, T. and Zigmond, M. J. (2003). Neuroprotective effects of prior limb use in 6-hydroxydopamine-treated rats: Possible role of GDNF. *J. Neurochem.* **85,** 299-305.

Colla, E., Coune, P., Liu, Y., Pletnikova, O., Troncoso, J. C., Iwatsubo, T., Schneider, B. L. and Lee, M. K. (2012). Endoplasmic reticulum stress is important for the manifestations of alpha-synucleinopathy in vivo. *J. Neurosci.* **32,** 3306-3320.

Colla, E., Jensen, P. H., Pletnikova, O., Troncoso, J. C., Glabe, C. and Lee, M. K. (2012). Accumulation of toxic alpha-synuclein oligomer within endoplasmic reticulum occurs in alpha-synucleinopathy in vivo. *J. Neurosci.* **32,** 3301-3305.

Cookson, M. R. (2005). The biochemistry of parkinson's disease*. *Annu. Rev. Biochem.* **74,** 29-52.

Cookson, M. R., Hardy, J. and Lewis, P. A. (2008). Genetic neuropathology of parkinson's disease. *Int. J. Clin. Exp. Pathol.* **1,** 217-231.

Cooper, S. E., McIntyre, C. C., Fernandez, H. H. and Vitek, J. L. (2012). Association of deep brain stimulation washout effects with parkinson disease duration *Arch. Neurol.*, 1-5.

D'Orazio, N., Gammone, M. A., Gemello, E., De Girolamo, M., Cusenza, S. and Riccioni, G. (2012). Marine bioactives: Pharmacological properties and potential applications against inflammatory diseases. *Marine drugs* **10,** 812-833.

De Dreu, M., Van der Wilk, A., Poppe, E., Kwakkel, G. and Van Wegen, E. (2012). Rehabilitation, exercise therapy and music in patients with parkinson's disease: A meta-analysis of the effects of music-based movement therapy on walking ability, balance and quality of life. *Parkinsonism Relat. Disord.* **18,** S114-S119.

De Erausquin, G. A., Hyrc, K., Dorsey, D. A., Mamah, D., Dokucu, M., Masco, D. H., Walton, T., Dikranian, K., Soriano, M., Garcia Verdugo, J. M. et al. (2003). Nuclear translocation of nuclear transcription factor-kappa B by alpha-amino-3-hydroxy-5-methyl-4-isoxazolepropionic acid receptors leads to transcription of p53 and cell death in dopaminergic neurons. *Mol. Pharmacol.* **63,** 784-790.

De Zeeuw, C. I. and Yeo, C. H. (2005). Time and tide in cerebellar memory formation. *Curr. Opin. Neurobiol.* **15,** 667-674.

Decressac, M., Mattsson, B. and Björklund, A. (2012). Comparison of the behavioural and histological characteristics of the 6-OHDA and α-synuclein rat models of parkinson's disease. *Exp. Neurol.* **235,** 306-315.

Dimant, H., Kalia, S. K., Kalia, L. V., Zhu, L. N., Kibuuka, L., Ebrahimi-Fakhari, D., McFarland, N. R., Fan, Z., Hyman, B. T. and McLean, P. J. (2013). Direct detection of alpha synuclein oligomers in vivo. *Acta neuropathologica communications* **1,** 1-10.

Donato, R., Miljan, E. A., Hines, S. J., Aouabdi, S., Pollock, K., Patel, S., Edwards, F. A. and Sinden, J. D. (2007). Differential development of neuronal physiological responsiveness in two human neural stem cell lines. *BMC Neurosci.* **8,** 36.

Doyle, K. M., Kennedy, D., Gorman, A. M., Gupta, S., Healy, S. J. and Samali, A. (2011). Unfolded proteins and endoplasmic reticulum stress in neurodegenerative disorders. *J. Cell. Mol. Med.* **15,** 2025-2039.

Earhart, G. M. (2009). Dance as therapy for individuals with parkinson disease. *Eur. J. Phys. Rehabil. Med.* **45,** 231-238.

El Ayadi, A. and Zigmond, M. J. (2011). Low concentrations of methamphetamine can protect dopaminergic cells against a larger oxidative stress injury: Mechanistic study. *PloS one* **6,** e24722.

Emerit, J., Edeas, M. and Bricaire, F. (2004). Neurodegenerative diseases and oxidative stress. *Biomedicine & pharmacotherapy* **58,** 39-46.

Fabbri, M., Mario, M. Rosa., Abreu, D., Ferreira, J. J. (2015). Clinical pharmacology review of safinamide for the treatment of Parkinson's disease. *Neurodegenerative Disease Management.* **5,** 6, 481-496

Fahn, S. and Sulzer, D. (2004). Neurodegeneration and neuroprotection in parkinson disease. *NeuroRx* **1,** 139-154.

Fan, T. J., Han, L. H., Cong, R. S. and Liang, J. (2005). Caspase family proteases and apoptosis. *Acta Biochim. Biophys. Sin. (Shanghai)* **37,** 719-727.

Fan, T. J., Han, L. H., Cong, R. S. and Liang, J. (2005). Caspase family proteases and apoptosis. *Acta Biochim. Biophys. Sin. (Shanghai)* **37,** 719-727.

Ferro, M. M., Bellissimo, M. I., Anselmo-Franci, J. A., Angellucci, M. E. M., Canteras, N. S. and Da Cunha, C. (2005). Comparison of bilaterally 6-OHDA-and MPTP-lesioned rats as models of the early phase of parkinson's disease: Histological, neurochemical, motor and memory alterations. *J. Neurosci. Methods* **148,** 78-87.

Fischer, U., Janicke, R. U. and Schulze-Osthoff, K. (2003). Many cuts to ruin: A comprehensive update of caspase substrates *Cell Death Differ.* **10,** 76-100.

Flood, P. M., Qian, L., Peterson, L. J., Zhang, F., Shi, J. S., Gao, H. M. and Hong, J. S. (2011). Transcriptional factor NF-κB as a target for therapy in parkinson's disease. *Parkinson's disease* **2011,** 216298.

Frazzitta, G., Balbi, P., Maestri, R., Bertotti, G., Boveri, N. and Pezzoli, G. (2013). The beneficial role of intensive exercise on parkinson disease progression. *Am. J. Phys. Med. Rehabil.* **92,** 523-532.

Friedlander, R. M. (2003). Apoptosis and caspases in neurodegenerative diseases. *N. Engl. J. Med.* **348,** 1365-1375.

Friend, D. M. and Keefe, K. A. (2013). A role for D1 dopamine receptors in striatal methamphetamine-induced neurotoxicity. *Neurosci. Lett.* **555,** 243-247.

Fritz, S., Merlo-Rains, A., Rivers, E., Brandenburg, B., Sweet, J., Donley, J., Mathews, H., deBode, S. and McClenaghan, B. A. (2011). Feasibility of intensive mobility training to improve gait, balance, and mobility in persons with chronic neurological conditions: A case series *J. Neurol. Phys. Ther.* **35,** 141-147.

Gao, H., Jiang, J., Wilson, B., Zhang, W., Hong, J. and Liu, B. (2002). Microglial activation-mediated delayed and progressive degeneration of rat nigral dopaminergic neurons: Relevance to parkinson's disease. *J. Neurochem.* **81,** 1285-1297.

Gao, H. M., Zhou, H., Zhang, F., Wilson, B. C., Kam, W. and Hong, J. S. (2011). HMGB1 acts on microglia Mac1 to mediate chronic neuroinflammation that drives progressive neurodegeneration. *J. Neurosci.* **31,** 1081-1092.

Gal, S., Zheng, H., Fridkin, M. and Youdim, M. B. (2005). Novel multifunctional neuroprotective iron chelator-monoamine oxidase inhibitor drugs for neurodegenerative diseases. in vivo selective brain monoamine oxidase inhibition and prevention of MPTP-induced striatal dopamine depletion. *J. Neurochem.* **95,** 79-88.

Ganat, Y. M., Calder, E. L., Kriks, S., Nelander, J., Tu, E. Y., Jia, F., Battista, D., Harrison, N., Parmar, M., Tomishima, M. J. et al. (2012). Identification of embryonic stem cell-derived midbrain dopaminergic neurons for engraftment *J. Clin. Invest.* **122,** 2928-2939.

Gazewood, J. D., Richards, D. R. and Clebak, K. (2013). Parkinson disease: An update. *Am. Fam. Physician* **87,** 267-273.

Ghosh, A. P., Klocke, B. J., Ballestas, M. E. and Roth, K. A. (2012). CHOP potentially co-operates with FOXO3a in neuronal cells to regulate PUMA and BIM expression in response to ER stress. *PLoS One* **7,** e39586.

Ghosh, A., Roy, A., Liu, X., Kordower, J. H., Mufson, E. J., Hartley, D. M., Ghosh, S., Mosley, R. L., Gendelman, H. E. and Pahan, K. (2007). Selective inhibition of NF-kappaB activation prevents dopaminergic neuronal loss in a mouse model of parkinson's disease. *Proc. Natl. Acad. Sci. U. S. A.* **104,** 18754-18759.

Ghosh, A., Roy, A., Matras, J., Brahmachari, S., Gendelman, H. E. and Pahan, K. (2009). Simvastatin inhibits the activation of p21ras and prevents the loss of dopaminergic neurons in a mouse model of parkinson's disease. *J. Neurosci.* **29,** 13543-13556.

Ghosh, A., Saminathan, H., Kanthasamy, A., Anantharam, V., Jin, H., Sondarva, G., Harischandra, D. S., Qian, Z., Rana, A. and Kanthasamy, A. G. (2013). The peptidyl-prolyl isomerase Pin1 up-regulation and proapoptotic function in dopaminergic neurons: Relevance to the pathogenesis of parkinson disease. *J. Biol. Chem.* **288,** 21955-21971.

Ghribi, O., Herman, M. M., Pramoonjago, P. and Savory, J. (2003). MPP+ induces the endoplasmic reticulum stress response in rabbit brain involving activation of the ATF-6 and NF-kappaB signaling pathways *J. Neuropathol. Exp. Neurol.* **62,** 1144-1153.

Giasson, B. I. and Lee, V. M. (2001). Parkin and the molecular pathways of parkinson's disease. *Neuron* **31,** 885-888.

Giasson, B. I. and Lee, V. M. (2003). Are ubiquitination pathways central to parkinson's disease? *Cell* **114,** 1-8.

Gorton, L. M., Vuckovic, M. G., Vertelkina, N., Petzinger, G. M., Jakowec, M. W. and Wood, R. I. (2010). Exercise effects on motor and affective behavior and catecholamine neurochemistry in the MPTP-lesioned mouse. *Behav. Brain Res.* **213,** 253-262.

Graybiel, A. M. (2005). The basal ganglia: Learning new tricks and loving it. *Curr. Opin. Neurobiol.* **15,** 638-644.

Graybiel, A. M. (2008). Habits, rituals, and the evaluative brain. *Annu. Rev. Neurosci.* **31,** 359-387.

Grilli, M. and Memo, M. (1999). Nuclear factor-kappaB/Rel proteins: A point of convergence of signalling pathways relevant in neuronal function and dysfunction *Biochem. Pharmacol.* **57,** 1-7.

Haas C. T., (2009). Exercise and parkinsons disease. **verbal communication to discuss unpublished research carried out and the impact of exercise in future treatments,**.

Hacioglu, G., Seval-Celik, Y., Tanriover, G., Ozsoy, O., Saka-Topcuoglu, E., Balkan, S. and Agar, A. (2012). Docosahexaenoic acid provides protective mechanism in bilaterally MPTP-lesioned rat model of parkinson's disease. *Folia Histochemica et Cytobiologica* **50,**.

Hackney, M. E. and Earhart, G. M. (2009). Short duration, intensive tango dancing for parkinson disease: An uncontrolled pilot study. *Complement. Ther. Med.* **17,** 203-207.

Hackney, M. E., Kantorovich, S. and Earhart, G. M. (2007). A study on the effects of argentine tango as a form of partnered dance for those with parkinson disease and the healthy elderly. *American Journal of Dance Therapy* **29,** 109-127.

Hackney, M. E. and Earhart, G. M. (2009). Effects of dance on movement control in parkinson's disease: A comparison of argentine tango and american ballroom. *J. Rehabil. Med.* **41,** 475-481.

Hackney, M. E. and Earhart, G. M. (2010). Effects of dance on gait and balance in parkinson's disease: A comparison of partnered and nonpartnered dance movement. *Neurorehabil. Neural Repair* **24,** 384-392.

Hackney, M. E., Kantorovich, S., Levin, R. and Earhart, G. M. (2007). Effects of tango on functional mobility in parkinson's disease: A preliminary study. *J. Neurol. Phys. Ther.* **31,** 173-179.

Hald, A. and Lotharius, J. (2005). Oxidative stress and inflammation in parkinson's disease: Is there a causal link? *Exp. Neurol.* **193,** 279-290.

Han, B., Hu, J., Shen, J., Gao, Y., Lu, Y. and Wang, T. (2013). Neuroprotective effect of hydroxysafflor yellow A on 6-hydroxydopamine-induced parkinson's disease in rats. *Eur. J. Pharmacol.* **714,** 83-88.

Han, B. S., Hong, H. S., Choi, W. S., Markelonis, G. J., Oh, T. H. and Oh, Y. J. (2003). Caspase-dependent and -independent cell death pathways in primary cultures of mesencephalic dopaminergic neurons after neurotoxin treatment. *J. Neurosci.* **23,** 5069-5078.

Haque, M. E., Thomas, K. J., D'Souza, C., Callaghan, S., Kitada, T., Slack, R. S., Fraser, P., Cookson, M. R., Tandon, A. and Park, D. S. (2008). Cytoplasmic Pink1 activity protects neurons from dopaminergic neurotoxin MPTP. *Proc. Natl. Acad. Sci. U. S. A.* **105,** 1716-1721.

Hara, H., Kamiya, T. and Adachi, T. (2011). Endoplasmic reticulum stress inducers provide protection against 6-hydroxydopamine-induced cytotoxicity. *Neurochem. Int.* **58,** 35-43.

Hara, M. R. and Snyder, S. H. (2007). Cell signaling and neuronal death. *Annu. Rev. Pharmacol. Toxicol.* **47,** 117-141.

Hartmann, A., Troadec, J. D., Hunot, S., Kikly, K., Faucheux, B. A., Mouatt-Prigent, A., Ruberg, M., Agid, Y. and Hirsch, E. C. (2001). Caspase-8 is an effector in apoptotic death of dopaminergic neurons in parkinson's disease, but pathway inhibition results in neuronal necrosis. *J. Neurosci.* **21,** 2247-2255.

Hayden, M. S. and Ghosh, S. (2008). Shared principles in NF-κB signalling. *Cell* **132,** 344-362.

Heiberger, L., Maurer, C., Amtage, F., Mendez-Balbuena, I., Schulte-Monting, J., Hepp-Reymond, M. C. and Kristeva, R. (2011). Impact of a weekly dance class on the functional mobility and on the quality of life of individuals with parkinson's disease. *Front. Aging Neurosci.* **3,** 14.

Henn, I. H., Bouman, L., Schlehe, J. S., Schlierf, A., Schramm, J. E., Wegener, E., Nakaso, K., Culmsee, C., Berninger, B., Krappmann, D. et al. (2007). Parkin mediates neuroprotection through activation of IkappaB kinase/nuclear factor-kappaB signaling *J. Neurosci.* **27,** 1868-1878.

Herman, T., Giladi, N., Gruendlinger, L. and Hausdorff, J. M. (2007). Six weeks of intensive treadmill training improves gait and quality of life in patients with Parkinson's disease: A pilot study. *Arch. Phys. Med. Rehabil.* **88,** 1154-1158.

Hetz C. (2009). Endoplasmic Reticulum Stress and Protein Misfolding in Amyotrophic Lateral Sclerosis. *Protein Misfolding Disorders: A Trip into the ER.* Sharjah U.A.E. Bentham Science Publishers Ltd. **56-76**

Hetz, C. (2012). The unfolded protein response: controlling cell fate decisions under ER stress and beyond. *Nature Reviews Molecular Cell Biology.* **13**, 89-102

Higuchi, M., Tomioka, M., Takano, J., Shirotani, K., Iwata, N., Masumoto, H., Maki, M., Itohara, S. and Saido, T. C. (2005). Distinct mechanistic roles of calpain and caspase activation in

neurodegeneration as revealed in mice overexpressing their specific inhibitors. *J. Biol. Chem.* **280,** 15229-15237.

Ho, Y., Ho, S., Pawlak, C. R. and Yeh, K. (2011). Effects of d-cycloserine on MPTP-induced behavioral and neurological changes: Potential for treatment of parkinson's disease dementia. *Behav. Brain Res.* **219,** 280-290.

Ho, C. C., Rideout, H. J., Ribe, E., Troy, C. M. and Dauer, W. T. (2009). The parkinson disease protein leucine-rich repeat kinase 2 transduces death signals via fas-associated protein with death domain and caspase-8 in a cellular model of neurodegeneration. *J. Neurosci.* **29,** 1011-1016.

Holschneider, D., Yang, J., Guo, Y. and Maarek, J. (2007). Reorganization of functional brain maps after exercise training: Importance of cerebellar–thalamic–cortical pathway. *Brain Res.* **1184,** 96-107.

Holtz, W. A. and O'Malley, K. L. (2003). Parkinsonian mimetics induce aspects of unfolded protein response in death of dopaminergic neurons. *J. Biol. Chem.* **278,** 19367-19377.

Howells, F. M., Russell, V. A., Mabandla, M. V. and Kellaway, L. A. (2005). Stress reduces the neuroprotective effect of exercise in a rat model for parkinson's disease. *Behav. Brain Res.* **165,** 210-220.

Hunot, S., Brugg, B., Ricard, D., Michel, P. P., Muriel, M. P., Ruberg, M., Faucheux, B. A., Agid, Y. and Hirsch, E. C. (1997). Nuclear translocation of NF-kappaB is increased in dopaminergic neurons of patients with parkinson disease *Proc. Natl. Acad. Sci. U. S. A.* **94,** 7531-7536.

Husárová, I., Lungu, O. V., Mareček, R., Mikl, M., Gescheidt, T., Krupa, P. and Bareš, M. (2011). Functional imaging of the cerebellum and basal ganglia during predictive motor timing in early parkinson's disease. *Journal of Neuroimaging.*

Inamdar, N. N., Arulmozhi, D. K., Tandon, A. and Bodhankar, S. L. (2007). Parkinson's disease: Genetics and beyond. *Curr. Neuropharmacol.* **5,** 99-113.

Ischiropoulos, H. (2003). Oxidative modifications of α-Synuclein. *Ann. N. Y. Acad. Sci.* **991,** 93-100.

Ischiropoulos, H. and Beckman, J. S. (2003). Oxidative stress and nitration in neurodegeneration: Cause, effect, or association? *J. Clin. Invest.* **111,** 163-169.

Iwashita, A., Muramatsu, Y., Yamazaki, T., Muramoto, M., Kita, Y., Yamazaki, S., Mihara, K., Moriguchi, A. and Matsuoka, N. (2007). Neuroprotective efficacy of the peroxisome proliferator-activated receptor delta-selective agonists in vitro and in vivo. *J. Pharmacol. Exp. Ther.* **320,** 1087-1096.

Jaeger, A., Baake, J., Weiss, D. G. and Kriehuber, R. (2013). Glycogen synthase kinase-3beta regulates differentiation-induced apoptosis of human neural progenitor cells. *International Journal of Developmental Neuroscience* **31,** 61-68.

Jia, Z. and Misra, H. P. (2007). Reactive oxygen species in< i> in vitro</i> pesticide-induced neuronal cell (SH-SY5Y) cytotoxicity: Role of NFκB and caspase-3. *Free Radical Biology and Medicine* **42,** 288-298.

Jiang, N., Bo, H., Song, C., Guo, J., Zhao, F., Feng, H., Ding, H., Ji, L. and Zhang, Y. (2013). Increased vulnerability with aging to MPTP: The mechanisms underlying mitochondrial dynamics. *Neurol. Res.*

Jiang, P., Gan, M., Ebrahim, A. S., Lin, W., Melrose, H. L. and Yen, S. C. (2010). ER stress response plays an important role in aggregation of α-synuclein. *Molecular neurodegeneration* **5,** 1-15.

Jiang, T., Zhang, Y., Zhou, H., Wang, H., Tian, L., Liu, J., Ding, J. and Chen, S. (2013). Curcumin ameliorates the neurodegenerative pathology in A53T α-synuclein cell model of Parkinson's disease through the downregulation of mTOR/p70S6K signaling and the recovery of macroautophagy. *Journal of NeuroImmune Pharmacology* **8,** 356-369.

Jin, H., Kanthasamy, A., Ghosh, A., Anantharam, V., Kalyanaraman, B. and Kanthasamy, A. G. (2013). Mitochondria-targeted antioxidants for treatment of parkinson's disease: Preclinical and clinical outcomes. *Biochimica et Biophysica Acta (BBA)-Molecular Basis of Disease.*

Jin, S. M. and Youle, R. J. (2013). The accumulation of misfolded proteins in the mitochondrial matrix is sensed by PINK1 to induce PARK2/Parkin-mediated mitophagy of polarized mitochondria. *Autophagy* **9,** 1750-1757.

Jin, Y. N., Hwang, W. Y., Jo, C. and Johnson, G. V. (2012). Metabolic state determines sensitivity to cellular stress in Huntington disease: Normalization by activation of PPARgamma. *PLoS One* **7,** e30406.

Kadowaki, H. and Nishitoh, H. (2013). Signaling pathways from the endoplasmic reticulum and their roles in disease. *Genes* **4,** 306-333.

Kalivendi, S. V., Yedlapudi, D., Hillard, C. J. and Kalyanaraman, B. (2010). Oxidants induce alternative splicing of α-synuclein: Implications for parkinson's disease. *Free Radical Biology and Medicine* **48,** 377-383.

Karunakaran, S. and Ravindranath, V. (2009). Activation of p38 MAPK in the substantia nigra leads to nuclear translocation of NF-kappaB in MPTP-treated mice: Implication in parkinson's disease *J. Neurochem.* **109,** 1791-1799.

Kim, H. G., Ju, M. S., Kim, D., Hong, J., Cho, S., Cho, K., Park, W., Lee, E. H., Kim, S. Y. and Oh, M. S. (2010). Protective effects of chunghyuldan against ROS-mediated neuronal cell death in models of Parkinson's disease. *Basic & clinical pharmacology & toxicology* **107,** 958-964.

Kim, H. G., Park, G., Piao, Y., Kang, M. S., Pak, Y. K., Hong, S. and Oh, M. S. (2014). Effects of the root bark of< i> paeonia suffruticosa</i> on mitochondria-mediated neuroprotection in an MPTP-induced model of Parkinson's disease. *Food and Chemical Toxicology*.

Kim, I., Xu, W. and Reed, J. C. (2008). Cell death and endoplasmic reticulum stress: Disease relevance and therapeutic opportunities. *Nature Reviews Drug Discovery* **7,** 1013-1030.

Kroemer, G. and Blomgren, K. (2007). Mitochondrial cell death control in familial parkinson disease. *PLoS biology* **5,** e206.

Kruidering, M. and Evan, G. I. (2000). Caspase-8 in apoptosis: The beginning of "The end"? *IUBMB Life* **50,** 85-90.

Kumar, S. (2007). Caspase function in programmed cell death. *Cell Death & Differentiation* **14,** 32-43.

Krumschnabel, G., Sohm, B., Bock, F., Manzl, C. and Villunger, A. (2009). The enigma of caspase-2: The laymen's view *Cell Death Differ.* **16,** 195-207.

Kudo, T. (2003). Involvement of unfolded protein responses in neurodegeneration. *Nihon Shinkei Seishin Yakurigaku Zasshi* **23,** 105-109.

Lamkanfi, M., Declercq, W., Vanden Berghe, T. and Vandenabeele, P. (2006). Caspases leave the beaten track: Caspase-mediated activation of NF-kappaB *J. Cell Biol.* **173,** 165-171.

Lamkanfi, M., Festjens, N., Declercq, W., Vanden Berghe, T. and Vandenabeele, P. (2007). Caspases in cell survival, proliferation and differentiation *Cell Death Differ.* **14,** 44-55.

Lee do, Y., Lee, K. S., Lee, H. J., Kim do, H., Noh, Y. H., Yu, K., Jung, H. Y., Lee, S. H., Lee, J. Y., Youn, Y. C. et al. (2010). Activation of PERK signaling attenuates abeta-mediated ER stress. *PLoS One* **5,** e10489.

Lee, H., Kim, H., Lee, M., Chang, H., Lee, T., Jang, M., Shin, M., Lim, B., Shin, M. and Kim, Y. (2003). Treadmill exercise decreases intrastriatal hemorrhage-induced neuronal cell death via suppression on caspase-3 expression in rats. *Neurosci. Lett.* **352,** 33-36.

Lee, H., Kim, S., Kim, K., Um, J., Lee, H., Chung, B. and Kang, C. (2001). Antiapoptotic role of NF-κB in the auto-oxidized dopamine-induced apoptosis of PC12 cells. *J. Neurochem.* **76,** 602-609.

Lee, E. Y., Lee, J. E., Park, J. H., Shin, I. C. and Koh, H. C. (2012). Rosiglitazone, a PPAR-gamma agonist, protects against striatal dopaminergic neurodegeneration induced by 6-OHDA lesions in the substantia nigra of rats. *Toxicol. Lett.* **213,** 332-344.

Lee, G. H., Kim, H. K., Chae, S. W., Kim, D. S., Ha, K. C., Cuddy, M., Kress, C., Reed, J. C., Kim, H. R. and Chae, H. J. (2007). Bax inhibitor-1 regulates endoplasmic reticulum stress-associated reactive oxygen species and heme oxygenase-1 expression. *J. Biol. Chem.* **282,** 21618-21628.

LeWitt, P.A. (2015). New levodopa therapeutic strategies. *Parkinsonism and Related Disorders*. **22,**1 ,37-40

Li, F., Harmer, P., Fitzgerald, K., Eckstrom, E., Stock, R., Galver, J., Maddalozzo, G. and Batya, S. S. (2012). Tai chi and postural stability in patients with parkinson's disease *N. Engl. J. Med.* **366,** 511-519.

Li, N., Sarojini, H., An, J. and Wang, E. (2010). Prosaposin in the secretome of marrow stroma-derived neural progenitor cells protects neural cells from apoptotic death. *J. Neurochem.* **112,** 1527-1538.

Li, L., Zhao, X., Fei, X., Gu, Z., Qin, Z. and Liang, Z. (2008). Bilobalide inhibits 6-OHDA-induced activation of NF-κB and loss of dopaminergic neurons in rat substantia nigra. *Acta Pharmacol. Sin.* **29,**.

Li, Y., Hu, X., Liu, Y., Bao, Y., An, L., (2009). Nimodipine protects dopaminergic neurons against inflammation-mediated degeneration through inhibition of microglial activation. *Neuropharmacology.* **56,** 3, 580-589

Lim, K. and Tan, J. M. (2007). Role of the ubiquitin proteasome system in parkinson's disease. *BMC biochemistry* **8,** S13.

Lin, S., Vincent, A., Shaw, T., Maynard, K. I. and Maiese, K. (2000). Prevention of nitric oxide-induced neuronal injury through the modulation of independent pathways of programmed cell death. *Journal of Cerebral Blood Flow & Metabolism* **20,** 1380-1391.

Lin, X. Y., Choi, M. S. and Porter, A. G. (2000). Expression analysis of the human caspase-1 subfamily reveals specific regulation of the CASP5 gene by lipopolysaccharide and interferon-gamma. *J. Biol. Chem.* **275,** 39920-39926.

Lindholm, D., Wootz, H. and Korhonen, L. (2006). ER stress and neurodegenerative diseases. *Cell Death Differ.* **13,** 385-392.

Liou, A. K., Zhou, Z., Pei, W., Lim, T. M., Yin, X. M. and Chen, J. (2005). BimEL up-regulation potentiates AIF translocation and cell death in response to MPTP. *FASEB J.* **19,** 1350-1352.

Liu, T., Brouha, B. and Grossman, D. (2004). Rapid induction of mitochondrial events and caspase-independent apoptosis in survivin-targeted melanoma cells. *Oncogene* **23,** 39-48.

Liu, W., Chen, Y., Li, B., Lu, G. and Chen, S. (2004). Neuroprotection by pergolide against levodopa-induced cytotoxicity of neural stem cells. *Neurochem. Res.* **29,** 2207-2214.

Lo, Y., Shih, Y., Tseng, Y. and Hsu, H. (2012). Neuroprotective effects of san-huang-xie-xin-tang in the MPP< sup>. *Evidence-Based Complementary and Alternative Medicine* **2012,**.

Lumini-Oliveira, J., Magalhães, J., Pereira, C. V., Aleixo, I., Oliveira, P. J. and Ascensão, A. (2009). Endurance training improves gastrocnemius mitochondrial function despite increased susceptibility to permeability transition. *Mitochondrion* **9,** 454-462.

Mabandla, M. V. and Russell, V. A. (2010). Voluntary exercise reduces the neurotoxic effects of 6-hydroxydopamine in maternally separated rats. *Behav. Brain Res.* **211,** 16-22.

Mabandla, M., Kellaway, L., Gibson, A. S. C. and Russell, V. A. (2004). Voluntary running provides neuroprotection in rats after 6-hydroxydopamine injection into the medial forebrain bundle. *Metab. Brain Dis.* **19,** 43-50.

Machado, A. G., Deogaonkar, M. and Cooper, S. (2012). Deep brain stimulation for movement disorders: Patient selection and technical options *Cleve. Clin. J. Med.* **79 Suppl 2,** S19-24.

Magalhães, J., Gonçalves, I., Lumini-Oliveira, J., Marques-Aleixo, I., Passos, E., Rocha-Rodrigues, S., Machado, N., Moreira, A., Rizo, D. and Viscor, G. (2014). Modulation of cardiac mitochondrial permeability transition and apoptotic signaling by endurance training and intermittent hypobaric hypoxia. *Int. J. Cardiol.*

Malhotra, J. D. and Kaufman, R. J. (2007). Endoplasmic reticulum stress and oxidative stress: A vicious cycle or a double-edged sword? *Antioxid. Redox Signal.* **9,** 2277-2293.

Marti, M., Rodi, D., Li, Q., Guerrini, R., Fasano, S., Morella, I., Tozzi, A., Brambilla, R., Calabresi, P., Simonato, M. et al. (2012). Nociceptin/orphanin FQ receptor agonists attenuate L-DOPA-induced dyskinesias. *J. Neurosci.* **32,** 16106-16119.

Martini F.H. (2006). *The Fundamentals of Anatomy and Physiology*, pp. 700-380,461. San Francisco: Pearson Benjamin Cummings Ed Ltd.

Martini F.H, Nath J.N, Bartholomew E.F. (2014). *Fundamentals of Anatomy & Physiology*, pp. 112-45,250, 87. San Francisco: Pearson Benjamin Cummings Ed Ltd.

Martini F.H, Ober W. C. (2006). *Martinis Atlas of the Human Body*, pp. 100-18,23, 24. San Francisco: Pearson Benjamin Cummings Ed Ltd.

Massachusetts B. (2008). *ReNcell® VM neural stem cell line Models Parkinson's disease - new human disease model shows function of PINK1 gene in neural degeneration . Millipore Corporation* July 2009-1-5.

Masumoto, J., Dowds, T. A., Schaner, P., Chen, F. F., Ogura, Y., Li, M., Zhu, L., Katsuyama, T., Sagara, J., Taniguchi, S. et al. (2003). ASC is an activating adaptor for NF-kappa B and caspase-8-dependent apoptosis. *Biochem. Biophys. Res. Commun.* **303,** 69-73.

Matsuda, S., Kitagishi, Y. and Kobayashi, M. (2013). Function and characteristics of PINK1 in mitochondria. *Oxid Med. Cell. Longev* **2013,** 601587.

Mattson, M. P. (2007). Calcium and neurodegeneration. *Aging cell* **6,** 337-350.

Mattson, M. P. (2006). Neuronal life-and-death signaling, apoptosis, and neurodegenerative disorders. *Antioxid. Redox Signal.* **8,** 1997-2006.

Mattson, M. P., Duan, W., Wan, R. and Guo, Z. (2004). Prophylactic activation of neuroprotective stress response pathways by dietary and behavioral manipulations. *NeuroRx* **1,** 111-116.

Mattson, M. P., LaFerla, F. M., Chan, S. L., Leissring, M. A., Shepel, P. N. and Geiger, J. D. (2000). Calcium signaling in the ER: Its role in neuronal plasticity and neurodegenerative disorders. *Trends Neurosci.* **23,** 222-229.

Mattson, M. and Meffert, M. (2006). Roles for NF-*κ*B in nerve cell survival, plasticity, and disease. *Cell Death & Differentiation* **13,** 852-860.

Mattson, M. P., Pedersen, W. A., Duan, W., Culmsee, C. and Camandola, S. (1999). Cellular and molecular mechanisms underlying perturbed energy metabolism and neuronal degeneration in alzheimer's and parkinson's diseases. *Ann. N. Y. Acad. Sci.* **893,** 154-175.

Matus, S., Lisbona, F., Torres, M., Leon, C., Thielen, P. and Hetz, C. (2008). The stress rheostat: An interplay between the unfolded protein response (UPR) and autophagy in neurodegeneration. *Curr. Mol. Med.* **8,** 157-172.

McIlwain, D. R., Berger, T. and Mak, T. W. (2013). Caspase functions in cell death and disease. *Cold Spring Harb Perspect. Biol.* **5,** a008656.

McNeely, M. E. and Earhart, G. M. (2012). Medication and subthalamic nucleus deep brain stimulation similarly improve balance and complex gait in parkinson disease *Parkinsonism Relat. Disord.*

Merck Chemicals Ltd, Caspase-2 Inhibitor I - Calbiochem; MSDS No. 218744 [Online]; Merck Chemicals Ltd: Nottingham UK , June 2008, http://www.merckmillipore.com/GB/en/product/Caspase-2-Inhibitor-I---Calbiochem,EMD_BIO-218744#anchor_PDS (accessed January 15, 2012).

Merck Chemicals Ltd, Caspase-4 Inhibitor -Calbiochem (CAS 402832-01-3); MSDS No. 218755 [Online]; Merck Chemicals Ltd: Nottingham UK , March 2011, http://www.merckmillipore.com/GB/en/product/Caspase-4-Inhibitor-I---CAS-402832-01-3---Calbiochem,EMD_BIO-218755#anchor_COA (accessed January 15, 2012).

Merck Chemicals Ltd, Caspase-8 Inhibitor II - Calbiochem; MSDS No. 218759 [Online]; Merck Chemicals Ltd: Nottingham UK , February 2011,

http://www.merckmillipore.com/GB/en/product/Caspase-8-Inhibitor-II---Calbiochem,EMD_BIO-218759#anchor_CITATION (accessed January 15, 2012).

Merck Chemicals Ltd, IKK-2 Inhibitor, SC-514 - CAS 354812-17-2 - Calbiochem; MSDS No. 401479 [Online]; Merck Chemicals Ltd: Nottingham UK , April 2011, http://www.merckmillipore.com/GB/en/product/IKK-2-Inhibitor%2C-SC-514---CAS-354812-17-2---Calbiochem,EMD_BIO-401479(accessed January 15, 2012).

Midwinter, R., Cheah, F., Moskovitz, J., Vissers, M. and Winterbourn, C. (2006). IkappaB is a sensitive target for oxidation by cell-permeable chloramines: Inhibition of NF-kappaB activity by glycine chloramine through methionine oxidation. *Biochem. J.* **396,** 71-78.

Miljan, E. A. (2007). ReNcell human neural progenitors: Renewable and consistent supply of human functional neurons. *Millipore Corporation* July 2010-1-4.

Miljan, E. A. (2008). In vitro modellingof Parkinson's disease using Rencell VMhuman neural stem cell line. *Millipore Corporation* July 2010-1-20.

Minks, E., Mareček, R., Pavlík, T., Ovesná, P. and Bareš, M. (2011). Is the cerebellum a potential target for stimulation in parkinson's disease? results of 1-hz rTMS on upper limb motor tasks. *The Cerebellum* **10,** 804-811.

Miyazaki, I. and Asanuma, M. (2008). Dopaminergic neuron-specific oxidative stress caused by dopamine itself. *Acta Med. Okayama* **62,** 141.

Modugno, N., Iaconelli, S., Fiorlli, M., Lena, F., Kusch, I. and Mirabella, G. (2010). Active theater as a complementary therapy for parkinson's disease rehabilitation: A pilot study *ScientificWorldJournal* **10,** 2301-2313.

Moore, D. J., West, A. B., Dawson, V. L. and Dawson, T. M. (2005). Molecular pathophysiology of parkinson's disease. *Annu. Rev. Neurosci.* **28,** 57-87.

Morón, Ú. M. and Castilla-Cortázar, I. (2012). Protection against oxidative stress and "IGF-I deficiency conditions"

Mu, L., Sobotka, S., Chen, J., Su, H., Sanders, I., Nyirenda, T., Adler,C. H., Shill, H.A., Caviness, J.N., Samanta, J.E., Sue, L.I., Beach, T.G., the Arizona Parkinson's Disease

Consortium. (2013). Parkinson Disease Affects Peripheral Sensory Nerves in the Pharynx. *Journal of Neuropathology and Experimental Neurology*. **72**,7, 614–623.

Murlasits, Z., Cutlip, R. G., Geronilla, K. B., Rao, K. M. K., Wonderlin, W. F. and Alway, S. E. (2006). Resistance training increases heat shock protein levels in skeletal muscle of young and old rats. *Exp. Gerontol.* **41,** 398-406.

Murlasits, Z., Lee, Y. and Powers, S. K. (2007). Short-term exercise does not increase ER stress protein expression in cardiac muscle. *Med. Sci. Sports Exerc.* **39,** 1522-1528.

Murray, T. K., Whalley, K., Robinson, C. S., Ward, M. A., Hicks, C. A., Lodge, D., Vandergriff, J. L., Baumbarger, P., Siuda, E., Gates, M. et al. (2003). LY503430, a novel alpha-amino-3-hydroxy-5-methylisoxazole-4-propionic acid receptor potentiator with functional, neuroprotective and neurotrophic effects in rodent models of parkinson's disease. *J. Pharmacol. Exp. Ther.* **306,** 752-762.

Nakagawa, T. and Yuan, J. (2000). Cross-talk between two cysteine protease families. activation of caspase-12 by calpain in apoptosis. *J. Cell Biol.* **150,** 887-894.

Nakagawa, T., Zhu, H., Morishima, N., Li, E., Xu, J., Yankner, B. A. and Yuan, J. (2000). Caspase-12 mediates endoplasmic-reticulum-specific apoptosis and cytotoxicity by amyloid-beta. *Nature* **403,** 98-103.

Nakamura, T., Cho, D. and Lipton, S. A. (2012). Redox regulation of protein misfolding, mitochondrial dysfunction, synaptic damage, and cell death in neurodegenerative diseases. *Exp. Neurol.* **238,** 12-21.

Nakamura, K. and Edwards, R. H. (2007). Physiology versus pathology in parkinson's disease. *Proc. Natl. Acad. Sci. U. S. A.* **104,** 11867-11868.

Oakes, S. A., Lin, S. S. and Bassik, M. C. (2006). The control of endoplasmic reticulum-initiated apoptosis by the BCL-2 family of proteins. *Curr. Mol. Med.* **6,** 99-109.

Oakes, S.A., Papa, F.R.(2014) The Role of Endoplasmic Reticulum Stress in Human Pathology. *Annual Review of Pathology: Mechanisms of Disease.* **10,** 173-194

Oda, T., Kosuge, Y., Arakawa, M., Ishige, K. and Ito, Y. (2008). Distinct mechanism of cell death is responsible for tunicamycin-induced ER stress in SK-N-SH and SH-SY5Y cells. *Neurosci. Res.* **60,** 29-39.

Omura, T., Kaneko, M., Okuma, Y., Orba, Y., Nagashima, K., Takahashi, R., Fujitani, N., Matsumura, S., Hata, A. and Kubota, K. (2006). A ubiquitin ligase HRD1 promotes the degradation of pael receptor, a substrate of parkin. *J. Neurochem.* **99,** 1456-1469.

Oshitari, T., Hata, N. and Yamamoto, S. (2008). Endoplasmic reticulum stress and diabetic retinopathy. *Vasc. Health. Risk Manag.* **4,** 115-122.

Oyadomari, S. and Mori, M. (2004). Roles of CHOP/GADD153 in endoplasmic reticulum stress *Cell Death Differ.* **11,** 381-389.

Ozcan, L. and Tabas, I. (2012). Role of endoplasmic reticulum stress in metabolic disease and other disorders *Annu. Rev. Med.* **63,** 317-328.

Pagani, M., Fabbri, M., Benedetti, C., Fassio, A., Pilati, S., Bulleid, N. J., Cabibbo, A. and Silia, R. (2000). PROTEIN SYNTHESIS, POST-TRANSLATION MODIFICATION, AND DEGRADATION-endoplasmic reticulum oxidoreductin 1-lb (ERO1-lb), a human gene induced in the course of the unfolded protein response. *J. Biol. Chem.* **275,** 23685-23692.

Pain, S., Barrier, L., Deguil, J., Milin, S., Piriou, A., Fauconneau, B. and Page, G. (2008). A cell-permeable peptide inhibitor TAT-JBD reduces the MPP< sup> </sup>-induced caspase-9 activation but does not prevent the dopaminergic degeneration in< i> substantia nigra</i> of rats. *Toxicology* **243,** 124-137.

Panet, H., Barzilai, A., Daily, D., Melamed, E. and Offen, D. (2001). Activation of nuclear transcription factor kappa B (NF-kappaB) is essential for dopamine-induced apoptosis in PC12 cells *J. Neurochem.* **77,** 391-398.

Paterson, C., A Allen, J., Browning, M., Barlow, G. and Ewings, P. (2005). A pilot study of therapeutic massage for people with parkinson's disease: The added value of user involvement. *Complementary therapies in clinical practice* **11,** 161-171.

Pereira, C. M. (2013). Crosstalk between endoplasmic reticulum stress and protein misfolding in neurodegenerative diseases. *ISRN Cell Biology* **2013,**.

Perez, F. A., Curtis, W. R. and Palmiter, R. D. (2005). Parkin-deficient mice are not more sensitive to 6-hydroxydopamine or methamphetamine neurotoxicity. *BMC Neurosci.* **6,** 71.

Perez, F. A. and Palmiter, R. D. (2005). Parkin-deficient mice are not a robust model of parkinsonism. *Proc. Natl. Acad. Sci. U. S. A.* **102,** 2174-2179.

Perez, R. G., Waymire, J. C., Lin, E., Liu, J. J., Guo, F. and Zigmond, M. J. (2002). A role for alpha-synuclein in the regulation of dopamine biosynthesis. *J. Neurosci.* **22,** 3090-3099.

Perier, C., Bové, J. and Vila, M. (2012). Mitochondria and programmed cell death in parkinson's disease: Apoptosis and beyond. *Antioxidants & redox signaling* **16,** 883-895.

Petzinger, G. M., Walsh, J. P., Akopian, G., Hogg, E., Abernathy, A., Arevalo, P., Turnquist, P., Vuckovic, M., Fisher, B. E., Togasaki, D. M. et al. (2007). Effects of treadmill exercise on dopaminergic transmission in the 1-methyl-4-phenyl-1,2,3,6-tetrahydropyridine-lesioned mouse model of basal ganglia injury. *J. Neurosci.* **27,** 5291-5300.

Pienaar, I. S. and van de Berg, W. (2013). A non-cholinergic neuronal loss in the pedunculopontine nucleus of toxin-evoked parkinsonian rats. *Exp. Neurol.* **248,** 213-223.

Pišlar, A. H., Zidar, N., Kikelj, D. and Kos, J. (2013). Cathepsin X promotes 6-hydroxydopamine-induced apoptosis of PC12 and SH-SY5Y cells. *Neuropharmacology*.

Poole, A. C., Thomas, R. E., Andrews, L. A., McBride, H. M., Whitworth, A. J. and Pallanck, L. J. (2008). The PINK1/Parkin pathway regulates mitochondrial morphology. *Proc. Natl. Acad. Sci. U. S. A.* **105,** 1638-1643.

Pothakos, K., Kurz, M. J. and Lau, Y. S. (2009). Restorative effect of endurance exercise on behavioral deficits in the chronic mouse model of parkinson's disease with severe neurodegeneration. *BMC Neurosci.* **10,** 6-2202-10-6.

Pourmoghaddam, A., Dettmer, M., O'Connor, D.P., Paloski, W.H., Layne, C.S. (2015). Identification of Changing Lower Limb Neuromuscular Activation in Parkinson's Disease during Treadmill Gait with and without Levodopa Using a Nonlinear Analysis Index. *Parkinsons Disease*. **2015,** 1-8

Promega, CaspACE™ Assay System, Colorimetric 1272/2008 V; MSDS No. 57501 [Online]; Promega: SouthamptonUK UK , August 2010, https://www.promega.co.uk/~/media/files/resources/msds/g57501(accessed January 15, 2012).

Rath, A., Klein, A., Papazoglou, A., Pruszak, J., Garcia, J., Krause, M., Maciaczyk, J., Dunnett, S. B. and Nikkhah, G. (2013). Survival and functional restoration of human fetal ventral mesencephalon following transplantation in a rat model of parkinsons disease. *Cell Transplant.* **22,** 1281-1293.

Redmond, L. and Ghosh, A. (2005). Regulation of dendritic development by calcium signaling. *Cell Calcium* **37,** 411-416.

Reynolds, A., Laurie, C., Lee Mosley, R. and Gendelman, H. E. (2007). Oxidative stress and the pathogenesis of neurodegenerative disorders. *Int. Rev. Neurobiol.* **82,** 297-325.

Ribar, T. J., Rodriguiz, R. M., Khiroug, L., Wetsel, W. C., Augustine, G. J. and Means, A. R. (2000). Cerebellar defects in Ca2 /calmodulin kinase IV-deficient mice. *J. Neurosci.* **20,**.

Rocchi, L., Carlson-Kuhta, P., Chiari, L., Burchiel, K. J., Hogarth, P. and Horak, F. B. (2012). Effects of deep brain stimulation in the subthalamic nucleus or globus pallidus internus on step initiation in parkinson disease *J. Neurosurg.*

Rochet, J. C. (2007). Novel therapeutic strategies for the treatment of protein-misfolding diseases. *Expert Rev. Mol. Med.* **9,** 1-34.

Rodríguez-Nogales,C., Garbayo, E., Carmona-Abellán, M.M., Luquin, M.R., Blanco-Prieto, M. J. 2015. Brain aging and Parkinson's disease: New therapeutic approaches using drug delivery systems. *Maturitas.* **84,** 25–31

Rolland, A. S., Herrero, M. T., Garcia-Martinez, V., Ruberg, M., Hirsch, E. C. and Francois, C. (2007). Metabolic activity of cerebellar and basal ganglia-thalamic neurons is reduced in parkinsonism. *Brain* **130,** 265-275.

Roy, A., Ghosh, A., Jana, A., Liu, X., Brahmachari, S., Gendelman, H. E. and Pahan, K. (2012). Sodium phenylbutyrate controls neuroinflammatory and antioxidant activities and protects dopaminergic neurons in mouse models of Parkinson's disease. *PloS one* **7,** e38113.

Samann, J., Hegermann, J., von Gromoff, E., Eimer, S., Baumeister, R. and Schmidt, E. (2009). Caenorhabditits elegans LRK-1 and PINK-1 act antagonistically in stress response and neurite outgrowth. *J. Biol. Chem.* **284,** 16482-16491.

Samantaray, S., Knaryan, V., Guyton, M., Matzelle, D., Ray, S. and Banik, N. (2007). The parkinsonian neurotoxin rotenone activates calpain and caspase-3 leading to motoneuron degeneration in spinal cord of lewis rats. *Neuroscience* **146,** 741-755.

Sano, R., Reed, J.C. (2013). ER stress-induced cell death mechanisms, *Biochimica et Biophysica Acta - Molecular Cell Research.* **1833,** 12, 3460-3470

Santa Cruz Biotechnology, Salubrinal (CAS 405060-95-9); MSDS No. 5717801 [Online]; Santa Cruz Biotechnology: Heidelberg, Germany , November 2011, http://www.scbt.com/datasheet-202332-salubrinal.html (accessed January 15, 2012).

Schulz, J. (2006). Anti-apoptotic gene therapy in Parkinson's disease. In *Parkinson's Disease and Related Disorders*, pp. 467-476: Springer.

See, V., Boutillier, A. L., Bito, H. and Loeffler, J. P. (2001). Calcium/calmodulin-dependent protein kinase type IV (CaMKIV) inhibits apoptosis induced by potassium deprivation in cerebellar granule neurons. *FASEB J.* **15,** 134-144.

Shang, T., Kotamraju, S., Kalivendi, S. V., Hillard, C. J. and Kalyanaraman, B. (2004). 1-methyl-4-phenylpyridinium-induced apoptosis in cerebellar granule neurons is mediated by transferrin receptor iron-dependent depletion of tetrahydrobiopterin and neuronal nitric-oxide synthase-derived superoxide. *J. Biol. Chem.* **279,** 19099-19112.

Sharma, R. and Gow, A. (2007). Minimal role for caspase 12 in the unfolded protein response in oligodendrocytes in vivo *J. Neurochem.* **101,** 889-897.

Sheline, C. T., Zhu, J., Zhang, W., Shi, C. and Cai, A. L. (2013). Mitochondrial inhibitor models of huntington's disease and parkinson's disease induce zinc accumulation and are attenuated by inhibition of zinc neurotoxicity in vitro or in vivo. *Neurodegener Dis.* **11,** 49-58.

Shibata, N. and Kobayashi, M. (2008). The role for oxidative stress in neurodegenerative diseases. *Brain Nerve* **60,** 157-170.

Shih, Y. T., Chen, I. J., Wu, Y. C. and Lo, Y. C. (2011). San-huang-xie-xin-tang protects against activated microglia- and 6-OHDA-induced toxicity in neuronal SH-SY5Y cells. *Evid Based. Complement. Alternat Med.* **2011,** 429384.

Shimoke, K., Amano, H., Kishi, S., Uchida, H., Kudo, M. and Ikeuchi, T. (2004). Nerve growth factor attenuates endoplasmic reticulum stress-mediated apoptosis via suppression of caspase-12 activity. *J. Biochem.* **135,** 439-446.

Shimoke, K., Kishi, S., Utsumi, T., Shimamura, Y., Sasaya, H., Oikawa, T., Uesato, S. and Ikeuchi, T. (2005). NGF-induced phosphatidylinositol 3-kinase signaling pathway prevents thapsigargin-triggered ER stress-mediated apoptosis in PC12 cells. *Neurosci. Lett.* **389,** 124-128.

Shrivastava, P., Vaibhav, K., Tabassum, R., Khan, A., Ishrat, T., Khan, M. M., Ahmad, A., Islam, F., Safhi, M. M. and Islam, F. (2013). Anti-apoptotic and anti-inflammatory effect of piperine on 6-OHDA induced parkinson's rat model. *J. Nutr. Biochem.* **24,** 680-687.

Sigma-Aldrich UK. (2011). Endoplasmic Reticulum Isolation Kit. *Biofiles Sigma.* **6.** 5. 1-6

Singer, C. (2012). Managing the patient with newly diagnosed parkinson disease *Cleve. Clin. J. Med.* **79 Suppl 2,** S3-7.

Skovronsky, D. M., Lee, V. M. and Trojanowski, J. Q. (2006). Neurodegenerative diseases: New concepts of pathogenesis and their therapeutic implications. *Annu.Rev.Pathol.Mech.Dis.* **1,** 151-170.

Smith, A., Kozlowski, D., Bohn, M. and Zigmond, M. (2005). Effect of AdGDNF on dopaminergic neurotransmission in the striatum of 6-OHDA-treated rats. *Exp. Neurol.* **193,** 420-426.

Smith, M. I. and Deshmukh, M. (2007). Endoplasmic reticulum stress-induced apoptosis requires bax for commitment and apaf-1 for execution in primary neurons. *Cell Death Differ.* **14,** 1011-1019.

Smith, W. W., Jiang, H., Pei, Z., Tanaka, Y., Morita, H., Sawa, A., Dawson, V. L., Dawson, T. M. and Ross, C. A. (2005). Endoplasmic reticulum stress and mitochondrial cell death pathways mediate A53T mutant alpha-synuclein-induced toxicity. *Hum. Mol. Genet.* **14,** 3801-3811.

Soreq, L., Ben-Shaul, Y., Israel, Z., Bergman, H. and Soreq, H. (2012). Meta-analysis of genetic and environmental parkinson's disease models reveals a common role of mitochondrial protection pathways. *Neurobiol. Dis.* **45,** 1018-1030.

Sokka, A. L., Putkonen, N., Mudo, G., Pryazhnikov, E., Reijonen, S., Khiroug, L., Belluardo, N., Lindholm, D. and Korhonen, L. (2007). Endoplasmic reticulum stress inhibition protects against excitotoxic neuronal injury in the rat brain. *J. Neurosci.* **27,** 901-908.

Sonsalla, P. K., Coleman, C., Wong, L., Harris, S. L., Richardson, J. R., Gadad, B. S., Li, W. and German, D. C. (2013). The angiotensin converting enzyme inhibitor captopril protects nigrostriatal dopamine neurons in animal models of parkinsonism. *Exp. Neurol.* **250,** 376-383.

Stallibrass, C., Sissons, P. and Chalmers, C. (2002). Randomized controlled trial of the alexander technique for idiopathic parkinson's disease. *Clin. Rehabil.* **16,** 695-708.

Subramaniam, S. R. and Chesselet, M. (2013). Mitochondrial dysfunction and oxidative stress in parkinson's disease. *Prog. Neurobiol.* **106,** 17-32.

Sun, D. and Chang, H. (2003). Differential regulation of JNK in caspase-3-mediated apoptosis of MPP -treated primary cortical neurons. *Cell Biol. Int.* **27,** 769-777.

Surmeier, D. J. (2007). Calcium, ageing, and neuronal vulnerability in parkinson's disease. *The Lancet Neurology* **6,** 933-938.

Surmeier, D. J., Guzman, J. N. and Sanchez-Padilla, J. (2010). Calcium, cellular aging, and selective neuronal vulnerability in parkinson's disease. *Cell Calcium* **47,** 175-182.

Sutoo, D. and Akiyama, K. (2003). Regulation of brain function by exercise. *Neurobiol. Dis.* **13,** 1-14.

Szegezdi, E., Logue, S. E., Gorman, A. M. and Samali, A. (2006). Mediators of endoplasmic reticulum stress-induced apoptosis. *EMBO Rep.* **7,** 880-885.

Szegezdi, E., Herbert, K. R., Kavanagh, E. T., Samali, A. and Gorman, A. M. (2008). Nerve growth factor blocks thapsigargin-induced apoptosis at the level of the mitochondrion via regulation of bim. *J. Cell. Mol. Med.* **12,** 2482-2496.

Tajiri, N., Yasuhara, T., Shingo, T., Kondo, A., Yuan, W., Kadota, T., Wang, F., Baba, T., Tayra, J. T. and Morimoto, T. (2010). Exercise exerts neuroprotective effects on parkinson's disease model of rats. *Brain Res.* **1310,** 200-207.

Tanaka, Y., Engelender, S., Igarashi, S., Rao, R. K., Wanner, T., Tanzi, R. E., Sawa, A., L Dawson, V., Dawson, T. M. and Ross, C. A. (2001). Inducible expression of mutant alpha-synuclein decreases proteasome activity and increases sensitivity to mitochondria-dependent apoptosis. *Hum. Mol. Genet.* **10,** 919-926.

Tanriover, G., Seval-Celik, Y., Ozsoy, O., Akkoyunlu, G., Savcioglu, F., Hacioglu, G., Demir, N. and Agar, A. (2010). The effects of docosahexaenoic acid on glial derived neurotrophic factor and neurturin in bilateral rat model of parkinson's disease. *Folia Histochemica et Cytobiologica* **48,** 434-433.

Terzioglu, M. and Galter, D. (2008). Parkinson's disease: Genetic versus toxin-induced rodent models. *FEBS journal* **275,** 1384-1391.

Tillerson, J. L., Cohen, A. D., Caudle, W. M., Zigmond, M. J., Schallert, T. and Miller, G. W. (2002). Forced nonuse in unilateral parkinsonian rats exacerbates injury. *J. Neurosci.* **22,** 6790-6799.

Tillerson, J. L., Cohen, A. D., Philhower, J., Miller, G. W., Zigmond, M. J. and Schallert, T. (2001). Forced limb-use effects on the behavioral and neurochemical effects of 6-hydroxydopamine. *J. Neurosci.* **21,** 4427-4435.

Tiwary, R., Yu, W., Li, J., Park, S. K., Sanders, B. G. and Kline, K. (2010). Role of endoplasmic reticulum stress in alpha-TEA mediated TRAIL/DR5 death receptor dependent apoptosis *PLoS One* **5,** e11865.

Thomas, M., Le, W. D., (2004) Minocycline: Neuroprotective Mechanisms in Parkinsons Disease, *Current Pharmaceutical Design*.**10,** 6, 679-686

Todd, D. J., Lee, A-H., Glimcher, L.H. (2008).The endoplasmic reticulum stress response in immunity and autoimmunity. *Nature Reviews Immunology*. **8,** 663-674

Tomlinson, C. L., Patel, S., Meek, C., Clarke, C. E., Stowe, R., Shah, L., Sackley, C. M., Deane, K. H., Herd, C. P. and Wheatley, K. (2012). Physiotherapy versus placebo or no intervention in Parkinson's disease. *Cochrane Database Syst. Rev.* **7,**.

Ton, T. G., Heckbert, S. R., Longstreth Jr, W., Rossing, M. A., Kukull, W. A., Franklin, G. M., Swanson, P. D., Smith-Weller, T. and Checkoway, H. (2007). Calcium channel blockers and< i> β</i>-blockers in relation to parkinson's disease. *Parkinsonism Relat. Disord.* **13,** 165-169.

Toxopeus, C. M., Maurits, N. M., Valsan, G., Conway, B. A., Leenders, K. L. and de Jong, B. M. (2012). Cerebral activations related to ballistic, stepwise interrupted and gradually modulated movements in parkinson patients. *PloS one* **7,** e41042.

Tusi, S. K., Khalaj, L., Ashabi, G., Kiaei, M. and Khodagholi, F. (2011). Alginate oligosaccharide protects against endoplasmic reticulum-and mitochondrial-mediated apoptotic cell death and oxidative stress. *Biomaterials* **32,** 5438-5458.

Ugarte, S. D., Lin, E., Klann, E., Zigmond, M. J. and Perez, R. G. (2003). Effects of GDNF on 6-OHDA-induced death in a dopaminergic cell line: Modulation by inhibitors of PI3 kinase and MEK. *J. Neurosci. Res.* **73,** 105-112.

Usha, R., Muralikrishnan, D., Thomas, B., Ghosh, S., Mandal, C. and Mohanakumar, K. P. (2000). Region-specific attenuation of a trypsin-like protease in substantia nigra following dopaminergic neurotoxicity by 1-methyl-4-phenyl-1, 2, 3, 6-tetrahydropyridine. *Brain Res.* **882,** 191-195.

Venderova, K. and Park, D. S. (2012). Programmed cell death in parkinson's disease. *Cold Spring Harb Perspect. Med.* **2,** 10.1101/cshperspect.a009365.

Vivas, J., Arias, P. and Cudeiro, J. (2011). Aquatic therapy versus conventional land-based therapy for parkinson's disease: An open-label pilot study *Arch. Phys. Med. Rehabil.* **92,** 1202-1210.

von Bohlen Und Halbach, O. (2005). Modeling neurodegenerative diseases in vivo review. *Neurodegener Dis.* **2,** 313-320.

Wang, H. Q. and Takahashi, R. (2007). Expanding insights on the involvement of endoplasmic reticulum stress in parkinson's disease. *Antioxid. Redox Signal.* **9,** 553-561.

Wang, X., Chen, S., Ma, G., Ye, M. and Lu, G. (2005). Involvement of proinflammatory factors, apoptosis, caspase-3 activation and Ca2+ disturbance in microglia activation-mediated dopaminergic cell degeneration. *Mech. Ageing Dev.* **126,** 1241-1254.

Wayman, G. A., Lee, Y., Tokumitsu, H., Silva, A. and Soderling, T. R. (2008). Calmodulin-kinases: Modulators of neuronal development and plasticity. *Neuron* **59,** 914-931.

Weerkamp, N. J., Tissingh, G., Poels, P. J., Zuidema, S. U., Munneke, M., Koopmans, R. T. and Bloem, B. R. (2013). Parkinson disease in long term care facilities: A review of the literature. *Journal of the American Medical Directors Association*.

Williams, A. C., Cartwright, L. S. and Ramsden, D. B. (2005). Parkinson's disease: The first common neurological disease due to auto-intoxication? *QJM* **98,** 215-226.

Wilms, H., Zecca, L., Rosenstiel, P., Sievers, J., Deuschl, G. and Lucius, R. (2007). Inflammation in Parkinson's diseases and other neurodegenerative diseases: Cause and therapeutic implications. *Curr. Pharm. Des.* **13,** 1925-1928.

Wilms, H., Rosenstiel, P., Sievers, J., Deuschl, G., Zecca, L. and Lucius, R. (2003). Activation of microglia by human neuromelanin is NF-kappaB dependent and involves p38 mitogen-activated protein kinase: Implications for parkinson's disease. *FASEB J.* **17,** 500-502.

Wood-Kaczmar, A., Gandhi, S., Yao, Z., Abramov, A. S., Miljan, E. A., Keen, G., Stanyer, L., Hargreaves, I., Klupsch, K. and Deas, E. (2008). PINK1 is necessary for long term survival and mitochondrial function in human dopaminergic neurons. *PloS one* **3,** e2455.

Xiang, B., Fei, X., Zhuang, W., Fang, Y., Qin, Z. and Liang, Z. (2011). Cathepsin L is involved in 6-hydroxydopamine induced apoptosis of SH-SY5Y neuroblastoma cells. *Brain Res.* **1387,** 29-38.

Xu, C., Qu, R., Zhang, J., Li, L. and Ma, S. (2013). Neuroprotective effects of madecassoside in early stage of parkinson's disease induced by MPTP in rats. *Fitoterapia* **90,** 112-118.

Yamaguchi, H. and Wang, H. G. (2004). CHOP is involved in endoplasmic reticulum stress-induced apoptosis by enhancing DR5 expression in human carcinoma cells *J. Biol. Chem.* **279,** 45495-45502.

Yamamoto, Y., Gaynor, R. B. (2001). Role of the NFκB Pathway in the Pathogenesis of Human Disease States. *Current Molecular Medicine,***1,** 3, 287-296

Yan, N. and Shi, Y. (2005). Mechanisms of apoptosis through structural biology. *Annu. Rev. Cell Dev. Biol.* **21,** 35-56.

Yang, W., Tiffany-Castiglioni, E., Koh, H. C. and Son, I. H. (2009). Paraquat activates the IRE1/ASK1/JNK cascade associated with apoptosis in human neuroblastoma SH-SY5Y cells. *Toxicol. Lett.* **191,** 203-210.

Yang, J., Weissman, L., Bohr, V. A. and Mattson, M. P. (2008). Mitochondrial DNA damage and repair in neurodegenerative disorders. *DNA repair* **7,** 1110-1120.

Ye, J., Liu, Z., Wei, J., Lu, L., Huang, Y., Luo, L. and Xie, H. (2013). Protective effect of SIRT1 on toxicity of microglial-derived factors induced by LPS to PC12 cells via the p53-caspase-3-dependent apoptotic pathway. *Neurosci. Lett.* **553,** 72-77.

Yoon, M., Shin, M., Kim, T., Kim, B., Ko, I., Sung, Y., Kim, S., Lee, H., Kim, Y. and Kim, C. (2007). Treadmill exercise suppresses nigrostriatal dopaminergic neuronal loss in 6-hydroxydopamine-induced parkinson's rats. *Neurosci. Lett.* **423,** 12-17.

Yoshida, H. (2007). ER stress and diseases *FEBS J.* **274,** 630-658.

Zhang, C., Jin, Y., Ziemba, K., Fletcher, A., Ghosh, B., Truit, E., Yurek, D. and Smith, G. (2013). Long distance directional growth of dopaminergic axons along pathways of netrin-1 and GDNF. *Exp. Neurol.* **250,** 156-164.

Zhang, Y., Liu, W., Ma, C., Geng, J., Li, Y., Li, S., Yu, F., Zhang, X. and Cong, B. (2012). Endoplasmic reticulum stress contributes to CRH-induced hippocampal neuron apoptosis. *Exp. Cell Res.* **318,** 732-740.

Zhang, L., Xue, Y., Yang, C., Yang, W., Chen, L., Zhang, Q., Qu, T., Huang, S., Zhao, L. and Wang, X. (2012). Human albumin prevents 6-hydroxydopamine-induced loss of tyrosine hydroxylase in vitro and in vivo. *PloS one* **7,** e41226.

Zhang, L., Huang, L., Chen, L., Hao, D. and Chen, J. (2013). Neuroprotection by tetrahydroxystilbene glucoside in the MPTP mouse model of parkinson's disease. *Toxicol. Lett.* **222,** 155-163.

Zhang, F., Qian, L., Flood, P. M., Shi, J. S., Hong, J. S. and Gao, H. M. (2010). Inhibition of IkappaB kinase-beta protects dopamine neurons against lipopolysaccharide-induced neurotoxicity. *J. Pharmacol. Exp. Ther.* **333,** 822-833.

Zhang, F., Qian, L., Flood, P. M., Shi, J. S., Hong, J. S. and Gao, H. M. (2010). Inhibition of IkappaB kinase-beta protects dopamine neurons against lipopolysaccharide-induced neurotoxicity. *J. Pharmacol. Exp. Ther.* **333,** 822-833.

Zigmond, M. J., Cameron, J. L., Hoffer, B. J. and Smeyne, R. J. (2012). Neurorestoration by physical exercise: Moving forward. *Parkinsonism Relat. Disord.* **18,** S147-S150.

Zigmond, M. J., Cameron, J. L., Leak, R. K., Mirnics, K., Russell, V. A., Smeyne, R. J. and Smith, A. D. (2009). Triggering endogenous neuroprotective processes through exercise in models of dopamine deficiency. *Parkinsonism Relat. Disord.* **15,** S42-S45.

Zigmond, M. J. and Smeyne, R. J. (2014). Exercise: Is it a neuroprotective and if so, how does it work? *Parkinsonism Relat. Disord.* **20,** S123-S127.

Appendix 1
Reagents

		Product Name	Supplier	Use
Antibodies				
	AB1872	Anti-Caspase 1 (Rabbit)	Abcam 330 Cambridge Science Park Cambridge CB4 0FL UK	WB
	AB7979	Anti-Caspase 2 Active (Rabbit)	Abcam 330 Cambridge Science Park Cambridge CB4 0FL UK	WB IF
	AB3623	Anti-Caspase 3 Cleaved (Rabbit)	Millipore Ltd 3-5 The Courtyards Hatters Lane Watford Hertfordshire WD18 8YH UK	IF WB
	04-439	Anti-Caspase 3 Active (Rabbit)	Millipore Ltd 3-5 The Courtyards Hatters Lane Watford Hertfordshire WD18 8YH UK	IF
	AB52183	Anti-Caspase 4 Active (Rabbit)	Abcam 330 Cambridge Science Park Cambridge CB4 0FL UK	IF WB
	AB97318	Anti-Caspase 4 (Rabbit)	Abcam 330 Cambridge Science Park Cambridge CB4 0FL UK	IF WB
	AB25897	Anti-Caspase 8 Active (Rabbit)	Abcam 330 Cambridge Science Park Cambridge CB4 0FL UK	IF WB

04-444	Anti-Caspase 9 Active (Rabbit)	Millipore Ltd 3-5 The Courtyards Hatters Lane Watford Hertfordshire WD18 8YH UK	WB
AB62484	Anti-Caspase 12 Cleaved (Rabbit)	Abcam 330 Cambridge Science Park Cambridge CB4 0FL UK	WB
04-1078	Anti-CAMK IV Active (Rabbit)	Millipore Ltd 3-5 The Courtyards Hatters Lane Watford Hertfordshire WD18 8YH UK	WB
MAB3026	Anti-NFκB Cleaved (Mouse)	Millipore Ltd 3-5 The Courtyards Hatters Lane Watford Hertfordshire WD18 8YH UK	IF WB
MAB318	Anti-Tyrosine Hydroxylase (Mouse)	Millipore Ltd 3-5 The Courtyards Hatters Lane Watford Hertfordshire WD18 8YH UK	IF
AB152	Anti-Tyrosine Hydroxylase (Rabbit)	Millipore Ltd 3-5 The Courtyards Hatters Lane Watford Hertfordshire WD18 8YH UK	IF
AQ300R	Sheep Anti Mouse IgG Rhodamine	Millipore Ltd 3-5 The Courtyards Hatters Lane Watford Hertfordshire WD18 8YH UK	IF

	AP123R	Goat Anti Rabbit IgG Rhodamine	Millipore Ltd 3-5 The Courtyards Hatters Lane Watford Hertfordshire WD18 8YH UK	IF
	AQ300F	Sheep Anti Mouse IgG FITC	Millipore Ltd 3-5 The Courtyards Hatters Lane Watford Hertfordshire WD18 8YH UK	IF
	AB6791	Sheep anti Rabbit IgG FITC	Abcam 330 Cambridge Science Park Cambridge CB4 0FL UK	IF
	AP192F	Donkey Anti Mouse IgG FITC	Millipore Ltd 3-5 The Courtyards Hatters Lane Watford Hertfordshire WD18 8YH UK	IF
	12-348	Goat anti Rabbit HRP conjugate	Millipore Ltd 3-5 The Courtyards Hatters Lane Watford Hertfordshire WD18 8YH UK	WB
	AP192P	Donkey Anti-Mouse HRP conjugate	Millipore Ltd 3-5 The Courtyards Hatters Lane Watford Hertfordshire WD18 8YH UK	WB
Cell Culture				
	SCM008	ReNVM cell	Millipore Ltd 3-5 The Courtyards Hatters Lane Watford Hertfordshire WD18 8YH UK	Cell culture

SCM005	ReNcell NSC Maintenance Medium	Millipore Ltd 3-5 The Courtyards Hatters Lane Watford Hertfordshire WD18 8YH UK	Cell culture
SCM007	ReNcell NSC Freezing Medium	Millipore Ltd 3-5 The Courtyards Hatters Lane Watford Hertfordshire WD18 8YH UK	Cell culture
L2020	Laminin	Sigma-Aldrich Ltd The Old Brickyard New Road Gillingham Dorset SP8 4XT UK	Cell culture
D5796	DMEM	Sigma-Aldrich Ltd The Old Brickyard New Road Gillingham Dorset SP8 4XT UK	Cell culture
A6964	Accutase	Sigma-Aldrich Ltd The Old Brickyard New Road Gillingham Dorset SP8 4XT UK	Cell culture
GF003	EGF	Millipore Ltd 3-5 The Courtyards Hatters Lane Watford Hertfordshire WD18 8YH UK	Cell culture
GF144	FGF	Millipore Ltd 3-5 The Courtyards Hatters Lane Watford Hertfordshire WD18 8YH UK	Cell culture

H116	6OHDA	Sigma-Aldrich Ltd The Old Brickyard New Road Gillingham Dorset SP8 4XT UK	Cell culture
S-1000	Goat serum	Vector Laboratories 3 Accent Park Pakewell Road Southgate Peterborough PE2 6XS UK	IF
158127	Paraformaldehyde	Sigma-Aldrich Ltd The Old Brickyard New Road Gillingham Dorset SP8 4XT UK	IF
N150	Triton X	Sigma-Aldrich Ltd The Old Brickyard New Road Gillingham Dorset SP8 4XT UK	IF
T8787	BSA	Vector Laboratories 3 Accent Park Pakewell Road Southgate Peterborough PE2 6XS UK	IF
158127	Vector shield Mounting Medium	Vector Laboratories 3 Accent Park Pakewell Road Southgate Peterborough PE2 6XS UK	IF
BT30006	MTT	Cambridge BioScience Munro House Trafalgar Way Bar Hill Cambridge, CB23 8SQ UK	Calorimetric

G7351	CaspACE assay system	Promega Delta House Southampton Science Park Southampton SO16 7NS UK	Calorimetric
482830K	**TUNEL**	Trevigen 8405 Helgerman Ct Gauthersburg Maryland MD 20877 USA	**TUNEL assay**
401479	Insolution IKK2 inhibitor	Merck Chemicals Ltd Boulevard Industrial Park Padge Road Nottingham NG9 2JR UK	**TUNEL assay** Calorimetric IF WB
SC-202332	Salubrinal	Santa Cruz Biotechnology Bergheimer Str.89-2 69115 Heidelberg Germany	**TUNEL assay** Calorimetric IF WB
G7351	zVADfmk	Promega Delta House Southampton Science Park Southampton SO16 7NS UK	**TUNEL assay** Calorimetric IF WB
107920	*zATADfmk*	Merck Chemicals Ltd Boulevard Industrial Park Padge Road Nottingham NG9 2JR UK	**TUNEL assay** Calorimetric IF WB c
218755	*zLEVDfmk*	Merck Chemicals Ltd Boulevard Industrial Park Padge Road Nottingham NG9 2JR UK	**TUNEL assay** Calorimetric IF WB

218759	*zIETDfmk*	Merck Chemicals Ltd Boulevard Industrial Park Padge Road Nottingham NG9 2JR UK	**TUNEL assay** Calorimetric IF WB
218744	*zVDVADfmk*	Merck Chemicals Ltd Boulevard Industrial Park Padge Road Nottingham NG9 2JR UK	**TUNEL assay** Calorimetric IF WB
302050	Tris base	Severn Biotech Unit 2 Park Lane Kidderminster Worcestershire DY11 6TJ UK	WB
303310	SDS	Severn Biotech Unit 2 Park Lane Kidderminster Worcestershire DY11 6TJ UK	WB
302125	Glycine	Severn Biotech Unit 2 Park Lane Kidderminster Worcestershire DY11 6TJ UK	WB
30-20-60	30% acryl amide Mix	Sigma-Aldrich Ltd The Old Brickyard New Road Gillingham Dorset SP8 4XT UK	WB
30-33-10	Ammonium persulphate	Sigma-Aldrich Ltd The Old Brickyard New Road Gillingham Dorset SP8 4XT UK	WB

30-21-60	BSA	Perbio Science Unit 9, Atley Way North Nelson Industrial Estate Cramlington Northumberland NE231WA UK	WB
A3574	BCA Protein Assay Kit	Pierce Biotechnology 3747 Meridian Road Rockford IL 61105 USA	Protein Assay
A3678	DTT	Sigma-Aldrich Ltd The Old Brickyard New Road Gillingham Dorset SP8 4XT UK	WB
23209	TEMED	Sigma-Aldrich Ltd The Old Brickyard New Road Gillingham Dorset SP8 4XT UK	WB
23227	Glycerol	Sigma-Aldrich Ltd The Old Brickyard New Road Gillingham Dorset SP8 4XT UK	WB
43819	Bromophenol Blue	Sigma-Aldrich Ltd The Old Brickyard New Road Gillingham Dorset SP8 4XT UK	WB
P5493	Prestained marker	Invitrogen 3 Fountain Drive Inchinnan Business Park Paisley PA4 9RF UK	WB
T9281	Coomaisse	Sigma-Aldrich Ltd The Old Brickyard New Road	WB

		Gillingham Dorset SP8 4XT UK	
G8773	Glacial acetic acid	Fisher Scientific Bishop Meadow Road Loughborough Leicestershire LE11 5RG UK	WB
B5525	Methanol	Fisher Scientific Bishop Meadow Road Loughborough Leicestershire LE11 5RG UK	WB
B7920	Analytical water	Fisher Scientific Bishop Meadow Road Loughborough Leicestershire LE11 5RG UK	WB
A040025	Ponceau solution	Sigma-Aldrich Ltd The Old Brickyard New Road Gillingham Dorset SP8 4XT UK	WB
M/3950/15	EDTA	Severn Biotech Unit 2 Park Lane Kidderminster Worcestershire DY11 6TJ UK	WB
W/0100/21	ECL solution	Perbio Science Unit 9, Atley Way North Nelson Industrial Estate Cramlington Northumberland NE231WA UK	WB
81462	PBS	Sigma-Aldrich Ltd The Old Brickyard New Road Gillingham Dorset SP8 4XT UK	Cell Culture IF WB
P1379	Tween20	Sigma-Aldrich Ltd The Old Brickyard New Road Gillingham	WB

30-232-60	Kodak developer solution	Dorset SP8 4XT UK Sigma-Aldrich Ltd The Old Brickyard New Road Gillingham Dorset SP8 4XT UK	WB
34087	Kodak fixer solution	Sigma-Aldrich Ltd The Old Brickyard New Road Gillingham Dorset SP8 4XT UK	WB
FMXOB0101824	Kodak MXB Blue film 18 x 24	Xograph Healthcare Xograph House Ebley Road Stonehouse Gloucestershire GL10 2LU UK	WB
P8307	Kodak 18 x 24 cassette	Xograph Healthcare Xograph House Ebley Road Stonehouse Gloucestershire GL10 2LU UK	WB

Appendix 2
Ethics Approval

PIERWSZA WARSZAWSKA KOMISJA ETYCZNA
do Doświadczeń na Zwierzętach
Instytut Biologii Doświadczalnej im. M. Nenckiego PAN
02-093 Warszawa, ul. Pasteura 3
Tel. 659-85-71 w. 212, 326, Fax: 822-53-42

Nr opinii	320/2005
Data	2005-07-15
Nr wniosku	320/2005
Data	2005-07-13

OPINIA
LOKALNEJ KOMISJI ETYCZNEJ
(Kopia wniosku jest integralną częścią opinii)

LOKALNA KOMISJA ETYCZNA Nr 1 w WARSZAWIE
rozpatrzyła na posiedzeniu w dniu 14 lipca 2005 r. wniosek o realizację projektu p.n.:

WPŁYW WZMOŻONEJ AKTYWNOŚCI RUCHOWEJ O RÓŻNEJ CHARAKTERYSTYCE NA SZLAK NO/cGMP I ŚMIERĆ NEURONÓW DOPAMINERGICZNYCH W ZWIERZĘCYM MODELU CHOROBY PARKINSONA.

złożony przez Dr MAŁGORZATĘ CHALIMONIUK
zatrudnioną w INSTYTUCIE MEDYCYNY DOŚWIADCZALNEJ I KLINICZNEJ
im. M. MOSSAKOWSKIEGO PAN

i uznała realizację tego projektu za:

D	Dopuszczalną (D)		niedopuszczalną (N)

Ustalono, że:
1. Doświadczenia należy zaliczyć do kategorii:

• badania na żywych kręgowcach	X
• testy na żywych kręgowcach	
• doświadczenia na żywych kręgowcach dla celów dydaktycznych	

2. Najwyższa wartość stopnia uważności proponowanych procedur nie przekracza

3. Doświadczenia mogą być wykonywane na zwierzętach

Lp.	Gatunek	Liczba zwierząt
1)	szczur	0

Szczegółowe uzasadnienie

Wniosek dotyczy przedłużenia ważności opinii LKE Nr 1 w Warszawie Nr 324/2002004 z dnia 29.01.2004, która aprobowała badania na 300 szczurach, z terminem ważności do końca roku 2006. Badania nie zostały podjęte z powodu braku finansowania, wobec czego Autorka wnioskuje o przedłużenie ważności opinii do końca roku 2008. Komisja zgodziła się na takie przedłużenie ważności opinii, bez zmiany innych warunków wykonywania doświadczeń. Niniejsza opinia jest ważna w połączeniu z uprzednią opinią Nr 324/2004.

Odwołanie od niniejszej opinii do KKE w Warszawie przysługuje kierownikowi jednostki i wnioskodawcy. Odwołanie składa się za pośrednictwem lokalnej komisji, która wydała opinię, w terminie jednego miesiąca od dnia otrzymania tej opinii (Dz. U. Nr 38 poz. 351 art. 30 z dnia 21 kwietnia 1997r).

Doc. dr hab. Krzysztof Turlejski
Przewodniczący Lokalnej Komisji Etycznej Nr 1
w Warszawie

Miejsce: Warszawa
Data: 15 lipiec 2005 r.

[illegible]
im. Mirosława Mossakowskiego
Polskiej Akademii Nauk
02-106 Warszawa, ul. Pawińskiego 5
tel. 608-60-17, 668-54-56
[illegible]

Zezwolenie Nr 9

NA PRZEPROWADZANIE DOŚWIADCZEŃ NA ZWIERZĘTACH

Na podstawie art. 16 ust. 2 pkt. 1 ustawy z dnia 21 stycznia 2005 r. o doświadczeniach na zwierzętach (Dz. U. Nr 33, poz. 289)

ZEZWALAM

Pani/u **prof. dr hab. n. med. Józef Langfort**

Tytuł naukowy lub stopień naukowy prof. dr hab. n. med.

Stanowisko profesor

Tytuł zawodowy biolog medyczny - fizjolog

na przeprowadzanie doświadczeń na następujących zwierzętach:

1. szczury
2. myszy
3. gerbile
4. króliki

Zezwolenie dotyczy wyłącznie doświadczeń na zwierzętach przeprowadzanych w ramach działalności

Zakład Farmakologii Doświadczalnej

(nazwa i adres jednostki doświadczalnej)

Zezwolenie jest ważne do dnia 31.12.2010 r.

2005.10.19
(data)

Z-ca DYREKTORA
ds. Ogólnych
[illegible]
(podpis kierownika jednostki doświadczalnej)

UWAGA

Doświadczenia na zwierzętach mogą być przeprowadzane wyłącznie po uzyskaniu zgody lokalnej komisji etycznej do spraw doświadczeń na zwierzętach lub Krajowej Komisji Etycznej do Spraw Doświadczeń na Zwierzętach oraz zezwolenia kierownika jednostki doświadczalnej.

[illegible]
im. Mirosława Mossakowskiego
Polskiej Akademii Nauk
02-106 Warszawa, ul. A. Pawińskiego 5
13.04.2009 r.

Za zgodność z oryginałem

STARSZY SPECJALISTA
mgr [illegible]

ReNeuron
pioneering stem cell therapeutics

ReNeuron Ltd

10 Nugent Road
Surrey Research Park
Guildford
Surrey
GU2 7AF, U.K.
Tel: +44-1483 302560
Fax: +44-1483 534864

Cell Line Regulatory Statement

I the undersigned declare the cell lines provided to Millipore by ReNeuron for further distribution under catologue numbers CX: SCC007 and VM:SCC008 were derived from tissue donations;

1. Procured with appropriate consent of the donor
2. Developed under ethically approved protocols
3. Reported to be free of HIV, HTLV, Hepatitus B & C infections as serologic tests applied to donor blood samples

Signed: 

Dr John Sinden, Chief Scientific Officer

Appendix 3
Data Analysis : PD Animal Model

Figure 3.3: Investigating the Amount of Active Caspase-2 in Brain Cortex of Untreated, Exercised. MPTP and MPTP Treated with Exercise Rat PD model

	DETERMINING CASPASE- 2 ACTIVITIES IN BRAIN CORTEX OF C, Ex, PD & PD-Ex GROUP			
	MEAN C	**MEAN Ex**	**MEAN PD**	**MEAN PD-Ex**
Active Caspase-2 Assay 1	0.98	1.11	1.78	1.25
Active Caspase-2 Assay 2	1.28	1.17	1.75	1.03
Active Caspase-2 Assay 3	1.35	1.50	1.81	1.15
Active Caspase-2 Assay 4	1.43	1.15	1.61	1.40
Active Caspase-2 Assay 5	1.35	0.83	1.51	0.96
Mean of All Assays	1.28	1.15	1.69	1.16
Mean of All Assays %	**100**	**90**	**132**	**91**
SD	0.17	0.24	0.13	0.18
SD (%)	17.49	23.99	12.74	17.54
T Test			**0.003**	**0.001**

ANOVA

Groups	*Count*	*Sum*	*Average*	*Variance*
MEAN C	5	6.397	1.2794	0.030058
MEAN Ex	5	5.7623	1.1524	0.057598
MEAN PD	5	8.4047	1.6898	0.016244
MEAN PD-Ex	5	5.7592	1.1506	0.030753

ANOVA

Source of Variation	*SS*	*df*	*MS*	*F*	*P-value*	*F crit*
Between Groups	0.961189	3	0.320396	9.401	0.000775	3.238715
Within Groups	0.540581	16	0.033786			
Total	1.501771	19				

Figure 3.5: Investigating the Amount of Cleaved Caspase-3 in Brain Cortex of Untreated, Exercised. MPTP and MPTP Treated with Exercise Rat PD model

	DETERMINING CASPASE-3 ACTIVITIES IN BRAIN CORTEX OF C, Ex, PD & PD-Ex GROUP			
	MEAN C	**MEAN Ex**	**MEAN PD**	**MEAN PD-Ex**
Cleaved Caspase-3 Assay 1	1.23	1.19	1.49	0.91
Cleaved Caspase-3 Assay 2	1.38	1.11	1.78	1.18
Cleaved Caspase-3 Assay 3	1.48	1.10	1.92	1.33
Cleaved Caspase-3 Assay 4	1.42	1.19	1.70	0.86
Cleaved Caspase-3 Assay 5	1.52	0.86	1.76	0.86
Mean of All Assays	1.41	1.09	1.73	1.03
Mean of All Assays %	**100**	**78**	**123**	**73**
SD	0.11	0.13	0.16	0.21
SD (%)	11.36	13.41	15.73	21.42
T Test			**0.007**	**0.001**

ANOVA

Groups	*Count*	*Sum*	*Average*	*Variance*
MEAN C	5	7.029	1.405	0.012983
MEAN Ex	5	5.4511	1.0903	0.017922
MEAN PD	5	8.647	1.729	0.024372
MEAN PD-Ex	5	5.1432	1.0286	0.004545

ANOVA

Source of Variation	*SS*	*df*	*MS*	*F*	*P-value*	*F crit*
Between Groups	1.56276	3	0.520920	20.53107	9.86E-06	3.23887
Within Groups	0.40595	16	0.002537			
Total	1.96872	19				

Figure 3.7: Investigating the Amount of Active Caspase-8 in Brain Cortex of Untreated, Exercised. MPTP and MPTP Treated with Exercise Rat PD model

	DETERMINING CASPASE-8 ACTIVITIES IN BRAIN CORTEX OF C, Ex, PD & PD-Ex GROUP			
	MEAN C	**MEAN Ex**	**MEAN PD**	**MEAN PD-Ex**
Active Caspase-8 Assay 1	1.30	1.59	1.89	1.20
Active Caspase-8 Assay 2	1.36	1.17	1.61	1.09
Active Caspase-8 Assay 3	1.49	1.41	1.89	1.27
Active Caspase-8 Assay 4	1.36	1.34	1.79	1.17
Active Caspase-8 Assay 5	1.52	1.28	1.91	0.88
Mean of All Assays	1.41	1.36	1.82	1.12
Mean of All Assays %	**100**	**96**	**129**	**80**
SD	0.09	0.16	0.13	0.15
SD (%)	9.46	15.81	12.71	15.07
T Test			**0.001**	**0.0001**

ANOVA

Groups	*Count*	*Sum*	*Average*	*Variance*
MEAN C	5	7.047226949	1.409445389	0.008950505
MEAN Ex	5	6.787427455	1.357485491	0.010725107
MEAN PD	5	9.092001	1.818400162	0.016162
MEAN PD-Ex	5	5.624678467	1.124935693	0.022712323

ANOVA

Source of Variation	*SS*	*df*	*MS*	*F*	*P-value*	*F crit*
Between Groups	1.255306065	3	0.418435355	22.97974749	4.829E-06	3.23871
Within Groups	0.291342089	16	0.018208389			
Total	1.546648154	19				

Figure 3.9: Investigating the Amount of Active Caspase-9 in Brain Cortex of Untreated, Exercised. MPTP and MPTP Treated with Exercise Rat PD model

	DETERMINING CASPASE-9 ACTIVITIES IN BRAIN CORTEX OF C, Ex, PD & PD-Ex GROUP			
	MEAN C	**MEAN Ex**	**MEAN PD**	**MEAN PD-Ex**
Active Caspase-9 Assay 1	1.32	1.27	1.26	1.68
Active Caspase-9 Assay 2	1.16	1.16	1.20	1.71
Active Caspase-9 Assay 3	1.14	1.22	1.47	1.66
Active Caspase-9 Assay 4	1.37	1.33	1.41	1.66
Active Caspase-9 Assay 5	1.26	1.38	1.48	1.75
Mean of All Assays	1.25	1.27	1.36	1.69
Mean of All Assays %	**100**	**102**	**109**	**135**
SD	0.10	0.09	0.13	0.04
SD (%)	10.04	8.80	12.62	4.06
T Test			**0.2**	**0.003**

ANOVA

Groups	*Count*	*Sum*	*Average*	*Variance*
MEAN C	5	6.2461	1.249228	0.010074
MEAN Ex	5	6.35887	1.271774	0.007707
MEAN PD	5	6.812869	1.362574	0.015916
MEAN PD-Ex	5	8.457162	1.691432	0.000446

ANOVA

Source of Variation	*SS*	*df*	*MS*	*F*	*P-value*	*F crit*
Between Groups	0.608267392	3	0.202089131	23.61306	4.054E-06	3.238715
Within Groups	0.140415576	16	0.008778474			
Total	0.748682968	19				

Figure 3.11: Investigating the Amount of Cleaved Caspase-12 in Brain Cortex of Untreated, Exercised. MPTP and MPTP Treated with Exercise Rat PD model

	DETERMINING CASPASE-12 ACTIVITIES IN BRAIN CORTEX OF C, Ex, PD & PD-Ex GROUP			
	MEAN C	**MEAN Ex**	**MEAN PD**	**MEAN PD-Ex**
Cleaved Caspase-12 Assay 1	1.18	1.13	1.51	0.94
Cleaved Caspase-12 Assay 2	1.12	1.33	1.66	0.84
Cleaved Caspase-12 Assay 3	1.17	1.16	1.36	0.81
Cleaved Caspase-12 Assay 4	1.10	1.20	1.35	0.81
Cleaved Caspase-12 Assay 5	1.10	0.94	1.43	0.86
Mean of All Assays	1.13	1.15	1.46	0.85
Mean of All Assays %	**100**	**102**	**129**	**75**
SD	0.04	0.14	0.13	0.05
SD (%)	3.74	14.40	12.82	5.27
T Test			**0.003**	**0.0001**

ANOVA

Groups	*Count*	*Sum*	*Average*	*Variance*
MEAN C	5	5.628	1.1256	0.00140
MEAN Ex	5	5.733	1.1466	0.00207
MEAN PD	5	7.2974	1.4594	0.00164
MEAN PD-Ex	5	4.260	0.8521	0.00027

ANOVA

Source of Variation	*SS*	*df*	*MS*	*F*	*P-value*	*F crit*
Between Groups	0.9238	3	0.3079	29.796	8.763E-07	3.2387
Within Groups	0.1653	16	0.0103			
Total	1.0892	19				

Figure 3.13: Investigating the Amount of Active Caspase-2 in Cerebellum of Untreated, Exercised. MPTP and MPTP Treated with Exercise Rat PD model

	DETERMINING CASPASE- 2 ACTIVITIES IN CEREBELLUM OF C, Ex, PD & PD-Ex GROUP			
	MEAN C	**MEAN Ex**	**MEAN PD**	**MEAN PD-Ex**
Active Caspase-2 Assay 1	1.64	1.25	1.71	0.22
Active Caspase-2 Assay 2	1.66	1.23	1.51	0.68
Active Caspase-2 Assay 3	1.50	1.11	1.39	0.48
Active Caspase-2 Assay 4	1.76	1.26	1.62	0.65
Active Caspase-2 Assay 5	1.44	1.04	1.58	0.56
Mean of All Assays	1.60	1.18	1.56	0.52
Mean of All Assays %	**100**	**74**	**98**	**32**
SD	0.13	0.10	0.12	0.18
SD (%)	12.64	9.68	12.26	18.24
T Test			**0.662**	**0.00001**

ANOVA

Groups	*Count*	*Sum*	*Average*	*Variance*
MEAN C	5	7.951025	1.599002	0.015987
MEAN Ex	5	5.890937	1.178187	0.009781
MEAN PD	5	7.816545	1.563309	0.030314
MEAN PD-Ex	5	2.591509	0.518302	0.033271

ANOVA

Source of Variation	*SS*	*df*	*MS*	*F*	*P-value*	*F crit*
Between Groups	3.776582	3	1.259527	68.37939	2.27E-09	3.238715
Within Groups	0.294663	16	0.018416			
Total	4.072325	19				

Figure 3.15: Investigating the Amount of Cleaved Caspase-3 in Cerebellum of Untreated, Exercised. MPTP and MPTP Treated with Exercise Rat PD model

	DETERMINING CASPASE-3 ACTIVITIES IN CEREBELLUM OF C, Ex, PD & PD-Ex GROUP			
	MEAN C	**MEAN Ex**	**MEAN PD**	**MEAN PD-Ex**
Cleaved Caspase-3 Assay 1	1.14	0.88	1.18	0.96
Cleaved Caspase-3 Assay 2	1.00	0.97	1.37	0.87
Cleaved Caspase-3 Assay 3	1.02	0.89	1.54	1.06
Cleaved Caspase-3 Assay 4	1.21	1.05	1.45	1.13
Cleaved Caspase-3 Assay 5	1.10	1.04	1.40	0.86
Mean of All Assays	1.09	0.97	1.39	0.98
Mean of All Assays %	**100**	**88**	**127**	**89**
SD	0.09	0.08	0.13	0.12
SD (%)	8.78	7.89	13.23	11.68
T Test			**0.004**	**0.001**

ANOVA

Groups	*Count*	*Sum*	*Average*	*Variance*
MEAN C	5	5.465	1.093	0.007
MEAN Ex	5	4.829	0.965	0.006
MEAN PD	5	6.942	1.388	0.088
MEAN PD-Ex	5	4.808	0.976	0.013

ANOVA

Source of Variation	*SS*	*df*	*MS*	*F*	*P-value*	*F crit*
Between Groups	0.582	3	0.194	17.23	2.86E-05	3.238
Within Groups	0.180	16	0.011			
Total	0.763	19				

Figure 3.17: Investigating the Amount of Active Caspase-8 in Cerebellum of Untreated, Exercised. MPTP and MPTP Treated with Exercise Rat PD model

	DETERMINING CASPASE-8 ACTIVITIES IN CEREBELLUM OF C, Ex, PD & PD-Ex GROUP			
	MEAN C	**MEAN Ex**	**MEAN PD**	**MEAN PD-Ex**
Active Caspase-8 Assay 1	1.24	0.91	1.51	1.02
Active Caspase-8 Assay 2	1.20	0.97	1.49	1.20
Active Caspase-8 Assay 3	1.24	1.00	1.44	1.27
Active Caspase-8 Assay 4	1.24	1.13	1.53	1.14
Active Caspase-8 Assay 5	1.10	1.16	1.53	1.27
Mean of All Assays	1.20	1.03	1.50	1.18
Mean of All Assays %	**100**	**86**	**125**	**98**
SD	0.06	0.11	0.04	0.11
SD (%)	6.19	10.56	3.58	10.60
T Test			**0.00001**	**0.001**

ANOVA

Groups	*Count*	*Sum*	*Average*	*Variance*
MEAN C	5	6.011653	1.202331	0.003282
MEAN Ex	5	5.166077	1.033215	0.011141
MEAN PD	5	7.500025	1.500005	0.000128
MEAN PD-Ex	5	5.902974	1.180595	0.002778

ANOVA

Source of Variation	*SS*	*df*	*MS*	*F*	*P-value*	*F crit*
Between Groups	0.574913	3	0.191638	27.84674	1.37E-06	3.238715
Within Groups	0.109325	16	0.006833			
Total	0.684238	19				

Figure 3.19: Investigating the Amount of Active Caspase-9 in Cerebellum of Untreated, Exercised. MPTP and MPTP Treated with Exercise Rat PD model

	DETERMINING CASPASE-9 ACTIVITIES IN CEREBELLUM OF C, Ex, PD & PD-Ex GROUP			
	MEAN C	**MEAN Ex**	**MEAN PD**	**MEAN PD-Ex**
Active Caspase-9 Assay 1	1.01	1.01	1.20	1.63
Active Caspase-9 Assay 2	1.17	0.85	1.27	1.41
Active Caspase-9 Assay 3	1.01	0.81	0.98	1.60
Active Caspase-9 Assay 4	1.05	0.92	1.32	1.30
Active Caspase-9 Assay 5	1.20	1.01	1.26	1.62
Mean of All Assays	1.09	0.92	1.21	1.51
Mean of All Assays %	**100**	**85**	**111**	**139**
SD	0.09	0.09	0.13	0.15
SD (%)	9.11	9.18	13.18	15.03
T Test			**0.1**	**0.01**

ANOVA

Groups	*Count*	*Sum*	*Average*	*Variance*
MEAN C	5	5.440	1.088	0.008
MEAN Ex	5	4.6031	0.9206	0.0043
MEAN PD	5	6.030	1.206	0.0173
MEAN PD-Ex	5	7.5552	1.5105	0.0225

ANOVA

Source of Variation	*SS*	*df*	*MS*	*F*	*P-value*	*F crit*
Between Groups	0.929971	3	0.309904	21.875	6.612E-06	3.2385
Within Groups	0.226735	16	0.014171			
Total	1.156706	19				

Figure 3.21: Investigating the Amount of Cleaved Caspase-12 in Cerebellum of Untreated, Exercised. MPTP and MPTP Treated with Exercise Rat PD model

	DETERMINING CASPASE-12 ACTIVITIES IN CEREBELLUM OF C, Ex, PD & PD-Ex GROUP			
	MEAN C	**MEAN Ex**	**MEAN PD**	**MEAN PD-Ex**
Cleaved Caspase-12 Assay 1	1.34	1.07	1.78	0.85
Cleaved Caspase-12 Assay 2	1.19	1.13	1.87	1.11
Cleaved Caspase-12 Assay 3	1.20	0.98	1.54	0.97
Cleaved Caspase-12 Assay 4	1.22	1.05	1.76	1.22
Cleaved Caspase-12 Assay 5	1.41	0.93	1.42	1.32
Mean of All Assays	1.27	1.03	1.67	1.09
Mean of All Assays %	**100**	**81**	**132**	**86**
SD	0.10	0.08	0.19	0.19
SD (%)	9.75	7.65	18.92	19.10
T Test			**0.01**	**0.001**

ANOVA

Groups	*Count*	*Sum*	*Average*	*Variance*
MEAN C	5	6.355	1.271	0.009
		5.1	1.02	0.005
MEAN Ex	5	6.3	1.26	0.007
		8.3	1.66	
MEAN PD	5	6.2	1.24	0.035
		5.4	1.08	0.036
MEAN PD-Ex	5	4.201	0.84	0.047

ANOVA

Source of Variation	*SS*	*df*	*MS*	*F*	*P-value*	*F crit*
Between Groups	1.248	3	0.416	18.99	1.5E-05	3.2387
Within Groups	0.350	16	0.021			
Total	1.598	19				

Figure 3.23: Investigating the Amount of Active Caspase-2 in Midbrain of Untreated, Exercised. MPTP and MPTP Treated with Exercise Rat PD model

	DETERMINING CASPASE- 2 ACTIVITIES IN MIDBRAIN OF C, Ex, PD & PD-Ex GROUP			
	MEAN C	**MEAN Ex**	**MEAN PD**	**MEAN PD-Ex**
Active Caspase-2 Assay 1	1.20	1.00	1.76	0.00
Active Caspase-2 Assay 2	1.28	1.20	1.63	0.00
Active Caspase-2 Assay 3	1.24	0.95	1.73	0.00
Active Caspase-2 Assay 4	1.14	1.17	1.85	0.00
Active Caspase-2 Assay 5	1.16	1.37	2.24	0.00
Mean of All Assays	1.20	1.14	1.84	0.00
Mean of All Assays %	**100**	**94**	**153**	**0**
SD	0.06	0.17	0.24	0.00
SD (%)	5.92	16.90	23.79	0.00
T Test			**0.003**	**0.0001**

ANOVA

Groups	*Count*	*Sum*	*Average*	*Variance*
MEAN C	5	6.021804	1.204368	0.003052
MEAN Ex	5	5.685127	1.137025	0.028199
MEAN PD	5	9.199392	1.839878	0.056194
MEAN PD-Ex	5	0	0	0

ANOVA

Source of Variation	*SS*	*df*	*MS*	*F*	*P-value*	*F crit*
Between Groups	8.789337	3	2.929779	132.1529	1.68E-11	3.238871
Within Groups	0.354697	16	0.022168			
Total	9.144034	19				

Figure 3.25: Investigating the Amount of Cleaved Caspase-3 in Midbrain of Untreated, Exercised. MPTP and MPTP Treated with Exercise Rat PD model

	DETERMINING CASPASE-3 ACTIVITIES IN MIDBRAIN OF C, Ex, PD & PD-Ex GROUP			
	MEAN C	**MEAN Ex**	**MEAN PD**	**MEAN PD-Ex**
Cleaved Caspase-3 Assay 1	0.99	1.00	1.50	0.83
Cleaved Caspase-3 Assay 2	1.14	1.10	1.68	1.23
Cleaved Caspase-3 Assay 3	1.25	1.19	1.77	0.87
Cleaved Caspase-3 Assay 4	1.27	1.27	1.45	1.06
Cleaved Caspase-3 Assay 5	1.06	0.97	1.54	1.07
Mean of All Assays	1.14	1.10	1.59	1.01
Mean of All Assays %	**100**	**97**	**139**	**89**
SD	0.12	0.13	0.14	0.16
SD (%)	12.29	12.59	13.51	16.28
T Test			**0.001**	**0.0003**

ANOVA

Groups	*Count*	*Sum*	*Average*	*Variance*
MEAN C	5	5.705	1.141	0.015106
		5.9198	1.1839	0.041065
MEAN Ex	5	5.5126	1.1025	0.015852
		7.9342	1.5868	0.018247
MEAN PD	5	5.0589	1.0117	0.026518
MEAN PD-Ex	5	5.0932	1.0186	0.041

ANOVA

Source of Variation	*SS*	*df*	*MS*	*F*	*P-value*	*F crit*
Between Groups	0.994	3	0.331	17.519	2.6E-05	3.2388
Within Groups	0.302	16	0.0189			
Total	1.2976	19				

Figure 3.27: Investigating the Amount of Active Caspase-8 in Midbrain of Untreated, Exercised. MPTP and MPTP Treated with Exercise Rat PD model

	DETERMINING CASPASE-8 ACTIVITIES IN MIDBRAIN OF C, Ex, PD & PD-Ex GROUP			
	MEAN C	**MEAN Ex**	**MEAN PD**	**MEAN PD-Ex**
Active Caspase-8 Assay 1	1.32	1.10	1.85	0.00
Active Caspase-8 Assay 2	1.33	0.94	1.58	0.00
Active Caspase-8 Assay 3	1.07	0.86	1.83	0.00
Active Caspase-8 Assay 4	1.14	0.86	1.89	0.00
Active Caspase-8 Assay 5	1.06	1.15	1.40	0.00
Mean of All Assays	1.18	0.98	1.71	0.00
Mean of All Assays %	**100**	**83**	**145**	**0**
SD	0.13	0.13	0.21	0.00
SD (%)	13.37	13.31	21.15	0.00
T Test			**0.01**	**0.0001**

ANOVA

Groups	*Count*	*Sum*	*Average*	*Variance*
MEAN C	5	5.9115783	1.182315794	0.017879779
MEAN Ex	5	4.913697	0.982739402	0.017706055
MEAN PD	5	8.504318	1.700860418	0.004474402
MEAN PD-Ex	5	0	0	0

ANOVA

Source of Variation	*SS*	*df*	*MS*	*F*	*P-value*	*F crit*
Between Groups	7.658526	3	2.552842	127.1206	2.2E-11	3.238715
Within Groups	0.321305	16	0.020081			
Total	7.979831	19				

Figure 3.29: Investigating the Amount of Active Caspase-9 in Midbrain of Untreated, Exercised. MPTP and MPTP Treated with Exercise Rat PD model

	DETERMINING CASPASE-9 ACTIVITIES IN MIDBRAIN OF C, Ex, PD & PD-Ex GROUP			
	MEAN C	**MEAN Ex**	**MEAN PD**	**MEAN PD-Ex**
Active Caspase-9 Assay 1	1.19	0.84	1.29	0.83
Active Caspase-9 Assay 2	1.07	0.79	1.33	0.77
Active Caspase-9 Assay 3	1.00	0.62	1.37	0.82
Active Caspase-9 Assay 4	1.11	0.87	1.41	0.92
Active Caspase-9 Assay 5	1.18	0.86	1.41	0.86
Mean of All Assays	1.11	0.80	1.36	0.84
Mean of All Assays %	**100**	**72**	**123**	**76**
SD	0.08	0.10	0.05	0.06
SD (%)	8.08	10.46	5.10	5.56
T Test			**0.001**	**0.0000003**

ANOVA

Groups	*Count*	*Sum*	*Average*	*Variance*
MEAN C	5	5.546886	1.109377	0.006052
MEAN Ex	5	3.979411	0.795882	0.001022
MEAN PD	5	6.807661	1.361532	0.002302
MEAN PD-Ex	5	4.206995	0.841399	0.000329

ANOVA

Source of Variation	*SS*	*df*	*MS*	*F*	*P-value*	*F crit*
Between Groups	1.033104	3	0.344436	59.46539	6.77E-09	3.238715
Within Groups	0.092650	16	0.005791			
Total	1.125754	19				

Figure 3.31: Investigating the Amount of Cleaved Caspase-12 in Midbrain of Untreated, Exercised. MPTP and MPTP Treated with Exercise Rat PD model

	DETERMINING CASPASE-12 ACTIVITIES IN MIDBRAIN OF C, Ex, PD & PD-Ex GROUP			
	MEAN C	**MEAN Ex**	**MEAN PD**	**MEAN PD-Ex**
Cleaved Caspase-12 Assay 1	0.92	0.79	1.88	0.49
Cleaved Caspase-12 Assay 2	1.32	0.85	1.64	0.20
Cleaved Caspase-12 Assay 3	1.26	0.80	1.96	0.39
Cleaved Caspase-12 Assay 4	0.97	0.80	1.58	0.45
Cleaved Caspase-12 Assay 5	0.87	0.72	1.58	0.18
Mean of All Assays	1.07	0.79	1.73	0.34
Mean of All Assays %	**100**	**74**	**162**	**32**
SD	0.21	0.05	0.18	0.14
SD (%)	20.82	4.61	17.94	14.36
T Test			**0.001**	**0.000001**

ANOVA

Groups	*Count*	*Sum*	*Average*	*Variance*
MEAN C	5	5.336671	1.067334	0.043357
MEAN Ex	5	3.958142	0.791628	0.002124
MEAN PD	5	8.634099	1.726820	0.032022
MEAN PD-Ex	5	1.705812	0.341162	0.006087

ANOVA

Source of Variation	*SS*	*df*	*MS*	*F*	*P-value*	*F crit*
Between Groups	5.046902	3	1.682301	68.46085	2.04E-09	3.238715
Within Groups	0.393701	16	0.024605731			
Total	5.440724	19				

Figure 3.33: Investigating the Amount of Active Caspase-2 in Striatum of Untreated, Exercised. MPTP and MPTP Treated with Exercise Rat PD model

	DETERMINING CASPASE- 2 ACTIVITIES IN STRIATUM OF C, Ex, PD & PD-Ex GROUP			
	MEAN C	**MEAN Ex**	**MEAN PD**	**MEAN PD-Ex**
Active Caspase-2 Assay 1	1.32	0.99	1.63	0.00
Active Caspase-2 Assay 2	1.26	0.93	1.82	0.00
Active Caspase-2 Assay 3	1.33	0.79	1.84	0.00
Active Caspase-2 Assay 4	1.22	0.90	1.98	0.00
Active Caspase-2 Assay 5	1.38	0.84	1.94	0.00
Mean of All Assays	1.30	0.89	1.84	0.00
Mean of All Assays %	**100**	**69**	**142**	**0**
SD	0.06	0.08	0.14	0.00
SD (%)	6.27	7.64	13.55	0.00
T Test			**0.0003**	**0.00001**

ANOVA

Groups	*Count*	*Sum*	*Average*	*Variance*
MEAN C	5	6.497725	1.299545	0.003293
MEAN Ex	5	4.459181	0.891836	0.005083
MEAN PD	5	9.207415	1.841483	0.005488
MEAN PD-Ex	5	0	0	0

ANOVA

Source of Variation	*SS*	*df*	*MS*	*F*	*P-value*	*F crit*
Between Groups	9.046249	3	3.015416	842.8956	1.72E-15	3.238871
Within Groups	0.012503	16	0.000781			
Total	9.058752	19				

Figure 3.35: Investigating the Amount of Cleaved Caspase-3 in Striatum of Untreated, Exercised. MPTP and MPTP Treated with Exercise Rat PD model

	DETERMINING CASPASE-3 ACTIVITIES IN STRIATUM OF C, Ex, PD & PD-Ex GROUP			
	MEAN C	**MEAN Ex**	**MEAN PD**	**MEAN PD-Ex**
Cleaved Caspase-3 Assay 1	1.28	0.74	1.41	0.38
Cleaved Caspase-3 Assay 2	1.38	1.20	1.48	0.46
Cleaved Caspase-3 Assay 3	1.21	0.99	1.49	0.43
Cleaved Caspase-3 Assay 4	1.28	1.21	1.64	0.46
Cleaved Caspase-3 Assay 5	1.31	0.86	1.59	0.43
Mean of All Assays	1.29	1.00	1.52	0.43
Mean of All Assays %	**100**	**77**	**118**	**33**
SD	0.06	0.21	0.09	0.03
SD (%)	6.10	20.76	9.37	3.30
T Test			**0.003**	**0.000002**

ANOVA

Groups	*Count*	*Sum*	*Average*	*Variance*
MEAN C	5	6.459401	1.291880	0.003725
MEAN Ex	5	4.998957	0.999791	0.043108
MEAN PD	5	7.606752	1.521350	0.007875
MEAN PD-Ex	5	2.154970	0.430994	0.010871

ANOVA

Source of Variation	*SS*	*df*	*MS*	*F*	*P-value*	*F crit*
Between Groups	3.329457	3	1.109819	78.29049	8.876E-10	3.238871
Within Groups	0.226810	16	0.014175			
Total	3.556267	19				

Figure 3.37: Investigating the Amount of Active Caspase-8 in Striatum of Untreated, Exercised. MPTP and MPTP Treated with Exercise Rat PD model

	DETERMINING CASPASE-8 ACTIVITIES IN STRIATUM OF C, Ex, PD & PD-Ex GROUP			
	MEAN C	**MEAN Ex**	**MEAN PD**	**MEAN PD-Ex**
Active Caspase-8 Assay 1	1.41	1.03	1.72	0.00
Active Caspase-8 Assay 2	1.26	1.08	1.80	0.00
Active Caspase-8 Assay 3	1.33	1.06	1.85	0.00
Active Caspase-8 Assay 4	1.50	1.02	1.50	0.00
Active Caspase-8 Assay 5	1.31	1.05	1.41	0.00
Mean of All Assays	1.36	1.05	1.66	0.00
Mean of All Assays %	**100**	**77**	**122**	**0**
SD	0.10	0.02	0.19	0.00
SD (%)	9.51	2.38	18.87	0.00
T Test			**0.03**	**0.00004**

ANOVA

Groups	*Count*	*Sum*	*Average*	*Variance*
MEAN C	5	6.803	1.360	0.009
MEAN Ex	5	5.235	1.047	0.000
MEAN PD	5	8.275	1.655	0.035
MEAN PD-Ex	5	0	0	0

ANOVA

Source of Variation	*SS*	*df*	*MS*	*F*	*P-value*	*F crit*
Between Groups	7.802	3	2.600	23.055	2.2E-13	3.238
Within Groups	0.180	16	0.011			
Total	7.983	19				

Figure 3.39: Investigating the Amount of Active Caspase-9 in Striatum of Untreated, Exercised. MPTP and MPTP Treated with Exercise Rat PD model

	DETERMINING CASPASE-9 ACTIVITIES IN STRIATUM OF C, Ex, PD & PD-Ex GROUP			
	MEAN C	**MEAN Ex**	**MEAN PD**	**MEAN PD-Ex**
Active Caspase-9 Assay 1	1.00	0.97	1.38	0.45
Active Caspase-9 Assay 2	1.08	0.86	1.24	0.58
Active Caspase-9 Assay 3	1.00	0.82	1.26	0.76
Active Caspase-9 Assay 4	1.18	0.88	1.22	0.75
Active Caspase-9 Assay 5	1.17	0.89	1.16	0.69
Mean of All Assays	1.09	0.88	1.25	0.65
Mean of All Assays %	**100**	**81**	**115**	**60**
SD	0.09	0.05	0.08	0.13
SD (%)	8.60	5.49	8.14	12.90
T Test			**0.01**	**0.0001**

ANOVA

Groups	*Count*	*Sum*	*Average*	*Variance*
MEAN C	5	5.428507	1.085701	0.007303
MEAN Ex	5	4.417383	0.883477	0.003101
MEAN PD	5	6.259030	1.251806	0.006206
MEAN PD-Ex	5	3.232463	0.646493	0.001615

ANOVA

Source of Variation	*SS*	*df*	*MS*	*F*	*P-value*	*F crit*
Between Groups	1.024810	3	0.341603	40.58947	1.047E-07	3.238715
Within Groups	0.134166	16	0.008385			
Total	1.158976	19				

Figure 3.41: Investigating the Amount of Cleaved Caspase-12 in Striatum of Untreated, Exercised. MPTP and MPTP Treated with Exercise Rat PD model

	DETERMINING CASPASE-12 ACTIVITIES IN STRIATUM OF C, Ex, PD & PD-Ex GROUP			
	MEAN C	**MEAN Ex**	**MEAN PD**	**MEAN PD-Ex**
Cleaved Caspase-12 Assay 1	1.08	0.92	1.87	0.00
Cleaved Caspase-12 Assay 2	0.99	0.87	1.95	0.00
Cleaved Caspase-12 Assay 3	1.14	0.80	1.91	0.00
Cleaved Caspase-12 Assay 4	1.00	0.88	1.86	0.00
Cleaved Caspase-12 Assay 5	1.28	0.80	1.67	0.00
Mean of All Assays	1.10	0.85	1.85	0.00
Mean of All Assays %	**100**	**78**	**169**	**0**
SD	0.12	0.05	0.10	0.00
SD (%)	11.93	5.17	10.49	0.00
T Test			**0.00001**	**0.000002**

ANOVA

Groups	*Count*	*Sum*	*Average*	*Variance*
MEAN C	5	5.488	1.0977	0.01425
MEAN Ex	5	4.2065	0.8413	0.00202
MEAN PD	5	9.2755	1.8551	0.00109
MEAN PD-Ex	5	0	0	0

ANOVA

Source of Variation	*SS*	*df*	*MS*	*F*	*P-value*	*F crit*
Between Groups	8.7275	3	2.90918	417.0104	2.1E-15	3.2387
Within Groups	0.11620	16	0.00697			
Total	8.83916	19				

Figure 3.43: Investigating the Amount of Active CAMK-IV in Cerebellum of Untreated, Exercised. MPTP and MPTP Treated with Exercise Rat PD model

	DETERMINING CAMK-IV ACTIVITIES IN CEREBELLUM OF C, Ex, PD & PD-Ex GROUP			
	MEAN C	**MEAN Ex**	**MEAN PD**	**MEAN PD-Ex**
Active CAMK-IV Assay 1	2.40	2.31	1.87	2.39
Active CAMK-IV Assay 2	2.85	2.47	1.61	2.49
Active CAMK-IV Assay 3	2.07	2.07	1.99	3.11
Active CAMK-IV Assay 4	1.74	2.25	1.68	2.72
Active CAMK-IV Assay 5	2.27	2.67	1.86	1.89
Mean of All Assays	2.27	2.35	1.80	2.52
Mean of All Assays %	**100**	**104**	**80**	**111**
SD	0.41	0.22	0.16	0.45
SD (%)	41.17	22.48	15.54	44.51
T Test			**0.06**	**0.02**

ANOVA

Groups	*Count*	*Sum*	*Average*	*Variance*
MEAN C	5	11.32500039	2.265000078	0.169000653
MEAN Ex	5	11.76793	2.353586	0.050054877
MEAN PD	5	9.015422	1.803084	0.024124138
MEAN PD-Ex	5	12.60643409	2.521286819	0.109898081

ANOVA

Source of Variation	*SS*	*df*	*MS*	*F*	*P-value*	*F crit*
Between Groups	1.417362154	3	0.472454	4.26572	0.021422	3.238715
Within Groups	1.769842184	16	0.110615			
Total	3.187204338	19				

Figure 3.45: Investigating the Amount of Active CAMK-IV in Brain Cortex of Untreated, Exercised. MPTP and MPTP Treated with Exercise Rat PD model

	DETERMINING CAMK-IV ACTIVITIES IN BRAIN CORTEX OF C, Ex, PD & PD-Ex GROUP			
	MEAN C	**MEAN Ex**	**MEAN PD**	**MEAN PD-Ex**
Active CAMK-IV Assay 1	1.80	1.52	1.32	1.96
Active CAMK-IV Assay 2	1.80	3.13	1.67	2.81
Active CAMK-IV Assay 3	2.54	2.89	2.03	2.36
Active CAMK-IV Assay 4	1.85	1.76	1.23	2.47
Active CAMK-IV Assay 5	1.54	1.49	1.49	2.30
Mean of All Assays	1.91	2.16	1.54	2.38
Mean of All Assays %	**100**	**113**	**81**	**125**
SD	0.37	0.79	0.32	0.31
SD (%)	37.45	78.95	31.63	30.93
T Test			**0.1**	**0.003**

ANOVA

Groups	*Count*	*Sum*	*Average*	*Variance*
MEAN C	5	9.529	1.9059	0.140427
MEAN Ex	5	10.78	2.1563	0.623236
MEAN PD	5	7.724	1.5448	0.100044
MEAN PD-Ex	5	11.89	2.3782	0.095065

ANOVA

Source of Variation	*SS*	*df*	*MS*	*F*	*P-value*	*F crit*
Between Groups	1.93	3	0.64	2.67	0.08	3.24
Within Groups	3.83	16	0.24			
Total	5.76	19				

Figure 3.47: Investigating the Amount of Active CAMK-IV in Midbrain of Untreated, Exercised. MPTP and MPTP Treated with Exercise Rat PD model

	DETERMINING CAMK-IV ACTIVITIES IN MIDBRAIN OF C, Ex, PD & PD-Ex GROUP			
	MEAN C	**MEAN Ex**	**MEAN PD**	**MEAN PD-Ex**
Active CAMK-IV Assay 1	2.20	3.45	0.88	4.60
Active CAMK-IV Assay 2	2.41	2.33	1.26	3.34
Active CAMK-IV Assay 3	2.44	2.10	0.93	3.95
Active CAMK-IV Assay 4	2.15	2.31	1.11	3.33
Active CAMK-IV Assay 5	2.03	3.08	1.20	2.76
Mean of All Assays	2.25	2.65	1.08	3.59
Mean of All Assays %	**100**	**118**	**48**	**160**
SD	0.18	0.21	0.17	0.13
SD (%)	17.66	21.00	16.55	13.00
T Test			**0.00001**	**0.001**

ANOVA

Groups	*Count*	*Sum*	*Average*	*Variance*
MEAN C	5	11.2245	2.24490	0.031280
MEAN Ex	5	13.54274	2.708567	0.036965
MEAN PD	5	5.378	1.07623	0.027376
MEAN PD-Ex	5	17.9777	3.59554	0.492138

ANOVA

Source of Variation	*SS*	*df*	*MS*	*F*	*P-value*	*F crit*
Between Groups	16.34063	3	5.446876	24.53671	3.163E-06	3.23871
Within Groups	3.551816	16	0.221988			
Total	19.89245	19				

Figure 3.49: Investigating the Amount of Active CAMK-IV in Striatum of Untreated, Exercised. MPTP and MPTP Treated with Exercise Rat PD model

	DETERMINING CAMK-IV ACTIVITIES IN STRIATUM OF C, Ex, PD & PD-Ex GROUP			
	MEAN C	**MEAN Ex**	**MEAN PD**	**MEAN PD-Ex**
Active CAMK-IV Assay 1	2.50	2.72	0.95	3.98
Active CAMK-IV Assay 2	2.62	3.64	0.79	4.65
Active CAMK-IV Assay 3	3.17	2.79	0.88	3.39
Active CAMK-IV Assay 4	2.59	4.13	1.05	3.78
Active CAMK-IV Assay 5	3.14	2.28	0.97	4.10
Mean of All Assays	2.80	3.11	0.93	3.98
Mean of All Assays %	**100**	**111**	**33**	**142**
Standard Deviation	0.32	0.40	0.10	0.36
Standard Deviation (%)	32.37	40.00	9.91	36.00
T Test			**0.0001**	**0.0001**

ANOVA

Groups	*Count*	*Sum*	*Average*	*Variance*
MEAN C	5	14.019	2.803	0.104
MEAN Ex	5	15.562	3.112	0.516
MEAN PD	5	4.639	0.927	0.009
MEAN PD-Ex	5	19.893	3.978	0.223

ANOVA

Source of Variation	*SS*	*df*	*MS*	*F*	*P-value*	*F crit*
Between Groups	24.789	3	8.263	36.672	2.1E-07	3.238
Within Groups	3.6051	16	0.2253			
Total	28.394	19				

Appendix 4
Data Analysis : ReNcell VM

Figure 4.3: 6OHDA Triggered Death of dDCN

		OPTIMISING 6OHDA CONCENTRATION IN dDCN				
		NOT TREATED	MEAN 50µM 6OHDA	MEAN 100µM 6OHDA	MEAN 150µM 6OHDA	MEAN 200µM 6OHDA
TIME INTERVAL	30 min	100.0	98.6	92.7	86.2	59.7
	1 hour	100.0	76.9	74.4	67.7	49.9
	1 hour 30 mins	100.0	72.4	68.3	59.4	36.0
	2 hour	100.0	73.8	57.5	39.1	28.0
	2 hour 30 min	100.0	51.6	38.5	28.3	28.1
	3 hour	100.0	37.5	28.0	28.4	14.3
	3 hour 30 min	100.0	32.6	23.4	15.5	11.2
	4 hour	100.0	27.2	22.9	12.0	5.2
	5 hour	100.0	25.6	12.7	6.5	4.0

Figure 4.6: 6OHDA Increased Induction of Activated Caspases-2,-3 and -8 in dDCN

	DETERMINING THE PROPORTION OF ACTIVE CASPASES-2,-3 AND -8 EXPRESSED IN TH POSITIVE NOT TREATED AND 6OHDA dDCN											
	NOT TREATED - 6OHDA		TREATED +6OHDA		NOT TREATED -6OHDA		TREATED +6OHDA		NOT TREATED -6OHDA		TREATED +6OHDA	
	TH	ACTIVE CASPASE-2	TH	ACTIVE CASPASE-2	TH	CLEAVED CASPASE-3	TH	CLEAVED CASPASE-3	TH	ACTIVE CASPASE-8	TH	ACTIVE CASPASE-8
Mean of Assay 1	20.13	17.07	12.60	12.60	19.67	6.73	8.47	8.47	24.47	8.87	10.80	10.80
Mean of Assay 2	26.40	16.93	13.67	13.67	24.20	7.00	8.40	8.40	27.53	9.13	12.27	12.27
Mean of Assay 3	26.87	18.53	15.07	15.07	26.40	7.00	8.40	8.40	23.67	8.53	11.20	11.20
Mean of All Assays	24.47	17.51	13.78	13.78	23.42	6.91	8.42	8.42	25.22	8.84	11.42	11.42
Mean of All Assays %	100.0	71.6	56.3	56.3	100.0	29.5	36.0	36.0	100.0	35.1	45.3	45.3
Total Ratio	0.72		1.00		0.30		1.00		0.35		1.00	
Total Ratio (%)	**72**		**100**		**30**		**100**		**35**		**100**	
T TEST	**0.02**				**0.000001**				**0.003**			

Figure 4.8: The Proportion of Active Caspases-2 and -8 in Caspase-3 positive Untreated and Treated 6OHDA dDCN

	PROPORTION OF ACTIVE CASPASEe-2 PRESENT IN CASPASE-3 POSITIVE NOT TREATED AND 6OHDA TREATED dDCN				PROPORTION OF ACTIVE CASPASE-8 PRESENT IN CASPASE-3 POSITIVE NOT TREATED AND 6OHDA TREATED dDCN			
	Non Treated (No 6OHDA)		Treated (6OHDA Induced)		Non Treated (No 6OHDA)		Treated (6OHDA Induced)	
	ACTIVE CASPASE-2	ACTIVE CASPASE-3	ACTIVE CASPASE-2	ACTIVE CASPASE-3	ACTIVE CASPASE-8	ACTIVE CASPASE-3	ACTIVE CASPASE-8	ACTIVE CASPASE-3
Mean of Assay 1	11.13	4.27	3.93	5.93	3.53	2.80	5.20	5.20
Mean of Assay 2	10.73	4.67	4.53	7.20	3.93	3.13	6.27	6.27
Mean of Assay 3	10.67	4.20	4.00	5.20	4.13	3.00	5.53	5.53
Mean of All Assays	10.84	4.38	4.16	6.11	3.87	2.98	5.67	5.67
Mean RATIO	**0.40**		**1.47**		**0.77**		**1.00**	
T TEST	**0.02**				**0.04**			

Figure 4.10: 6OHDA Triggered Caspase Mediated Death of dDCN

	DETERMINING IF 6OHDA TRIGGERS CASPASE MEDIATED DEATH IN dDCN			
	MEAN NOT TREATED	**MEAN zVADfmk**	**MEAN 6OHDA**	**MEAN 6OHDA & zVADfmk**
Mean of Assay 1	0.048	0.026	0.124	0.059
Mean of Assay 2	0.062	0.052	0.183	0.090
Mean of Assay 3	0.033	0.029	0.144	0.080
Mean of All Assays	**0.048**	**0.036**	**0.150**	**0.076**
Mean of All Assays %	**100**	**75**	**315**	**160**
SD	0.014	0.012	0.012	0.021
(n)	3	3	3	3
SQR	1.732	1.732	1.732	1.732
SE	0.008	0.007	0.007	0.012
SE %	0.786	0.716	0.699	1.209
T Test				**0.031**

Figure 4.12: zVADfmk Reduced Amount of Active Caspase-2 in 6OHDA Treated dDCN

	DETERMINING THE AMOUNT OF ACTIVE CASPASE-2 IN 6OHDA TREATED dDCN			
	MEAN NOT TREATED	**MEAN 6OHDA & zVADfmk**	**MEAN 6OHDA**	**MEAN 6OHDA & zVADfmk**
Active Caspase-2 Assay 1	0.981	0.830	1.509	1.262
Active Caspase-2 Assay 2	1.105	0.667	1.448	0.980
Active Caspase-2 Assay 3	0.942	0.739	1.744	1.110
Mean of All Assays	1.010	0.745	1.567	1.117
Mean of All Assays %	**100.0**	**74**	**155**	**111**
SD	0.085	0.081	0.156	0.141
SD (%)	8.517	8.138	15.623	14.11
T Test				**0.02**

Figure 4.14: zVADfmk Reduced Amount of Active Caspase-3 in 6OHDA Treated dDCN

	DETERMINING THE AMOUNT OF CLEAVED CASPASE-3 IN 6OHDA TREATED dDCN			
	MEAN NOT TREATED	**MEAN 6OHDA & zVADfmk**	**MEAN 6OHDA**	**MEAN 6OHDA & zVADfmk**
Cleaved Caspase-3 Assay 1	1.117	0.216	1.725	0.668
Cleaved Caspase-3 Assay 2	0.957	0.269	1.899	0.925
Cleaved Caspase-3 Assay 3	1.188	0.345	1.559	0.713
Mean of All Assays	1.087	0.276	1.728	0.769
Mean of All Assays %	**100**	**25**	**159**	**70**
SD	0.12	0.06	0.17	0.14
SD (%)	11.83	6.48	17.01	13.74
T Test				**0.002**

Figure 4.16: zVADfmk Reduced Amount of Active Caspase-8 in 6OHDA Treated dDCN

	DETERMINING THE AMOUNT OF ACTIVE CASPASE-8 IN 6OHDA TREATED dDCN			
	MEAN NOT TREATED	**MEAN 6OHDA & zVADfmk**	**MEAN 6OHDA**	**MEAN 6OHDA & zVADfmk**
Active Caspase-8 Assay 1	0.952	0.217	1.713	1.048
Active Caspase-8 Assay 2	1.036	0.365	1.973	1.150
Active Caspase-8 Assay 3	1.019	0.362	1.842	1.099
Mean of All Assays	1.003	0.315	1.843	1.099
Mean of All Assays %	**100.0**	**31**	**184**	**110**
SD	0.0442	0.0849	0.1298	0.0509
SD (%)	4.4204	8.4872	12.9768	5.0933
T Test				**0.005**

Figure 4.18: 6OHDA Triggered Caspases, PERK and NFκB Apoptotic Death of dDCN

	DETERMINING IF 6OHDA TRIGGERS APOPTOTIC DEATH IN dDCN							
	MEAN NOT TREATED	MEAN 6OHDA	MEAN 6OHDA & SALUBRINAL	MEAN 6OHDA & IKK	MEAN 6OHDA & zVADfmk	MEAN 6OHDA & zLEVDfmk	MEAN 6OHDA & zIETDfmk	MEAN 6OHDA & zVDVADfmk
Mean of Assay 1	0.79	2.15	1.05	1.36	0.98	1.14	1.26	1.04
Mean of Assay 2	0.82	2.19	1.09	1.27	0.99	1.13	1.30	1.06
Mean of Assay 3	0.77	2.10	1.08	1.28	1.00	1.14	1.27	1.08
Mean of All Assays	0.79	2.15	1.07	1.31	0.99	1.14	1.28	1.06
Mean of All Assays %	**100**	**271**	**136**	**165**	**125**	**144**	**161**	**134**
SD	0.023	0.047	0.021	0.047	0.011	0.005	0.019	0.017
(n)	3	3	3	3	3	3	3	3
SQR	1.73	1.73	1.73	1.73	1.73	1.73	1.73	1.73
SE	0.013	0.027	0.012	0.027	0.006	0.003	0.011	0.010
SE %	1.343	2.711	1.187	2.689	0.611	0.295	1.069	0.976
T Test			**0.00009**	**0.00003**	**0.0003**	**0.0006**	**0.0002**	**0.0002**

Anova

SUMMARY

Groups	Count	Sum	Average	Variance
Mean 6OHDA	24	51.48533333	2.145222222	0.003086683
Mean 6OHDA and Salubrinal	24	25.76033333	1.073347222	0.002407261
Mean 6OHDA and IKK	24	31.33233333	1.305513889	0.003584676
Mean 6OHDA and zVADfmk	24	23.69266667	0.987194444	0.001239207
Mean 6OHDA and zLEVDfmk	24	27.332	1.138833333	0.000981729
Mean 6OHDA and zIETDfmk	24	30.62166667	1.275902778	0.002239193
Mean 6OHDA and zVDVADfmk	24	25.403	1.058458333	0.000912955

ANOVA

Source of Variation	SS	df	MS	F	P-value	F crit
Between Groups	22.71938126	6	3.786563543	1834.105192	2.037E-145	2.155302264
Within Groups	0.332389185	161	0.002064529			
Total	23.05177044	167				

Appendix 5
Data Analysis : NFκB

Figure 5.3: Presence of NFκB Expressed in Untreated and 6OHDA Treated dDCN

	DETERMINING THE PROPORTION p65 NFκB EXPRESSED IN TH POSITIVE NOT TREATED AND 6OHDA dDCN			
	Non Treated (No 6OHDA)		Treated (6OHDA)	
	Active TH	Cleaved NFκB	Active TH	Cleaved NFκB
Mean of Assay 1	34.60	17.06	9.67	10.00
Mean of Assay 2	36.13	18.22	10.13	11.00
Mean of Assay 3	32.73	20.36	11.93	10.60
Mean of All Assays	34.49	18.55	10.58	10.53
Mean of All Assays %	100.00	53.78	30.67	30.54
Total Ratio	0.54		1.00	
Total Ratio (%)	**54**		**100**	
T TEST	**0.01**			

Figure 5.5: 6OHDA Triggers Activation NFκB in dDCN

	6OHDA INCREASED ACTIVATION OF NFκB IN dDCN	
	MEAN NOT TREATED	**MEAN TREATED 6OHDA**
Cleaved NFκB Assay 1	0.824	1.360
Cleaved NFκB Assay 2	0.686	1.217
Cleaved NFκB Assay 3	0.955	1.349
Cleaved NFκB Assay 4	0.363	1.438
Cleaved NFκB Assay 5	0.310	1.542
Mean Assay	0.627	1.381
Mean Assay(%)	**100**	**220**
SD	0.28	0.12
SD (%)	28.31	11.99
T Test		**0.002**

Figure 5.8: Proportion of Active Caspases-2,-3 and -8 Expressed in NFκB Positive Untreated and 6OHDA Treated dDCN

	DETERMINING THE PROPORTION OF ACTIVE CASPASES-2,-3 AND -8 EXPRESSED IN NFκB POSITIVE NOT TREATED AND 6OHDA dDCN											
	Non Treated (No 6OHDA)		Treated (6OHDA)		Non Treated (No 6OHDA)		Treated (6OHDA)		Non Treated (No 6OHDA)		Treated (6OHDA)	
	Cleaved NFκB	Active Caspase-2	Cleaved NFκB	Active Caspase-2	Cleaved NFκB	Cleaved Caspase-3	Cleaved NFκB	Cleaved Caspase-3	Cleaved NFκB	Active Caspase-8	Cleaved NFκB	Active Caspase-8
Mean of Assay 1	36.67	19.33	10.00	8.13	41.93	11.00	10.47	5.47	19.67	7.60	9.87	9.87
Mean of Assay 2	42.33	16.01	8.00	8.33	41.40	11.20	9.93	6.00	24.20	8.21	10.40	10.40
Mean of Assay 3	41.93	18.56	10.87	8.80	39.67	12.00	10.53	5.27	26.40	8.13	12.00	12.00
Mean of All Assays	40.31	17.97	9.62	8.42	41.00	11.40	10.31	5.58	23.42	10.31	10.76	10.76
Mean of All Assays %	100.00	44.57	23.87	20.89	100.00	30.60	25.15	13.60	100.00	34.03	45.92	45.92
Total Ratio	0.45		0.88		0.31		0.54		0.34		1.00	
Total Ratio (%)	**45**		**88**		**31**		**54**		**34**		**100**	
T TEST	**0.02**				**0.02**				**0.01**			

Figure 5.10: Optimising the Concentration of IKK in 6OHDA Treated dDCN

	DETERMINING THE EFFECT OF IKK IN 6OHDA dDCN									
	MEAN NOT TREATED	**MEAN IKK**	**MEAN 6OHDA**	**MEAN 6OHDA & IKK 10µM**	**MEAN 6OHDA & IKK 30µM**	**MEAN 6OHDA & IKK 50µM**	**MEAN 6OHDA & IKK 70µM**	**MEAN 6OHDA & IKK 80µM**	**MEAN 6OHDA & IKK 100µM**	**MEAN 6OHDA & IKK 120µM**
Mean of Assay 1	2.26	2.26	0.73	0.75	0.78	0.71	1.29	1.33	1.32	1.33
Mean of Assay 2	2.27	2.20	0.69	0.66	0.67	0.71	1.31	1.35	1.38	1.37
Mean of Assay 3	2.29	2.26	0.65	0.70	0.69	0.73	1.25	1.29	1.27	1.19
Mean of All Assays	2.27	2.24	0.69	0.70	0.71	0.72	1.29	1.32	1.32	1.30
Mean of All Assays %	**100**	**99**	**30**	**31**	**31**	**32**	**57**	**58**	**58**	**57**
SD	0.018	0.031	0.041	0.045	0.059	0.010	0.030	0.033	0.054	0.097
(n)	3	3	3	3	3	3	3	3	3	3
SQR	1.732	1.732	1.732	1.732	1.732	1.732	1.732	1.732	1.732	1.732
SE	0.010	0.018	0.023	0.026	0.034	0.006	0.017	0.019	0.031	0.056
SE %	1.033	1.767	2.344	2.621	3.427	0.597	1.708	1.903	3.139	5.611
T Test							**0.0001**			

Figure 5.12: IKK and zVADfmk Promote Survival of 6OHDA Treated dDCN

	6OHDA TRIGGERS NFκB CLASSICAL AND CASPASE MEDIATED DEATH OF dDCN						
	MEAN NOT TREATED	**MEAN IKK**	**MEAN zVADfmk**	**MEAN 6OHDA**	**MEAN 6OHDA & zVADfmk**	**MEAN 6OHDA & IKK**	**MEAN 6OHDA & zVADfmk & IKK**
Mean of Assay 1	2.059	2.035	2.103	0.535	1.004	1.285	1.539
Mean of Assay 2	2.121	2.099	2.051	0.671	0.955	1.203	1.545
Mean of Assay 3	2.114	2.109	2.123	0.631	1.205	0.934	1.539
Mean of All Assays	2.098	2.081	2.092	0.612	1.055	1.141	1.541
Mean of All Assays %	**100**	**99**	**100**	**29**	**50**	**54**	**73**
SD	0.03	0.04	0.04	0.07	0.13	0.18	0.00
(n)	3	3	3	3	3	3	3
SQR	1.73	1.73	1.73	1.73	1.73	1.73	1.73
SE	0.02	0.02	0.02	0.04	0.08	0.11	0.00
SE %	1.97	2.31	2.15	4.04	7.65	10.60	0.20
T Test					**0.014**	**0.026**	**0.002**

Figure 5.14: Determining the Amount of Cleaved NFκB in IKK Treated 6OHDA dDCN

	CLEAVED NFκB IS SUPPRESSED BY IKK IN 6OHDA dDCN			
	MEAN NOT TREATED	**MEAN IKK**	**MEAN 6OHDA**	**MEAN 6OHDA & IKK**
Cleaved NFκB Assay 1	0.918	0.000	1.488	0.000
Cleaved NFκB Assay 2	1.069	0.000	1.572	0.000
Cleaved NFκB Assay 3	1.148	0.000	1.444	0.000
Mean Assay	1.045	0.000	1.502	0.000
Mean Assay(%)	**100**	**0**	**144**	**0**
SD	0.12	0.00	0.07	0.00
SD (%)	11.69	0.00	6.50	0.00
T Test			**0.009**	

Figure 5.16: IKK and zIETDfmk Promote Survival of 6OHDA Treated dDCN

	DETERMINING IF CASPASE-8 IS ACTIVE IN NFκB CLASSICAL PATHWAY OF 6OHDA dDCN						
	MEAN NOT TREATED	**MEAN IKK**	**MEAN zIETDfmk**	**MEAN 6OHDA**	**MEAN 6OHDA & IKK**	**MEAN 6OHDA & zIETDfmk**	**MEAN 6OHDA & IKK & zIETDfmk**
Mean of Assay 1	2.109	2.108	2.157	0.694	1.215	1.206	1.272
Mean of Assay 2	2.091	2.116	2.124	0.694	1.282	1.298	1.266
Mean of Assay 3	2.115	2.102	2.102	0.657	1.328	1.456	1.482
Mean of All Assays	2.105	2.109	2.128	0.682	1.275	1.320	1.340
Mean of All Assays %	**100**	**100**	**101**	**32**	**61**	**63**	**64**
SD	0.013	0.007	0.028	0.022	0.057	0.126	0.123
(n)	3	3	3	3	3	3	3
SQR	1.73	1.73	1.73	1.73	1.73	1.73	1.73
SE	0.01	0.00	0.02	0.01	0.03	0.07	0.07
SE %	0.74	0.38	1.60	1.24	3.28	7.29	7.11
T Test					**0.001**	**0.01**	**0.01**
					0.62		
						0.472	**0.852**

Figure 5.19: Proportion of Active Caspase-8 Expressed in NFκB Positive 6OHDA, IKK, zIETDfmk Treated dDCN

	DETERMINING THE PROPORTION OF ACTIVE CASPASES-8 EXPRESSED IN NFκB NOT TREATED AND 6OHDA TREATED dDCN															
	NOT TREATED (-6OHDA)								TREATED (+6OHDA)							
			IKK		zIETDfmk		IKK & zIETDfmk				IKK		zIETDfmk		IKK & zIETDfmk	
	NFκB	ACTIVE CASPASE-8	NFκB	ACTIVE CASPASE-8	NFκB	ACTIVE CASPASE-8	NFκB	ACTIVE CASPASE-8	NFκB	ACTIVE CASPASE-8	NFκB	ACTIVE CASPASE-8	NFκB	ACTIVE CASPASE-8	NFκB	ACTIVE CASPASE-8
Mean of Assay 1	22.67	5.53	0.00	0.00	19.53	0.00	0.00	0.00	12.00	12.00	0.00	0.00	9.13	0.00	0.00	0.00
Mean of Assay 2	20.13	6.13	0.00	0.00	20.73	0.00	0.00	0.00	8.07	8.07	0.00	0.00	9.93	0.00	0.00	0.00
Mean of Assay 3	15.27	4.87	0.00	0.00	14.33	0.00	0.00	0.00	7.93	7.93	0.00	0.00	8.73	0.00	0.00	0.00
Mean of All Assays	19.36	5.51	0.00	0.00	18.20	0.00	0.00	0.00	9.33	9.33	0.00	0.00	9.27	0.00	0.00	0.00
Mean of All Assays %	**100**	**28**	**0**	**0**	**94**	**0**	**0**	**0**	**100**	**100**	**0**	**0**	**99**	**0**	**0**	**0**
Total Ratio	0.28		0.00		0.00		0.00		1.00		0.00		0.00		0.00	
Total Ratio (%)	**28**		**0**		**0**		**0**		**100**		**0**		**0**		**0**	

Figure 5.21 : Determining the Amount of Active Caspase-8 in IKK Treated 6OHDA dDCN

	ACTIVE CASPASE-8 IS SUPPRESSED BY IKK IN 6OHDA dDCN			
	MEAN NOT TREATED	**MEAN IKK**	**MEAN 6OHDA**	**MEAN 6OHDA & IKK**
Active Caspase-8 Assay 1	0.883	0.000	2.164	0.000
Active Caspase-8 Assay 2	0.924	0.000	1.937	0.000
Active Caspase-8 Assay 3	1.133	0.000	1.515	0.000
Mean Assay	0.980	0.000	1.872	0.000
Mean Assay(%)	**100**	**0**	**191**	**0**
SD	0.13	0.00	0.33	0.00
SD (%)	13.43	0.00	32.91	0.00
T Test			**0.029**	

Figure 5.23: IKK and zVDVADfmk Promote Survival of 6OHDA Treated dDCN

	DETERMINING IF CASPASE-2 IS ACTIVE IN NFκB CLASSICAL PATHWAY OF 6OHDA dDCN						
	MEAN NOT TREATED	**MEAN IKK**	**MEAN zVDVADfmk**	**MEAN 6OHDA**	**MEAN 6OHDA & IKK**	**MEAN 6OHDA & zVDVADfmk**	**MEAN 6OHDA & IKK & zVDVADfmk**
Mean of Assay 1	2.07	2.03	2.09	0.65	1.23	1.63	1.67
Mean of Assay 2	2.10	2.11	2.11	0.67	1.16	1.59	1.66
Mean of Assay 3	2.03	2.05	2.06	0.56	1.16	1.40	1.52
Mean of All Assays	2.07	2.06	2.09	0.62	1.18	1.54	1.61
Mean of All Assays %	**100**	**100**	**101**	**30**	**57**	**75**	**78**
SD	0.04	0.04	0.03	0.06	0.04	0.13	0.08
(n)	3.00	3.00	3.00	3.00	3.00	3.00	3.00
SQR	1.73	1.73	1.73	1.73	1.73	1.73	1.73
SE	0.02	0.02	0.01	0.03	0.02	0.07	0.05
SE %	2.18	2.45	1.50	3.47	2.41	7.23	4.76
T Test					**0.0004**	**0.002**	**0.0001**
					0.03		
						0.004	**0.449**

Figure 5.26: Proportion of Active Caspase-2 Expressed in NFκB Positive 6OHDA, IKK, zVDVADfmk Treated dDCN

	DETERMINING THE PROPORTION OF ACTIVE CASPASES-2 EXPRESSED NFκB POSITIVE NOT TREATED AND 6OHDA TREATED dDCN															
	NOT TREATED (-6OHDA)								TREATED (+6OHDA)							
			IKK		zVDVA Dfmk		IKK & zVDVA Dfmk				IKK		zVDVA Dfmk		IKK & zVDVA Dfmk	
	NFκB	ACTIVE CASPASE-2	NFκB	ACTIVE CASPASE-2	NFκB	ACTIVE CASPASE-2	NFκB	ACTIVE CASPASE-2	NFκB	ACTIVE CASPASE-2	NFκB	ACTIVE CASPASE-2	NFκB	ACTIVE CASPASE-2	NFκB	ACTIVE CASPASE-2
Mean of Assay 1	23.13	8.20	0.00	0.00	24.20	0.00	0.00	0.00	13.07	13.00	0.00	0.00	11.20	0.00	0.00	0.00
Mean of Assay 2	27.20	11.47	0.00	0.00	26.47	0.00	0.00	0.00	9.80	9.80	0.00	0.00	9.60	0.00	0.00	0.00
Mean of Assay 3	25.93	12.80	0.00	0.00	22.13	0.00	0.00	0.00	9.53	9.53	0.00	0.00	9.40	0.00	0.00	0.00
Mean of All Assays	25.42	10.82	0.00	0.00	24.27	0.00	0.00	0.00	10.80	10.78	0.00	0.00	10.07	0.00	0.00	0.00
Mean of All Assays %	**100**	**43**	**0**	**0**	**95**	**0**	**0**	**0**	**100**	**100**	**0**	**0**	**93**	**0**	**0**	**0**
Total Ratio	0.43		0.00		0.00		0.00		1.00		0.00		0.00		0.00	
Total Ratio (%)	**43**		**0**		**0**		**0**		**100**		**0**		**0**		**0**	

Figure 5.28: Determining the Amount of Active Caspase-2 in IKK Treated 6OHDA dDCN

	ACTIVE CASPASE-2 IS SUPPRESSED BY IKK IN 6OHDA dDCN			
	MEAN NOT TREATED	**MEAN IKK**	**MEAN 6OHDA**	**MEAN 6OHDA & IKK**
Active Caspase-2 Assay 1	0.830	0.000	1.647	0.000
Active Caspase-2 Assay 2	0.869	0.000	1.252	0.000
Active Caspase-2 Assay 3	0.643	0.000	1.352	0.000
Mean Assay	0.781	0.000	1.417	0.000
Mean Assay(%)	**100**	**0**	**181**	**0**
SD	0.12	0.00	0.21	0.00
SD (%)	12.06	0.00	20.55	0.00
T Test			**0.016**	

Figure 5.29: zVDVADfmk and IKK Provide Further Survival of 6OHDA Treated dDCN

	DETERMINING IF CASPASES-2 AND -8 ARE ACTIVE IN NFκB CLASSICAL PATHWAY OF 6OHDA dDCN										
	MEAN NOT TREATED	MEAN IKK	MEAN zVDVADfmk	MEAN zIETDfmk	MEAN 6OHDA	MEAN 6OHDA & IKK	MEAN 6OHDA & zVDVADfmk	MEAN 6OHDA & zIETDfmk	MEAN 6OHDA & IKK & zIETDfmk	MEAN 6OHDA & IKK & zVDVADfmk	MEAN 6OHDA & IKK & zIETDfmk & zVDVADfmk
Mean of Assay 1	2.167	2.190	2.195	2.162	0.541	1.224	1.542	1.235	1.260	1.594	1.649
Mean of Assay 2	2.201	2.118	2.139	2.184	0.554	1.241	1.506	1.213	1.225	1.563	1.595
Mean of Assay 3	2.105	2.115	2.133	2.136	0.560	1.133	1.601	1.120	1.182	1.699	1.731
Mean of All Assays	2.158	2.141	2.156	2.160	0.552	1.199	1.550	1.189	1.222	1.619	1.659
Mean of All Assays %	**100**	**99**	**100**	**100**	**26**	**56**	**72**	**55**	**57**	**75**	**77**
SD	0.05	0.04	0.03	0.02	0.01	0.06	0.05	0.06	0.04	0.07	0.07
(n)	3	3	3	3	3	3	3	3	3	3	3
SQR	1.73	1.73	1.73	1.73	1.73	1.73	1.73	1.73	1.73	1.73	1.73
SE	0.03	0.02	0.02	0.01	0.01	0.03	0.03	0.04	0.02	0.04	0.04
SE %	2.83	2.45	1.98	1.39	0.56	3.36	2.79	3.54	2.26	4.12	3.95
T Test						**0.002**	**0.001**	**0.003**	**0.001**	**0.0012**	**0.001**
							0.001	**0.848**	**0.603**	**0.002**	**0.001**
									0.482	**0.247**	
									0.003		
									0.001	**0.002**	
										0.002	**0.522**

Anova

SUMMARY				
Groups	Count	Sum	Average	Variance
6OHDA	24	13.24	0.55	0.00
6OHDA + IKK	24	28.78	1.20	0.00
6OHDA + zVDVADfmk	24	37.19	1.55	0.01
6OHDA + zIETDfmk	24	28.54	1.19	0.00
6OHDA + IKK + zIETDfmk	24	29.33	1.22	0.00
6OHDA + IKK + zVDVADfmk	24	38.85	1.62	0.01
6OHDA + IKK + zIETDfmk + zVDVADfmk	24	39.80	1.66	0.01

ANOVA

Source of Variation	SS	df	MS	F	P-value	F crit
Between Groups	21.0907477	6	3.515124617	635.7417172	2.455E-109	2.155302264
Within Groups	0.890196519	161	0.005529171			
Total	21.98094422	167				

Figure 5.34 : IKK and zLEVDfmk Promote Survival of 6OHDA Treated dDCN

	DETERMINING IF CASPASE-4 IS ACTIVE IN NFκB CLASSICAL PATHWAY OF 6OHDA dDCN						
	MEAN NOT TREATED	**MEAN IKK**	**MEAN zLEVDfmk**	**MEAN 6OHDA**	**MEAN 6OHDA & IKK**	**MEAN 6OHDA & zLEVDfmk**	**MEAN 6OHDA & IKK & zLEVDfmk**
Mean of Assay 1	2.075	2.166	2.143	0.586	1.082	1.238	1.560
Mean of Assay 2	2.075	2.106	2.107	0.605	1.066	1.239	1.568
Mean of Assay 3	2.019	2.048	2.036	0.598	1.096	1.230	1.603
Mean of All Assays	2.056	2.106	2.095	0.596	1.082	1.236	1.577
Mean of All Assays %	**100**	**102**	**102**	**29**	**53**	**60**	77
SD	0.03	0.06	0.05	0.01	0.01	0.01	0.02
(n)	3.00	3.00	3.00	3.00	3.00	3.00	3.00
SQR	1.73	1.73	1.73	1.73	1.73	1.73	1.73
SE	0.02	0.03	0.03	0.01	0.01	0.00	0.01
SE %	1.89	3.41	3.14	0.57	0.86	0.29	1.32
T Test					**0.00001**	**0.000002**	**0.00002**
					0.001		
						0.00002	**0.001**

Figure 5.37: Proportion of Active Caspase-4 Expressed in NFκB Positive 6OHDA, IKK, zLEVDfmk Treated dDCN

	DETERMINING THE PROPORTION OF ACTIVE CASPASES-4 EXPRESSED IN NFκB NOT TREATED AND 6OHDA TREATED dDCN															
	NOT TREATED (-6OHDA)								TREATED (+6OHDA)							
			IKK		zLEVDfmk		IKK & zLEVDfmk				IKK		zLEVDfmk		IKK & zLEVDfmk	
	NFκB	ACTIVE CASPASE-4	NFκB	ACTIVE CASPASE-4	NFκB	ACTIVE CASPASE-4	NFκB	ACTIVE CASPASE-4	NFκB	ACTIVE CASPASE-4	NFκB	ACTIVE CASPASE-4	NFκB	ACTIVE CASPASE-4	NFκB	ACTIVE CASPASE-4
Mean of Assay 1	15.80	4.67	0.00	5.73	13.07	0.00	0.00	0.00	5.93	7.67	0.00	7.93	6.47	0.00	0.00	0.00
Mean of Assay 2	12.33	6.80	0.00	7.00	12.00	0.00	0.00	0.00	6.33	8.40	0.00	7.20	6.40	0.00	0.00	0.00
Mean of Assay 3	11.73	7.60	0.00	8.20	14.00	0.00	0.00	0.00	5.67	6.93	0.00	9.13	5.53	0.00	0.00	0.00
Mean of All Assays	13.29	6.36	0.00	6.98	13.02	0.00	0.00	0.00	5.98	7.67	0.00	8.09	6.13	0.00	0.00	0.00
Mean of All Assays %	**100**	**48**	**0**	**53**	**98**	**0**	**0**	**0**	**100**	**128**	**0**	**135**	**103**	**0**	**0**	**0**
Total Ratio	0.48		0.00		0.00		0.00		1.28		0.00		0.00		0.00	
Total Ratio (%)	**48**		**0**		**0**		**0**		**128**		**0**		**0**		**0**	

Figure 5.39: Determining the Amount of Active Caspase-4 in IKK Treated 6OHDA dDCN

	DETERMINING THE AMOUNT OF ACTIVE CASPASE-4 IN IKK TREATED 6OHDA dDCN			
	MEAN NOT TREATED	**MEAN IKK**	**MEAN 6OHDA**	**MEAN 6OHDA & IKK**
Active Caspase-4 Assay 1	1.013	0.983	1.666	1.760
Active Caspase-4 Assay 2	0.940	0.877	2.123	1.899
Active Caspase-4 Assay 3	0.805	1.304	1.733	2.177
Mean Assay	0.920	1.055	1.840	1.945
Mean Assay(%)	**100**	**115**	**200**	**212**
SD	0.106	0.222	0.247	0.212
SD (%)	10.56	22.23	24.66	21.23
T Test			**0.013**	**0.607**

Figure 5.40: zLEVDfmk and IKK Provide Further Survival of 6OHDA Treated dDCN

	DETERMINING THE EFFECT OF CASPASES-2 AND -8 ACTIVITIES IN NFκB CLASSICAL PATHWAY OF 6OHDA dDCN													
	MEAN NOT TREATED	MEAN IKK	MEAN zVDVADfmk	MEAN zLEVDfmk	MEAN zIETDfmk	MEAN 6OHDA	MEAN 6OHDA & IKK	MEAN 6OHDA & zVDVADfmk	MEAN 6OHDA & zLEVDfmk	MEAN 6OHDA & zIETDfmk	MEAN 6OHDA & IKK & zVDVADfmk	MEAN 6OHDA & IKK & zLEVDfmk	MEAN 6OHDA & IKK & zIETDfmk	MEAN 6OHDA & IKK & zVDVADfmk & zLEVDfmk & zIETDfmk
Mean of Assay 1	2.078	2.075	2.039	2.027	2.038	0.491	1.159	1.418	1.180	1.195	1.469	1.687	1.186	1.725
Mean of Assay 2	2.046	2.027	2.021	2.021	1.996	0.375	1.135	1.509	1.278	1.143	1.360	1.760	1.106	1.801
Mean of Assay 3	2.011	2.031	2.109	2.109	2.036	0.422	1.148	1.443	1.196	1.176	1.490	1.720	1.173	1.760
Mean of All Assays	2.045	2.044	2.057	2.052	2.023	0.430	1.147	1.457	1.218	1.171	1.439	1.722	1.155	1.762
Mean of All Assays %	**100**	**100**	**100**	**100**	**99**	**21**	**56**	**71**	**60**	**57**	**70**	**84**	**56**	**86**
SD	0.03	0.03	0.05	0.05	0.02	0.06	0.01	0.05	0.05	0.03	0.07	0.04	0.04	0.04
(n)	3	3	3	3	3	3	3	3	3	3	3	3	3	3
SQR	1.73	1.73	1.73	1.73	1.73	1.73	1.73	1.73	1.73	1.73	1.73	1.73	1.73	1.73
SE	0.02	0.02	0.03	0.03	0.01	0.03	0.01	0.03	0.03	0.02	0.04	0.02	0.02	0.02
SE %	1.93	1.5	2.70	2.86	1.40	3.37	0.68	2.72	3.03	1.52	4.02	2.12	2.47	2.21

		5												
T Test						**0.002**	**0.00003**	**0.001**	**0.004**	**0.0001**	**0.00003**	**0.001**	**0.00002**
							0.005	**0.139**	**0.250**	**0.016**	**0.001**	**0.788**	**0.001**
											0.005	**0.265**	**0.0001**
										0.746	**0.0003**	**0.609**	
											0.007		
											0.0001		
										0.008			

Anova

SUMMARY

Groups	Count	Sum	Average	Variance
MEAN 6OHDA + IKK	24	27.53433333	1.147263889	0.002159063
MEAN 6OHDA + zVDVADfmk	24	34.95633333	1.456513889	0.006126309
MEAN 6OHDA + zLEVDfmk	24	29.22566667	1.217736111	0.005338522
MEAN 6OHDA + zIETDfmk	24	28.11183333	1.171326389	0.002020492
MEAN 6OHDA + IKK + zVDVADfmk	24	36.508	1.521166667	0.010800686
MEAN 6OHDA + IKK + zLEVDfmk	24	39.6466	1.651941667	0.011186528
MEAN 6OHDA + IKK + zIETDfmk	24	27.72	1.155	0.00315399
MEAN 6OHDA + IKK + zVDVADfmk + zLEVDfmk + zIETDfmk	24	42.061	1.752541667	0.004240037

ANOVA

Source of Variation	SS	df	MS	F	P-value	F crit
Between Groups	9.913130631	7	1.416161519	251.5940169	1.2052E-90	2.0596375
Within Groups	1.035691241	184	0.005628757			
Total	10.94882187	191				

Figure 5.42

Various treatments used by combining different inhibitors such as IKK, zVDVADfmk, zLEVDfmk and zIETDfmk to determine if maximal cell survival could be achieved by suppression of Caspases-2,-4,-8 and NFκB activity in 6OHD treated dDCN

	Treatment 1	Treatment 2	Treatment 3	Treatment 4	Treatment 5	Treatment 6	Treatment 7	Treatment 8	
	6OHD IKK	6OHD zVDVADfmk	6OHD zLEVDfmk	6OHD zIETDfmk	6OHD IKK zVDVADfmk	6OHD IKK zLEVDfmk	6OHD IKK zIETDfmk	6OHD IKK zVDVADfmk zLEVDfmk zIETDfmk	p-value obtained
Comparison 1	+	+	-	-	-	-	-	-	0.005
Comparison 2	+	-	+	-	-	-	-	-	0.139
Comparison 3	+	-	-	+	-	-	-	-	0.250
Comparison 4	+	-	-	-	+	-	-	-	0.016
Comparison 5	+	-	-	-	-	+	-	-	0.001
Comparison 6	+	-	-	-	-	-	+	-	0.788
Comparison 7	+	-	-	-	-	-	-	+	0.001
Comparison 8	-	-	-	-	+	-	-	+	0.005
Comparison 9	-	-	-	-	-	+	-	+	0.265
Comparison 10	-	-	-	-	-	-	+	+	0.0001
Comparison 11	-	-	-	-	+	+	-	-	0.008

Comparison 12	-	-	-	-	+	-	+	-	**0.007**
Comparison 13	-	-	-	-	-	+	+	-	**0.0001**
Comparison 14	-	+	-	-	+	-	-	-	**0.746**
Comparison 15	-	-	+	-	-	+	-	-	**0.0003**
Comparison 16	-	-	-	+	-	-	+	-	**0.609**
	6OHDIKK	**6OHDzVDVADfmk**	**6OHDzLEVDfmk**	**6OHDzIETDfmk**	**6OHDIKKzVDVADfmk**	**6OHDIKKzLEVDfmk**	**6OHDIKKzIETDfmk**	**6OHDIKKzVDVADfmkzLEVDfmkzIETDfmk**	**p-value obtained**
	Treatment 1	**Treatment 2**	**Treatment 3**	**Treatment 4**	**Treatment 5**	**Treatment 6**	**Treatment 7**	**Treatment 8**	

Appendix 6
Data Analysis : ER Stress

Figure 6.2: Salubrinal Promoted Survival of 6OHDA Treated dDCN

	DETERMINING THE EFFECT OF SALUBRINAL IN 6OHDA dDCN			
	MEAN NOT TREATED	**MEAN SALUBRINAL**	**MEAN 6OHDA**	**MEAN 6OHDA & SALUBRINAL**
Mean of Assay 1	1.613	1.500	0.561	1.042
Mean of Assay 2	1.523	1.391	0.533	1.117
Mean of Assay 3	1.344	1.278	0.707	1.078
Mean of All Assays	1.494	1.390	0.600	1.079
Mean of All Assays %	**100**	**93**	**40**	**72**
SD	0.14	0.11	0.09	0.04
(n)	3.000	3.000	3.000	3.000
SQR	1.732	1.732	1.732	1.732
SE	0.08	0.06	0.05	0.02
SE %	7.90	6.42	5.38	2.17
T Test				**0.006**

Figure 6.4: Optimising the Concentration of Salubrinal in 6OHDA Treated dDCN

	DETERMINING THE EFFECT OF SALUBRINAL AND zVADfmk IN 6OHDA dDCN							
	MEAN NOT TREATED	MEAN 6OHDA	MEAN SALUBRINAL 30µM	MEAN SALUBRINAL 50µM	MEAN SALUBRINAL 70µM	MEAN SALUBRINAL 80µM	MEAN SALUBRINAL 100µM	MEAN SALUBRINAL 120µM
Mean of Assay 1	1.800	0.684	1.214	1.236	1.303	1.283	1.276	1.285
Mean of Assay 2	2.063	0.827	1.543	1.581	1.609	1.597	1.599	1.600
Mean of Assay 3	1.858	0.610	1.264	1.239	1.311	1.265	1.251	1.252
Mean of All Assays	1.907	0.707	1.340	1.352	1.408	1.382	1.375	1.379
Mean of All Assays %	**100**	**37**	**70**	**71**	**74**	**72**	**72**	**72**
SD	0.14	0.11	0.18	0.20	0.17	0.19	0.19	0.19
(n)	3	3	3	3	3	3	3	3
SQR	1.73	1.73	1.73	1.73	1.73	1.73	1.73	1.73
SE	0.08	0.06	0.10	0.11	0.10	0.11	0.11	0.11
SE %	7.95	6.37	10.23	11.47	10.06	10.78	11.21	11.08
T Test			**0.01**					

Figure 6.6: Salubrinal and zVADfmk Promote Survival of 6OHDA Treated dDCN

	DETERMINING THE EFFECT OF SALUBRINAL AND zVADfmk IN 6OHDA dDCN						
	MEAN NOT TREATED	**MEAN SALUBRINAL**	**MEAN zVADfmk**	**MEAN 6OHDA**	**MEAN 6OHDA & zVADfmk**	**MEAN 6OHDA & SALUBRINAL**	**MEAN 6OHDA & SALUBRINAL & zVADfmk**
Mean of Assay 1	1.98	1.87	1.89	0.65	1.18	1.50	1.82
Mean of Assay 2	1.85	1.75	1.76	0.56	1.06	1.51	1.68
Mean of Assay 3	2.05	1.94	1.99	0.61	1.08	1.55	1.84
Mean of All Assays	1.96	1.85	1.88	0.61	1.11	1.52	**1.78**
Mean of All Assays %	**100**	**94**	**96**	**31**	**56**	**78**	**91**
SD	0.10	0.09	0.11	0.05	0.06	0.03	0.09
(n)	3.00	3.00	3.00	3.00	3.00	3.00	3.00
SQR	1.73	1.73	1.73	1.73	1.73	1.73	1.73
SE	0.06	0.05	0.07	0.03	0.04	0.02	0.05
SE %	5.74	5.47	6.59	2.67	3.58	1.68	5.07
T Test					**0.001**	**0.00004**	**0.0002**

Figure 6.8 : Salubrinal and zVDVADfmk Promote Survival of 6OHDA Treated dDCN

	DETERMINING IF CASPASE-2 IS ACTIVE IN ER STRESS PATHWAY OF 6OHDA dDCN						
	MEAN NOT TREATED	**MEAN SALUBRINAL**	**MEAN zVDVADfmk**	**MEAN 6OHDA**	**MEAN 6OHDA & SALUBRINAL**	**MEAN 6OHDA & zVDVADfmk**	**MEAN 6OHDA & SALUBRINAL & zVDVADfmk**
Mean of Assay 1	2.08	2.13	2.10	0.65	1.44	1.52	1.51
Mean of Assay 2	2.18	2.19	2.14	0.55	1.27	1.39	1.52
Mean of Assay 3	2.12	2.11	2.15	0.73	1.46	1.35	1.48
Mean of All Assays	2.13	2.14	2.13	0.64	1.39	1.42	1.50
Mean of All Assays %	**100**	**101**	**100**	**30**	**65**	**67**	**71**
SD	0.048	0.041	0.027	0.087	0.104	0.090	0.023
(n)	3	3	3	3	3	3	3
SQR	1.73	1.73	1.73	1.73	1.73	1.73	1.73
SE	0.028	0.023	0.016	0.050	0.060	0.052	0.013
SE %	2.755	2.348	1.557	5.031	6.026	5.214	1.313
T Test					**0.001**	**0.0004**	**0.002**
						0.716	
						0.199	**0.257**

Figure 6.11: Proportion of Active Caspase-2 Expressed in TH Positive 6OHDA, IKK, zVDVADfmk Treated dDCN

	DETERMINING THE PROPORTION OF ACTIVE CASPASES-2 EXPRESSED NOT TREATED AND 6OHDA TREATED dDCN															
	NOT TREATED (-6OHDA)								TREATED (+6OHDA)							
			SALUBRINAL		zVDVADfmk		SALUBRINAL & zVDVADfmk				SALUBRINAL		zVDVADfmk		SALUBRINAL & zVDVADfmk	
	TH	ACTIVE CASPASE-2	TH	ACTIVE CASPASE-2	TH	ACTIVE CASPASE-2	TH	ACTIVE CASPASE-2	TH	ACTIVE CASPASE-2	TH	ACTIVE CASPASE-2	TH	ACTIVE CASPASE-2	TH	ACTIVE CASPASE-2
Mean of Assay 1	39.40	27.47	36.27	0.00	35.87	0.00	36.73	0.00	8.73	8.73	9.27	0.00	13.00	0.00	11.33	0.00
Mean of Assay 2	38.40	29.27	39.07	0.00	37.00	0.00	36.40	0.00	7.80	7.80	6.67	0.00	11.67	0.00	14.33	0.00
Mean of Assay 3	37.07	27.33	37.07	0.00	36.47	0.00	36.40	0.00	7.07	7.07	7.40	0.00	12.67	0.00	11.00	0.00
Mean of All Assays	38.29	28.02	37.47	0.00	36.44	0.00	36.51	0.00	7.87	7.87	7.78	0.00	12.44	0.00	12.22	0.00
Mean of All Assays %	**100**	**73**	**98**	**0**	**95**	**0**	**95**	**0**	**100**	**100**	**99**	**0**	**158**	**0**	**155**	**0**
Total Ratio	0.73		0.00		0.00		0.00		1.00		0.00		0.00		0.00	
Total Ratio (%)	**73**		**0**		**0**		**0**		**100**		**0**		**0**		**0**	

Figure 6.13: Determining the Amount of Active Caspase-2 in Salubrinal Treated 6OHDA dDCN

	ACTIVE CASPASE-2 IS SUPPRESSED BY SALUBRINAL IN 6OHDA dDCN			
	MEAN NOT TREATED	**MEAN SALUBRINAL**	**MEAN 6OHDA**	**MEAN 6OHDA & SALUBRINAL**
Active Caspase-2 Assay 1	1.069	0.000	1.702	0
Active Caspase-2 Assay 2	1.117	0.000	1.604	0
Active Caspase-2 Assay 3	0.959	0.000	1.746	0
Active Caspase-2 Assay 4	0.529	0.000	1.529	0
Active Caspase-2 Assay 5	0.421	0.000	2.416	0
Mean of All Assays	0.819	0.000	1.799	0.000
Mean of All Assays %	**100**	**0**	**220**	**0**
SD	0.321	0.000	0.355	0.000
SD (%)	32.13	0.00	35.48	0.00
T Test			**0.02**	

Figure 6.15 : Salubrinal and zLEVDfmk Promote Survival of 6OHDA Treated dDCN

	DETERMINING IF CASPASE-4 IS ACTIVE IN ER STRESS PATHWAY OF 6OHDA dDCN						
	MEAN NOT TREATED	**MEAN SALUBRINAL**	**MEAN zLEVDfmk**	**MEAN 6OHDA**	**MEAN 6OHDA & SALUBRINAL**	**MEAN 6OHDA & zLEVDfmk**	**MEAN 6OHDA & SALUBRINAL & zLEVDfmk**
Mean of Assay 1	2.03	2.02	2.10	0.72	1.43	1.22	1.57
Mean of Assay 2	2.03	2.07	2.11	0.67	1.38	1.26	1.61
Mean of Assay 3	2.04	2.05	2.06	0.60	1.36	1.17	1.54
Mean of All Assays	2.03	2.05	2.09	0.66	1.39	1.22	1.57
Mean of All Assays %	**100**	**101**	**103**	**33**	**68**	**60**	77
SD	0.010	0.025	0.025	0.059	0.036	0.045	0.036
(n)	3	3	3	3	3	3	3
SQR	1.73	1.73	1.73	1.73	1.73	1.73	1.73
SE	0.006	0.014	0.015	0.034	0.021	0.026	0.021
SE %	0.585	1.437	1.461	3.391	2.101	2.578	2.057
T Test					**0.0002**	**0.0003**	**0.0001**
					0.007		
						0.004	**0.001**

Figure 6.18: Proportion of Active Caspase-4 Expressed in TH Positive 6OHDA, IKK, zLEVDfmk Treated dDCN

	DETERMINING THE PROPORTION OF ACTIVE CASPASES-4 EXPRESSED NOT TREATED AND 6OHDA TREATED dDCN															
	NOT TREATED (-6OHDA)								TREATED (+6OHDA)							
			SALUBRINAL		zLEVDfmk		SALUBRINAL & zLEVDfmk				SALUBRINAL		zLEVDfmk		SALUBRINAL & zLEVDfmk	
	TH	ACTIVE CASPASE-4	TH	ACTIVE CASPASE-4	TH	ACTIVE CASPASE-4	TH	ACTIVE CASPASE-4	TH	ACTIVE CASPASE-4	TH	ACTIVE CASPASE-4	TH	ACTIVE CASPASE-4	TH	ACTIVE CASPASE-4
Mean of Assay 1	37.07	13.60	30.20	14.07	31.27	0.00	30.20	0.00	13.33	13.33	12.87	12.87	17.33	0.00	18.60	0.00
Mean of Assay 2	36.87	14.00	35.60	15.53	32.80	0.00	28.80	0.00	11.40	11.40	14.07	14.07	16.67	0.00	19.47	0.00
Mean of Assay 3	24.80	12.87	29.80	15.27	29.33	0.00	34.20	0.00	14.13	14.13	14.07	14.07	18.67	0.00	19.40	0.00
Mean of All Assays	32.91	13.49	31.87	14.96	31.13	0.00	31.07	0.00	12.96	12.96	13.67	13.67	17.56	0.00	19.16	0.00
Mean of All Assays %	**100**	**41**	**97**	**45**	**95**	**0**	**94**	**0**	**100**	**100**	**105**	**105**	**136**	**0**	**148**	**0**
Total Ratio	0.41		0.47		0.00		0.00		1.00		1.00		0.00		0.00	
Total Ratio (%)	**41**		**47**		**0**		**0**		**100**		**100**		**0**		**0**	

Figure 6.20: Determining the Amount of Active Caspase-4 in Salubrinal Treated 6OHDA dDCN

	DETERMINING THE AMOUNT OF ACTIVE CASPASE-4 IN SALUBRINAL TREATED 6OHDA dDCN			
	MEAN NOT TREATED	**MEAN SALUBRINAL**	**MEAN 6OHDA**	**MEAN 6OHDA & SALUBRINAL**
Active Caspase-4 Assay 1	1.117	1.100	1.520	0.978
Active Caspase-4 Assay 2	0.942	0.965	1.356	1.057
Active Caspase-4 Assay 3	1.164	1.134	1.468	1.576
Active Caspase-4 Assay 4	0.586	1.637	2.545	3.223
Active Caspase-4 Assay 5	1.117	0.657	1.348	1.295
Mean of All Assays	0.985	1.099	1.647	1.626
Mean of All Assays %	**100**	**112**	**167**	**165**
SD	0.239	0.355	0.507	0.325
SD (%)	23.89	35.50	50.71	32.51
T Test			**0.04**	**0.965**

Figure 6.21: zLEVDfmk and Salubrinal Provide Further Survival of 6OHDA Treated dDCN

	DETERMINING IF CASPASES-2 AND -4 ARE ACTIVE IN PERK ER STRESS PATHWAY OF 6OHDA dDCN										
	MEAN NOT TREATED	MEAN SALUBRINAL	MEAN zVDVADfmk	MEAN zLEVDfmk	MEAN 6OHDA	MEAN 6OHDA & SALUBRINAL	MEAN 6OHDA & zVDVADfmk	MEAN 6OHDA & zLEVDfmk	MEAN 6OHDA & SALUBRINAL & zVDVADfmk	MEAN 6OHDA & SALUBRINAL & zLEVDfmk	MEAN 6OHDA & SALUBRINAL & zVDVADfmk & zLEVDfmk
Mean of Assay 1	2.06	2.10	2.02	2.15	0.69	1.40	1.39	1.14	1.42	1.66	1.71
Mean of Assay 2	2.13	2.12	1.95	1.95	0.45	1.31	1.28	1.06	1.27	1.59	1.66
Mean of Assay 3	2.05	2.06	2.02	2.02	0.64	1.37	1.38	1.09	1.36	1.49	1.64
Mean of All Assays	2.08	2.09	2.00	2.04	0.59	1.36	1.35	1.10	1.35	1.58	1.67
Mean of All Assays %	**100**	**99**	**99**	**98**	**28**	**65**	**65**	**53**	**65**	**76**	**80**
SD	0.04	0.03	0.04	0.10	0.13	0.05	0.06	0.04	0.08	0.08	0.04
(n)	3	3	3	3	3	3	3	3	3	3	3
SQR	1.73	1.73	1.73	1.73	1.73	1.73	1.73	1.73	1.73	1.73	1.73
SE	0.03	0.02	0.02	0.06	0.07	0.03	0.04	0.02	0.04	0.05	0.02
SE %	2.55	1.86	2.41	5.78	7.44	2.76	3.63	2.40	4.43	4.72	2.25
T Test						**0.005**	**0.003**	**0.014**	**0.002**	**0.001**	**0.003**
							0.825	**0.002**	**0.812**	**0.024**	**0.001**
									0.023		
										0.003	
										0.008	**0.181**

Anova

SUMMARY

Groups	Count	Sum	Average	Variance
MEAN 6OHDA	24	14.201	0.591708333	0.01389124
MEAN 6OHDA & SALUBRINAL	24	32.652	1.3605	0.005065778
MEAN 6OHDA & zVDVADfmk	24	32.39233333	1.349680556	0.007106381
MEAN 6OHDA & zLEVDfmk	24	26.37883333	1.099118056	0.003887373
MEAN 6OHDA & SALUBRINAL & zVDVADfmk	24	32.329	1.347041667	0.009138766
MEAN 6OHDA & SALUBRINAL & zLEVDfmk	24	37.901	1.579208333	0.014660945
MEAN 6OHDA & SALUBRINAL & zVDVADfmk & zLEVDfmk	24	40.10966667	1.671236111	0.007173164

ANOVA

Source of Variation	SS	df	MS	F	P-value	F crit
Between Groups	18.35216541	6	3.058694236	351.4375867	9.09191E-90	2.155302264
Within Groups	1.401243892	161	0.008703378			
Total	19.75340931	167				

Figure 6.26 : Salubrinal and zIETDfmk Promote Survival of 6OHDA Treated dDCN

	DETERMINING IF CASPASE-8 IS ACTIVE IN ER STRESS PATHWAY OF 6OHDA dDCN						
	MEAN NOT TREATED	MEAN SALUBRINAL	MEAN zIETDfmk	MEAN 6OHDA	MEAN 6OHDA & zIETDfmk	MEAN 6OHDA & SALUBRINAL	MEAN 6OHDA & SALUBRINAL & zIETDfmk
Mean of Assay 1	2.14	2.14	2.15	0.67	1.48	1.26	1.76
Mean of Assay 2	2.16	2.12	2.12	0.67	1.51	1.32	1.78
Mean of Assay 3	1.99	2.04	2.10	0.67	1.57	1.36	1.83
Mean of All Assays	2.10	2.10	2.12	0.67	1.52	1.31	1.79
Mean of All Assays %	**100**	**100**	**101**	**32**	**72**	**63**	**85**
SD	0.09	0.05	0.02	0.00	0.05	0.05	0.04
(n)	3	3	3	3	3	3	3
SQR	1.73	1.73	1.73	1.73	1.73	1.73	1.73
SE	0.05	0.03	0.01	0.00	0.03	0.03	0.02
SE %	5.39	2.78	1.35	0.20	2.74	3.00	2.10
T Test					**0.001**	**0.002**	**0.0003**
					0.007		
						0.002	**0.0004**

Figure 6.29: Proportion of Active Caspase-8 Expressed in TH Positive 6OHDA, IKK, zIETDfmk Treated dDCN

	DETERMINING THE PROPORTION OF ACTIVE CASPASES-8 EXPRESSED NOT TREATED AND 6OHDA TREATED dDCN															
	NOT TREATED (-6OHDA)								TREATED (+6OHDA)							
			SALUBRINAL		zIETDfmk		SALUBRINAL & zIETDfmk				SALUBRINAL		zIETDfmk		SALUBRINAL & zIETDfmk	
	TH	ACTIVE CASPASE-8	TH	ACTIVE CASPASE-8	TH	ACTIVE CASPASE-8	TH	ACTIVE CASPASE-8	TH	ACTIVE CASPASE-8	TH	ACTIVE CASPASE-8	TH	ACTIVE CASPASE-8	TH	ACTIVE CASPASE-8
Mean of Assay 1	40.93	13.00	38.73	11.00	38.60	0.00	38.47	0.00	14.13	14.13	16.27	16.27	16.73	0.00	19.53	0.00
Mean of Assay 2	41.07	12.07	39.07	12.33	38.47	0.00	40.13	0.00	14.00	14.00	14.73	14.73	16.33	0.00	17.33	0.00
Mean of Assay 3	38.20	16.67	39.00	11.20	37.87	0.00	37.93	0.00	11.40	11.40	13.33	13.33	15.93	0.00	17.40	0.00
Mean of All Assays	40.07	13.91	38.93	11.51	38.31	0.00	38.84	0.00	13.18	13.18	14.78	14.78	16.33	0.00	18.09	0.00
Mean of All Assays %	**100**	**35**	**97**	**29**	**96**	**0**	**97**	**0**	**100**	**100**	**112**	**112**	**124**	**0**	**137**	**0**
Total Ratio	0.35		0.30		0.00		0.00		1.00		1.00		0.00		0.00	
Total Ratio (%)	**35**		**30**		**0**		**0**		**100**		**100**		**0**		**0**	

Figure 6.31: Determining the Amount of Active Caspase-8 in Salubrinal Treated 6OHDA dDCN

	DETERMINING THE AMOUNT OF ACTIVE CASPASE-8 IN SALUBRINAL TREATED 6OHDA dDCN			
	MEAN NOT TREATED	**MEAN SALUBRINAL**	**MEAN 6OHDA**	**MEAN 6OHDA & SALUBRINAL**
Active Caspase-8 Assay 1	0.970	0.945	1.876	1.359
Active Caspase-8 Assay 2	0.980	1.082	1.336	2.154
Active Caspase-8 Assay 3	0.912	0.968	1.473	1.520
Active Caspase-8 Assay 4	0.871	0.830	1.954	2.373
Active Caspase-8 Assay 5	0.974	1.485	1.861	1.543
Mean of All Assays	0.941	1.062	1.700	1.790
Mean of All Assays %	**100**	**113**	**181**	**190**
SD	0.048	0.253	0.276	0.445
SD (%)	4.79	25.28	27.63	44.49
T Test			**0.003**	**0.713**

Figure 6.32: zLEVDfmk, zIETDfmk and Salubrinal Provide Further Survival of 6OHDA Treated dDCN

	DETERMINING THE EFFECT OF CASPASES-2,-4 AND -8 ACTIVITIES IN PERK ER STRESS PATHWAY OF 6OHDA dDCN													
	MEAN NOT TREATED	MEAN SALUBRINAL	MEAN zVDVADfmk	MEAN zLEVDfmk	MEAN zIETDfmk	MEAN 6OHDA	MEAN 6OHDA & SALUBRINAL	MEAN 6OHDA & zVDVADfmk	MEAN 6OHDA & zLEVDfmk	MEAN 6OHDA & zIETDfmk	MEAN 6OHDA & SALUBRINAL & zVDVADfmk	MEAN 6OHDA & SALUBRINAL & zLEVDfmk	MEAN 6OHDA & SALUBRINAL & zIETDfmk	MEAN 6OHDA & SALUBRINAL & zVDVADfmk & zLEVDfmk & zIETDfmk
Mean of Assay 1	2.06	2.02	2.07	2.03	2.01	0.66	1.32	1.33	1.14	1.33	1.31	1.56	1.73	1.85
Mean of Assay 2	2.08	2.01	2.05	2.05	2.06	0.78	1.41	1.43	1.19	1.30	1.41	1.60	1.70	1.84
Mean of Assay 3	2.05	2.03	2.00	2.00	1.96	0.62	1.40	1.37	1.17	1.35	1.38	1.61	1.71	1.87
Mean of All Assays	2.06	2.02	2.04	2.03	2.01	0.69	1.38	1.38	1.17	1.33	1.36	1.59	1.71	1.85
Mean of All	**100**	**102**	**102**	**98**	**97**	**33**	**67**	**67**	**57**	**64**	**66**	**77**	**83**	**90**

Assays %														
SD	0.02	0.01	0.04	0.02	0.05	0.08	0.05	0.05	0.03	0.03	0.05	0.03	0.01	0.02
(n)	3	3	3	3	3	3	3	3	3	3	3	3	3	3
SQR	1.73	1.73	1.73	1.73	1.73	1.73	1.73	1.73	1.73	1.73	1.73	1.73	1.73	1.73
SE	0.01	0.01	0.02	0.01	0.03	0.05	0.03	0.03	0.02	0.02	0.03	0.02	0.01	0.01
SE%	0.95	0.71	2.04	1.29	2.77	4.74	2.85	3.12	1.66	1.66	2.86	1.52	0.82	0.90
T Test							**0.001**	**0.001**	**0.01**	**0.003**	**0.001**	**0.001**	**0.002**	**0.001**
								0.94	**0.01**	**0.2**	**0.74**	**0.01**	**0.004**	**0.002**
												0.002	**0.004**	**0.0003**
											0.8066	**0.001**	**0.003**	
											0.006			
												0.005		
												0.004		

Anova

SUMMARY

Groups	Count	Sum	Average	Variance
MEAN 6OHDA	24	16.5012	0.68755	0.007345
MEAN 6OHDA & SALUBRINAL	24	33.09333	1.378888889	0.003563
MEAN 6OHDA & zVDVADfmk	24	33.009	1.375375	0.00608
MEAN 6OHDA & zLEVDfmk	24	28.015	1.167291667	0.004312
MEAN 6OHDA & zIETDfmk	24	31.81433	1.325597222	0.003816
MEAN 6OHDA & SALUBRINAL & zVDVADfmk	24	32.74333	1.364305556	0.006285
MEAN 6OHDA & SALUBRINAL & zLEVDfmk	24	38.13	1.588763	0.005

		033	889	599
MEAN 6OHDA & SALUBRINAL & zIETDfmk	24	41.11	1.712916 667	0.002 739
MEAN 6OHDA & SALUBRINAL & zVDVADfmk & zLEVDfmk & zIETDfmk	24	44.46 233	1.852597 222	0.000 858

ANOVA

Source of Variation	SS	df	MS	F	P-value	F crit
Between Groups	21.73 443	8	2.71680 4008	602.27 89	7.423E-139	1.983 337
Within Groups	0.933 751	207	0.00451 0874			
Total	22.66 818	215				

Figure 6.34

Various treatments used by combining different inhibitors such as salubrinal, zVDVADfmk, zLEVDfmk and zIETDfmk to determine if maximal cell survival could be achieved by suppression of Caspases-2,-4,-8 and PERK activity in 6OHD treated dDCN

	Treatment 1	Treatment 2	Treatment 3	Treatment 4	Treatment 5	Treatment 6	Treatment 7	Treatment 8	
	6OHD SALUBRINAL	6OHD zVDVADfmk	6OHD zLEVDfmk	6OHD zIETDfmk	6OHD SALUBRINAL zVDVADfmk	6OHD SALUBRINAL zLEVDfmk	6OHD SALUBRINAL zIETDfmk	6OHD SALUBRINAL zVDVADfmk zLEVDfmk zIETDfmk	p-value obtained
Comparison 1	+	+	-	-	-	-	-	-	0.94
Comparison 2	+	-	+	-	-	-	-	-	0.01
Comparison 3	+	-	-	+	-	-	-	-	0.2
Comparison 4	+	-	-	-	+	-	-	-	0.74
Comparison 5	+	-	-	-	-	+	-	-	0.01
Comparison 6	+	-	-	-	-	-	+	-	0.004
Comparison 7	+	-	-	-	-	-	-	+	0.002
Comparison 8	-	-	-	-	+	-	-	+	0.002
Comparison 9	-	-	-	-	-	+	-	+	0.0004
Comparison	-	-	-	-	-	-	+	+	0.003

10									
Comparison 11	-	-	-	-	+	+	-	-	**0.006**
Comparison 12	-	-	-	-	+	-	+	-	**0.004**
Comparison 13	-	-	-	-	-	+	+	-	**0.005**
Comparison 14	-	+	-	-	+	-	-	-	**0.807**
Comparison 15	-	-	+	-	-	+	-	-	**0.0001**
Comparison 16	-	-	-	+	-	-	+	-	**0.0003**
	6OHDSALUBRINAL	**6OHDzVDVADfmk**	**6OHDzLEVDfmk**	**6OHDzIETDfmk**	**6OHDSALUBRINALzVDVADfmk**	**6OHDSALUBRINALzLEVDfmk**	**6OHDSALUBRINALzIETDfmk**	**6OHDSALUBRINALzVDVADfmkzLEVDfmkzIETDfmk**	**p-value obtained**
	Treatment 1	**Treatment 2**	**Treatment 3**	**Treatment 4**	**Treatment 5**	**Treatment 6**	**Treatment 7**	**Treatment 8**	

Figure 6.37: IKK and Salubrinal Provide Further Survival of 6OHDA Treated dDCN

	6OHDA TRIGGERS PERK ER STRESS & NFκB CLASSICAL PATHWAY IN dDCN						
	MEAN NOT TREATED	MEAN SALUBRINAL	MEAN IKK	MEAN 6OHDA	MEAN 6OHDA & SALUBRINAL	MEAN 6OHDA & IKK	MEAN 6OHDA & SALUBRINAL & IKK
Mean of Assay 1	2.059	2.035	2.038	0.643	1.357	1.089	1.620
Mean of Assay 2	2.008	2.057	1.957	0.645	1.301	1.044	1.601
Mean of Assay 3	2.018	2.027	2.041	0.649	1.313	1.021	1.624
Mean of All Assays	2.028	2.040	2.012	0.646	1.323	1.051	1.615
Mean of All Assays %	**100**	**101**	**99**	**32**	**65**	**52**	**80**
SD	0.03	0.02	0.05	0.00	0.03	0.03	0.01
(n)	3	3	3	3	3	3	3
SQR	1.73	1.73	1.73	1.73	1.73	1.73	1.73
SE	0.015	0.009	0.028	0.002	0.017	0.020	0.007
SE %	1.547	0.898	2.755	0.180	1.702	2.013	0.691
T Test					**0.0006**	**0.0023**	**0.00002**
					0.0006		
						0.0011	**0.0004**

Figure 6.41: zVADfmk, IKK and Salubrinal Provide Further Survival of 6OHDA Treated dDCN

	DETERMINING THE EFFECT OF PERK ER STRESS, NFκB AND CASPASE ACTIVITIES OF 6OHDA INDUCED dDCN								
	MEAN NOT TREATED	MEAN SALUBRINAL	MEAN zVADfmk	MEAN IKK	MEAN 6OHDA	MEAN 6OHDA & zVADfmk	MEAN 6OHDA & SALUBRINAL	MEAN 6OHDA & IKK	MEAN 6OHDA & SALUBRINAL & zVADfmk & IKK
Mean of Assay 1	2.123	2.122	2.137	2.172	0.688	1.096	1.526	1.178	1.939
Mean of Assay 2	2.066	2.066	2.072	1.988	0.643	1.050	1.517	1.152	1.886
Mean of Assay 3	2.039	1.914	1.921	1.888	0.586	1.033	1.484	1.137	1.842
Mean of All Assays	2.076	2.034	2.043	2.016	0.639	1.060	1.509	1.156	1.889
Mean of All Assays %	**100**	**98**	**98**	**98**	**31**	**51**	**73**	**56**	**91**
SD	0.04	0.11	0.11	0.14	0.05	0.03	0.02	0.02	0.05
(n)	3	3	3	3	3	3	3	3	3
SQR	1.73	1.73	1.73	1.73	1.73	1.73	1.73	1.73	1.73
SE	0.025	0.062	0.064	0.083	0.029	0.019	0.013	0.012	0.028
SE %	2.480	6.220	6.399	8.320	2.931	1.893	1.296	1.191	2.803
T Test						**0.001**	**0.0002**	**0.001**	**0.00001**
							0.00004		
						0.0001			
							0.02		
							0.00005	**0.0016**	**0.0003**

Anova

SUMMARY

Groups	Count	Sum	Average	Variance
MEAN6OHDA	24	15.334	0.638917	0.006718
MEAN 6OHDA & zVADfmk	24	25.4347	1.059779	0.003327
MEAN 6OHDA & SALUBRINAL	24	36.21266667	1.508861	0.005377
MEAN 6OHDA & IKK	24	27.73233333	1.155514	0.005202
MEAN 6OHDA & SALUBRINAL & zVADfmk & IKK	24	45.3345	1.888938	0.004093

ANOVA

Source of Variation	SS	df	MS	F	P-value	F crit
Between Groups	21.45081119	4	5.362703	1084.836	2.76E-90	2.450570518
Within Groups	0.568482844	115	0.004943			
Total	22.01929447	119				

Appendix 7
Publications

Publication (Academic Journal)

Chaudhry ZL, Ahmed BY, 2014, The Role of Caspases in Parkinson's disease Pathogenesis: A brief look at the Mitochondrial Pathway, Journal of Austin Alzheimer and Parkinson disease, 1, 4, 1-5.

Chaudhry ZL, Ahmed BY, 2013, Caspase-2 and caspase-8 trigger caspase-3 activation following 6-OHDA-induced stress in human dopaminergic neurons differentiated from ReNVM stem cells, Neurol Res, 35, 4, 435-440

Conference platform and poster presentations

Chaudhry Z L, Ahmed B, 'Inhibition of PERK and NFKB pathway can reduce death of stressed dopaminergic neurons differentiated from human stem cell line', XXI International Parkinson Congress, Milan, Italy (December 2015).

Chaudhry Z L, Ahmed B, 'The Role of Caspases in ER and NFκB Mediated Death of 6OHDA treated dopaminergic neurons', XXI International Parkinson Congress, Milan, Italy (December 2015).

Chaudhry Z L, Paige A J W. Ahmed BY, Protective role of zVADfmk and Salubrinal against 6OHD-induced neurotoxicity in dopaminergic neurons, University of Bedfordshire Conference, Bedfordshire , UK (July 2011)

Chaudhry Z, Chalimoniuk M. Langfort J. and Ahmed BY. "A Study of Caspases and Exercise in Parkinsons Disease: Does Exercise Suppress Cell Death?"Abstr. the 10th International Conference on Alzheimer's & Parkinson's Diseases Barcelona, Spain (March 2011)

Chaudhry Z L, and Ahmed BY, Caspases 2 and 8 trigger Caspase 3 activation in 6OHD treated dDCN, University of Bedfordshire Conference, Bedfordshire , UK(July 2010)

Chaudhry Z, Ahmed BY., Chalimoniuk M. and Langfort J. "The Role of Caspases & Exercise in Parkinson's disease. Abstr. XVIII International Parkinson Congress, Miami, Florida, USA (Dec 2009).

Chaudhry ZL, (2009), 'Examining the effect of exercise on different PD brain regions in animal model', *SPRING Exercise International conference*, London, UK, September 2009,

Ahmed BY., Chalimoniuk M, Chaudhry Z, Ali H and Langfort J. "Exercise as a neuroprotective mechanism in Parkinson's disease" Abstr. SPRING Exercise International conference, London, UK (Invited speaker, Sept 2009)

Chaudhry Z L, Ahmed BY, Chalimoniuk M, and Langfort J., The effect of exercise on Caspase and CAMK IV levels in Parkinson's Disease, University of Bedfordshire Conference, Bedfordshire , UK(July 2009)

Chaudhry Z, group presentation (Ahmed BY. Ayub R , Ali H and Fathy S), August 2008, Research seminar Exercise and Parkinson disease, (invited, UoB staff and students, general public and members of Parkinson Disease Society, UK and SPRING (Special Parkinson disease research group)

Chaudhry Z, Western Blot Analysis on CAMK IV in Normal and Parkinsonian Rat Brain, The Science, Engineering & Technology Awards Limited, London, UK (July 2008)

Prizes and awards

2008 Dr Mike Daniel Memorial Prize	Awarded
2008 Science, Engineering & Technology Student of the Year Award	Nominee
2007 Mentoring Gold	Awarded
2007 Duke of Edinburgh Gold	Awarded
2007 Millennium Volunteers Silver	Awarded